

# **Development of a New General Click Chemistry Method and Applications in Bioconjugation:**

**Part I: Rewiring Bacteria Cell Surfaces with Bio-Orthogonal Chemistry**

**Part II: A Novel General Dialdehyde Click Chemistry for Primary Amine Conjugation**

Sina Elahipanah

**A Dissertation Submitted to the Faculty of Graduate Studies in Partial Fulfillment  
of the Requirements for the Degree of Doctor of Philosophy**

Graduate Program in Chemistry

York University

Toronto, Ontario

May 2017

© Sina Elahipanah, 2017

## Abstract

The ability to tailor cell surfaces with non-native molecules is critical to advance the study of cellular communication, cell behavior, and for next-generation therapeutics. There has been a tremendous effort to tailor mammalian cell surfaces with organic functional groups; however, there are few reliable and non-invasive methods for re-wiring the bacterial cell surface. Current methods to re-engineer bacteria surfaces rely on complicated, slow, and often expensive molecular biology and metabolic manipulation methods with a limited scope on the type of molecules installed onto the surface. In the first part of this report, we introduce a new straightforward method based on liposome fusion to re-engineer Gram-negative bacteria cell surface with bio-orthogonal groups that can subsequently be conjugated to a range of molecules (biomolecules, small molecules, probes, proteins) for further studies and programmed behavior of bacteria. This method is fast, efficient, inexpensive, and useful for installing a broad scope of ligands and biomolecules to Gram-negative bacteria surfaces.

The development of methods to conjugate a range of molecules to primary amine functional groups have revolutionized the fields of chemistry, biology and material science. Due to its abundance, the primary amine is the most convenient functional group handle in molecules for ligation to other molecules for a broad range of applications that affect all scientific fields. Current conjugation methods with primary amines include the use of activated carboxylic acids, isothiocyanates, Michael addition type systems and reaction with ketones or aldehydes followed by in situ reductive amination. In the second part, we introduce a new traceless, high yield, fast; click chemistry method based on the rapid and

efficient trapping of amine groups via a functionalized dialdehyde group. The click reaction occurs in mild conditions in organic solvents or aqueous media, proceeds in high yield. Moreover, no catalyst or activating group is required and the only by-product is water. The dialdehyde headgroup was used for applications in cell surface engineering and for tailoring surfaces for material science applications. We anticipate broad utility of the general dialdehyde click chemistry to primary amines in all areas of chemical research ranging from polymers, bioconjugation to material science and nanoscience.

## **Dedication**

This thesis is dedicated to my parents, who have always been there in good and bad times with me. To my mother Manijeh, my backbone, my spine, my strength and my hope to live, for her unconditional love and compassion; a woman who has taught me the true meaning of persistence and optimism. To my father Shokrollah, from whom I have learned humbleness, wisdom, reason and literacy.

*Sina Elahipanah*



## Acknowledgments

I would like to get started from my PI Prof. **Muhammad N. Yousaf**. Muhammad has a very distinctive characteristic that I can claim with confidence very few of his other students have been or will ever be exposed to as I experienced. In the past years, we have developed a unique relation that is only possible with the humblest of advisors. He showed me to see the true “other sides” and to have a different vision of life. Looking at his ambitious personality, I learned not to submit easy and always climb up one more step. I learned to be my hardest critic of my own work, to take a step back along with a deep breath, and look at the “big picture” of my work. Perhaps the most important souvenir I took from his training was to take responsibility. His greatest training was “no training” and made me dig in and fight for knowledge. Not because he did not care, rather for the trust he had in me. He convinced me that I should always ask “why” and don’t give up until I found the answers to it. He taught me how to catch a fish beside other competitive fishermen. He gave me the opportunity explore science the way I wanted to, He guided me through each step and realigned me back onto the right path, a quality that very few advisors share with him. He gave me the opportunity to help him put his new lab together, a unique chance than no other graduate student experiences in a lifetime. His ability to train the new generation of thinkers is an admirable and exclusive quality of Muhammad.

He has served as an academic advisor, a mentor and a true friend. During the past years, I have seen many colleagues and compared their relations with their PIs. He and I have serious differences and conflict of ideas, but this only led to remarkable developments

in our work. Although I have always chosen to call him “boss”, for that reason, I am proud to have had a “friend” more than a “boss”.

Besides my advisor, I would like to thank the rest of my thesis committee: Prof. **P.G Potvin**, Prof. **G. Audette**, Prof. **Yingfu Li** and Prof. **Z.H Zhu** for their insightful comments and encouragement, but also for the hard question, which incited me to widen my research from various perspectives.

In this regard, I would like to extend my deepest special gratitude to Prof **P.G Potvin** for his help and guidance that is simply beyond what I can state in a short paragraph of a thesis. Perhaps it would take an entire chapter to thank him. He took me as an undergraduate thesis student in 2008 and trained me to be a professional student. He has been a true friend, mentor and extraordinary influence in my life. While I have benefited enormously from his infinite knowledge of chemistry, we have shared many non-science moments with each other, during which, I have learnt how to approach and tackle life problems.

I would also like to extend my special gratitude to Prof. **G. Audette** for accepting to be on my committee on a late notice. I have most certainly enjoyed my discussions and conversations with him about the project and biological experiments conducted in this work. He served to be the sole biologist/biochemist on my committee, who truly kept me excited and motivated about the field, and encouraged me to constantly learn more about the principles of my work. His challenging questions and comments only made me dig in deeper.

My sincere thanks also go to **Dr. W. Luo, Dr. Hunter, Dr. Donaldson, Dr. Johnson,** and **Dr. Jamie Kwan** for their help in synthesis, NMR spectroscopy, biological experiments, consultation and advising. Without their precious support, it would not have been possible to conduct this research.

I thank my current and previous fellow lab mates for their humble and warm company and stimulating discussions, for the efforts in making our research meaningful and for all the fun, we have had in the last four years. In addition, I thank my friends:

- **Mohandes (Siamak):** Perhaps the biggest influence in my life from the age of seven. Life would have been completely different without you, not sure, what I would have turned out to be in your absence. You have been closer to me than any other individual I can think of. Thank you for being there.
- **Hesam e baba:** Probably the two most different, yet immensely similar people on the face of this planet, who have gone far in friendship to be two true inseparable complementary souls dwelling one body.
- **Shahin:** 2005 was the year buddy, not sure how life would have been without you. Interacting with you felt more like having a science therapist, OR an internal dopamine stimulant hooked up in my Cortico-Basal-Ganglia-Thalamo-Cortical loop.
- **Paul:** You know what I am going to say, but I will stay civil. Perhaps nobody knows the past 5/6 years as well as you do. All those nights, all those failed

experiments; all those meaningless data and all those moments back from  
Mohammad's office could not have been meaningful without you buddy.

- All other friends who helped me to be a better warrior. Cheers folks!

# Table of Contents

<i>Abstract</i> .....	<i>ii</i>
<i>Dedication</i> .....	<i>iv</i>
<i>Acknowledgments</i> .....	<i>v</i>
<i>Table of Contents</i> .....	<i>ix</i>
<i>List of Figures</i> .....	<i>xiv</i>
<i>List of Schemes</i> .....	<i>xix</i>
<i>List of Abbreviations</i> .....	<i>xxi</i>
<i>Publications</i> .....	<i>xxiv</i>
<b>1CHAPTER ONE</b> .....	<b>1</b>
1.1 Introduction .....	1
1.2 Classes of Bioconjugation Reactions .....	3
1.2.1 Thiol.....	4
1.2.2 Hydroxyl .....	6
1.2.3 Carboxylate.....	8
1.2.4 Amino .....	9
1.3 Classes of Biorthogonal Reactions .....	15
1.3.1 Amine/Carbonyl Condensation .....	17
1.3.2 Oxime Ligation.....	20
1.3.3 Staudinger Ligation to Triarylphosphine.....	22
1.3.4 Cycloaddition.....	25
1.3.5 Cycloaddition Enzymatic Conjugation and Labelling.....	29
<b>2CHAPTER TWO</b> .....	<b>37</b>
2.1 Introduction .....	37
2.2 Results and Discussion .....	48
2.3 Experimental Procedures .....	62
2.3.1 Liposome Preparation (Figure 2.5).....	62

2.3.2	Functionalized Fluorescent Assay (Figure 2.9) .....	62
2.3.3	Transient Transfection Assay (Figure 2.11) .....	63
2.3.4	Protein-Ligand Interaction Analysis, Through Biorthogonal Ligation (Figure 2.12) .....	64
2.3.5	Aldehyde Surface Adhesion Analysis (Figure 2.13) .....	65
2.3.6	Protein-Ligand Material Surface Adhesion Analysis (Figure 2.14) .....	66
2.4	Conclusion .....	67
<b>3CHAPTER THREE .....</b>		<b>69</b>
3.1	Introduction .....	69
3.1.1	Carbonyl and Imine .....	74
3.1.2	Glutaraldehyde.....	78
3.2	Results and Discussion .....	97
3.2.1	Substrate Type A .....	104
3.2.2	Substrate Type B .....	111
3.2.3	Substrate Type C .....	126
3.2.4	Substrate Type D .....	133
3.2.5	Kinetic Study .....	141
3.2.6	Synthesis of Small Organic Reporter Molecules.....	150
3.2.7	Synthesis of Crosslinker Dialdehyde.....	155
3.3	Materials and Method .....	161
3.3.1	Synthesis of Molecules 1-4.....	161
3.3.2	Synthesis of Molecules 5-7.....	163
3.3.3	Synthesis of Molecules 8-10.....	164
3.3.4	Synthesis of Molecules 12-19.....	166
3.3.5	Synthesis of Molecules 20-23.....	170
3.3.6	Synthesis of Molecules 24-27.....	172
3.3.7	Synthesis of Molecules 28-31.....	174
3.3.8	Synthesis of Molecules 33-37.....	177
3.3.9	Synthesis of Molecules 38-43.....	179
3.3.10	Synthesis of Molecules 44-46.....	182
3.3.11	Synthesis of Molecules 47-49.....	184

3.3.12	Synthesis of Molecules 51-53.....	186
3.3.13	Synthesis of Molecules 55-58.....	188
3.3.14	Synthesis of Molecules 59-63.....	190
3.3.15	Synthesis of Molecules 64-67.....	193
3.3.16	Synthesis of Molecules 68-73.....	195
3.3.17	Synthesis of Molecules 75-76.....	196
<b>4CHAPTER FOUR.....</b>		<b>199</b>
4.1	Introduction .....	199
4.2	Results and Discussion .....	201
4.2.1	Delivery of Ligands via Functionalized Liposome .....	201
4.2.2	Preparation and Delivery of Dialdehyde Lipids Conjugate.....	203
4.2.3	Preparation and Delivery of Dialdehyde Reagents.....	210
4.2.4	Non-Liposomal Application of Dialdehyde Conjugating System.....	214
4.3	Materials and Method .....	232
4.3.1	General Dialdehyde Liposomes (Pathway A) (Figure 4.2) .....	232
4.3.2	General Blank Liposomes (Figure 4.2) .....	232
4.3.3	General Control Liposomes (No Dialdehyde) (Figure 4.2).....	233
4.3.4	General Quenched Dialdehyde Liposomes (Figure 4.2) .....	233
4.3.5	DNP-Dialdehyde Conjugation Liposome Preparation (Pathway A) (Figure 4.2) .....	233
4.3.6	Biotin-Dialdehyde Conjugation Liposome Preparation (Pathway A) (Figure 4.2) .....	234
4.3.7	FLAG-Dialdehyde Conjugation Liposome Preparation (Pathway A) (Figure 4.2) .....	234
4.3.8	DNPC-Dialdehyde Conjugation Liposome Preparation (Pathway B) (Figure 4.2) .....	234
4.3.9	Biotin-Dialdehyde Conjugation Liposome Preparation (Pathway B) (Figure 4.2) .....	235
4.3.10	FLAG-Dialdehyde Conjugation Liposome Preparation (Pathway B) (Figure 4.2) .....	236
4.3.11	DNPC-Dialdehyde Conjugate Liposome Delivery (Mammalian Cell) (Figure 4.3) .....	236

4.3.12 Biotin-Dialdehyde Conjugate Liposome Delivery (Mammalian Cell) (Figure 4.3) .....	237
4.3.13 FLAG-Dialdehyde Conjugate Liposome Delivery (Mammalian Cell) (Figure 4.3) .....	238
4.3.14 Biotin-Dialdehyde Conjugate Liposome Delivery (Bacteria Cell) (Figure 4.3) .....	239
4.3.15 General Dodecylamine Liposomes (Pathway A) (Figure 4.6) .....	239
4.3.16 General Blank Liposomes (Pathway A) (Figure 4.6) .....	240
4.3.17 General Control Liposomes (No Dodecylamine) (Figure 4.6) .....	240
4.3.18 General Quenched Dodecylamine Liposomes (Pathway A) (Figure 4.6) .	241
4.3.19 DNPC-Dialdehyde-Dodecylamine Conjugation Liposome Preparation (Pathway A) (Figure 4.6) .....	241
4.3.20 Biotin-Dialdehyde-Dodecylamine Conjugation Liposome Preparation (Pathway A) (Figure 4.6) .....	241
4.3.21 DNPC-Dialdehyde Conjugation Liposome Preparation (Pathway B) (Figure 4.6) .....	242
4.3.22 Biotin-Dialdehyde-Dodecylamine Conjugation Liposome Preparation (Pathway A) (Figure 4.6) .....	243
4.3.23 DNPC-Dialdehyde-Dodecylamine Conjugate Liposome Delivery (Mammalian Cell) (Figure 4.7) .....	243
4.3.24 Biotin-Dialdehyde-Dodecylamine Conjugate Liposome Delivery (Mammalian Cell) (Figure 4.7) .....	244
4.3.25 DNP-Dialdehyde-dodecylamine Conjugate Liposome Delivery (Bacteria Cell) (Figure 4.7) .....	245
4.3.26 Biotin-Dialdehyde-dodecylamine Conjugate Liposome Delivery (Bacteria Cell) (Figure 4.7) .....	246
4.3.27 Conjugation of L-lysine ethyl ester dihydrochloride with dialdehyde substrate 53 (Scheme 4-1) .....	246
4.3.28 Decoupling of L-Lysine Ethyl Ester Dihydrochloride with Dialdehyde Substrate 53 (Scheme 4-3) .....	247
4.3.29 Crosslinking of Protein LAR D1D1 and CS2 Domain (Figure 4.11) .....	247
4.3.30 Crosslinking/Stapling of Protein EA22 (Figure 4.12) .....	248
4.3.31 Crosslinking of Protein PP16 (Figure 4.12) .....	249



4.3.32 Dialdehyde Crosslinking of Commercial Latex-Amine Beads in Aqueous Solution (Figure 4.13).....	250
4.3.33 Crosslinker Dialdehyde Generation of Tissue Constructs (Figure 4.15)...	252
4.3.34 Functionalization of a Solid Surface with Dialdehyde Headgroup (Figure 4.16).....	254
4.3.35 Immobilization of Beads on the Functionalized Dialdehyde Surface Substrate (Figure 4.17) .....	255
4.3.36 Streptavidin-FITC Adhesion to Liposomes Functionalized with Dialdehyde Lipid (42) .....	255
4.3.37 Rabbit IgG-FITC Adhesion to Liposomes Functionalized with Dialdehyde Lipid (42) .....	256
<b>5CHAPTER FIVE .....</b>	<b>258</b>
<b>References .....</b>	<b>263</b>
<b>Appendix (NMR Spectroscopy) .....</b>	<b>284</b>

## List of Figures

Figure 1.1 Thiol liberation for conjugation reaction.....	5
Figure 1.2 Thiol nucleophilic conjugate addition to maleimide .....	6
Figure 1.3 Tyrosine conjugation via $S_NAr$ reaction.....	7
Figure 1.4 Tyrosine bioconjugation via Mannich reaction.....	8
Figure 1.5 Carboxylic acid conversion into an amide linkage.....	9
Figure 1.6 Guanidyl group stabilization .....	10
Figure 1.7 Rearrangement of O-acylisourea to a stable urea.....	11
Figure 1.8 Alternative peptide coupling activators.....	12
Figure 1.9 Amin conjugation via formation of thiourea .....	12
Figure 1.10 Amine conjugation via formation of an imine bond .....	13
Figure 1.11 Amine conjugation via azaelectrocyclization reaction.....	14
Figure 1.12 List of biorthogonal reactions.....	16
Figure 1.13 Energy level of HOMO and LUMO.....	20
Figure 1.14 Overview of Staudinger ligation in bioconjugation .....	23
Figure 1.15 Overview of traceless Staudinger ligation.....	25
Figure 1.16 Overview of Huisgen Click chemistry .....	26
Figure 1.17 Overview of catalytic cycle of CuAAC.....	27
Figure 1.18 Overview of strained alkyne and azide click chemistry .....	28
Figure 1.19 Examples of activated strained alkynes.....	29
Figure 1.20 Synthesis of protein with un-natural amino acid tag .....	30
Figure 1.21 Cell surface re-engineering using metabolic pathways .....	32
Figure 2.1 Delivery of reporter onto cell surface.....	38
Figure 2.2 Cell membrane surface components.....	39
Figure 2.3 Bacteria cell surface engineering.....	42
Figure 2.4 Drug delivery via liposome fusion .....	43
Figure 2.5 Liposome reengineering with biorthogonal head group.....	45
Figure 2.6 Tissue assembly using biorthogonal ligation .....	46

Figure 2.7 Overview membrane structure of bacteria .....	47
Figure 2.8 General scheme of biorthogonal oxime ligation and cell labelling .....	49
Figure 2.9 Quantitative analysis of fluorescent probe on bacteria surface .....	51
Figure 2.10 The interplay of liposome composition, liposome fusion/incubation time and the amount of ketone molecules Transient transfection of engineered bacteria .....	54
Figure 2.11 Transient depletion of bio-orthogonal groups on a bacteria surface over time .....	56
Figure 2.12 Bacteria surface engineering with bio-orthogonal groups for further ligand and protein conjugation.....	58
Figure 2.13 Surface immobilization of bacteria using biorthogonal chemistry.....	60
Figure 2.14 Surface immobilization of bacteria using biorthogonal chemistry via Protein-Ligand interaction .....	61
Figure 3.1 Illustration of linking macromolecules with reporters via formation of a “lock” .....	70
Figure 3.2 General presentation of conjugating a biomolecule to a dialdehyde headgroup .....	71
Figure 3.3 General presentation of decoupling of a conjugate between an amine biomolecule and dialdehyde headgroup.....	73
Figure 3.4 Dipole moment of carbonyl.....	74
Figure 3.5 General structural representation of dialdehyde substrate.....	97
Figure 3.6 Reaction mechanism proposed for formation of vicinal 1,2 diol through oxidation of an alkene .....	99
Figure 3.7 Reaction mechanism proposed for oxidative cleavage of 1,2 diol using NaIO <sub>4</sub> .....	100
Figure 3.8 Catalytic cycle of UpJohn dihydroxylation using OsO <sub>4</sub> and NMO as re-oxidant .....	101
Figure 3.9 Enantioselective oxidation of an alkene using AD-mix- $\alpha$ and AD-mix- $\beta$ chiral ligands .....	102
Figure 3.10 General representation of synthesis for a C3 substitution of cyclopentene. ....	104
Figure 3.11 Conversion of a carboxylic acid moiety to an amide bond with a nucleophilic substitution on activated ester .....	105
Figure 3.12 <sup>1</sup> H-NMR spectrum of molecule 4.....	107

Figure 3.13 Possible formation of an amide conjugate using propylamine and phenethylamine .....	108
Figure 3.14 Possible products propylamine conjugation to substrate Type A .....	109
Figure 3.15 Installation of a methyl group to generate a quaternary carbon at C3 position .....	111
Figure 3.16 <sup>1</sup> H-NMR spectrum of molecule 18.....	113
Figure 3.17 Resonance structure of enamine contributing to up/downfield NMR chemical shift .....	115
Figure 3.18 Partial NMR spectrum of substrate 14 .....	116
Figure 3.19 Possible conjugation products of substrate 22 using different size nucleophile methylamine and propylamine.....	118
Figure 3.20 2D-COSY Spectrum of substrate 22 conjugate with methylamine.....	119
Figure 3.21 2D-HSQC spectrum of substrate 22 conjugate with methylamine .....	120
Figure 3.22 2D-COSY Spectrum of substrate 22 conjugate with propylamine .....	121
Figure 3.23 2D-HSQC spectrum of substrate 22 conjugate with propylamine .....	122
Figure 3.24 Reduction of N=C bond using mild reductant sodium cyanoborohydride..	123
Figure 3.25 <sup>1</sup> H-NMR spectrum overlay of substrate 22 conjugations with methylamine vs reduced products .....	124
Figure 3.26 <sup>1</sup> H-NMR spectrum overlay of substrate 22 conjugations with propylamine vs reduced products .....	125
Figure 3.27 <sup>1</sup> H-NMR spectrum of molecule 36.....	129
Figure 3.28 <sup>1</sup> H-NMR spectrum of molecule 37 .....	130
Figure 3.29 <sup>1</sup> H-NMR spectrum of molecule 42.....	132
Figure 3.30 <sup>1</sup> H-NMR spectrum of molecule 43.....	132
Figure 3.31 General structure of an optimized dialdehyde substrate template type D ...	134
Figure 3.32 General mechanism pathway for deprotection of t-butyl ester protecting group .....	137
Figure 3.33 Chemical shift of the two distinctive diagnostic protons of substrate 44....	139
Figure 3.34 Pseudo first order reaction of substrate 53 with propylamine.....	143
Figure 3.35 Plot of 1,4dihydropyridine formation through enamine peak monitor.....	144
Figure 3.36 Graph of carbonyl consumption over 175 seconds of nucleophilic addition .....	145

Figure 3.37 Examination of dialdehyde conjugate stability with pH changes over extended time .....	147
Figure 3.38 Examination of dialdehyde conjugate stability with pH changes after 5 minutes .....	148
Figure 3.39 Effect of protonation/ deuteration of enamine moieties of 1,4-dihydropyridine conjugate .....	149
Figure 3.40 Different variations of biotin molecule with different oxidation state of S	152
Figure 3.41 Comparison of fluorescein-amine reporter nucleophilicity .....	155
Figure 3.42 Inactivation illustration of terminal electrophilic centers due to TEG coordination to a cationic species .....	158
Figure 3.43 General trend of reactivity for dialdehyde headgroup .....	160
Figure 4.1 Cartoon depiction of functionalized liposome delivery of reporters via fusion onto surface of mammalian and bacterial cell .....	202
Figure 4.2 Cartoon depiction of functionalized liposome SUV particle preparation .....	204
Figure 4.3 Cartoon depiction of dialdehyde conjugation to a variety of ligands, further delivery of the complex onto the surface of the mammalian and bacterial membrane. .	206
Figure 4.4 The number of delivered antigen molecules via ligation to dialdehyde-functionalized liposome .....	208
Figure 4.5 The number of delivered biotin molecules via ligation to dialdehyde functionalized liposome .....	209
Figure 4.6 Cartoon depiction of functionalized liposome SUV particle preparation .....	211
Figure 4.7 Cartoon depiction of dialdehyde reporter conjugation to a dodecylamine liposome, further delivery of the complex onto the surface of the mammalian and bacterial membrane. ....	213
Figure 4.8 <sup>1</sup> H-NMR spectrum of conjugating L-lysine ethyl ester with substrate 53 ....	215
Figure 4.9 Spectral comparison of unreacted L-lysine and conjugated L-lysine after reacting with dialdehyde 53 .....	216
Figure 4.10 <sup>1</sup> H-NMR spectrum of acid treated L-lysine ethyl ester conjugate with substrate 53 .....	219
Figure 4.11 Cartoon depiction of Protein LAR D1D2l and Caskin 2 SAM2 crosslinking to form a robust covalent bond .....	221
Figure 4.12 Illustration of protein PP16 and EA22 crosslinking to form a robust covalent bond.....	222

Figure 4.13 A cartoon depiction of non-selective crosslinking of proteins using glutaraldehyde .....	223
Figure 4.14 Demonstration of an application in conjugation and releasing through acid catalysis in fluorescent beads .....	225
Figure 4.15 Construction of a multilayer tissue using dialdehyde crosslinker and tissue viability assay.....	227
Figure 4.16 Cartoon depiction of functionalizing a surface with dialdehyde headgroup	228
Figure 4.17 Demonstration and characterization of dialdehyde headgroup synthesized on surface via conjugation to fluorescent reporter beads.....	230
Figure 5.1 Cartoon depiction of a Swiss army molecule with three locations for functionality .....	261

## List of Schemes

Scheme 3-1 Glutaraldehyde products in aqueous solution with cationic catalyst .....	83
Scheme 3-2 Glutaraldehyde $\alpha,\beta$ -unsaturated polymer.....	84
Scheme 3-3 Glutaraldehyde cyclic hemiacetal polymer.....	85
Scheme 3-4 Glutaraldehyde polymerization reaction.....	86
Scheme 3-5 Glutaraldehyde product in alkaline solution .....	87
Scheme 3-6 Glutaraldehyde products at low concentration .....	88
Scheme 3-7 Reactions of primary amine with glutaraldehyde in solution (Michael addition, Schiff Base).....	90
Scheme 3-8 Reactions of primary amine with glutaraldehyde in solution (Crosslinking)	91
Scheme 3-9 Dimeric cyclic glutaraldehyde reaction with proteins under alkaline conditions.....	92
Scheme 3-10 Glutaraldehyde reaction with proteins under Acidic conditions.....	93
Scheme 3-11 Glutaraldehyde reaction with proteins under alkaline conditions.....	94
Scheme 3-12 General synthesis of a glutaraldehyde molecule.....	97
Scheme 3-13 A general reaction scheme for synthesis of a C3' substituted dialdehyde substrate using metathesis.....	102
Scheme 3-14 Model reaction for synthesis of substrate Type A .....	106
Scheme 3-15 General synthesis of a substrate model Type B .....	112
Scheme 3-16 General synthesis of a substrate model Type C-1.....	127
Scheme 3-17 General synthesis of a lipid substrate model Type C-2 .....	129
Scheme 3-18 Conjugation of propylamine to dialdehyde substrate 36 .....	130
Scheme 3-19 General synthesis of a bislipid substrate model Type C-2.....	131
Scheme 3-20 Conjugation of propylamine to dialdehyde substrate 42 .....	131
Scheme 3-21 Synthetic approaches for finding a suitable linker for dialdehyde substrate template using 3-bromopropanoic acid.....	135
Scheme 3-22 Lactonization of 3-bromopropanoic acid into $\beta$ -propiolactone .....	136
Scheme 3-23 Synthetic approaches for finding a suitable linker for dialdehyde substrate template using 2-((6-bromohexyl)oxy)tetrahydro-2H-pyran.....	138

Scheme 3-24 General synthesis of optimized dialdehyde substrate template Type D ...	138
Scheme 3-25 Illustration of a synthetic pathway for generation of a typical dialdehyde substrate, followed by conjugation to a biomolecule.....	140
Scheme 3-26 Alternative synthetic proposal to generate substrate 45 .....	141
Scheme 3-27 General synthesis of crosslinker dialdehyde molecule using model substrate Type C.....	156
Scheme 3-28 Conjugation of crosslinker molecule 66 to propylamine .....	157
Scheme 3-29 General synthesis of hydrophilic TEG crosslinker dialdehyde molecule 70 using model substrate Type D.....	159
Scheme 4-1 Conjugation of L-lysine ethyl ester dihydrochloride with substrate 53.....	215
Scheme 4-2 Deuteration of enamine moiety with exposure to D <sub>2</sub> O.....	217
Scheme 4-3 Examination of reverse reaction of conjugate to starting material at lower pH .....	217



## List of Abbreviations

2D	Two dimensional
3D	Three dimensional
AA	Amino acid
ACN	Acetonitrile
ADC	Antibody Drug Conjugates
Cat	Catalytic
CFU	Colony forming units
COFs	Covalent organic framework
COSY	2D-NMR Correlation Spectroscopy
CuAAC	Copper-Catalyzed Azide-Alkyne
d	Doublet
DAPI	4',6-diamidino-2-phenylindole
DCC	<i>N,N'</i> -Dicyclohexylcarbodiimide
DCM	Dichloromethane
DEPT	Distortionless Enhancement by Polarization Transfer
DMEM	Dulbecco's Modified Eagle's medium
DMF	Dimethylformamide
DMPG	1,2-dimyristoyl-sn-glycero-3-phospho-(1'-rac-glycerol)
DMSO	Dimethyl sulfoxide
DNP	2,4-Dinitrophenol
DOTAP	<i>N</i> -[1-(2,3-Dioleoyloxy)propyl]- <i>N,N,N</i> -trimethylammonium chloride
DPPC	1,2-dipalmitoyl-sn-glycero-3-phosphocholine
<i>E. coli</i>	<i>Escherichia coli</i>
EDC	1-Ethyl-3-(3-dimethylaminopropyl)carbodiimide
EDTA	Ethylenediaminetetraacetic acid
EtOAc	Ethyl acetate
FBS	Fetal bovine serum

FITC	Fluorescein isothiocyanate
h	Hour
HATU	1-[Bis(dimethylamino)methylene]-1H-1,2,3-triazolo[4,5-b]pyridinium 3-oxid hexafluorophosphate <i>O</i> -(Benzotriazol-1-yl)- <i>N,N,N',N'</i> -tetramethyluronium
HBTU	hexafluorophosphate <i>O</i> -(6-Chlorobenzotriazol-1-yl)- <i>N,N,N',N'</i> -tetramethyluronium
HCTU	hexafluorophosphate
HEPES	4-(2-hydroxyethyl)-1-piperazineethanesulfonic acid
HMBC	Heteronuclear Multiple-Bond Correlation Spectroscopy
HNMR	Proton nuclear magnetic resonance
HOMO	Highest occupied molecular orbital
HRP	Horseradish peroxidase
HSQC	Heteronuclear Single-Quantum Correlation Spectroscopy
IR	Infrared
ITO	Indium tin oxide
LB	Lysogeny broth
LD <sub>50</sub>	Lethal dose 50
LDA	Lithium diisopropylamide
LPS-A	Lipopolysaccharide
LUMO	Lowest unoccupied molecular orbital
MeOH	Methanol
MOFs	Metal-organic frameworks
MS	Mass spectrometry
NMO	<i>N</i> -methyl morpholine oxide
NMR	Nuclear magnetic resonance
Nu	Nucleophile
OD	Optical density
<i>P. aeruginosa</i>	<i>Pseudomonas aeruginosa</i>
PBS	Phosphate buffered
PEG	Polyethylene glycol

POPC	1-palmitoyl-2-oleoyl-sn-glycero-3-phosphocholine
ppm	Parts per million
	Benzotriazole-1-yl-oxy-tris-pyrrolidino-phosphonium
PyBOP	hexafluorophosphate
RCF	Relative centrifugal forces
RT	Room temperature
SDS	Sodium dodecyl sulfate
SUV	Small unilamellar vesicles
t	Triplet
	<i>O</i> -(1H-6-Chlorobenzotriazole-1-yl)-1,1,3,3-
TBTU	tetramethyluronium hexafluorophosphate
TCEP	tris(2-carboxyethyl)phosphine
TEA	Triethylamine
THF	Tetrahydrofuran
TLC	Thin layer chromatography
TRITC	Tetramethylrhodamine
UV	Ultra violet

## Publications

Some portions of this work and other related research contributions appear in the following publications, there are some major parts that are in process of submission for publication:

- 1- **Elahipanah, S.** et al. Rewiring Gram-Negative Bacteria Cell Surfaces with Bio-Orthogonal Chemistry via Liposome Fusion. *Bioconjug. Chem.* **27**, 1082–1089 (2014).
- 2- Rogozhnikov, D., Luo, W., **Elahipanah, S.**, O'Brien, P. J. & Yousaf, M. N. Generation of a Scaffold-Free Three-Dimensional Liver Tissue via a Rapid Cell-to-Cell Click Assembly Process. *Bioconjug. Chem.* **27**, 1991–1998 (2016)
- 3- Rogozhnikov, D., O'Brien, P. J., **Elahipanah, S.** & Yousaf, M. N. Scaffold Free Bio-orthogonal Assembly of 3-Dimensional Cardiac Tissue via Cell Surface Engineering. *Scientific Reports* **6**, 39806 (2016)
- 4- **Elahipanah, S.**, O'Brien, P. J., Rogozhnikov, D. & Yousaf, M. N. General Dialdehyde Click Chemistry for Amine Bioconjugation. *Bioconjug. Chem.* **28**, 1422–1433 (2017).
- 5- O'Brien, P. J., **Elahipanah, S.**, Rogozhnikov, D. & Yousaf, M. N. Bio-Orthogonal Mediated Nucleic Acid Transfection of Cells via Cell Surface Engineering. *ACS Central Science* **3**, 489–500 (2017).
- 6- Highlighted in C&E News “Genetic engineering through click chemistry” 2017, **96**, p.06, 23

# **1 CHAPTER ONE**

## **Bioconjugation Chemistry and Chemical Ligation to Macromolecules: Background Principals and Current Methods**

---

### **1.1 Introduction**

Macromolecule conjugation is an attractive area of research in biochemistry and biotechnology. Methods developed for a mild and highly selective conjugation of macromolecules allow for novel discoveries in derivatization of proteins, DNA/RNA and manipulation of carbohydrates. Such applications have proven to be central to the advancement of biochemistry, biotechnology and medicine. The strength of such reactions lies in their ability to modify a native macromolecule without disturbing regular function in the physiological environment. Improvement of these chemical reactions has led to the development of an increasingly growing field of “Bioconjugate chemistry”. This field highlights the derivatization of macromolecules through a covalent connection to a foreign body. Among such molecules, carbohydrates, glycans, amino acids and proteins bear exceptional significance with important biological properties. All of these molecules play important role in cellular activities and are fundamental in sustaining homeostasis of the living organism. Manipulation of these molecules has offered a new gateway to study the cell function in more details and also to use them in molecular biology for diagnostic and therapeutic purposes. However, complexity and sensitivity of these macromolecules have made such modifications often very difficult, laborious and expensive. The innovation of reactions that would be biocompatible and silent to regular cellular hydrolytic actions has

demanded conjugation strategies arising from organic chemists' toolbox. Many discovered reactions could conjugate ligands to macromolecules and act as probes or reporters in binding studies.<sup>1-3</sup> High-throughput approaches have been the result of innovation of reporters like biotin,<sup>4,5</sup> NMR probes<sup>6</sup> and immobilized ligand on surfaces.<sup>7-9</sup>

Appended small molecules to larger structures have opened a new gateway in methods to study protein behavior and other biochemical experiments. FRET reporters can be modified to reveal invaluable information about the conformational changes of protein-protein interaction as low as 10 nm range.<sup>10</sup> Non-fluorescent probes also play important part in bioconjugation experiments and are heavily used in understanding of integral proteins and channels on cell surfaces.<sup>11</sup>

Protein conjugation has always been the major spotlight among bioconjugation chemists for the development of methods that would allow for ligation with retention of the native function. Protein pegylation,<sup>12-14</sup> probe installation, protein-protein interaction, immobilization<sup>15-17</sup> and antibody-drug conjugation<sup>18-21</sup> are only a short list of the attributions. The growing field of novel therapeutics for cancer therapy has focused on selective and highly efficient targeting of the affected cells via conjugation of a toxin to an antibody that is recognized by the corresponding antigen on cell surface.<sup>22-24</sup> Approval of Adcetris® (brentuximab vedotin) and Kadcyla® (ado-trastuzumab emtansine), by the Food and Drug Administration (FDA) in 2015 is the product of such efforts and a great step forward for materializing antibody drug conjugates (ADC) therapies.<sup>23</sup> An important pre-requisite of a successful ADC complex is its ability to release the payload in the most available form into the cytoplasm. Although there is a tremendous ongoing effort to

optimize the efficiency of therapeutic index, there are some serious drawbacks and limitations associated with their efficacy.

There has been enormous developments and contributions in the biomedical and biotechnology field from organic chemistry in the past 50 years. There are great improvements in the organic reactions that facilitate all the mentioned objectives above. Although the search for reactions that would accommodate for all the necessary conditions of a successful bioconjugation is a difficult task, there is a long list of reagents and functional groups available for chemical biologists.<sup>18</sup> Typically, a bioconjugation reaction could either be “biorthogonal” or simply a biocompatible protocol that would lead to the formation of a covalent bond. Biorthogonal reactions are a sub-class of bioconjugation field, that occur under physiological conditions, at 37 °C, neutral pH and are invisible to other reactive functional groups found in biology. Such reactions do not produce side-products and do not exhibit reactivity towards reactive moieties in the cellular environment. For this reason, they are often hidden from enzymatic metabolic processes or clearance from the cytoplasm. All mentioned criteria must be fulfilled so that a functional group could be considered a biorthogonal pair.

## **1.2 Classes of Bioconjugation Reactions**

An important feature of bioconjugation reaction is the ability of the reactive centers to remain highly selective for each other to ensure a specific site is targeted in a heterogeneous environment. Poor control of such modifications will often result in loss of physiological function of the macromolecule<sup>25</sup>. Many research groups have focused on

development and design of a conjugation strategy that would facilitate attachment of biological molecules without disturbing their native structures. Most of these developments take advantage of a selected number of functional groups already present within the structure of the native biomolecule. Rich in hydroxyl functional groups, carbohydrates could participate in nucleophilic addition type conjugations; similarly, amino acids both in protein structure and as independent signalling peptides, also offer a versatile reactive center for conjugation. However, this could create both limitation and opportunity for their use in chemical ligations. Many of these functional groups serve merely as a general nucleophile and present limited selectivity towards other electrophiles. Best selectivity could be achieved with cysteine, lysine, and histidine and in some cases serine.<sup>26</sup> The thiol of cysteine is one of the most studied reactive centers to tether proteins with other biologic and non-biological bodies. However, reversibility of reaction and relatively low abundance of available cysteine in the protein structures has provided the opportunity for a better reactive center in bioconjugation.<sup>27</sup> In contrast to thiol, lysine offers a more reactive yet less selective primary amine, which could be applied in multiple quantitative conjugations independent of site specificity<sup>28</sup>. Conjugation of the primary amine requires a relatively harder electrophilic center such as an activated ester,<sup>29</sup> sulfonyl chloride<sup>30</sup> and isothiocyanate residue.<sup>31</sup> Here we highlight some of the most common bioconjugation strategies that use the active functional group of a side chain residues.

### **1.2.1 Thiol**

Thiols are the most nucleophilic centers found in the biological macromolecules.<sup>32</sup> Although they are more reactive at lower pH ranges in comparison with a primary amine,



they are often found to be bound by a disulfide bond. In order to generate a reactive thiol center, the thioester or the oxidized disulfide bond must be reduced using mild reagents such as dithiothreitol<sup>33</sup> or phosphine derivatives (TCEP).<sup>34</sup>

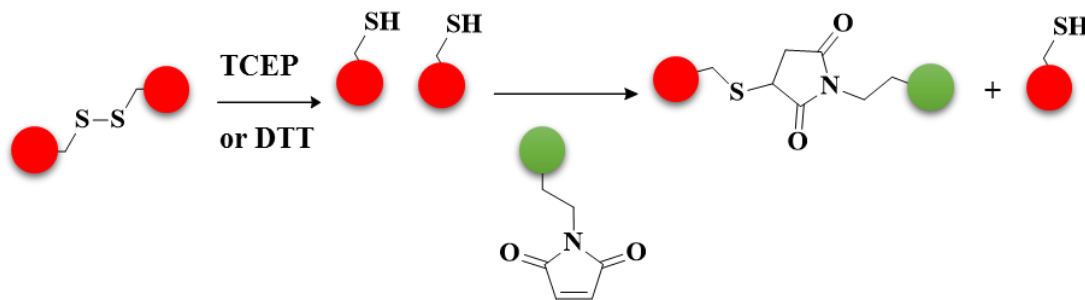


*Figure 1.1 Thiol liberation for conjugation reaction*

A cartoon presentation of a disulfide bond reduction using an appropriate reducing agent to afford two sulfhydryls, which could further form a covalent bond with a maleimide reporter on any exogenous macromolecule. For every reduction, there are two molecules of thiol produced that could engage in two independent bioconjugation reactions.

*In-situ* preparation of a thiol group could allow for a nucleophilic addition to forming thioether bonds. For example, maleimide reacts readily with sulfhydryls in high selectivity<sup>35</sup> or alternatively an alkylation reaction could be conducted using iodoacetamide. The presence of electron withdrawing carbonyl makes this reagent a good alkylating agent for thiols. In spite of selectivity, iodoalkanes are known to react with methionine in a heterogeneous sample.<sup>36</sup> Other protocols have reported the reaction of thiols with allyl halide to form the allylic thioether, but the scope has remained restricted to peptide modification.<sup>37</sup>

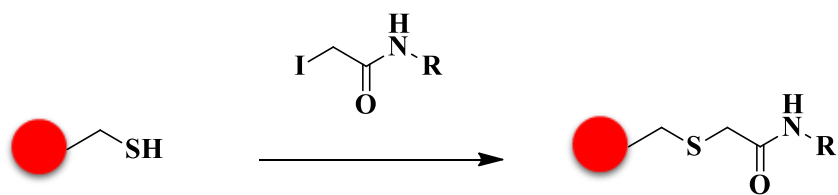


*Figure 1.2 Thiol nucleophilic conjugate addition to maleimide*

An available thiol could react with a haloalkane that is incorporated onto a biomacromolecule chemical structure, thus could be used as a chemical reporter that generates a robust covalent bond in a 1,2-nucleophilic conjugate addition reaction. Alkylation of a thiol using such haloalkanes is an irreversible process and would result in a permanent labelling of the subject.

While chemical modification of thiols with reagents has been a common practice in biochemical experiments, unnecessary exposure of proteins to chemicals often leads to undesired consequences. Furthermore, low abundance of cysteine in the biology and its fundamental role within the core of a protein for maintaining a functional structure, makes it a relatively unpreserved candidate for bioconjugation reactions.<sup>38</sup> In spite of all shortcomings, thiol is proven to be one of the most effective sites used in the protein bioconjugation in modern practice.

### 1.2.2 Hydroxyl

Tyrosine residue could also be used as a peptide handle, acting as a nucleophile through its hydroxyl. The preliminary attempts in tyrosine conjugation were exploited through ( $S_NAr$ ) reaction of *azo* derivatives with phenol at *ortho* position.<sup>39</sup> Depending on the photostability and photochemical properties of the substituents on the azo aryl, the resulting tyrosine-azo aryl conjugate may not have significant reporting characteristics.

Introducing an electron-withdrawing group in the *para* position allows for an easy reduction into the aniline that could be further transformed into a stable benzoxazine with a substituted acrylamide. Eventually, an electrophilic center could be installed on the azo aryl ring and serve as a chemical handle. For example, installation of a ketone group could allow for a ligation to a hydroxylamine or hydrazine.<sup>40</sup>

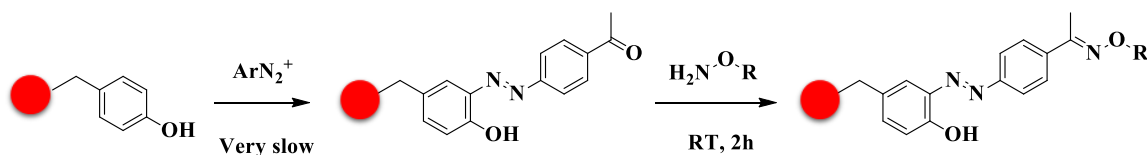


*Figure 1.3 Tyrosine conjugation via  $\text{S}_{\text{N}}\text{Ar}$  reaction*

Tyrosine residue could be labeled with an azo aryl moiety through a nucleophilic aromatic substitution at the *para* position. The *azo* aryl molecule could be armed with an electrophilic center and further act as a secondary chemical trap for bioconjugation.

Other useful protocols offer high selectivity for tyrosine conjugation but rely on the use of multiple reagents. In a three-component variation of Mannich reaction, an amine and aldehyde could react to form an intermediate imine, which produces a good electrophilic center for a substitution reaction at the *ortho* position of a phenol. This reaction is highly efficient and its most effective at lower pH ranges of 5.0 with a low millimolar concentration of reactants. Since tyrosine residue is mostly abundant in the core structure of hydrolytic polypeptides, Mannich conjugation is considered to be a highly selective reaction for tyrosine labelling. However, reproducibility of this protocol is dependent on the nature of protein and tyrosine microenvironment.<sup>41,42</sup>

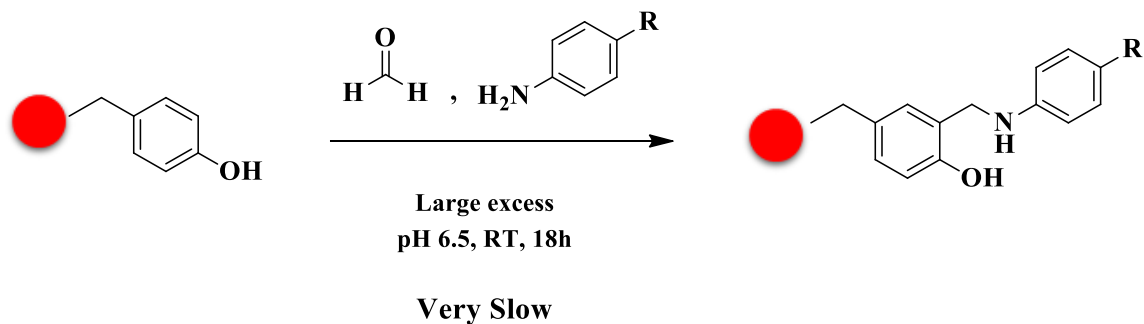


*Figure 1.4 Tyrosine bioconjugation via Mannich reaction*

Tyrosine could be selectively labeled with an aniline derivative, in presence of catalytic formaldehyde. Similar to Figure 1.3, upon successful nucleophilic aromatic substitution of tyrosine, a chemical reporter could be installed on the rear end of aniline to present a reactive moiety for secondary conjugation.

### 1.2.3 Carboxylate

Carboxylates are found in literally every protein structure as the C-terminus, and as a side chain in glutamate and aspartate residues. Conjugation to any of these moieties requires a standard peptide coupling protocol through the formation of an activated ester of the carboxylate. There are many reagents introduced in the recent years for generation of an amide bond through coupling with a water soluble reagent, however, most of coupling agents are susceptible to rapid hydrolysis under physiological conditions.<sup>43</sup>

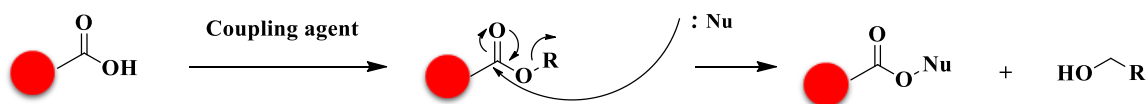


*Figure 1.5 Carboxylic acid conversion into an amide linkage*

Carboxylic moieties could be transformed into an activated ester and undergo a nucleophilic substitution with suitable nucleophiles. Reaction with amines could secure a robust amide bond that irreversibly labels the target.

#### 1.2.4 Amino

Lysine residues are an important component of protein structures that play significant functional and catalytic role in biology. Those buried deep in the core structure and binding site of proteins participate in enzymatic reactions, but surface residues show little responsibility in protein function. For that reason, surface lysine residues become outstanding reactive centers for protein labelling. Other amino acids containing a nitrogen in their side chain like tryptophan, asparagine, glutamine, arginine and histidine have little to no importance in bioconjugation chemistry. Either most are key players in catalytic actions or simply do not offer a reactive nitrogen center. For example, electrically charged side chains guanidyl group with pKa of 12.5, is a resonance stable structure of a diamine functional group that shows minimum nucleophilicity in organic chemistry<sup>44</sup> and chemical biology.<sup>45</sup>

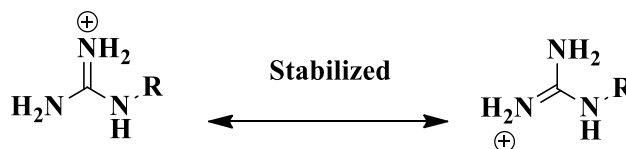


*Figure 1.6 Guanidyl group stabilization*

Stabilization of charges on the guanidyl group renders this functional group to be an ineffective moiety for bioconjugation.

In contrast, lysine carries a primary amino group on its side chain that is often the most available nucleophile on any protein structure. Primary amines are known to sustain its reactivity even at low pH ranges, where functional groups are protonated. High abundance and availability, unique chemical properties and superior reactivity of this side chain make lysine the most important labelling target in bioconjugation chemistry.

Engaging an amine in a covalent bond outside of physiological conditions is not a difficult task, but mostly remain to be only plausible in an organic reaction vessel. There has been many reported protocols and reagents for amine coupling in the context of chemical biology. The reaction of a primary amine with activated esters, isothiocyanates and ketone are well known processes commonly used in organic reactions. Although each one delivers a specialized purpose for a set of conditions, activated esters have maintained a more general role in the polypeptide and artificial protein synthesis. While the method remains to be a major route for the synthesis of larger molecules (polypeptides), it has limited scope for *in-vivo* applications. A classic example of such activators is *N*-hydroxysuccinimide that generates a convenient electrophilic center for any reactive amine

to make an amide linkage. A major factor contributing to a significantly low yield of *N*-hydroxysuccinimide activation is the rearrangement of *O*-acylisourea to the stable *N*-acylurea, which quenches the ester and renders it unreactive towards other amines. In addition to low yield, purification of by-products is often very difficult, which adds to the drawback of *in-vivo* applications and cost of the experiment. Subsequently, synthetic infeasibility, poor yield, the release of by-products and instability of *N*-hydroxysuccinimide demanded more exotic coupling molecules.

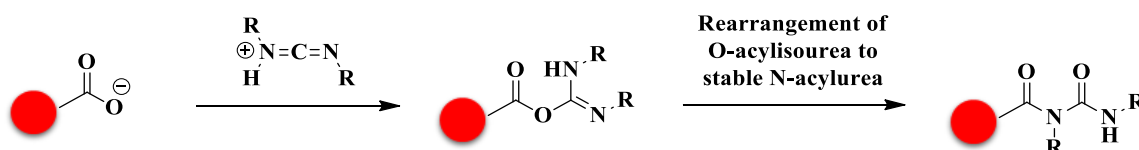


*Figure 1.7 Rearrangement of O-acylisourea to a stable urea*

Anionic carboxylates could be easily transformed into activated centers that present unique electrophilic moieties for nucleophilic substitutions. However, *O*-acylisourea intermediate could rapidly rearrange into a more stable acylurea and become unavailable for any further substitution reactions. This type of side reaction leaves DCC/EDC type coupling agents an ineffective approach for the formation of amide bonds.

There is a large library of activating molecules, intended to overcome such obstacles of amine conjugation; among all HBTU, HATU, HCTU, TBTU, PyBOP has offered the best synthetic feasibility in the reaction vessel, however, the very limited application has been sought for any *in vivo* practice.

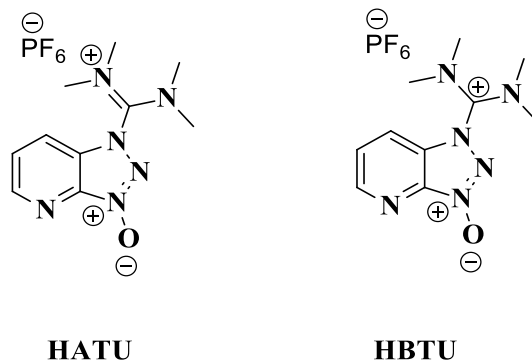


*Figure 1.8 Alternative peptide coupling activators*

HATU and HBTU are common examples of safe triazoles that could be used in peptide coupling reactions and afford the corresponding amide linkage in high yield.

Isothiocyanates are also useful functional groups in amine coupling techniques. Their operating pH range (9.0-9.5) is slightly higher than esters, which makes them unsuitable for some proteins. Furthermore, they provide no selectivity for the targeted amino acid residue and show reactivity towards most nucleophiles.

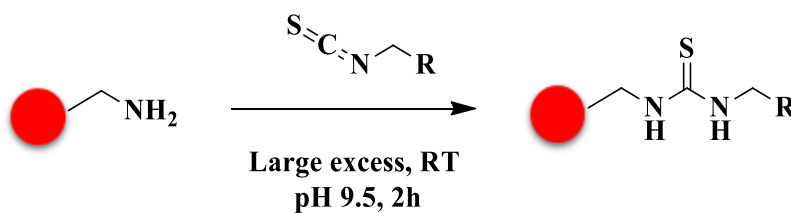


*Figure 1.9 Amin conjugation via formation of thiourea*

The amino group could be easily trapped in a covalent bond with isothiocyanates to form a stable thiourea linkage at RT and alkaline conditions.



Reductive amination of an imine bond is a very common approach to secure a robust bond between the primary amine of a lysine and any molecule carrying a carbonyl group.<sup>46</sup> Dearborn et al have demonstrated in their work in 1979 that a protein could be successfully labeled at lysine residues and the N- terminus. All similar protocols use a mild reducing agent that would convert the imine bond into a secondary amine.

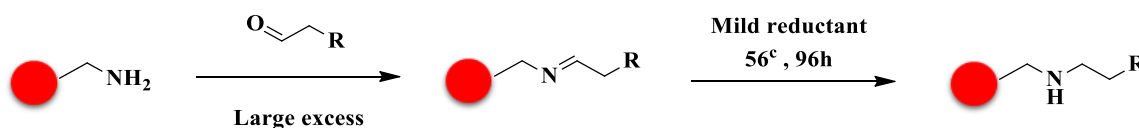


*Figure 1.10 Amine conjugation via formation of an imine bond*

The amino group could react with a carbonyl moiety to generate an imine bond. The addition of a mild reductant could secure a robust  $sp^3$  bond that will no longer reverse to yield starting material.

Other reported exotic amine coupling reactions show limited practical scope for *in-vivo* applications. For example, primary amines could undergo a nucleophilic addition reaction with 1H-benzo[d][1,3]oxazine-2,4-dione, to irreversibly open the ring to yield orthoaminebenzamide. A slight variation of this protocol using oxidative cleavage method and aniline tethered protein is reported by Hooker's work in 2006.<sup>47</sup> Tanaka et al have introduced another technique that uses  $6\pi$ -azaelectrocyclization of a beta keto reagent with amine to form a charged ring structure.<sup>48,49</sup>

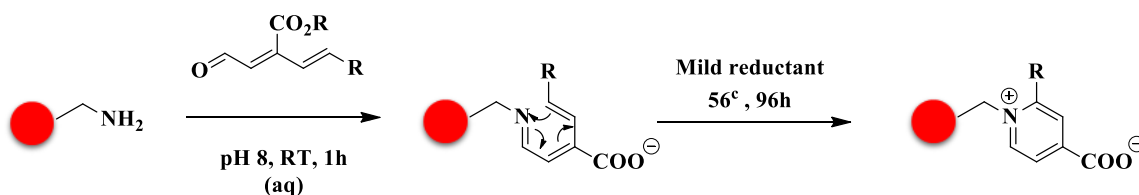


*Figure 1.11 Amine conjugation via azaelectrocyclization reaction*

A dione molecule could react with the primary amine side group of lysine, and further form an irreversible intermediate orthoaminebenzamide molecule. An intramolecular process of azaelectrocyclization could afford a pyridinium ion that is stable enough to serve as a bioconjugation product for lysine labelling.

Although providing a suitable electrophilic center could result in a chemical ligation, not all conjugates would produce a stable structure. Most of the mentioned procedures lead to the formation of an unstable species that could easily collapse in an aqueous environment. Others are either inefficient in reaction or require many chemical modifications on the protein itself, which then introduce further complexities into the system. There remains a demand for a conjugation strategy that would generate a robust reliable bond and offer high selectivity for amines with no dependence on exogenous reactants. A suitable system would also necessitate minimum chemical reaction performed on the biomacromolecule as well. Although reversibility is a drawback of most strategies, it could also be an important requirement of some biological applications. For example, the efficacy of ADC is heavily dependent on the ability of the complex to release the toxic payload through some reversible process. However, most techniques do not sustain a stable preliminary bond needed for conjugation and render the purpose ineffective.

### **1.3 Classes of Biorthogonal Reactions**

The exploration of biomolecules has always been a challenge for scientists. In order to investigate cell behavior in its native state, they have always designed their approaches to impose minimum modification on the cellular machinery system. This is an exceedingly delicate task to accomplish without disrupting a biomolecule's native structure. In order to address this concern, biologists and chemists collaborated to introduce new methodologies that could create non-native centers on biomolecules. These functional groups had to serve as a chemical handle to react only with their reactive pair in the plethora of other functional groups present in biological settings. Such pairs must be highly selective, kinetically competent and deficient of any toxins; furthermore, they must fulfil all ligation requirements under physiological conditions.

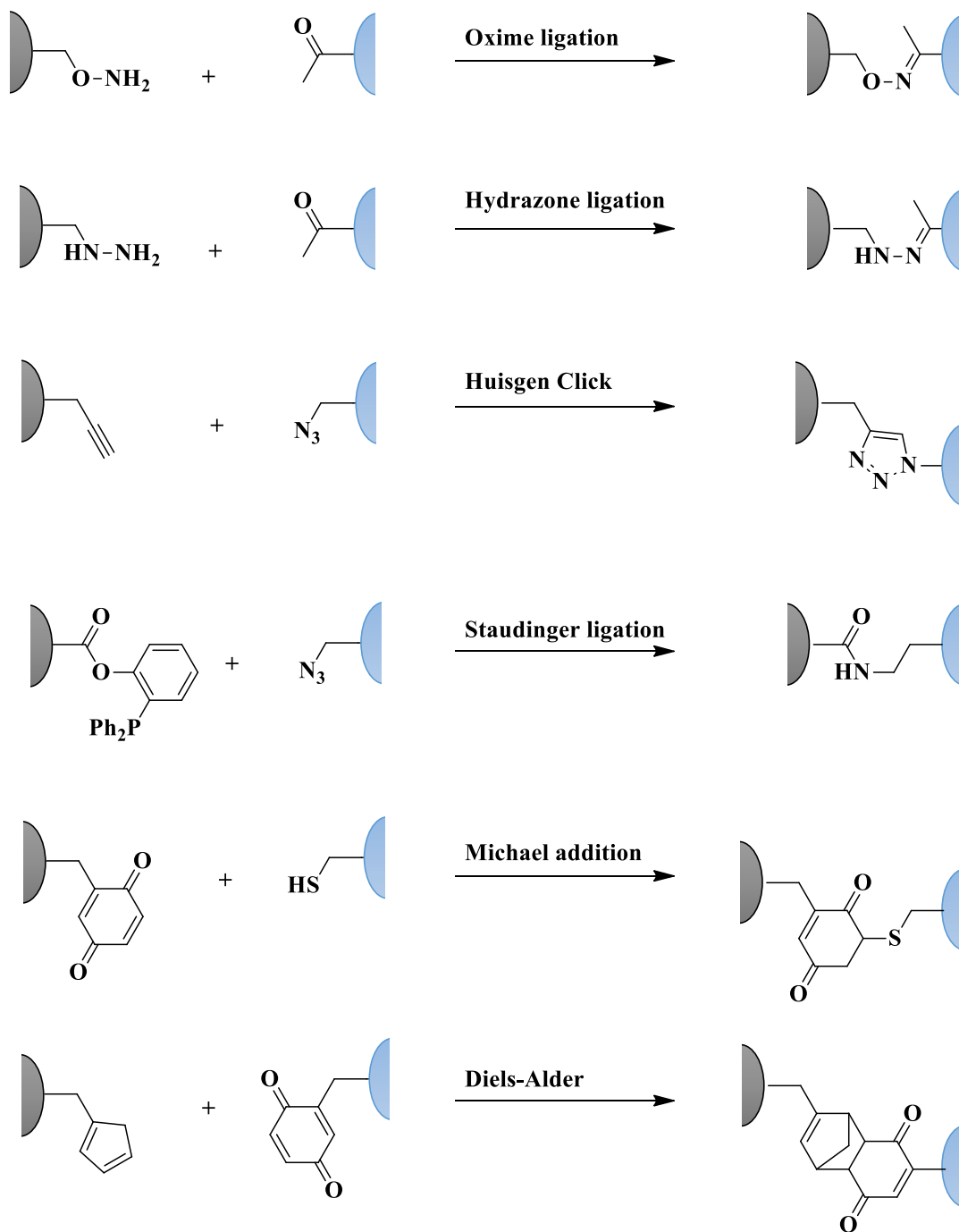


*Figure 1.12 List of biorthogonal reactions*

Some examples of biorthogonal pairs are presented here that could produce a traceless, efficient and biocompatible linkage between macromolecules without engaging in side reaction with cellular endogenous reactive moieties.

The combined effort of biologists and chemists gave rise to remarkable innovations in biochemistry and molecular probing. A Nobel prize was granted in this area for the synthesis of a genetically encoded fluorescent protein (GFP) in 2008.<sup>50</sup> While some macro-biomolecules are manipulated via genetic encoding, others like glycans, carbohydrates cannot be modified after biosynthesis. In order to introduce modifications, a hand full of reactions have been carefully selected from an organic chemist's toolbox that leads to the development of a considerably useful field of biorthogonal chemistry. This term was first coined by Carolyn Bertozzi in 2003 and refers to a set of reactions that do not interfere nor interact with other functional groups in physiological environments.<sup>51</sup> In spite of her work and contributions to the field, biorthogonal chemistry is a relatively older concept that was initially intended to address the reactivity of amino acid side chains with chemical reporters. However, the new definition limits the list of functional groups to only those non-naturally occurring moieties in biomolecules. Some of the most important biorthogonal reactions worth looking in a great detail are the reaction of hydroxylamine and hydrazide with carbonyl, Staudinger ligation to triarylphosphine and various dipole cycloaddition reactions.

### **1.3.1 Amine/Carbonyl Condensation**

Reactions of the carbonyl groups are among the most important of the organic reactions in chemistry. In addition to the dipole moment of the carbonyl groups, which locates a partial positive charge on the carbon, their  $\alpha$  carbon is also considerably acidic. These features enable a carbonyl compound to act both as an electrophile and as a nucleophile. The reaction of carbonyl towards nucleophiles has been extensively studied;

there are two possible mechanisms by which a better electrophilic center is generated: acid catalysis mechanism and base catalysis mechanism. Stronger nucleophiles tend to undergo *base catalyzed additions* during which they attack the carbon of the carbonyl to generate a tetrahedral transition state that pushes the electron density towards the oxygen. The negatively charged oxygen is perceived as a relatively strong alkoxide ion, which could abstract a proton to further stabilize the intermediate. In contrast, weaker nucleophiles require pre-activation of the carbonyl group in order to add to the carbonyl of the carbonyl. While there are many nucleophiles that could engage in a nucleophilic addition to the carbonyl group, hydroxyl, amine and thiol are the most important in the context of bioconjugation chemistry.

Amines have proven to be the single most nucleophilic and accessible reactive moiety available on the side chain of amino acids. Their reactions with most electrophiles are usually efficient and feasible under physiological conditions. A common reaction for amine conjugation is the condensation of amines with carbonyls in the form of ketone or aldehyde. Primary amines are nucleophilic at neutral pH and could readily add to carbonyl groups. The addition of primary nitrogen to aldehyde and ketone would usually proceed with the loss of water to form an imine bond also known as a Schiff base. This addition would generate an unstable carbinolamine, which is a term referring to a species containing  $\text{-NR}_n$  and hydroxyl on the same carbon. Under acidic conditions, a proton could facilitate the loss of hydroxyl group in the form of water. This step is significantly faster than a typical dehydration of an alcohol. The final imine product could also abstract a proton on the nitrogen, analogous to a carbonyl, and undergo further nucleophilic addition with any

immediately available nucleophile. Therefore, removal of the water by-product or any other nucleophile would further increase the yield of product.

The  $sp^2$ -hybridized carbonyl groups are reactive towards both primary and secondary amines. The formation of a stable product in the reaction of a primary amine with a single carbonyl group is highly dependent on the solution and microenvironment of the reaction. Nucleophilic addition of a primary amine to a carbonyl in aqueous solution forms an imine, which is a reversible process and would not be a sustainable method to generate a conjugate.<sup>52</sup> Other factors such as pH, temperature and concentration of reactant are crucial in the overall kinetics and feasibility of reaction. Higher pH ranges tend to accommodate more effectively for solubilisation and stabilization of a final Schiff base product. In any event, lowering the pH would rapidly favour the reversion to starting material and complete dissipation of C=N bond. In contrast, the same reaction is more tolerant in an organic solvent and could withhold a stable imine product. Contrary to aqueous solutions, pH has a completely different definition in an organic environment; hence acidity and proton availability would also be an atypical concept. Temperature, for most reactions, enhances the progression of the chemical reaction. This principle could be true for reverse reactions towards the formation of the starting material as is considered a form of product on the other side of the reaction arrow. The reaction of an amine with carbonyl is no exception from this notion either.<sup>52</sup> Beyond pH of the environment, the concentration of reactants is the most influential factor in the formation of the product as it has an immediate impact on the direction of equilibrium. Excess equivalence of attacking amine, even in aqueous solution, would always help to maintain some amount of product in the form of Schiff base. As discussed earlier, deprotonation of a primary amine at its

acidic dissociation constant range is a reversible process. There leaves some finite amount of deprotonated amine available in a solution that facilitates a nucleophilic addition, and further consumption of carbonyl. However kinetically slow, this minor amount of deprotonated amine is substantial enough to push the reaction forward towards complete depletion of carbonyl in solution over extended time.<sup>52</sup>

### 1.3.2 Oxime Ligation

Condensation of amines and carbonyls is not as efficient under physiological settings, as the imine product is not stable enough to sustain a robust covalent bond under aqueous environment. Nucleophilic additions could be perceived as sharing electrons between the HOMO and LUMO orbitals. Some  $\alpha$  electronegative heteroatom would increase the HOMO energy level of the attacking nucleophile. Reversibility of imine and enamine are due to lack of a mechanism to delocalize the  $\pi$ -bond. This instability is resolved in nucleophiles carrying and  $\alpha$  electronegative heteroatom.

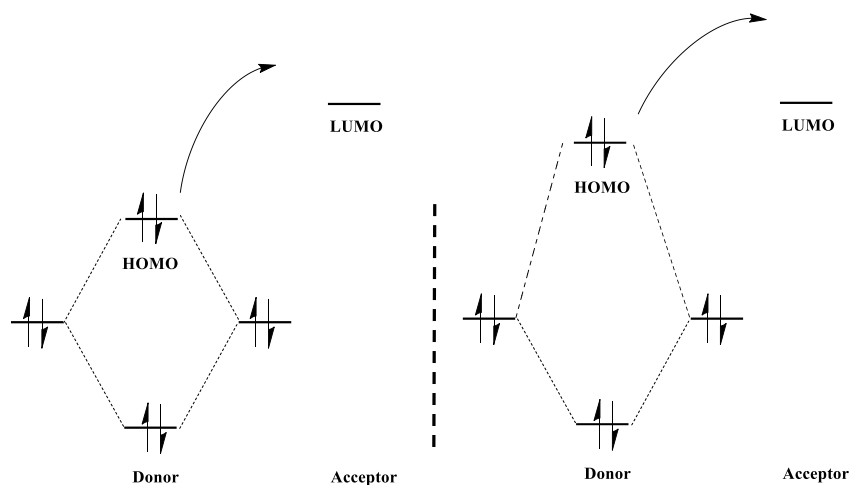


Figure 1.13 Energy level of HOMO and LUMO



Effect of the alpha donor, with a lone pair of electrons, on a nucleophilic heteroatom, would increase the energy level of HOMO; hence results in a substantially increased nucleophilicity.

The interaction of the HOMO energy levels of the two adjacent heteroatoms will consequently cause a significant electron repulsion or splitting, which would result in a rise in energy levels. This effect will lead to a discrete reduction of the HOMO/LUMO energy level, therefore enhances the electron transfer process. In addition to enhanced nucleophilicity of the attacking atom, the increased electron density of the heteroatom also delocalizes the partial  $\delta^+$  charge on the carbon sharing the  $\pi$ -bond. This contribution also increases the LUMO level of the electrophile hence relegates the chance of further nucleophilic attacks.

While such nucleophiles are generally stronger in their ability to engage in nucleophilic addition reactions, they do not necessarily have the same contributions in acid/base reactions. Their interactions with a proton are much less affected by the frontier orbital, hence their influence will be smaller in an acid/base reaction. This chemical phenomenon resulting in an enhanced nucleophilicity of the attacking functional group is referred to as an *alpha effect*.<sup>53,54,55</sup> Eminent examples of such nucleophiles are hydrazine and hydroxylamine and their products are hydrozone and oxime respectively. The products are easily characterized by their IR absorption stretch at  $1400\text{ cm}^{-1}$ .<sup>55,56</sup> While catalytic amounts of  $\text{H}^+$  would significantly improve the rate of oxime/hydrozone formation, such condition is not a prerequisite for dehydration. In fact, the formation of an oxime bond has been extensively studied in our group and has proven to be just as rapid as a neutral

condition. In spite of the slight abundance of aldehyde and ketones in the cell, in the form of hormones and carbohydrates, there are many reports in the literature that incorporate artificial carbonyl and use this type of chemistry in biological experiments. Schultz and co-workers have demonstrated a site-specific protein labeling procedure using a ketone functional group that could serve as a chemical handle.<sup>57</sup> Perhaps a better approach to chemically modify macromolecules is to modify integral or surface proteins on the cell membrane, where enzymes do not recognize carbonyls. Bertozzi has demonstrated in two different works, that a metabolic process could convert carbohydrates into keto-sugars. The delivery of such sugars onto the cell surface will allow for incorporation of a keto chemical handle, which could be detected using a hydroxylamine reporter.<sup>58,59</sup>

Utilization of non-native supernucleophile in biochemical settings has also gained tremendous attention in the recent years, as they are easily prepared in using simple synthetic processes. Such nucleophiles offer a unique opportunity to substitute the weaker amine or thiol nucleophiles, in chemical reactions that stability of the final product become crucial to the feasibility of the experiment. Their solvent compatibility, pH suitability and fast kinetics make them exceptional functional groups in biology. More importantly, they are often *in-cognito* to most of the biochemical enzymatic machinery, hence could selectively target a particular region of the cell.

### **1.3.3 Staudinger Ligation to Triarylphosphine**

Ligation of an azide and a triarylphosphine has offered an interesting resolution to the non-selective interactions of carbonyl and hydroxylamines *in vivo* studies with other

exogenous molecules and hormones. This method is a slight modification of azide reduction, using arylphosphines, in which the hydrolyzed product is an amino group. However, the  $N^-$  could be easily trapped in an amide bond, through a fast intermolecular process, by the installation of an ester moiety *ortho* to the azo-yilde intermediate. In the absence of an ester, the intermediate would simply hydrolyze to release the corresponding amine and phosphine oxide.<sup>60</sup>

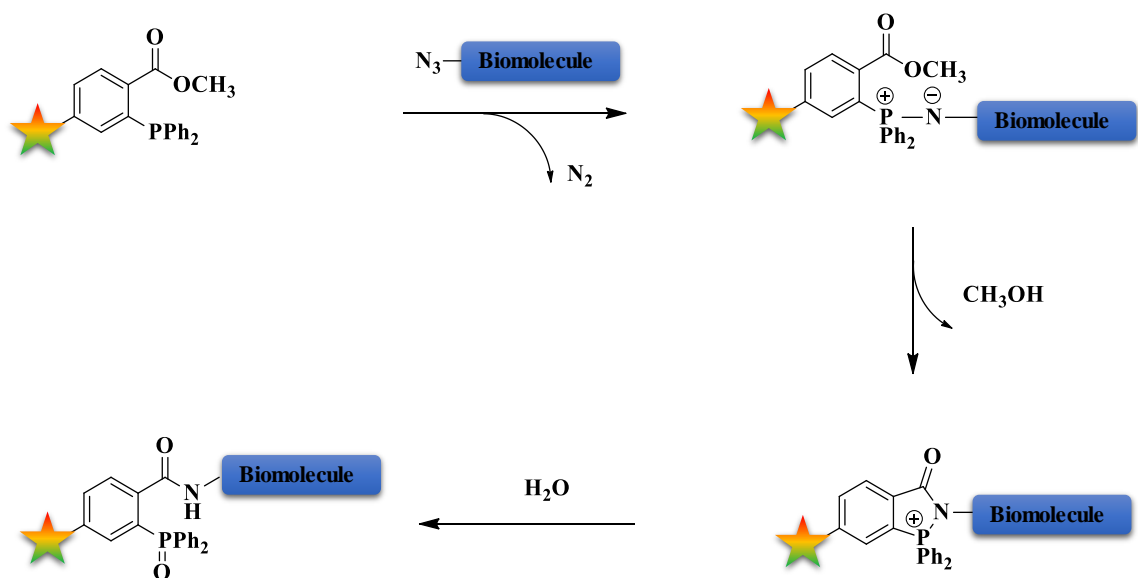


Figure 1.14 Overview of Staudinger ligation in bioconjugation

Triarylphosphines with a *para* ester substitution could act as a unique amine trap for any attacking primary amino group. A macromolecule could be labeled with an azide group and undergo Staudinger ligation with triphenylphosphine to liberate  $N_2$ . Installation of an accessible ester in the vicinity of nitrogen anion would allow for a rapid intermolecular process of substitution. Once the negative charge is stabilized and an amide bond is established, the addition of water would yield phosphine oxide.

In spite of reasonable selectivity of ligation between azide and triarylphosphines, there are other functional groups that could competitively reduce the azido group. Thiols

and disulfides are examples of such exogenous moieties that could serve as mild reductants for azides in the cytosol. Glutathione is a rich source of redox interactions in the cytosol that plays a significant role in biological processes.<sup>61-63</sup> This issue has been dealt with by Bertozzi group through pre-reduction of thiols using TCEP.<sup>64</sup> The only disadvantage of this alternative is the increased generation of free sulfhydryl in cytosol or solution.

An advantage of Staudinger ligation is exploited in its flexibility to carry a variety of reporters on the aryl groups. There are many protocols that utilize a derivative of the triarylphosphine armed with a fluorogenic reporter. Such reagents are extremely useful for real-time imaging and monitoring of organelles or cells.<sup>65</sup> Among other modifications of this ligation, we could highlight Raines and co-workers report on the preparation of a traceless Staudinger ligation that uses a thioester moiety for the formation of an amide bond between two distinct peptides carrying an azide.<sup>66</sup> In addition to the redox complexities of the reaction, a toxic by-product is released in the form of methanol. Although in very small quantity, yet it could act as a negative stimulant for some biological samples.

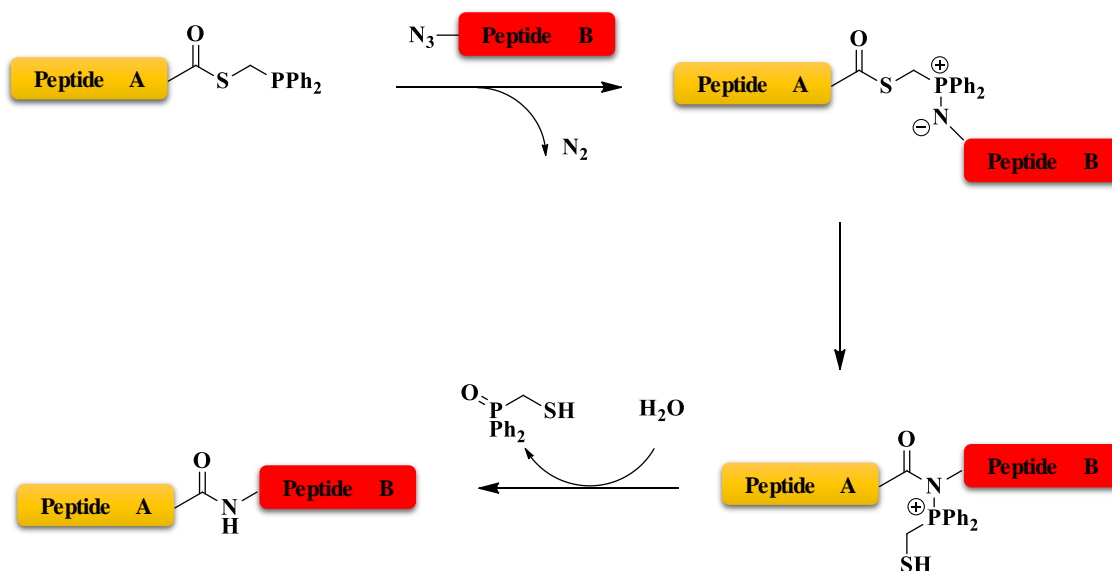


*Figure 1.15 Overview of traceless Staudinger ligation*

A slight modification on the original Staudinger ligation takes advantage of the tendency of S to act as a good leaving group in substitution/addition reactions. Although it leaves no traces of the reactants on the final conjugated products, it releases by-products in the form of phosphine thiol species.

Staudinger ligation has introduced a purely organic approach in bioconjugation field and has added many probe variations to the library of reagents. In spite of all efforts, it suffers from low kinetic profiles and release of undesired byproducts. There have been many attempts to improve its reactivity by introducing electron donating substituents, but they have only served to accelerate phosphine oxidation in air.<sup>67</sup>

### 1.3.4 Cycloaddition

Azides are very useful functional groups in the context of biological reactions. They are completely non-native and absent in the world of biology. This feature makes them a unique candidate to serve as a highly selective biorthogonal pair for chemical ligation

without engaging in any other chemical reaction with other endogenous functional groups. Azide chemical reaction with alkynes has been introduced in the late 19<sup>th</sup> century by Arthur Michael<sup>68</sup> but studies mechanistically by Professor Rolf Huisgen in the 50s during which, a concerted mechanism for the formation of the cyclic product was proposed in 1963.<sup>69</sup>

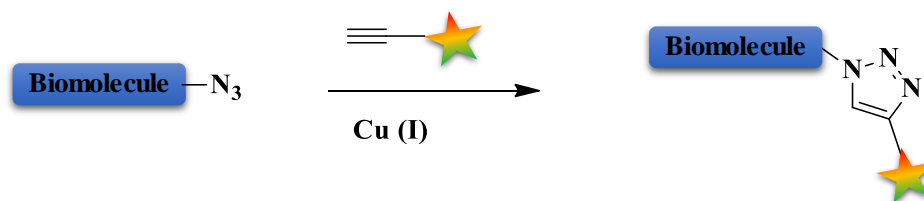


*Figure 1.16 Overview of Huisgen Click chemistry*

An alkyne and azide could react in a 1,3dipolar cycloaddition in presence of catalytic Cu (I) to afford a stable triazole ring.

However, it was not a suitable reaction to be conducted under physiological conditions. A major drawback was a relatively higher energy requirement for the aromatization of reactants to form a triazole product, which is an impossible endeavor to achieve in the vicinity of the cellular environment. Independently from one another, Sharpless and Meldal proposed that copper(I) could, in fact, catalyze the preparation of a 1,4disubstituted 1,2,3-triazole with great enhancement of up to 7 orders of magnitude faster.<sup>70,71,72</sup>

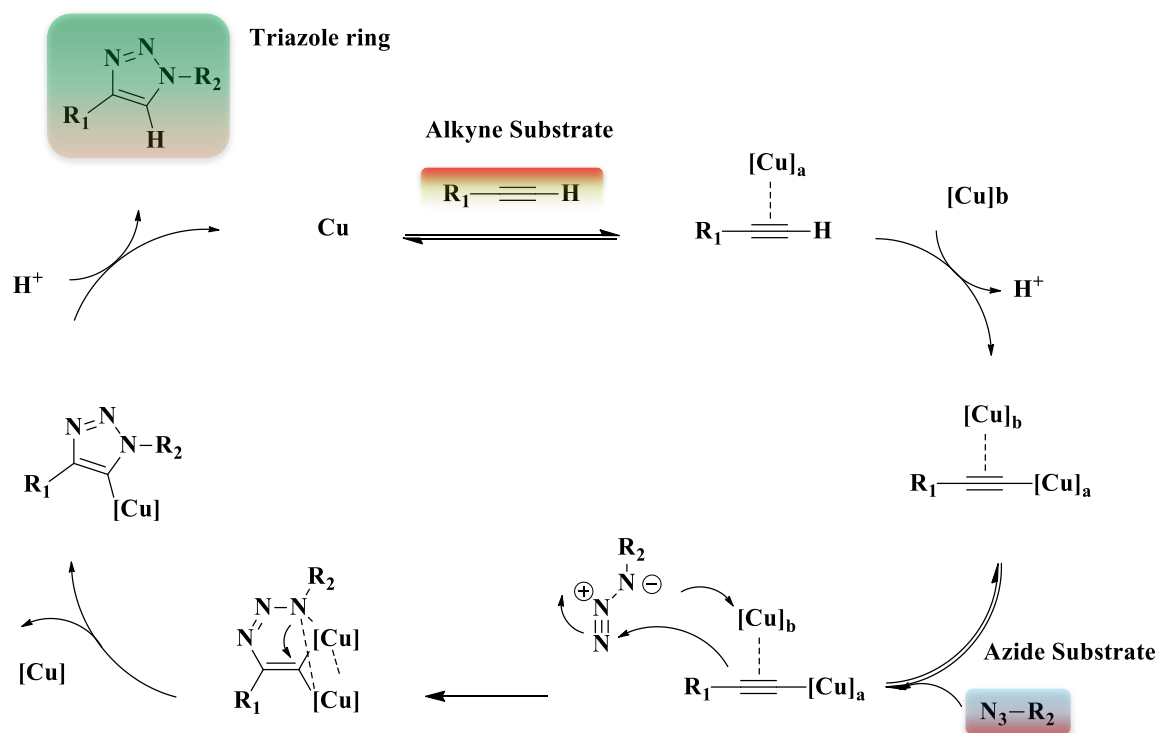


Figure 1.17 Overview of catalytic cycle of CuAAC

A catalytic cycle of Copper-Catalyzed Azide-Alkyne 1,3dipolar cycloaddition is presented.

Copper-catalyzed azide-alkyne 1,3 dipolar cycloaddition (CuAAC) attracted tremendous attention and was further developed to be a powerful tool in synthetic organic reactions, combinatorial chemistry, material chemistry, polymer chemistry, and chemical biology.<sup>73–78</sup> However, it was first utilized as a bioconjugate technique in Finn’s group for attachment of reporters to cowpea mosaic virus in 2003.<sup>79</sup> Later same year Köhn also reported the use of this type of chemistry in tagging viral infections.<sup>80</sup>

Although there was a great hope for the CuAAC reaction to secure a promising position to selectively tie biomolecules in a heterogeneous sample, it presented serious toxicity towards living cells and inhibited their further growth. *E. coli* cells, subjected to

small concentration of CuBr 100 $\mu$ M, failed to divide after a 16h exposure.<sup>81,82</sup> Similar to bacterial cells, mammalian cells also showed a concentration dependent survival rate towards Cu(I) inorganic salt. It was evident that an alternative catalysis should be explored to eliminate the need for Cu (I) exposure. In an effort to replace metal catalysis, Bertozzi developed ring strain conditions that were first introduced by Alder and Stein.<sup>83</sup> They had shown that reactivity of azide enhanced tremendously towards dicyclopentadiene in contrast with a cyclopentadiene. Inspired by this discovery, Wittig and Krebs proposed that cyclooctyne has an “explosive like” reaction once brought into contact with phenylazide.<sup>84</sup> Intrigued by their discovery, Bertozzi successfully labeled cell surface glycan with an azide functional group and detected it using a synthesized biotin reporter tethered to a strained cyclooctyne with no toxic effects.<sup>85</sup>

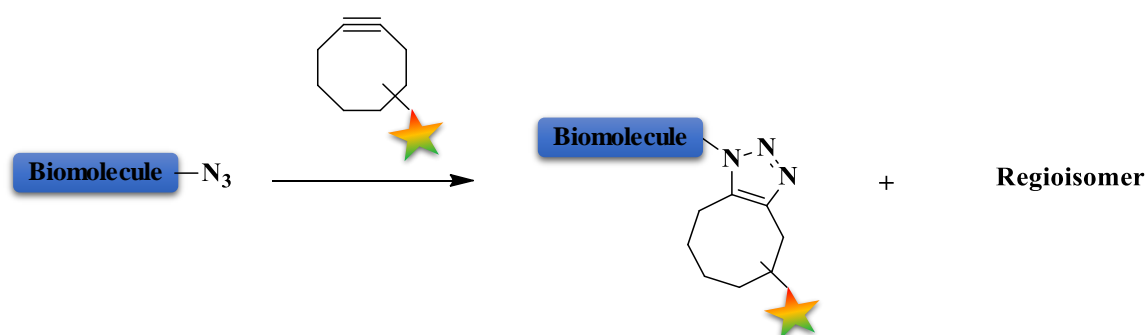


*Figure 1.18 Overview of strained alkyne and azide click chemistry*

Introducing a strained alkyne, in the form of octyne ring, eliminates the need for a catalytic process of click chemistry in the formation of a triazole ring.



The preliminary results led to the development of series of other synthetic biomolecules decorated with strained alkynes and solved the problem with metal catalysis of Huisgen reactions. Since then, there has not been much ground breaking advancement in the “click chemistry” other than installation of electron-withdrawing groups that led to 60 fold kinetics improvement.<sup>86,87</sup>

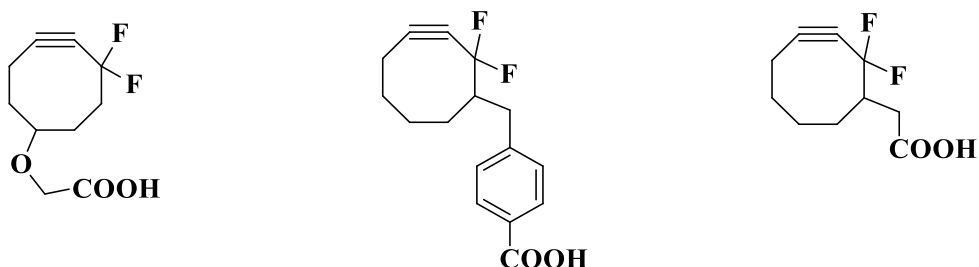


*Figure 1.19 Examples of activated strained alkynes*

Development of multiple substrates derived from monofluorosubstituted cyclooctyne (MFCO) and substantial positive feedback from their reactivity, led to significant improvements in the synthesis of DIFO strained alkyne rings.

### 1.3.5 Cycloaddition Enzymatic Conjugation and Labelling

In addition to the remarkable contributions of organic chemistry to the developments of bioconjugation field, biochemists also deserve credit for their efforts in functionalization of native biomolecules. Incorporation of a selective functional group on protein, glycan and lipid is the greatest achievement of such efforts. All these protocols depend on cell's enzymatic machinery to install a particular residue on the macromolecule. While they seem to be the product of cell's natural behavior, they still depend on the manipulation of some enzymatic function.

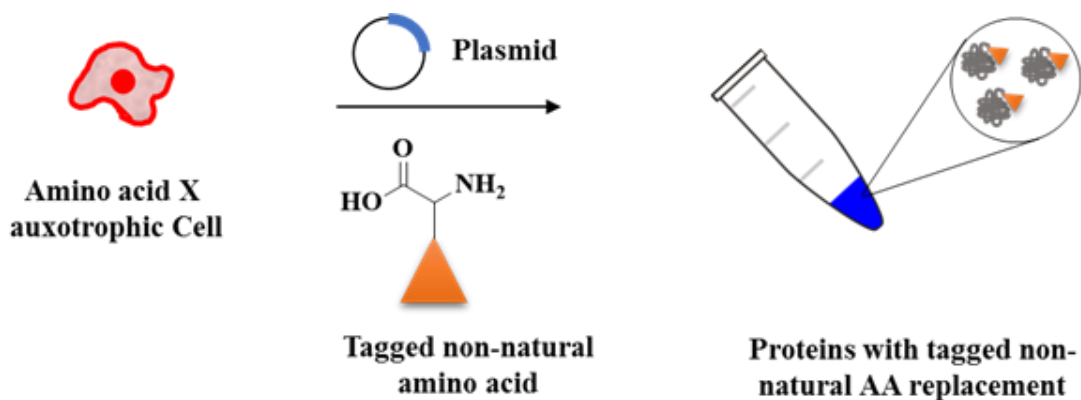


*Figure 1.20 Synthesis of protein with un-natural amino acid tag*

Unnatural amino acids could be incorporated into the sequence of protein using auxotrophic cell lines. The resulting protein synthesis is a macromolecule that offers an unnatural residue.

For example, Tirrel and co-workers pioneered protein labelling using metabolic residue-specific modification. The cell is fed with non-natural amino acids that could undergo metabolic conversion to install a chemical handle on a macromolecule.<sup>88-90</sup> There has been a tremendous effort and development in the incorporation of such biorthogonal functional groups on proteins that have proven to be useful in imaging and cellular trafficking experiments.<sup>91</sup> A concerning challenge for biochemists lies in the functional incompatibility of some non-natural amino acids with their parent molecular structure to serve equally in hydrolytic functions. Such dissimilarities require special attention and modified protocols for the experiment intended. For example, aminonacyl-tRNA synthetases (aaRSs) must be genetically mutated to remain tolerant for unnatural substrates.<sup>92,93</sup>

While this technique seems to be an easy approach for a highly selective bioconjugation experiment, there are many uncertain check points in the proper metabolism of the non-natural amino acid using its enzyme. This technique leaves a lot of uncertainties regarding the fate of the metabolite and their destination. Furthermore, there is no systematic control over the toxicity of the metabolite nor the starting material in the cell. For the mentioned reasons, it cannot serve as a universal approach towards macromolecule labelling for more clinical experiments.

A reasonable alternative for metabolic incorporation of functional groups would be the genetic encoding of proteins to carry a functional group on their native structure. In this method, a terminating codon (UAG) is replaced with a code that encodes a non-natural amino acid onto the complementary template of tRNA.<sup>94</sup> Despite the elegant design of this protocol, it suffers from poor yield and only a small amount of the functional group is installed on the target; from this population, only a few remain to be effective for labelling purposes.<sup>95</sup> In spite of all limitations, genetic encoding methods served many research groups and contributed to much of mechanistic explorations of protein folding and structural analysis in the past years.<sup>96–99</sup> Many functional groups such as amino acids carrying an azide,<sup>100</sup> alkynes,<sup>101</sup> carbonyl<sup>102,103</sup> and alkenes<sup>104</sup> have been successfully incorporated into protein structure using *in-vivo* protocols. In addition to the basic functional groups on organic chemistry lists, there are more advanced and complex residues installed on the structure of a macromolecule protein such as aryl halides,<sup>105</sup> anilines,<sup>106,107</sup> boronic acids,<sup>108</sup> photoisomerizable and crosslinkers.<sup>109,110</sup> The extent of improvement of these approaches seemed to be endless that even a complete structure of a fluorophore was successfully installed on the protein structure.<sup>111,112</sup>

Glycans can also be engineered to carry a biorthogonal pair on their structure. The principle is virtually identical to protein metabolic labelling methods.<sup>113</sup> Since glycans do not contain the same translational template as proteins do, genetically encoding them is not as applicable as other biomolecules. However, incorporation of a functional group via metabolic modifications on a non-natural carbohydrate is a well-practiced protocol. This method is called metabolic oligosaccharide engineering, which was first reported by Reutters et al by altering the acyl side chain on precursor *N*-acetylmannosamine (ManNAc) derivatives.<sup>113,114</sup> In an extension of this protocol, Bertozzi transferred a ketone functional group on the cell surface using ManNAc derivative.<sup>115,116</sup> The carbonyl group was easily detected using a biorthogonal pair, like an activated amino group, hydroxylamine or a hydrazine reporter.

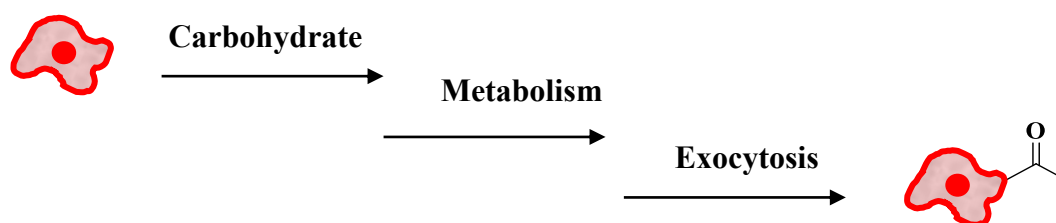


*Figure 1.21 Cell surface re-engineering using metabolic pathways*

A non-native organic functional group could be incorporated onto cell surface via the metabolic action of cells on a precursor carbohydrate. Enzymatic processes could transform a precursor residue on the carbohydrate structure into the corresponding metabolite that will be excreted from the cell through exocytosis. The functional group could get incorporated into the membrane to be used as a chemical handle.

Similar to glycans, lipids are also synthesized without flexibility for post-translational modification, therefore installation of a probe on lipid products remain to be more challenging than proteins. There are numerous reports on modification of lipids

through myristoylation and palmitoylation to embed a biorthogonal pair on the backbone. Berthiaume et al have used this technique to study the effects and contributions of myristoylation to apoptosis using Staudinger ligation.<sup>117</sup> Or in a similar study, a novel protein lipidation mechanism was studied in the liver by labelling the mitochondrial palmitoylation product.<sup>118</sup> A number of farnesyl precursors have been synthesized to carry a biorthogonal functional pair that is used to study protein modification.<sup>119–122</sup> While functionalization of lipids would not have much physiological importance itself, it could serve as a powerful mean to conduct mechanistic *in vivo* studies of proteins, cellular inter-components and lipid metabolism.

Organic chemistry, molecular biology and genetics have all offered various methods to intervene with the basic cellular function and introduce a unique foreign body on biomacromolecules. Each field has exhausted the resources to design a minimally invasive method through which, a cell could be decorated with a non-native moiety that could serve as a chemical reporter. Inspired by nature's way of molecular interactions, organic chemists have modified and diverted their reactions out of round bottom flasks to fill in some of the gaps. Molecular biologists have designed new methods that would compel cells to synthesize proteins and other biological entities suited for an intended purpose. In spite of all collective efforts, there remains a huge gap to satisfy all the needs for a clean, healthy and green conjugation.

While genetic encoding, metabolic pathways and other biochemical procedures leave the impression of flawless approaches, they are often highly laborious, expensive and require trained personnel to execute a successful experiment. The available techniques are often complex and associated with uncertainties that may either interrupt cell physiology

or jeopardize cell viability. They are often dependent on countless factors that are simply beyond what researchers could monitor and control. Therefore, much of the result obtained could be skewed by uncertain aspects unknown. Genetic and metabolic manipulation of cells towards the production of proteins and other biologics would obviously permanently change the identity of the cell's hereditary codes. Once a new set of genetic codes are dictated to the cell, the subject is no longer an accurate model of that cell line for prospect experiments. In addition to the loss of native identity, each reformation requires a new set of genetically encoding procedure. The tasks are often very laborious and could not be easily performed without long term preparations. All key molecular players in life are very sensitive and could be susceptible to damages upon exposure to any chemical or biological modifications. Proteins, in particular, become a victim of such modifications. They are often very expensive and difficult to purify in the lab, thus labelling and experimentation on them should be conducted with caution. The efficiency of such protocols must remain exceptionally high as the starting materials are usually available in small quantities. Furthermore, exposure of chemical reagents could easily change the native folding and structural feature of a functioning protein. The result of such manipulations could lead to inaccurate and distorted operation of the macromolecule. Hence the protein would no longer serve as a true model and representative of its native state. The currently available methods and reagents for bioconjugation often suffer from the release of unnecessary by-products that could pose threat to the homeostasis of cell's microenvironment. However traceless the current chemical reactions are, there still remains some residues or by-products that could be potentially cytotoxic for living organelles. Selectivity for an isolated target is another concern and challenge for accurate labelling of macromolecules. In spite

of the range of nucleophiles present in the heterogeneous cellular sample, fishing for a segregated target becomes detrimental for a successful conjugation. The field of bioconjugation is in need for an approach that eliminates the need for any modifications of the macromolecule. The serious restrictions associated with the available techniques in biochemistry have left tremendous opportunity for organic chemistry to improve upon reactions that could replace the unambiguous protocols offered by other biochemical methods.

Here in the first part of this work, we report a novel strategy to insert an organic biorthogonal functional group on the surface of a model organism bacteria cell, using the common cellular practice of liposome fusion. These functional groups could then serve as counterfeit handles/receptors on the cell surface to enable temporal and spatial control over its default command. This technique offers a safe incorporation of organic chemistry into lipid vesicle structures that are essentially made from materials recognized by the cell as plasma membrane. Such procedures are routinely executed to deliver nutrients and toxins in and out of the cell. Traditionally, liposome fusion has been used to overcome the challenges of delivering pharmaceutical ingredients into the cell via binding to exclusive receptors. The chemistry incorporated onto the cell-surface does not interact with any of the endogenous or surficial glycoproteins, yet offers efficiency, simplicity and compatibility with cell's biochemistry and physiology, which would sustain cells normal cell activity. Preliminary research has shown successful cell-surface engineering on eukaryotic mammalian cells; yet introducing such exogenous integrals onto the prokaryotic cell-surface remains to develop. This research explores the feasibility of prokaryotic cell-surface engineering using the liposome-fusion technique.

In the second part of this work, we introduce a novel amine conjugation system that would eliminate the need for any chemical/physical modifications on the biomolecules or cell surfaces. This is the first time, to the best of our knowledge, that a unique strategy allows for a successful conjugation and release of a primary amine in the context of organic chemistry and biological applications. This method is highly selective for the intended target with rapid ligation and no residual by-products. The functional group designed is biocompatible and could easily operate under physiological conditions. It is synthetically flexible and could be installed on a variety of small organic molecule reporters to label carbohydrates, glycans and amino acids. It is also applicable to a wide range of larger macromolecules in the form of proteins and even crosslinks a whole cell to other micro/macrosopic entities.



## 2 CHAPTER TWO

### **Re-Engineering Gram Negative Bacteria Cell Surfaces with Bio-Orthogonal Chemistry via Liposome Fusion**

---

#### **2.1 Introduction**

Bioconjugation chemistry has offered a new insight into targeted labelling of cellular components in the past years.<sup>123,124</sup> A number of organic functional groups have been introduced that would allow for a high discrimination of a particular recipient within the cytoplasm of a cell. Biochemists have also introduced novel methods to incorporate such chemical handles on macromolecules to serve as an essential communication medium. In spite of all efforts, there is an existing gap to fill in the delivery of such chemistries onto biological subjects. Although there are many organic reactions that could satisfy the objectives in bioconjugation, there remains a method that could successfully deliver them. We already discussed the recent advancements in the re-engineering of cell surfaces using metabolic incorporation of functional groups<sup>115,58</sup> or the installation of non-natural amino acids onto the complementary template of tRNA.<sup>94</sup> Molecular biology and genetics have offered various methods to intervene with the basic cellular trafficking by designing genetic codes, which would compel cell to synthesize proteins and other biological entities to decorate the cell surface. The available techniques suffer from complexities and uncertainties that would either interrupt cell physiology or render the cell futile. Although these techniques have served in many experimental procedures to unravel scientific ambiguities, they do not offer a non-invasive tactic in the delivery of chemistry. In the

recent years, it has become evident that the novel delivery approaches of chemical handles onto cell deserve equal attention to designing innovative chemical reactions.

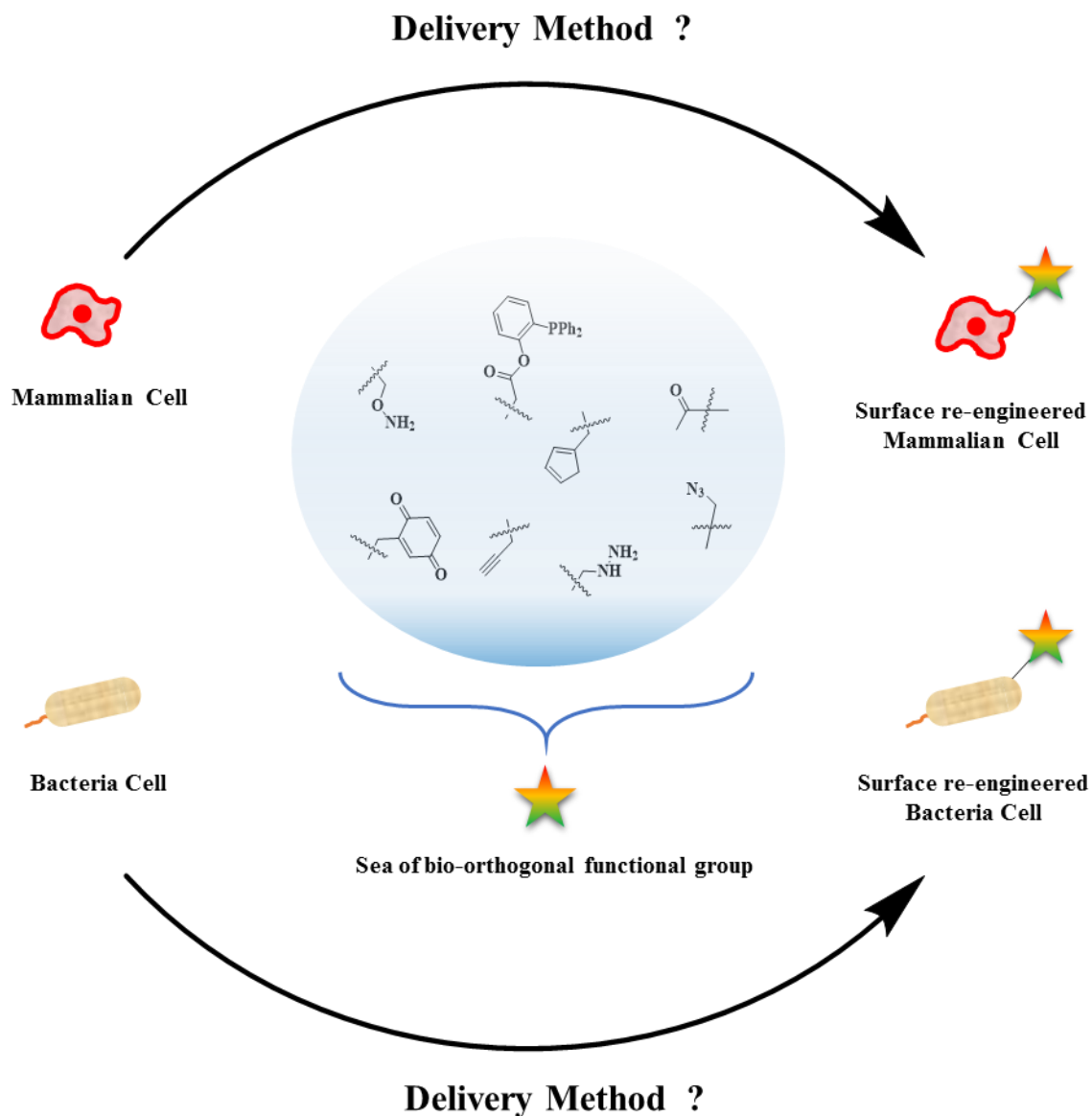


*Figure 2.1 Delivery of reporter onto cell surface*

A delivery method is required to reliably transfer a chemical handle onto cell surface without disrupting regular cellular function. Although there are many organic functional groups available in the literature, there is still a need for a new strategy to safely deliver them onto the membrane.

Biological membranes are primarily designed to serve as barriers, with minimal tendency to expose cell compartments to the endogenous variables. Nonetheless, a cell's viability is heavily dependent on communication with external environment for energy resources, migration, recognition, protection and replication processes. To accommodate for such survival factors, membranes are decorated with complex receptors and biological regulators, which mediate cellular activities. Among such activities, membrane fusion plays a central role not only in cell-cell fusion, or fertilization and myogenesis but also in endocytosis, exocytosis and other transport processes between cellular organelles. All cellular fusions occur in a highly controlled fashion to avoid admitting intruders into the cell.<sup>125–128</sup>

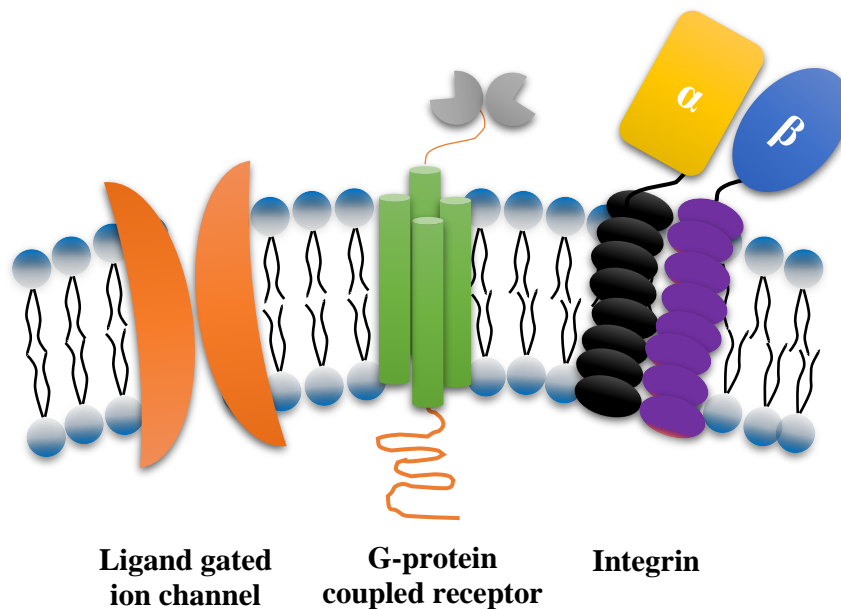


*Figure 2.2 Cell membrane surface components*

The surface of a membrane is decorated with a variety of macromolecules that regulate normal activities. These molecules serve as antenna and receiver for the cell through which external communications are possible.

The understanding and manipulation of the bacteria cell surface are important for a range of fundamental studies of bacterial behaviour and for therapeutic applications to improve human health.<sup>129</sup> The first studies of modifying bacteria surface proteins were performed in the 1980's and led to the critical development of tools to tailor bacteria cells with biological macromolecules and synthetic man-made molecules for applications in microbiology, vaccine development and biotechnology.<sup>130,131</sup> In particular, gram-negative bacteria including *Pseudomonas aeruginosa* and *E. coli* have shown increasing importance due to their implications in infection and pathogenesis.<sup>132,133</sup> These bacteria also serve as model single cell organisms to study fundamental cell behaviour as well as various bacteria associated diseases. Methods to tailor bacterial cell surfaces are essential to generate new bacterial platforms that have the ability to display a wide range of molecules to further explore and manipulate bacterial behaviour and to design next generation of therapeutics.

Due to the complexity of the bacteria cell surface, few straightforward and robust technologies exist to add biomacromolecules or synthetic small molecules and ligands to the membrane with high efficiency and fidelity. Current methods use three main strategies, all of which have been extensively discussed in Chapter 1: 1. A molecular biology approach that uses genetic surface display technologies. 2. A metabolic engineering approach where foreign substrate ligands are fed to bacteria and then processed through the bacteria enzymatic machinery to be displayed on the cell surface and 3. Direct chemical display of molecules to the bacteria cell surface via chemical ligation to membrane proteins or carbohydrates. Through genetic surface display technologies, a range of applications including environmental remediation,<sup>134</sup> biofuel production,<sup>135</sup> biocatalysts,<sup>136</sup> bio-

sensing,<sup>137</sup> protein library screening,<sup>138</sup> cancer therapeutics,<sup>139</sup> vaccine development,<sup>140,141</sup> and intestinal probiotic therapy<sup>142</sup> have been investigated. However, these technologies traditionally cannot be applied to install non-genetically encoded molecules such as lipids, carbohydrates, and a variety of non-native chemical compounds. To address this limitation, chemical surface display technologies, which allow for installation of non-native compounds onto cell surfaces, have become increasingly interesting to researchers over recent years. These technologies are commonly based on metabolic labelling of small peptides, which relies on intercepting the machinery pathways of cell-wall biosynthesis. Thus, they are well suited for manipulating the surface glycans as well as subsequent conjugation of other attachable compounds. These technologies led to many studies including directed evolution,<sup>143</sup> proteomic analysis,<sup>81</sup> immunotherapy,<sup>144,145</sup> molecular imaging,<sup>146</sup> and host–pathogen interactions.<sup>147</sup>

Herein, we introduce a rapid and straightforward gram-negative bacteria surface engineering method that bypasses traditional genetic and metabolic manipulations. This approach relies on integrating a robust delivery system (liposome fusion) with bio-orthogonal lipids to tailor bacteria surfaces. The liposome fusion method combined with bio-orthogonal ligation strategies allows for the presentation of stealth like molecules on the bacteria surface for subsequent decoration with a wide variety of ligands to simultaneously track bacteria, augment bacteria behaviour and to provide theranostic type studies and applications.

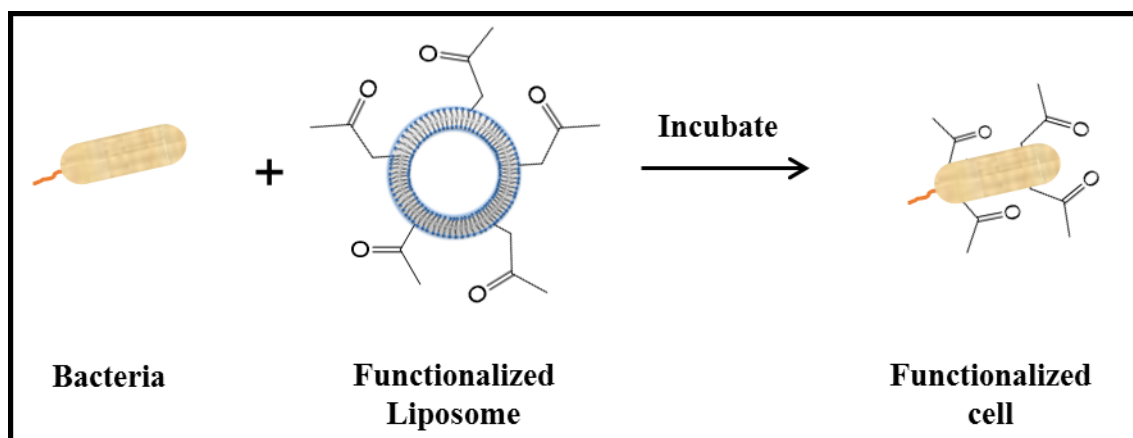


*Figure 2.3 Bacteria cell surface engineering*

Bacteria cells are incubated with the ketone-functionalized liposomes. Through liposome fusion, the bacteria surface can be engineered to present ketone groups, which can subsequently react with an oxyamine tailored reporter molecule via bio-orthogonal oxime conjugation. Based on this bacteria surface engineering system, a range of ligands, proteins, small molecules, and probes containing the oxyamine group can be installed onto the bacteria surface through oxime ligation.

In this report we use, for the first time, an oxime reaction to tailor *Pseudomonas aeruginosa* and *E. coli* bacteria cell surfaces with a range of ligands. Based on this powerful, fast and straightforward surface engineering technique, a wide range of functional molecules can be installed onto the bacteria surface without disturbing regular cellular activities. In this work, we fully characterize and demonstrate this new strategy by employing flow cytometry, phase contrast microscopy, membrane isolation, mass spectrometry and surface chemistry methods to study the tailoring of bacteria cell surfaces.

Liposome fusion has been used as a technique for the delivery of chemical and biological cargoes into mammalian cells for many years.<sup>148–150</sup> In this study, we used the liposome strategy to deliver novel lipid-like functional molecules efficiently to a bacteria

surface. The liposome fusion method takes advantage of hydrophobic interactions of liposome vesicles and lipid bilayers to insert into the outer membrane structure. Although such interactions are electrostatic in nature and thermodynamically favoured, the composition of the liposome nanostructure plays a significant role in inducing adhesion and fusion.

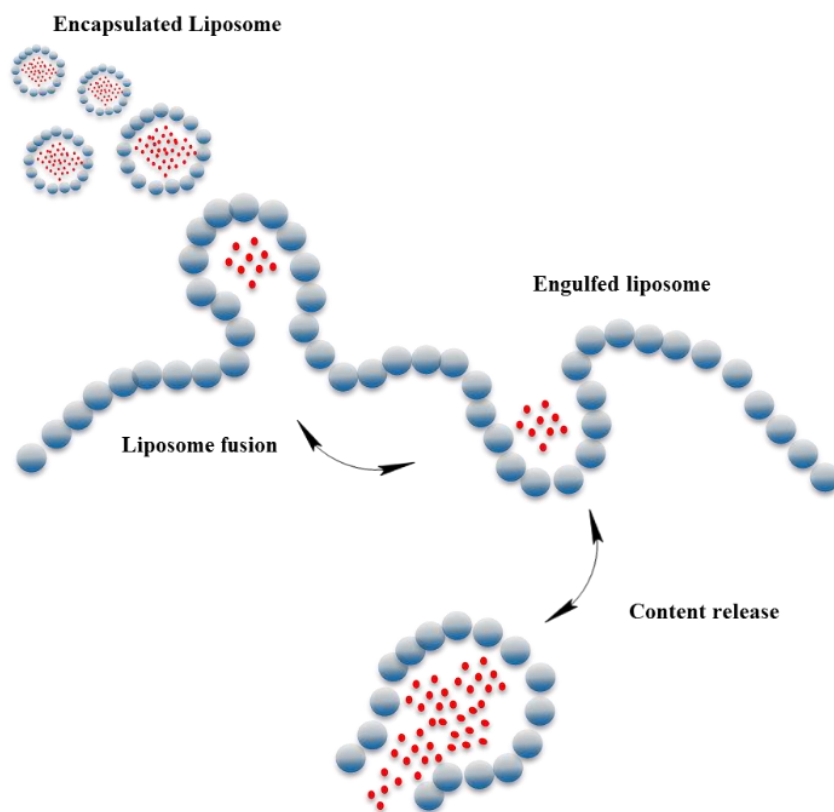


*Figure 2.4 Drug delivery via liposome fusion*

Active pharmaceutical ingredients could be encapsulated in a liposome micelle and fed to a cell in a culture. If the liposome composition remains compatible with cellular membrane lipid composition, they could be recognized as normal building blocks of membrane and fuse into the lipid bilayer. Once engulfed, they could release their cargo content in the target area and elicit their therapeutic effect. This strategy is inspired by cell's natural trafficking mechanism. Nutrients are regularly taken up through endocytosis and toxins are excreted through exocytosis via liposome fusion principle.

In order to tailor bacteria surfaces with a range of molecules, a general class of reactions that can be performed at physiological conditions without side reactions in a biological environment is required. Tremendous research has been performed to investigate and expand the scope of these special chemical reactions termed bio-orthogonal chemistry<sup>151–153</sup>. Several new types of bio-orthogonal reactions have been discovered including click, hydrazone, thiol-ene, diels-alder, etc.. However, the most popular click reaction is the copper catalyzed Huisgen [3+2] alkyne and azide reaction, hydrazone and oxime chemistry. Pioneering efforts by several researchers have shown the utility of these reactions for many biological applications ranging from *in vivo* targeting, drug delivery, antibody drug conjugates, protein engineering, proteomics, imaging and biosensing.<sup>154–156</sup>

A proficient novel alternative is proposed in this research to insert an organic functional group on the surface of the cell, using the common cellular practice of liposome fusion.<sup>157</sup> These functional groups could then serve as counterfeit handles/receptors on the surface to enable temporal and spatial control over the cell's default command. This technique incorporates a safe organic chemistry into lipid vesicle structures that are essentially made from materials recognized by the cell as plasma membrane. Such procedures are routinely executed to deliver nutrients and toxins in and out of the cell.<sup>158,159</sup> Historically, it has been used to conveniently avoid the challenges of dispensing pharmaceutical ingredients into the cell that require binding to exclusive receptors.<sup>160,161</sup> The chemistry incorporated onto the cell-surface does not interact with bio-active molecules and glycoproteins, yet offers efficiency, simplicity and compatibility with cell's biochemistry and physiology, which would sustain cells normal activity.



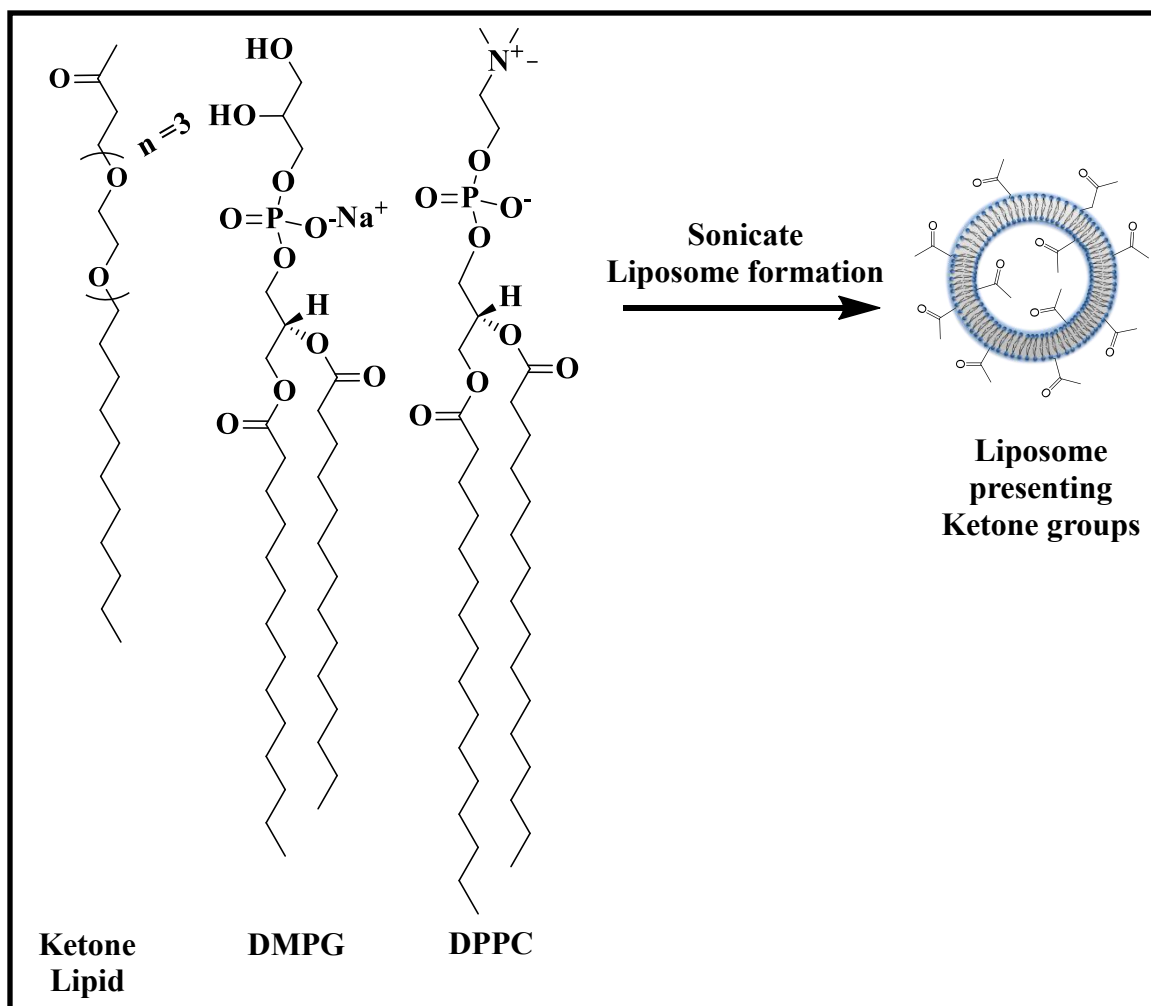


*Figure 2.5 Liposome reengineering with biorthogonal head group*

A ketone-terminated lipid-like molecule is mixed with 1,2-dipalmitoyl-sn-glycero-3-phosphocholine (DPPC) and 1,2-dimyristoyl-sn-glycero-3-phospho-(1'-rac-glycerol) (DMPG) to form ketone-functionalized liposomes.

Preliminary research has shown successful cell-surface engineering achievements on eukaryotic mammalian cells; yet introducing such exogenous integrals onto the prokaryotic cell-surface remains a challenge. This research explores the feasibility of prokaryotic cell-surface engineering using liposome-fusion technique.<sup>162,163</sup>

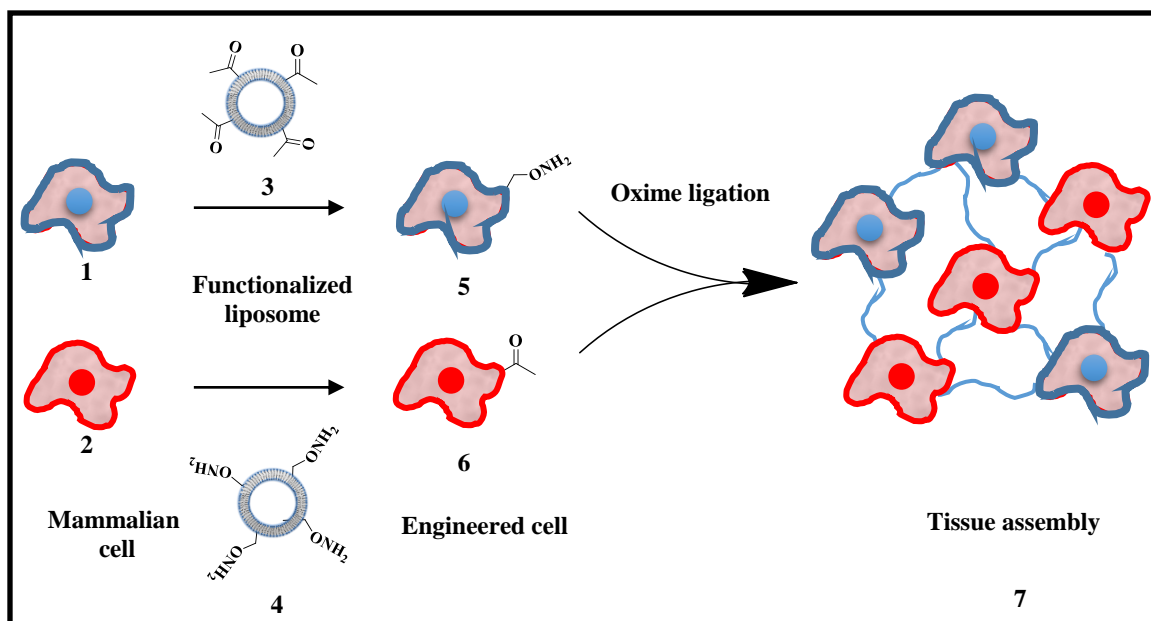
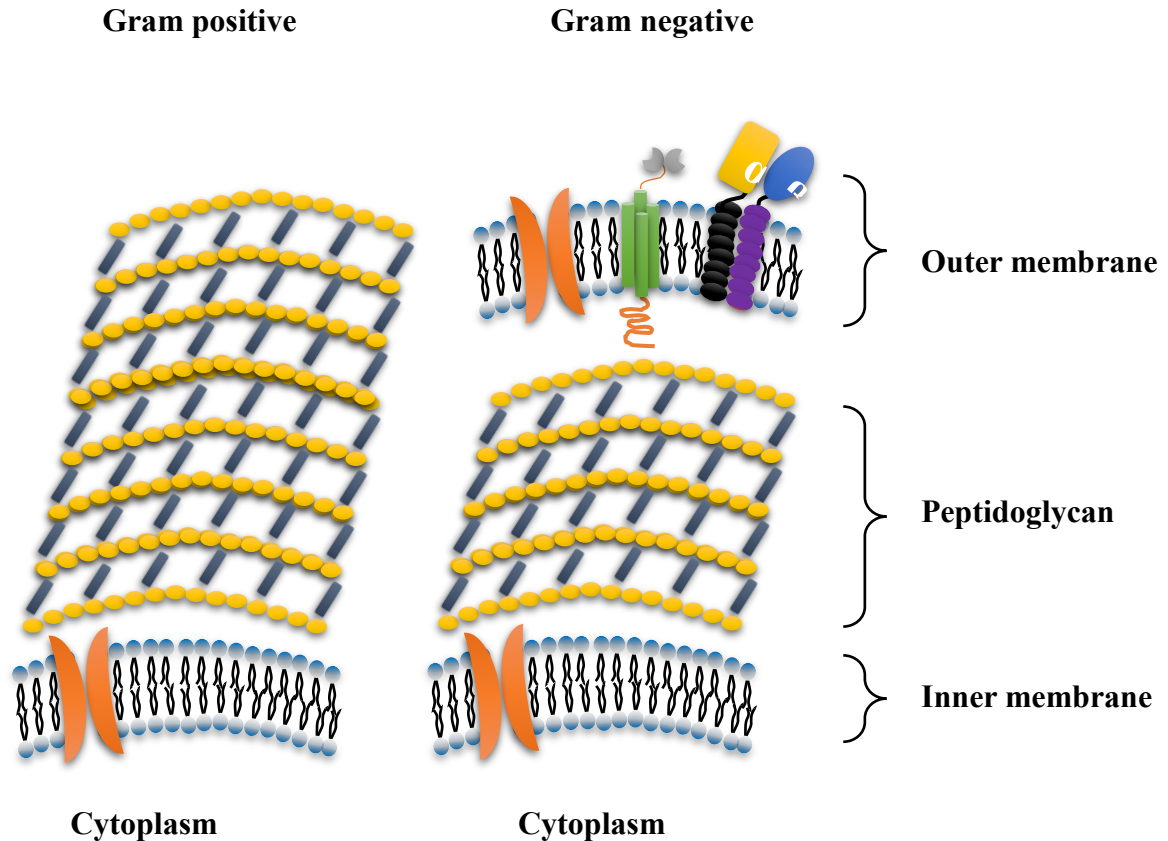


Figure 2.6 Tissue assembly using biorthogonal ligation

Native mammalian cells (1) and (2) were incubated with functionalized liposomes (3) and (4) to re-engineer the surface membrane with the corresponding biorthogonal pair. The resulting engineered cells (5) and (6) were mixed and incubated to form a viable tissue assembly construct (7).

Prokaryotic cell permeability is a highly organized task, regulated by the cell wall to maintain cell's viability and organelles integrity. The membrane structures are the fundamental differences between the gram-negative and positive bacteria. The cell wall of a gram-negative bacterium is comprised of an outer membrane, periplasmic space (peptidoglycan) and cytoplasmic membrane. However, peptidoglycan layer in a gram-positive bacteria is far more robust and thicker.<sup>164</sup> For this reason, liposome fusion attempts on gram-positive *Bacillus subtilis* did not produce any promising results. Flow cytograms obtained from those attempts presented minor auto fluorescence emitting from their surface.



*Figure 2.7 Overview membrane structure of bacteria*

Bacteria membrane are significantly different between gram positive and negative cells. While the surface of gram-negative bacteria contains the outer lipid bilayer membrane, gram positive cells contain a thick layer of peptidoglycan. The unusual thick peptidoglycan allows for additional impermeability of the cell wall. This feature is also partially responsible for cell wall stability.

Because of their effective permeability function of their outer membrane, both structures are resistant to the majority of foreign agents. Nonetheless, some hydrophobic macromolecules have better diffusion probability by the virtue of either hydrophobic interactions with an outer leaflet or simply cell's routine admission for regular biochemical requirements.<sup>165</sup> Some small hydrophilic molecules could also enter cells inner structure

from water-filled porin channels, but such transfers are highly disfavoured, as serious damage could be inflicted upon cell's structure. Among most important factors influencing cell trafficking of a gram-negative cell, lies the composition of the lipopolysaccharide (LPS-A), found on the outer membrane, and cationic interactions ( $\text{Ca}^{2+}$ ,  $\text{Mg}^{2+}$ ,  $\text{Na}^{+}$ ) on the surface.<sup>159,166,167,168</sup> LPS molecules bind to cations and form a polycationic “roof” on the surface of the cell; these molecules are further stabilized by divalent charges available across the cell wall.<sup>169</sup> Large number of antibiotics act on disrupting the interaction between LPS crosslinkers, which would eventually result in cell wall instability and trigger collapse.<sup>170</sup> For the very same reason, diffusion of even highly hydrophobic foreign entities through the outer membrane requires moderate, yet effective, disruption of LPS-cationic interactions. Low concentration of chelating agents, in particular, EDTA, have served well in compelling the cell to permit incorporation of some hydrophobic molecules into the membrane structure.<sup>165,171</sup>

## 2.2 Results and Discussion

In previous studies from our laboratory, nanostructure liposomes made from POPC/DOTAP and bio-orthogonal lipids have shown broad scope results in decorating the surface of mammalian cells.<sup>172–177</sup> However, this particular liposome composition may not be necessarily compatible with the majority of gram-negative bacterial cell membranes. Recent reports have shown successful delivery of antimicrobial cargo into the cytoplasm of bacterial cells using DPPC/DMPG lipids.<sup>157</sup> Therefore, we designed our bio-orthogonal/liposome delivery system based on a combination of 1,2-dimyristoyl-sn-glycero-3-phospho-(1'-rac-glycerol) (DMPG) and 1,2-dipalmitoyl-sn-glycero-3-

phosphocholine (DPPC) and a bio-orthogonal lipid like molecule (**Figure 2.8**). This combination will result in a negatively charged liposome, while cells also retain anionic surface properties. This seems counterintuitive to the principles of charge attractions; however, the negative charges of the liposome are not as concentrated to be repelled from their target cell membrane.

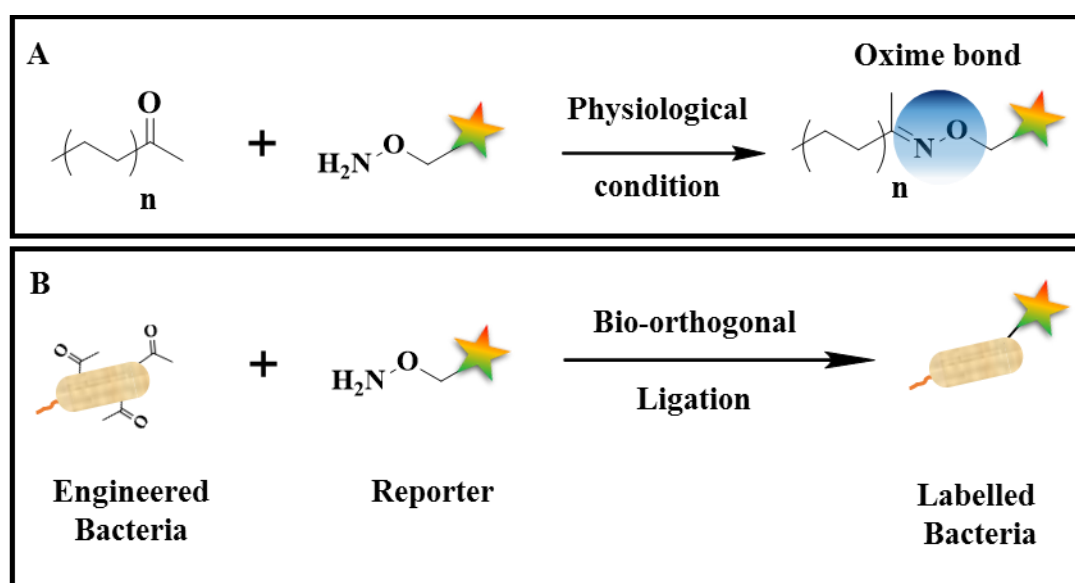


*Figure 2.8 General scheme of biorthogonal oxime ligation and cell labelling*

(A) A general representation of a ketone lipid-like molecule and hydroxylamine tethered to a reporter probe is shown. The biorthogonal pairs could ligate to form a stable oxime bond under physiological conditions. (B) Bacteria cells are incubated with the ketone-functionalized liposomes at pH 4.5 buffer at 37 °C for 1h. Through liposome fusion, the bacteria surface can be engineered to present ketone groups, which can subsequently react with a hydroxylamine tailored reporter molecule via bio-orthogonal oxime conjugation. Based on this bacteria surface engineering system, a range of ligands, proteins, small molecules, and probes containing the hydroxylamine group can be installed onto the bacteria surface through oxime ligation.

As shown in **(Figure 2.8)**, 2-dodecanone, DMPG, and DPPC were mixed together at various ratios to prepare ketone-presenting liposomes to be delivered to bacteria for display on their cell surfaces. After fusion, the bacteria surface presents ketone molecules, which can subsequently be reacted with hydroxylamine ( $\text{RONH}_2$ ) containing ligands, proteins or small molecules via oxime ligation.

A reasonable speculation may suggest that ketone-lipid molecules alone could also deliver the same purpose in the formation of a micelle, however, the addition of the dodecanone molecules directly to cells, not in liposome format, did not result in insertion onto the bacteria cell membrane. We also reasoned it might require the same procedural sonication, but it still produced the same consistent negative results.

As a representative application, a synthetically modified fluorescent probe FITC- $\text{ONH}_2$  was synthesized to click with the ketone group on the bacteria surface and thus label the bacteria with a fluorescent probe. Through the bio-orthogonal oxime conjugation between hydroxylamine and ketone, the bacteria surface can be fluorescently labelled with the FITC moiety. It was observed that cells treated with these liposomes were indistinguishable in behaviour and morphological integrity from untreated bacteria. The oxime reaction conjugate offers a very powerful ligation method that is well tolerated by living cells. This reaction is also very efficient with no side reactions or by-products under physiological conditions.

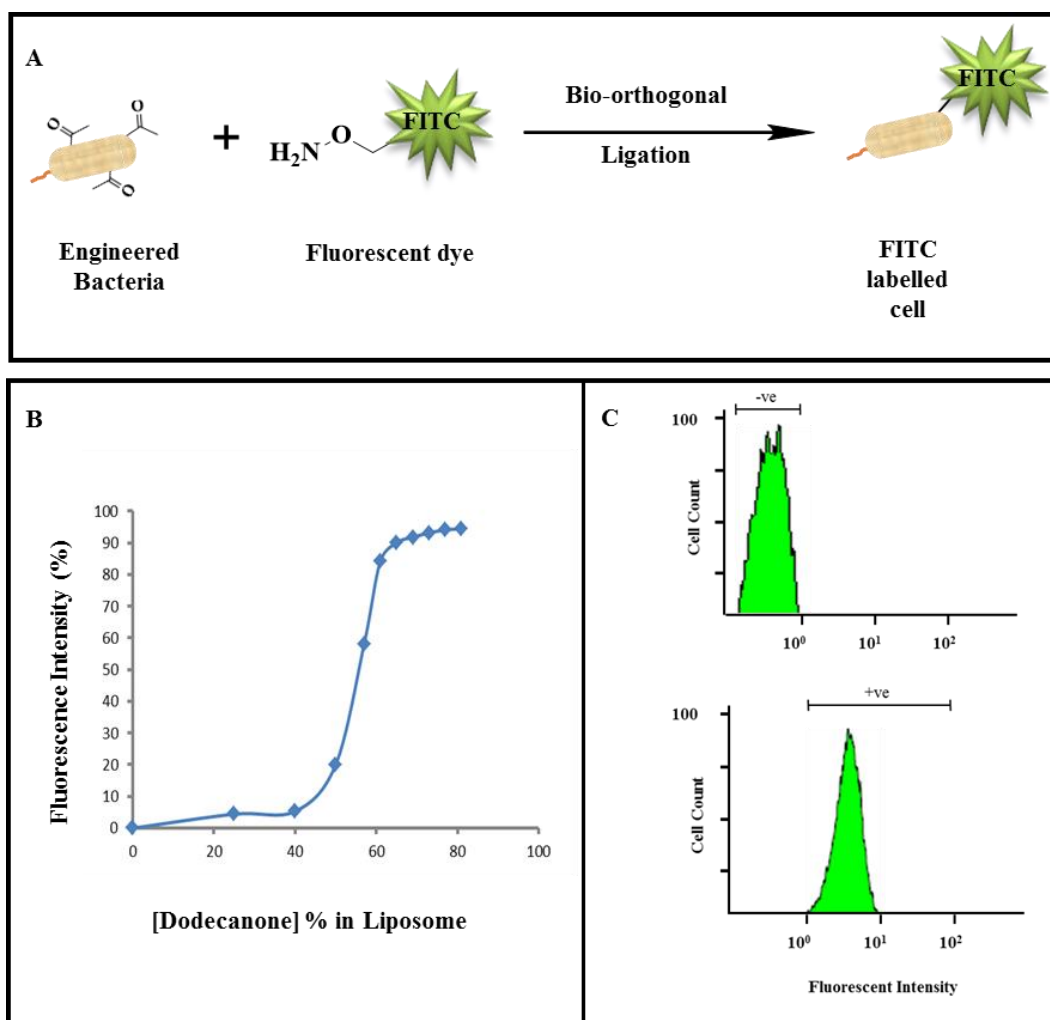


*Figure 2.9 Quantitative analysis of fluorescent probe on bacteria surface*

Quantitative characterization of bacteria surface engineering via bio-orthogonal chemistry and liposome fusion by flow cytometry. **(A)** Schematic of the process of bacteria surface engineering. Through liposome fusion, bacteria cells were surface-engineered to present ketone groups, which subsequently reacted with a hydroxylamine tailored fluorescent reporter (FITC-ONH<sub>2</sub>) to generate FITC-conjugated bacteria. **(B)** Flow cytometry analysis of the relationship between ketone concentration in the liposome and ketone installed onto the bacteria cell surface. The amount of ketone on the cell surface correlates with the amount of conjugated FITC-ONH<sub>2</sub> and can be analyzed by fluorescence intensity. It is observed that controlling ketone concentration in the liposome results in tuning a number of ketone molecules installed onto the cell surface. **(C)** Flow cytometry characterization shows that control bacteria cells treated with blank liposomes containing no ketone and then FITC-ONH<sub>2</sub> produced no fluorescent signal. Bacteria cells treated with ketone tailored liposomes and then FITC-ONH<sub>2</sub> resulted in fluorescent bacteria due to oxime ligation

To characterize the bio-orthogonal liposome fusion and conjugation method to tailor cell surfaces we used hydroxylamine probes and flow cytometry (**Figure 2.9A**). Bacteria cells were treated with liposomes for 1 hr containing different amounts of ketone groups and then exposed to FITC-ONH<sub>2</sub> (a fluorescent-hydroxylamine). Only cells presenting ketone groups reacted via a bio-orthogonal oxime ligation and became fluorescent. These cells were then quantified for fluorescence intensity, which directly corresponds to the successful liposome fusion and therefore the amount of ketone presentation on bacteria surfaces with flow cytometry. The data shows that the FITC-ONH<sub>2</sub> efficiently clicked to the ketone-presenting bacteria and reported positive fluorescent signal after thoroughly washing and removing excess FITC-ONH<sub>2</sub>. In contrast, the control bacteria (liposome exposure but without ketone-lipid) reported no fluorescent signal under the same conditions. We also conducted a further study to determine the role of the amount of bio-orthogonal lipid group (ketone) concentration within the liposome on the oxime conjugation of the fluorescent probe (FITC-ONH<sub>2</sub>) (**Figure 2.9B**). It was clear that increasing the ketone concentration of the liposome resulted in increased ketone group content on the cell surface through a standard titration curve.

To further explore the parameters that affect bacteria cell surface engineering, we investigated how the interplay of liposome composition, liposome fusion/incubation time affected the amount of bio-orthogonal group displayed on the bacteria surface. Moreover, the ability to precisely determine and therefore tune the number of bio-orthogonal groups (ketones) on the bacteria surface may be relevant for a number of applications that require precise amounts of ligands or proteins to be conjugated to the cell surface. Furthermore, interfacial kinetic information for conjugation may be obtained for further biophysical



studies of membrane dynamics. To quantitatively analyze the number of ketone groups on the bacteria surface, a standard fluorescence quantification kit (Quantum<sup>TM</sup> FITC-5 MESF from Bangs Laboratories, Inc.) was used for measuring the amount of fluorescence from the FITC-ONH<sub>2</sub> treated ketone-presenting bacteria. The 3D plot shows that the number of ketone groups on the bacteria surface is directly related to the concentration of ketones within the liposome and the duration of liposome fusion (**Figure 2.10**). Therefore, the amount of bio-orthogonal group on the cell surface can be quantitatively determined by controlling parameters that directly influence the liposome fusion conditions. It was also determined that only a small amount (several thousand) of bio-orthogonal groups installed onto the cell surface was required for ligand immobilization detection. An important feature of the liposome fusion onto cell surface method described have the ability to rapidly alter cell surfaces and to precisely tune the amount of bio-orthogonal lipid and therefore control ligand conjugation without the use of cumbersome molecular biology or metabolic engineering strategies. Furthermore, due to the mild liposome fusion conditions and the fast bio-orthogonal surface conjugation method, no toxicity or disruption of regular cellular activity was observed. The data in the 3D plot provides a systematic matrix of conditions to tailor cell surface ligands and proteins that could prove valuable in clinical applications where precise amounts of ligand bio-conjugation are required. For example, various cancer biomarkers, viral infections, adjuvants and other immunophenotyping analyses are all diagnosed via their relative abundance on the cell surface.<sup>178</sup>

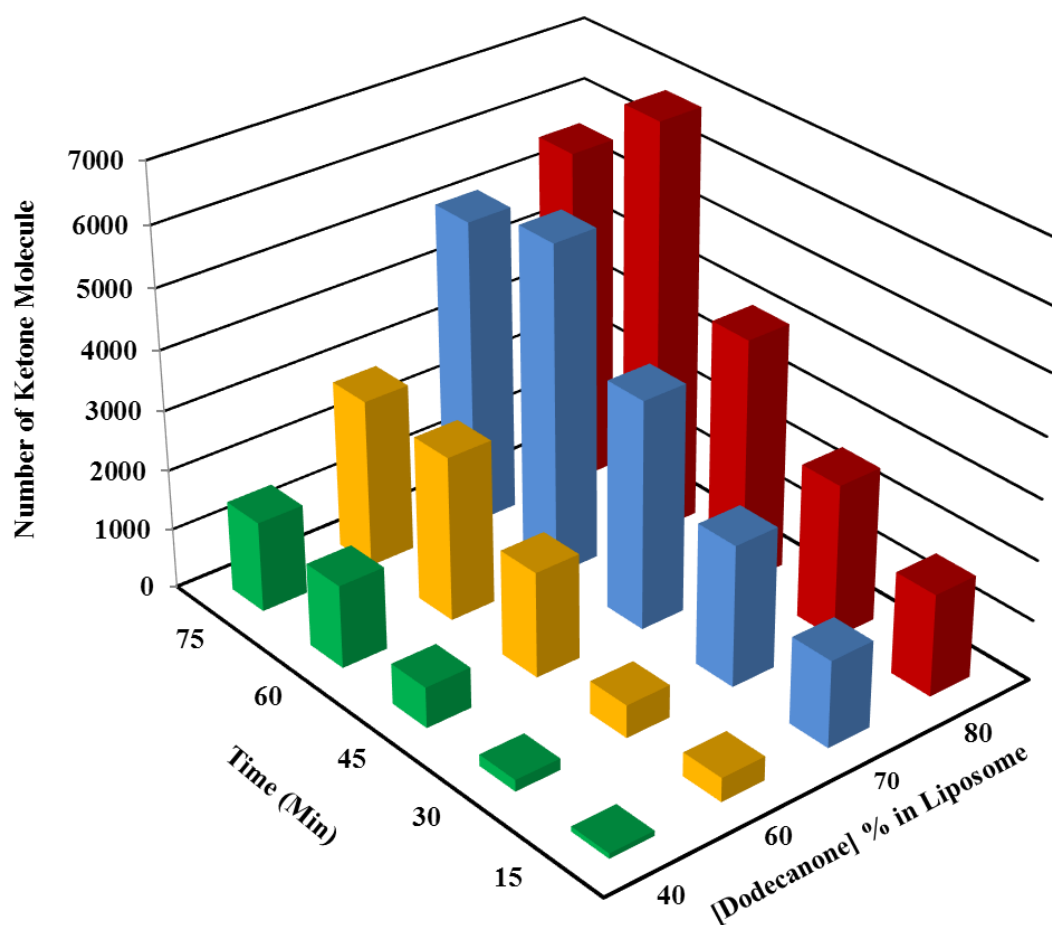


*Figure 2.10 The interplay of liposome composition, liposome fusion/incubation time and the amount of ketone molecules Transient transfection of engineered bacteria*

A three-dimensional (3D) plot describing the interplay between liposome composition, liposome fusion/incubation time and the number of ketone molecules on the bacteria cell surface. The ketone groups on the cell surface were conjugated with a fluorescent probe FITC-ONH<sub>2</sub> and then quantified per bacteria cell using flow cytometry. From the data, the number of ketone molecules on the bacteria surface is directly related to the ketone content in the liposome as well as the liposome fusion/incubation duration. By tuning the ketone content in the liposome and incubation time (liposome fusion time), the amount of ketone on the cell surface can be directly modulated.

To investigate the retention of (bio-orthogonal groups) ketone groups on the cell surface over time we analyzed the amount of ketone via flow cytometry (**Figure 2.11**). This transient transfection may be valuable in modifying bacteria for specific time-sensitive applications. To determine the quantities of available ketone molecules on the bacteria cell surface, a fluorescent molecule FITC-ONH<sub>2</sub> was used to conjugate with the ketone on the bacteria membrane. An aliquot withdrawn from the culture incubated in fresh LB media showed a significant reduction in the number of ketones reported after 4h growth and showed negligible amounts after 12h of growth. The fluorescently labelled bacteria were characterized using flow cytometry and the quantity of fluorescent molecule was calibrated based on a standard fluorescence quantification kit (Quantum<sup>TM</sup> FITC-5 MESF from Bangs Laboratories, Inc.). The quantification kit contains a group of fluorescent beads labelled with varying amounts of FITC. A QuickCal<sup>®</sup> analysis template is provided with the kit. After using flow cytometry to measure the FITC intensity of the group of beads, a standardized calibration system can be established based on the analysis template. Therefore, the FITC intensity can be directly translated into the amount of surface conjugation. This transient feature may be useful for applications that require the bacteria to only present probes or ligands for short periods of time sensitive assays and tracking.

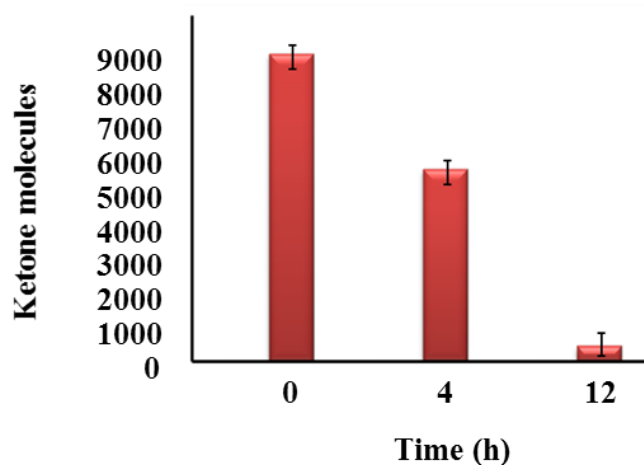


*Figure 2.11 Transient depletion of bio-orthogonal groups on a bacteria surface over time*

Transient transfection of bio-orthogonal groups on a bacteria surface. Time course of ketone content and viability of functionalized cells studied over 12h, with incubating in fresh LB media at 37°C. After 12h incubation in fresh media, cells completely dilute the ketone content and are no longer surface tailored with bio-orthogonal groups and are indistinguishable from non-tailored bacteria.

To further demonstrate the scope of the bio-orthogonal bacteria surface method for protein display, we used the classic association of biotin and streptavidin. After the introduction of ketone groups to the bacteria surface, biotin-ONH<sub>2</sub> was added to the cells to ligate an oxime bond. Then streptavidin was added and the ligand-protein association characterized by flow cytometry, mass spectrometry and western blotting (**Figure 2.12**). First, biotin-ONH<sub>2</sub> (Quanta Biodesign) was conjugated to the ketone presenting bacteria surface. The presence of biotin on the surface was then confirmed with the bio-specific association of FITC-conjugated streptavidin and quantified by flow cytometry (**Figure 2.12A**). A western blot analysis showed the bacteria cell wall contained streptavidin only

when bacteria presented biotin groups via bio-orthogonal oxime conjugation (**Figure 2.12B**). Briefly, after biotin display and streptavidin addition, bacteria cells were lysed and the membrane protein content was isolated according to a straightforward protocol (**Figure 2.12C**). Samples were then run on SDS gel, blotted and stained with anti-streptavidin antibody HRP and detected using luminol. Furthermore, the bands in the gel lanes were excised, trypsinized and analyzed using mass spectrometry. (**Figure 2.12D**) clearly, shows tandem MS/MS analysis of the bacteria surface containing streptavidin. Several control experiments were performed: 1. Bacteria that did not present ketones on the surface showed no streptavidin binding. 2. Bacteria exposed to liposomes without ketones (blank liposomes) showed no streptavidin binding. 3. Bacteria presenting ketones were reacted with a sacrificial hydroxylamine and then exposed to biotin-ONH<sub>2</sub> and then to streptavidin showed no streptavidin binding. These experiments showed that only upon liposome fusion of ketone groups followed by biotin-ONH<sub>2</sub> oxime conjugation, followed by streptavidin addition resulted in protein tailoring of the bacteria surface.

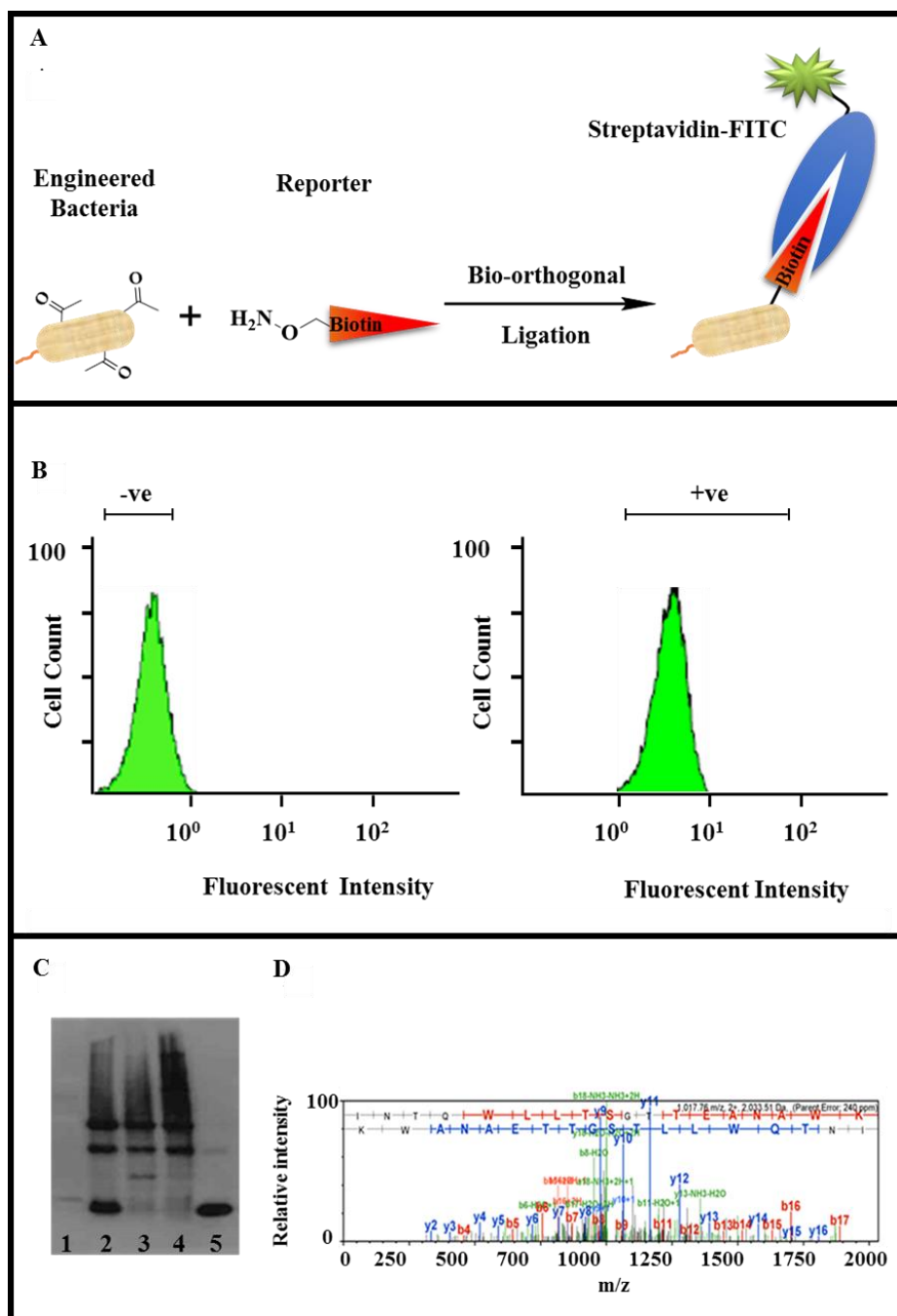


*Figure 2.12 Bacteria surface engineering with bio-orthogonal groups for further ligand and protein conjugation*

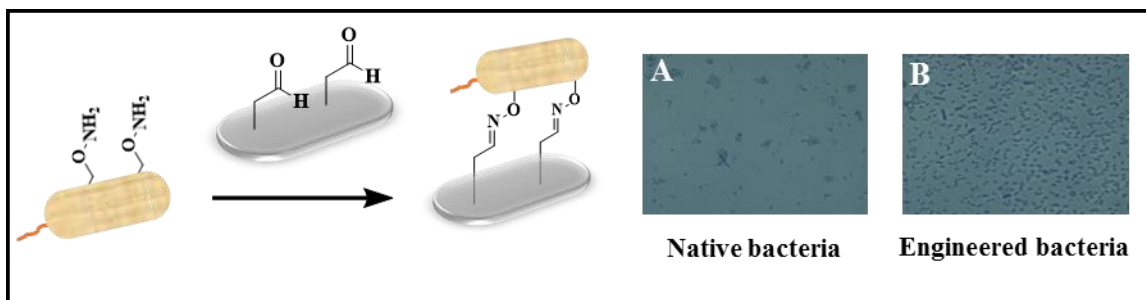
(A) Bacteria surface-engineered with ketone groups via liposome fusion can be further modified by the conjugation of hydroxylamine tailored ligands such as Biotin-ONH<sub>2</sub>. The biotin ligand present on bacteria surface can then be recognized with Streptavidin labelled with an FITC reporter (Streptavidin-FITC) and characterized by flow cytometry. (B) Cells treated with blank liposomes containing no ketone molecules do not show any

fluorescent signal, while cells treated with ketone liposomes showed a fluorescent signal (C) Cells with the biotin-streptavidin complex were lysed and the plasma membrane content isolated. The total plasma protein content was analyzed on 0.1% SDS-12% PAGE and the western blot was stained with anti-streptavidin antibody and then detected with luminol. Lane 1 is a protein ladder intended for molecular weight measurement. Lane 2 is the positive analyte of ketone-engineered cells treated with biotin-ONH<sub>2</sub> and then streptavidin (ketone-engineered cells + Biotin-ONH<sub>2</sub> + Streptavidin). Lane 2 is a negative control sample of ketone-engineered cells without biotin-ONH<sub>2</sub> and treated only with streptavidin (ketone-engineered cells + Streptavidin). Lane 3 is a negative control of cells treated with blank liposome with no ketone (blank cells + Biotin-ONH<sub>2</sub> + Streptavidin). Lane 4 is a positive standard of pure streptavidin. (D) Mass spectrometry analysis of digested lane 1 sample.

The interaction of gram negative bacteria with a range of materials and other cells has important implications in a variety of diverse fields including bioenergy, biofuel, biofilm formation, and the infection of plants and animals.<sup>179,180</sup> Networks of biofilms are often associated with cardiovascular diseases and could form chronic artery plaques around the valves. A study in 2014, utilized a fluorescent tag to reveal the role of bacterial infection, contributed by at least 10 different types of bacteria in the formation of a plaque through biofilm secretion.<sup>181,182</sup> In particular, *P. aeruginosa* becomes pathogenic upon cell-cell interactions in a biofilm.<sup>183</sup> To further explore the utility of this bacteria surface engineering system, we showed the specific association between tailored *Pseudomonas aeruginosa* bacteria and tailored materials via bio-orthogonal ligation and ligand-protein interaction.

In our previous work, we established a methodology to rapidly fabricate aldehyde presenting indium tin oxide (ITO) materials for material science, biomaterial and solar cell applications.<sup>184,185</sup> ITO is a conductive and transparent material and ideal for surface

chemistry studies. In the present study, we employed the aldehyde-tailored ITO substrates and seeded surface-engineered bacteria presenting hydroxylamines onto these substrates to evaluate the specific binding of bacteria to ITO substrates via an interfacial oxime ligation (**Figure 2.13**). It was observed that control bacteria with no hydroxylamines present on the surface adhered poorly to the aldehyde-tailored ITO, while the hydroxylamine-presenting bacteria showed high amounts of binding and significant adherence to the aldehyde-tailored ITO even after washing.



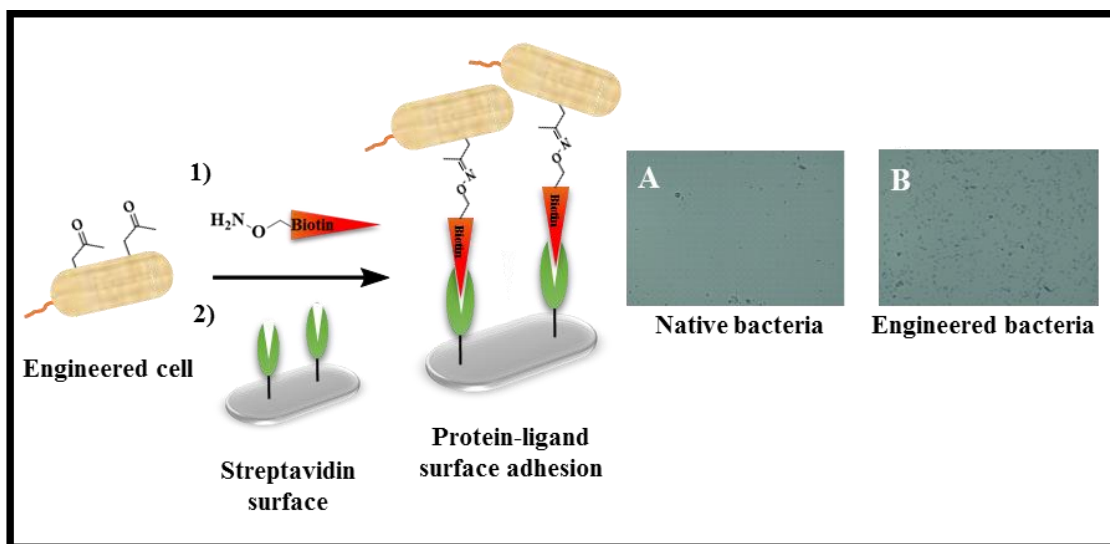
*Figure 2.13 Surface immobilization of bacteria using biorthogonal chemistry*

Illustration showing surface-engineered bacteria presenting hydroxylamine adhered to aldehyde-tailored indium tin oxide (ITO) material via oxime immobilization. (A) Images showing that control bacteria with no hydroxylamine present on the surface do not adhere well to aldehyde-tailored indium tin oxide (ITO). (B) Images showing significant adherence of surface-engineered bacteria, which present hydroxylamine and bound to the aldehyde-tailored ITO via oxime bonding.

In this context, we determined that ligand-presenting bacteria should adhere to protein-coated slides via a bio-specific protein-ligand interaction (**Figure 2.14**). Ketone presenting bacteria that were subsequently reacted with biotin-hydroxylamine showed significant levels of biotin conjugation via oxime ligation as described above. This biotin presenting bacteria were then added to streptavidin coated glass substrates (Arrayit) and



adhered efficiently. Control experiments deficient of ketone, biotin or streptavidin were showed no adhesion to the material surface. By re-wiring the bacteria surface with ketone groups or hydroxylamine groups, it is possible to sort or capture these bacteria in complex mixtures with polymers, beads or materials presenting complementary bio-orthogonal groups.



*Figure 2.14 Surface immobilization of bacteria using biorthogonal chemistry via Protein-Ligand interaction*

An illustration describing ligand immobilization (Biotin- $\text{ONH}_2$ ) on ketone-presenting bacteria and subsequent ligand-protein (Biotin-Streptavidin) interaction at the interface of bacteria and material. **(A)** Microscopy showing no adherence of control bacteria onto a Streptavidin-coated glass substrate; the particles are merely artifacts on the surface. **(B)** Microscopy showing that Biotin-tailored bacteria adhered to a Streptavidin-coated glass substrate via Biotin-Streptavidin recognition.

## 2.3 Experimental Procedures

### 2.3.1 Liposome Preparation (Figure 2.5)

Liposomes were prepared with DPPC, DMPG and the corresponding bio-orthogonal pair in various ratios. For example, 160  $\mu\text{L}$  of DPPC 10mg/mL stock, 10  $\mu\text{L}$  DMPG 10 mg/mL and 55  $\mu\text{L}$  of 10 mg/mL ketone/hydroxylamine were mixed in chloroform. After thorough evaporation of the organic solvent using air stream, content was re-suspended in an HEPES buffer and sonicated for 4h using tip-sonicator that is placed in an ice bath to avoid overheating.

### 2.3.2 Functionalized Fluorescent Assay (Figure 2.9)

Bacteria *E. coli* B121, were grown to  $\text{OD}^{650} = 0.6$ , corresponding to approximately  $4 \times 10^8$  CFU/mL. The cells were harvested by centrifugation at 4000 RCF for 10 minutes, washed with 100 mM  $\text{CaCl}_2$  and resuspended in 6 mL of 100 mM  $\text{CaCl}_2$  for 2h at 4 °C. Aliquot cells were suspended in 10 mL of 0.5 mM HEPES buffer pH 4.3. Cells were then treated with 6  $\mu\text{L}$  EDTA 50 mM pH 8.4 and incubated at 37 °C for 1h. Liposome fusion was attempted by the addition of various concentrations of Ketone-SUV (10%, 20%, 30%, etc..) to the competent cells at 37 °C for 1h. Aliquot samples were withdrawn and washed with PBS buffer pH 7.0. 5  $\mu\text{L}$  of 1.6mMol FITC-PEG-hydroxylamine was added to the suspension for 5 minutes at 4 °C. Unbound probe was washed thoroughly three times with PBS buffer to reduce non-specific binding to cells. The extent of fusion was assessed by measuring fluorescence signal using a Nikon camera fluorescent microscopy at 492 nm

excitation and 518 nm emission, along with Beckman Coulter Flow Cytometer at 600 nm excitation for FITC based probe.

**Control (Blank liposome).** Liposomes were prepared with 160  $\mu$ L DPPC 10 mg/mL stock and 10  $\mu$ L DMPG 10 mg/mL, mixed in chloroform. After thorough evaporation of the organic solvent, content was re-suspended in an HEPES buffer and sonicated for 4h using tip-sonicator in an ice bath. This composition results in the formation of a plain liposome deficient of biorthogonal pairs.

**Control (Quenched liposome).** Liposomes were prepared with 160  $\mu$ L DPPC 10 mg/mL stock and 10  $\mu$ L DMPG 10 mg/mL and 55  $\mu$ L of 10 mg/mL dodecanone mixed in chloroform. The solution was then treated with excess sacrificial methyl hydroxylamine to quench the ketone on the liposome. After thorough evaporation of the organic solvent, content was re-suspended in an HEPES buffer and sonicated for 4h using tip-sonicator in an ice bath. This composition results in the formation of an oxime ligated liposome deficient of any reactive bio-orthogonal pairs.

### 2.3.3 Transient Transfection Assay (Figure 2.11)

An aliquoted sample of functionalized bacteria with ketone and FITC-PEG-hydroxylamine label was placed into fresh LB culture over a monitored period of time. A sample was withdrawn at a particular time interval to determine OD<sup>650</sup> as well as fluorescent intensity corresponding to the number of oxime-FITC residue on the surface.

### 2.3.4 Protein-Ligand Interaction Analysis, Through Biorthogonal Ligation

#### (Figure 2.12)

Bacteria *E. coli* BL21, were grown to  $OD^{650} = 0.6$ , corresponding to approximately  $4 \times 10^8$  CFU/mL. The cells were harvested by centrifugation at 4000 RCF for 10 minutes, washed with 100 mM  $CaCl_2$  and resuspended in 6 mL of 100 mM  $CaCl_2$  for 2h at 4°C. Aliquot cells were suspended in 10 mL of 0.5 mM HEPES buffer pH 4.3. Cells were then treated with 6  $\mu$ L EDTA 50 mM pH 8.4 and incubated at 37 °C for 1h. Liposome fusion was attempted by the addition of 70% concentrations of Ketone-SUV to the competent cells at 37 °C for 1h. Aliquot samples were withdrawn and washed with PBS buffer pH 7.0. Series of different volume 20, 40, 60, 80, 100, 120  $\mu$ L of Biotin-PEG-hydroxylamine 50 mg/mL were added to the suspension and incubated for 3h minutes at 4 °C. Unbound biotin was washed thoroughly three times with PBS buffer to reduce non-specific binding to cells. Conjugated cells were then treated with 50  $\mu$ L of Streptavidin-FITC for 30 minutes at 37 °C. The extent of fusion was assessed by measuring fluorescence signal using a Beckman Coulter Flow Cytometer at 600 nm excitation for FITC based probe. A control experiment was conducted parallel to other trials, with the addition of plain liposomes deficient of bio-orthogonal pairs.

**Control (Blank liposome).** Liposomes were prepared with 160  $\mu$ L DPPC 10mg/mL stock and 10  $\mu$ L DMPG 10 mg/mL, mixed in chloroform. After thorough evaporation of the organic solvent, content was re-suspended in an HEPES buffer and sonicated for 4h using tip-sonicator in an ice bath. This composition results in the formation of a plain liposome deficient of bio-orthogonal pairs.

**Control (Quenched liposome).** Liposomes were prepared with 160  $\mu$ L DPPC 10 mg/mL stock and 10  $\mu$ L DMPG 10 mg/mL and 55  $\mu$ L of 10 mg/mL dodecanone mixed in chloroform. The solution was then treated with excess sacrificial methyl hydroxylamine to quench the ketone on the liposome. After thorough evaporation of the organic solvent, content was re-suspended in an HEPES buffer and sonicated for 4h using tip-sonicator in an ice bath. This composition results in the formation of an oxime ligated liposome deficient of any reactive bio-orthogonal pairs.

### 2.3.5 Aldehyde Surface Adhesion Analysis (Figure 2.13)

Bacteria *E. coli* BL21, were grown to  $OD^{650} = 0.6$ , corresponding to approximately  $4 \times 10^8$  CFU/mL. The cells were harvested by centrifugation at 4000 RCF for 10 minutes, washed with 100 mM  $CaCl_2$  and resuspended in 6 mL of 100 mM  $CaCl_2$  for 2h at 4 °C. Aliquot cells were suspended in 10 mL of 0.5 mM HEPES buffer pH 4.3. Cells were then treated with 6  $\mu$ L EDTA 50 mM pH 8.4 and incubated at 37 °C for 1h. Liposome fusion was attempted by the addition of hydroxylamine-SUV 70% to the competent cells. Aliquot samples were withdrawn and washed with PBS buffer pH 7.0. ITO plates coated with aldehyde functionality were submerged in 10 mL of cell suspension for 4h. Plates were removed and washed thoroughly with PBS buffer and gram stained for phase contrast microscopic analysis. Surface adhesion experiments were replicated with Arrayit® Premium Superaldehyde glass and Streptavidin/Avidin glass substrates.

**Control (Native cells).** Native *E. coli* BL21 cells were treated with glass plates presenting ketone functional groups and incubated for 30 minutes. Plates were removed

and washed thoroughly with PBS buffer and gram stained for phase contrast microscopic analysis

**(Quenched plate).** Glass plates presenting ketone functional groups were submerged into a solution of methyl hydroxylamine in chloroform and incubated for 30 minutes. The resulting surface will no longer present a reactive ketone moiety.

### 2.3.6 Protein-Ligand Material Surface Adhesion Analysis (Figure 2.14)

Bacteria *E. coli* BL21, were grown to  $OD^{650} = 0.6$ , corresponding to approximately  $4 \times 10^8$  CFU/mL. The cells were harvested by centrifugation at 4000 RCF for 10 minutes, washed with 100 mM  $CaCl_2$  and resuspended in 6 mL of 100 mM  $CaCl_2$  for 2h at 4 °C. Aliquot cells were suspended in 10 mL of 0.5 mM HEPES buffer pH 4.3. Cells were then treated with 6  $\mu$ L EDTA 50 mM pH 8.4 and incubated at 37 °C for 1h. Liposome fusion was attempted by the addition of ketone-SUV 70% to the competent cells. Aliquot samples were withdrawn and washed with PBS buffer pH 7.0 then treated with a 5-fold excess of biotin-hydroxylamine for 15 minutes. Arrayit® Streptavidin/Avidin glass (1x1 cm) was submerged in 10 mL of cell suspension for 4h. Plates were removed and washed thoroughly with PBS buffer and gram stained for phase contrast microscopic analysis.

**Control (Native cells).** Arrayit® Streptavidin/Avidin glass (1x1 cm) presenting protein molecules was submerged into a PBS pH 7.0 buffer with native *E. coli* BL21 cells and incubated for 30 minutes. Plates were then removed and washed thoroughly with PBS buffer and gram stained for phase contrast microscopic analysis

**Control (Quenched plate).** A solution of biotin hydroxylamine was treated with excess acetone for 30 minutes. Then acetone was evaporated for 5h and Arrayit® Streptavidin/Avidin glass (1x1 cm) was submerged into the quenched solution of biotin-oxime in PBS pH 7.0 and incubated for 1h. The resulting surface will no longer present a reactive ketone moiety.

## 2.4 Conclusion

In summary, a novel and rapid gram-negative bacteria surface engineering method was developed and demonstrated for *E. coli* and *P. aeruginosa*. We introduced a new method based on liposome fusion to engineer gram-negative bacteria cells with bio-orthogonal groups. These groups can subsequently be conjugated to a range of molecules (biomolecules, small molecules, probes, proteins, nucleic acids, ligands, nanostructures, radiolabels, etc...). This method can be universal for tailoring a variety of gram-negative bacteria for various applications in sensing and therapeutics. We showed this strategy is efficient for tailoring *E. coli* and the *P. aeruginosa* bacteria strains. This straightforward method is 1. Fast 2. Efficient 3. General for a range of ligand conjugations and bypasses molecular biology and metabolic interference processes to tailor cell surfaces. This method could be of crucial importance to a range of applications including bacteria labelling and probing, interfacial kinetic study, bacteria-material interaction, bacteria-mammalian cell interaction and vaccine development. Due to the liposome delivery method, many different types of bio-orthogonal chemical reactions may be installed onto the cell surface. Furthermore, a wide range of molecules with lipid-like features may be incorporated into a liposome and subsequently delivered and displayed on a bacteria surface including

ligands, probes and proteins. This method also provided an open platform for easily installing any functional groups, probes, ligands, proteins, and nanostructures for biological and tissue engineering studies and applications.<sup>186-192</sup> Although this approach provides a unique opportunity to incorporate a functional group onto the surface of a cell, it still remains to be an inadequate technique to allow for macromolecule conjugation. Presentation of a biorthogonal group on the surface would require its functional group sister to be installed on the other substrate to form a covalent bond. This means that both systems need modifications and synthesis to be armed with one of the reactive moieties. Synthesis of a hydroxylamine, or a ketone, on biological molecules is not a simple task to accomplish without suffering from synthetic consequences. Such limitations leave a tremendous gap for improvement in designing a system, which would minimize the number of modification steps performed on either component. The exploration and developments to address such concerns will be elaborated in details in the following chapter.



## 3 CHAPTER THREE

### Novel Chemo-Selective Bio-conjugation for Primary amines

---

#### 3.1 Introduction

In the previous Chapter 2, we introduced a novel method that allows for an efficient delivery of functional groups onto the surface of a model bacterial organism without interfering with their natural physiological operations. The system uses lipid like molecules to deliver a biorthogonal pair that does not react with cellular components, hence serves as a chemical handle for further bioconjugation. This technique offers a specialized approach in delivering functional groups and it always requires two compatible reactive partners for a successful conjugation. The functional groups delivered are often chosen from a library of biorthogonal pairs that are proven to be exceptionally chemoselective for their partner reactant. For this reason, conjugation of two biological bodies to one another using this approach requires the installation of two functional groups on both analysts. Although the performance of liposome fusion delivery system is independent of this prerequisite, it would not eliminate the need for chemical modifications on biomolecules. While the cell surface could be easily re-engineered with a particular organic functional group using liposome fusion, tethering it to a macromolecule (ie. antibody) still requires chemical incorporation of the other pair onto protein's structure. For this reason, liposome fusion delivery does not address the concerns and challenges of minimizing chemical reactions performed on biomolecules. As demonstrated in Chapter 1, it is important to recognize the

tedious and cumbersome challenges of modifying a macromolecule through organic synthesis or biochemical re-engineering. In order to resolve this conundrum, one should seek an alternative that would only require modification on one of the reactants, leaving the biomolecule unaffected. Such dilemmas leave the gap open for the discovery of a new method through which, a biomolecule could be selectively discriminated in a heterogeneous environment. Ideally, a suitable system should be designed to target a reliable, available and highly reactive counterpart on the biomolecule. The challenge is analogous to designing a universal organic functional trapping “Master lock” that could easily react and link macromolecules together. It would also be beneficial to hold a key to this “lock” to reverse the effect upon demand.

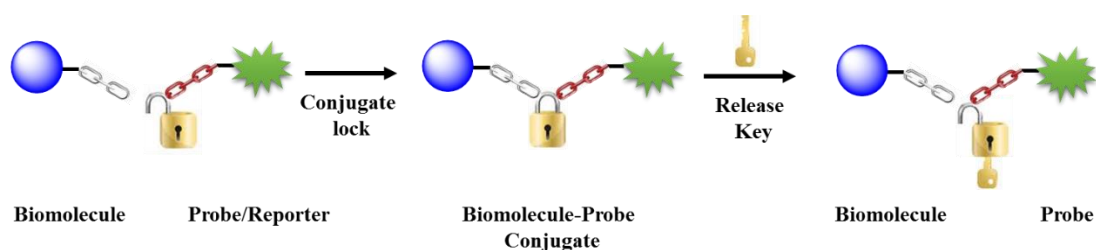


*Figure 3.1 Illustration of linking macromolecules with reporters via formation of a “lock”*

Bioconjugation researchers have always been in pursuit of such trapping “locks” and “master keys”, however, the complexity of biological environment makes it an extremely difficult objective to achieve. In spite of all difficulties, proteins offer some breaks through their amino acid side chain residues. We introduced the collective effort of researchers to identify and label the reactive side chains on different locations of protein structure in Chapter 1. Among the long list of chemical reactions performed on amino acids, “amines” deserve special attention as they are highlighted as the most effective

targets. Amines are the single most available nucleophilic centers in biological environments. They participate in nucleophilic addition reactions under a relatively broad pH spectrum. They are highly abundant in protein structures that dominate the biological world. They often do not engage, or have small activity, in catalytic operations of macromolecules. Unlike thiols, which are mostly trapped in disulfide bridges, they are not essential for maintaining the structural integrity of proteins. In spite of the long list of existing amine-conjugating systems, the area demands an improved, efficient and green conjugation strategy that eliminates the flaws of previous techniques.

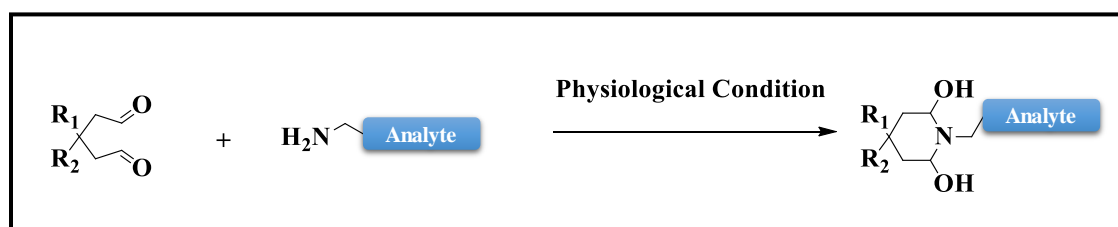


*Figure 3.2 General presentation of conjugating a biomolecule to a dialdehyde headgroup*

Herein we introduce a novel amine-conjugation strategy that offers a unique opportunity to chemoselectively conjugate to any accessible primary amine found on biomacromolecules. This approach is not limited to its use in bioconjugation chemistry; it could very well serve as a fresh method in organic synthetic reactions. The conjugate headgroup we introduce in this work is an inspiration from the glutaraldehyde crosslinker that has been effectively used in biochemistry for labelling and crosslinking of proteins. Our active headgroup dialdehyde structure allows for two consecutive nucleophilic additions of amino groups; however, unlike glutaraldehyde, it would rapidly trap the attacking amine in an annulated ring structure that would not easily collapse under physiological conditions. This system provides exceptional chemoselectivity for primary

amines, fast kinetic profile, steady atom economy, green reaction and on-demand reversibility.

Although proteins are rich in primary amines, in the form of lysine side chains, there are other functional groups that could either react or contribute to increased nucleophilicity of other active centers in the vicinity of any electrophile. It is important to design a strategy, which could discriminate among those unwanted nucleophiles and only click with a primary amine of a lysine. Failure to maintain chemoselectivity leads to destruction and possibly denaturation of native structures and defeats the purpose. Our dialdehyde system allows for successful ligation with only one primary amine and remains unreactive towards other nucleophiles like thiols and hydroxyls. In unusual cases, it may allow for hydroxyl conjugation, however, it would be rapidly outcompeted with the more strongly nucleophilic amine.

The reaction kinetics is highly comparable with cellular natural reactions, thus secures an excellent place among other biochemical reaction processes. Its rapid conjugation makes this approach a unique method for biochemical experiments in which reactants are susceptible to time-sensitive degradations. Bioconjugation is obtained within seconds and the reaction proceeds to completion within minutes at room temperature at neutral pH. Increasing the temperature works only to enhance reactivity. In contrast, dialdehyde molecules remain highly stable at freezing temperatures for prolonged storage time and subsequent use.

This reaction deserves special attention for its good atom economy. A successful conjugation produces no organic by-products and would not undergo any side-reactions.

In organic solvent conditions, it would only produce two moles of water that could be easily excluded from reaction vessel; and under physiological conditions, it preserves those hydroxy moieties on the parent molecule. This quality of our system becomes a powerful trait in practicing green chemistry both in the contexts of organic synthesis and bioconjugation. This property differentiates dialdehyde conjugation from all other conjugation systems that produce some by-product residues, and require further purification. It also delivers the main purpose in designing a novel method in which the need for delicate chemical modification and laborious purification procedures on valuable biomolecule samples are completely eliminated.

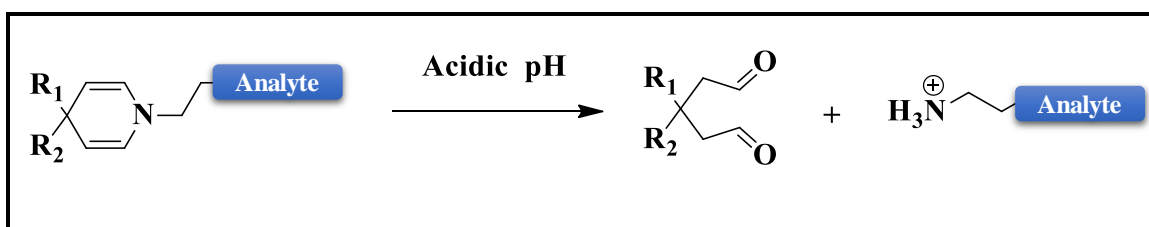


*Figure 3.3 General presentation of decoupling of a conjugate between an amine biomolecule and dialdehyde headgroup*

Perhaps the single most important feature of our system is its on-demand reversibility. Once an amine is trapped in the dialdehyde annulated structure, it could easily undergo a reverse process under lower pH ranges to release the reactants. This quality becomes extremely valuable in applications that depend on the release of a payload, toxin or simply withdrawal of labelling effect. We believe that our technology has the opportunity to serve as a promising alternative for the current antibody-drug conjugates.

### 3.1.1 Carbonyl and Imine

Our dialdehyde system uses two carbonyl centers to trap the attacking amine; hence, it is important to develop a robust understanding of carbonyl chemistry before discussing the system in detail. An aldehyde consists of a carbon double bonded to a  $sp^2$ -hybridized oxygen with a bond angle of approximately  $120^\circ$ . Chemical properties of carbonyl groups are often compared against alkenes. Much like an alkene, the bond is made up of a sigma and a pi bond, but oxygen's greater electronegativity, makes it slightly more polar, which contributes to the larger molecular dipole moments (D) of aldehydes and ketones.

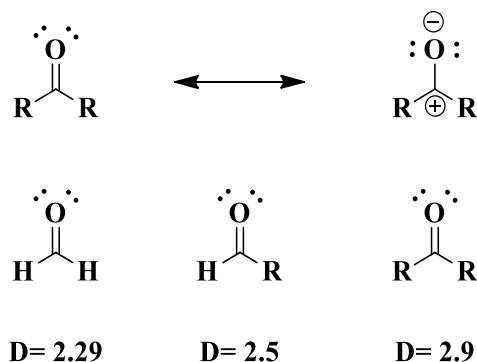


*Figure 3.4 Dipole moment of carbonyl*

The molecular dipole moments (coulomb-meter) of a carbonyl functional group increase with the addition of electron-donating substituent from formaldehyde to a ketone.

The resonance structure of carbonyl generates a carbocation that is significantly stabilized by any inductive effect of a  $sp^3$  center. The oxygen contains two non-bonding electron pairs through which it forms hydrogen bond.<sup>193</sup>

In addition to the dipole moment of the carbonyl compound which locates a partial positive charge on the carbon, their  $\alpha$  carbon is also considerably acidic. These features would enable a carbonyl compound to act as both an electrophile and a nucleophile. The reaction of carbonyls towards nucleophiles has been extensively studied; there are two possible mechanisms for nucleophilic addition reactions: acid-catalysis mechanism and base catalysis mechanism. Stronger nucleophiles tend to undergo *base-catalyzed additions* during which they attack the carbon of the carbonyl to generate a tetrahedral transition state that pushes pi electron density towards the oxygen. The negatively charged oxygen is perceived as a relatively strong base, which could abstract a proton to further stabilize the intermediate. In contrast, weaker nucleophiles require pre-activation of the carbonyl group in order to add to the carbocation of the carbonyl. While there are many nucleophiles that could engage in a nucleophilic addition to the carbonyl group, hydroxyl, amines and thiols are the most important in the context of bioconjugation chemistry. Primary amines are nucleophilic at the neutral state and could readily add to carbonyl groups. The addition of the amine to aldehyde and ketone would usually proceed with the loss of water to form an imine bond also known as a Schiff base. The addition reaction to an aldehyde/ketone proceeds through the generation of an unstable carbinolamine, which is a term referring to a species containing  $\text{-NR}_n$  and hydroxyl on the same carbon. Under acidic conditions, a proton could facilitate the loss of hydroxyl group in the form of water. This step is significantly faster than a typical dehydration of an alcohol. The final imine product could also abstract a proton on the nitrogen, as it is an analogue to a carbonyl, and undergo further nucleophilic addition with any immediately available nucleophile. Therefore, removal of the water by-product or any other nucleophile would further increase the yield of product.

The  $sp^2$ -hybridized carbonyl groups are reactive towards both primary and secondary amines. The formation of a stable product in the reaction of a primary amine with a single carbonyl group is highly dependent on the solution and microenvironments of the reagents. Nucleophilic addition of a primary amine to a carbonyl in aqueous solution forms an imine, which is a reversible process and would not be a sustainable method to generate a conjugate<sup>52</sup>. Other factors such as pH, temperature and concentration are also crucial in the overall kinetics and feasibility of reaction. While higher pH ranges tend to be more suitable for solubilisation and stabilization of a final Schiff base product, lowering the pH would rapidly favour the reversion to starting material and complete dissipation of C=N bond. In contrast, the same reaction has a higher chance of success in an organic solvent and could withhold a stable imine product. Temperature, for most reactions, enhances the progression of the chemical reaction and favours the formation of products. This principle could hold true in reverse reactions for formation of starting material, as they would also be considered a form of product on the other side of the reaction arrow. The reaction of an amine with carbonyl is no exception from this notion either.<sup>52</sup> Beyond pH of the environment, concentration of reactants is the most influential factor in the formation of the product as it has an immediate impact on the direction of equilibrium. Excess equivalence of attacking amine, even in aqueous solution, would always help to maintain some amount of product in the form of Schiff base. However, deprotonation of a primary amine at its acidic dissociation constant range is a reversible process. This leaves some finite amount of deprotonated amine available in a solution that facilitates a nucleophilic addition, and further consumption of carbonyl. However kinetically slow, this minor



amount of deprotonated amine is substantial enough to push the reaction forward towards complete depletion of carbonyl in solution.<sup>52</sup>

Unlike a primary amine, the addition of a secondary amine to carbonyl tends to form an enamine bond. Enamines are more versatile and reactive intermediates that could act both as a nucleophile and base but not as an electrophile. Gilbert Stork in 1963 demonstrated the ability of an enamine to act as a nucleophile to form a robust C-C  $sp^3$  bond with a reasonably activated electrophile.<sup>194</sup> Since then, reactions of enamines have been extensively studied and has led to the development of many established synthetic methods for a  $\beta$ -substitution of amines.<sup>195–204</sup>

The dialdehyde reactive headgroup consists of two  $sp^2$ -hybridized carbonyl groups with planar carbon centers that are five carbons away from one another. The flat chain is substituted at position C3 with a chemical handle that carries the rest of the molecule. The incorporation of a chemical handle in the structure of a general substrate allows for installation of specialized components on the molecule specific to experiments. Later, during the next chapter, influences of functionality and electronics on the yield of conjugation will be discussed in great details. There are two parallel additions to carbonyl centers resulting in the formation of a secondary amine intermediate. While carbinolamine is known to be relatively unstable and short-lived, a 6-membered ring could easily secure a stable structure that would not further collapse to other species. In addition to that, the attacking amine is no longer considered a primary, therefore the formation of an imine bond would not be conceivable; later, and dehydration will result in the formation of two enamine bonds inside the ring. As mentioned previously, the fate of the 1,4-dihydropyridine ring versus the hydrated aminated species in solution is heavily dependent

on the microenvironment of the reaction, such as solvent and pH. The unique characteristic of the dialdehyde system, in contrast to another carbonyl reactive moiety, lies in its ability to form a thermodynamically stable ring that locks the attacking amine in a 6-membered ring. Unlike any other amine conjugation systems, which use carbonyl as a chemical trap, a dialdehyde headgroup minimizes the chance of imine formation, hence eliminates the concerns over the stability of the conjugate. The conjugate will not require further stabilization or chemical treatments with reducing agents to secure a robust molecule.

### **3.1.2 Glutaraldehyde**

In depth understanding of the dialdehyde system requires a comprehensive examination of its parent molecule, glutaraldehyde. This involves reactivity, stability and conjugation mode of action through which glutaraldehyde has served in the previous biochemical reactions. It is of great importance to recognize that the dialdehyde system is essentially an improved extension of its parent molecule glutaraldehyde. An absolute knowledge of glutaraldehyde chemistry becomes a pre-requisite for the logical understanding of the remaining of this work. In this section, we will focus on glutaraldehyde chemistry in a comprehensive elaboration.

Glutaraldehyde essentially consists of two terminal aldehyde groups. Aldehydes are generally less stable than their ketone counterpart is and are often susceptible to air oxidation over time. Once hydrated, they tend to adopt various structures that result in chain polymerization which often but not always, lead to the generation of some irreversible products that no longer share the same reactivity as a carbonyl. Presence of

nucleophilic centers in the vicinity of a carbonyl, or in the same solution could lead to addition reactions to the aldehyde or creation of bonds and functional groups that facilitate the rotation or inaccessibility of reactive centers for further chemical reactions.<sup>205–208</sup> The most important side-reaction of aldehyde is acid/base catalysis of the aldol reaction. Aldol reaction usually initiates further polymerization to indistinguishable long chains.

Glutaraldehyde has been the subject of research for almost 60 years owing to its unique ability to immobilize proteins, cross-link macromolecule and fix cellular components. There is a limited class of macromolecules that are reactive towards glutaraldehyde or other carbonyl centers. Their ability to react with carbonyl centers is essentially determined by the availability of the proper type of nucleophilic moieties. Most carbohydrates<sup>209</sup> and lipids<sup>210</sup> have proven to be inert towards molecules, unless an artificial nucleophilic center is incorporated into their backbone. Glucosamine is an example of a naturally occurring amino sugar that contains the right functional group to present some reactivity with carbonyl groups. Lipids that are armed with a source of primary or secondary amine, like phosphatidylserine, also have moderate non-selective reactivity for electrophilic moieties.<sup>211</sup> Nucleic acid polymers are reactive towards formaldehyde, which is a small carbonyl-carrying molecule and could be easily used in fixation of the entire DNA through reaction of the corresponding nucleotides amino sugars with formaldehyde,<sup>212</sup> however, the reaction of other aldehyde-containing molecules like glutaraldehyde with DNA itself, remains to be investigated.<sup>213</sup>

In addition to the crosslinking utility of glutaraldehyde, techniques used to immobilize enzymes were also an attractive area of research that gained attention after much data was collected on protein crosslinking using glutaraldehyde. The technique is

often dependent on the formation of a robust covalent bond between a hydrophobic molecule and a macromolecule through coupling with a glutaraldehyde bridge. A similar principle could be thought of in crosslinking use of glutaraldehyde between enzymes.<sup>214</sup> The role of a bifunctional immobilization reagents was first explored in the 1950's by Zahn.<sup>215</sup> Other crosslinking utilities of glutaraldehyde were developed for the purpose of protein stabilization and further X-ray crystallographic analysis by Quicho and Richards<sup>216</sup> and microscopic analysis of fixed tissues conducted by Robertson and Schultz in 1970.<sup>217</sup> In the later years, glutaraldehyde attracted tremendous attention in crosslinking chemistry and enzyme interaction for its exceptional ability to form a 3D network of intermolecular species, conjugation of hydrophobic molecules and protein structure analysis. Furthermore, there is a limited list of class of molecules that show reactivity towards aldehyde in biological settings. Each one of the mentioned applications would require a particular set of conditions exclusive to that experiment, which are often determined empirically through trial and error. Such limitations predominantly arise from protein insolubility and natural behavior<sup>218,219</sup> protein concentration,<sup>220</sup> the optimal pH,<sup>221</sup> operating temperature,<sup>222</sup> ionic strength of medium<sup>223</sup> and reaction time.<sup>224</sup>

General use of glutaraldehyde was first illustrated in the 1960s for fixation of tissues through, back then an unknown mechanism, which later discovered to be crosslinking of internal proteins.<sup>225</sup> Glutaraldehyde's highly efficient reactivity towards proteins in aqueous solution near neutral pH, made this reagent a very attractive and essential ingredient in crosslinking experiments. Glutaraldehyde reacts with many functional groups either on the surface or sometime embedded within relatively deeper layers of a macromolecule. Amine, thiol, phenol and imidazole are all nucleophilic centers

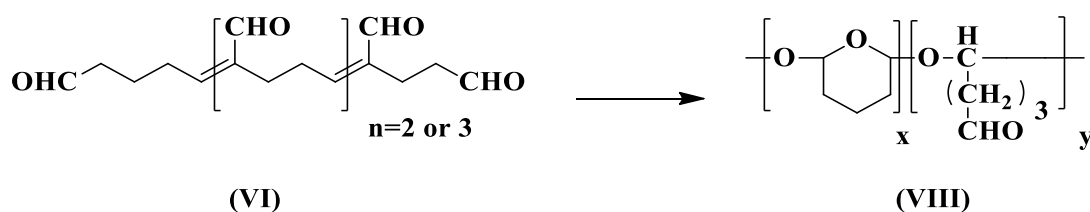
that have shown reactivity towards glutaraldehyde. While the complexity of glutaraldehyde conformation has a crucial determinant on the reaction mechanism with each of the nucleophiles, the purpose of conjugation is often always fulfilled by the formation of some kind of bridge between the glutaraldehyde and the macromolecule. Enzyme immobilization studies, in particular, have presented a suitable model study for such complexities, which we will examine later in the discussion. Studies on amino acid's reactivity towards aldehydes have provided substantial information about the condition of reaction, hence the suitability of glutaraldehyde for crosslinking of proteins in an aqueous environment at different pH ranges. The preliminary investigation of reactivity of the following amino acids was conducted from the early 1960s to late 1970s; Lysine,<sup>226</sup> Tyrosine, phenylalanine and tryptophan,<sup>227</sup> cysteine, serine, proline, histidine, glycine, arginine and glycylglycine<sup>228</sup> are the major amino acids that have been reported in the mentioned literature for their side chain functional group nucleophilicity. While different types of molecules containing an aldehyde had been used in the mentioned studies, collective results obtained suggest that there is different reactivity between amino acids towards the carbonyl functional group. The order of decreasing reactivity of the side chain is as following  $\epsilon$ -amino,  $\alpha$ -amino, guanidyl, secondary amine and hydroxyl group. Avrameas and Ternynck have demonstrated the poor reactivity of the guanidyl towards glutaraldehyde and speculated that rapid consumption of the reagent by other more reactive amino groups would retard any reaction with guanidyl.<sup>219</sup> Another study conducted by Okuda et al in 1991 revealed that thiols only react with glutaraldehyde in biological settings if a primary amino group is available in the vicinity of the reaction site.<sup>229</sup>

Since the  $\epsilon$ -amino of the R chain on lysine presents the most reactivity and application in bioconjugation, herein we will focus on some of the preliminary studies that have speculated and proposed possible mechanism for the formation of a conjugate between  $\epsilon$ -amino and glutaraldehyde in aqueous solution. This explanation will be an analogue to dialdehyde's reactivity with lysine side chain. Formation of a Schiff base in the reaction of a primary amine with a carbonyl center is widely studied over the pH spectrum. While there is a significant reversibility at relatively lower pH ranges, pH 7-9 ranges are an optimal window for minimum reversibility. The immobilization and conjugation of a protein to a glutaraldehyde bridge, or any other carrier of a similar electrophilic center, is generally, but not always, a direct implication of lysyl moiety ligation to the electrophile handle.<sup>214</sup> Although pKa (acid dissociation constant) of  $\epsilon$ -amino is greater than 9.5, upon successful establishment of an equilibrium there will be some finite amount of unprotonated amines that remain available and reactive at acidic pH ranges. Such small amount of unprotonated amine in solution is sufficient to react with glutaraldehyde, which then shifts the equilibrium towards complete consumption of the reagent. Since lysine is mostly abundant on the surface and outer core of protein structures, and does not participate in crucial enzymatic or other biological regulatory functions of the protein, it is available for chemical ligations. Consequently its ligation does not necessarily disturb protein function or structure.<sup>216</sup>

### **3.1.2.1 Structural Analysis**

The structural variations of glutaraldehyde have a substantial impact on the stability and reactivity. Glutaraldehyde molecule could easily adopt different structures depending

on the environment it resides in. The solution conditions have an important effect on the final configuration of the molecule, consequently would also influence the application of the crosslinking molecule. pH, temperature, solvent, concentration are some of the consideration in working with glutaraldehyde. There are 13 well-studied forms of glutaraldehyde that each is to behave differently in interaction with other macromolecules like protein. There is an abundance of data on the structural conformation of the glutaraldehyde in the literature that has been collected over 40 years of research on the crosslinking ability of glutaraldehyde. Aso and Aito studied the effect of catalysts on the polymerization of glutaraldehyde and observed comparable results in aqueous solution at room temperature. The products were characterized to be a tetra- and pentamer making approximately one aldehyde group per multimer.<sup>230,231</sup>

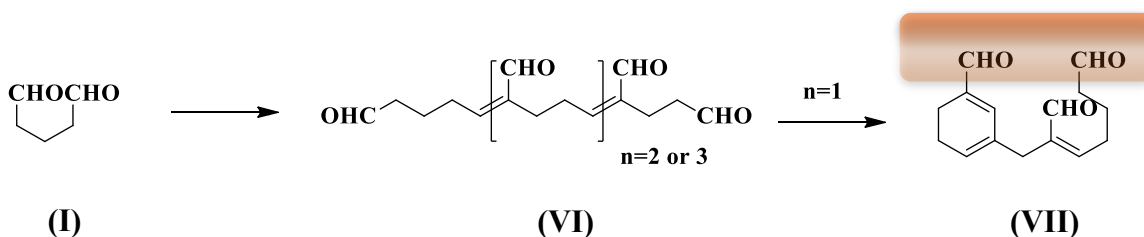


*Scheme 3-1 Glutaraldehyde products in aqueous solution with cationic catalyst*

Glutaraldehyde could spontaneously form a polymer in presence or absence of a cationic catalyst in aqueous solution. Structure (**VIII**) was identified as a soluble tetramer or pentamer comprising one free aldehyde group per molecule formed through the intramolecular-intermolecular propagation polymerization with ring formation.

Richards and Knowles conducted comprehensive studies using NMR spectroscopy and examined the protons in the commercially available aqueous solution. Their spectra analysis was in a disagreement with the formation of a dimer, cyclic dimer, trimer or any

bicyclic trimer in single abundance, rather a mixture of all multimeric sub-units as well as the polymeric structure was observed. Their observations were consistent with the formation of  $\alpha,\beta$ -unsaturated aldehydes which could subsequently lead to the formation of other heavy chain polymeric units or cyclize through aldol condensation. Their proposed structure would make many carbonyls available for further reactions.<sup>232</sup>



*Scheme 3-2 Glutaraldehyde  $\alpha,\beta$ -unsaturated polymer*

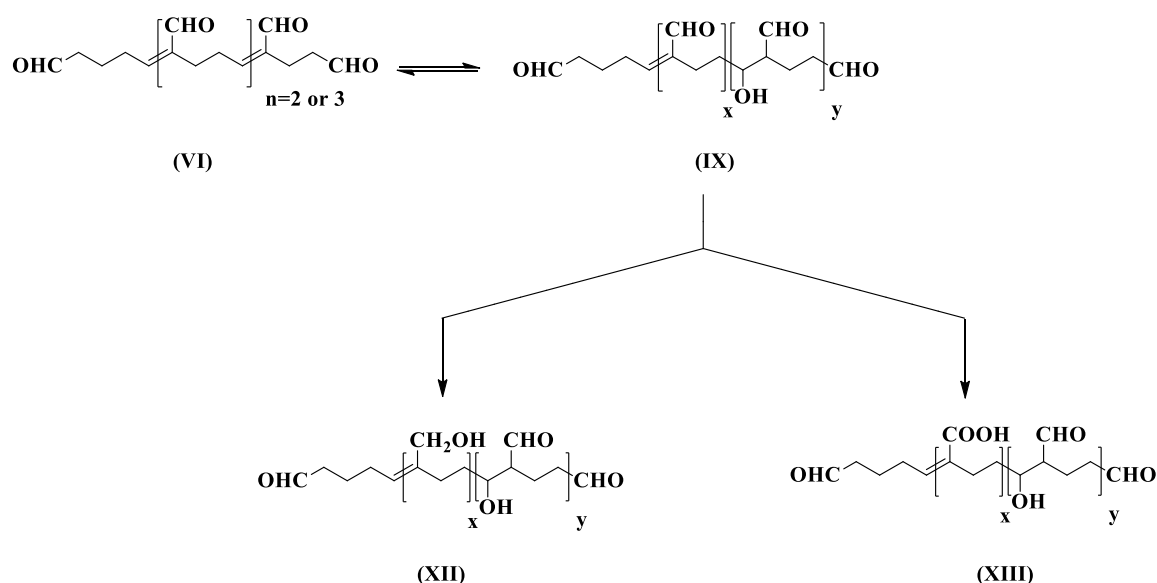
A solution of commercial glutaraldehyde is largely polymeric and comprises significant concentrations of  $\alpha,\beta$ -unsaturated elements (**VI**). Such species could form rings (**VII**) by the loss of water molecules through aldol condensation. Although structure (**VI**) is a representative of an average structure containing the unsaturated polymerized glutaraldehyde ( $\alpha,\beta$ -unsaturated compound), the carbonyls would be hydrated.

A year later, Hardy et al conjoined two techniques of UV spectrometry in tandem with HNMR spectroscopy to further confirm the presence of  $\alpha,\beta$ -unsaturated aldehydes in the organic extracts of the mixture. However, low abundance of such species revealed by trivial integration of the corresponding peak at 235 nm demanded further structural analysis on purified samples. Conversely, a purification procedure using organic extraction was only helpful to recover 50 % of the original sample; even then, the obtained glutaraldehyde underwent rapid rehydration that rendered the spectroscopic analysis ineffective. The combined information extracted from this study was in a strong agreement with Aso and





at medium to high pH ranges. Their observations were consistent with Monsen's findings in the formation of what they had earlier called "poly-glutaraldehyde". The  $\alpha$ -hydroxy aldehyde polymer is very sensitive to solvent, pH and oxygen content in the solvent and would easily proceed to form other by-products.<sup>236</sup>

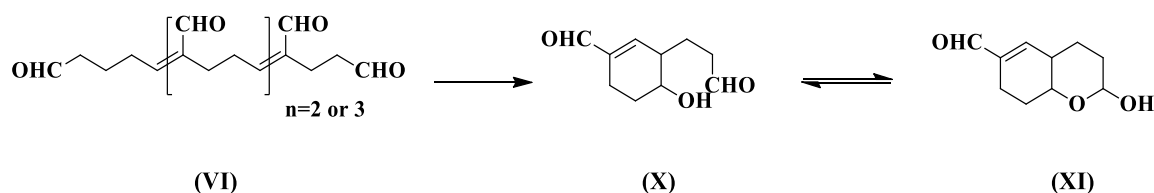


*Scheme 3-4 Glutaraldehyde polymerization reaction*

Investigation of aldol condensation of glutaraldehyde in the pH range of 7.0 to 13.5 reveals a poly-glutaraldehyde that could remain soluble or insoluble in water. The extent of functionalization i.e. hydroxyl, carboxylic acid, carbonyl is largely dependent on pH, oxygen content and other kinetic parameters leading to the structures (XII) and (XIII).

In the later studies conducted by Tashima et al, some novel forms of smaller subunits of polymer were observed at moderately alkaline pH. Functional group analysis performed on the mentioned structures, using IR and UV spectroscopy, suggested the presence of hydroxyl and formyl group in a tangled conformation. Later confirmation by

GC and elemental analysis, a more vivid image of the structure was obtained. An exact mass of 182 g/mol for the corresponding molecular formula  $C_{10}H_{14}O_3$ , further examined by 2D  $^1H$ -NMR, indicated an annulated structure below <sup>237</sup>.

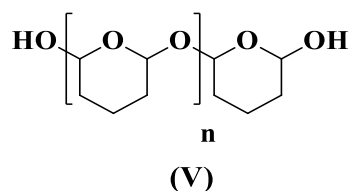


*Scheme 3-5 Glutaraldehyde product in alkaline solution*

Treatment of glutaraldehyde with an alkaline solution will result in the formation of some dimers characterized by IR spectroscopy. Data suggests formation of some  $\alpha,\beta$ -unsaturation formyl and hydroxyl groups

Although glutaraldehyde structure has always gained its attraction due to its unique ability to crosslink proteins in water, the effect of the solvent remained to be neglected for almost 20 years. While all studies had agreed that a solution of glutaraldehyde will not contain much of the monomeric parent molecule, Kawahara et al argued that not all of the parameters had been considered in the adopted structure of the polymer. They looked at the effect of the solvent on the possible formation of the polymers, and its interaction with the polymer. They suggested that water would be a relatively suitable nucleophile that would present some reactivity towards the carbonyl moieties thus change its availability in the form of free aldehyde groups. Kawahara suggested that since studies conducted by Monsan<sup>235</sup> have all been performed in organic phase their outcome would suffer from factors affecting the feedback. While structural analysis of glutaraldehyde, from a chemical perspective, would not be hindered if performed in an organic setting, the feedback of such studies would not remain useful for biological conditions. Such disparagements led to the

further prosecution of other results accumulated in the course of 20 years. In a wider reconsideration, the efforts of Richards, Knowles<sup>232</sup> and Hardy<sup>230</sup> were also reassessed for the use of deuterated water in their NMR spectroscopic analysis. Monitoring the peak of interest in both of their independent <sup>1</sup>H-NMR studies, which much of the conclusions were drawn from, presented inconsistent integration for the  $\alpha$ -carbon proton.<sup>233</sup> In addition to integration discrepancies, the equilibrium of most polymers fluctuated between water and deuterated water.<sup>238</sup> Whipple and Ruta's <sup>234</sup> studies also had looked at <sup>13</sup>C-NMR peak intensities that could not reveal accurate quantitative measurements for any convincing conclusion. Consequently, Kawahara et al <sup>239</sup> employed UV spectroscopy and light scattering technique to look at the same structures previously claimed to be dominant but used commercially available 70% (w/v) glutaraldehyde aqueous solution which would also present a consistent sample with that of used in biological experiments. This study suggested that concentration, solvent and pH would all collectively determine the stable structure of glutaraldehyde in solution. Lower concentrations and pH ranges of 3.5 to 8 would shift the equilibrium to the formation of some deconvoluted monomeric hemiacetal units. In 1997, same authors revealed that concentrations of up to 10% glutaraldehyde in water could be suitable for maintaining a monomeric structure and that the  $\alpha,\beta$ -unsaturated products could be present only in negligible amounts.<sup>240</sup>



*Scheme 3-6 Glutaraldehyde products at low concentration*

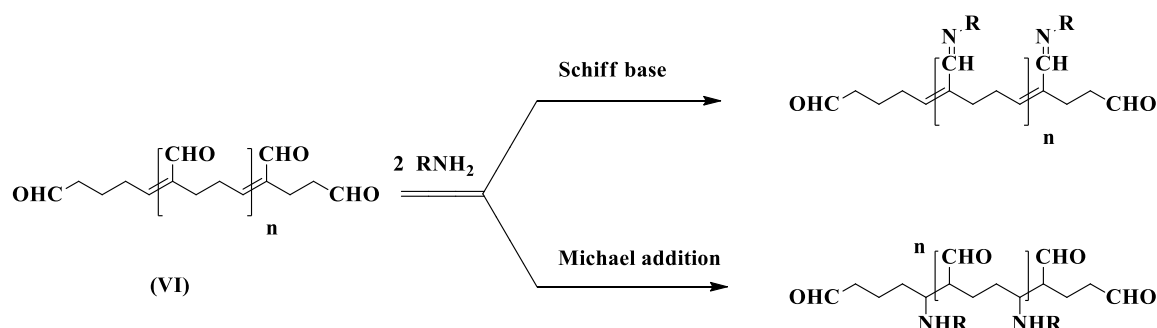
Upon dilution, large quantities of polymeric species that contain cyclic hemiacetal structure (**V**) slowly convert to monomers.

Comprehensive studies conducted in the past 50 years on the structural behavior of glutaraldehyde in organic or aqueous solutions, unanimously suggest of the formation of multiplex subunits of mono, di, tri, tetrameric polymers that would present an inconsistent number of carbonyl functional group for the crosslinking application. The concentration, pH, temperature and buffer system used in downstream applications remain to be assessed based on individual applications and analytes of interest. Hence, the effectiveness of glutaraldehyde in crosslinking could not be generalized and must be exploited only in the contexts of a particular experiment.

#### **3.1.2.2 Mechanism of Glutaraldehyde Bio-conjugation**

As previously discussed, glutaraldehyde could exist in different conformations in aqueous solutions; therefore, there is not a single apparent mechanism of conjugation proposed in studies. However, observing the structure of the products of such ligations at higher pH ranges generates more stable species that would allow for a more detailed structural characterization. These studies would then help to postulate a more accurate mechanism for the formation of the products. Richards and Knowles in the 1968<sup>232</sup> and Monsen et al<sup>235</sup> in 1973 proposed some possible pathways through which the amino group of the protein reacts with  $\alpha,\beta$ -unsaturated aldehydes in an aldol condensation. In their mechanism, amino group undergoes a conjugate addition to the ethylenic double bond on

the  $\alpha,\beta$ -unsaturated aldehyde oligomer in a Michael-type addition reaction. In contrast, Monsen et al suggested that aldehydic carbonyl groups are the target of the nucleophilic addition. This mechanism is obviously bound to encompass the formation of a Schiff base that must be stabilized by conjugation. The reported results of both studies are in an agreement that glutaraldehyde exists in some kind of polymeric conformation and is not present in its monomeric unit. Boucher's research presented a conflicting mechanism in the 1970s and suggested of a monomeric starting material of glutaraldehyde in aqueous solution.<sup>241,242</sup>



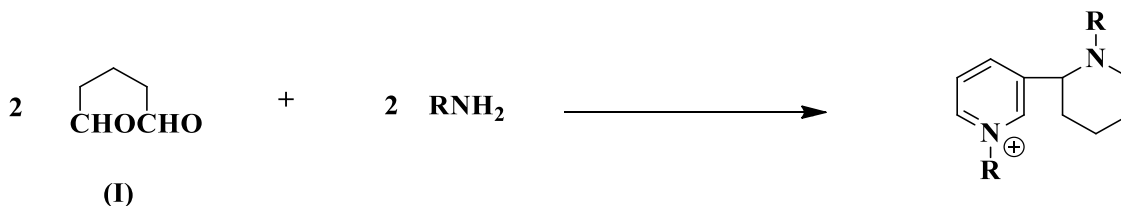
*Scheme 3-7 Reactions of primary amine with glutaraldehyde in solution (Michael addition, Schiff Base)*

A mechanism proposed an addition reaction on the aldehydic part of the  $\alpha,\beta$ -unsaturated polymers (and poly-glutaraldehyde) towards the formation of a Schiff base (imine) stabilized by conjugation. A different postulated pathway involves the reaction of the protein amino group with  $\alpha,\beta$ -unsaturated aldehydes formed by aldol condensation of glutaraldehyde. There is evidence of a conjugate addition of amino groups to ethylenic double bonds through a Michael-type addition. This mechanism was supported through demonstration of nucleophilic addition on the ethylenic double bond with a large excess of amine.

Boucher's findings suggested that the active form of glutaraldehyde that reacts in solution is strictly dependent on the pH of the solution and that the oligomeric forms of it

could easily revert to their monomers upon treatment with heat or ultrasonic radiations. Unlike acidic conditions, alkaline pH would not allow for such reversions and force glutaraldehyde to stay as oligomers. The rationale behind the latter observation was solely based on the slow rates of interchanges between glutaraldehyde oligomer and monomer with temperature and time. Years later, Ruijgrok<sup>243</sup> in 1990 confirmed the conclusion drawn by Boucher, by exploring the effect of heat generated by microwave irradiation versus conventional heating on the aldehyde moiety in glutaraldehyde aqueous solutions.

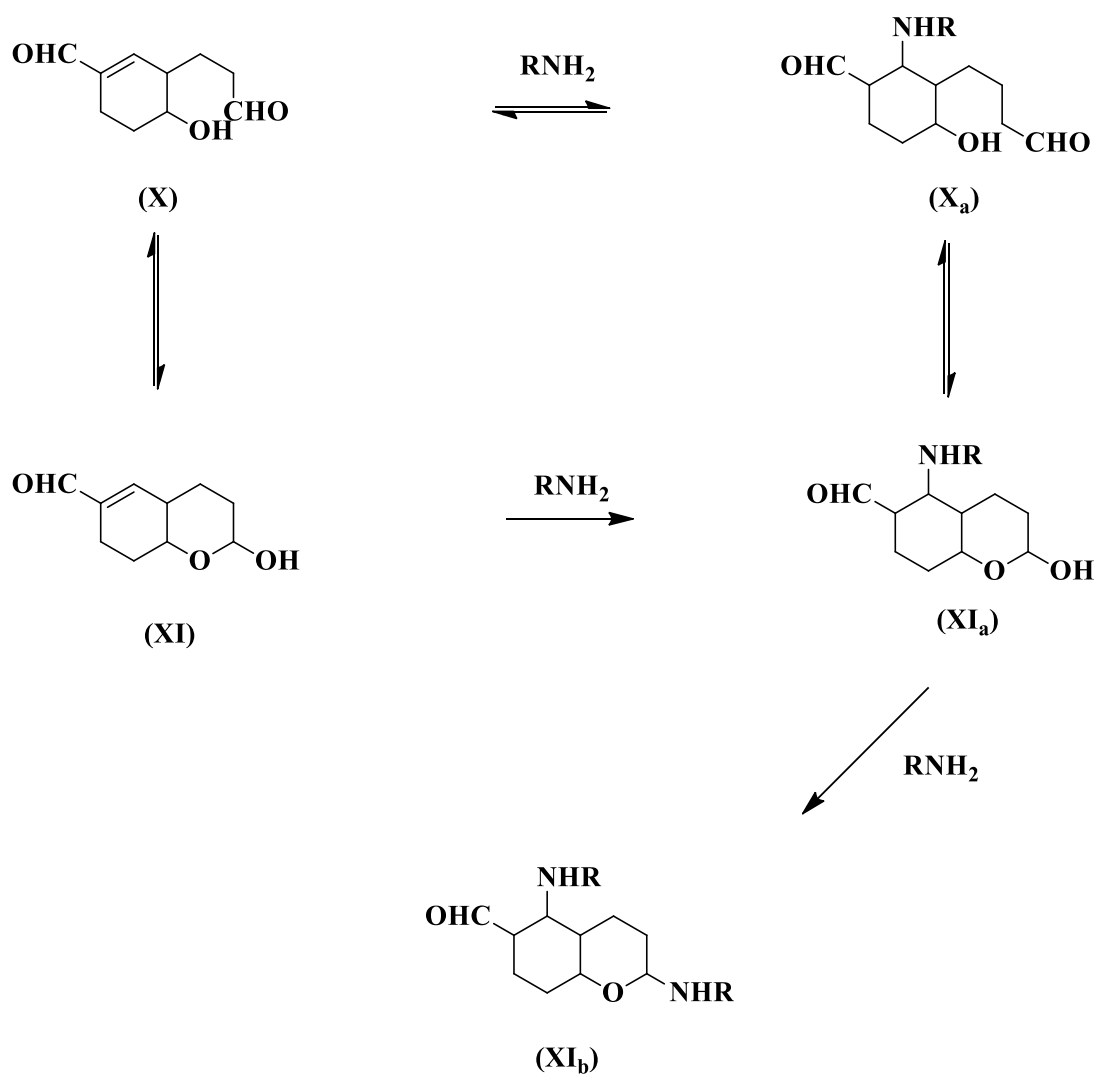
The nature of the glutaraldehyde starting material remained a controversial subject among active research groups. In 1976 Hardy et al<sup>244</sup> and Lubig et al<sup>245</sup> argued that an  $\alpha,\beta$ -unsaturated aldehyde could not be the primary species that offers a reactive center. Rather, in the presence of amino groups, some dimer structure arising from an  $\alpha,\beta$ -unsaturated precursor is more likely to be responsible for providing a more reactive moiety for conjugation. This mechanism requires two equivalence of the monomeric units to undergo concerted nucleophilic addition of a single amine to form, possibly, a quaternary structure of amine. Although a definite mechanism could not be postulated at the time, a pathway involving cyclization, dehydration and even internal redox reaction was proposed. A pyridinium-containing dimer was later isolated by the same group and characterized using UV spectroscopy that produced a consistent UV absorption consistent with the Bowes and Carter report of 1968.<sup>226</sup>



*Scheme 3-8 Reactions of primary amine with glutaraldehyde in solution (Crosslinking)*

Upon reaction of a protein amino group with glutaraldehyde, some dimers could form products that contain quaternary pyridinium compounds, rather than glutaraldehyde polymers reacting with amino groups.

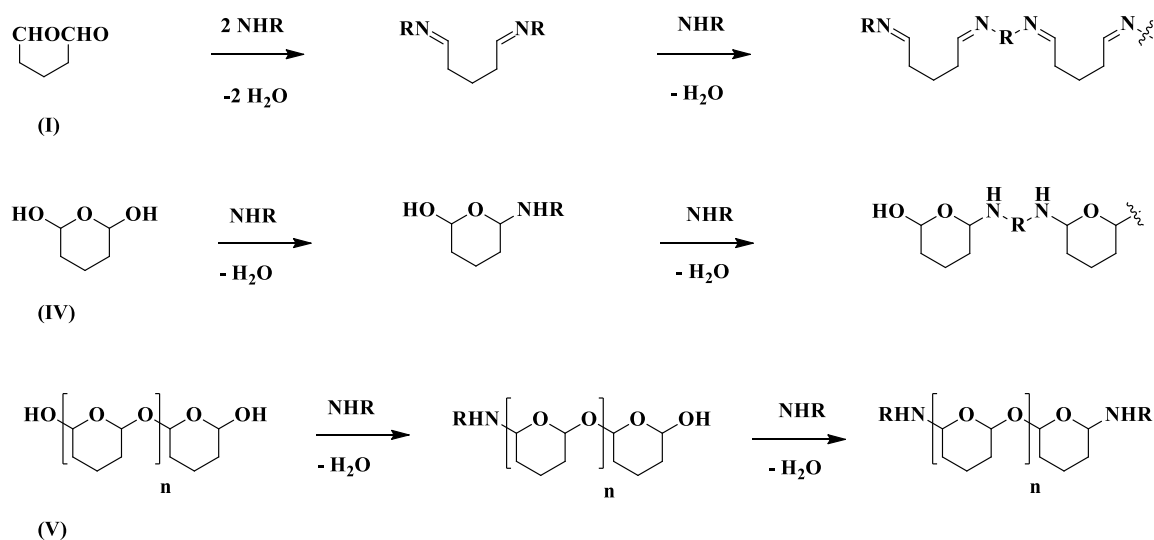
Tashima et al<sup>237</sup> reported a study in 1991 that confirmed the Michael addition to the ethylenic double bond in alkaline condition and that an excess of the amino group would eliminate the need for a redox pathway.



*Scheme 3-9 Dimeric cyclic glutaraldehyde reaction with proteins under alkaline conditions*



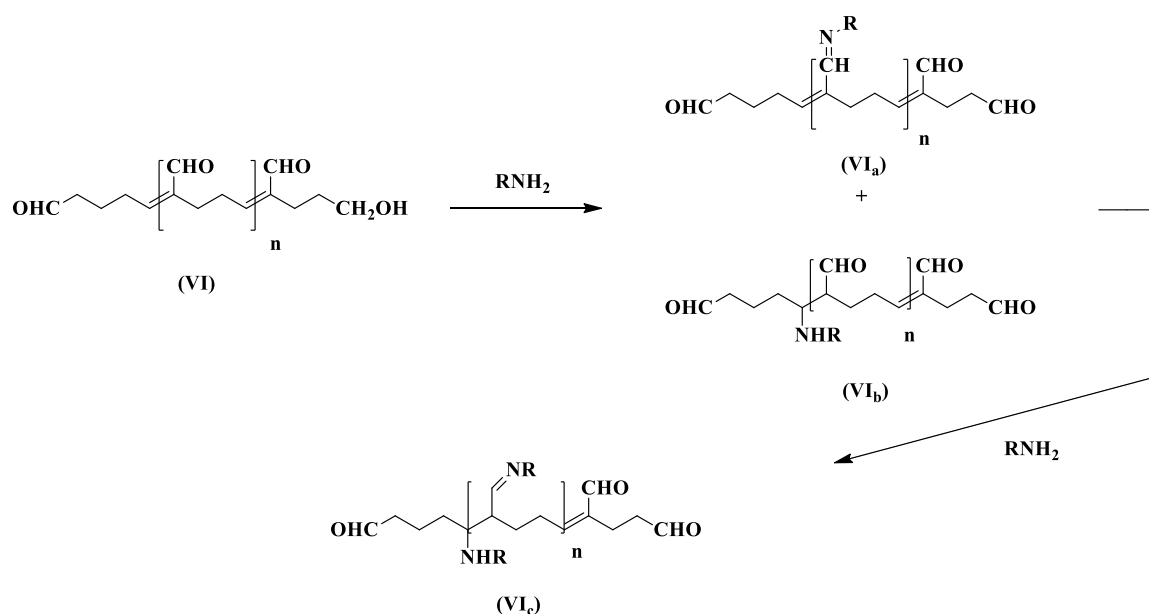
In the mid-1990s, Walt and Agayn<sup>246</sup> conducted a more detailed and systematic approach to explore the effect of pH and the reactivity of different forms of glutaraldehyde in solution. They proposed that conjugation of an amino group with any aldehydic center of any kind is not favourable as it will form a Schiff base. However, there are two possible outcomes under acidic conditions, which both would contain a polymeric unit of bridged protein. Polymeric units of connected hemiacetal are more plausible to form as the result of an amine nucleophilic addition, which definitely will generate a polymeric structure.



*Scheme 3-10 Glutaraldehyde reaction with proteins under Acidic conditions*

Multiple reaction products were proposed depending on the pH profile of reaction. A mixture of monomers ranging from free aldehyde form (I) or cyclic hemiacetal (IV), cyclic hemiacetal oligomer (V) could exist under acidic or neutral conditions. A nucleophilic attack by lysine residues is expected to induce the formation of a Schiff base in solution. However, Schiff bases are known to reverse under acidic conditions and are not favoured, leading to a reaction of monomeric cyclic hemiacetals (IV) and multimeric form (V).

In contrast, under alkaline conditions, two different Schiff base products are predominant that are robust and unreactive in an acid hydrolysis reaction. The stability of the Schiff base products is due to a stronger stabilization through repeating internal double bonds with the aldehyde groups and formation of the Michael addition product. The presence of an excess amine in solution would eventually react with the exposed aldehyde groups and produce more Schiff bases that are labile to acid hydrolysis and contribute to overall unsuccessful conjugation. This concern could be addressed by reducing the Schiff bases to a secondary amine that is a promising alternative to secure a robust conjugation system.



*Scheme 3-11 Glutaraldehyde reaction with proteins under alkaline conditions*

Under basic conditions, the reaction of  $\alpha,\beta$ -unsaturated oligomeric aldehydes (VI) with amine could produce two products robust to acid hydrolysis under basic conditions : a Schiff base (VIa) and a Michael addition product (VIb). If the excess amino reactant is present, some mixed product of (VIc) could also exist in solution but susceptible to loss of resonance stabilization under acidic condition.

Finally, Kawahara et al<sup>240</sup> in 1997 demonstrated that presence of amino group would catalyze polymerization reactions and favours aldol condensation in solution. This reaction would produce large polymer units containing many aldehydes and  $\alpha,\beta$ -unsaturated aldehydes that are available for formation of both Schiff base and Michael addition reactions. This study suggested that glutaraldehyde aqueous solutions are more likely to act as a staining brush that would crosslink proteins in massive mixture rather than small-localized patches in solution.

While there is still a considerable disagreement in the aqueous structure of a commercially available glutaraldehyde solution, it is still an important reagent in protein conjugation experiments. Regardless of its mechanism of bioconjugation, it has proven to be an extremely effective reagent for highly specialized experiments. Although there is not a single mechanism that could be proposed to accurately describe the formation of conjugates with protein, its effectiveness could not be dismissed. Over the years, efforts to solve conjugation mechanism has been shifted towards more advanced and applied utility of such reagents.

### **3.1.2.3 General Synthesis of Aldehyde and Glutaraldehyde**

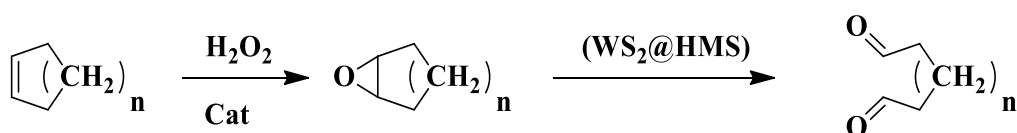
There are multiple synthetic routes available in the literature to conveniently synthesize a carbonyl group in the form of an aldehyde or a ketone, alcohol oxidation, Friedel-Crafts acylation, alkyne hydration and oxidative cleavage.<sup>193,247–249</sup> However, the extensive utility of carbonyl groups in organic chemistry has demanded highly adaptable synthetic methods that would allow for installation of such electrophilic centers in

molecules. Such synthetic approaches are not limited to reactions inside an organic chemist's reaction flask but have advanced onto biologist's toolbox. Biologists can now incorporate carbonyls onto larger macromolecules using enzymatic interaction and other catalytic protocols *in-vitro* studies. While there are many ways to synthesize a carbonyl group, oxidation of an alcohol is the ideal route in the laboratory or industrial settings. However, the disadvantage of these methods lies in the relatively toxic reagents that facilitate the reaction. Chromium salts and pyridinium salts are the cheapest reagents used that also produce undesirable by-products, which are not environmentally friendly. Organic oxidants such as iodated organic catalysts have been developed to overcome such shortcomings; however, they often require difficult laborious purification. In contrast to selective and mild oxidants, safer reagents like permanganate salts are sometimes used in preparations of carbonyl groups but suffer from over oxidation to a carboxylic acid.

Friedel-Craft acylation is also a powerful method to generate aldehydes or ketone using carbon monoxide or acyl groups. This method is obviously strictly designed for aromatic molecules to be armed with a carbonyl reactive moiety. Hydration of alkyne is another method through which a carbonyl group could be installed on a substrate. However, alkynes are equally important in bioconjugation and play a crucial role in some types of click-chemistry, therefore are not often used as a suitable precursor for carbonyl synthesis. Mercuric salts are used in at lower pH ranges or hydroboration-Oxidation to hydrate the alkyne and produce the corresponding carbonyl.<sup>193,247–249</sup>

There are many methods reported in the literature for general synthesis of a glutaraldehyde, but only a few are industrially practical. There are many limitations in the stability of the final product. Use of toxins and harsh conditions also pose serious

restrictions in the manufacturing process. There are some general methods reported for the synthesis of  $\text{CHO}-(\text{CH}_2)_n-\text{CHO}$  that are discriminate of the  $n$ . For instance, while oxidation of ethylene glycol and acetaldehyde are the preferred methods for glyoxal production, oxidative ring opening of cycloalkene or addition of a vinyl ether to acrolein are often used to make glutaraldehyde.<sup>250</sup> Wei-Lin Dai et al have reported a green method which uses catalytic amount of peroxide and some mesoporous silica catalyst ( $\text{WS}_2@\text{HMS}$ ) material as the catalyst to open a cyclopentene oxide into final product in reasonable yields<sup>251</sup>.



*Scheme 3-12 General synthesis of a glutaraldehyde molecule*

In another report, acrolein could undergo Diels-alder [4+2] cycloaddition with methyl vinyl ether in the gas phase to yield 3,4-dihydro-2-methoxy-2*H*-pyran. An acidic work up of the reaction would yield glutaraldehyde.<sup>250</sup>

### 3.2 Results and Discussion

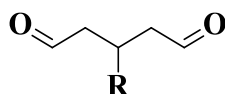


*Figure 3.5 General structural representation of dialdehyde substrate*

The synthesis of all amine-conjugating molecules in this work are designed to produce a 5-membered aliphatic structure. Synthesis of a substituted symmetrical five

carbon aliphatic chain with dicaronyl terminal functional groups is not an easy task to accomplish without sacrificing selectivity, stereochemistry, functionality, and yield and in some cases, synthetic feasibility.

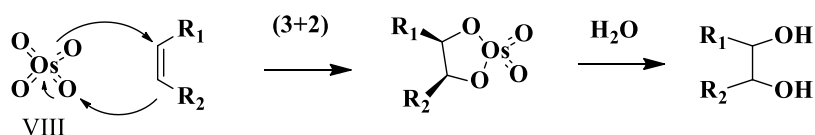
In addition to those challenges, there are not many synthetic routes reported in the literature to eliminate or minimize difficulties. Furthermore, synthetic protocols are usually developed to satisfy a need for a highly demanding application; otherwise, specialized molecules are synthesized through a custom synthetic route. Insufficiency of such methods for synthesis of a terminal dicarbonyl molecule is partly due to lack of a broad application for this class of molecules. In addition to that, proposed synthetic route must account for a reactive handle group at position C3' in all substrate models without limiting the cyclization to a 6-membered ring. A functionalized C3' aliphatic molecule with terminal an electrophilic center on a 5-carbon backbone is far more specialized to be found among the common commercially available options. The biological exploitation of this work is focused on a highly specialized application, therefore a novel synthetic route had to be designed in house to fulfil all the requirements for downstream functions.

A general look at the final structure of a dialdehyde substrate, it becomes evident that using a 5-carbon backbone precursor is the most convenient approach. In an attempt to seek functional groups that could be converted to aldehydes in high yields, olefin becomes the first choice as it offers great reactivity, stability and commercial diversity. Furthermore, starting from an olefin, two aldehyde groups could be installed on the same molecule with a single reaction. Olefin could be easily converted to vicinal hydroxyls that are excellent precursors to carbonyl groups on the same backbone. Oxidative cleavage would then yield two carbonyl groups that could either stay on the same chain or simply

split into two independent molecules. While all other synthetic methods are limited to use in a fume-hood in presence of harsh solvents and reagents, oxidative cleavage could be easily performed using mild conditions. For this reason, it is a powerful tool for *in-vivo* or *in-vitro* installation of the carbonyl group on biological molecules like protein, sugar and artificial amino acid. Alternatively,  $O_3$  could add to an accessible alkene to form an ozonide intermediate, which under mild reducing environment, cleaves to generate two carbonyl groups. A variety of reducing agents could be used for this purpose, but DMS and zinc are the common reagents. Oxidative cleavage is also feasible under oxidizing environments using  $H_2O_2$  or  $KMnO_4$  but both would further oxidize the aldehyde product to a carboxylic acid.

The laborious procedure of ozonolysis of olefin in some laboratory settings demanded the development of more practical methods. Lemieux–Johnson oxidation in 1956, inspired by Milas hydroxylation in the 1930s, introduced a promising method in which a combination of two steps could conveniently substitute the need for  $O_3$ .<sup>252,253,254</sup>

#### Mechanism A



#### Mechanism B

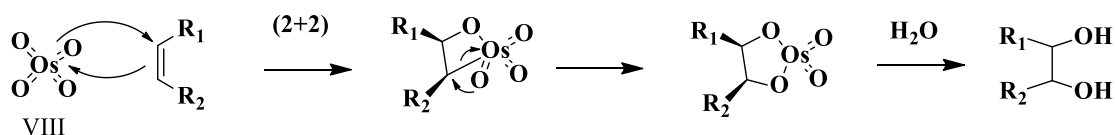


Figure 3.6 Reaction mechanism proposed for formation of vicinal 1,2 diol through oxidation of an alkene

During the first step, the olefin would be converted to vicinal diol in an *syn* addition reaction using OsO<sub>4</sub>, which could be easily oxidatively cleaved into the corresponding carbonyl groups. There are some disagreements in the order of addition to the OsO<sub>4</sub>, however, experimental observations have demonstrated the possible mechanism of 1,3-dipolar cycloaddition or a (2+2)-addition to the metal center.

Sodium periodate in aqueous solutions would serve the same purpose as ozonolysis, and is compatible with polar protic solvents. After preparation of the diol, hydroxyl groups attack the NaIO<sub>4</sub> to reduce the iodine (VII) to (V), the cyclic iodate ester then undergoes a reverse cycloaddition, which breaks the C-C and forms two separate C-O π bonds. This mechanism is analogous to the second step of ozonolysis with an additional proton transfer step; it is also quite similar to periodic acid and leads to a tetra-acetate cleavage. The resulting inorganic by-products are easily filtered and the desired organic carbonyl compounds are taken up in an organic solvent.<sup>255,256,257</sup>

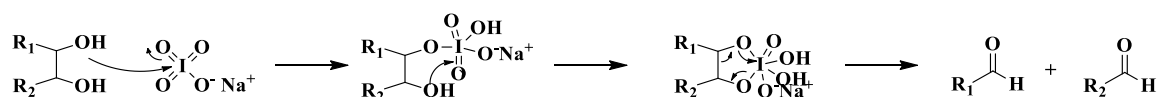


Figure 3.7 Reaction mechanism proposed for oxidative cleavage of 1,2 diol using NaIO<sub>4</sub>

While Lemieux–Johnson oxidation proved to be an important synthetic route in the preparation of aldehydes and ketone for biological studies, the OsO<sub>4</sub> used in the preparation of its precursor diol raised serious health concerns. Its relatively low LD<sub>50</sub> of 200 µg/m<sup>3</sup> along with its reactivity towards the abundant unsaturated molecules in the optic nervous system and its ability to penetrate plastic make it a poor candidate in practice. A more convenient and less toxic method of dihydroxylation was then introduced by Van Rhee-*en*,<sup>258</sup>



R. C. Kelly and D. Y. Cha of the Upjohn Company that uses a mild re-oxidant NMO for re-generation of  $\text{OsO}_4$  in a catalytic cycle.<sup>258,259</sup>

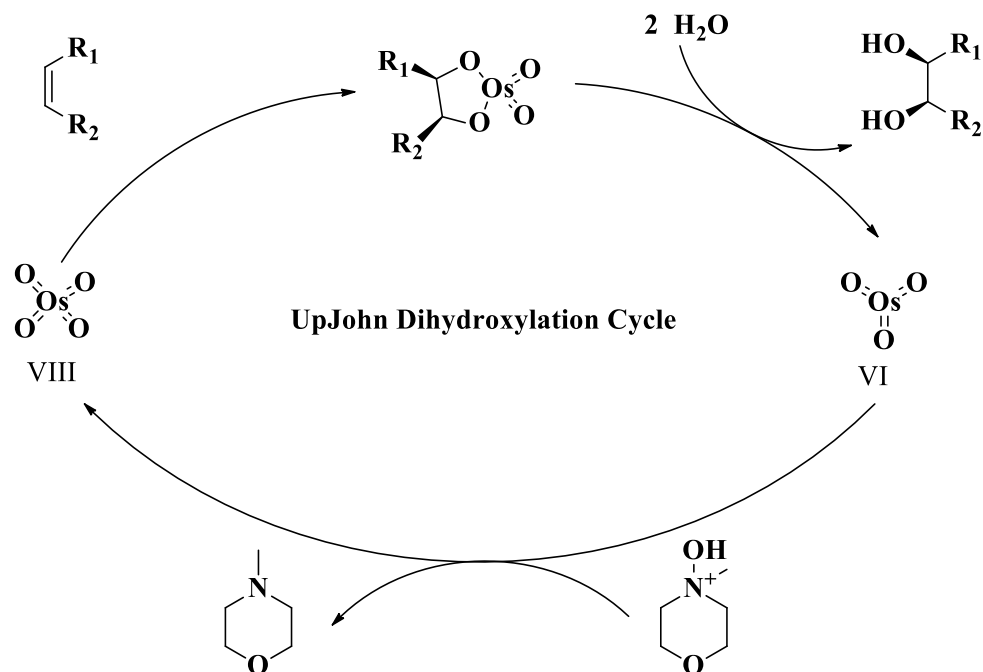


Figure 3.8 Catalytic cycle of UpJohn dihydroxylation using  $\text{OsO}_4$  and NMO as re-oxidant

Further improvement of this reaction by K. Barry Sharpless yielded a more selective and reliable method that would produce enantiopreferred isomer of the vicinal diol in high yields using  $(\text{DHQ})_2\text{-PHAL}$  called AD-mix- $\alpha$  and  $(\text{DHQD})_2\text{-PHAL}$  called AD-mix- $\beta$  chiral ligands.<sup>258,260–262</sup>

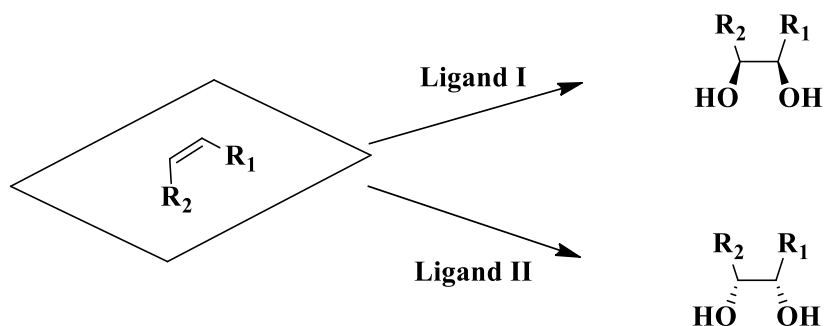
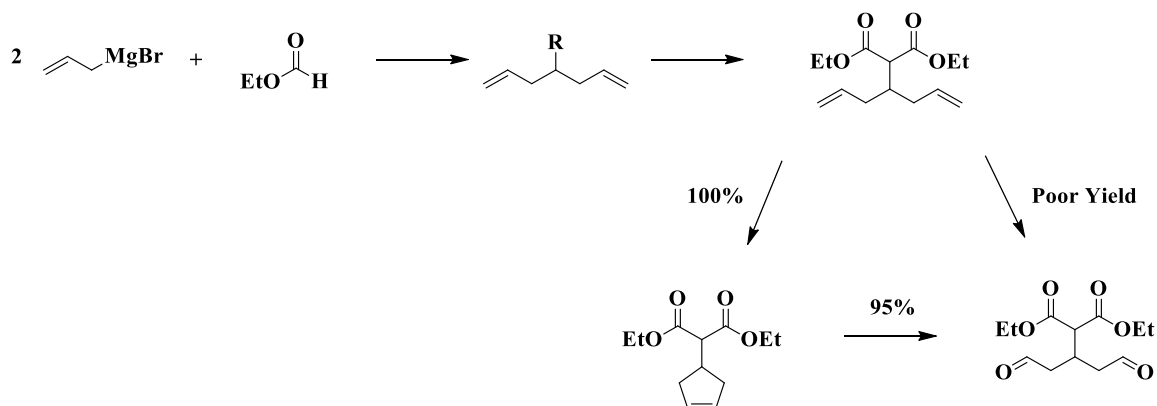


Figure 3.9 Enantioselective oxidation of an alkene using AD-mix- $\alpha$  and AD-mix- $\beta$  chiral ligands

Yang et al<sup>263</sup> reported a method for conversion of less substituted olefins to aldehyde without further oxidation to a carboxylic acid. They took advantage of a  $\text{RuCl}_3$  catalyst in their work that could convert an olefin to aldehyde in different solvent systems. The paper introduces the use of three different combinations of the catalyst, solvent and other salts that are specific for the olefin substrate used. A 3.5% mol  $\text{RuCl}_3$ –Oxone– $\text{NaHCO}_3$  in  $\text{CH}_3\text{CN}$ – $\text{H}_2\text{O}$  (1.5:1) is used to generate aromatic aldehydes,  $\text{RuCl}_3$ – $\text{NaIO}_4$  in 1,2-dichloroethane– $\text{H}_2\text{O}$  (1:1) would convert aliphatic olefins and  $\text{RuCl}_3$ – $\text{NaIO}_4$  in  $\text{CH}_3\text{CN}$ – $\text{H}_2\text{O}$  (6:1) proves to be the most effective combination for terminal aliphatic olefin.



Scheme 3-13 A general reaction scheme for synthesis of a C3' substituted dialdehyde substrate using metathesis

Hutchison<sup>264</sup> in 2006 (**Scheme 3-13**) reported the synthesis of a 6,6-bicyclic malonamide that contains useful information about installation of a chemical handle on C3' position of a 5 membered aliphatic carbon structure. Although their scope of synthesis stays limited to designing ligands with a binding site for f-block trivalent lanthanide ions, some of their synthetic steps are a valuable demonstration for the generation of a generic dialdehyde substrate. After the making of an aliphatic diene, their attempts to convert the olefin directly to dialdehyde, followed by an ozonolysis protocol, failed to be effective as it posed some complexities in the reduction of the ozonide intermediate. Therefore, a ring-closing metathesis was performed using Grubb's ruthenium catalyst to generate a C3' substituted cyclopentene ring, which was then successfully converted to a dialdehyde.

While synthesis of a dicarbonyl headgroup itself is not a difficult task, development of a sustainable method that would allow for the further multilateral synthesis of a suite of the substrate becomes a great challenge. Targeting of an amino group from a biological source is a delicate endeavor that is often affected by many factors in an acutely convoluted environment. The competing reactive centers, solvent, solubility, pH, temperature and concentration concerns are only a few examples that could be mentioned. Other regulatory functions and physiological interactions such as enzymatic processes, trafficking and signal transduction of small molecules in a cell become a great concern in the fate of any introduced non-native molecules. The conjugating substrate could interact with these factors in many ways and adopt an unexpected behavior, which would not be consistent with predicted observations. For this reason, it is important to obtain a tangible understanding of conjugating substrate's behavior and connections with each of possible influential parameters in an isolated study. In order to mimic the ability of a dialdehyde

molecule to successfully react with an amine, a set of substrates were synthesized and reacted with a sacrificial primary amine. Propylamine is chosen as a model nucleophile to satisfy the resemblance to R chain of a lysine, furthermore, its volatility would allow for convenient and fast isolation of the conjugate product. Looking at combined synthetic routes reported in the literature as well as an extensive examination of possible pathways, series of substrates were synthesized to serve as a novel amine conjugation system, which we will elaborate in the next subsections.

### 3.2.1 Substrate Type A

Earlier in the chapter, we introduced the criteria for an ideal and safe route to synthesize a dicarbonyl compound with a place holder for a chemical handle at position C3'. A close look at the commercially available precursors containing an alkene within a 5-carbon open chain or cyclic aliphatic backbone, cyclopentene is an obvious option, however, lack of a convenient synthetic direction to selectively install a handle at C3' makes it an unsuitable molecule for further reactions.

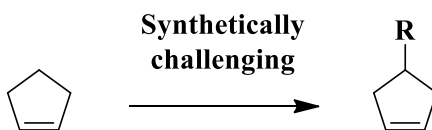


*Figure 3.10 General representation of synthesis for a C3 substitution of cyclopentene*

A commercially available 3-cyclopentenecarboxylic acid is an excellent choice, which offers a carboxylic acid on C3' and could be used for installation of a variety of functional groups. Carboxylic acids are not generally considered highly reactive moieties

but they could be easily translated to other reactive centers. They are superb starting material for the formation of a robust amide bond, which is an abundant and important linkage in the native biological system. Conversion of a carboxylic acid to an amide bond has been studied extensively for its importance in securing a robust connection both using organic reagents<sup>265–271</sup> and enzymatic reactions.<sup>272</sup> While this conversion in presence of an organic solvent could be achieved in great yields and selectivity, it is far less efficient in an aqueous environment as most activated carboxylic acids are susceptible to substantial hydrolysis. It is evident that this ligation is also dependent on the availability of an attacking amine on the carrier molecule. Most primary and secondary amines are proven to be reactive both in neutral or quaternary salt in alkaline conditions.

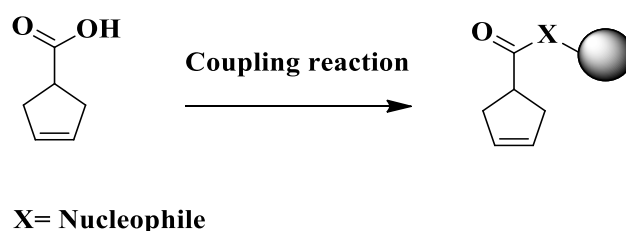
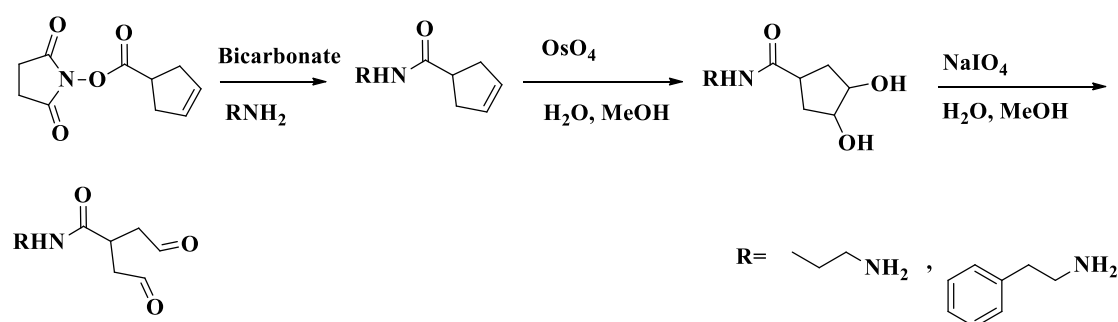


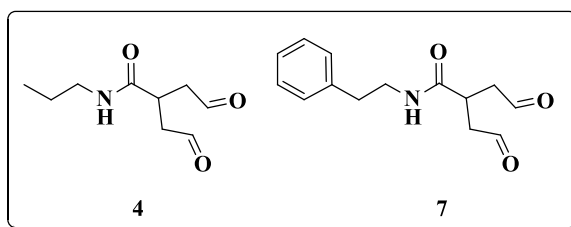
*Figure 3.11 Conversion of a carboxylic acid moiety to an amide bond with a nucleophilic substitution on activated ester*

We initially started with using 3-cyclopentenecarboxylic acid in two separate model systems, to form an amide linkage, with a propylamine and phenethylamine carriers using *N*-hydroxysuccinimide and DCC under alkaline conditions to afford molecule **2** and **5** with reasonable yields (**Scheme 3-14**). The often-relative low yields of such amide syntheses using *N*-hydroxysuccinimide, through the generation of an activated ester, lies in the rapid rearrangements of *O*-acylisourea to a highly stable *N*-acylurea. The limitations and inadequacies of activated esters formed from first generation DCC/EDC coupling

protocols have been elaborated in details in Chapter 1 (**Figure 1.7**). Oxidation of the olefin to vicinal diol **3** and **6** proceeds through a concerted interaction of two oxygens from OsO<sub>4</sub> with the alkene interface. The resulting 5-member osmate ester transition state is then reduced in aqueous solution to generate the two diastereoisomer *syn* (*3R,4S*) and (*3S,4R*) products. It is evident that the dialdehyde product of the subsequent oxidative cleavage step performed on the vicinal diol in this reaction does not have any particular stereochemistry associated with it. Although for this reason, the 1,2 diol compounds could be isolated in as a mixture of diastereoisomers, some are reported and characterized as isolated products in this work.



**Type A**



*Scheme 3-14 Model reaction for synthesis of substrate Type A*

An activated ester was generated using DCC/ *N*-hydroxysuccinimide and bicarbonate in THF. The addition of propylamine and phenethylamine to the intermediate affords substrate **4** and **7**. Substrate Type I is a model molecule that contains an amide linkage directly attached to the C3' tertiary carbon.

Following the isolation of 1,2 diols, both isomers were oxidized to the corresponding **4** and **7** dialdehyde substrates. Characterization of a dialdehyde molecule is an extremely difficult task using conventional analytical techniques for the reasons explained in details in analogous structural investigations and elucidation of glutaraldehyde (**Section 3.1.2.1**). Similar to glutaraldehyde, a dialdehyde substrate tends to form a hydrated hemiacetal headgroup that is consistent with the presence of some multiplet in the 4.5 to 5.6 ppm region of the  $^1\text{H}$ -NMR spectrum (**Figure 3.12**). In addition to hydrated structures of a dialdehyde head group, there is a great prospect for polymerization progression in the solution.

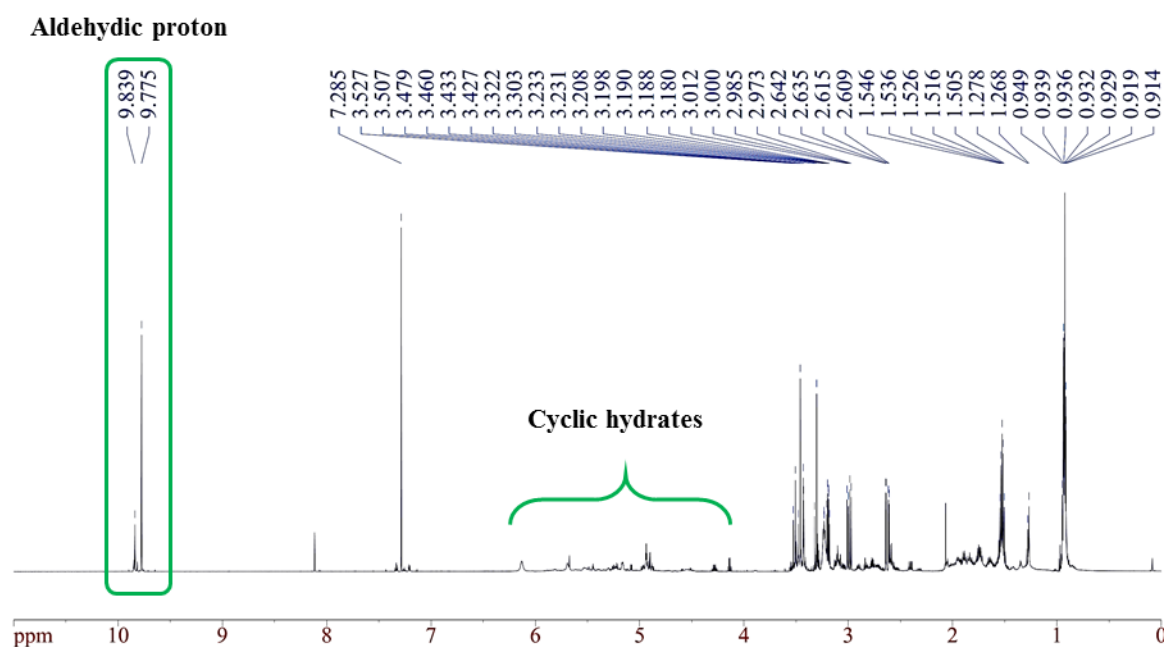
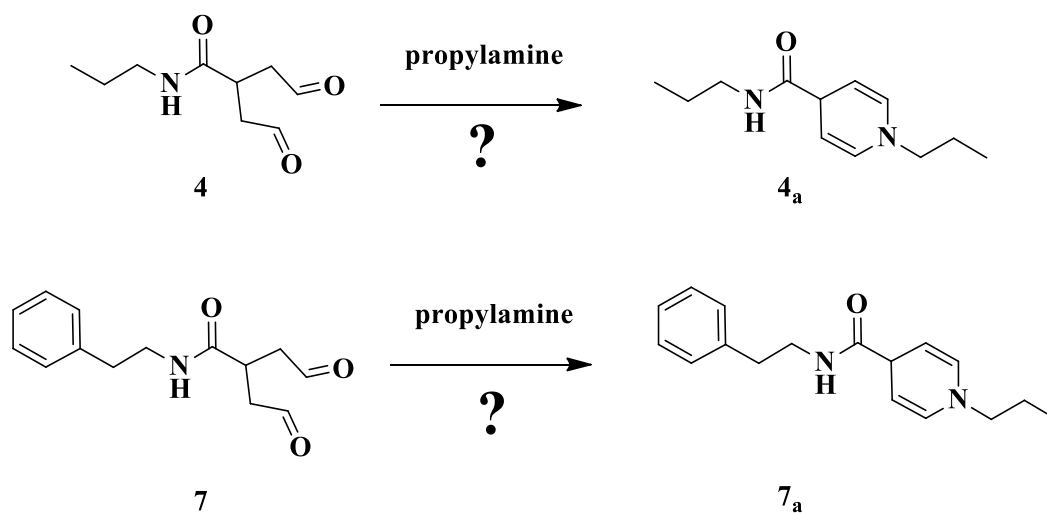


Figure 3.12  $^1\text{H}$ -NMR spectrum of molecule 4

NMR spectroscopy indicates presence of two distinctive aldehydic protons and a set of complex multiplet consistent with signals belonging to a cyclic hemiacetal or hydrated aldehyde

In order to address this concern, an aliquot of the dialdehyde sample was placed in a sealed desiccator with P<sub>2</sub>O<sub>5</sub> and dried over 48h, however, the shortest time exposure to air or saturated water level in any deuterated solvent is sufficient to rapidly hydrate the sample and render the effort ineffective. Based on the information regarding glutaraldehyde reactivity reported in the literature,<sup>214,216,217,225,240,242,243,245,251</sup> those carbonyls that are hydrated or otherwise engaged in an oligomeric chain, remain reactive towards amino groups.<sup>232</sup> Such behavior is demonstrated in glutaraldehyde's ability to crosslink and immobilize macromolecules while assuming unresolved structures. This information gives confidence that there is a promising chance for dialdehyde substrate to also behave similarly and readily react with an attacking amino group. Although characterization of a dialdehyde itself is a strenuous task, formation of conjugate and derivatives will be of great value in further characterization of precursors.



*Figure 3.13 Possible formation of an amide conjugate using propylamine and phenethylamine*

The addition of a primary amine (propylamine) to substrate **4<sub>a</sub>** and **7<sub>a</sub>** should presumably yield an annulated conjugate.



To investigate the reactivity of molecules **4** and **7**, a sacrificial primary propylamine was introduced in an organic solvent and reacted for 2h (**Figure 3.13**). The resulting conjugates were then analyzed by  $^1\text{H}$ -NMR in  $\text{CDCl}_3$  to obtain preliminary structural information.

The obtained NMR spectra of molecules **4<sub>a</sub>** and **7<sub>a</sub>** contain a very ambiguous set of signals that are difficult to correlate with any reasonable structure consistent with the formation of the desired product. The abundance of unresolved signals spread over most of the spectrum **4<sub>a</sub>** suggests the formation of multiple species in reaction with propylamine (**Figure 3.14**). A very little correlation exists to link the signals with any expected structures in the spectrum. Furthermore, there is no evidence supporting the formation of any enamine or even imine bonds in this reaction. A close look at the structure of **4** and **7** substrates, there is a single  $\beta$ -proton to carbonyl that could possibly allow for a rearrangement into different structures that do not share the same electronics or chemical properties with a 1,4-dihydropyridine ring. A  $\beta$ -hydride shift could lead to the formation of many structures like 1,2-dihydropyridine, 2,3-dihydropyridine and pyridinium ion that may not produce distinctive signals in  $^1\text{H}$ -NMR spectrum if carrying a charge.

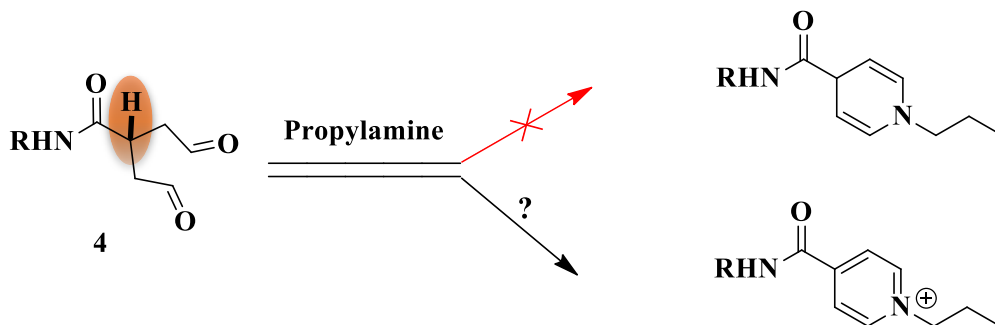


*Figure 3.14 Possible products propylamine conjugation to substrate Type A*

<sup>1</sup>H-NMR spectrum suggests the formation of a species that is not consistent with the structure of a 1,4 dihydropyridine. Since the peaks are relatively undefined and broad, one could speculate the formation of some form of a polymer or a charged moiety.

All undesired reactions discussed above are only the outcome of the addition of one amino group to the dialdehyde; however, the addition of multiple amines to the same substrate should not be forgotten. Such side reactions would allow for two amine additions to carbonyls and engage them in a covalent imine bond. TLC attempts using different solvent systems also produced streaking patterns that added to the uncertainty of a clean reaction between sacrificial amine and dialdehyde substrate Type A.

Observations obtained from conjugation, motivated us to examine the substrate in a detail to find possible reasons and drawbacks, which could lead to unsuccessful ligation. Although <sup>1</sup>H-NMR spectroscopy failed to reveal useful feedback on an effective conjugation, it is evident that upon nucleophilic addition of amino group, the aldehydic peaks at 9.5 ppm were no longer present. While the characterization of a product by means of isolation is not practical, such observations suggest a chemical reaction between **4** and **7** with the attacking amine. Therefore, complete consumption of aldehydic signals from the spectra leaves the desire for further investigation into other alternative models that would allow for a more vivid representation of the system. Furthermore, an unambiguous characterization could reveal invaluable information about the mechanism and behavior of dialdehyde system in bioconjugation contexts.

### 3.2.2 Substrate Type B

In an attempt to address the possibility of a rearrangement, contributed by the  $\beta$ -proton, a methyl ( $-\text{CH}_3$ ) was installed in  $\beta$  position in replacement of proton.

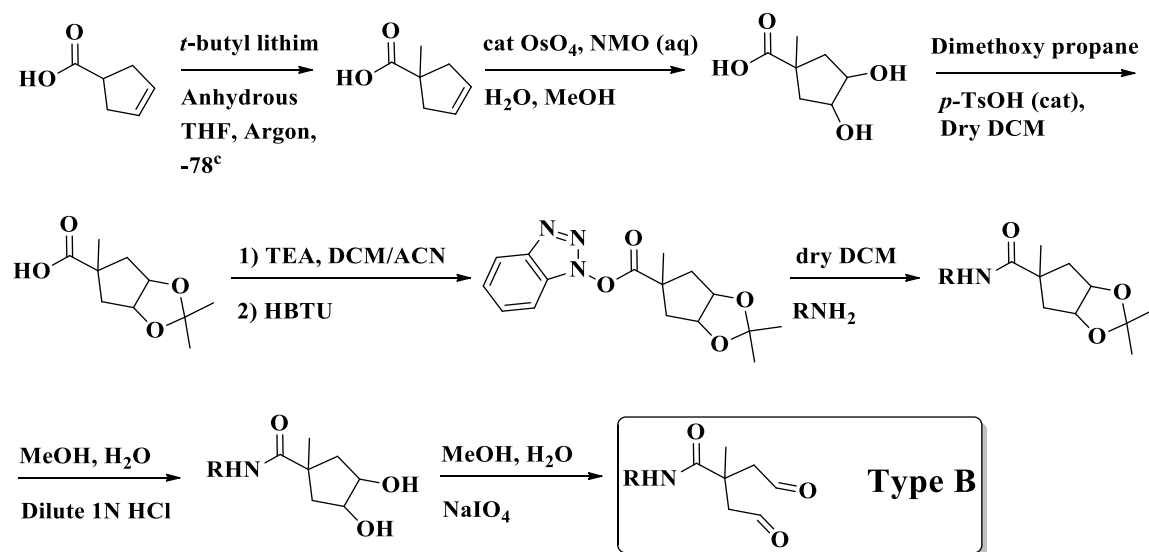


*Figure 3.15 Installation of a methyl group to generate a quaternary carbon at C3 position*

The considerable acidity of the  $\alpha$ -keto proton would allow for the formation of a C-C bond through alkylation of the dianion enolate.

A carboxylic acid dianion was generated using *t*-butyl lithium in THF at  $-78^\circ\text{C}$ , to which excess methyl iodide was added (**Scheme 3-15**). In spite of common over alkylation reactions at the  $\beta$ -keto positions, the product of the first alkylation will be a quaternary carbon that would not suffer from such side reactions. A simple acid/base separation would afford product **12** in an exceptionally high yield. Although LDA is a more common base used for the generation of enolate within the working pKa range (18-21), deprotonation using *t*-butyl lithium was much more effective in the generation of the dianion carboxylate. Molecule **13** is obtained similarly to previous oxidation reactions using  $\text{OsO}_4$  with NMO in a catalytic cycle to afford two diastereomer products in a relatively lower yield compared to **3** and **6**. The 1,2 diol product should be preferably protected to prevent any competition with amines during the formation of amide bridge. Protection of **13** will generate two diastereomers **14**, hence an interesting set of complex signals arise from stereochemistry of the protecting group and splitting pattern with neighboring nuclei. Unlike previous

routes, a triazole-activating group was used for enhanced efficiency and yield. Incorporation of a tetramethylammonium salt in the body of the coupling activator is a significant improvement in increasing the yield of securing an amide bond. The new class of reagents is extraordinary replacements for *N*-hydroxysuccinimide/DCC or EDC combination, as they do not allow rearrangements to *N*-acylurea.



Scheme 3-15 General synthesis of a substrate model Type B

Surprisingly, the activated ester product of triazole salt with any carboxylic acid is sufficiently stable to be isolated and stored for 6 months with minimum degradation. The addition of a primary amine to it will rapidly form the amide bond and leave behind *N*-hydroxytriazole as well as the corresponding tetramethylammonium salt. Formation of 1,2 vicinal diol through dihydroxylation could be done either early on during the synthesis or accommodated at the end. However, if attempted after amide formation the excess NMO present in the reaction vessel could possibly cause oxidation of the amide to *N*-oxide. In contrast, early oxidation followed by protection of the 1,2 diols prevents such side reactions

and also allows for a long-term storage of a stable precursor, which could be converted to fresh dialdehyde in a convenient quick step without any degradations.

Inspecting the NMR spectrum (**Figure 3.16**) of **18**, it is apparent that the tolerance of the dialdehyde headgroup towards the formation of hydrated states drastically improves, such that, there are much more resolved signals spread out in the aliphatic region.

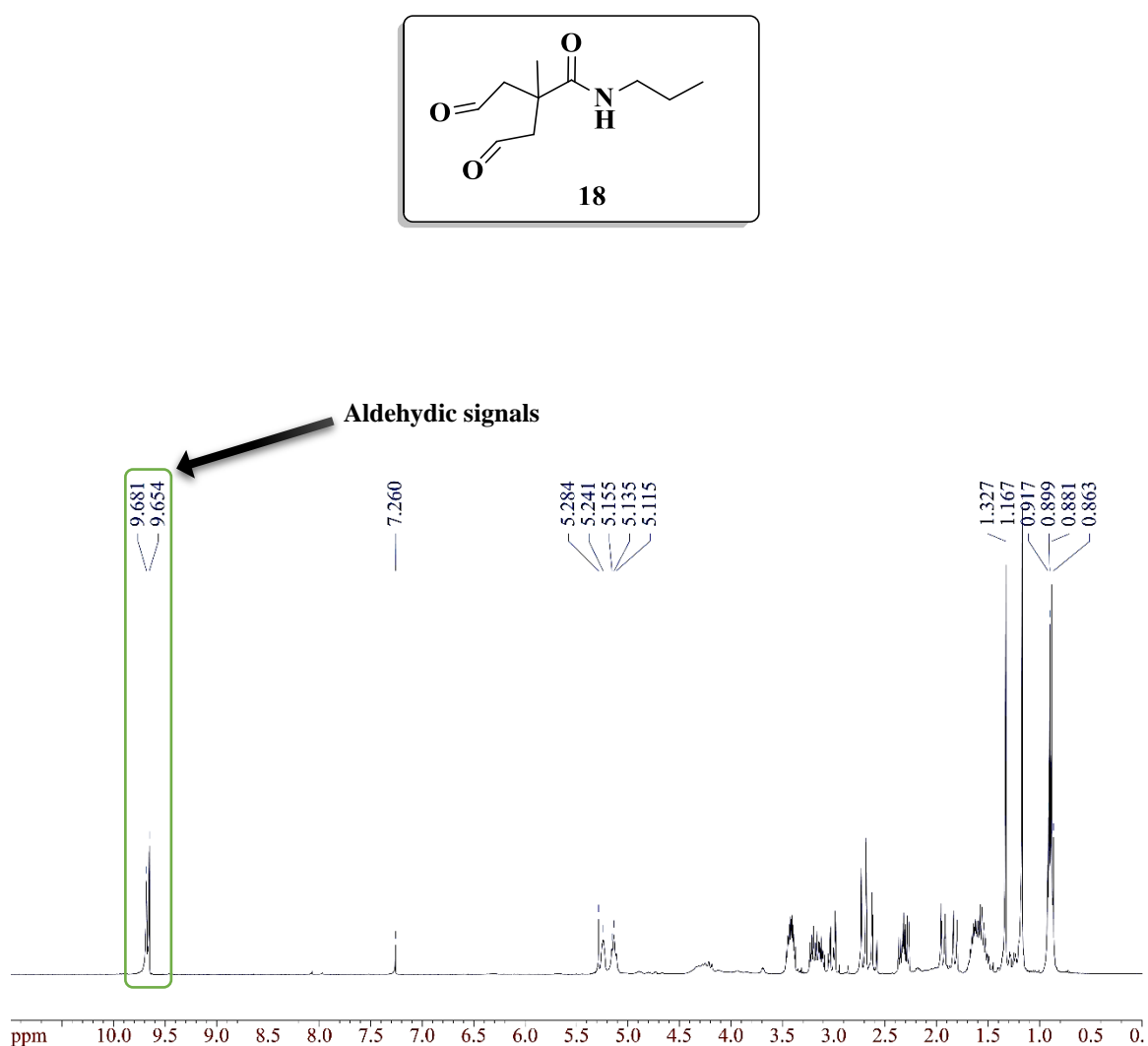
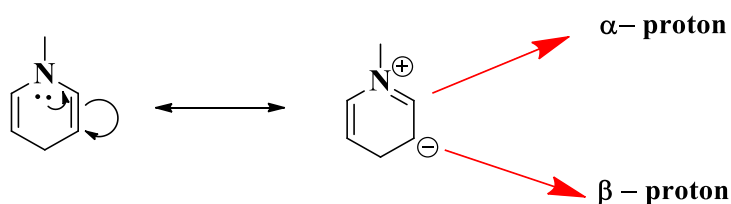


Figure 3.16 <sup>1</sup>H-NMR spectrum of molecule 18

The two distinctive signals at 1.132 and 1.167 ppm belong to the newly installed -CH<sub>3</sub> protons. This information suggests that there should be two different molecules present in the solution. While there are two  $\alpha$ -keto diastereotopic protons that could contribute to different environments around other nuclei, the presence of two independent set of CH<sub>3</sub> proton signals could only be justified by a polymeric structure of hemiacetals. There are also two peaks at 9.654 and 9.681 ppm characteristic of aldehyde signals. Although the spectrum presents some cleaner and more resolved signals corresponding to dialdehyde products, substantial evidence of hydrated headgroup and oligomers are still persistent at 5.0 to 5.5 ppm region.

In order to address this concern, similar to previous attempts, an aliquot of the dialdehyde sample was placed in a sealed desiccator with P<sub>2</sub>O<sub>5</sub> and dried over 48h, however, the same behavior, similar to first model reactions, was observed and analyte quickly formed hydrates in NMR tube. TLC experiments also generated the same streak smears that could not be resolved into isolated spots. While a column chromatography appeared to be a tempting approach for purification to a single molecule, results obtained from TLC were not convincing enough to proceed with any separation. A conjugation trial using propylamine was performed to investigate the formation of 1,4-dihydropyridine with the dialdehyde **18** substrate. As stated before, it is expected for all isomers to exhibit some reactivity towards an attacking nucleophile of the proper valance. The addition was conducted in DCM and solution was stirred for 2h, then the solvent was stripped off and the sample was analyzed by <sup>1</sup>H-NMR spectroscopy in CDCl<sub>3</sub>. The results are much more encouraging than previous attempts in Type A substrates, as there are many resolved peaks that could help solve a possible structure. It is evident that the chemical shift of enamine

bonds are unusual, experiencing a symmetrical environment, they are usually around 4.0 ppm and 6.0 ppm. The significant difference in the chemical shift of two vinylic protons lies in the increased electron density contributed by the lone pair of nitrogen released onto the  $\beta$  position that explains the upfield signal.



*Figure 3.17 Resonance structure of enamine contributing to up/downfield NMR chemical shift*

Looking at the spectrum of **19**, the conjugated propylamine to substrate **18**, there is a doublet of doublet between the range of 5.101-5.124 ppm ( $j = 6.8$  Hz); and an unresolved set of peaks at 5.031-5.047 ppm ( $j = 6.4$  Hz) both chemical shifts are indicative of a set of nuclei that are not in the vicinity of an electron donor heteroatom (**Figure 3.18**). However, the chemical shift of these protons is highly consistent with a polymeric structure of the dialdehyde substrate engaged in a hemiaminal chain. The persistent formation of a hemiaminal chain is easily justified by the formation of a kinetic product intermediate that is rapidly trapped as a stable product, hence would no longer undergo the entropically favoured process of losing water and remain as hydrated hemiaminals.

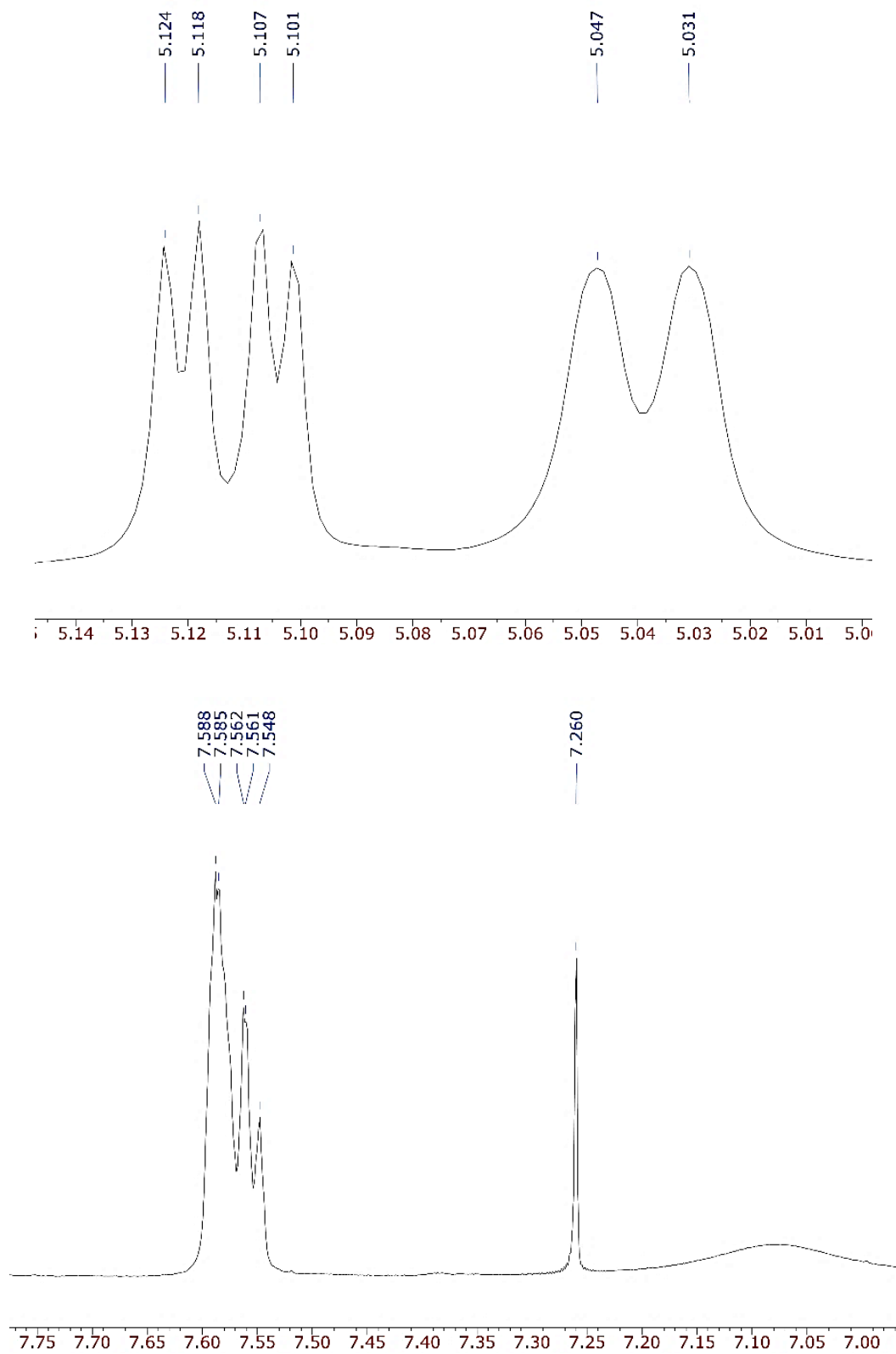
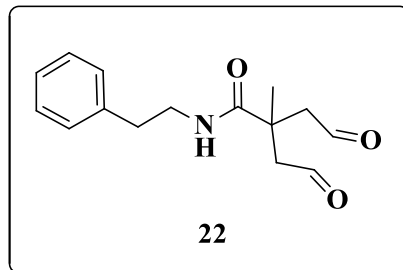


Figure 3.18 Partial NMR spectrum of substrate 14



Furthermore, the complex signal at approximately 7.5 ppm is consistent with the formation of imine bonds with the condensation of attacking amine with the two aldehydes in the parent molecule. Although there is an equilibrium between the kinetic product in the form of imine versus the thermodynamic product 1,4-dihydropyridine, the imine product is more favoured in a deuterated organic solvent. To investigate whether time would favour complete shift of equilibrium towards thermodynamic imine product, a fresh aliquot of **18** was treated with a stoichiometric amount of propylamine and incubated for a longer period; however, the resulting spectrum presented an identical set of signals.

To better understand the system, an analogue substrate was synthesized that held an aromatic ring for better differentiation of starting material dialdehyde against the conjugate.



This model substrate was treated with two different attacking nucleophiles methylamine and propylamine. Methylamine was chosen to mimic a slightly less hindered and more available amine, which may eliminate any ambiguity regarding the influence of larger attacking amines on the system (**Figure 3.19**). A thorough 1D-NMR and 2D-NMR Correlation Spectroscopy (COSY), Heteronuclear Single-Quantum Correlation Spectroscopy (HSQC) and Heteronuclear Multiple-Bond Correlation Spectroscopy

(HMBC) analysis were conducted to resolve a possible structure (**Figure 3.20, Figure 3.21, Figure 3.22, Figure 3.23**).

Interestingly methylamine reacting with substrate **22** produced a mixture of products that presented substantial signals highly consistent with the formation of a 1,4-dihydropyridine ring in great abundance.

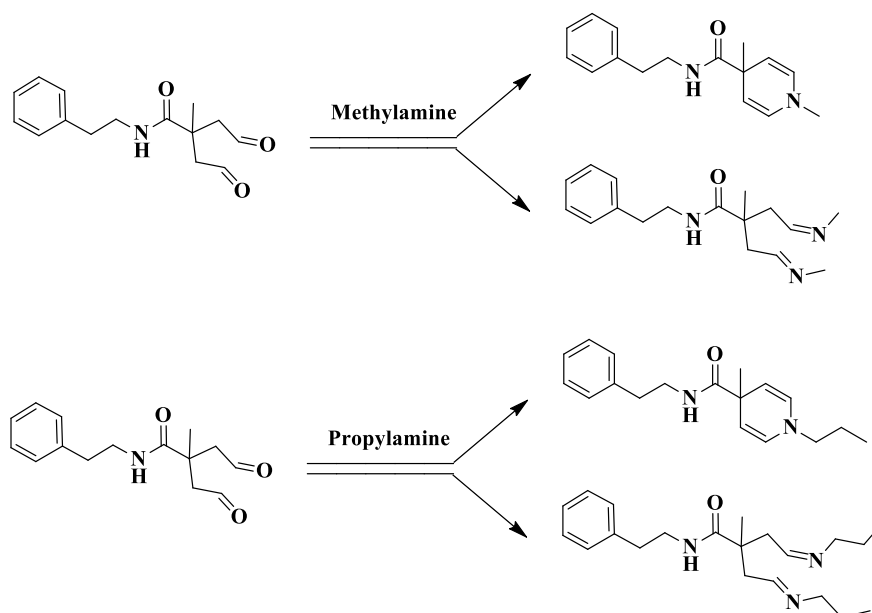


*Figure 3.19 Possible conjugation products of substrate **22** using different size nucleophile methylamine and propylamine*

Substrate **22** was treated with methylamine in THF to investigate the possible outcome products. NMR spectroscopy is suggestive of formation of two products in the form of annulated conjugate AND disubstituted carbonyls in the form of imine residue. In contrast, there is very little evidence for the formation of an annulated conjugate with propylamine. The appearance of persistent signals at 7.645 ppm is predominantly consistent with the formation of imine product. This behaviour could be rationalized based on the size and accessibility of smaller primary methylamine as opposed to larger nucleophiles.

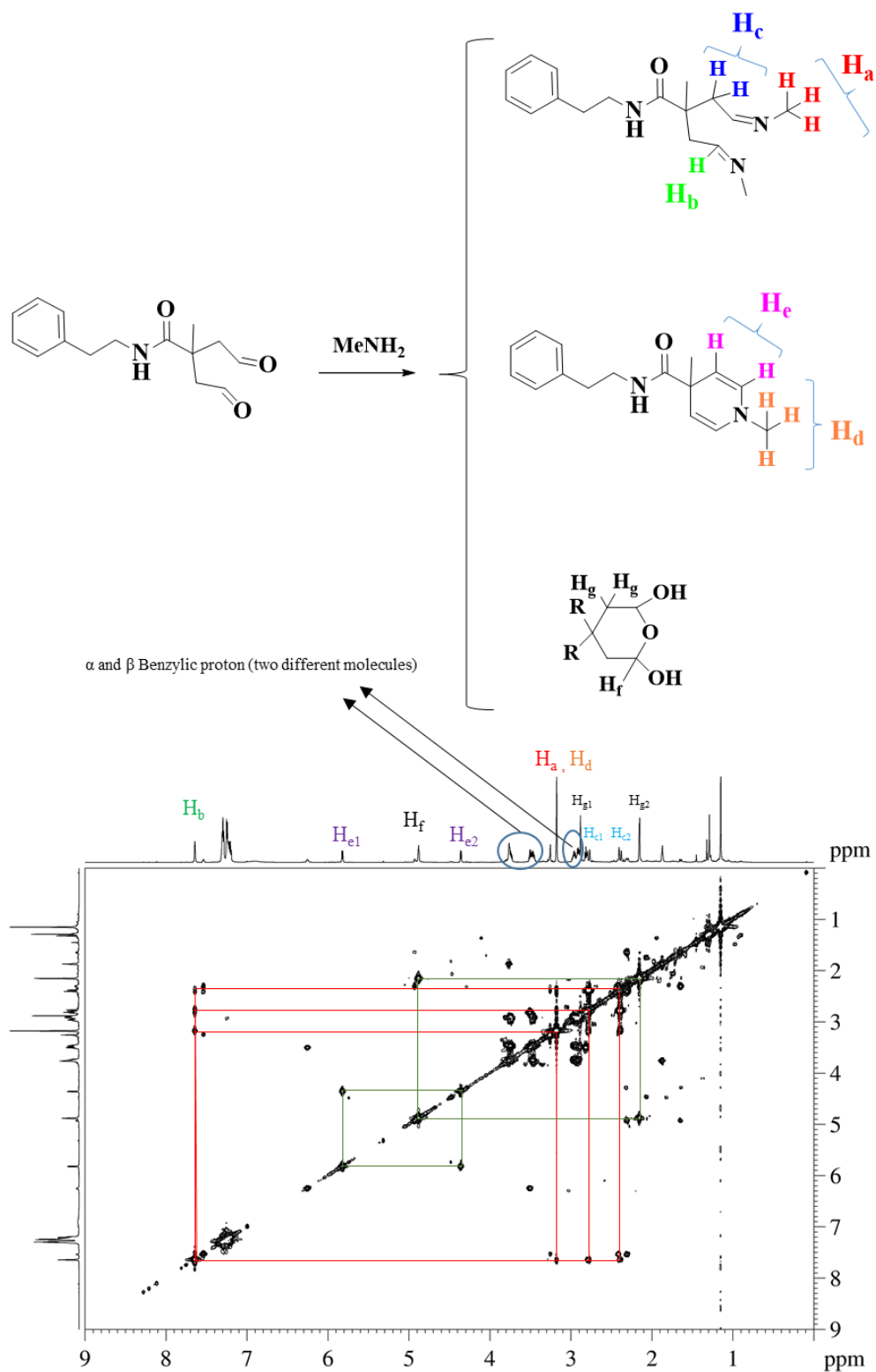
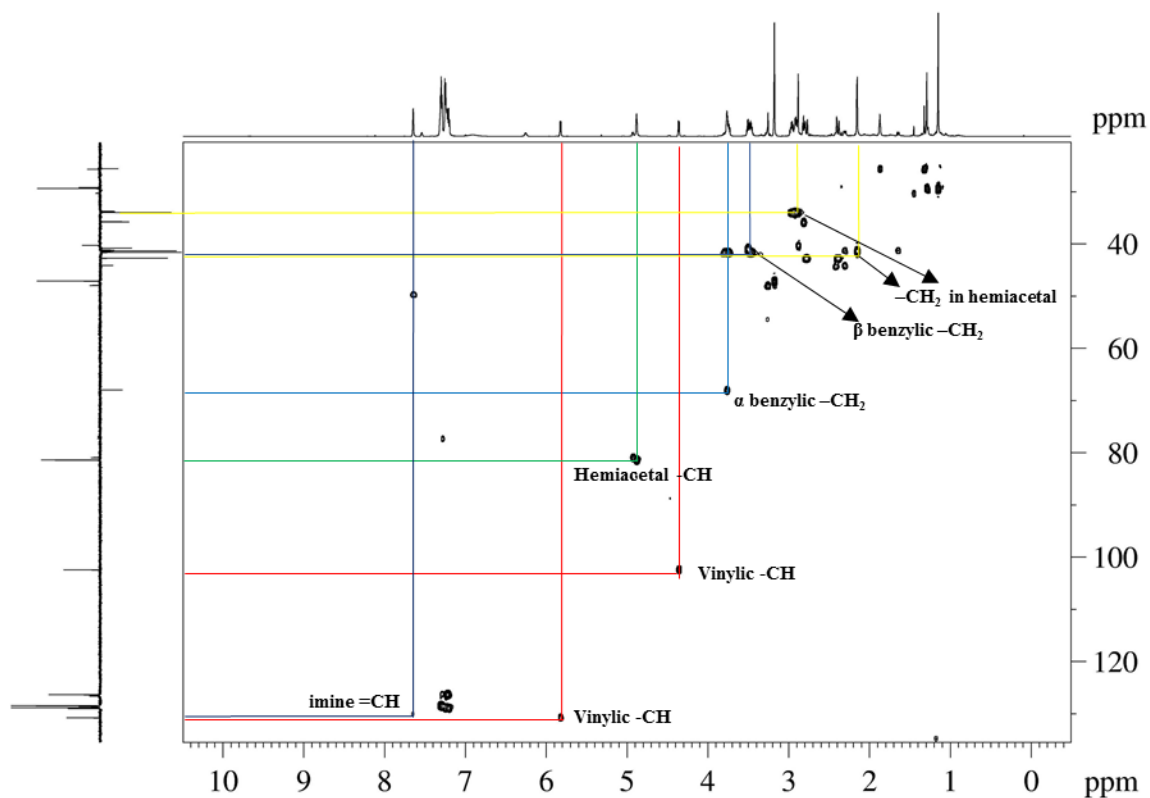


Figure 3.20 2D-COSY Spectrum of substrate 22 conjugate with methylamine

Conjugate products of substrate **22** with methylamine produce an approximately equal amount of imine and enamine product. Although 1D proton NMR is self-explanatory, 2D-NMR spectroscopy provides essential information about the nature of the protons and the carbon they are attached to. There spin system and the splitting pattern available in the COSY spectrum (**Figure 3.20**) is highly consistent with the existence of both products at the same time, as well as some unreacted dialdehyde that assumes a hydrated structure. Further, the 2D-NMR spectrum of HSQC in conjunction with DEPT analysis (**Figure 3.21**) confirms the number of nuclei attached to the corresponding carbon on each product.



*Figure 3.21 2D-HSQC spectrum of substrate 22 conjugate with methylamine*

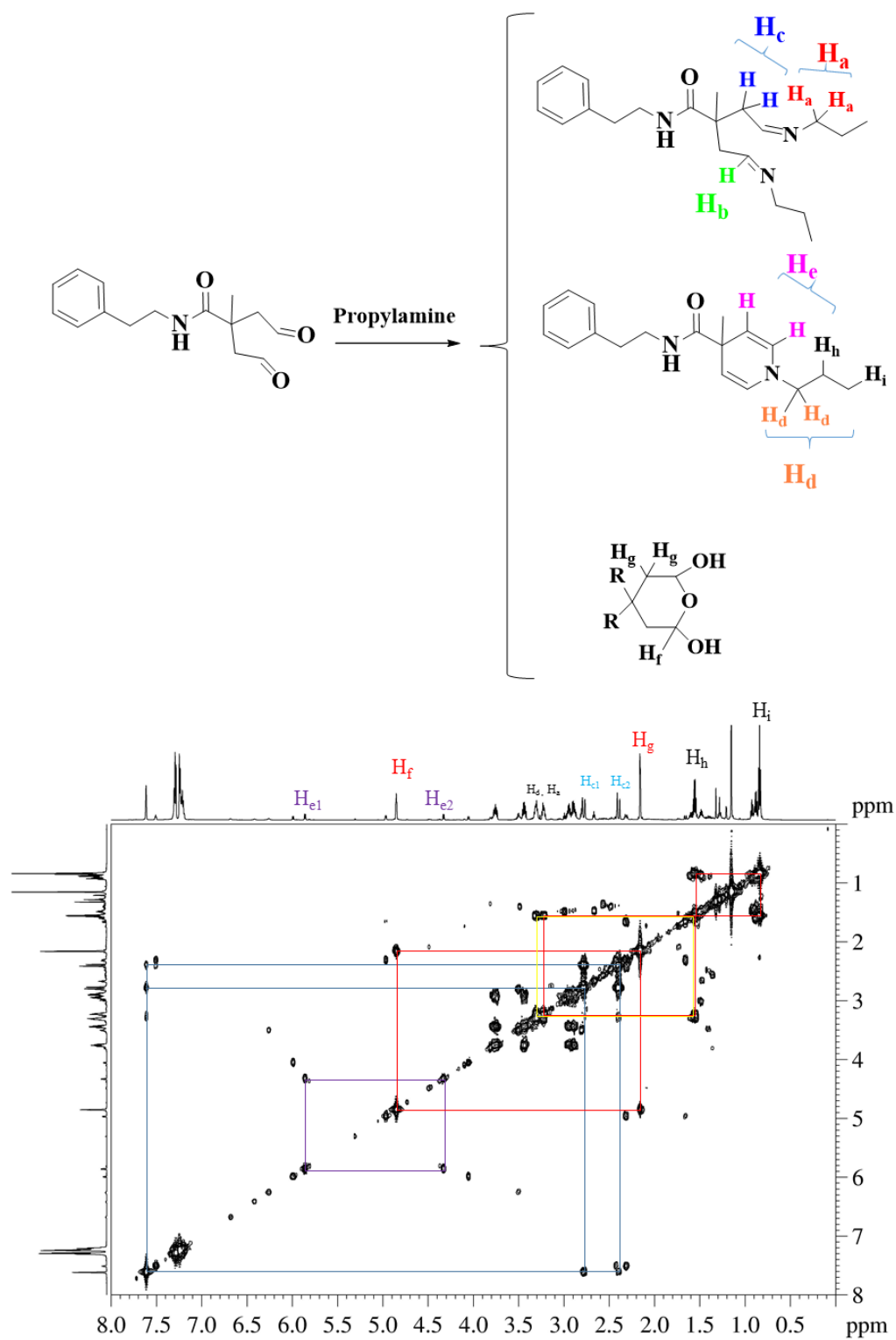
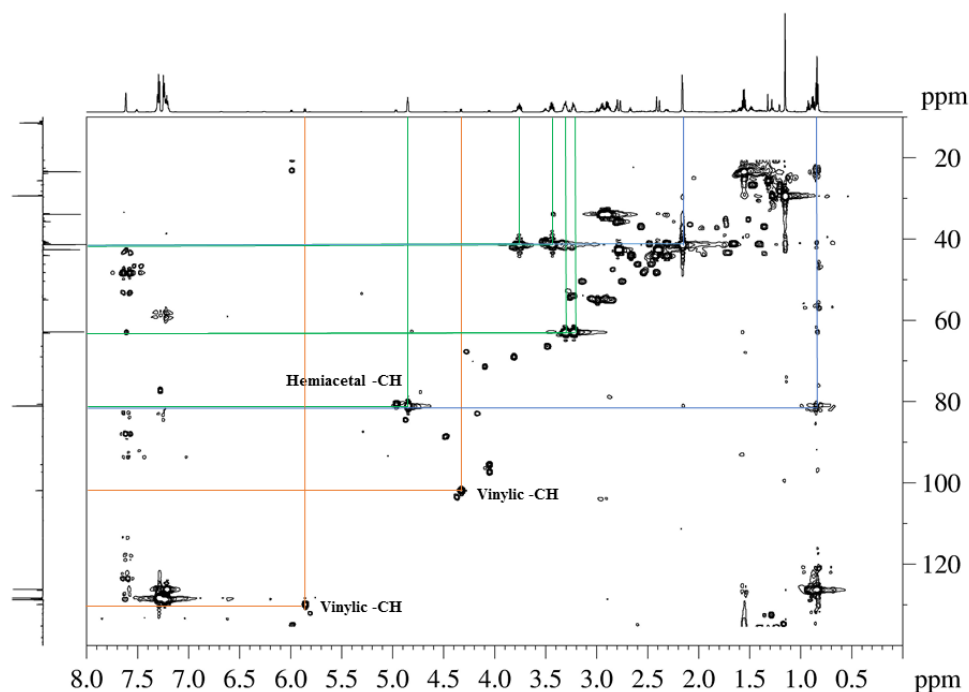


Figure 3.22 2D-COSY Spectrum of substrate 22 conjugate with propylamine

Similarly, substrate **22** was conjugated to propylamine and the resulting products were analyzed using 2D-NMR spectroscopy (**Figure 3.22**, **Figure 3.23**). Although very analogous results are observed, imine product is far more abundant than enamine. Formation of hydrated dialdehyde in the form of cyclic hemiacetal is also observed in the spectrum. In another speculation, the signals consistent with the formation of the hemiacetal could be equally related to the formation of some polymeric cyclic hemiaminal products.



*Figure 3.23 2D-HSQC spectrum of substrate 22 conjugate with propylamine*

In order to distinguish between an imine and enamine bond, and to further confirm the above speculations, we attempted to take advantage of their differences in behavior in the reduction reaction. Reduction of an imine bond to the corresponding N-C bond is a common practice in organic chemistry. While imines are readily reduced in aqueous

solutions, enamines require certain pH window for the same reaction. Cyclic enamines suffer even more from such special lower pH conditions. For this reason, any attempt to reduce a cyclic enamine under neutral conditions would remain ineffective; in contrast, an imine bond is expected to readily reduce. The conjugate product of substrate **22** with methylamine and propylamine were both exposed to cyanoborohydride in water pH 7.4 and stirred for 1h at room temperature (**Figure 3.24**). The NMR spectra obtained from both reaction vessels corroborates with the speculations made in complete disappearance of the imine signals and persistence of signals for the enamine peaks (**Figure 3.25**, **Figure 3.26**).

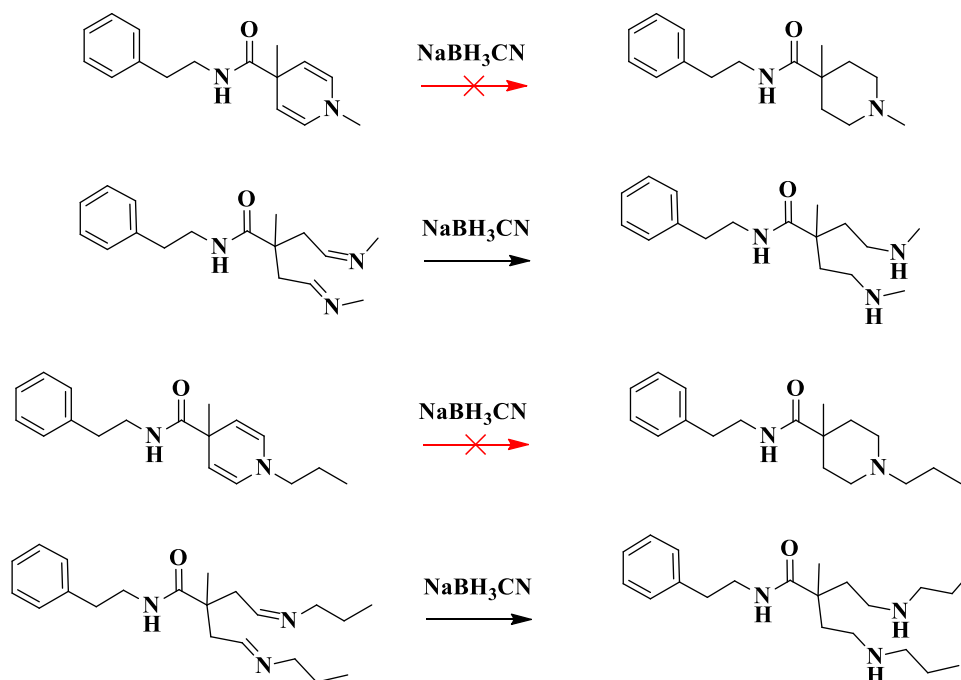


*Figure 3.24 Reduction of N=C bond using mild reductant sodium cyanoborohydride*

The impure conjugate mixture of both methylamine and propylamine ligated products were reduced using sodium cyanoborohydride under a neutral condition in MeOH. A simple analysis of the  $^1\text{H}$ -NMR spectra obtained from the product of this reaction could reveal valuable information about the possible ligated products of amine conjugation.

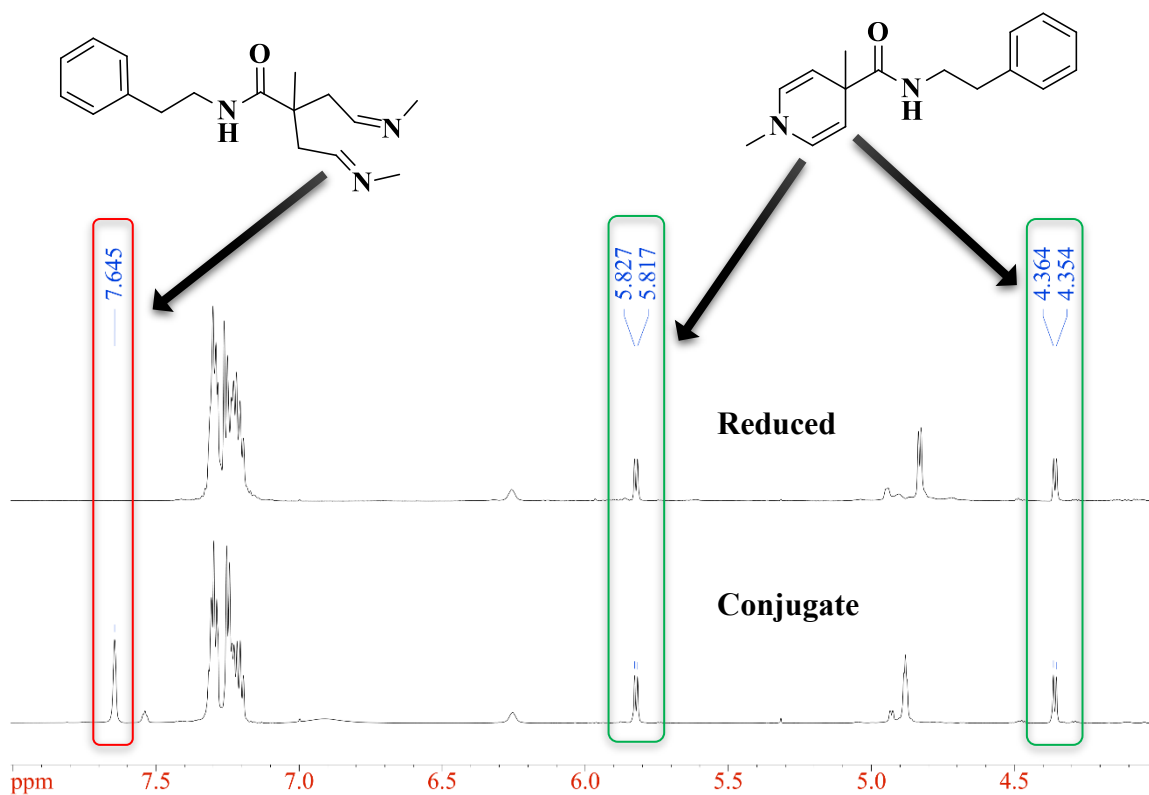


*Figure 3.25  $^1\text{H}$ -NMR spectrum overlay of substrate 22 conjugations with methylamine vs reduced products*

Upon treatment of the conjugate mixture of substrate **22** with methylamine, it is evident that imine peak is collapsed and the enamine peaks remain intact. This result is highly consistent with the expected outcome of reduction reaction of a simple imine and a cyclic enamine moiety. Imine products are easily reduced under neutral mild reducing environment; however, cyclic enamines require considerably lower pH conditions to convert to N-C bonds.



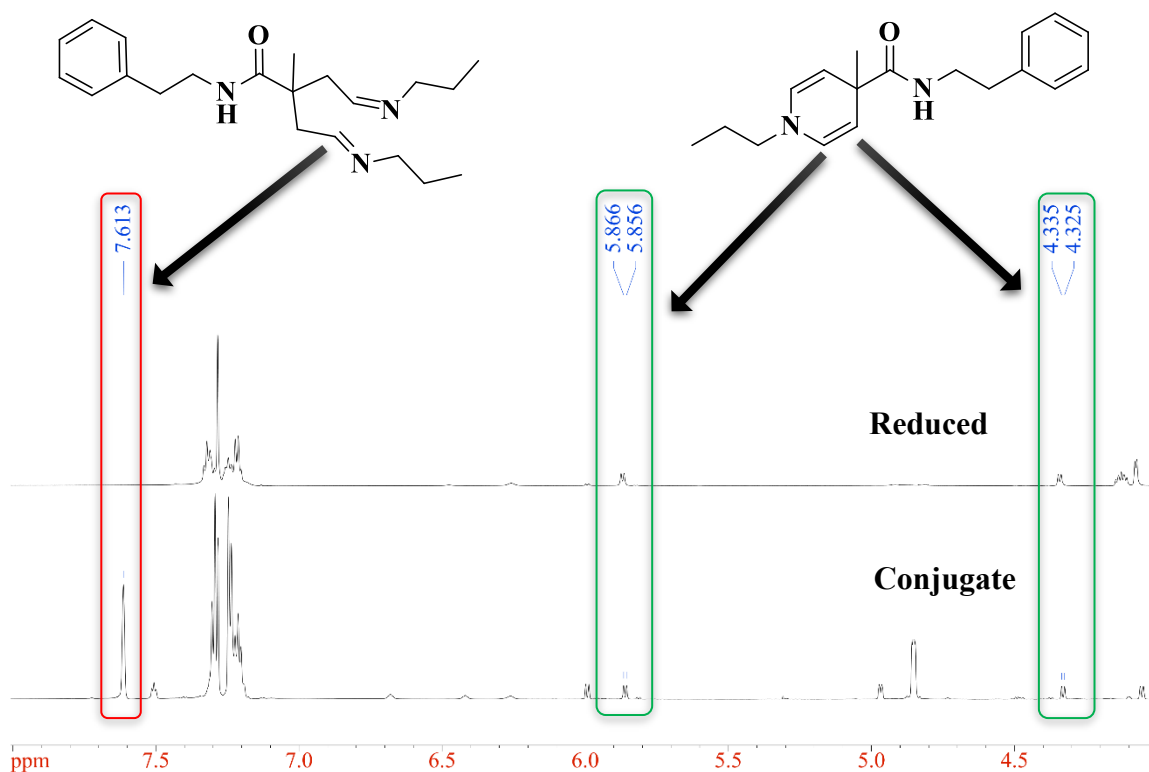


*Figure 3.26  $^1\text{H}$ -NMR spectrum overlay of substrate **22** conjugations with propylamine vs reduced products*

Upon treatment of the conjugate mixture of substrate **22** with propylamine, it is evident that an annulated product concentration in the form of dienamine is trivial in the impure mixture of the analyte. The substantial imine peak is highly suggestive of formation of  $\text{N}=\text{C}$  bond in the conjugate molecule. Upon treatment with a mild reducing agent under neutral conditions, the imine peak is collapsed and the trivial enamine peaks remain intact. This result is another supporting evidence for the formation of imine products in considerably higher abundance to dienamine product while conjugating with propylamine.

There is undeniable evidence that there is some imine formed during the nucleophilic addition to the dicarbonyl systems. This phenomenon could be rationalized based on kinetic vs thermodynamic products of nucleophilic additions. Although imines are generally more stable than enamines, in the case of an annulated 1,4 dihydropyridine, the formation of the 6-member ring outcompetes the stability over imine products.

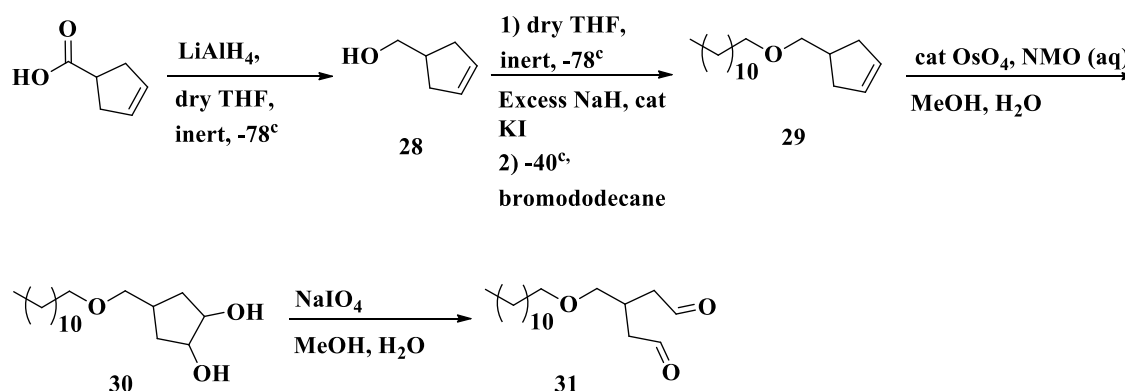
However, the formation of an imine product could be explained through thermodynamic favourability and is expected to gradually transform into the kinetic product.

### **3.2.3 Substrate Type C**

In spite of the reasonable improvements in results and illustration of a successful conjugation in the previous two model systems, we remained intrigued to address the remaining uncertainties in the characterization of the product. It is believed that reducing chemical functionality in the vicinity of a highly reactive center could potentially minimize the effect of other factors in the fate of conjugate. While amide bonds are proven fairly inert and robust in connecting two foreign structures, we speculated that they still might influence the stereochemistry and electronics of the molecule. In an attempt to address this issue, we replaced the amide bond with an ether linkage. Ether bonds are generally inert and do not elicit any reactivity towards other functional groups nor contribute to changes in electronics of molecules. They often participate in chemical reactions only at extreme temperature and pH ranges; their stability is also reasonable at physiological conditions.

Synthesizing substrate models that contain only a small carrier moiety would merely satisfy the requirements for studying physical organic criterions, disregarding other possible modes of characterizations in biological settings. Such limited one-directional approaches would be a waste of time and resources. For the explained reasons, this time a lipid-like substrate was synthesized to allow for a genuine characterization of amine ligation, AND demonstration of its ability to deliver amine containing ligands in a biological application using liposome fusion.

Synthesis and isolation of molecule **28** proved to be much more challenging than expected, due to its low molecular weight and considerably low boiling point (approximately  $< 80\text{ }^{\circ}\text{C}$ ) (**Scheme 3-16**). The close boiling point of the product and solvent THF in the reduction step led to a significant loss of the alcohol in the distillation of solvent. The subsequent alkylation of alcohol also required inert and anhydrous conditions, which demanded a thorough purification from any residual solvents from previous reduction step. Substitution of THF with anhydrous ether in the reduction step, followed by the minimum amount of aqueous work up allowed for significant improvement of product yield. Substrate **32** was tested with propylamine to demonstrate its ability to form the expected conjugate structure, however, it failed to produce any species characterizable via NMR spectroscopy. Therefore, it was quickly disregarded as a suitable precursor candidate for prospect models.



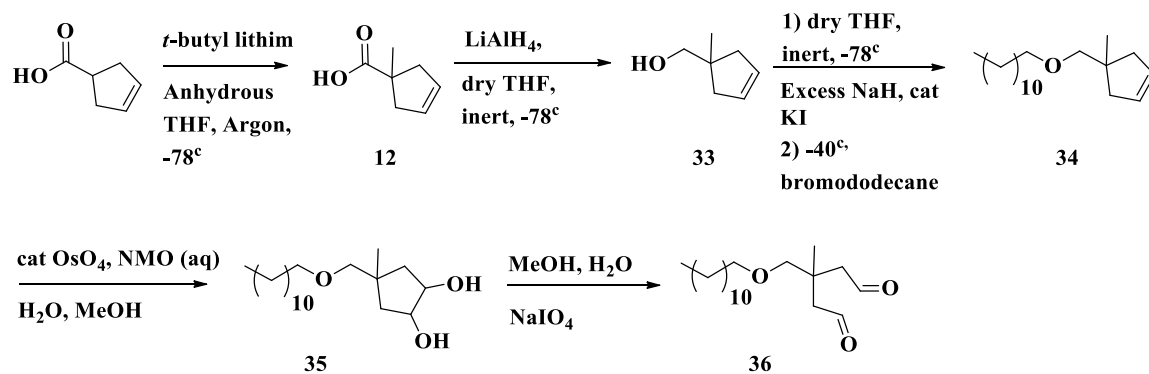
*Scheme 3-16 General synthesis of a substrate model Type C-1*

Later in the biological applications, we revisited molecule **31**, for liposome delivery purposes and surprisingly learned that it is competently efficient to deliver amine-containing ligands via liposome fusion. We learnt that such discrepancies between results

obtained from abortive preliminary organic reactions in organic vessel versus biological applications could be miss-interpreted, hence diverge us away from many potential valuable developments.

Although at the time preliminary results of ether linkage failed to produce satisfying outcome, our last hypothesis towards a promising conjugation was left to be examined in (**Scheme 3-17**), in which, a lipid like substrate was synthesized to contain an *ether linkage* as well as a *methyl* ( $-CH_3$ ) *substitution* at position C3'.

Unlike molecule **28**, the analogous alcohol **33** had enough molecular weight and higher boiling point to be easily isolated and fully characterized. Overall, subsequent alkylation and dihydroxylation products were obtained in reasonable yield; however, alkoxide of **33** is a relatively bulky anion and contributes to some product loss via deprotonation of bromododecane and formation of minor *E2* products. The oxidative cleavage of 1,2 diol to the corresponding dialdehyde **36** yielded a rather unclean mixture of expected scattered signals that could not be easily related to an isolated dialdehyde. Although it is evident that the sample is a mixture of oligomers and other possible hydrated structures, successful conversion of 1,2 diol to dialdehyde is a definite fact supported by aldehydic signals at 9.836-9.84 ppm (**Figure 3.27**).



*Scheme 3-17 General synthesis of a lipid substrate model Type C-2*

### Aldehydic signals

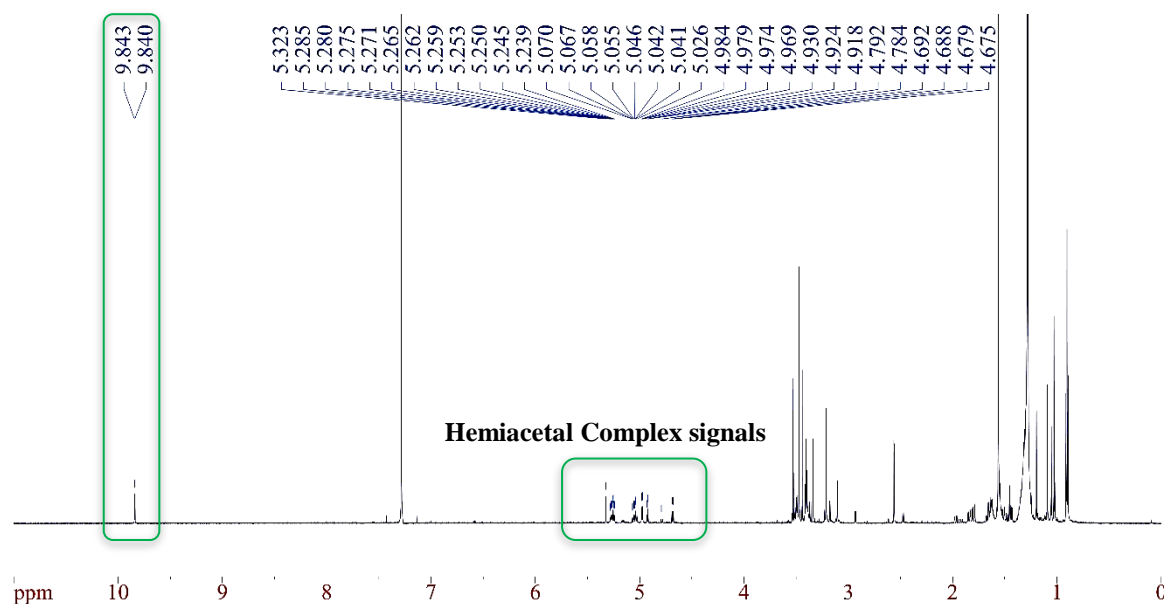
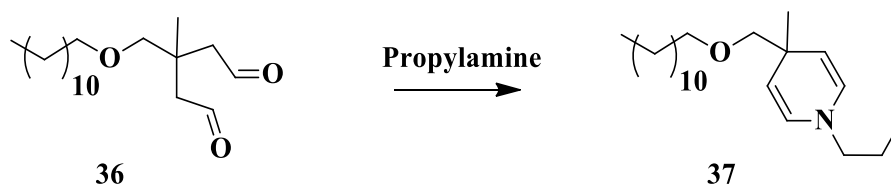


*Figure 3.27  $^1\text{H}$ -NMR spectrum of molecule 36*

Following the previous logics, expecting some degree of conjugation to any variation of dialdehyde molecules, we treated substrate **36** with propylamine (**Scheme 3-18**) and examined it with  $^1\text{H}$ -NMR spectroscopy. Surprisingly, for the first time, the product of an amine conjugation to a dialdehyde substrate produced the purely anticipated product that did not require any purification or work up whatsoever (**Figure 3.28**).



*Scheme 3-18 Conjugation of propylamine to dialdehyde substrate 36*

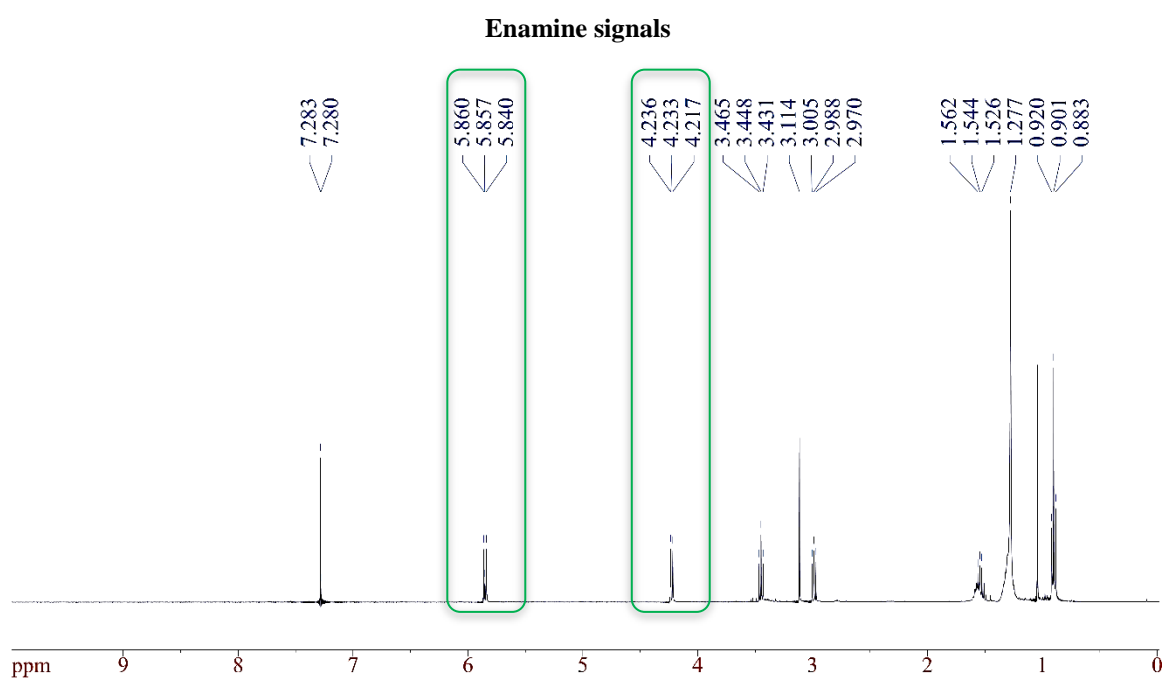


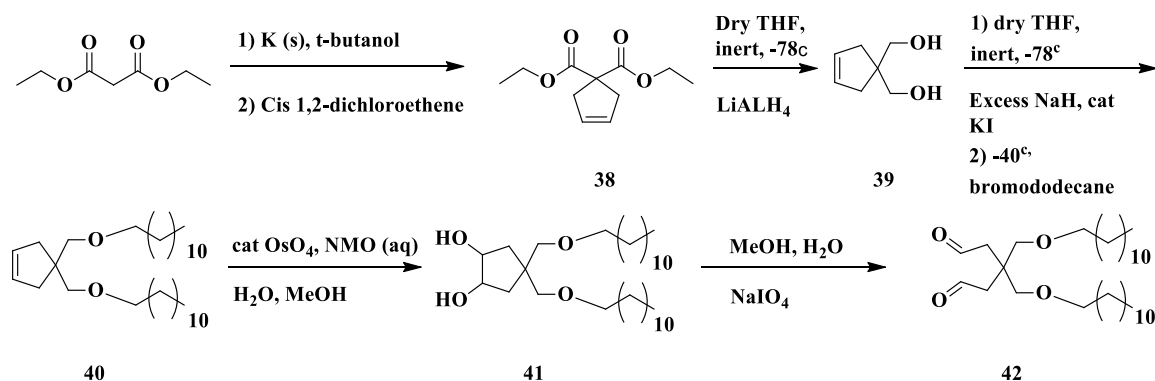
*Figure 3.28 <sup>1</sup>H-NMR spectrum of molecule 37*

Treatment of molecule **37** with propylamine produced a single product that requires no further purification. Evaporation of excess amine would result in a quantitative, pure and clean product.

This experiment illustrated the certainty of previous speculations, that even though dialdehyde head groups could be engaged in polymeric or hydrated structures, a primary

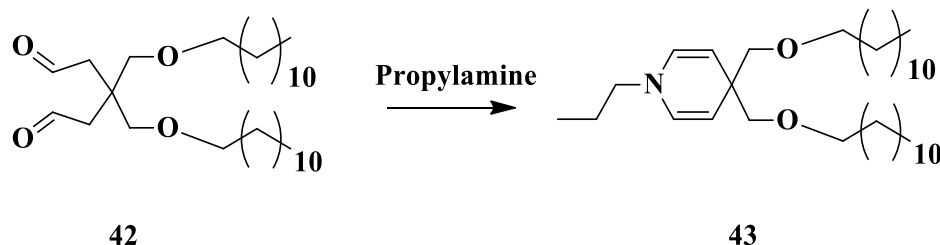
amino group could still engage them in a reaction to form 1,4-dihydropyridine conjugate. Therefore, the structural and chemical configuration that a dialdehyde molecule assumes in solution is proven irrelevant in its ability to ligate into a single final product.

A similar molecule was synthesized to improve the non-polar interactions of the lipid tails and the liposome hydrophobic residue (**Scheme 3-19**). Installation of an extra carbon chain would force a certain steric hindrance and minimizes polymerization of the dialdehyde headgroup, hence would make it more accessible for nucleophiles.



*Scheme 3-19 General synthesis of a bislipid substrate model Type C-2*

The NMR spectra obtained from **42** and **43** both remain consistent with previous observations from successful ligations (**Figure 3.29**, **Figure 3.30**).



*Scheme 3-20 Conjugation of propylamine to dialdehyde substrate 42*

**Aldehydic**

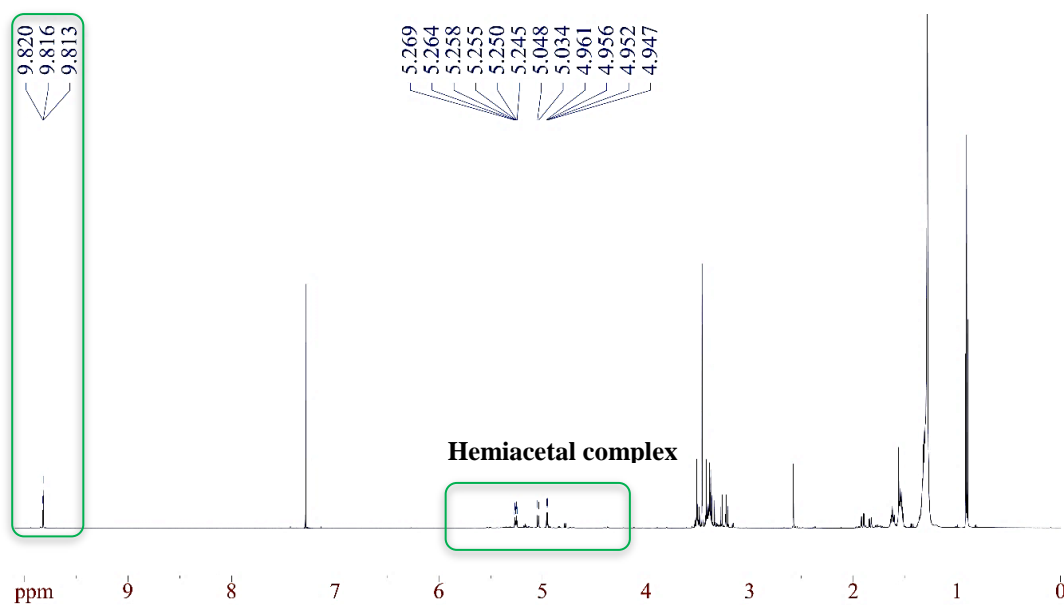


Figure 3.29  $^1\text{H}$ -NMR spectrum of molecule 42

**Enamine signals**

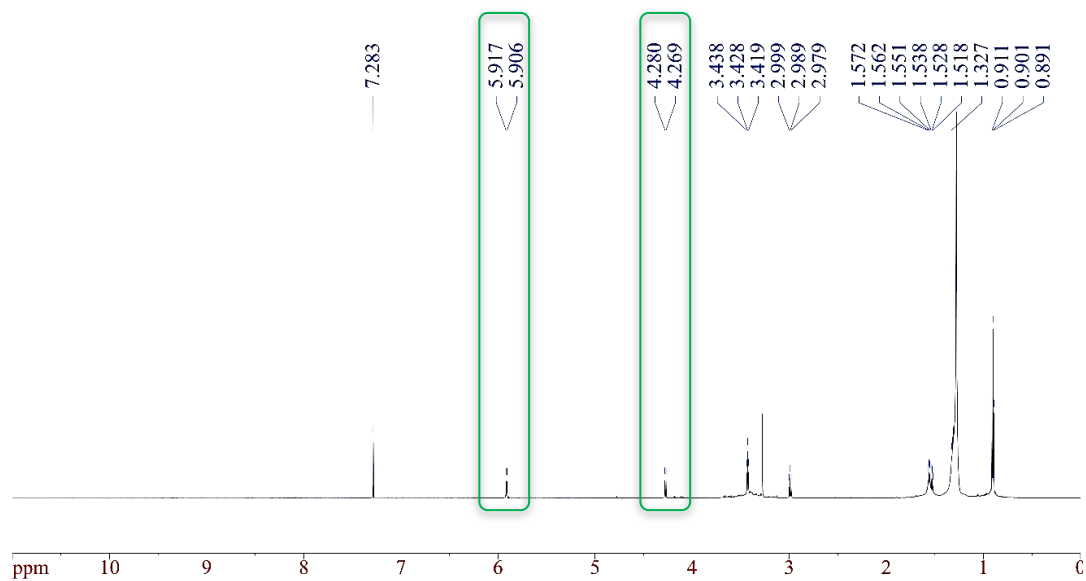


Figure 3.30  $^1\text{H}$ -NMR spectrum of molecule 43



### 3.2.4 Substrate Type D

Summarizing all the information obtained in the previous attempts, we identified the essential intrinsic features of a suitable substrate. A list of all the key elements required for achieving a successful conjugation was prepared. All these elements would satisfy both the organic chemistry criteria AND the chemical biology applications. Due to a wide range of applications for our amine conjugation system exploited in different areas of biotechnology, much effort was invested in producing a single parent substrate that could be installed on a variety of molecules (ie Reporters, adjuvants, antibody, proteins etc). The multilateral synthesis of this parent molecule had to fulfil all requirements such as synthetic flexibility, stability, kinetic competence, characterizations, solubility and synthetic feasibility.

The incorporation of a feature in the parent molecule that facilitates further installation of any handle group suited for any practice is an absolute prerequisite for an ideal synthetic route. This unique trait in the design of such precursors is an important quality of synthetic routes for organic and biological applications, which allows for the integration of any probe or component into the structure of a dialdehyde molecule. Stability of the precursor is also very important in offering a reliable substrate that would withstand long shelf life and remain invincible to degradations. Any designed precursor should remain kinetically competent with other biological reactions. Although conjugation to dialdehyde headgroup itself has proven to be an extremely fast and efficient ligation, the influence of other functional groups within the vicinity of carbonyls should not be neglected. We have already demonstrated the effect of some organic functional groups and their stereochemistry/electronics on the outcome of ligation. Furthermore, any design that could

not offer a comprehensive characterization of synthesized molecules would be an inadequate approach in establishing a viable protocol. Although characterization of most of the dialdehyde molecules is limited due to the structure, they assume in solution, they still should allow for a full identification via derivatization. Such models should also be soluble in aqueous solutions, be reactive at 37 °C and neutral pH and refrain from interacting with untargeted physiological components. These requirements demand an approach for the synthesis of a biocompatible molecule, which could easily operate under physiological conditions. To conclude, the design should also present a practical synthetic route that could be conveniently translated from the chalkboard and be materialized in the fume-hood. Retrosynthesis of a precursor that would satisfy all of the features explained is a difficult task.

In an attempt to introduce a novel design, we proposed the ideal candidate (**Figure 3.31**), which offered a reactive carboxylic acid moiety handle (Part A), sufficient distance of carbonyls from the end product 1,4 dihydropyridine ring (Part B) and synthetic feasibility for oxidative cleavage (Part C).

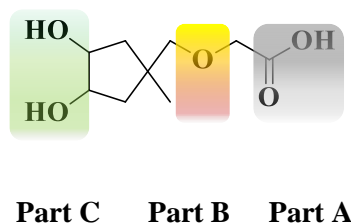
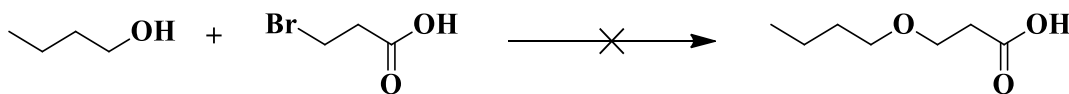


*Figure 3.31 General structure of an optimized dialdehyde substrate template type D*

Many attempts were made to design a substrate that would contain a relatively longer linker from ether linkage point (part B) to minimize functionality in the vicinity of

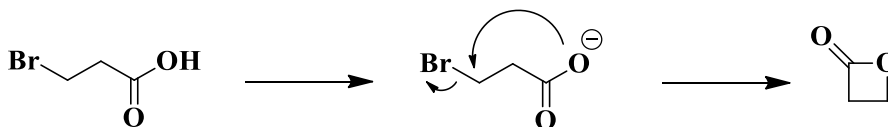
the dialdehyde headgroup (part C), but they all proved to be inefficient and in some cases, synthetically impractical. Some of the attempted synthesis will be briefly highlighted below:

Butoxide was selected to represent any alkoxide for convenient purification and 3-bromopropionic acid was chosen to serve as a potential linker (**Scheme 3-21**). Butoxide anion was generated in cold THF and NaH under inert pressure, to which the electrophile was added. Since the carboxylic acid would immediately reprotonate the alkoxide, excess NaH was used in the reaction vessel. The suspension was then stirred at a lower temperature to ensure the alkoxide is regenerated, then brought to room temperature and stirred for 1h. the mixture was then moderately heated at 55 °C overnight. After an acid/base work up, there is no trace of any desired product generated.



*Scheme 3-21 Synthetic approaches for finding a suitable linker for dialdehyde substrate template using 3-bromopropanoic acid*

The addition of 3-bromopropionic acid to a source of NaH, the carboxylic acid would immediately lose its proton and push the reaction towards a much faster and favoured intramolecular process of cyclization into a lactone (**Scheme 3-22**). This process completely quenches the electrophile and make it unavailable for further S<sub>N</sub>2 type additions.



*Scheme 3-22 Lactonization of 3-bromopropanoic acid into  $\beta$ -propiolactone*

Although lactones are well known to undergo ring-opening processes through activation of the carbonyl and generate useful reagent *in-situ*, such procedures require a source of a proton or other Lewis acid; both of which are difficult to exist under alkaline conditions. In another attempt, KI was added to enhance the rate of alkoxide addition, yet it only served towards an even faster lactonization. The solution to the problem seemed so easy by protecting the carboxylic acid moiety with a *t*-butyl ester-protecting group. However, 3-bromopropionic acid with a corresponding protecting group was not commercially available and protecting 3-bromopropionic acid in the lab was not an endeavor to accomplish when slightly different suitable commercially available reagent was readily available. Therefore, the reaction was performed using 2-bromoethanoic acid, with a *t*-butyl ester-protecting group, at 4°C with in THF and excess NaH under inert pressure followed by dilute HCl aqueous wash. *t*-butyl ester protecting group is among the most enduring protections and its removal is not as easy as a simple dilute acid work up. In spite of its persistence, the isolated product had already lost its protection after column chromatography. There are many inorganic catalysts and harsh acidic/basic conditions reported in the literature for the removal of such groups<sup>273–275</sup> (**Figure 3.32**). Sale et al<sup>274</sup> have used NaH and DMF to generate NaNMe<sub>2</sub> *in-situ* which then deprotonates the  $\beta$  carbon and proceed with deprotection into the corresponding carboxylic acid. Although NaH itself is not strong enough to abstract a proton from  $\beta$  carbon and generate the

corresponding carboxylate and isobutylene, refluxing for a long time may convert it to NaOH, which then could hydrolyze the protecting group in long reaction times.

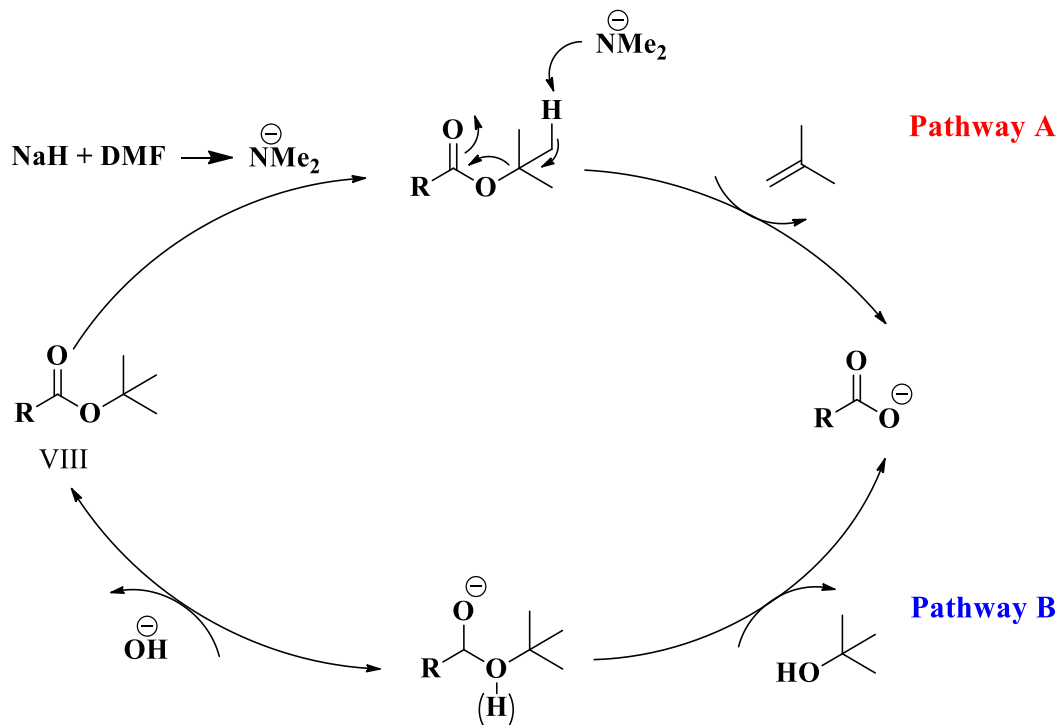
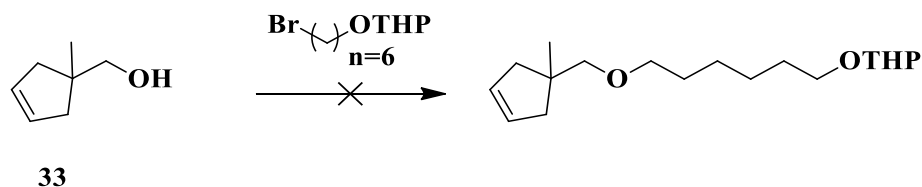


Figure 3.32 General mechanism pathway for deprotection of *t*-butyl ester protecting group

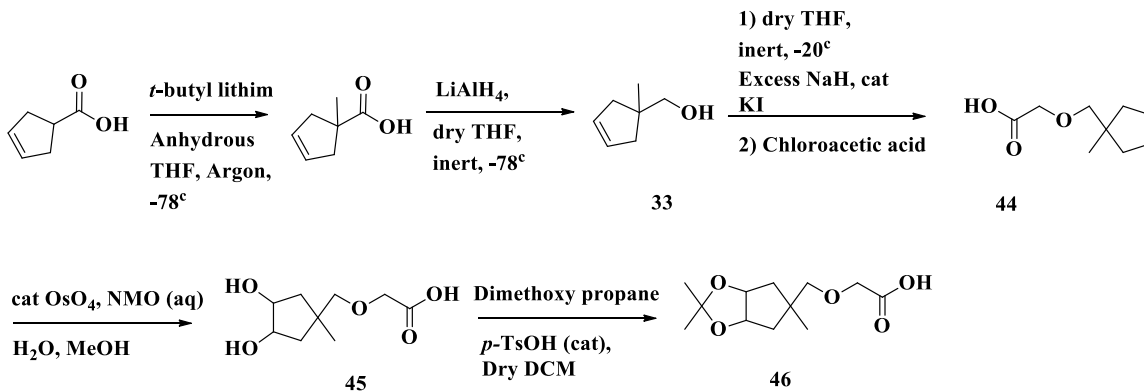
Even though a successful trial for alkylation of a linker with a carboxylic terminal moiety was conducted, the reaction exhibited much lower yields using hindered alcohols. Despite the recent successful alkylation attempt, challenges in translating conditions from the model reaction that uses an unhindered primary alcohol to a relatively sterically hindered alcohol compound **33**, led us to consider other alternatives. 6-bromohexanol seemed to be a suitable alkylating agent that would make an accessible electrophilic center for nucleophilic additions (**Scheme 3-23**). The terminal alcohol could be easily protected to allow the electrophilic center react with other alkoxides, then deprotected and converted into a carboxylic acid. Although the design seemed to be very promising, the isolated

product's yields were still not as effective as anticipated. Elimination products were much more predominant, hence led us to use other synthetic routes and use another alkylating agent that was bound to undergo  $S_N2$  addition.



*Scheme 3-23 Synthetic approaches for finding a suitable linker for dialdehyde substrate template using 2-((6-bromohexyl)oxy)tetrahydro-2H-pyran*

Eventually, compound **44** was synthesized through alkylation of the smallest unit possible, chloroacetic acid, which would not cyclize into a lactone ring nor has the opportunity to form *E2* by-products (**Scheme 3-24**). A thorough chemical spectral analysis of the obtained product was conducted through  $^1\text{H-NMR}$ ,  $^{13}\text{C-NMR}$ , HMBC 2D-NMR spectroscopy and to ensure an ether linkage is established. The elaborative examination of **44** assisted to understand the structural and chemical properties of the molecule to determine whether it could serve as a standard template for prospect syntheses.



*Scheme 3-24 General synthesis of optimized dialdehyde substrate template Type D*

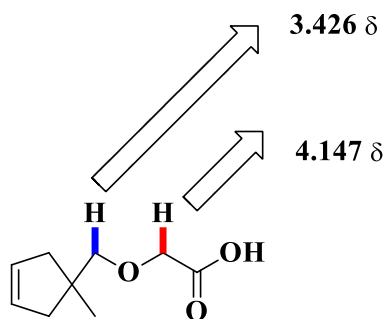
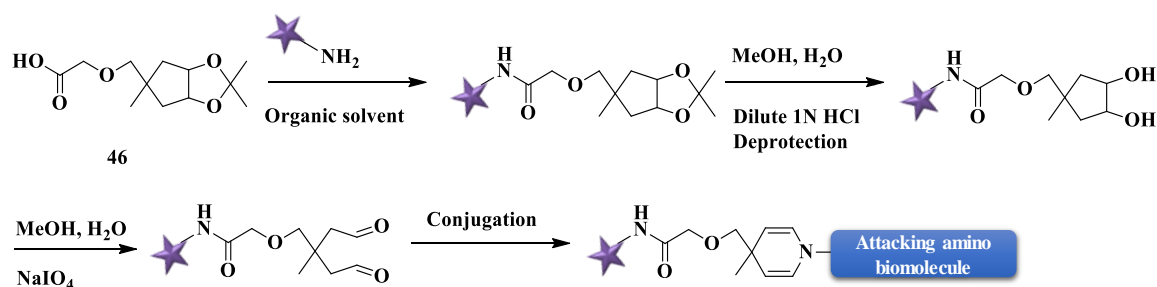


*Figure 3.33 Chemical shift of the two distinctive diagnostic protons of substrate 44*

Unlike previous experiences in dihydroxylation of other molecules, substrate **45** was synthesized in a relatively low yield of 72%. While the reported yield is the best obtained in the lab, most trials attempted suffered from significantly lower yields. The inefficiency in synthesis is not entirely due to chemical processes during the reaction, work up and purification also contributes to these considerable poor yields. The chemical features of the product and the nature of other chemicals present in the reaction vessel would not allow for a simple take-up of desired organic product in an organic solvent. Since oxidation of the olefin requires an excess amount of NMO, the crude product must be washed with some aqueous solution. In addition to solubility concerns, the catalytic re-oxidation of  $\text{OsO}_4$  is most efficient at higher pH windows, therefore NMO solutions are often supplied 50% in water at pH 9.0. However, substrate **45** would no longer be a neutral molecule at that pH and must be re-protonated. Compound **45**, with two hydroxyls and a carboxylic acid, allows for strong and persistent hydrogen bonding, thus exhibit noticeable hydrophilic properties. To address all concerns above, the crude was treated with a minimum amount of a dilute acidic solution, then dried over  $\text{MgSO}_4$  and quickly dry loaded onto silica gel. While this seemed to be the best solution to the problem, most of the product was still lost in column chromatography process. Inadequacy in yield proved to be the most important

drawback of this design that could not be addressed using other alternatives. Contrary to this disadvantage, the applications intended for dialdehyde substrates do not require concentrated samples, therefore obtaining higher yields has never been the scope of optimization in this research.



*Scheme 3-25 Illustration of a synthetic pathway for generation of a typical dialdehyde substrate, followed by conjugation to a biomolecule.*

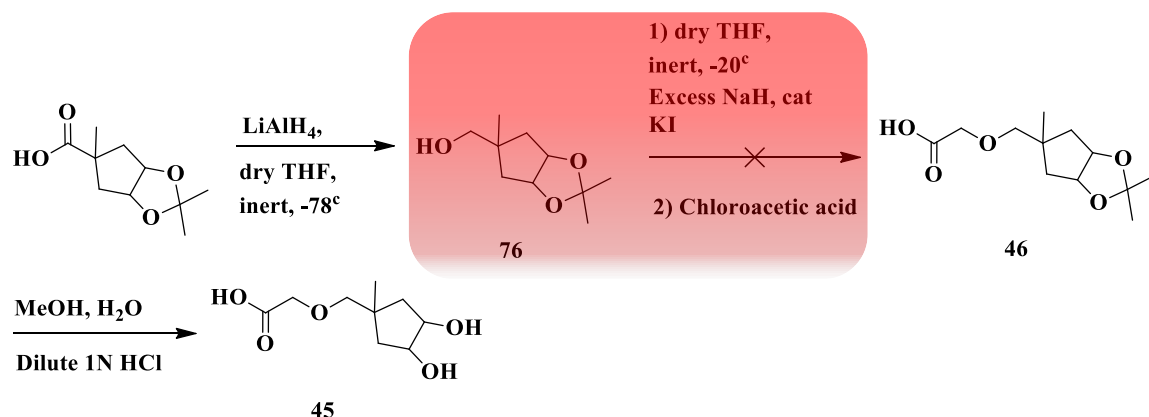
Acetonide protected dialdehyde headgroup could be conveniently installed on any reporter molecule (presented by a purple star) and made available through a simple deprotection step. A biomolecule armed with a primary amine could effectively conjugate to this complex and detected using the appropriate analytical method.

Substance **45** allowed for a convenient conversion of the carboxylic acid moiety to many different substituents that could carry another reporter (**Scheme 3-25**). To ensure a long-term storage ability, the 1,2 diol moiety was protected with acetonide to afford molecule **46**, which could be stored indefinitely and converted into fresh dialdehyde for experimentation. A triazole-activated carboxylic acid of substrate **46** is also stable enough to be stored for a long period of time, which makes it a unique precursor for subsequent reactions. In particular, any carrier molecule armed with an amine could form an amide bond with the substrate that remains to be robust under physiological conditions. Once the target substrate is made, the dialdehyde headgroup could be easily synthesized through



quick deprotection, followed by oxidative cleavage of 1,2 diol. Some example reporter molecules are highlighted in the next subsection.

It is noteworthy to mention that in parallel attempts, precursor olefin was first converted to a 1,2 diol, then protected with acetonide and reduced to afford a primary alcohol (**Scheme 3-26**). In spite of higher yield obtained in overall product, its bulky anion has greater chance to participate in *E2* reactions rather than  $S_N2$ . Although 2-chloroacetic acid does not allow for any elimination reaction, nucleophilic substitution is also not a favoured process. For this reason, it could not be used for subsequent reactions.



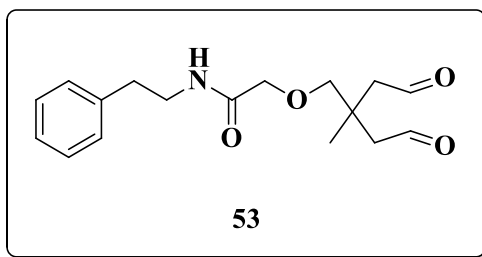
*Scheme 3-26 Alternative synthetic proposal to generate substrate 45*

Generation of a bulky anion will be a hindered nucleophile that does not serve well as an accessible nucleophilic center.

### 3.2.5 Kinetic Study

Our conjugation system is designed to serve in tandem with other biological structures and chemical machinery, thus it is very important to ensure that it delivers the purpose rapidly tuned with other biological reactions under physiological condition. An

amphiphilic model substrate **53** was synthesized to investigate the kinetics of this system in organic ( $\text{CDCl}_3$ ) and the aqueous ( $\text{D}_2\text{O}$ ) environment.



Although compound **53** contains an aromatic ring, it is readily soluble in water at room temperature. This unique and powerful physical property of **53** enabled us to mimic the behavior of dialdehyde head group and its reactivity in aqueous solutions. Other substrates that would allow for a thorough investigation in both aqueous and organic solvent would entail installation of a PEG moiety, which adds enormous synthetic complexity and inconvenience in the purification of dialdehyde.

The kinetic studies (**Figure 3.34**, **Figure 3.35**) were carried out through a pseudo-first order reaction using propylamine as a nucleophile to annulate into the 1,4-dihydropyridine ring. Kinetic parameters were obtained by monitoring the disappearance of the dialdehyde peaks after 25 seconds and growth of the vinylic peaks over 3.3h. The aldehydic region is omitted in this figure as it collapses rapidly within seconds of the reaction.

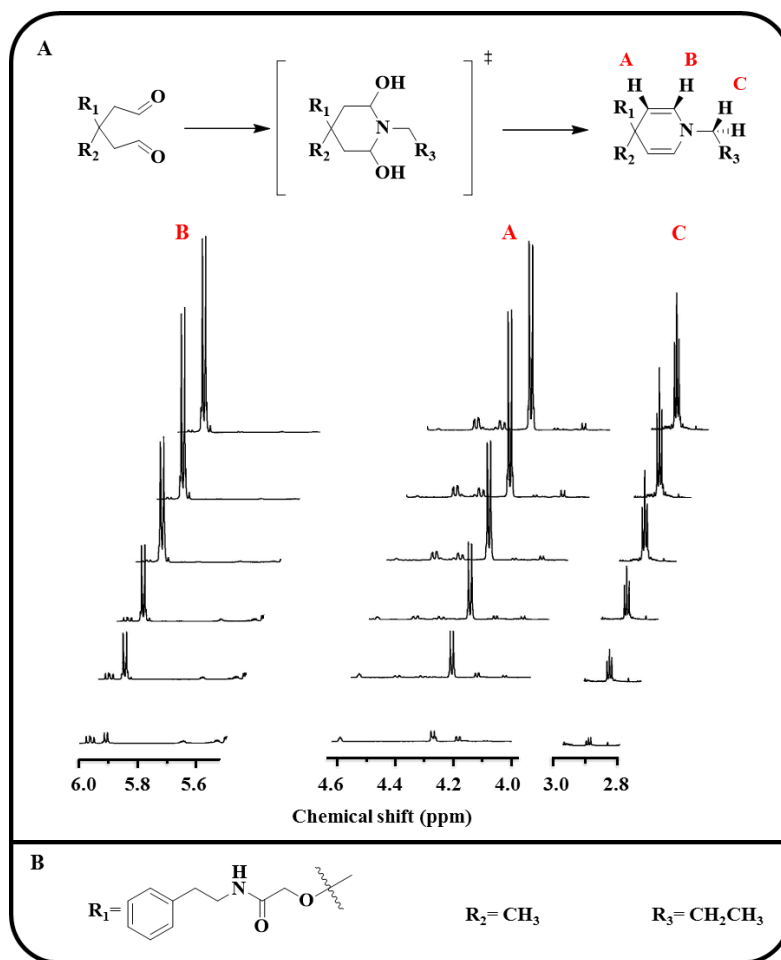
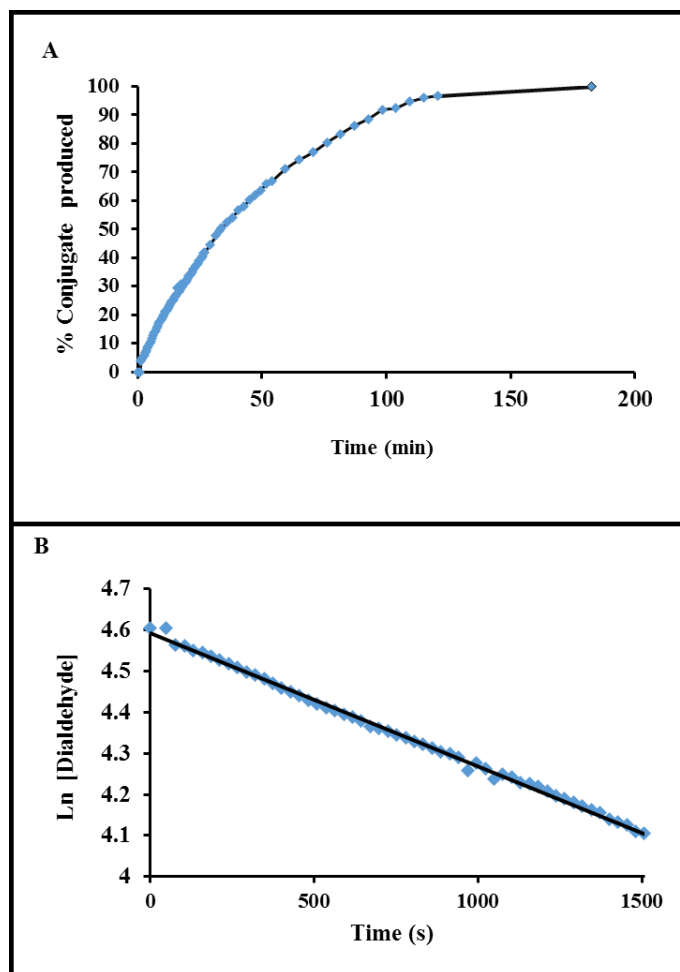


Figure 3.34 Pseudo first order reaction of substrate 53 with propylamine

A 50 mM solution of molecule 53 was reacted with 10X excess sacrificial model propylamine in  $\text{CDCl}_3$  and analyzed using a 700 MHz NMR over 180 minutes at room temperature in NMR tube. The reaction progress reveals a rapid initial nucleophilic addition of the amine to a carbonyl, followed by the second intramolecular addition to forming a 6-membered hydrated dihydropyridine ring. The aldehydic peaks were fully consumed within seconds of initiation, followed by immediate formation of the distinctive enamine peaks and N-alpha protons on the conjugate. The mechanism suggests a rapid elimination of water to form the stable saturated dihydropyridine with a short half-life of 30 minutes.



*Figure 3.35 Plot of 1,4dihydropyridine formation through enamine peak monitor*

A sustainable bioconjugation is achieved within seconds of the reaction indicated by the disappearance of carbonyl peaks. Any intermediate formed would rapidly proceed to lose the element of water and form a dihydropyridine ring. The graph is drawn based on observing the appearance of the vinylic protons and alpha amino protons.

Since the reaction is extremely fast, obtaining meaningful data points using aldehydic peaks is not plausible. It is evident that a successful ligation is established rapidly to sustain a conjugation with targeting nucleophile. This affords an intermediate that would

eventually transform into a 1,4 dihydropyridine ring. However, structural elucidation of the actual intermediate formed is a difficult proposition and depends on postulated mechanisms for the reaction. Formation of carbinolamine or imine are two credible routes, but both remain to be merely a speculation. Since the determination of the actual structure is not within the scope of our research, further investigation was halted. Peaks representing the vinylic protons reach their half-life within the first 30 minutes of exposure to propylamine and reached maximum abundance at 100 minutes. However, it is important to recognize that a successful viable ligation is achieved within the first 25 seconds of reaction (**Figure 3.36**).

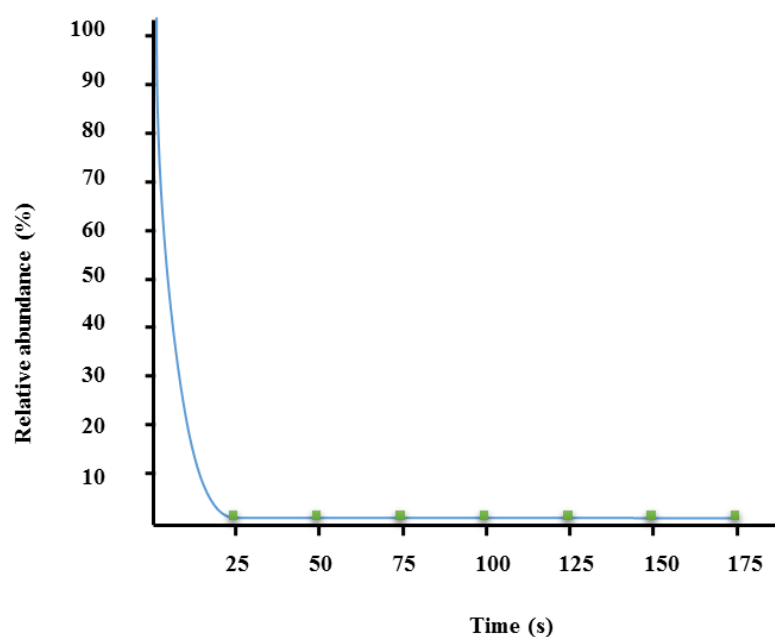


*Figure 3.36 Graph of carbonyl consumption over 175 seconds of nucleophilic addition*

The aldehydes are completely consumed within the first 25 seconds of nucleophile exposure. Although conjugation of dialdehyde moiety is very fast, the transformation of any intermediate into a final product is a relatively longer process.

In 1974 Sayer et al<sup>276</sup> have conducted a very thorough study on the formation of carbinolamines in the reaction of a primary amine with substituted benzaldehydes. They revealed that pH plays a major role in the kinetics and the mechanism of product formation; hence they focused on kinetics and structural reactivity of the carbonyl molecules at various pH conditions. Their data suggests two different pathways of reaction: **(I)** At relatively lower pH ranges below 7, a general nucleophilic addition of a reactive amine to carbonyl through a concerted mechanism under acid catalysis is believed to be plausible, whereas, **(II)** a formation of a zwitterionic intermediate is more favoured in a stepwise uncatalyzed addition reaction, followed by a proton transfer facilitated by water or other proton sources. The reaction of a weakly basic amine, the hydronium catalyzed process in the formation of the carbinolamine, is more credible through the pathway (I) and remains independent of the polarity of the substituents on the reactants. In contrast, for stronger attacking amines with larger rate constants, the intermediate is rapidly stabilized by the “proton switch” from the quaternary amine, which is proven highly sensitive to the polarity of the electrophile. It is noteworthy to mention that formation of carbinolamine is only plausible in an aqueous environment where most double bonds between N and C are hydrated. Changing the solvent to some organic would result in the formation of imine bonds. In contrast to a primary amine, nucleophilic substituted amines would generate an enamine compound, which is less stable than an imine bond. Lack of any hydrogens on the nitrogen atom in the carbinolamine makes the imine formation an impossible option. Alternatively,  $\alpha$ -hydrogen to carbonyl would stabilize the intermediate and facilitate the  $\beta$ -elimination to secure a  $\pi$ -bond.

A pH profile study was conducted to investigate the effect of different acidic/basic environment on the reversibility feature of the system (**Figure 3.37**). It is evident that the 1,4-dihydropyridine rapidly hydrolyzes within seconds to release the conjugated amine, while it remains stable at higher pH ranges for an extended period of time. Such superior stability of the conjugate structure makes this system a good strategy for payload delivery and prolonged biological applications that require a robust link but also depend on reversibility to release the payload messenger.

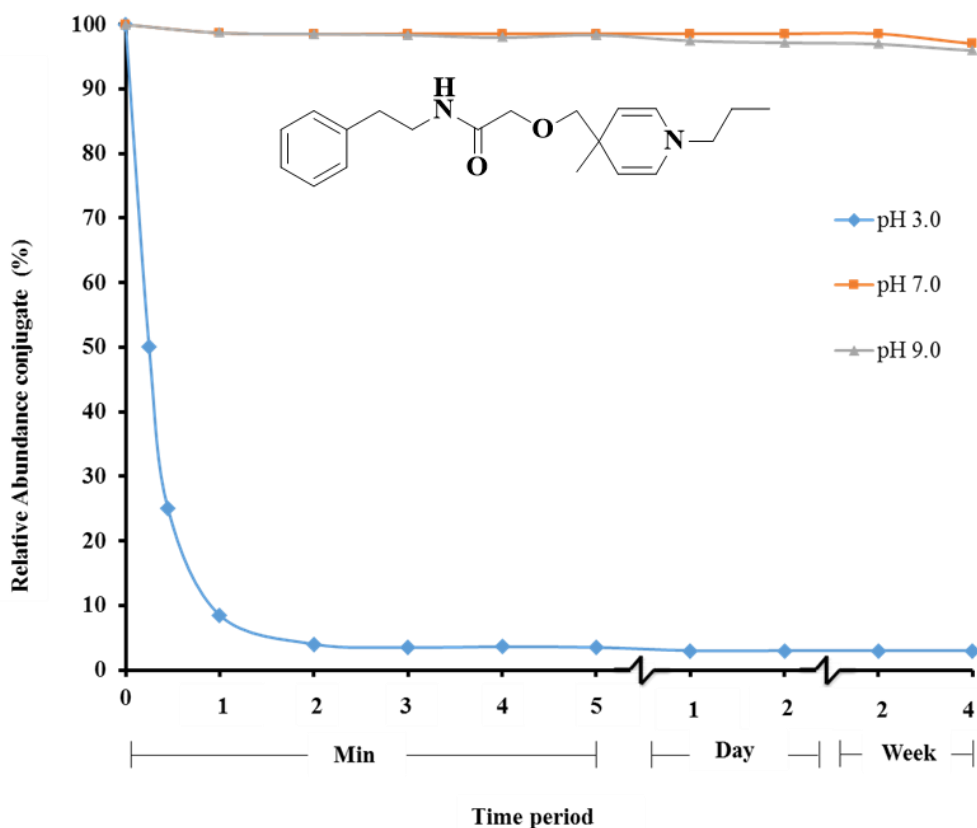


*Figure 3.37 Examination of dialdehyde conjugate stability with pH changes over extended time*

The effect of pH was investigated on the conjugate formed in the kinetic experiment over three ranges of pH spectrum. The stability of the product was carefully monitored over one month by observing the persistence of key peaks and formation of other residual signals. The conjugate rapidly undergoes hydrolysis under acidic conditions to form the starting material, while it remains highly stable at higher pHs over months.

Since the dienamine collapses within seconds of acid treatment, a closer look at a shorter period was necessary to establish the abundance of the reverse product. (Figure 3.38) demonstrates the stability of the conjugate at different pH ranges after 3 minutes of exposure to  $H^+/OH^-$ . The concentration of the conjugate decreases to 10 % of its original amount within 3 minutes.

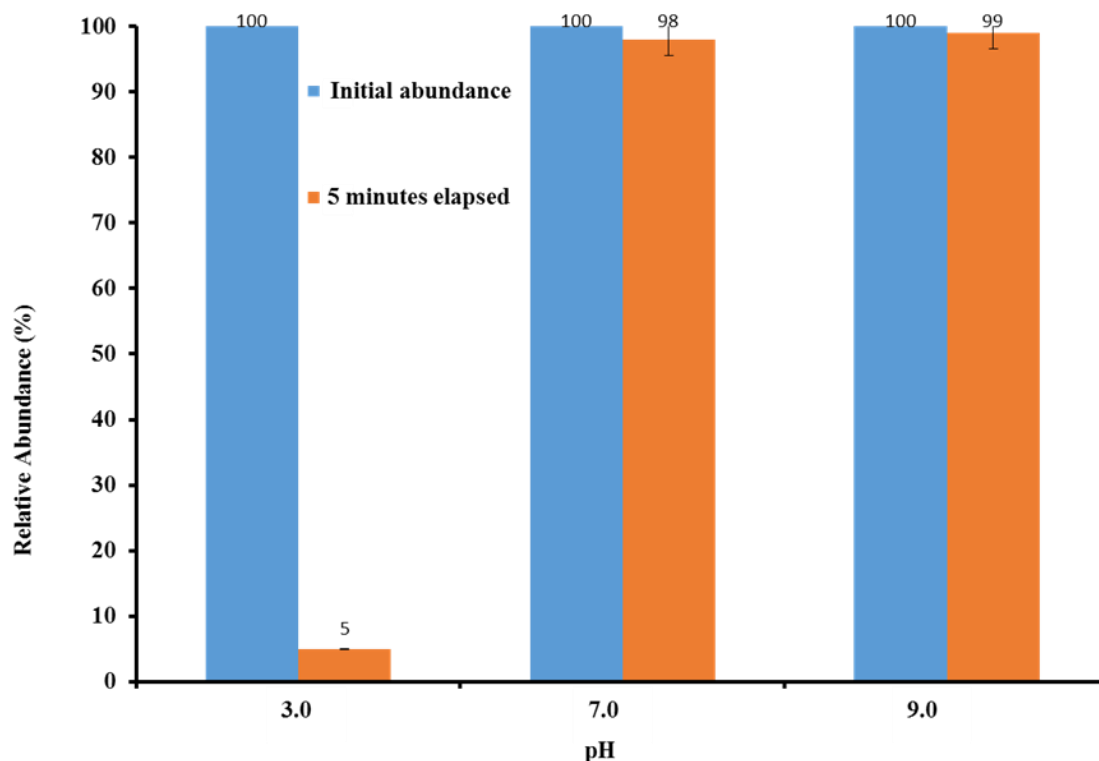


*Figure 3.38 Examination of dialdehyde conjugate stability with pH changes after 5 minutes*

Lowering pH initiates the reverse process of breaking enamine bonds to release the primary amine and possibly regenerate the starting material aldehyde. However, higher pH ranges remain ineffective towards any chemical changes

It is important to replicate the analysis in aqueous solutions; however, conducting kinetic studies in  $D_2O$  would suffer from hydration/deuteration of both enamine bonds.



This will make the vinylic enamine peaks unavailable for rate diagnosis (**Figure 3.39**). The disappearance of the aldehyde would also be seriously affected by hydrated conformations that could skew the results. The only useful peak for screening would be the accumulation of the corresponding signal to  $\alpha$ -proton on attacking amine.

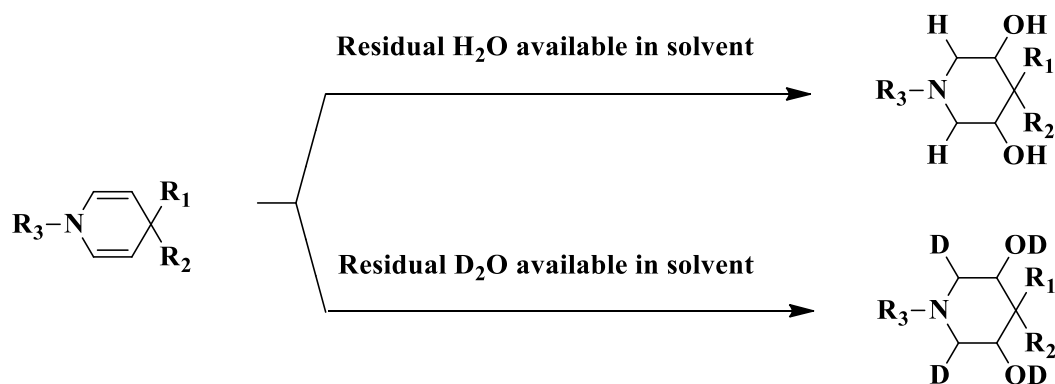


*Figure 3.39 Effect of protonation/ deuteration of enamine moieties of 1,4-dihydropyridine conjugate*

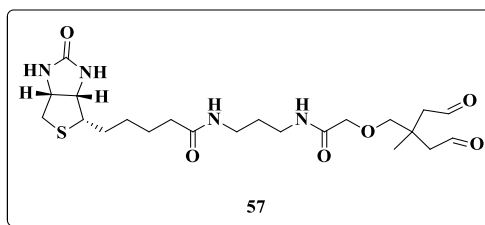
Exposure of a 1,4 dihydropyridine conjugate ring to a protonating solvent will result in the formation of a hydrate structure that would restrict a proper and unambiguous detection of vinylic protons via NMR spectroscopy.

Stability of synthesized dialdehyde molecules used in this study is often compared against a commercially available glutaraldehyde in aqueous solution. Unlike a simple glutaraldehyde that could serve as a multipurpose crosslinking reagent, the molecules synthesized in this work are generally chemically different from one another, therefore are designed for dissimilar applications. While the backbone of the structure remains somewhat consistent, the carrier tail away from dialdehyde headgroups is designed for a distinctive task. For that reason, the stability of the molecules may slightly vary among the same class of molecule. The overall stability of such substrates has been investigated by

$^1\text{H}$ -NMR,  $^{13}\text{C}$ -NMR, MS and monitoring the successful downstream conjugation in biological settings. The stability and durability of the final product are also investigated using  $^1\text{H}$ -NMR,  $^{13}\text{C}$ -NMR and MS over 6 months for sustaining the molecular integrity of a 1,4-dihydroxyridine moiety in an organic solvent. The stability of the product **54** was also considered at three pH's of 3.0, 7.0 and 9.0 over one month in both organic and aqueous solvents.

### 3.2.6 Synthesis of Small Organic Reporter Molecules

The compelling evidence for an effective conjugation using substrate **46** as a template was adequate for biological applications in which, all requirements for establishment of a robust bio-conjugation was satisfied. Resolving all uncertainties and addressing questions regarding the suitability of a method for an effective conjugation system, we shifted the focus from characterization towards producing more practical molecules for *in-vivo* applications. There is a vast pool of molecules that could be armed with a dialdehyde warhead. Medical imaging probes, immunoassay ligands, fluorescent reporters, immobilization factors, nanotubes and colloids, oligosaccharide antigens, nucleic acids, synthetic polymers, antibodies, crosslinking bridges, stapling polymers are only some of the examples and much more that would simply overwhelm the field. We chose to focus on relatively modest probes through which, we found great utility in our own multidisciplinary field of research. Biotin, DNP, FITC, and peptides were the first class of molecules we attempted to arm with our amine coupling molecules. Despite many efforts, due to time restraints and laboratory limitations, only the first two on the attempted list could be successfully synthesized.



Synthesis of a biotin-dialdehyde is one of the greatest synthetic challenges in this work with the limited available analytical and purification techniques. There are many reported protocols that afford an elegant modification of a biotin molecule for click chemistry, bio-conjugation or protein studies; however, isolation of such products requires advanced analytical resources such as HPLC or prep-column chromatography. Even then, the product is often obtained in very small amount, only enough for reduced number of *in-vivo* experiments.

Formation of an amide linkage between a commercially available biotin-cadaverine HCl salt and substrate **46** proceeds through the generation of an activated *N*-hydroxytriazole ester with the carboxylic acid handle. Most previous amidation reactions were conducted in DCM/ACN, but biotin cadaverine is insoluble in most organic solvents including those with high dielectric constants like DMF and DMSO. Surprisingly the reaction proceeds with no problem in MeOH/ACN mixture in alkaline conditions. Although neutral MeOH could serve as a moderate competing nucleophile towards highly reactive electrophiles, keeping the temperature and addition of the amine simultaneously with *N*-hydroxy triazole would minimize the effect of solvolysis of any kind. Synthesis of **57** posed another major problem during which, sulfur-containing substrates could easily oxidize to their higher oxidation states. The oxidative cleavage step of 1,2 diols is bound to generate sulfoxide and sulfone. Therefore, purification of such molecules becomes

inevitably impossible using the conventional methods available in our laboratory practice. In addition to purification challenges, depending on the stoichiometry of oxidizing agent, multiple species of the product could be afforded in a mixture of sulfide oxidation state variations. Although this particular concern could be rectified through the use of an excess oxidizing agent, the purification challenges remain in effect. In addition to synthetic obstacles, we assumed an even more serious challenge concerning the biological activity of biotin sulfone/sulfoxide's and their affinity towards the corresponding Avidin molecules.

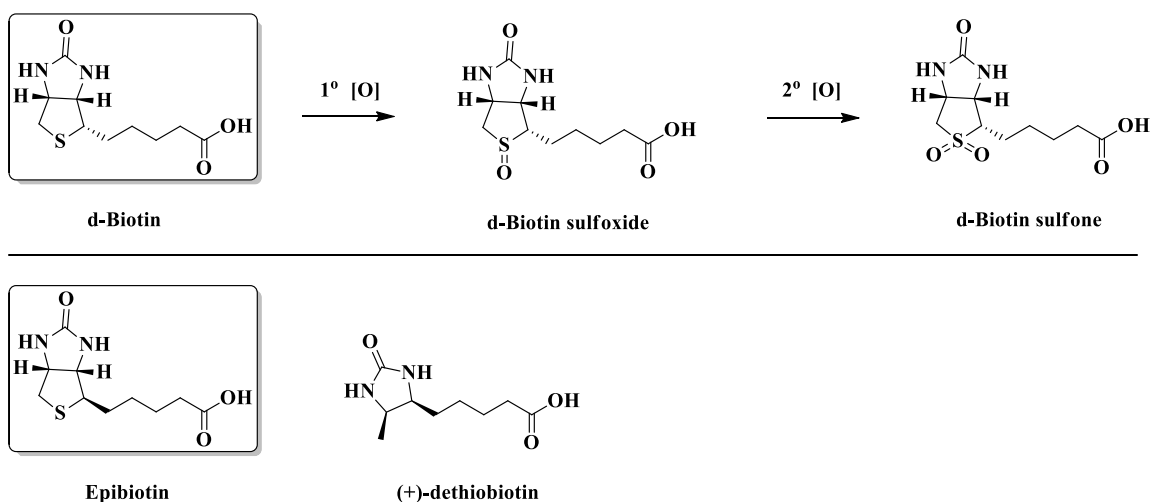


*Figure 3.40 Different variations of biotin molecule with different oxidation state of S*

The binding affinity of a biotin molecule decreases with increasing oxidation state of S, however, there is still a substantial affinity for *d*-biotin sulfone. Such variations are so subtle that a complete removal of S from the parent structure will still result in a sustainable attraction with protein pocket.

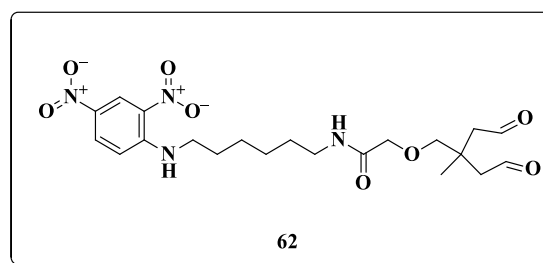
However, there is an abundance of research conducted investigating the differences in binding affinity for streptavidin among biotin sulfide, sulfoxide and sulfone variations

(Figure 3.40). Surprisingly, while the parent molecule biotin sulfide has the highest affinity for streptavidin  $10^{-14}$  mol/L,<sup>277</sup> other oxides are not significantly lower either. However, the difference between *R* and *S* stereochemistry of any biotin oxide becomes decisive in their ability to find the proper orientation within the binding pocket. Bolbach et al have conducted an extensive study on the variation for binding ability and efficiency of different derivatives synthesized from the parent biotin molecule.<sup>278</sup> they have reported that (*S*) absolute configuration at C6',  $\alpha$  to -S heteroatom is essential for high-affinity binding to Avidin class of biomolecules. Once biotin/protein interaction is established in the binding pocket, the tetrahedral oxyanion generated is rapidly stabilized through interaction with amino acid residues. The superior affinity of streptavidin for biotin lies in the ability of the complex to overcome the oxyanion charge. Surprisingly, the -S atom does not take vital role in such attractions as both dethiobiotin and sulfone analogs still bind with reasonable  $K_d$  constants of  $5 \times 10^{-13}$  and  $10^{-13}$  respectively.<sup>277</sup>

Antibody recruiting molecules (ARM) are another attractive class of substrates in biology for their applications in both biotechnology and other therapeutic purposes. DNP or Sanger's reagent is a useful example of ARM molecule that was initially used as a staining probe for nucleophilic moieties in biological settings. It was first used in 1945 by Frederick Sanger,<sup>279</sup> who demonstrated its ability to probe the N-terminal amino acid in polypeptide chains, in particular, insulin molecules. its structure and ability to serve as a probe was explored in the later years in great detail using NMR spectroscopy.<sup>280–282</sup> Other non-therapeutic applications of DNP could be exploited in dye, pesticide and other industrial applications; but perhaps it is most valuable to this work for its unique ability to enhance antibody production in a biological environment. Subsequently, it has proven to

be an effective probe that is easily recognized by other monoclonal antibodies in molecular experiments.<sup>283–287</sup> DNP or its analogous derivatives are found naturally in living cells and participate in ionophore proton transfer processes across the membrane. It's essential role in biological environments makes it a good probe for synthetic modifications and improved utility in biotechnology.

A DNP molecule was tethered to an amino linker in a mixture of MeOH/H<sub>2</sub>O solvent in presence of bicarbonate. Since the amino linker precursor is essentially a homobifunctional amino molecule, it either should be protected at one end or should be already available in a reaction vessel, to which, DNP is slowly added.



The product would be the anion salt of aniline and must be reprotonated with dilute acid to cationic salts for purification purposes. It could then be coupled with **46** to generate substrate **60** in reasonable yields. Substrate **60** is then treated with dilute acid in MeOH to afford **61** and oxidized to the corresponding dialdehyde **62**. Although excess periodate could presumably oxidize the amide bond to *N*-oxide, no evidence supporting this side reaction was observed in the NMR spectrum. The dialdehyde substrate **62** was conjugated to propylamine to demonstrate its ability to trap an attacking amine and form the expected 1,4-dihydropyridine. The <sup>1</sup>H-NMR spectrum confirms an effective ligation to the attacking amine and displays the characteristic enamine peaks at 4.181 and 6.946 ppm in the

spectrum. There is no evidence of imine formation even at higher concentrations of an amino group, which reiterates the efficiency in ligation to a stable annulated conjugate. The growth of a triplet at 3.091 ppm, correlating with an alpha proton on the attacking amine, is another event in the spectrum that helps to monitor the reaction progression.

In an attempt to expand this suite of small reporter molecules, we tried to synthesize FITC-dialdehyde using FITC-amine precursors. However, the aniline type substituents on a FITC dye is considered to be very poorly nucleophilic, due to resonance stabilization of the lone pair if amine electrons, thus do not participate in nucleophilic additions effectively. The analog 5-FAM-cadaverine offers a much better primary nucleophilic amine residue (**Figure 3.41**). Despite our attempts, there are not much convincing evidence that a nucleophilic substitution has occurred towards the formation of an amide bond with substrate **46**. In addition to synthetic challenges, purification of such delicate compounds would also require alternatives that are more advanced.

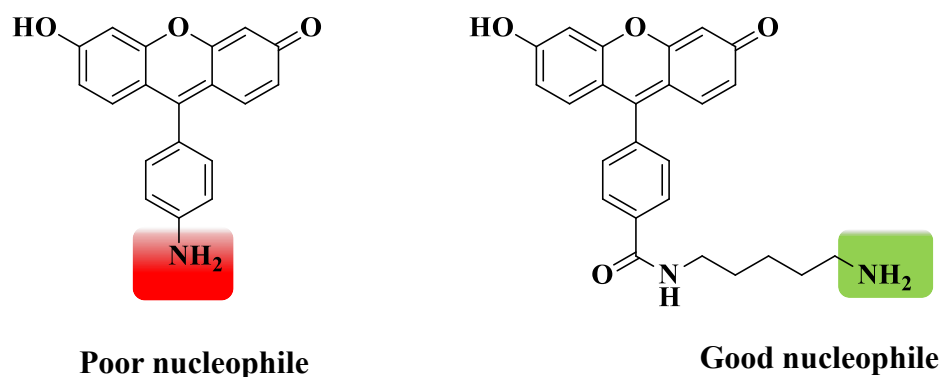
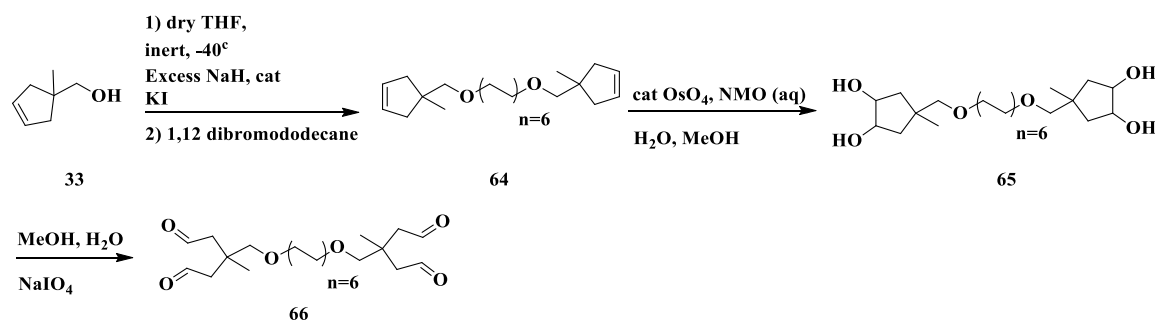


*Figure 3.41 Comparison of fluorescein-amine reporter nucleophilicity*

### 3.2.7 Synthesis of Crosslinker Dialdehyde

Motivated by the results of an effective ligation strategy, we began to develop methods to extend the utility towards protein conjugation applications. Since crosslinking of macromolecules is an eminent field of study in biotechnology/biochemistry, it inspired us to explore the practicality of our technology in this interesting area.

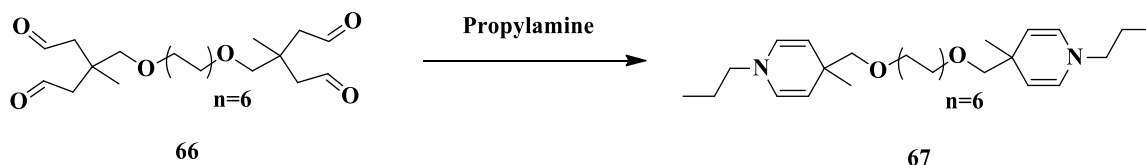


*Scheme 3-27 General synthesis of crosslinker dialdehyde molecule using model substrate Type C*

We designed a homobifunctional crosslinker armed with two dialdehyde centers on either end of the linker (**Scheme 3-27**). The synthesis begins with a nucleophilic substitution of alkoxides of **33**, generated in dry THF under inert pressure and excess NaH at -20°, with the half equivalence of 1,8-dibromododecane in presence of catalytic amount of KI. Although the formation of *E2* product is inevitable with the use of a relatively hindered nucleophile, adding the electrophile at rather low temperatures (ie. -10 to 4°) favours more S<sub>N</sub>2 products. Since the final product **6** is a non-polar analyte, a normal phase chromatography using silica gel is not a very effective purification technique; hence, it was not purified as an isolated product. Substrate **64** was then oxidized to the corresponding diol product **65** and isolated as a mixture of diastereomers.

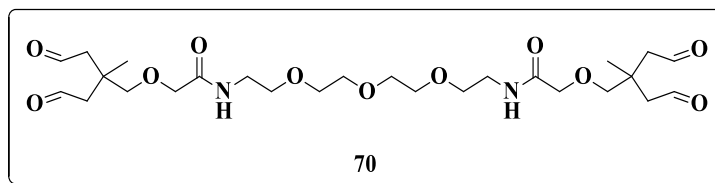


The NMR spectrum of **65** is quite interesting and complex as it's a spectrum obtained from the mixture of isomers with multiple diastereomer centers. Purification of any of those isomers is a dreadful task using conventional normal phase silica gel chromatography. We made multiple attempts to obtain a purified sample of a single isomer to investigate their reactivity based on individual dialdehyde head group, but it was proven to be more challenging to invest much time on. Conversion of **65** to **66** follows our standard protocol using sodium periodate in MeOH/H<sub>2</sub>O at room temperature for 2h. The resulting product was treated with propylamine to obtain two 1,4-dihydropyridines (**Scheme 3-28**).



*Scheme 3-28 Conjugation of crosslinker molecule 66 to propylamine*

Although substrate **66** is a very useful crosslinker, it suffered from poor solubility in aqueous solution, therefore, did not serve as effective as other available crosslinkers with hydrophilic moieties. In order to address solubility concerns, an analogous crosslinker was synthesized with a tetraethylene glycol (TEG) arm.



Using any precursor containing TEG moiety is an intricate task for an organic chemist. Such products are often extremely difficult to purify in reasonable quantities using

normal phase chromatography, and reverse phase chromatography is not always an available resource in laboratory settings using manual flash or gravity systems.

Starting material used in the synthetic route designed to produce **70** was quite different from **66**. In an attempt to synthesize **70** using the similar protocol as **46**, the alkoxides of **33** (-OI) were reacted with a doubly tosylated terminal TEG linker, however, the *E2* products were obtained in higher abundance than  $S_N2$  desired products (**Figure 3.42**). In additions to high yield of side products, TEG arm is a very good cation-coordinating linker that could wind up around its own core to form cyclic coordinated ethers to subsequently make reactive electrophilic centers less accessible for displacement.

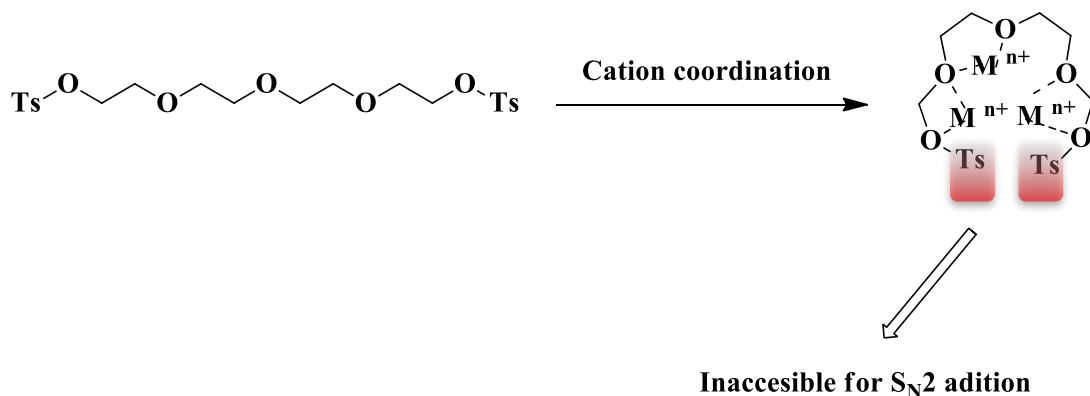
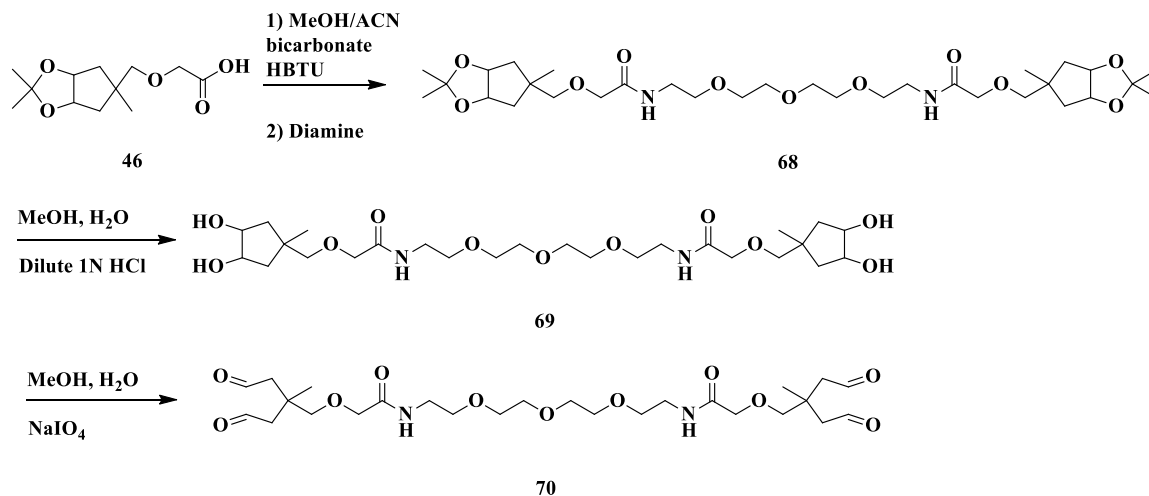


*Figure 3.42 Inactivation illustration of terminal electrophilic centers due to TEG coordination to a cationic species*

Coordination of oxygen with cationic species will result in a coagulated structure that hinders the accessibility of the terminal tosylated parts for nucleophilic substitutions.

Therefore, we sought other alternative methods to generate the same class of crosslinker using our retrosynthetic template **46**. A hydrophilic homobifunctional

crosslinker **70** was successfully synthesized according to (Scheme 3-29) and further conjugated to propylamine to examine its efficiency in trapping a primary amine.



*Scheme 3-29 General synthesis of hydrophilic TEG crosslinker dialdehyde molecule 70 using model substrate Type D*

The successful ligation of crosslinker **70** led to many interesting biological applications, which will be discussed in the following chapter.

In addition to all the systemic approaches in the synthesis of a dialdehyde substrate, there have been many other molecules synthesized, that assisted us in the development of a robust model system. Although some did not eventually deliver the conjugation purpose in biological experiments, they have been an essential part of the research. Despite the failure in obtaining reasonable results in the preliminary model systems A and B, there are also some probes synthesized within the same class of molecules that presented reasonable competitive conjugation *in-vivo*. All of these molecules deserve attention and will be catalogued in the synthesis appendix section, but will not be discussed.

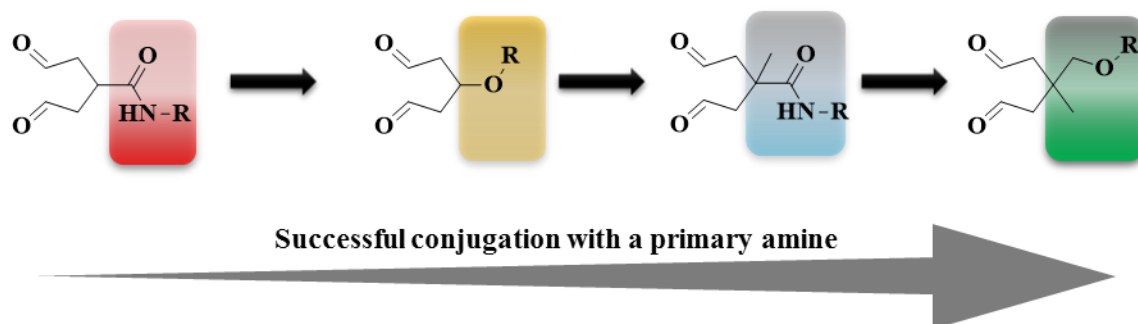


*Figure 3.43 General trend of reactivity for dialdehyde headgroup*

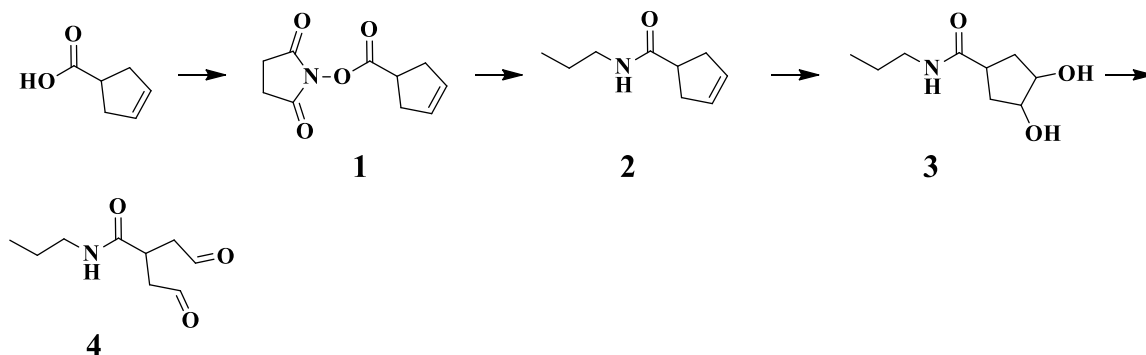
Reducing functionality in the vicinity of the headgroup results in a more clear and higher yield of conjugation.

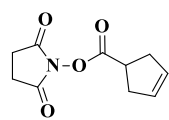
Evolution of the substrates synthesized for trapping a primary amine suggests that as we reduce the functionality around the vicinity of the headgroup, the reactivity of amines towards the trapping hole increases significantly (**Figure 3.43**). Although in many cases a bioconjugation in the context of starting material consumption is achieved, the formation of a characterizable structure is more convincing as we move to the right side of the trend.

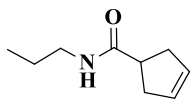
### 3.3 Materials and Method

All reagents and chemical used in the syntheses procedures below are purchased from Sigma Aldrich and characterized by NMR spectroscopy prior to use. The inert atmosphere pressure has been established using 5.0 Argon gas provided by Praxair.

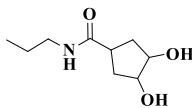
#### 3.3.1 Synthesis of Molecules 1-4



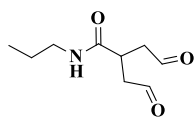
 **2,5-dioxopyrrolidin-1-yl cyclopent-3-enecarboxylate (1).** 3-Cyclopentenecarboxylic acid (0.5000g, 4.45mmol), *N,N'*-Methanetetraylbis[cyclohexanamine] (1.104g, 5.35 mmol, 1.2 eq) and *N*-Hydroxysuccinimide (0.6206 g, 5.35 mmol, 1.2 eq) were all mixed in 50 mL dry DCM and stirred for 6h. DCM was distilled off under vacuum and the mixture was purified with silica Hex:EtOAc (2:8) to afford a white solid (2.60 mmol, 58%). <sup>1</sup>H-NMR (300 MHz; CDCl<sub>3</sub>): δ 5.69 (s, 2H), 3.47-3.36 (m, 1H), 2.84 (s, 4H), 2.17 (s, 2H) ppm.



***N*-propylcyclopent-3-enecarboxamide (2).** To a solution of **(1)** (0.5439 g, 2.60 mmol) in dry DCM was added large excess of propylamine (0.780 g, 0.013mmol). Mixture was stirred for 1h, then concentrated and flushed through a pad of silica to afford white solid (2.34 mmol, , 95%). <sup>1</sup>H-NMR (300 MHz; CDCl<sub>3</sub>): δ 5.70-5.65 (m, 2H), 3.23 (td, *J* = 7.1, 5.9 Hz, 2H), 2.95 (dt, *J* = 16.1, 8.1 Hz, 1H), 2.66-2.59 (m, 4H), 1.59-1.47 (m, 2H), 0.95-0.90 (m, 3H) ppm. <sup>13</sup>C-NMR (300 MHz; CDCl<sub>3</sub>): δ 176.0, 129.2, 77.5, 77.1, 76.6, 43.6, 41.2, 37.0, 22.9, 11.3 ppm. HRMS Anal. Calcd for C<sub>9</sub>H<sub>15</sub>NO 154.1232 (m/z). [M<sup>+</sup>] Found: 154.1219(m/z).

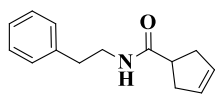
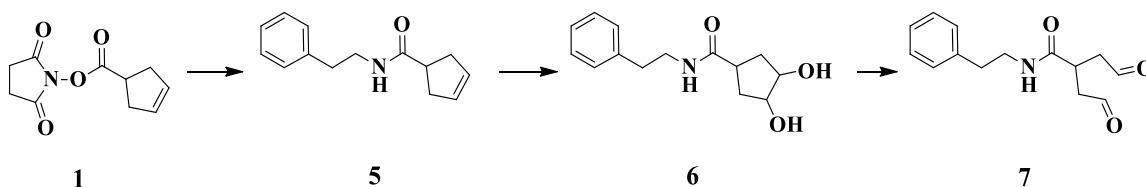


***3,4*-dihydroxy-*N*-propylcyclopentanecarboxamide (3).** To a solution of **(2)** (0.3585 g, 2.34 mmol) in acetone: acetonitrile (1:1) was added catalytic amount of OsO<sub>4</sub> and excess *N*-Methylmorpholine *N*-oxide 50% in H<sub>2</sub>O. Reaction was monitored with TLC for complete disappearance of starting material. Solvent was distilled off under vacuum and the product was taken into diethyl ether and dried over MgSO<sub>4</sub>, further two separate diastereomers were purified with silica Hex:EtOAc (3:7) to afford white solid (2.106 mmol, 90%) <sup>1</sup>H-NMR (700 MHz; MeOD) Isomer I: δ 4.10 (dd, *J* = 4.7, 3.9 Hz, 2H), 3.11 (t, *J* = 7.1 Hz, 2H), 3.01-2.98 (m, 1H), 1.95-1.91 (m, 2H), 1.89-1.85 (m, 2H), 1.50 (sextet, *J* = 7.2 Hz, 2H), 0.91 (t, *J* = 7.4 Hz, 3H) ppm. <sup>1</sup>H-NMR (700 MHz; MeOD) Isomer II: δ 3.94-3.92 (m, 2H), 3.31 (dt, *J* = 3.3, 1.7 Hz, 1H), 3.12 (t, *J* = 7.1 Hz, 2H), 2.72 (tt, *J* = 9.3, 6.5 Hz, 1H), 2.12 (dddt, *J* = 13.9, 6.9, 4.7, 2.3 Hz, 2H), 1.81-1.77 (m, 2H), 1.51 (dd, *J* = 14.3, 7.3 Hz, 2H), 0.92 (t, *J* = 7.4 Hz, 3H) ppm. <sup>13</sup>C-NMR (700 MHz; MeOD): δ 178.06, 178.04, 73.5, 40.9, 40.2, 34.3, 22.2, 10.26, 10.24 ppm. HRMS Anal. Calcd for C<sub>9</sub>H<sub>17</sub>NO<sub>3</sub> 250.1443 (m/z). [M<sup>+</sup>] Found: 250.1431 (m/z).

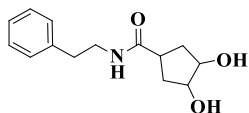


**4-oxo-2-(2-oxoethyl)-N-propylbutanamide (4).** To a solution of **(3)** (0.3940 g, 2.106 mmol) in H<sub>2</sub>O:methanol (1:9) was added NaIO<sub>4</sub> (0.4504 g, 2.106 mmol). Mixture was stirred for 1h until a flakey white, solid iodate salt, was obtained. Solvent was distilled off under vacuum and the product was taken into diethyl ether and dried over MgSO<sub>4</sub> and used for subsequent reactions.

### 3.3.2 Synthesis of Molecules 5-7

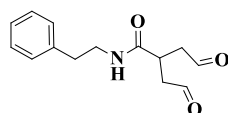


**N-phenethylcyclopent-3-enecarboxamide (5).** To a solution of **(1)** (0.04162 g, 0.198 mmol) in water and sodium bicarbonate(excess) was added Phenethylamine (0.0221 g, 0.1824 mmol, 1.1 eq). Mixture was stirred for 1h, then concentrated and flushed through a pad of silica to afford white solid (0.165 mmol, 83%).  
<sup>1</sup>H-NMR (400 MHz; CDCl<sub>3</sub>): δ 7.34-7.20 (m, 5H), 5.67 (d, *J* = 5.7 Hz, 2H), 3.54 (q, *J* = 6.5 Hz, 2H), 2.87 (dt, *J* = 26.1, 7.5 Hz, 3H), 2.59 (d, *J* = 8.0 Hz, 4H) ppm. <sup>13</sup>C-NMR (400 MHz; CDCl<sub>3</sub>): δ 176.0, 139.0, 129.2, 128.8, 126.4, 77.5, 77.1, 76.8, 43.5, 40.7, 35.7 ppm.  
 HRMS Anal. Calcd for C<sub>14</sub>H<sub>17</sub>NO. 216.1388 (m/z). [M<sup>+</sup>] Found: 216.1374 (m/z).



**3,4-dihydroxy-N-phenethylcyclopentanecarboxamide (6).** To a solution of **(5)** (0.4257 g, 0.198 mmol) in acetone: acetonitrile (1:1)

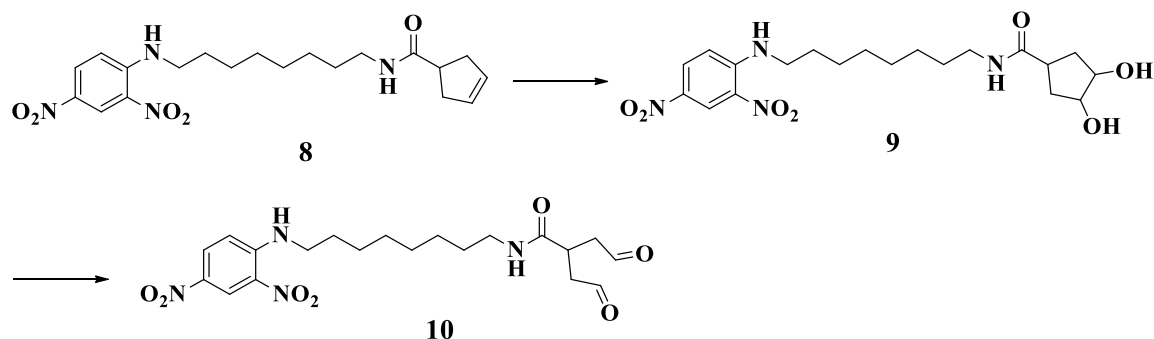
was added catalytic amount of OsO<sub>4</sub> and excess *N*-Methylmorpholine *N*-oxide 50% in H<sub>2</sub>O. Reaction was monitored with TLC for complete disappearance of starting material. Solvent was distilled off under vacuum and the product was taken into diethyl ether and dried over MgSO<sub>4</sub>, further the product was isolated as white solid. (0.148 mmol, 58 %) <sup>1</sup>H-NMR (300 MHz; MeOD): δ 7.32-7.19 (m, 6H), 4.10 (t, *J* = 4.2 Hz, 2H), 3.42-3.31 (m, 2H), 2.96 (s, 1H), 2.79 (t, *J* = 7.3 Hz, 2H), 1.87 (tdd, *J* = 6.9, 4.1, 2.7 Hz, 4H) ppm. <sup>13</sup>C-NMR (300 MHz; MeOD): δ 177.4, 139.1, 128.4, 128.0, 125.9, 73.55, 73.48, 48.4, 48.2, 47.9, 47.3, 47.0, 46.7, 40.6, 40.2, 35.1, 34.43, 34.26 ppm.



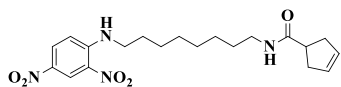
*N*-benzyl-4-oxo-2-(2-oxoethyl)butanamide (**7**). To a solution of (**6**) in

H<sub>2</sub>O:methanol (1:9) was added NaIO<sub>4</sub>. The mixture was stirred for 1h until a flakey white, solid iodate salt, was obtained. The solvent was distilled off under vacuum and the product was taken into diethyl ether and dried over MgSO<sub>4</sub> and used for subsequent reactions.

### 3.3.3 Synthesis of Molecules 8-10

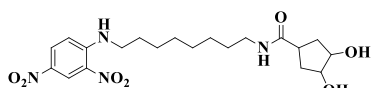






***N*-(8-(2,4-dinitrophenylamino)octyl)cyclopent-3-enecarboxamide (8)**

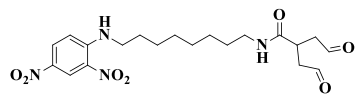
To a solution of *N*<sup>1</sup>-(2,4-dinitrophenyl)octane-1,8-diamine (0.5000 g, 1.2376 mmol) (**1**) in MeOH was added (0.2845 g, 1.361 mmol, 1.1eq) of (**1**). Mixture was stirred for 1h, then concentrated and flushed through a pad of silica to afford yellow solid (1.076 mmol, 87%). <sup>1</sup>H-NMR (700 MHz; MeOD): δ 9.06 (t, *J* = 2.3 Hz, 1H), 8.32-8.30 (m, 1H), 7.18 (d, *J* = 9.6 Hz, 1H), 5.66 (s, 2H), 3.51 (t, *J* = 7.2 Hz, 2H), 3.19 (t, *J* = 7.1 Hz, 2H), 3.03-3.00 (m, 1H), 2.61-2.55 (m, 4H), 1.77 (dt, *J* = 14.7, 7.4 Hz, 2H), 1.54-1.36 (m, 10H) ppm. <sup>13</sup>C-NMR (700 MHz; MeOD): δ 177.3, 148.4, 129.7, 128.6, 123.4, 114.3, 47.99, 47.87, 47.75, 42.92, 42.87, 39.0, 36.6, 29.00, 28.87, 28.83, 28.3, 26.49, 26.43 ppm.



***N*-(8-(2,4-dinitrophenylamino)octyl)-3,4-dihydroxycyclopentanecarboxamide (9)**

To a solution of (**8**) (0.4347 g, 1.076mmol) in acetone: acetonitrile (1:1) was added catalytic amount of OsO<sub>4</sub> and excess *N*-methylmorpholine *N*-oxide 50% in H<sub>2</sub>O. Reaction was monitored with TLC for complete disappearance of starting material. Solvent was distilled off under vacuum and the product was taken into ethyl acetate and dried over MgSO<sub>4</sub>, further purified with silica Hex:EtOAc (3:7) to afford two separate diastereomers as yellow solid (0.7854 mmol, 73%) <sup>1</sup>H-NMR (700 MHz; MeOD) Isomer I: δ 9.06-7.17 (m, 3H), 4.13-4.11 (m, 2H), 3.50 (t, *J* = 7.2 Hz, 2H), 3.16 (d, *J* = 14.2 Hz, 2H), 3.01-2.99 (m, 1H), 1.96-1.86 (m, 4H), 1.77 (dt, *J* = 14.7, 7.4 Hz, 2H), 1.53-1.35 (m, 10H) ppm. <sup>1</sup>H-NMR (700 MHz; MeOD) Isomer II: δ 9.05-7.17 (m, 3H), 3.95 (tt, *J* = 4.1, 1.9 Hz, 2H), 3.50 (t, *J* = 7.2 Hz, 2H), 3.17 (t, *J* = 7.1 Hz, 2H), 2.74-2.72 (m, 1H), 2.15-2.11 (m, 2H), 1.82-1.76 (m, 4H), 1.53-1.36 (m,

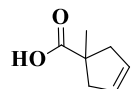
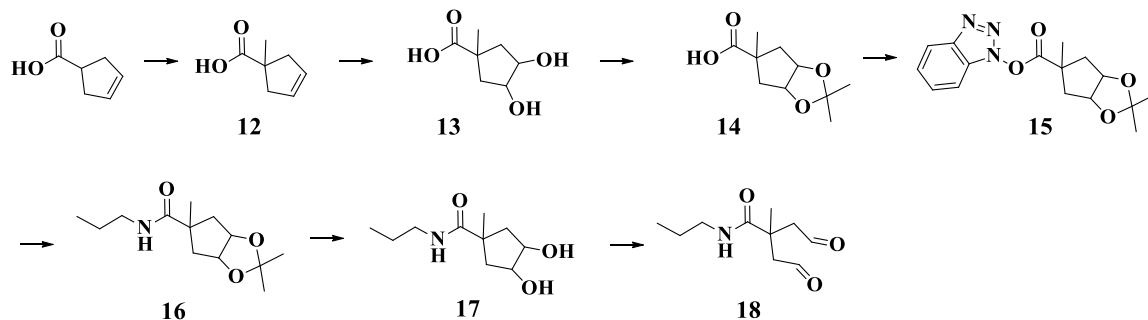
10H) ppm.  $^{13}\text{C}$ -NMR (700 MHz; MeOD):  $\delta$  177.4, 148.3, 135.4, 129.7, 123.4, 114.3, 73.6, 47.9, 42.9, 40.3, 39.0, 34.5, 28.96, 28.87, 28.82, 28.3, 26.49, 26.42 ppm.



*N*-(8-(2,4-dinitrophenylamino)octyl)-4-oxo-2-(2-oxoethyl)butanamide (**10**) To a solution of (**9**) in

H<sub>2</sub>O:methanol (1:9) was added NaIO<sub>4</sub>. The mixture was stirred for 1h until a flakey white, solid iodate salt, was obtained. The solvent was distilled off under vacuum and the product was taken into methanol and dried over MgSO<sub>4</sub> and used for subsequent reactions.

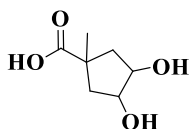
### 3.3.4 Synthesis of Molecules 12-19



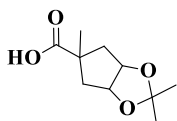
*1-methylcyclopent-3-enecarboxylic acid* (**12**). To a solution of cyclopent-3-enecarboxylic acid (0.5000 g, 4.459 mmol) in 50 mL dry THF at -78 °C under

inert atmosphere was added *t*-butyl lithium 1.7 M (9 mL, 13.37 mmol, 3 eq) over 1h. The mixture was stirred at the same temperature for an additional 30 minutes until dianion is successfully generated, then excess iodomethane was added gently. A white precipitate forms and produces a suspension which dissolves at higher temperature overnight. The

mixture is quenched by 1 mL of H<sub>2</sub>O and stirred for 15 minutes, then THF is stripped off under vacuum and remaining crude is diluted with DCM. The organic solution was filtered and washed with H<sub>2</sub>O (6 x 50 mL), saturated NH<sub>4</sub>Cl (3 x 50 mL), and H<sub>2</sub>O (2 x 50 mL), dried over MgSO<sub>4</sub>, and purified with silica Hex:EtOAc (2:8) to afford a clear oil solid (3.121 mmol, 70%), repeating the experiment on the crude will yield 100% product. <sup>1</sup>H-NMR (700 MHz; CDCl<sub>3</sub>): δ 5.64 (s, 2H), 2.98 (d, *J* = 14.7 Hz, 2H), 2.28 (d, *J* = 14.8 Hz, 2H), 1.36 (s, 3H) ppm. <sup>13</sup>C-NMR (700 MHz; CDCl<sub>3</sub>): δ 184.1, 128.2, 47.6, 44.6, 25.7 ppm. HRMS Anal. Calcd for C<sub>9</sub>H<sub>14</sub>O<sub>3</sub> 171.1021 (m/z). [M<sup>+</sup>] Found: 171.1014 (m/z).

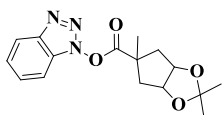


**3,4-dihydroxy-1-methylcyclopentanecarboxylic acid (13).** To a solution of (12) (0.5000 g, 4.459 mmol) in acetone: acetonitrile (1:1) was added a catalytic amount of OsO<sub>4</sub> and excess *N*-Methylmorpholine *N*-oxide 50% in H<sub>2</sub>O. The reaction was monitored by TLC for complete disappearance of starting material. Solvent was distilled off under vacuum and the product was taken into ethyl acetate and dried over MgSO<sub>4</sub>, further purified with silica MeOH:EtOAc (0.5:9.5) to afford a white solid (3.121 mmol, 70%) <sup>1</sup>H-NMR (700 MHz; MeOD): δ 4.05 (td, *J* = 5.3, 1.5 Hz, 1H), 3.33 (dt, *J* = 3.2, 1.6 Hz, 3H), 2.41-2.38 (m, 2H), 1.66-1.64 (m, 2H), 1.39 (s, 3H) ppm. <sup>13</sup>C-NMR (700MHz; MeOD): δ 180.9, 73.4, 44.9, 42.3, 26.5 ppm.



**2,2,5-trimethyltetrahydro-3aH-cyclopenta[d][1,3]dioxole-5-carboxylic acid (14).** To a solution of (13) (0.5000 g, 3.121 mmol) in dry THF and catalytic amount of *p*-TsOH was added large excess of 2,2-dimethoxypropane. Reaction

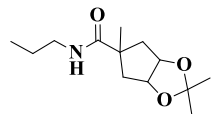
was monitored with TLC for complete disappearance of starting material. THF was distilled off under vacuum and the mixture was diluted with DCM. The organic solution was filtered and washed with H<sub>2</sub>O (2 x 50 mL), dried over MgSO<sub>4</sub>, and purified with silica Hex:EtOAc (7:3) to afford mixture of diastereomers as white solid (2.964 mmol, 95%) <sup>1</sup>H-NMR (700 MHz; CDCl<sub>3</sub>): δ 4.74-4.74 (m, 2H), 2.67 (d, *J* = 14.5 Hz, 1H), 2.27 (dd, *J* = 14.7, 5.0 Hz, 2H), 1.92 (d, *J* = 14.6 Hz, 2H), 1.50 (d, *J* = 15.7 Hz, 3H), 1.32 (q, *J* = 26.9 Hz, 6H) ppm. <sup>13</sup>C-NMR (700 MHz; CDCl<sub>3</sub>): δ 183.4, 182.5, 110.6, 109.8, 81.2, 80.7, 50.0, 49.0, 42.6, 26.3, 26.1, 25.2, 24.2, 23.7 ppm.



***1H-benzo[d][1,2,3]triazol-1-yl 2,2,5-trimethyltetrahydro-3aH-cyclopenta[d][1,3]dioxole-5-carboxylate (15).*** To a solution of (14)

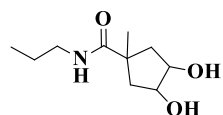
mixed isomers (0.5936 g, 2.964 mmol) in DCM/ACN and excess of TEA was added HBTU (1.239 g, 3.261 mmol, 1.1 eq). Reaction was monitored with TLC for complete disappearance of starting material. DCM/ACN was distilled off under vacuum and the mixture was purified with silica Hex:EtOAc (4:1) to afford two separate diastereomers as white solid (2.371 mmol, 80%, combined isomers) <sup>1</sup>H-NMR (700 MHz; CDCl<sub>3</sub>) Isomer I: δ 8.08 (d, *J* = 8.4 Hz, 1H), 7.55 (t, *J* = 7.6 Hz, 1H), 7.45-7.42 (m, 1H), 7.36 (d, *J* = 8.3 Hz, 1H), 4.86-4.85 (m, 2H), 2.52-2.49 (m, 2H), 2.27 (d, *J* = 14.7 Hz, 2H), 1.84 (s, 3H), 1.57 (s, 3H), 1.34 (s, 3H) ppm. <sup>13</sup>C-NMR (700 MHz; CDCl<sub>3</sub>): δ 172.6, 143.5, 128.6, 128.2, 124.7, 120.3, 110.3, 109.1, 80.3, 48.3, 42.9, 25.7, 25.1, 23.8 ppm. <sup>1</sup>H-NMR (700 MHz; CDCl<sub>3</sub>) Isomer II: δ 8.05 (d, *J* = 8.4 Hz, 1H), 7.59 (d, *J* = 8.3 Hz, 1H), 7.51 (ddd, *J* = 8.1, 7.1, 0.9 Hz, 1H), 7.41 (ddd, *J* = 8.3, 7.1, 1.0 Hz, 1H), 4.78 (dd, *J* = 3.9, 1.5 Hz, 3H), 2.94 (d, *J* = 15.0 Hz, 4H), 1.74 (ddd, *J* = 15.0, 4.1, 1.4 Hz, 3H), 1.71 (s, 6H), 1.32 (s, 6H), 1.25 (s, 6H)

ppm.  $^{13}\text{C}$ -NMR (700 MHz;  $\text{CDCl}_3$ ):  $\delta$  172.6, 143.5, 128.2, 124.7, 120.3, 110.3, 109.1, 80.3, 48.3, 42.9, 25.7, 25.1, 23.8 ppm.



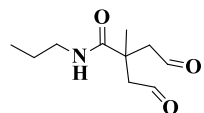
**2,2,5-trimethyl-N-propyltetrahydro-3aH-cyclopenta[d][1,3]dioxole-5-carboxamide (16).** To a solution of **(15)** (0.3769 g, 1.1876 mmol) in dry

DCM was added large excess of propylamine. Mixture was stirred for 0.5h, then concentrated and flushed through a pad of silica to afford white solid (1.1876 mmol, 100%).  $^1\text{H}$ -NMR (700 MHz;  $\text{CDCl}_3$ ):  $\delta$  4.76 (d,  $J$  = 2.7 Hz, 2H), 3.22-3.19 (m, 2H), 2.27-2.25 (m, 2H), 1.84 (d,  $J$  = 14.2 Hz, 2H), 1.55-1.51 (m, 8H), 1.47 (s, 3H), 1.30 (s, 3H), 0.92 (t,  $J$  = 7.3 Hz, 3H) ppm.  $^{13}\text{C}$ -NMR (700 MHz;  $\text{CDCl}_3$ ):  $\delta$  177.3, 110.2, 50.5, 43.0, 41.4, 26.2, 24.7, 23.6, 22.9, 11.3 ppm.



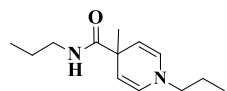
**3,4-dihydroxy-1-methyl-N-propylcyclopentanecarboxamide (17).** To a solution of **(16)** (0.2687 g, 1.1876 mmol) in methanol 50 mL, 3 drops

of 1 N HCl was added. Reaction was monitored with TLC for complete disappearance of starting material. Solvent was distilled off under vacuum and the product was taken into ethyl acetate and dried over  $\text{MgSO}_4$ , further purified with silica MeOH:EtOAc (0.5:9.5) to afford a white solid.  $^1\text{H}$ -NMR (400 MHz;  $\text{CDCl}_3$ ):  $\delta$  4.26 (t,  $J$  = 2.5 Hz, 2H), 3.25-3.21 (m, 2H), 2.46-2.41 (m, 2H), 2.15 (d,  $J$  = 3.7 Hz, 2H), 1.66 (dd,  $J$  = 13.7, 5.4 Hz, 2H), 1.45 (s, 3H), 1.28 (d,  $J$  = 2.5 Hz, 3H), 0.93 (t,  $J$  = 7.3 Hz, 3H) ppm.



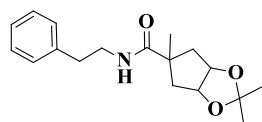
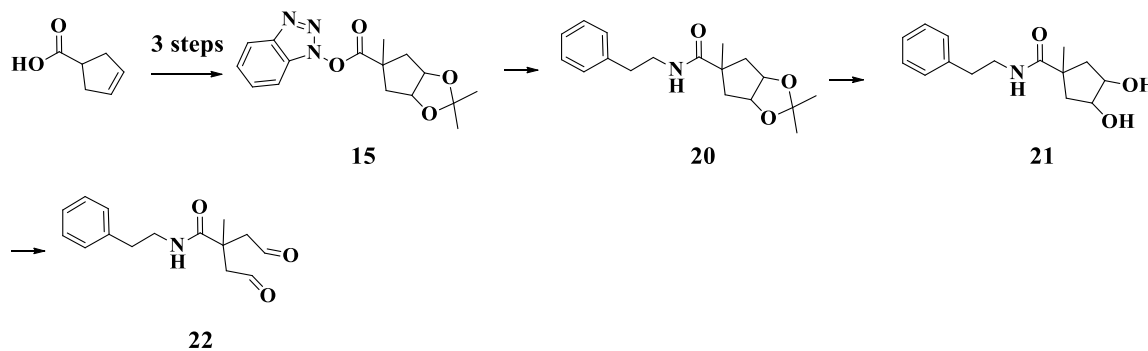
**2-methyl-4-oxo-2-(2-oxoethyl)-N-propylbutanamide (18).** To a solution of **(17)** in  $\text{H}_2\text{O}$ :methanol (1:9) was added  $\text{NaIO}_4$ . The mixture was stirred

for 1h until a flakey white, solid iodate salt, was obtained. The solvent was distilled off under vacuum and the product was taken into diethyl ether and dried over MgSO<sub>4</sub> and used for subsequent reactions.



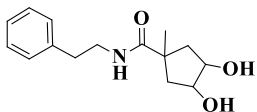
**4-methyl-N,1-dipropyl-1,4-dihydropyridine-4-carboxamide (19).** To a solution of **(18)** (20 mg, 0.4032 mmol) in DCM was added excess propylamine and stirred for 15 minutes at RT. Solvent and excess propylamine were distilled off under vacuum and the final product was taken into diethyl ether and dried over MgSO<sub>4</sub> to clear oil.

### 3.3.5 Synthesis of Molecules 20-23



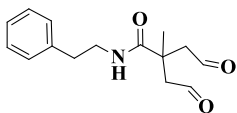
**2,2,5-trimethyl-N-phenethyltetrahydro-3aH-cyclopenta[d][1,3]dioxole-5-carboxamide (20).** To a solution of **(15)** (0.3769 g, 1.1876 mmol) in dry DCM was added of phenethylamine (0.22699 g, 1.1876 mmol). Mixture was stirred for 0.5h, then concentrated and flushed through a pad of silica to afford white solid (1.1876 mmol, 100%). <sup>1</sup>H-NMR (700 MHz; CDCl<sub>3</sub>): δ 7.34-7.22 (m, 5H), 3.52 (q, J = 6.4 Hz, 2H), 2.85 (t, J = 7.2 Hz, 2H), 2.41 (d, J = 14.9 Hz, 2H),

2.32-2.21 (m, 2H), 1.88 (dd,  $J = 101.4, 14.5$  Hz, 2H), 1.64-1.61 (m, 2H), 1.53 (t,  $J = 8.2$  Hz, 2H), 1.36 (s, 3H), 1.27 (d,  $J = 6.4$  Hz, 6H) ppm.



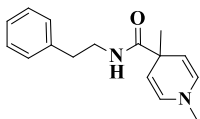
**3,4-dihydroxy-1-methyl-N-phenethylcyclopentanecarboxamide**

**(21).** To a solution of **(20)** (0.1000 g, 0.330 mmol) in methanol 50 mL, 3 drops of 1 N HCl was added. Reaction was monitored with TLC for complete disappearance of starting material. Solvent was distilled off under vacuum and the product was taken into ethyl acetate and dried over  $\text{MgSO}_4$ , further purified with silica MeOH:EtOAc (0.5:9.5) to afford a white solid as mixture of isomers (0.3131 mmol, 95%)  $^1\text{H}$  NMR (400 MHz,  $\text{CDCl}_3$ ):  $^1\text{H}$ -NMR (400 MHz;  $\text{CDCl}_3$ ):  $\delta$  7.35-7.19 (m, 5H), 4.20 (t,  $J = 4.4$  Hz, 2H), 4.10 (d,  $J = 3.9$  Hz, 2H), 3.53 (dd,  $J = 11.3, 6.1$  Hz, 2H), 2.87-2.81 (m, 2H), 2.35 (dd,  $J = 13.6, 6.3$  Hz, 2H), 2.08 (dd,  $J = 14.3, 4.3$  Hz, 2H), 1.75 (dd,  $J = 14.1, 6.0$  Hz, 2H), 1.61 (dd,  $J = 13.6, 5.2$  Hz, 2H), 1.34 (s, 3H), 1.21 (s, 3H) ppm.



**2-methyl-4-oxo-2-(2-oxoethyl)-N-phenethylbutanamide (22).** To a solution of **(21)** in  $\text{H}_2\text{O}$ :methanol (1:9) was added  $\text{NaIO}_4$ . The mixture

was stirred for 1h until a flakey white, solid iodate salt, was obtained. The solvent was distilled off under vacuum and the product was taken into diethyl ether and dried over  $\text{MgSO}_4$  and used for subsequent reactions.

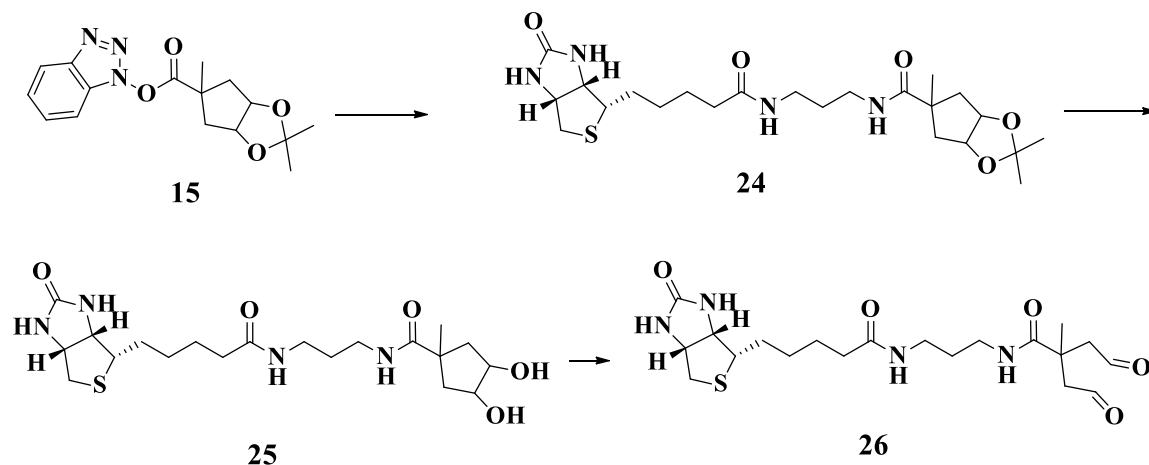


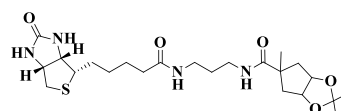
**1,4-dimethyl-N-phenethyl-1,4-dihydropyridine-4-carboxamide (23).** To

a solution of **(22)** (20 mg, 0.4032 mmol) in DCM was added excess propylamine and stirred for 15 minutes at RT. Solvent and excess propylamine were

distilled off under vacuum and the final product was taken into diethyl ether and dried over  $\text{MgSO}_4$  to clear oil.

### 3.3.6 Synthesis of Molecules 24-27

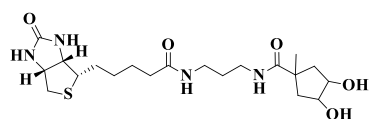



**2,2,5-trimethyl-N-(3-(5-((3*aS*,4*S*,6*aR*)-2-oxohexahydro-1*H*-thieno[3,4-*d*]imidazol-4-yl)pentanamido)propyl)tetrahydro-3*aH*-cyclopenta[*d*][1,3]dioxole-5-carboxamide (24).**

To a solution of **(15)** (42.0 mg, 0.1482 mmol) in methanol, *N*-(+)-Biotinyl-3-aminopropylammonium trifluoroacetate (50 mg, 0.1206 mmol) was added. Mixture was stirred for 10 minutes in presence of excess sodium bicarbonate, then concentrated and purified with silica EtOAc:MeOH (4.5:0.5) to afford white solid (0.1334 mmol, 90%).  $^1\text{H}$ -NMR (700 MHz; MeOD):  $\delta$  4.74 (d,  $J$  = 5.5 Hz, 1H), 4.68 (d,  $J$  = 4.7 Hz, 1H), 4.51 (dd,  $J$  = 7.7, 5.0 Hz, 1H), 4.33 (dt,  $J$  = 7.6, 3.7 Hz, 1H), 3.33 (s, 3H), 2.95 (dd,  $J$  = 12.7, 4.9 Hz, 1H), 2.72 (d,  $J$  = 12.7 Hz, 1H), 2.55 (d,  $J$  = 14.6 Hz, 1H), 2.25-2.23 (m, 2H), 2.18 (dd,  $J$  =

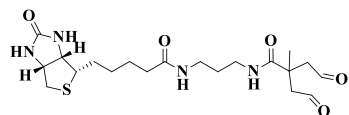


14.0, 4.6 Hz, 1H), 1.88 (d,  $J = 14.4$  Hz, 1H), 1.78-1.60 (m, 8H), 1.47 (dt,  $J = 11.4, 5.8$  Hz, 4H), 1.33-1.25 (m, 9H) ppm.  $^{13}\text{C}$ -NMR (700 MHz; MeOD):  $\delta$  179.1, 177.9, 174.8, 164.7, 109.9, 109.6, 81.2, 80.7, 62.0, 60.2, 55.6, 50.5, 49.8, 48.0, 46.5, 41.95, 41.92, 39.6, 36.6, 36.36, 36.31, 36.13, 35.5, 28.91, 28.77, 28.4, 28.1, 26.6, 25.49, 25.45, 25.0, 24.7, 24.4, 22.52, 22.33 ppm.



**3,4-dihydroxy-1-methyl-N-(3-(5-((3a*S*,4*S*,6a*R*)-2-oxohexahydro-1*H*-thieno[3,4-*d*]imidazol-4-**

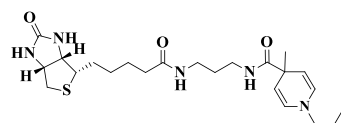
**yl)pentanamido)propyl)cyclopentanecarboxamide (25).** To a solution of (24) (57.64 mg, 0.1195 mmol) in methanol 50 mL, 3 drops of 1 N HCl was added. Reaction was monitored with TLC for complete disappearance of starting material. Solvent was distilled off under vacuum and the product was taken into methanol and neutralized with sodium bicarbonate and dried over  $\text{MgSO}_4$ , further purified with silica MeOH:EtOAc (0.5:9.5) to afford a white solid (0.1135 mmol, 95%).  $^1\text{H}$ -NMR (700 MHz; MeOD):  $\delta$  4.50 (dd,  $J = 7.7, 5.0$  Hz, 1H), 4.32 (dd,  $J = 7.7, 4.5$  Hz, 1H), 4.08 (t,  $J = 4.3$  Hz, 2H), 4.04-4.02 (m, 1H), 3.36-3.32 (m, 3H), 2.94 (dd,  $J = 12.7, 4.9$  Hz, 1H), 2.72 (d,  $J = 12.7$  Hz, 1H), 2.50-2.47 (m, ), 2.37 (dd,  $J = 13.4, 5.8$  Hz, 1H), 2.25-2.15 (m, 4H), 1.79-1.55 (m, 14H) ppm.



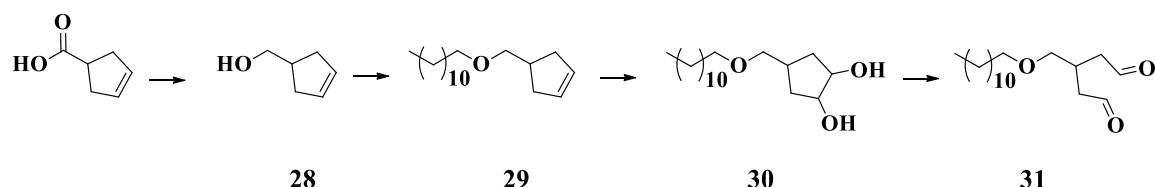
**N-(3-(2-methyl-4-oxo-2-(2-oxoethyl)butanamido)propyl)-5-((3a*S*,4*S*,6a*R*)-2-oxohexahydro-1*H*-thieno[3,4-*d*]imidazol-**

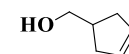
**4-yl)pentanamide (26)** To a solution of (25) (50.17 mg, 0.1135 mmol) in  $\text{H}_2\text{O}$ :methanol (1:9) was added  $\text{NaIO}_4$ . The mixture was stirred for 1h until a flakey white, solid iodate

salt, was obtained. The solvent was distilled off under vacuum and the product was taken into methanol and dried over MgSO<sub>4</sub> and used for subsequent reactions.

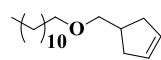
 **4-methyl-N-(3-(5-((3a*S*,4*S*,6a*R*)-2-oxohexahydro-1*H*-thieno[3,4-*d*]imidazol-4-yl)pentanamido)propyl)-1-propyl-1,4-dihydropyridine-4-carboxamide (27).** To a solution of (26) (20 mg, 0.0454 mmol) in MeOH was added excess propylamine and stirred for 15 minutes at RT. Solvent and excess propylamine were distilled off under vacuum and the final product was taken into diethyl ether and dried over MgSO<sub>4</sub> to clear oil.

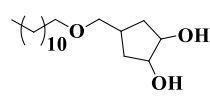
### 3.3.7 Synthesis of Molecules 28-31



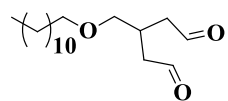
 **cyclopent-3-enylmethanol (28).** To a suspension of lithium aluminum hydride (0.5083 g, 13.37 mmol, 3 eq) in dry 100 mL THF at -78 °C, cyclopent-3-enecarboxylic acid (0.5000 g, 4.45 mmol) was added drop wise over 1h. The mixture was stirred for 6h and then quenched with 15 mL 1 M NaOH. Mixture was stirred for an additional 2h, then concentrated and taken up in diethyl ether and dried over MgSO<sub>4</sub> to afford clear liquid

(3.79 mmol, 85%).  $^1\text{H-NMR}$  (300 MHz,  $\text{CDCl}_3$ ): 2.12-2.16 (ttt 1H), 2.49-2.53 (dd, 2H), , 3.57-3.58 (d, 3H, 5.14Hz), 5.69 (s, 2H) ppm.

 **4-(dodecyloxymethyl)cyclopent-1-ene (29)**. To a suspension of excess NaH in dry 100 mL dry THF at  $-78\text{ }^\circ\text{C}$  was added compound **(28)** (0.3720 g, 3.79 mmol) and stirred for 1h. Temperature was gradually increased to  $-40\text{ }^\circ\text{C}$  and bromododecane (1.3828 g, 5.68 mmol, 1.5 eq) was added drop wise over 0.5h. The mixture was mildly refluxed overnight. THF was distilled off under vacuum and the mixture was diluted with DCM. The organic solution was filtered and washed with  $\text{H}_2\text{O}$  (6 x 50 mL), saturated  $\text{NH}_4\text{Cl}$  (3 x 50 mL), and  $\text{H}_2\text{O}$  (2 x 50 mL), dried over  $\text{MgSO}_4$ , and purified with silica Hex:EtOAc (2:8) to afford a clear oil solid (2.95 mmol, 78%)  $^1\text{H-NMR}$  (700 MHz;  $\text{CDCl}_3$ ):  $\delta$  5.65 (s, 2H), 3.41 (t,  $J = 6.7\text{ Hz}$ , 2H), 3.30 (d,  $J = 7.4\text{ Hz}$ , 2H), 2.56 (td,  $J = 8.4, 4.1\text{ Hz}$ , 1H), 2.47 (dd,  $J = 14.1, 8.7\text{ Hz}$ , 2H), 2.09 (dd,  $J = 14.1, 4.7\text{ Hz}$ , 2H), 1.57 (d,  $J = 7.1\text{ Hz}$ , 2H), 1.26 (s, 20H), 0.88 (t,  $J = 7.0\text{ Hz}$ , 3H) ppm.  $^{13}\text{C-NMR}$  (700 MHz;  $\text{CDCl}_3$ ):  $\delta$  129.5, 75.3, 71.1, 36.7, 36.0, 31.9, 29.70, 29.68, 29.65, 29.63, 29.50, 29.36, 26.2, 22.7, 14.1 ppm. HRMS Anal. Calcd for  $\text{C}_{18}\text{H}_{34}\text{O}$  267.1208 (m/z).  $[\text{M}^+]$  Found: 267.1197 (m/z).

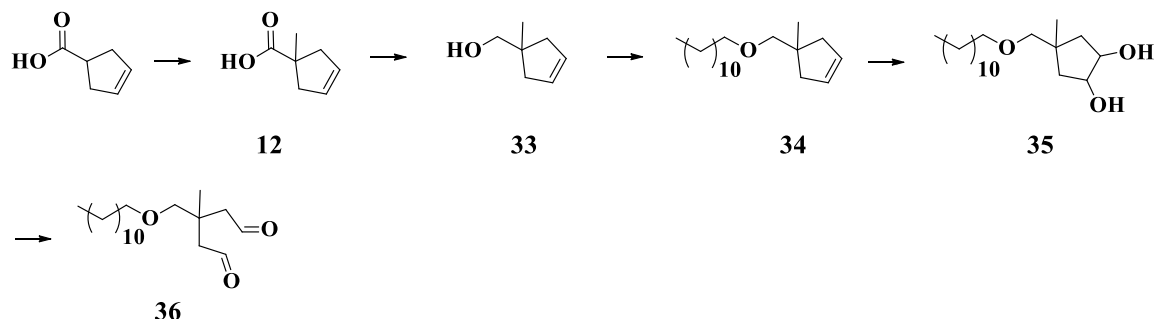
 **4-(dodecyloxymethyl)cyclopentane-1,2-diol (30)**. To a solution of **(29)** (3.541 g, 2.95 mmol) in acetone: acetonitrile (1:1) was added catalytic amount of  $\text{OsO}_4$  and excess *N*-Methylmorpholine *N*-oxide 50% in  $\text{H}_2\text{O}$ . Reaction was monitored with TLC for complete disappearance of starting material. Solvent was distilled off under vacuum and the product was taken into diethyl ether and dried over  $\text{MgSO}_4$ ,

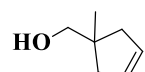
further purified with silica Hex:EtOAc (3:7) to afford a white solid (2.065 mmol, 70%)  $^1\text{H}$ -NMR (700 MHz;  $\text{CDCl}_3$ ):  $\delta$  4.15-4.15 (m, 2H), 3.40 (t,  $J$  = 6.6 Hz, 2H), 3.27 (d,  $J$  = 6.3 Hz, 2H), 2.58-2.56 (m, 1H), 2.10 (d,  $J$  = 2.4 Hz, 1H), 1.88 (td,  $J$  = 9.1, 4.1 Hz, 2H), 1.68 (dt,  $J$  = 13.3, 6.4 Hz, 2H), 1.58-1.55 (m, 2H), 1.34-1.28 (m, 18H), 0.90 (t,  $J$  = 7.0 Hz, 3H) ppm.  $^1\text{H}$ -NMR (700 MHz;  $\text{CDCl}_3$ ):  $\delta$  3.40 (t,  $J$  = 6.6 Hz, 2H), 3.28 (t,  $J$  = 5.4 Hz, 2H), 2.59-2.55 (m, 1H), 2.09 (t,  $J$  = 3.9 Hz, 1H), 1.87 (ddd,  $J$  = 13.8, 9.3, 4.5 Hz, 2H), 1.69-1.66 (m, 2H), 1.57 (d,  $J$  = 4.3 Hz, 6H), 1.32-1.28 (m, 20H), 0.91-0.89 (m, 3H) ppm.  $^{13}\text{C}$ -NMR (700 MHz;  $\text{CDCl}_3$ ):  $\delta$  77.63, 77.63, 77.61, 77.61, 77.57, 77.57, 77.45, 77.45, 75.01, 75.01, 73.97, 73.97, 71.17, 71.17, 34.84, 34.84, 34.62, 34.62, 31.93, 31.93, 29.68, 29.68, 29.63, 29.63, 29.50, 29.50, 29.43, 29.43, 29.36, 29.36, 26.20, 26.20, 22.70, 22.70, 14.13, 14.13 ppm.

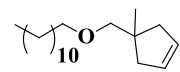


**3-(dodecyloxymethyl)pentanedial (31).** To a solution of **(30)** in  $\text{H}_2\text{O}$ :methanol (1:9) was added  $\text{NaIO}_4$ . The mixture was stirred for 1h until a flakey white, solid iodate salt, was obtained. The solvent was distilled off under vacuum and the product was taken into diethyl ether and dried over  $\text{MgSO}_4$  and used for subsequent reactions.

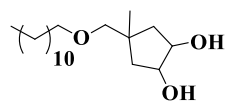
### 3.3.8 Synthesis of Molecules 33-37



 **(1-methylcyclopent-3-enyl)methanol (33)**. To a suspension of lithium aluminum hydride (0.3358 g, 8.837 mmol, 3 eq) in dry 100 mL THF at -78 °C, cyclopent-3-enecarboxylic acid (**12**) (0.3704 g, 2.945 mmol) was added drop wise over 1h. The mixture was stirred for 6h, and then quenched with 15 mL 1 M NaOH. Mixture was stirred for an additional 2h, then concentrated and up taken in diethyl ether and dried over MgSO<sub>4</sub> to afford clear liquid (1.885 mmol, 63%). <sup>1</sup>H-NMR (700 MHz; CDCl<sub>3</sub>): δ 5.64-5.63 (m, 2H), 3.47 (s, 3H), 2.35-2.32 (m, 2H), 2.12-2.07 (m, 2H), 1.13 (s, 3H) ppm. <sup>13</sup>C-NMR (700 MHz; CDCl<sub>3</sub>): δ 129.2, 71.4, 43.0, 24.9 ppm.

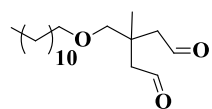
 **4-(dodecyloxymethyl)-4-methylcyclopent-1-ene (34)**. To a suspension of excess NaH in dry 100 mL dry THF at -78 °C was added (**33**) (0.2081 g, 1.885 mmol) and stirred for 1h. The temperature was gradually increased to -40 °C and bromododecane (0.6107 g, 2.450 mmol, 1.3 eq) was added drop wise over 0.5h. The mixture was mildly refluxed overnight. THF was distilled off under vacuum and the mixture was diluted with DCM. The organic solution was filtered and washed with H<sub>2</sub>O (6 x 50 mL), saturated

NH<sub>4</sub>Cl (3 x 50 mL), and H<sub>2</sub>O (2 x 50 mL), dried over MgSO<sub>4</sub>. Separation of bromododecane and the ether endured great difficulties; hence the molecule was never purified as isolated product and was directly used in the subsequent reaction.



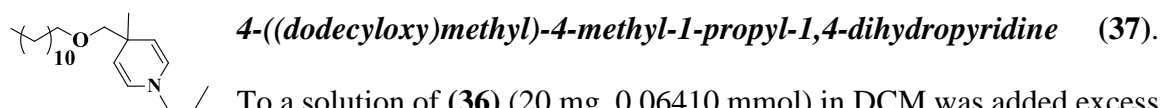
**4-(dodecyloxymethyl)-4-methylcyclopentane-1,2-diol (35).** To a

solution of the crude product in previous step **(34)** (0.5000 g, 1.785 mmol) in acetone: acetonitrile (1:1) was added a catalytic amount of OsO<sub>4</sub> and excess *N*-Methylmorpholine *N*-oxide 50% in H<sub>2</sub>O. The reaction was monitored with TLC for complete disappearance of starting material. Solvent was distilled off under vacuum and the product was taken into ethyl acetate and dried over MgSO<sub>4</sub>, further purified with silica Hex:EtOAc (2.5:2.5) to afford a white solid as mixture of isomers (1.214 mmol, 68%) <sup>1</sup>H-NMR (700 MHz; CDCl<sub>3</sub>): δ 4.16-4.14 (m, 1H), 3.98-3.95 (m, 1H), 3.53 (dd, *J* = 8.2, 5.1 Hz, 2H), 3.42-3.39 (m, 2H), 3.14 (s, 2H), 3.06 (s, 2H), 1.98-1.95 (m, 2H), 1.81-1.78 (m, 2H), 1.71-1.57 (m, 5H), 1.59-1.52 (m, 6H), 1.41-1.23 (m, 15H), 1.17-1.14 (m, 2H), 1.03-0.99 (m, 2H), 0.95-0.89 (m, 3H) ppm.



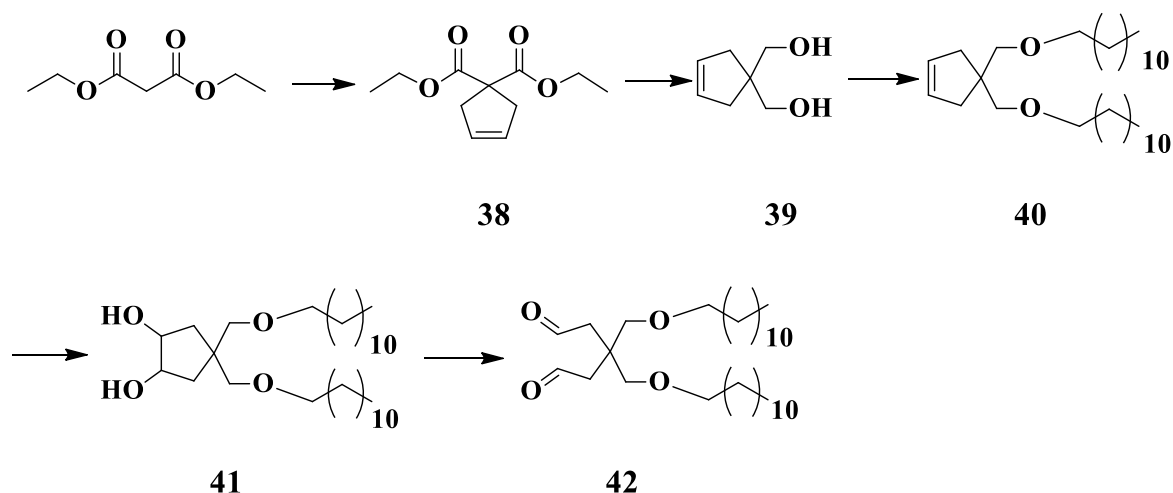
**3-(dodecyloxymethyl)-3-methylpentanedial (36).** To a solution of **(35)**

in H<sub>2</sub>O:methanol (1:9) was added NaIO<sub>4</sub>. The mixture was stirred for 1h until a flakey white, solid iodate salt, was obtained. The solvent was distilled off under vacuum and the product was taken into diethyl ether and dried over MgSO<sub>4</sub> and used for subsequent reactions.



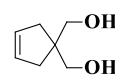
To a solution of **(36)** (20 mg, 0.06410 mmol) in DCM was added excess propylamine and stirred for 15 minutes at RT. Solvent and excess propylamine were distilled off under vacuum and the final product was taken into diethyl ether and dried over  $\text{MgSO}_4$  to clear oil.  $^1\text{H-NMR}$  (400 MHz;  $\text{CDCl}_3$ ):  $\delta$  5.85 (d,  $J = 7.9$  Hz, 2H), 4.23 (d,  $J = 7.9$  Hz, 2H), 3.45 (t,  $J = 6.8$  Hz, 3H), 3.11 (s, 2H), 2.99 (t,  $J = 7.0$  Hz, 2H), 1.59-1.51 (m, 7H), 1.28 (s, 32H), 0.90 (t,  $J = 7.3$  Hz, 10H) ppm.  $^{13}\text{C-NMR}$  (400 MHz;  $\text{CDCl}_3$ ):  $\delta$  129.4, 103.6, 55.0, 35.6, 31.9, 29.67, 29.63, 29.62, 29.61, 29.51, 29.50, 29.34, 26.1, 23.4, 22.7, 14.1, 11.1 ppm.

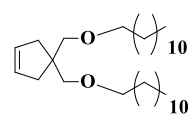
### 3.3.9 Synthesis of Molecules 38-43



**diethyl cyclopent-3-ene-1,1-dicarboxylate (38).** To a solution of diethyl malonate (2.00 g, 12.48 mmol) in 50 mL *t*-butanol and metallic Na (s) (0.287 g, 12.48 mmol) was added *cis*-1,4-dichlorobut-2-ene. The mixture was stirred until a yellow solution is obtained, only then another portion of (0.287 g, 12.48 mmol) metallic

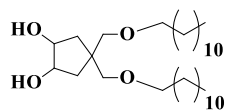
Na) was added and stirred for 12h. *tert*-butanol was distilled off under vacuum and the mixture was diluted with DCM. The organic solution was filtered and washed with H<sub>2</sub>O (6 x 50 mL), saturated NH<sub>4</sub>Cl (3 x 50 mL), and H<sub>2</sub>O (2 x 50 mL), dried over MgSO<sub>4</sub>, and purified with silica Hex:EtOAc (2:8) to afford a clear oil solid (11.23 mmol, 90%) <sup>1</sup>H-NMR (400 MHz; CDCl<sub>3</sub>): δ 5.62 (s, 2H), 4.21 (d, *J* = 7.1 Hz, 2H), 3.03 (s, 4H), 1.27 (d, *J* = 7.2 Hz, 3H) ppm. <sup>13</sup>C-NMR (700 MHz; CDCl<sub>3</sub>): δ 172.2, 127.8, 61.5, 58.8, 40.8, 14.0 ppm. HRMS Anal. Calcd for C<sub>11</sub>H<sub>16</sub>O<sub>4</sub> 213.1127 (m/z). [M<sup>+</sup>] Found: 213.1121 (m/z).

 **cyclopent-3-ene-1,1-diyl dimethanol (39).** To a suspension of lithium aluminum hydride (1.706 g, 44.92 mmol) in dry 100 mL THF at -78 °C, diethyl cyclopent-3-ene-1,1-dicarboxylate (**38**) (2.38 g, 11.23 mmol) was added drop wise over 1h. The mixture was stirred for 5h and then quenched with 15 mL 1M NaOH. Mixture was stirred for an additional 2h, then concentrated and up taken in diethyl ether and dried over MgSO<sub>4</sub> to afford white solid (9.54 mmol, 85%). <sup>1</sup>H-NMR (700 MHz; CDCl<sub>3</sub>): δ 5.65 (s, 2H), 3.73 (s, 4H), 2.24 (s, 4H) ppm.

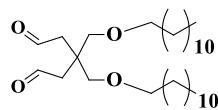
 **4,4-bis(dodecyloxymethyl)cyclopent-1-ene (40).** To a suspension of excess NaH in dry 100 mL dry THF at -78 °C was added cyclopent-3-ene-1,1-diyl dimethanol (**39**) (1.222 g, 9.54 mmol) and stirred for 1h. The temperature was gradually increased to -40 °C and bromododecane (7.104 g, 28.62 mmol) was added drop wise over 0.5h. The mixture was mildly refluxed overnight. THF was distilled off under vacuum and the mixture was diluted with DCM. The organic solution was filtered and



washed with H<sub>2</sub>O (6 x 50 mL), saturated NH<sub>4</sub>Cl (3 x 50 mL), and H<sub>2</sub>O (2 x 50 mL), dried over MgSO<sub>4</sub>, and purified with silica Hex:EtOAc (2:8) to afford a clear oil solid (7.60 mmol, 80%) <sup>1</sup>H-NMR (700 MHz; CDCl<sub>3</sub>): δ 5.60 (s, 2H), 3.43 (t, *J* = 6.7 Hz, 4H), 3.33 (s, 4H), 2.21 (s, 4H), 1.57 (dd, *J* = 9.4, 5.2 Hz, 4H), 1.28 (s, 20H), 0.90 (t, *J* = 7.1 Hz, 6H) ppm.

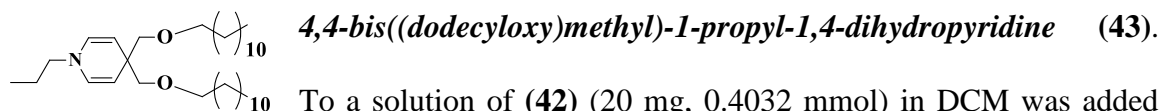


**4,4-bis(dodecyloxymethyl)cyclopent-1-ene-1,2-diol (41).** To a solution of 4,4-bis(dodecyloxymethyl)cyclopent-1-ene (**40**) (3.541 g, 7.60 mmol) in acetone: acetonitrile (1:1) was added catalytic amount of OsO<sub>4</sub> and excess *N*-methylmorpholine *N*-oxide 50% in H<sub>2</sub>O. Reaction was monitored with TLC for complete disappearance of starting material. Solvent was distilled off under vacuum and the product was taken into diethyl ether and dried over MgSO<sub>4</sub>, further purified with silica Hex:EtOAc (3:7) to afford a white solid (6.84 mmol, 90%) <sup>1</sup>H-NMR (700 MHz; CDCl<sub>3</sub>): δ 3.93 (d, *J* = 7.2 Hz, 2H), 3.53 (t, *J* = 6.7 Hz, 2H), 3.38 (t, *J* = 6.6 Hz, 2H), 3.29 (s, 2H), 3.16 (s, 2H), 1.85 (dd, *J* = 14.1, 6.2 Hz, 2H), 1.69 (dd, *J* = 14.2, 5.0 Hz, 2H), 1.63 (t, *J* = 7.3 Hz, 2H), 1.55 (t, *J* = 7.0 Hz, 2H), 1.31 (d, *J* = 6.8 Hz, 40H), 0.90 (t, *J* = 7.1 Hz, 6H) ppm. <sup>13</sup>C-NMR (700 MHz; CDCl<sub>3</sub>): δ 77.19, 77.01, 76.94, 76.83, 76.1, 74.4, 71.86, 71.68, 45.0, 37.6, 31.9, 29.68, 29.64, 29.62, 29.55, 29.49, 29.46, 29.40, 29.36, 26.17, 26.12, 22.7, 14.1 ppm. HRMS Anal. Calcd for C<sub>31</sub>H<sub>62</sub>O<sub>4</sub> 499.4726 (m/z). [M<sup>+</sup>] Found: 499.4720 (m/z).



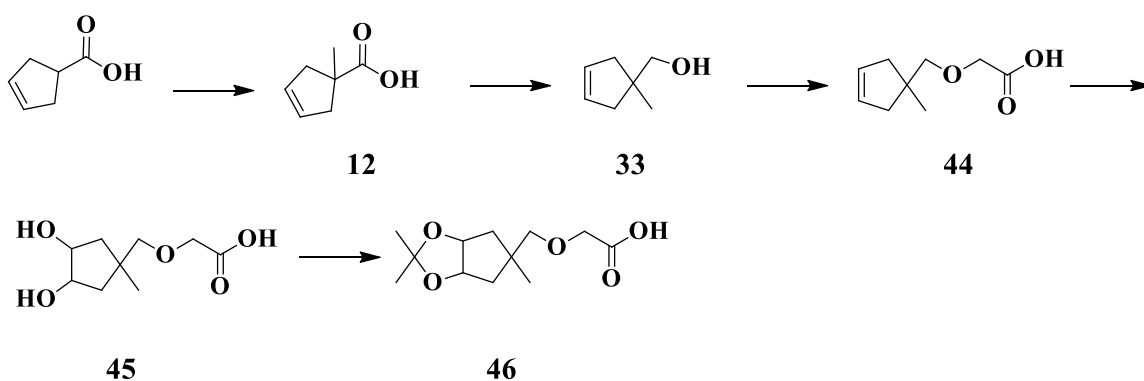
**3,3-bis(dodecyloxymethyl)pentanedial (42).** To a solution of (**41**) (3.4063 g, 6.84 mmol) in H<sub>2</sub>O:methanol (1:9) was added NaIO<sub>4</sub>.

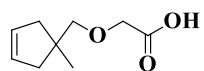
Mixture was stirred for 1h until a flakey white, solid iodate salt, was obtained. Solvent was distilled off under vacuum and the product was taken into diethyl ether and dried over  $\text{MgSO}_4$  and used for subsequent reactions.



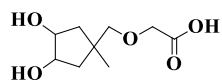
To a solution of **(42)** (20 mg, 0.4032 mmol) in DCM was added excess propylamine and stirred for 15 minutes at RT. Solvent and excess propylamine were distilled off under vacuum and the final product was taken into diethyl ether and dried over  $\text{MgSO}_4$  to afford pure clear oil.  $^1\text{H}$ -NMR (700 MHz;  $\text{CDCl}_3$ ):  $\delta$  5.91 (d,  $J = 7.7$  Hz, 2H), 4.27 (d,  $J = 7.8$  Hz, 2H), 3.43 (t,  $J = 6.7$  Hz, 4H), 3.28 (s, 4H), 2.99 (t,  $J = 7.0$  Hz, 2H), 1.55 (dq,  $J = 23.0, 7.3$  Hz, 6H), 1.32 (t,  $J = 6.9$  Hz, 36H), 0.90 (t,  $J = 7.1$  Hz, 9H) ppm.  $^{13}\text{C}$ -NMR (700 MHz;  $\text{CDCl}_3$ ):  $\delta$  130.8, 99.9, 71.7, 55.0, 40.6, 31.9, 29.71, 29.69, 29.67, 29.61, 29.55, 29.54, 29.52, 29.50, 29.44, 29.38, 26.22, 26.18, 23.4, 22.7, 14.1, 11.1 ppm.

### 3.3.10 Synthesis of Molecules 44-46

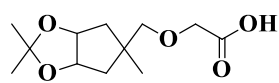




**2-((1-methylcyclopent-3-enyl)methoxy)acetic acid (44)** To a suspension of excess NaH in dry 100 mL dry THF at 0°C was added (1-methylcyclopent-3-enyl)methanol (**33**) (0.4494 g, 4.008 mmol) and stirred for 15 minutes. Then 2-chloroacetic acid (0.3767 g, 4.008 mmol, 1 eq) pre-dissolved in dry cool THF was added to the suspension via syringe. The mixture was mildly refluxed overnight. THF was distilled off under vacuum and the mixture was diluted with DCM. Content was treated with 1 N NaOH to remove the organic impurities, then treated with 1 N HCl and uptaken in DCM and dried over MgSO<sub>4</sub> to afford white solid (3.206 mmol, 80%) <sup>1</sup>H-NMR (700 MHz; CDCl<sub>3</sub>): δ 5.63 (s, 2H), 4.15 (s, 2H), 3.43 (s, 2H), 2.38 (d, *J* = 14.3 Hz, 2H), 2.11 (d, *J* = 14.2 Hz, 2H), 1.16 (s, 3H) ppm. <sup>13</sup>C-NMR (176 MHz; CDCl<sub>3</sub>): δ 172.3, 129.0, 80.4, 68.4, 42.1, 25.4 ppm.



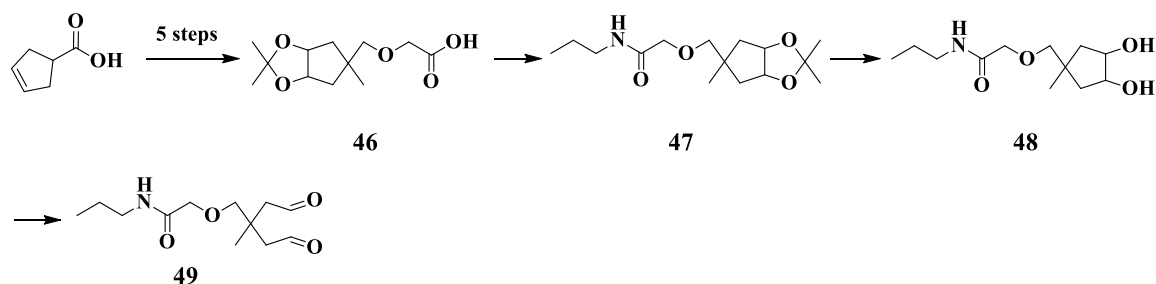
**2-((3,4-dihydroxy-1-methylcyclopentyl)methoxy)acetic acid (45)** To a solution of crude product in previous step (**44**) (0.5456 g, 3.206 mmol) in acetone: acetonitrile (1:1) was added catalytic amount of OsO<sub>4</sub> and excess *N*-methylmorpholine *N*-oxide 50% in H<sub>2</sub>O at pH 8.0. Reaction was monitored with TLC for complete disappearance of starting material. Solvent was distilled off under vacuum and the product was taken into ethyl acetate and dried over MgSO<sub>4</sub>, further purified with silica Hex:EtOAc (5:5) to afford a white solid as mixture of isomers (2.308 mmol, combined 72%) <sup>1</sup>H-NMR (700 MHz; CDCl<sub>3</sub>): <sup>1</sup>H-NMR (700 MHz; CDCl<sub>3</sub>): δ 4.16 (t, *J* = 4.4 Hz, 2H), 4.14 (s, 2H), 3.27 (s, 2H), 1.99 (dd, *J* = 13.7, 6.2 Hz, 2H), 1.61 (dd, *J* = 13.7, 4.9 Hz, 2H), 1.22 (s, 3H) ppm. <sup>13</sup>C-NMR (700 MHz; CDCl<sub>3</sub>): δ 171.1, 81.0, 76.6, 74.4, 68.1, 41.8, 39.8, 27.4 ppm.

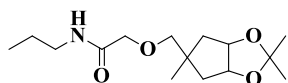


**2-((2,2,5-trimethyltetrahydro-3aH-cyclopenta[d][1,3]dioxol-5-yl)methoxy)acetic acid (46)** To a solution of (45) mixture of

isomers, (0.4713 g, 2.308 mmol) in dry THF and catalytic amount of *p*-TsOH was added large excess of 2,2-dimethoxypropane. Reaction was monitored with TLC for complete disappearance of starting material. THF was distilled off under vacuum and the mixture was diluted with DCM. The organic solution was filtered and washed with H<sub>2</sub>O (2 x 50 mL), dried over MgSO<sub>4</sub>, and purified with silica Hex:EtOAc (7:3) to afford mixture of diastereomers as white solid (2.193 mmol, combined 95%) <sup>1</sup>H-NMR (700 MHz; CDCl<sub>3</sub>) Isomer I: δ 4.73-4.72 (m, 2H), 4.13 (s, 2H), 3.29 (s, 2H), 1.87 (dt, *J* = 14.5, 2.2 Hz, 2H), 1.74 (d, *J* = 14.2 Hz, 2H), 1.54 (s, 3H), 1.32 (s, 3H), 1.26 (s, 3H) ppm. <sup>1</sup>H-NMR (700 MHz; CDCl<sub>3</sub>): δ 4.72 (dd, *J* = 3.4, 2.2 Hz, 3H), 4.16 (s, 2H), 4.13 (s, 2H), 3.61 (s, 2H), 3.28 (s, 2H), 2.01 (d, *J* = 14.8 Hz, 2H), 1.90 (ddd, *J* = 14.7, 4.9, 1.5 Hz, 2H), 1.72 (d, *J* = 14.1 Hz, 2H), 1.54 (s, 4H), 1.51 (s, 3H), 1.31 (d, *J* = 6.8 Hz, 6H), 1.25 (s, 3H), 1.10 (s, 3H) ppm. <sup>13</sup>C-NMR (700 MHz; CDCl<sub>3</sub>): δ 173.5, 172.6, 110.18, 110.06, 81.7, 81.4, 80.5, 78.6, 68.5, 68.2, 44.49, 44.46, 41.81, 41.71, 26.41, 26.23, 25.9, 24.5, 23.7, 23.4 ppm.

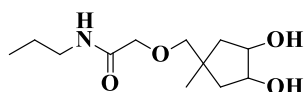
### 3.3.11 Synthesis of Molecules 47-49





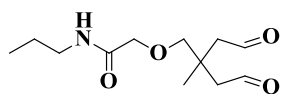
*N*-propyl-2-((2,2,5-trimethyltetrahydro-3aH-cyclopenta[d][1,3]dioxol-5-yl)methoxy)acetamide (**47**) To a

solution of (**46**) mixed isomers (0.2000 g, 0.8196 mmol) in DCM/ACN and excess of sodium bicarbonate was added HBTU (0.3426 g, 0.9016 mmol, 1.1eq). Reaction was monitored with TLC for complete disappearance of starting material. Once the activated carboxylic acid is generated, confirmed by disappearance of carboxylic acid intermediate, excess of propylamine was dispensed. Mixture was stirred for 0.5h, then concentrated and flushed through a pad of silica Hex:EtOAc (4:1) to afford clear oil (0.7786 mmol, 95%) Mixture of Isomers:  $^1\text{H-NMR}$  (400 MHz;  $\text{CDCl}_3$ ):  $\delta$  4.72 (t,  $J = 2.1$  Hz, 2H), 3.95 (s, 2H), 3.29 (q,  $J = 6.7$  Hz, 2H), 3.22 (s, 2H), 1.77 (d,  $J = 3.0$  Hz, 4H), 1.57 (dd,  $J = 13.3, 8.0$  Hz, 9H), 1.32 (s, 3H), 1.28 (s, 3H), 0.96 (t,  $J = 7.4$  Hz, 3H) ppm.



2-((3,4-dihydroxy-1-methylcyclopentyl)methoxy)-*N*-propylacetamide (**48**) To a solution of (**47**) (0.1900 g, 0.7786

mmol) in methanol:H<sub>2</sub>O (1:1), 3 drops of 1 N HCl was added. Reaction was monitored with TLC for complete disappearance of starting material. Solvent was distilled off under vacuum and the product was taken into ethyl acetate and dried over MgSO<sub>4</sub>, further purified with silica MeOH:EtOAc (0.5:9.5) to afford a white solid (0.7786mmol, 100%)  $^1\text{H-NMR}$  (700 MHz;  $\text{CDCl}_3$ ):  $\delta$  4.12 (t,  $J = 4.3$  Hz, 2H), 3.94 (s, 2H), 3.27 (q,  $J = 6.8$  Hz, 2H), 3.18 (s, 2H), 1.92-1.90 (m, 2H), 1.61-1.53 (m, 2H), 1.20 (s, 3H), 0.94 (t,  $J = 7.4$  Hz, 3H) ppm.  $^{13}\text{C-NMR}$  (700 MHz;  $\text{CDCl}_3$ ):  $\delta$  169.5, 80.8, 74.4, 70.9, 41.9, 40.5, 39.9, 27.5, 22.9, 11.3 ppm.

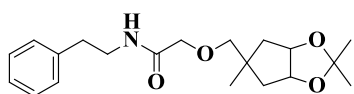
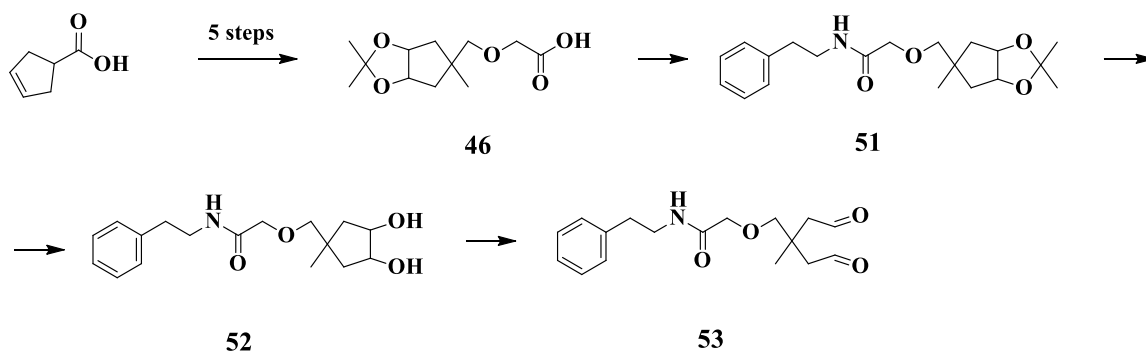


**2-(2-methyl-4-oxo-2-(2-oxoethyl)butoxy)-N-propylacetamide**

(49) To a solution of (48) (190.7 mg, 0.7786 mmol) in

H<sub>2</sub>O:methanol (1:9) was added NaIO<sub>4</sub> and stirred for 1h until a flakey white, solid iodate salt appeared. The solvent was distilled off under vacuum and the product was taken into diethyl ether and dried over MgSO<sub>4</sub> and used for subsequent reactions.

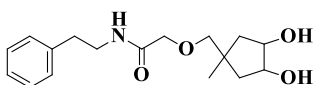
### 3.3.12 Synthesis of Molecules 51-53



**N-phenethyl-2-((2,2,5-trimethyltetrahydro-3aH-cyclopenta[d][1,3]dioxol-5-yl)methoxy)acetamide (51)** To

a solution of (46) mixed isomers (0.2000 g, 0.8196 mmol) in DCM/ACN and excess of sodium bicarbonate was added HBTU (0.3426 g, 0.9016 mmol, 1.1 eq). Reaction was monitored with TLC for complete disappearance of starting material. Once the activated carboxylic acid is generated, confirmed by TLC, phenethylamine (0.0991 g, 0.8196 mmol) is added to the reaction vessel. Mixture was stirred for 0.5h, then concentrated and flushed through a pad of silica Hex:EtOAc (4:1) to afford clear oil (0.7377mmol, 90 %) <sup>1</sup>H-NMR (700 MHz; CDCl<sub>3</sub>): δ 7.33-7.31 (m, 1H), 7.25-7.23 (m, 1H), 7.21-7.20 (m, 1H), 4.62-4.61

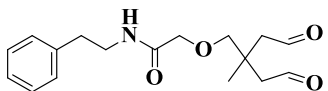
(m, 2H), 3.89 (s, 2H), 3.59 (q,  $J = 6.5$  Hz, 2H), 3.09 (s, 2H), 2.84 (t,  $J = 6.8$  Hz, 2H), 1.62 (d,  $J = 7.8$  Hz, 2H), 1.58 (s, 3H), 1.52 (s, 3H), 1.30 (s, 3H), 1.14 (s, 3H) ppm.  $^{13}\text{C}$ -NMR (700 MHz;  $\text{CDCl}_3$ ):  $\delta$  169.5, 138.6, 128.7, 126.7, 110.1, 81.5, 80.4, 70.8, 44.2, 41.7, 39.6, 35.5, 26.3, 24.4, 23.6 ppm.



**2-((3,4-dihydroxy-1-methylcyclopentyl)methoxy)-N-**

**phenethylacetamide (52):** To a solution of **(51)** (0.2560 g, 7.377

mmol) in methanol: $\text{H}_2\text{O}$  (1:1), 3 drops of 1 N HCl was added. Reaction was monitored with TLC for complete disappearance of starting material. Solvent was distilled off under vacuum and the product was taken into ethyl acetate and dried over  $\text{MgSO}_4$ , further purified with silica MeOH:EtOAc (0.5:9.5) to afford a clear oil (7.377 mmol, 100%)  $^1\text{H}$ -NMR (700 MHz;  $\text{CDCl}_3$ ):  $\delta$  7.33 (t,  $J = 7.5$  Hz, 1H), 7.24 (d,  $J = 7.3$  Hz, 1H), 7.21 (d,  $J = 7.4$  Hz, 1H), 3.96 (d,  $J = 3.5$  Hz, 2H), 3.90 (s, 2H), 3.61 (d,  $J = 19.4$  Hz, 2H), 3.07 (s, 2H), 2.85 (d,  $J = 13.4$  Hz, 2H), 1.76 (dd,  $J = 13.8, 6.4$  Hz, 2H), 1.49 (dd,  $J = 13.8, 5.2$  Hz, 2H), 1.08 (s, 3H) ppm.  $^{13}\text{C}$ -NMR (700 MHz;  $\text{CDCl}_3$ ):  $\delta$  169.5, 138.6, 128.89, 128.76, 126.6, 80.7, 74.3, 70.8, 41.7, 39.73, 39.55, 35.5, 27.4 ppm. HRMS Anal. Calcd for  $\text{C}_{17}\text{H}_{25}\text{NO}_4$  308.1861 (m/z).  $[\text{M}^+]$  Found: 308.1851 (m/z).



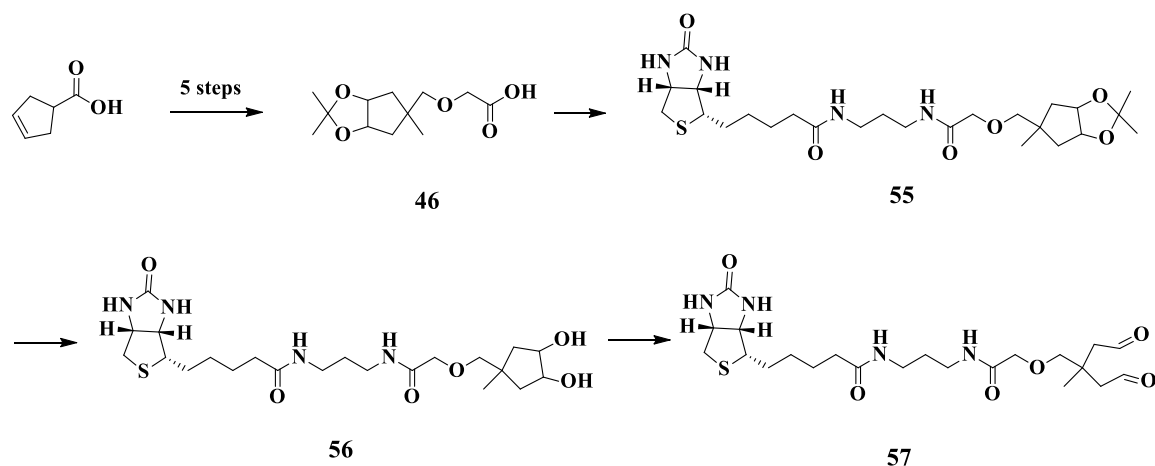
**2-(2-methyl-4-oxo-2-(2-oxoethyl)butoxy)-N-**

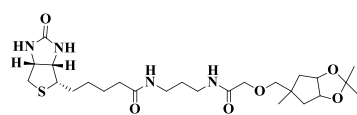
**phenethylacetamide (53)** To a solution of **(52)** (2.2647 g, 7.377

mmol) in  $\text{H}_2\text{O}$ :methanol (1:9) was added  $\text{NaIO}_4$  and stirred for 1h until a flakey white,

solid iodate salt appeared. The solvent was distilled off under vacuum and the product was taken into diethyl ether and dried over MgSO<sub>4</sub> and used for subsequent reactions.

### 3.3.13 Synthesis of Molecules 55-58

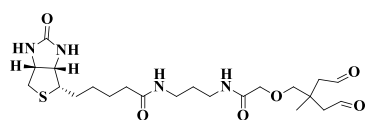


 **5-((3*aS*,4*S*,6*aR*)-2-oxohexahydro-1*H*-thieno[3,4-*d*]imidazol-4-yl)-N-(3-(2-((2,2,5-trimethyltetrahydro-3*aH*-cyclopenta[*d*][1,3]dioxol-5-yl)methoxy)acetamido)propyl)pentanamide** (55) To a

solution of (46) mixed isomers (0.0589 g, 0.2415 mmol) in MeOH/ACN and excess of sodium bicarbonate was added HBTU (0.0917 g, 0.2656 mmol, 1.1 eq). Reaction was monitored with TLC for complete disappearance of starting material. Once the activated carboxylic acid is generated, confirmed by TLC, biotin cadaverine trifluoroacetate (0.1000g, 0.2415 mmol, 1 eq) is added to the reaction vessel. Mixture was stirred for 0.5h, then concentrated and flushed through a pad of silica MeOH:EtOAc (1:4) to white crystal. <sup>1</sup>H-NMR (700 MHz; MeOD): δ 4.74-4.73 (m, 2H), 4.51 (dd, *J* = 7.8, 5.0 Hz, 1H), 4.32 (dd, *J*

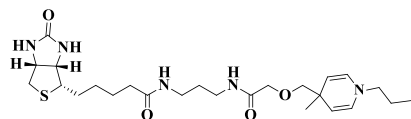


= 7.8, 4.5 Hz, 1H), 3.95 (s, 2H), 3.37 (s, 2H), 3.33 (q, 1H), 3.25 (s, 2H), 3.23 (d,  $J = 6.9$  Hz, 2H), 2.95 (dd,  $J = 12.7, 5.0$  Hz, 2H), 2.72 (d,  $J = 12.7$  Hz, 2H), 2.24 (t,  $J = 7.3$  Hz, 2H), 1.94 (dd,  $J = 14.2, 5.1$  Hz, 2H), 1.71-1.66 (m, 4H), 1.49 (d,  $J = 4.9$  Hz, 2H), 1.46 (d,  $J = 6.9$  Hz, 2H), 1.46 (s, 3H), 1.30 (s, 3H), 1.24 (s, 3H) ppm.



**2-(2-methyl-4-oxo-2-(2-oxoethyl)butoxy)-N-**

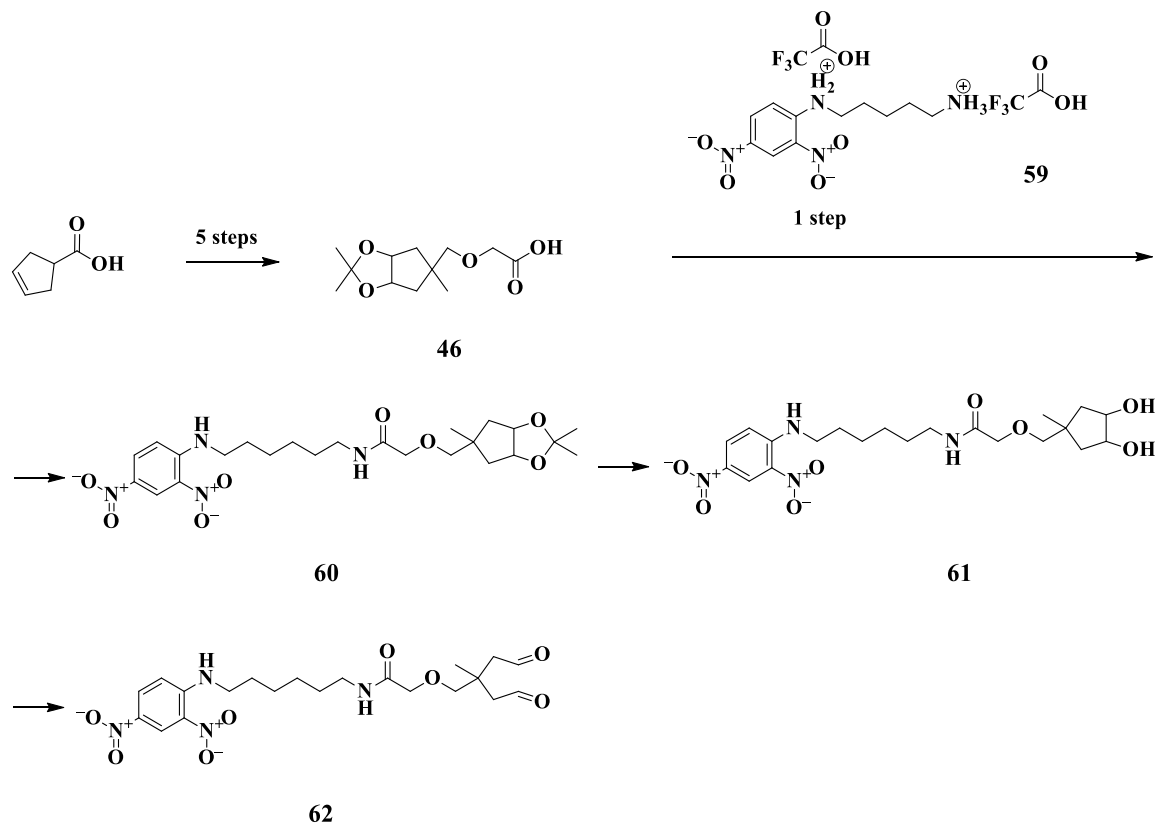
**phenethylacetamide (57)** To a solution of **(56)** (87.74 mg, 0.1800 mmol) in H<sub>2</sub>O:methanol (1:9) was added 3 drops of dilute acid and stirred for 0.5h, then NaIO<sub>4</sub> was added and stirred for 1h until a flakey white, solid iodate salt appeared. Solvent was distilled off under vacuum and the product was taken into diethyl ether and dried over MgSO<sub>4</sub> and used for subsequent reactions.



**N-(3-(2-((4-methyl-1-propyl-1,4-dihydropyridin-4-yl)methoxy)acetamido)propyl)-5-((3a*S*,4*S*,6a*R*)-2-**

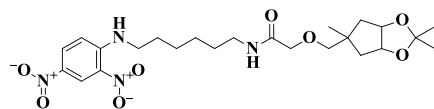
**oxohexahydro-1*H*-thieno[3,4-*d*]imidazol-4-yl)pentanamide (58).** To a solution of **(57)** (20 mg, 0.04132 mmol) in MeOH was added excess propylamine and stirred for 15 minutes at RT. Solvent and excess propylamine were distilled off under vacuum and the final product was taken into diethyl ether and dried over MgSO<sub>4</sub> to clear oil.

### 3.3.14 Synthesis of Molecules 59-63



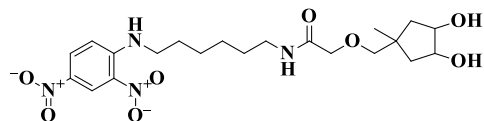
***N1-(2,4-dinitrophenyl)hexane-1,6-diamine trifluoroacetate*** (**59**) : To a solution of *N*-Boc-1,6-hexanediamine hydrochloride (0.2000 g, 0.793 mmol) in DMF/H<sub>2</sub>O in (9:1) and excess of sodium bicarbonate was added (0.1771 g, 0.9523 mmol, 1.2eq) and stirred overnight. The solvents were stripped off under high vacuum and the content was dissolved in MeOH and treated with 80 % TFA and stirred for 1h at RT. After complete evaporation of solvent, fresh MeOH was added and filtered. Final product was isolated as yellow crystals of trifluoroacetate quaternary salt. <sup>1</sup>H-NMR (700 MHz; MeOD): δ 9.05 (dd, *J* = 5.5, 2.9 Hz, 1H), 8.30 (ddd, *J* = 9.5, 2.4, 1.9 Hz, 1H), 7.19-7.18 (m, 1H), 3.53 (d, *J* = 7.1 Hz, 2H), 2.97-2.94 (m, 2H), 1.80 (t, *J* = 7.3 Hz, 2H), 1.72-1.70 (m, 2H), 1.55-1.49 (m, 4H) ppm. <sup>13</sup>C-NMR (700 MHz; MeOD): δ 161.74,

161.55, 148.3, 135.5, 130.1, 129.7, 123.38, 123.37, 119.3, 117.7, 116.0, 114.3, 42.7, 39.2, 28.1, 27.1, 26.0, 25.7 ppm.



*N*-(6-(2,4-dinitrophenylamino)hexyl)-2-((2,2,5-trimethyltetrahydro-3aH-cyclopenta[d][1,3]dioxol-5-

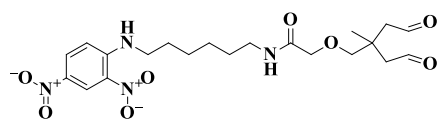
*yl)methoxy)acetamide (60)*: To a solution of **(46)** mixed isomers (0.2000 g, 0.8196 mmol) in MeOH/ACN and excess of sodium bicarbonate was added HBTU (0.3426 g, 0.901 mmol, 1.1 eq) and stirred for 1h at RT. Reaction was monitored with TLC for complete disappearance of starting material carboxylic acid. Once the activated carboxylic acid is generated, confirmed by TLC, **(59)** (0.4643 g, 0.901 mmol, 1.1 eq) was added to the reaction vessel. Mixture was stirred for 0.5h, then concentrated and flushed through a pad of silica Hex:EtOAc (4:1) to afford yellow crystal (0.737 mmol, 90%). <sup>1</sup>H-NMR (700 MHz; CDCl<sub>3</sub>): δ 9.17 (d, *J* = 2.5 Hz, 1H), 8.57 (s, 1H), 8.31-8.30 (m, 1H), 6.94 (d, *J* = 9.5 Hz, 1H), 6.63 (d, *J* = 5.9 Hz, 1H), 4.72 (d, *J* = 4.7 Hz, 2H), 3.99 (s, 2H), 3.54 (s, 2H), 3.43 (q, *J* = 6.4 Hz, 3H), 3.33 (q, *J* = 6.7 Hz, 3H), 1.99 (d, *J* = 14.7 Hz, 2H), 1.82 (t, *J* = 7.3 Hz, 3H), 1.62-1.59 (m, 3H), 1.57 (s, 2H), 1.54 (td, *J* = 9.8, 4.0 Hz, 6H), 1.49-1.48 (m, 4H), 1.46 (q, *J* = 7.5 Hz, 3H), 1.30 (s, 3H), 1.09 (s, 3H) ppm. <sup>13</sup>C-NMR (700 MHz; CDCl<sub>3</sub>): δ 170.1, 148.3, 136.0, 130.4, 124.4, 113.8, 110.0, 81.3, 70.7, 44.5, 43.5, 41.8, 38.5, 29.5, 28.6, 26.56, 26.43, 26.2, 26.0, 23.4 ppm.



2-((3,4-dihydroxy-1-methylcyclopentyl)methoxy)-

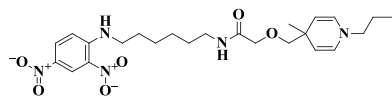
*N*-(6-(2,4-dinitrophenylamino)hexyl)acetamide

**(61)** To a solution of **(60)** (0.3747 g, 0.737 mmol) in methanol:H<sub>2</sub>O (1:1), 3 drops of 1 N HCl was added. Reaction was monitored with TLC for complete disappearance of starting material. Solvent was distilled off under vacuum and the product was taken into ethyl acetate and dried over MgSO<sub>4</sub>, further purified with silica MeOH:EtOAc (0.5:9.5) to afford yellow crystals (0.700 mmol, 95%). <sup>1</sup>H-NMR (700 MHz; CDCl<sub>3</sub>): δ 9.16 (d, *J* = 2.6 Hz, 1H), 8.57 (s, 1H), 8.30 (dd, *J* = 9.5, 2.5 Hz, 1H), 6.94-6.93 (m, 1H), 6.46 (s, 1H), 4.13 (q, *J* = 4.3 Hz, 2H), 4.03 (s, ), 3.96 (s, 2H), 3.43 (q, *J* = 6.2 Hz, 3H), 3.34 (q, *J* = 6.8 Hz, 3H), 3.32 (d, *J* = 10.3 Hz, 1H), 3.20 (d, *J* = 6.7 Hz, 2H) ppm. <sup>13</sup>C-NMR (700 MHz, CDCl<sub>3</sub>): δ 169.6, 148.3, 136.0, 130.4, 124.4, 113.9, 80.8, 74.4, 70.9, 43.5, 41.9, 39.8, 38.6, 29.5, 28.6, 27.5, 26.56, 26.45 ppm.



*N*-(6-(2,4-dinitrophenylamino)hexyl)-2-(2-methyl-4-oxo-2-(2-oxoethyl)butoxy)acetamide **(62)** To a

solution of **(61)** (32.7 mg, 0.700 mmol) in H<sub>2</sub>O:methanol (1:9) was added NaIO<sub>4</sub> and stirred for 1h until a flakey white, solid iodate salt appeared. The solvent was distilled off under vacuum and the product was taken into diethyl ether and dried over MgSO<sub>4</sub> and used for subsequent reactions.

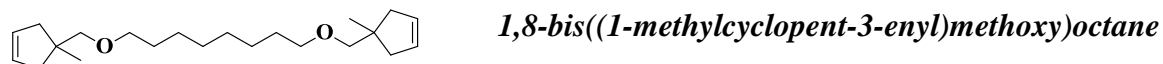
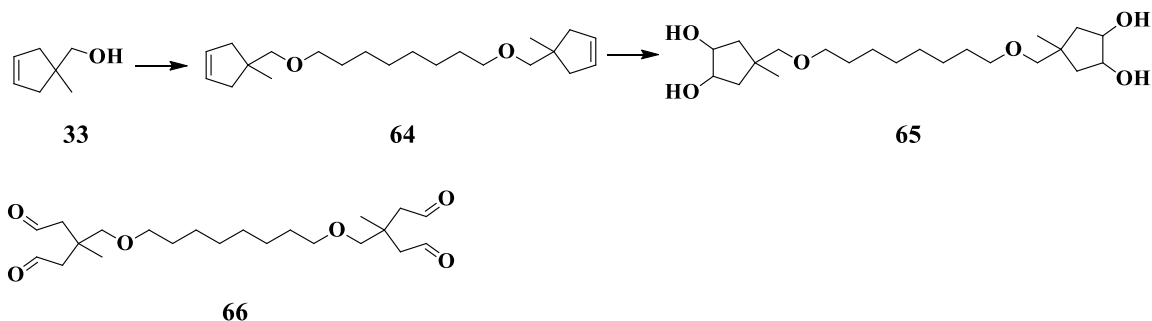


*N*-(6-((2,4-dinitrophenyl)amino)hexyl)-2-((4-methyl-1-propyl-1,4-dihydropyridin-4-yl)methoxy)acetamide **(63)**.

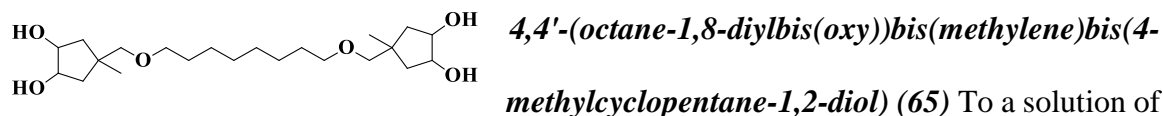
To a solution of **(62)** (20 mg, 0.04291 mmol) in MeOH was added excess propylamine and stirred for 15 minutes at RT. Solvent and excess propylamine were distilled off under

vacuum and the final product was taken into diethyl ether and dried over MgSO<sub>4</sub> to clear oil.

### 3.3.15 Synthesis of Molecules 64-67

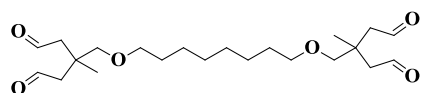


**(64)** To a suspension of excess NaH and cat KI in dry 100 mL dry THF at -20 °C was added **(33)** (0.3000 g, 2.678 mmol) and stirred for 1h. The temperature was gradually increased to 0 °C and 1,12 dibromododecane (2.0207 g, 6.167 mmol, 2.3 eq) was added drop wise over 0.5h. The mixture was mildly refluxed overnight. THF was distilled off under vacuum and the mixture was diluted with DCM. The organic solution was filtered and washed with H<sub>2</sub>O (6 x 50 mL), saturated NH<sub>4</sub>Cl (3 x 50 mL), and H<sub>2</sub>O (2 x 50 mL), dried over MgSO<sub>4</sub>, to afford a white solid. The product was not purified as an isolated compound; further used in subsequent steps.



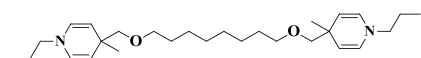
To a solution of crude product in previous step **(64)** (0.6978 g, 2.089 mmol) in acetone: acetonitrile (1:1)

was added catalytic amount of OsO<sub>4</sub> and excess *N*-methylmorpholine *N*-oxide 50% in H<sub>2</sub>O at pH 8.0. Reaction was monitored with TLC for complete disappearance of starting material. Solvent was distilled off under vacuum and the product was taken into ethyl acetate and dried over MgSO<sub>4</sub>, further purified with silica Hex:EtOAc (2.5:2.5) to afford a white solid as mixture of isomers (1.880mmol, 90%) <sup>1</sup>H-NMR (700 MHz; MeOD): δ 4.04-4.01 (m, 3H), 3.99 (t, *J* = 4.5 Hz, 2H), 3.58 (dd, *J* = 7.1, 2.9 Hz, 2H), 3.51-3.47 (m, 4H), 3.44-3.41 (m, 4H), 3.23 (s, 2H), 3.08 (s, 2H), 1.89-1.83 (m, 4H), 1.75 (dd, *J* = 13.6, 5.6 Hz, 4H), 1.63-1.56 (m, 7H), 1.50 (dt, *J* = 13.4, 5.4 Hz, 7H), 1.40-1.36 (m, 31H), 1.13 (s, 5H), 1.05 (s, 3H) ppm. <sup>13</sup>C-NMR (700 MHz; MeOD): δ 80.0, 79.8, 74.15, 74.05, 73.87, 71.9, 71.17, 71.00, 70.8, 66.0, 48.0, 47.4, 41.27, 41.11, 40.6, 40.1, 39.2, 38.9, 33.0, 29.45, 29.32, 29.28, 29.23, 29.16, 29.13, 26.6, 26.18, 26.02, 25.99, 25.91, 25.3 ppm.



**3,3'-(octane-1,8-diylbis(oxy))bis(methylene)bis(3-methylpentanedial) (66)** To a solution of (65) (0.7557

g, 1.880 mmol) in H<sub>2</sub>O:methanol (1:9) was added NaIO<sub>4</sub> and stirred for 1h until a flakey white, solid iodate salt appeared. The solvent was distilled off under vacuum and the product was taken into diethyl ether and dried over MgSO<sub>4</sub> and used for subsequent reactions.

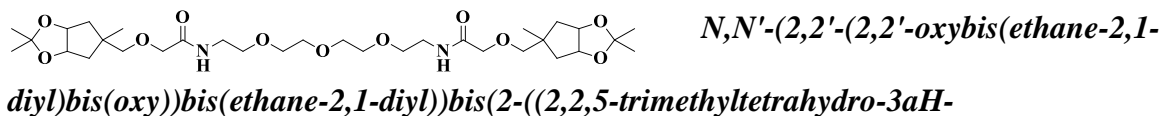
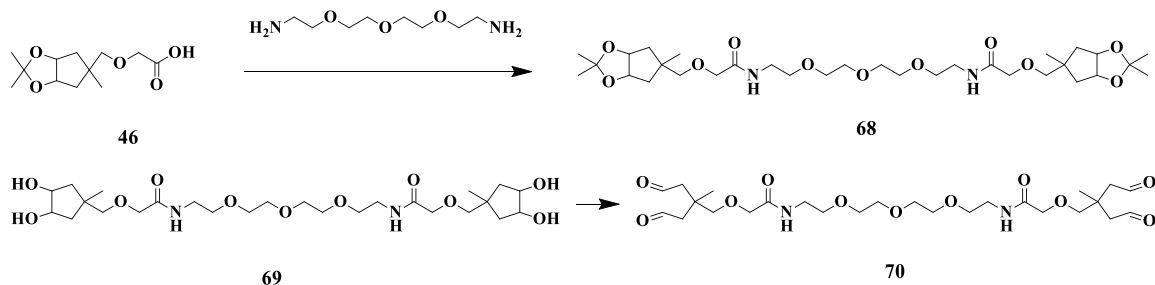


**1,8-bis((4-methyl-1-propyl-1,4-dihydropyridin-4-yl)methoxy)octane (67).** To a solution of (66) (20 mg, 0.05052 mmol) in DCM was added

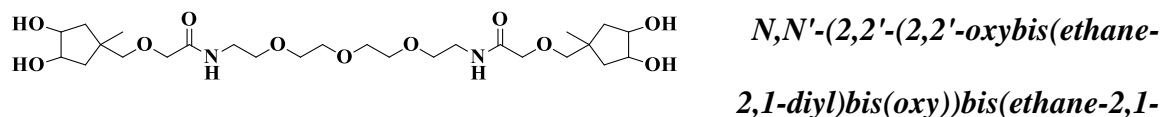
excess propylamine and stirred for 15 minutes at RT. Solvent and excess propylamine were

distilled off under vacuum and the final product was taken into diethyl ether and dried over MgSO<sub>4</sub> to clear oil.

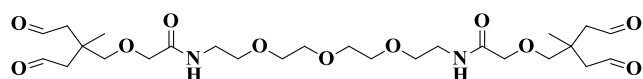
### 3.3.16 Synthesis of Molecules 68-73



*N,N'*-(2,2'-(2,2'-oxybis(ethane-2,1-diyl))bis(oxy))bis(ethane-2,1-diyl)bis(2-((2,2,5-trimethyltetrahydro-3aH-cyclopenta[d][1,3]dioxol-5-yl)methoxy)acetamide) (**68**) To a solution of (**46**) mixed isomers (0.0635 g, 0.2604 mmol) in MeOH/ACN and excess of sodium bicarbonate was added HBTU (0.2078 g, 0.546 mmol, 2.1 eq). Reaction was monitored with TLC for complete disappearance of starting material. Once the activated carboxylic acid is generated, confirmed by TLC, 1,11-Diamino-3,6,9-trioxaundecane (0.0250 g, 0.1302 mmol) is added to the reaction vessel. Mixture was stirred for 0.5h, then concentrated and flushed through a pad of silica MeOH:EtOAc (1:4) to afford clear oil (0.1236 mmol, 95%). The product was not purified as isolated compound; it was used in further steps.



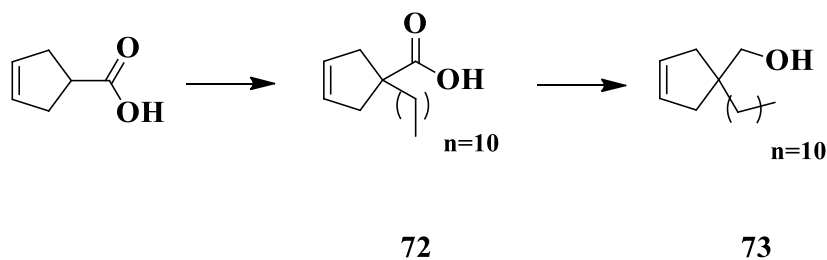
*diyl))bis(2-((3,4-dihydroxy-1-methylcyclopentyl)methoxy)acetamide) (69)* To a solution of **(68)** (0.8000 g ,0.1236 mmol) in methanol:H<sub>2</sub>O (1:1), 3 drops of 1 N HCl was added. Reaction was monitored with TLC for complete disappearance of starting material. Solvent was distilled off under vacuum and the product was taken into ethyl acetate and dried over MgSO<sub>4</sub>, further purified with silica MeOH:EtOAc (1:4) to afford a clear oil (0.1236 mmol, 100%) . <sup>1</sup>H-NMR (700 MHz, CDCl<sub>3</sub>): 1.28-1.39 (4s, 12H), 1.518 (s, 3H), 1.540 (s, 3H), 1.92- 1.95 (d, 2H, J= 14.59Hz), 2.28-2.30 (d, 2H), 2.68-2.70 (d, 2H, J= 14.51Hz), 4.682-4.689 (d, 1H , J= 4.38Hz), 4.760-4.769 (d, 1H) ppm.



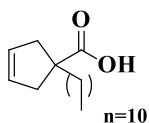
*N,N'-(2,2'-(2,2'-oxybis(ethane-2,1-diyl))bis(oxy))bis(ethane-2,1-*

*diyl))bis(2-(2-methyl-4-oxo-2-(2-oxoethyl)butoxy)acetamide)(70)* To a solution of **(69)** (0.8000 g ,0.1236 mmol) in H<sub>2</sub>O:methanol (1:9) was added NaIO<sub>4</sub> and stirred for 1h until a flakey white, solid iodate salt appeared. Solvent was distilled off under vacuum and the product was taken into diethyl ether and dried over MgSO<sub>4</sub> and used for subsequent reactions.

### 3.3.17 Synthesis of Molecules 75-76

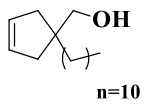






**1-dodecylcyclopent-3-enecarboxylic acid (72)** To a solution of cyclopent-3-

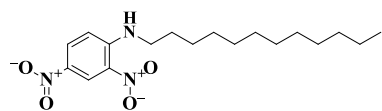
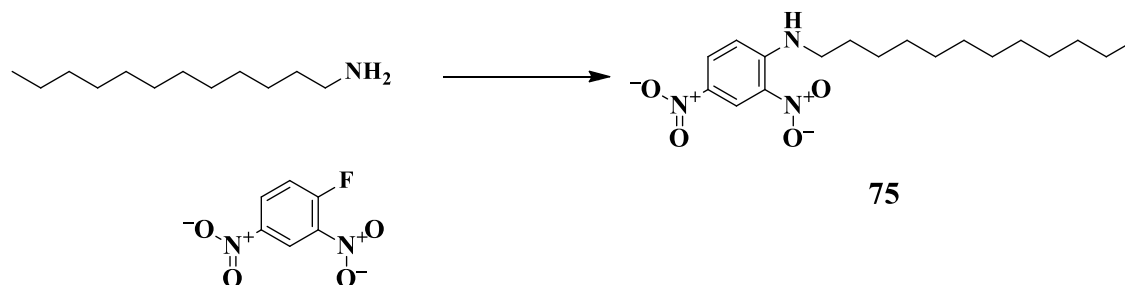
enecarboxylic acid (0.5000 g, 4.459 mmol) in 50 mL dry THF at -78 °C under inert atmosphere was added *tetr*-butyl lithium 1.7 M (9 mL, 13.37 mmol, 3 eq) over 1h. The mixture was stirred at the same temperature for an additional 30 minutes until dianion is successfully generated, then excess iodododecane was added gently. A white precipitate forms and produces a suspension which dissolves at higher temperature overnight. The mixture is quenched by 1 mL of H<sub>2</sub>O and stirred for 15 minutes, then THF is stripped off under vacuum and remaining crude is diluted with DCM. The organic solution was filtered and washed with H<sub>2</sub>O (6 x 50 mL), saturated NH<sub>4</sub>Cl (3 x 50 mL), and H<sub>2</sub>O (2 x 50 mL), dried over MgSO<sub>4</sub>, and purified with silica Hex:EtOAc (2:8) to afford a clear oil solid (2.006 mmol, 45 %),. <sup>1</sup>H-NMR (700 MHz; CDCl<sub>3</sub>): δ 5.63 (s, 2H), 2.96-2.93 (m, 2H), 2.35 (d, *J* = 16.4 Hz, 2H), 1.72 (t, *J* = 0.7 Hz, 2H), 1.29 (d, *J* = 28.9 Hz, 20H), 0.92-0.90 (m, 3H) ppm. <sup>13</sup>C-NMR (700 MHz; CDCl<sub>3</sub>): δ 183.2, 128.4, 52.4, 42.3, 39.4, 31.9, 30.0, 29.44, 29.31, 25.3, 22.7, 14.1 ppm. HRMS Anal. Calcd for C<sub>18</sub>H<sub>32</sub>O<sub>2</sub> 281.2481 (m/z). [M<sup>+</sup>] Found: 281.2471 (m/z).



**1-dodecylcyclopent-3-enecarboxylic acid (73)** To a suspension of lithium

aluminum hydride (0.3000 g, 6.000 mmol, 3 eq) in dry 100 mL THF at -78 °C, (**72**) (0.5618 g, 2.006 mmol) was added drop wise over 1h. The mixture was stirred for 6h, and then quenched with 15 mL 1 N NaOH. Mixture was stirred for an additional 2h, then concentrated and up taken in diethyl ether and dried over MgSO<sub>4</sub> to afford clear liquid (1.885 mmol, 63%).. <sup>1</sup>H-NMR (700 MHz; CDCl<sub>3</sub>): δ 5.62 (s, 2H), 3.48 (s, 2H), 2.25-2.15 (m, 4H), 1.46 (t, *J* = 7.6 Hz, 2H), 1.35-1.22 (m, 20H), 0.90 (t, *J* = 7.1 Hz, 3H) ppm. <sup>13</sup>C-

NMR (700 MHz; CDCl<sub>3</sub>):  $\delta$  129.3, 69.5, 46.1, 41.2, 37.5, 31.9, 30.6, 29.7, 29.4, 24.6, 22.7, 14.1 ppm. HRMS Anal. Calcd for C<sub>18</sub>H<sub>32</sub>O<sub>2</sub> 267.2688 (m/z). [M<sup>+</sup>] Found: 267.2679 (m/z).



***N*-dodecyl-2,4-dinitroaniline (75)**

To a solution of dodecylamine (0.1000 g, 5.276 mmol) and excess sodium bicarbonate in 100 mL MeOH at 0 °C, DNP-F (0.1000 g, 5.376 mmol) pre-dissolved in 5 mL of MeOH was added dropwise over 1h. The mixture was stirred for 6h then concentrated and up taken in DCM and dried over MgSO<sub>4</sub> to afford yellow crystals (4.677 mmol, 87%). <sup>1</sup>H-NMR (700 MHz; CDCl<sub>3</sub>):  $\delta$  9.17 (d, J = 2.7 Hz, ), 8.58 (s, 1H), 8.30-8.28 (m, 1H), 6.94 (d, J = 9.5 Hz, 1H), 3.43 (td, J = 7.1, 5.3 Hz, 2H), 1.80 (dt, J = 14.9, 7.4 Hz, 2H), 1.50-1.29 (m, 20H), 0.90 (t, J = 7.1 Hz, 3H) ppm. <sup>13</sup>C-NMR (700 MHz; CDCl<sub>3</sub>):  $\delta$  148.4, 135.9, 130.34, 130.26, 124.4, 113.9, 43.6, 31.9, 29.61, 29.53, 29.45, 29.34, 29.20, 28.7, 26.9, 22.7, 14.1 ppm.

## 4 CHAPTER FOUR

### Biological Studies and Application of Synthetic Molecules

---

#### 4.1 Introduction

This section will introduce the immense biological studies that illustrate the utility of our dialdehyde headgroup in the delivery of ligands onto the surface of mammalian and *E. coli* model organism using liposome fusion, protein-protein crosslinking, immobilization of amine-presenting beads, construction of multilayer mammalian cell tissues and surface substrates.

Previous studies have already demonstrated the ability of liposome fusion to deliver a lipid like functional group onto both prokaryotic and eukaryotic cells with high efficiency.<sup>172,288,289</sup> Unlike preliminary interests in using liposome fusion for cargo delivery, our work has exploited this system to deliver a functional group onto the surface of a cell. Although any lipid molecule with a reactive headgroup could be presumably installed on the membrane, only a handful has important application in conjugation chemistry. In Chapter 2, we illustrated the successful incorporation of a lipid-like molecule with a ketone functional group onto the surface of *E. coli*.<sup>289</sup> The presence of the ketone molecule was then detected using synthesized fluorescent probe, immunostaining with biotin-streptavidin, adhesion to hydroxylamine surface and isolation of membrane components followed by confirmation of MS/MS analysis. The results showed promising

opportunity for the incorporation of exogenous molecules on the surface without interruption of regular cellular functioning machinery.

Results reported in Chapter 2 inspired us to use our dialdehyde strategy in the context of liposome fusion, and deliver a bioconjugate pair onto lipid bilayer. Armed with an amino group handle, any exogenous body like protein, carbohydrate, peptides or small molecule carrying a primary amine could be easily installed on the surface of a cell. We explored the ability of a dialdehyde headgroup to deliver biological probes onto the surface of the mammalian and bacterial cell via amine coupling reactions; then we verified the presence of the probe using spectroscopic analysis, flow cytometry and immunostaining assays.

We also examined the unique ability of our homobifunctional crosslinker to link and /or staple one and two protein component systems with high efficiency competing with other commercially available crosslinkers. This method has a great opportunity to secure a promising position in the field of an antibody-drug conjugate (ADC). Coupled to a payload through a robust covalent bond, the ADC complex could successfully deliver its payload to a highly selective target, and further release it for an efficient therapeutic effect with reasonable yield.<sup>290</sup>

In continuation of exploring its capacity, we crosslinked polymer beads that are functionalized with primary amines together. This work also demonstrates the unique reversibility feature of our conjugation system. Releasing the amine from the dialdehyde to regenerate the starting material is a unique trait in our design that is absent from all other comparable systems. We also extrapolated the crosslinking ability of a hydrophilic

homobifunctional molecule to generate multilayers of mammalian tissue. To the best of our knowledge, this work is the first demonstration of such tissue engineering protocols that do not require any pre-treatments or prior modification of the tissue sample or scaffold design.<sup>291–293</sup>

In an attempt to synthesize a solid surface displaying dialdehyde, we functionalized a glass plate that proved to be highly effective in immobilizing any primary amine carrier. To investigate the immobilization ability of the surface, we introduced beads displaying an amine moiety on their interface. Subsequently, the releasing quality of our technology was reemphasized by decoupling the beads to recover the dialdehyde-functionalized surface.

## **4.2 Results and Discussion**

### **4.2.1 Delivery of Ligands via Functionalized Liposome**

Liposome fusion is a highly regulated task by the cellular membrane lipid bilayer. A cell is quite familiar with the mechanism of fusion through the development of endo/exocytosis processes (**Figure 2.4**). Since the lipid bilayer contents of cell lines could be drastically different, an appropriate charge and lipid tail are essential for the extent of fusion (**Figure 4.1**). In Chapter 2, we demonstrated that anionic lipid contents in the nanostructure are suitable for liposome fusion into the gram-negative bacteria cell membrane.

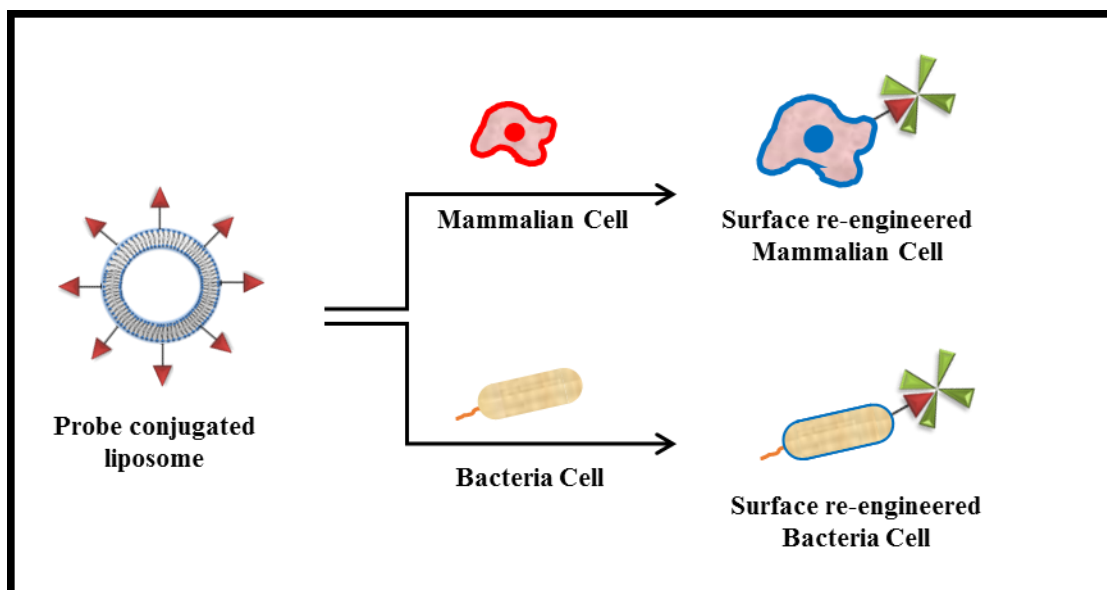


*Figure 4.1 Cartoon depiction of functionalized liposome delivery of reporters via fusion onto surface of mammalian and bacterial cell*

Functionalized liposomes could be incubated with cells for the appropriate time to present the reporter molecule on their surfaces. The probe could be easily detected through a variety of analytical techniques such as immunostaining, flow cytometry and fluorescent microscopy.

Although the use of such compositions is in a disagreement with bactericidal effects of such charged lipid molecules, appropriate concentration and composition allowed for a more effective fusion. The dialdehyde headgroup on a long lipid tail has proven to be insusceptible to polymerization in presence of moderate concentration of charged lipids, thus could be mixed with a variety of lipid compositions suited for any particular cell type.

It is evident that the ability of a cell to uptake liposome nanostructures is highly dependent on the cell line and its physiology. For example, while gram-negative bacteria could easily accept a liposome nanostructure and display a functional group on its surface, the thick peptidoglycan layer of gram-positive bacteria prevents the process (**Figure 2.7**).

The Same principle applies to mammalian cells, thus contributes to liposome content taken up by the lipid bilayer.

Herein we demonstrate the ability of functionalized liposomes onto different cell surfaces (**Figure 4.3, Figure 4.6**). The liposomes nanostructures obtained using pathways **A** and **B** were used to transfer a collection of ligands like DNP, biotin and FLAG peptide onto the surface of mammalian cells, and biotin to the surface of bacteria cell wall. All of these ligands were detected using flow cytometry, microscopy and immunostaining. Only cells with a successful conjugate of dialdehyde and reporter amine displayed interaction with antibody-fluorophore. In contrast, Cells treated with dialdehyde liposomes, which were quenched with sacrificial propylamine did not conjugate with amine probe and showed no affinity for their corresponding antibody.

#### **4.2.2 Preparation and Delivery of Dialdehyde Lipids Conjugate**

The application of our novel amine conjugation is not limited to its utility in the context of organic chemistry. Preparation and delivery of dialdehyde using liposomes onto cell surfaces were investigated via two routs illustrated in (**Figure 4.2**). We demonstrated that lipid-like dialdehyde molecule could be mixed with background lipids to form liposome nanostructures displaying the reactive site for amine conjugation (pathway A), OR, it could be coupled to any amine containing ligand and then incorporated into liposome nanostructures (pathway B). Similarly, an amine-lipid molecule could be mixed with the proper composition of lipids to form a liposome nanostructure. The delivered amine could be detected and quantified using a reporter armed with a dialdehyde headgroup.

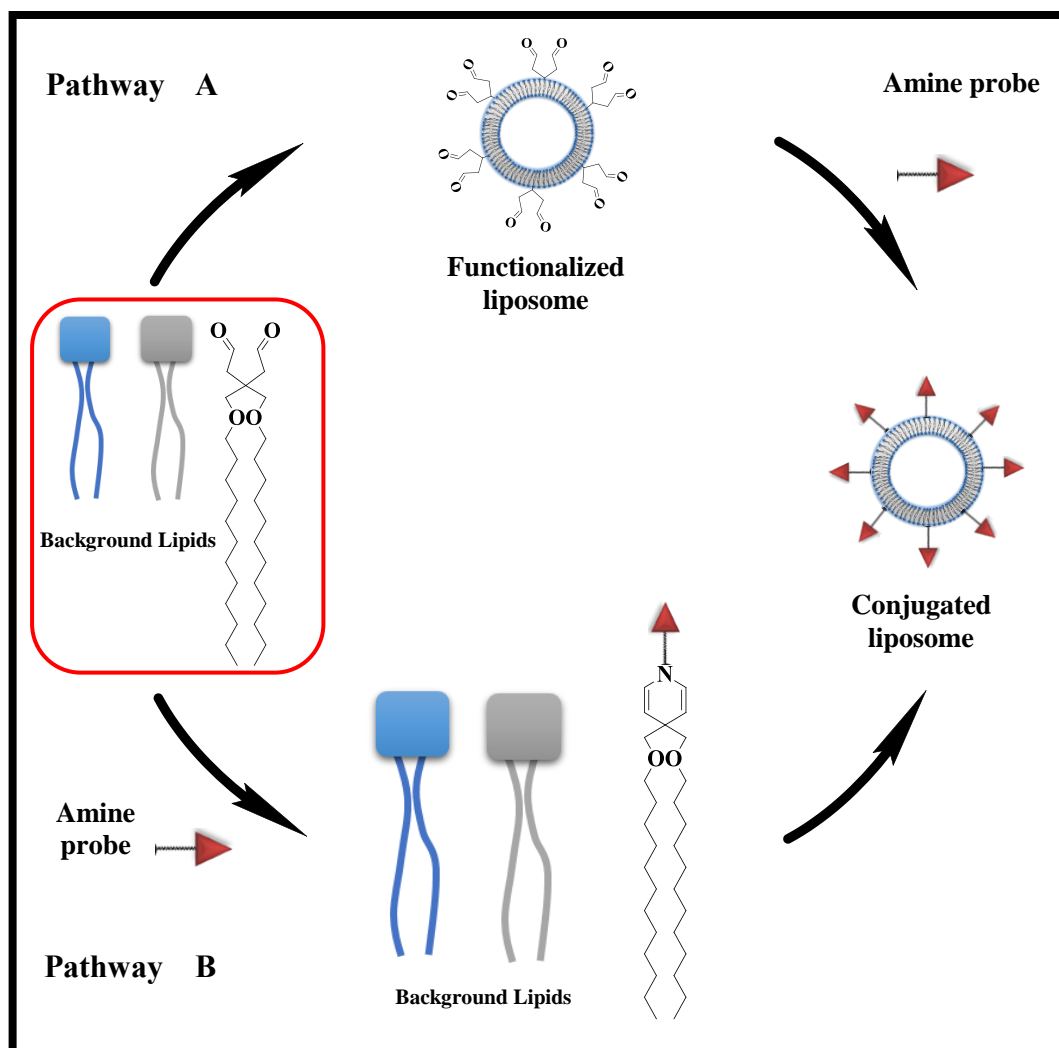


*Figure 4.2 Cartoon depiction of functionalized liposome SUV particle preparation*

Liposomes were formed by mixing the proper lipid composition with dialdehyde lipid molecule to form SUVs displaying dialdehyde functional headgroup, through two different pathways. In **Pathway A** dialdehyde functionalized liposomes were formed by mixing the proper concentration of background lipid molecules with lipid-dialdehyde then the nanostructures were treated with amine containing probe in water to generate a liposome nanostructure displaying the probe. In **pathway B**, dialdehyde lipid was first conjugated with a probe containing amine functional group, then sonicated to form liposomes displaying the probe. Both pathways will result in the formation of liposomes that could deliver their interface payload onto membrane surfaces via fusion.



This flexibility in functionalized liposome is critical for downstream applications, in which reactivity and non-selective interactions with other species become a concern. Liposomes were formed by mixing the proper composition of lipids and dialdehyde-lipid molecule (pathway A) to form SUVs displaying dialdehyde functional headgroup, then the nanostructures were treated with amine containing probe in aqueous buffer, and sonicated to generate a liposome nanostructure displaying the probe. In pathway B, the dialdehyde lipid is first conjugated to a probe and then sonicated with other lipids to form nanostructures displaying the probe. Both routes would result in a robust chemical ligation of the amine to the headgroup, and will successfully transfer the ligand to a lipid bilayer. Both conjugate and the dialdehyde starting material proved to be highly tolerant to sonication and insusceptible to hydrolysis in an aqueous environment. This is an important concern for long and complicated biochemical applications that simultaneously engage many different factors with the different nucleophilic center. This feature allows for the generation of flexible protocols designed for multicomponent biological experiments.

The liposomes containing the probe could be stored up to 3 weeks at -20 °C in aqueous conditions. While the extent of degradation has not been measured, the results obtained from downstream applications show no significant difference compared to freshly made batches. It is noteworthy to mention that the use of a bis-lipidated structure of dialdehyde **42** would allow for a higher efficiency of lipid insertion, thereby, more probe delivery per surface.



containing ligated probe showed an affinity for their corresponding fluorophore-antibody, hence generated fluorescent signals. Quenched dialdehyde liposomes and deficient liposomes fed to cells, did not display any interaction with the antibody hence did not generate any signals. Figure **A** to **C** show the delivery onto mammalian cells and **D** illustrates bacterial surface delivery. (**A**) Mammalian cells were treated with liposomes conjugated to a DNP-NH<sub>2</sub> (**59**) and detected using Anti-DNP antibody FITC using flow cytometry; further, a fluorescent image of the cells decorated with probe-antibody FITC was obtained using a microscope. (**B**) Mammalian cells were also treated with liposomes conjugated to Biotin-NH<sub>2</sub> and further detected using streptavidin-FITC using flow cytometry followed by microscopy. (**C**) Mammalian cells were treated with liposomes conjugated to FLAG peptide and were detected using FITC-anti-FLAG antibody via flow cytometry and microscopy analysis. (**D**) Shows a cartoon depiction of *E. coli* B121 cells treated with biotin-NH<sub>2</sub> further detected using streptavidin-FITC via flow cytometry and fluorescent microscopy.

The quantities of fluorescent molecules on both types cells were quantified based on a standard fluorescence quantification kit (Quantum<sup>TM</sup> FITC-5 MESF from Bangs Laboratories, Inc.) (**Figure 4.4**). The quantification kit contains a group of fluorescent beads labelled with varying amounts of FITC. A QuickCal® analysis template is provided with the kit. After using flow cytometry to measure the fluorescence intensity of beads, to generate a standard curve for the intensity of fluorescent. Therefore, the fluorescent intensity can be directly translated into the amount of surface conjugation.

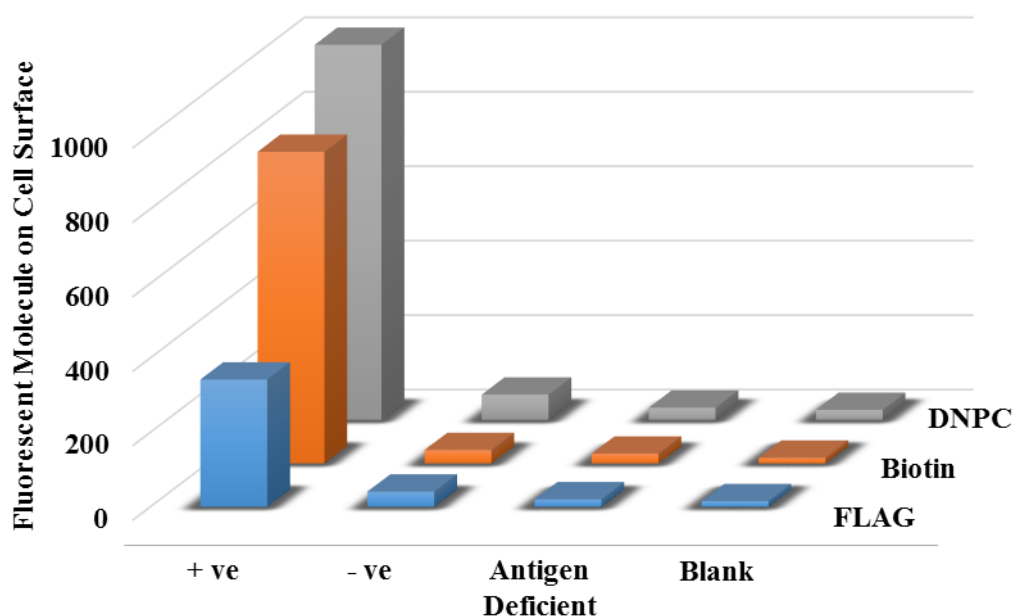


*Figure 4.4 The number of delivered antigen molecules via ligation to dialdehyde-functionalized liposome*

A two-dimensional (2D) plot describing a number of antigen molecules on the mammalian cell surface. The antigen molecules on the cell surface were conjugated to a dialdehyde lipid like molecule and mixed with appropriate composition and concentration of lipids to form liposome particles. Liposomes decorated with the probe were then incubated with cells in media and treated with a corresponding antibody-FITC reporter. The number of FITC molecules were quantified using Quantum<sup>TM</sup> FITC-5 MESF calibration kit via flow cytometric analysis.

In contrast to mammalian cells, the quantities of fluorescent molecules per surface of a bacterial cell are much more abundant (**Figure 4.5**). This is merely due to the significantly higher concentration of probe required to reengineer a bacterial surface.<sup>289</sup> Informed by previous observations on bacterial lipid bilayer and experiments performed in Chapter 2, the concentration of ligands required for clear detection was observed to be much higher

for prokaryotic cells. This also reveals the high tolerance of gram-negative membrane to allow such high liposome content to fuse within the lipid bilayer. While a maximum number of molecules observed on mammalian cell membrane was 1008 molecules/cell, *E. coli* could withstand up to 15000 molecules/cell.

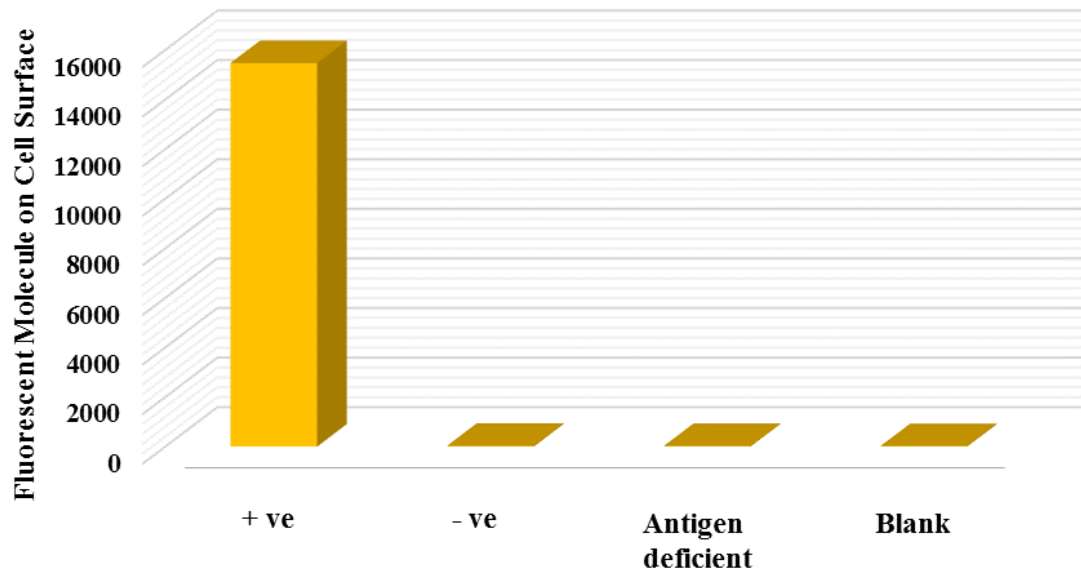


*Figure 4.5 The number of delivered biotin molecules via ligation to dialdehyde functionalized liposome*

A two-dimensional (2D) plot describing the number of biotin-NH<sub>2</sub> molecules on the *E. coli* B121 cell surface. The antigen molecule on the cell surface was conjugated to a dialdehyde lipid-like molecule and mixed with appropriate composition and concentration of lipids to form liposome particles. Liposomes decorated with the probe were then incubated with cells in media and treated with Streptavidin-FITC antibody fluorescent reporter. The number of FITC molecules were quantified using Quantum TM FITC-5 MESF calibration kit via flow cytometric analysis. The number of a fluorescent reporter on the surface is directly proportional to the number of biotin present on the cell surface.

### 4.2.3 Preparation and Delivery of Dialdehyde Reagents

In another project, we attempted to synthesize a suite of molecular probes with a dialdehyde headgroup on their backbone structure. Molecular probes have important utility in biotechnology and have been used extensively for cellular interaction studies. We have demonstrated and explained the synthesis of probes in Chapter 3. In this study, we conjugated a molecular probe to an amine lipid molecule and exploited their ability to insert into a membrane as immunostaining reporters (**Figure 4.6**). In an alternative attempt to generate reporter-presenting liposomes, SUVs were prepared by sonicating the appropriate composition of the lipids with dodecylamine to display a primary amine on their surface. A biomolecule armed with a dialdehyde headgroup was then mixed with the liposomes and incubated for 15 minutes to ensure chemical ligation is established. This approach allows for a successful incorporation of any biomarker with a dialdehyde functional group onto cell surface via liposome fusion. It is important to mention that such reporters could be used to directly tag any structure that contains a primary amine, ie proteins, antibody, carbohydrate, etc. However, in this study, they were utilized in the context of liposome fusion for a demonstration of delivery onto the cell surface.

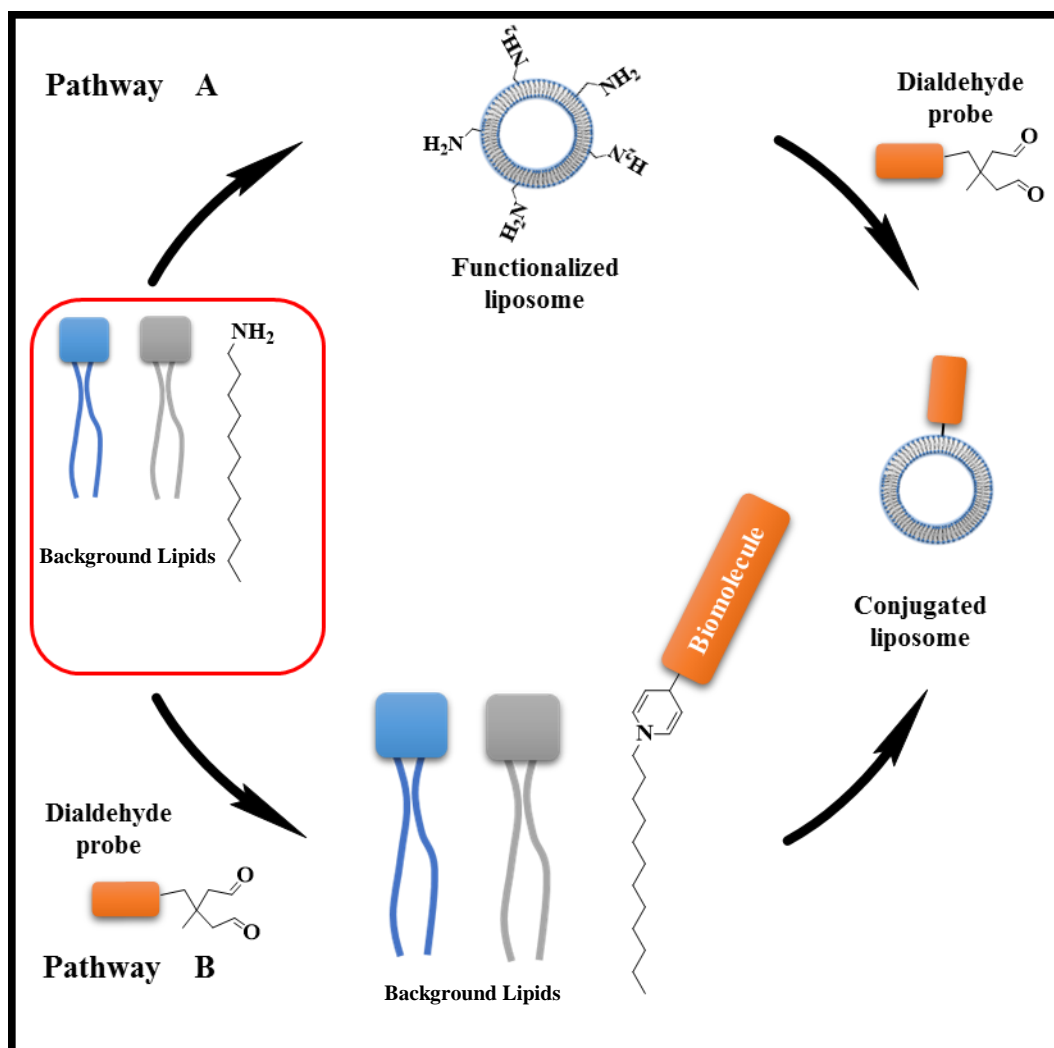


*Figure 4.6 Cartoon depiction of functionalized liposome SUV particle preparation*

Liposomes were formed by mixing the proper lipid composition with dodecylamine to form SUVs displaying a primary nucleophilic moiety. In **Pathway (A)** dodecylamine functionalized liposomes were formed by mixing the proper concentration of background lipid like molecules then the nanostructures were treated with dialdehyde biomolecule in water to generate a liposome nanostructure displaying the biomolecule reporter. In **pathway (B)**, dodecylamine lipid was first conjugated with a probe to secure a covalent bond, then sonicated to form liposomes displaying the reporter. Both pathways will result in the formation of liposomes that could deliver their interface payload onto membrane surfaces via fusion.

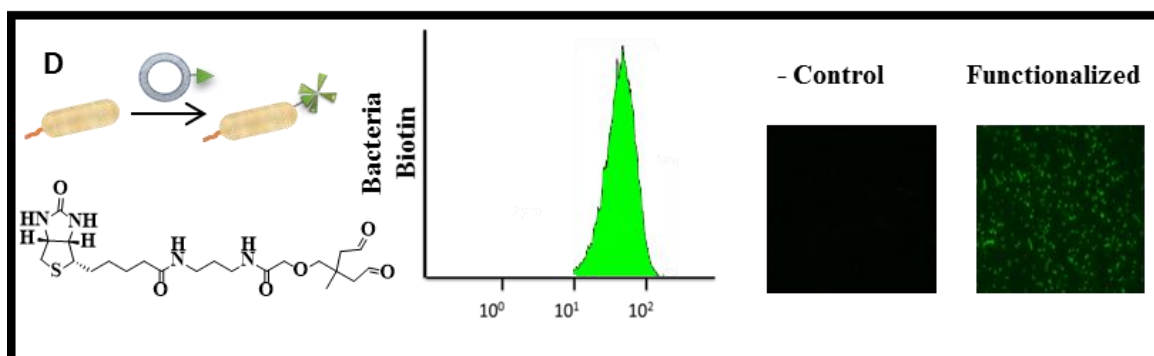
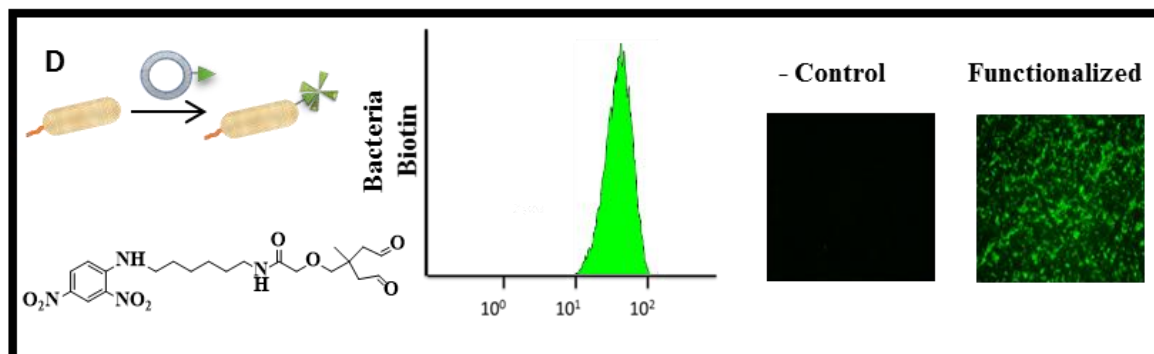
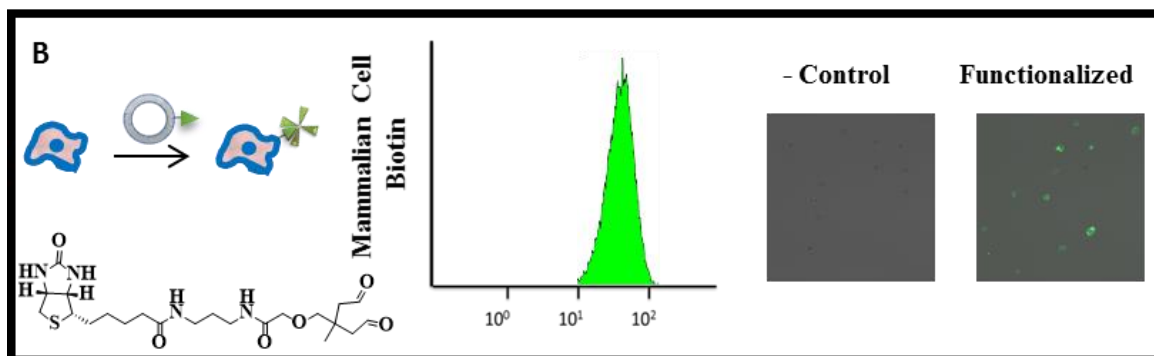
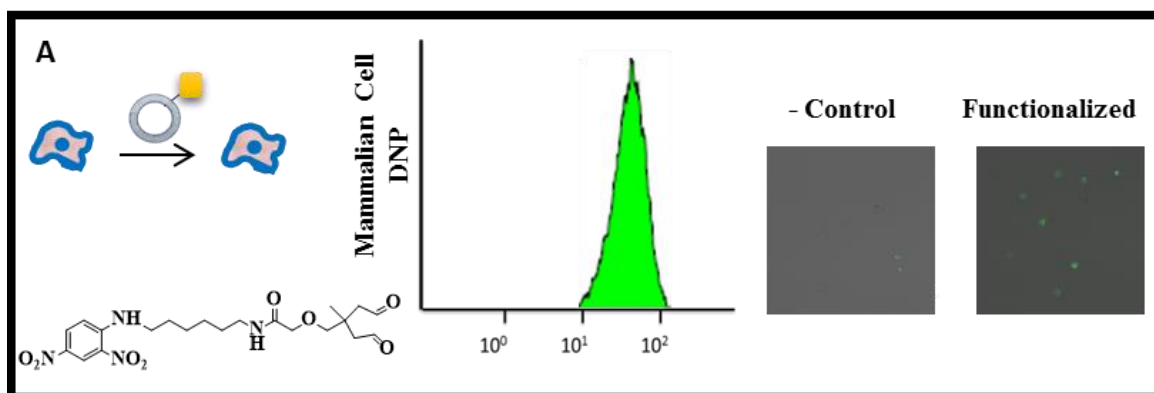




*Figure 4.7 Cartoon depiction of dialdehyde reporter conjugation to a dodecylamine liposome, further delivery of the complex onto the surface of the mammalian and bacterial membrane.*

Flow cytometry and fluorescent microscopic analysis of the successful liposome delivery of a dialdehyde bioreporter via ligation to dodecylamine functionalized liposome is presented, in which only cells treated with liposome containing ligated probe showed an affinity for their corresponding fluorophore-antibody, hence generated fluorescent signals. Quenched dialdehyde reporters and deficient liposomes fed to cells, did not display any interaction with the antibody hence did not generate any signals. Figure A to C show the delivery onto mammalian cells and D illustrates bacterial surface delivery. **(A)** Mammalian cells were treated with liposomes functionalized with a bioreporter DNP-dialdehyde (**62**) and detected using Anti-DNP antibody FITC using flow cytometry; further, a fluorescent image of the cells decorated with probe-antibody FITC was obtained using a microscope. **(B)** Mammalian cells were also treated with liposomes functionalized with a bioreporter biotin-dialdehyde (**57**) conjugated to dodecylamine and further detected using streptavidin-FITC using flow cytometry followed by microscopy. **(C)** Bacteria cells were treated with liposomes conjugated to DNP-dialdehyde (**62**) via ligation with dodecylamine and were detected using Anti-DNP antibody FITC via flow cytometry and microscopy analysis. **(D)** Shows a cartoon depiction of bacteria cells treated liposome functionalized with a bioreporter biotin-dialdehyde (**57**) further detected using streptavidin-FITC via flow cytometry and fluorescent microscopy.

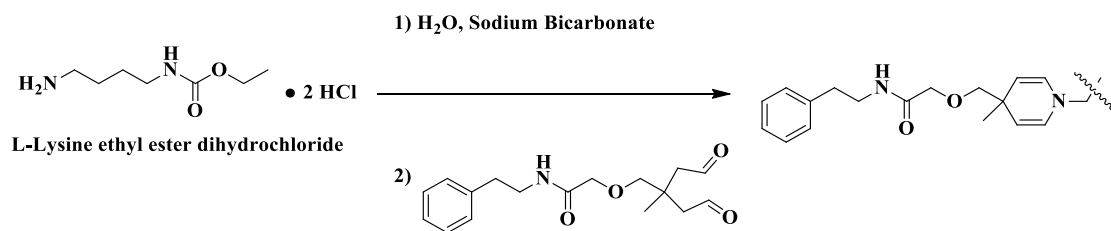
Similar to the previous experiment (**Figure 4.3**), we demonstrate the ability of dialdehyde reagents to conjugate to a primary amine and insert into the lipid bilayer of both mammalian and bacterial cell wall (**Figure 4.7**). Using two different preparation methods pathway **A** and **B**, we illustrate both the stability and effectiveness of our synthesized molecules, to participate in multicomponent studies in tandem with other biological macromolecules and deliver the purpose with high selectivity. The liposome nanostructures obtained using pathways **A** and **B** were used to transfer DNP-dialdehyde and biotin-dialdehyde onto the surface of mammalian cells and bacteria cell wall. All of these ligands were detected using flow cytometry, microscopy and immunostaining. Only

cells treated with amine-functionalized liposomes carrying a reporter interacted with the corresponding antibody. In contrast, Cells treated with quenched amine liposomes, which were acetylated did not conjugate with dialdehyde probe and showed no affinity for the antibody. Similarly, probes that were quenched with propylamine did not react with dodecylamine in a liposome, thus did not present any affinity for the antibody.

#### **4.2.4 Non-Liposomal Application of Dialdehyde Conjugating System**

##### **4.2.4.1 Examination of Lysine Conjugation with Dialdehyde Substrate**

The promising results obtained from the successful conjugation of amines inspired us to explore other possible utility for this system. Although incorporation of small ligands displaying a primary amine onto the cell surface via liposome fusion is a great achievement, delivery of macromolecules with complicated physiological roles is an exceptionally important endeavor. The results obtained from the successful conjugation of FLAG peptide to the dialdehyde lipid molecule was a demonstration for the practicality of our system to serve as a promising method in protein conjugation field. In order to better understand the protein conjugation, we attempted the reaction using a modified lysine with a hydrophilic dialdehyde substrate **53** (**Scheme 4-1**). This experiment played a key role in our understanding of amino acid conjugation behavior as the smallest subunit of larger biostructures.



*Scheme 4-1 Conjugation of L-lysine ethyl ester dihydrochloride with substrate 53*

Although the reaction was performed in aqueous solution, the characterization had to be carried out in a deuterated organic solvent for <sup>1</sup>H-NMR spectroscopy (**Figure 4.8**). The exposure of the dienamine to any protic/deuterated solvent would favour the equilibrium towards formation of a deuterated alkene. Therefore, obtaining the spectrum in D<sub>2</sub>O poses some challenges in identifying the appropriate signals (**Scheme 4-2**).

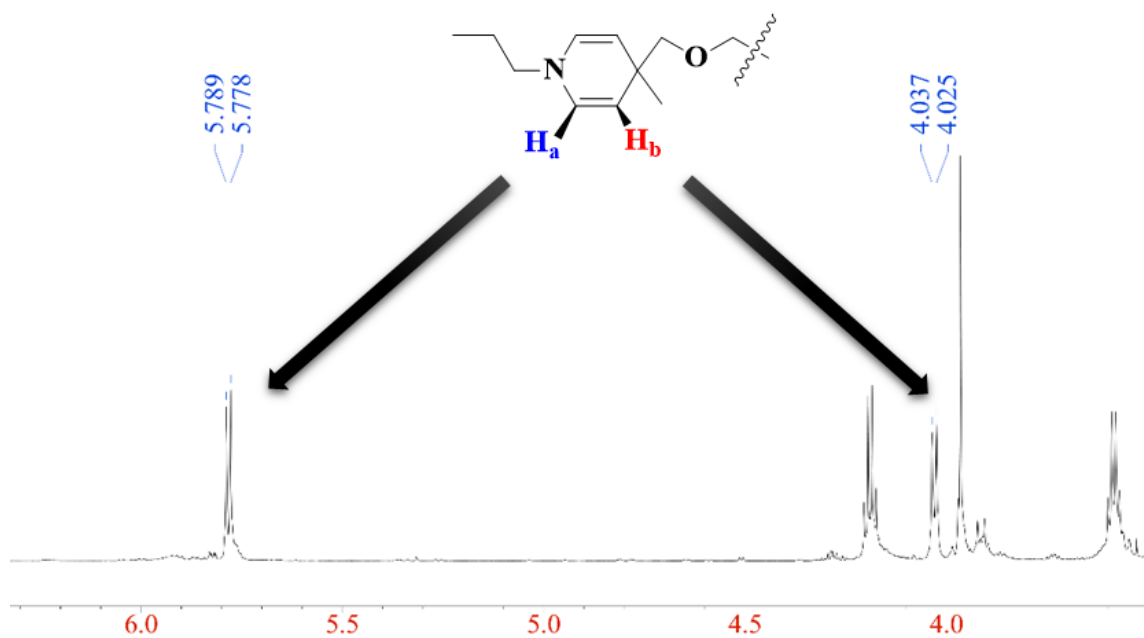


*Figure 4.8 <sup>1</sup>H-NMR spectrum of conjugating L-lysine ethyl ester with substrate 53*

The appearance of persistent signals at 4.025-5.789 ppm is a strong evidence for the formation of 1,4 dihydropyridine ring. The pair of signals could only be visualized

if the spectrum is obtained in an organic deuterated solvent. However, the reaction it self could easily be performed in an aqueous solution, then prepared in a non-protic NMR solvent.

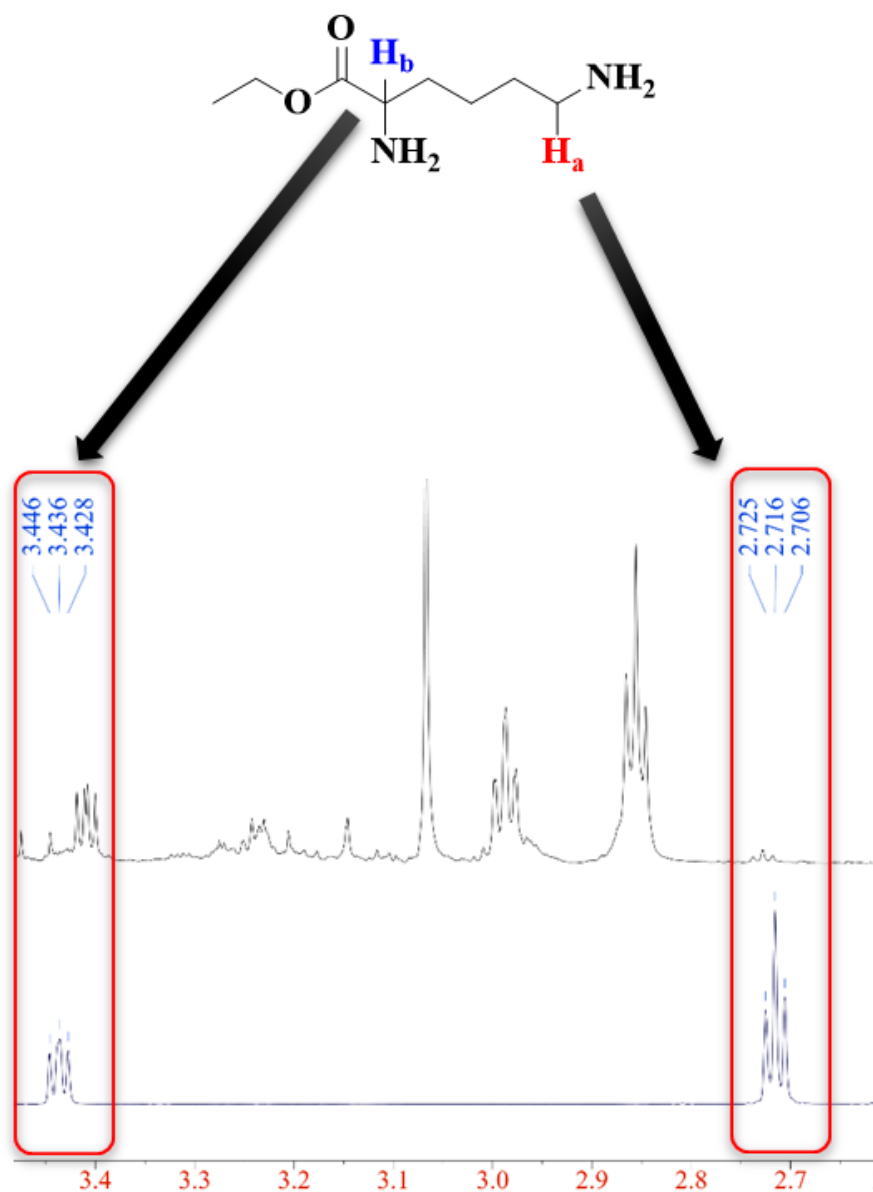
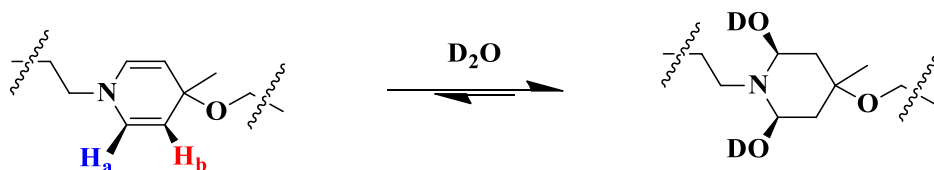


*Figure 4.9 Spectral comparison of unreacted L-lysine and conjugated L-lysine after reacting with dialdehyde 53*

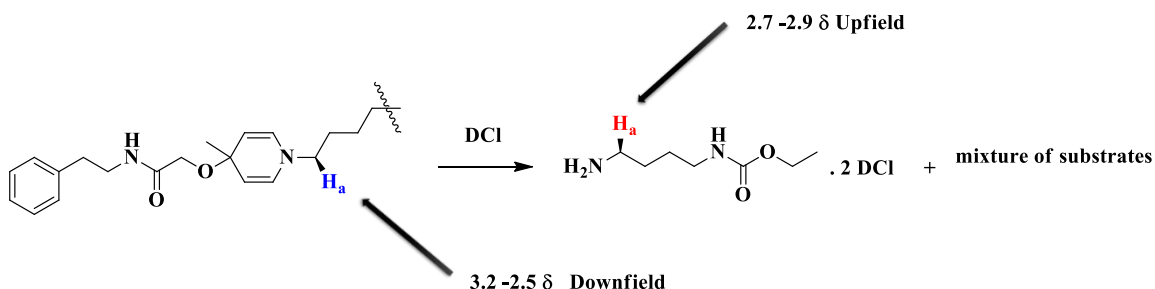
It is evident that α-protons to the amines have shifted consistently with the chemical shift of a tertiary amine

Although the spectrum is eventually obtained in an organic solvent, the corresponding enamine peaks in the final spectrum of the conjugated product are only observed if the conjugation has successfully completed, therefore it could unambiguously confirm the viability of the reaction.



*Scheme 4-2 Deuteration of enamine moiety with exposure to D<sub>2</sub>O*

The reversibility of our system was also investigated through treatment of the final conjugate with DCl in MeOD to afford species that no longer resemble any of the conjugates (**Scheme 4-3**).



*Scheme 4-3 Examination of reverse reaction of conjugate to starting material at lower pH*

The conjugate product of L-lysine ethyl ester with substrate **53** was treated with DCl and D<sub>2</sub>O and adjusted to pH 3.0, The <sup>1</sup>H-NMR spectrum of this mixture was obtained and analyzed for consistent peaks.

Although the products of acid treatment were not isolated and characterized independently, the spectrum of this reaction is consistent with the reformation of the attacking amine indicated by the slight upfield shift of  $\alpha$ -proton on amino, which is consistent with the chemical shift of primary amine residue at approximately 2.70 – 2.90  $\delta$  ppm (**Figure 4.10**). Reformation of some unresolved set of peaks at 5.2 -5.7  $\delta$  ppm regions of the spectrum is consistent with the formation of polymeric hydrates or hemiacetal structures that were reported in both structural elucidation of glutaraldehyde studies, and our dialdehyde substrate  $^1\text{H}$ -NMR spectra. While an explicit analysis of isolated product has not been performed to determine whether a “reusable” starting material is regenerated during the reverse process, it is clear that after 3 min of acid exposure, there are no longer any molecular associations between the attacking amine and dialdehyde substrate. This unique feature of dialdehyde conjugating system allows for the release of any conjugate upon demand. The ability of any conjugate to release a payload becomes enormously important in the delivery of a payload on an antibody.

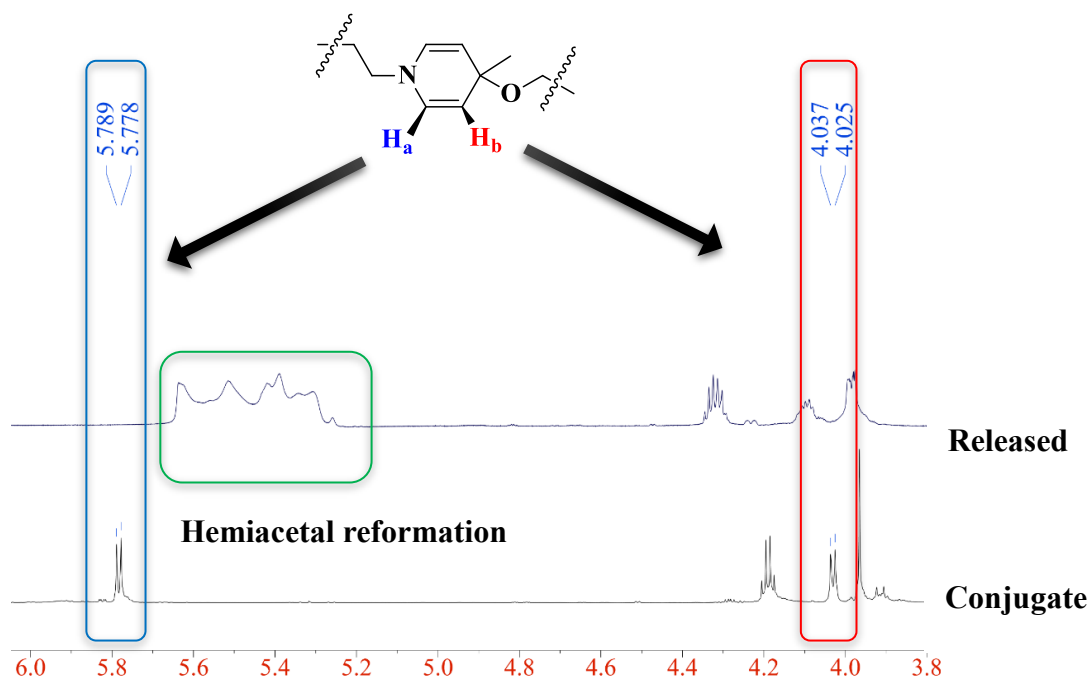


*Figure 4.10  $^1\text{H}$ -NMR spectrum of acid treated L-lysine ethyl ester conjugate with substrate **53***

The conjugate product of L-lysine ethyl ester with substrate **53** was treated with DCl and its results were analyzed via  $^1\text{H}$ -NMR spectroscopy. It is evident that at low pH, the enamine peaks have completely disappeared from the spectrum. The reappearance of a set of unresolved signals between 5.2 -5.7 ppm is highly consistent with the previous observation from a mixture of hydrated/polymeric dialdehyde structure. This is a reflection of a reverse reaction occurring to regenerate some of the starting material

#### 4.2.4.2 Protein Crosslinking Using Homobifunctional Dialdehyde Crosslinker

The promising results obtained from a successful reaction of the smallest building block of a protein with the dialdehyde headgroup inspired us to expand the method to use our homobifunctional crosslinker in protein bridging. In an effort to explore protein

conjugation field, many model systems such as antibodies and other classes of proteins were treated with ligands and crosslinkers containing dialdehyde headgroup. Since antibodies have become an important alternative to selectively deliver a potent payload to a cancerous target<sup>294</sup>, they deserve special attention in bioconjugation chemistry. Selectivity, efficient delivery and effective release of a cytotoxin to a target, demands an antibody-drug-conjugate interaction that is robust enough to successfully deliver the payload, and subsequently allow for an efficient release to the selected targets. While attempts on antibody conjugation using our technology have proven to be much more challenging than the currently available protocols, we successfully conjugated our dialdehyde headgroup to other classes of macromolecules and proteins (**Figure 4.11**).

Herein we introduce two protein systems that were successfully crosslinked using our homobifunctional dialdehyde substrate. A common leucocyte antigen release protein LAR D1D2, and Caskin2 SAM2 domain are two independent structures that would naturally form a complex with one another with high affinity. However, once run on a denaturing SDS gel they would fall apart due to lack of a covalent link. Therefore, the denatured fragments of the protein will be present as multiple distinctive precursor bands on the gel. Using a very small amount of dialdehyde crosslinker **70**, we successfully established a robust covalent bond between the two components and formed a multimer of the protein complex that would not break apart on SDS gel. The complex withstood the disrupting effect of SDS gel and a high temperature of 100 °C while staining with a  $\beta$ -mercaptoethanol.



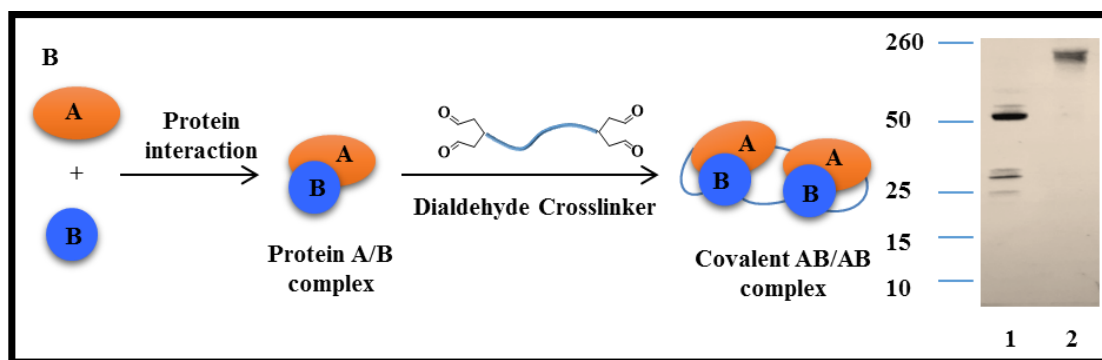


*Figure 4.11 Cartoon depiction of Protein LAR D1D2I and Caskin 2 SAM2 crosslinking to form a robust covalent bond*

Protein LAR D1D2I and Caskin 2 SAM2 were incubated to associate with each other in solution. To this complex was added 15  $\mu\text{L}$  amount of substrate (**70**) dialdehyde crosslinker and incubated for 15 minutes. The amine residue on proteins would rapidly be trapped with dialdehyde moiety and form a robust covalent bond. Since the interaction of the two protein is now secured through a real stable covalent bond, they would not dissociate under normal conditions used in electrophoresis analysis. **Lane 1** presents the electrophoretic separation of two proteins from each other deficient of any crosslinker. **Lane 2** presents the attempted electrophoretic separation of two proteins that are connected through a covalent bond. It is evident that complex in the lane 2 would not dissociate to regenerate two isolated proteins.

Similarly, a bacterial lamdaphage protein PP16 was crosslinked to another PP16 to form higher molecular weight complexes (**Figure 4.12**). In another example, EA22 a small molecular weight protein was successfully crosslinked to form a dimer and a tetramer. Although crosslinking of protein is a relatively challenging task, stapling of protein is a unique reproducible ability of dialdehyde reagent that has not been achieved using glutaraldehyde or other available commercial products.

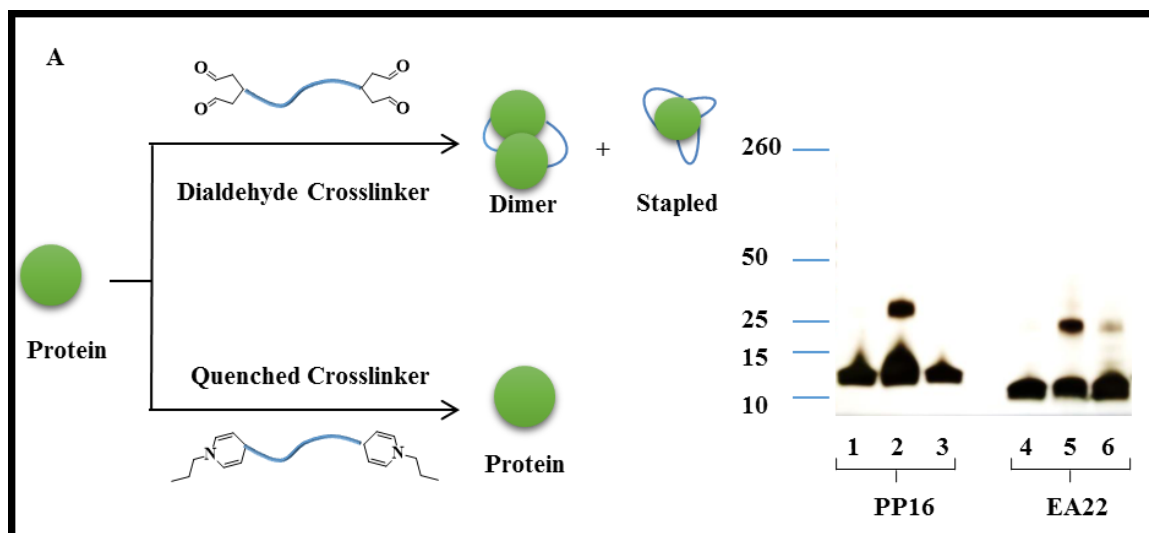


*Figure 4.12 Illustration of protein PP16 and EA22 crosslinking to form a robust covalent bond*

In separate vials, protein PP16 and EA22 were each incubated with 15  $\mu$ L amount of substrate (**70**) dialdehyde crosslinker for 15 minutes. the amine residue on proteins would rapidly be trapped with dialdehyde moiety and form a robust covalent bond between like proteins. The interaction of the complexed protein is now secured through a real stable covalent bond and forms a multimeric association that would not collapse under normal conditions used in electrophoresis analysis. **Lane 1** presents the native PP16 protein, **Lane 2** is protein PP16 treated with dialdehyde crosslinker and **lane 3** is a protein that has been treated with a propylamine-quenched crosslinker, hence will remain unreactive towards dialdehyde head group. **Lane 4** presents the native EA22 protein, **Lane 5** is protein EA22 treated with dialdehyde crosslinker and **lane 6** is a protein that has been treated with a propylamine-quenched crosslinker, hence will remain unreactive towards dialdehyde head group. The minor positive signal is merely a contrast concern and should not be interpreted as comparable binding to a typical positive trial.

Protein conjugation, and in particular crosslinking, is highly dependent on the type of the protein and substructures embedded within its outer surface. It is safe to say that

there does not exist a single reagent that would crosslink all kinds of protein. It is important to emphasize the importance of available amino groups on the outer layers of the protein for ligations. Although most proteins contain some lysine residues or display some nucleophilic amino group on their outer surface, not all proteins could participate in bioconjugation reactions in a predicted behavior.<sup>124,295–297</sup> (**Figure 4.13**)

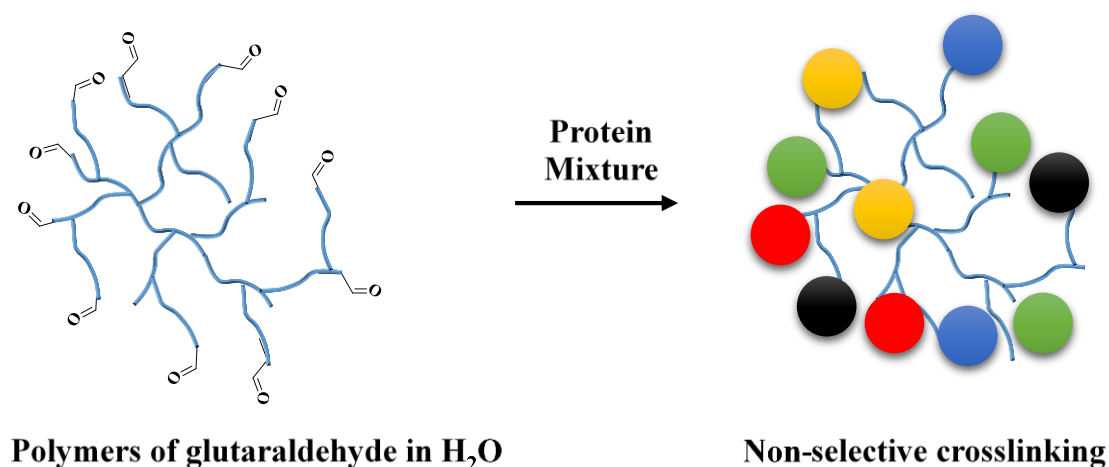


*Figure 4.13 A cartoon depiction of non-selective crosslinking of proteins using glutaraldehyde*

Glutaraldehyde has a unique ability to crosslink a protein mixture to form large structural coagulations that present no specificity for the region and type of protein connection. It often crosslinks all lysine rich regions of macromolecules without discriminating the structure, function, or folding nature of the proteins.

We have also compared the crosslinking ability of dialdehyde against glutaraldehyde to learn about their differences. It is evident that there are more multimeric species of the same protein is formed using glutaraldehyde reagent. This phenomenon is merely due to the formation of polymeric structures of glutaraldehyde molecules in an aqueous

environment, which could act as a massive network to react with many proteins and form a large coagulated structure. Although the extend of polymerization would be directly dependent on glutaraldehyde concentration, such samples often present multiple bands or a smear of proteins on a non-denaturing SDS gel. In contrast, a homobifunctional dialdehyde crosslinker would selectively yield only one of those multimers based on the concentration used in the final solution of the same protein.

#### **4.2.4.3 Bead Crosslinking Using Homobifunctional Dialdehyde Crosslinker**

We demonstrate the effectiveness of a homobifunctional crosslinker displaying two dialdehyde headgroups at the ends of TEG and C12 aliphatic arm to connect larger cell-like macroscopic structures (**Figure 4.14**). This approach takes advantage of the fact that cells are coated with layers of proteins and could act as a concentrated ball of amino groups. To examine the feasibility of crosslinking macrostructures using dialdehyde conjugation, a model system fluorescent yellow-green latex amine-modified polystyrene suspension of 1.0  $\mu\text{m}$  mean-particle size was used. This model system was chosen to resemble a macrostructure presenting a cell size. Although there is a size difference of up to 10-fold between the beads and mammalian cells, the macroscopic scale of 1.0  $\mu\text{m}$  is sufficiently large enough to qualify as a model system representing mammalian cells. Beads treated with the crosslinker formed aggregates of larger particles in solution and eventually settled down from the solvent. Upon treatment with dilute acid, beads were then released as single monomers. Similar to previous attempts, the reversibility of this system was assessed using dilute  $\text{H}^+$  and allowed for a complete control over the release of beads.

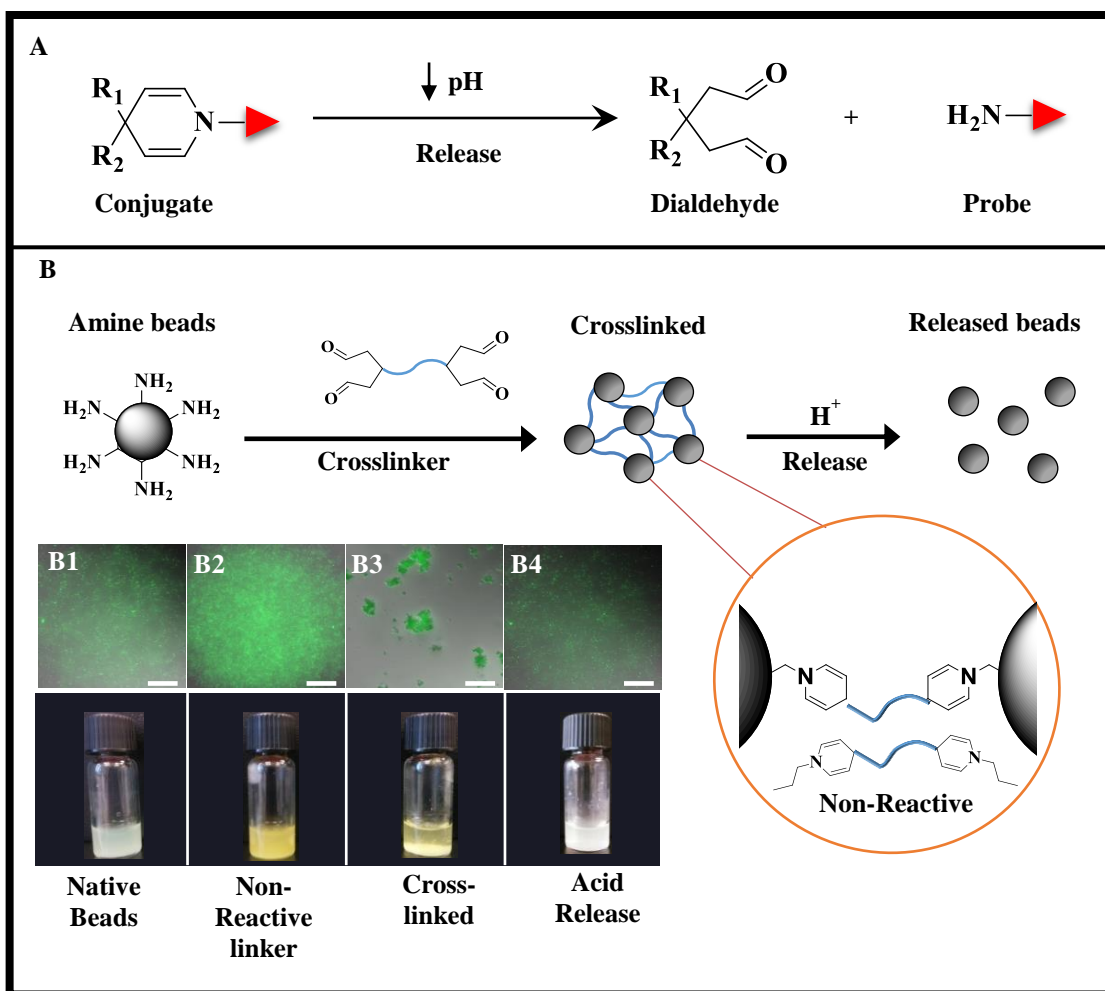


*Figure 4.14 Demonstration of an application in conjugation and releasing through acid catalysis in fluorescent beads*

(A) a general illustration of acid-release of a payload from the conjugate is presented. Lowered pH ranges would rapidly release the amine-payload from the dialdehyde head group to yield starting material. (B) Displays a cartoon depiction of fluorescent beads functionalized with amino groups crosslinking to form clumps that are easily observable with fluorescent microscopy. (B1) is a microscopy image of native beads. (B2) is a microscopy image of beads that are treated with quenched crosslinker heard the group, therefore beads remain unreactive towards the dialdehyde trapping center. (B3) is a microscopy image of fluorescent beads treated with a crosslinker (70) or (66) to generate connected coagulations on fluorescent particles. (B4) is a microscopy image of B3 sample, treated with dilute HCl, which results in a rapid hydrolysis of enamine bonds to release the amine bead (payload).

#### 4.2.4.4 Construction of Multilayer Tissue Using Homobifunctional Dialdehyde Crosslinker

We have previously demonstrated and generated a tissue construct using biorthogonal chemistry via cell surface engineering. A published work illustrated the use of liposome nanostructures, displaying ketone and hydroxylamine, in re-engineering the surface of hepatocytes could be used to generate 3D liver tissue construct.<sup>298</sup> In another study, we replicated the system to generate beating cardiac tissue construct.<sup>299</sup> Results of crosslinking of a large structure, demonstrated by coagulation of beads, led to a development of experiments in which, *C3H10T1/2* mammalian cells were mixed with the linker to form multilayers of up to 30  $\mu\text{m}$  in thickness using our crosslinker (**Figure 4.15**). In contrast, cells treated with a quenched linker that is no longer presenting the active dialdehyde head group did not form any layers of tissue. To ensure tissues generated are viable, Trypan Blue dye exclusion procedure viability assay was conducted after 16h. The mechanism of Trypan Blue dye exclusion procedure is well known and relies on the ability of cells to remove the compound from cytoplasm as toxins. Healthy cells could identify the blue dye and remove it through physiological processes in the cytoplasm, while dead cells remain stained under a microscope. Therefore, healthy cells were identified through deficiency of the dye within their cytoplasm in comparison with the dead stained cell. The exploration of release capability of the crosslinker in multilayer cells was omitted at this time as it would fall beyond the scope of this project, however, such studies would provide detail on the future application of tissue engineering with complete spatial and temporal control over the shape of an organ.

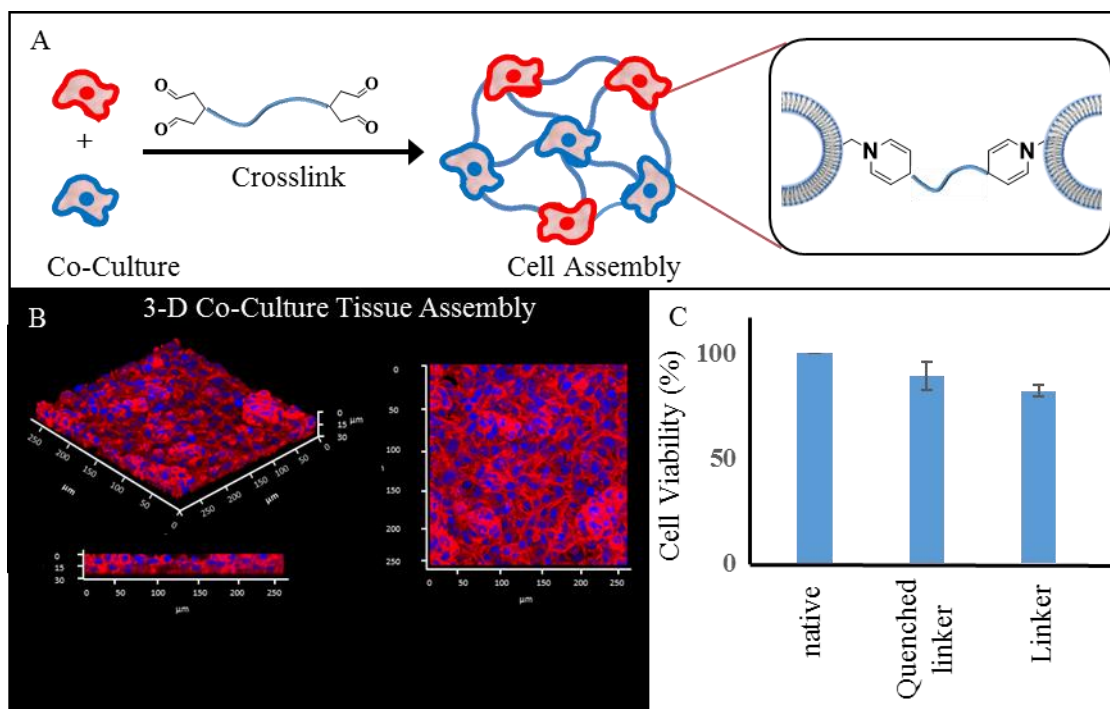


*Figure 4.15 Construction of a multilayer tissue using dialdehyde crosslinker and tissue viability assay*

(A) A general illustration of co-cultured mammalian cells with crosslinker substrate (**70**) is presented. This demonstration highlights the ability of substrate (**70**) to enforce cell-cell adhesion through the formation of a robust covalent bond. Such interactions would stimulate cells to fabricate a scaffold, on which, cell proliferation could occur naturally. (B) Cells were co-cultured in media and treated with substrate 2  $\mu\text{L}$  of a 20 mg/mL (**70**) overnight under physiological conditions. Confocal microscopy images reveal the formation of a 30  $\mu\text{m}$  tissue construct in thickness. (C) Cell viability assay was performed to determine the toxicity of reagents and viability of constructed tissue. Viability and health of crosslinked co-culture cell are significantly comparable to native cells, as well as cells treated with propylamine-quenched cells.

Construction of a tissue layer has been performed through many different methods.<sup>291–293</sup> We have previously developed a fully functional small tissue through forced contact, using re-functionalizing cell surface with biorthogonal pairs via liposome fusion. However, this approach offers a non-invasive route that does not require any

modification of the cells and solely relies on establishing forced-contact between the surfaces using dialdehyde crosslinker. We believe that this method could be a complementary step towards tissue reengineering protocols, and minimize the number of modification steps required in experiments.

#### 4.2.4.5 Functionalization of a Surface with Dialdehyde Headgroup

The final project focuses on the installation of a dialdehyde headgroup on a solid surface, like an ITO or a simple Supramine Arrayit ARYC plate. Such surfaces have a very broad scope of application in biology,<sup>300,301</sup> organic chemistry,<sup>302,303</sup> inorganic chemistry<sup>304,305</sup> and electrochemical experiments such as SAM synthesis. Solid surfaces have been used in the past to immobilize proteins, bacteria cell or even display antigens for mechanistic studies of their biochemistry. ITO surface is particularly attractive for its unique conductive properties as optoelectronic material and applications in photovoltaics systems,<sup>306</sup> organic light-emitting diodes<sup>307</sup> and as other conductive/optical coatings.<sup>308,309</sup>

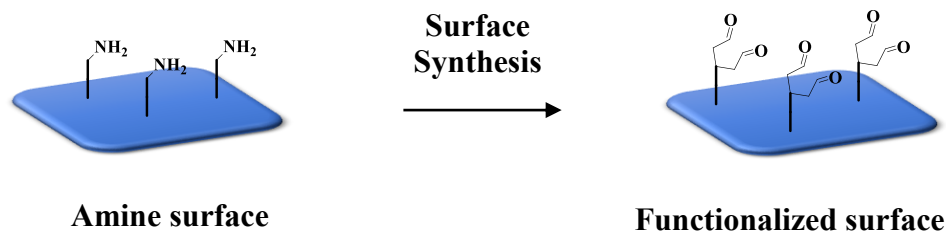


*Figure 4.16 Cartoon depiction of functionalizing a surface with dialdehyde headgroup*

A dialdehyde headgroup could be conveniently installed on a surface that has the proper starting functional group. An amino-group displaying surface was transformed into a dialdehyde-functionalized surface, which then could be used as a model system for surface immobilization applications.



Installation of an amine trapping functional group could allow for immobilization of species that display a reactive amine (**Figure 4.16**). Starting from a Superamine Arrayit ARYC plate that is coated with a density of  $2 \times 10^{12}$  molecule/mm<sup>2</sup> amino groups on a (25 x 76 mm) surface, we built a linker armed with exposed dialdehyde functional groups.

The surface displaying dialdehyde was then characterized using fluorescent green latex amine-modified polystyrene purchased from Sigma Aldrich. The surface was submerged into a solution of beads suspended in water for 1h, then washed with MeOH to reduce non-selective adhesions, and characterized using microscopy. The plates pretreated with propylamine were quenched and did not display any available dialdehyde head group, thus did not generate fluorescent signals. The surface coated with amine-modified beads was treated with dilute acid to regenerate the dialdehyde native plate (**Figure 4.17**).

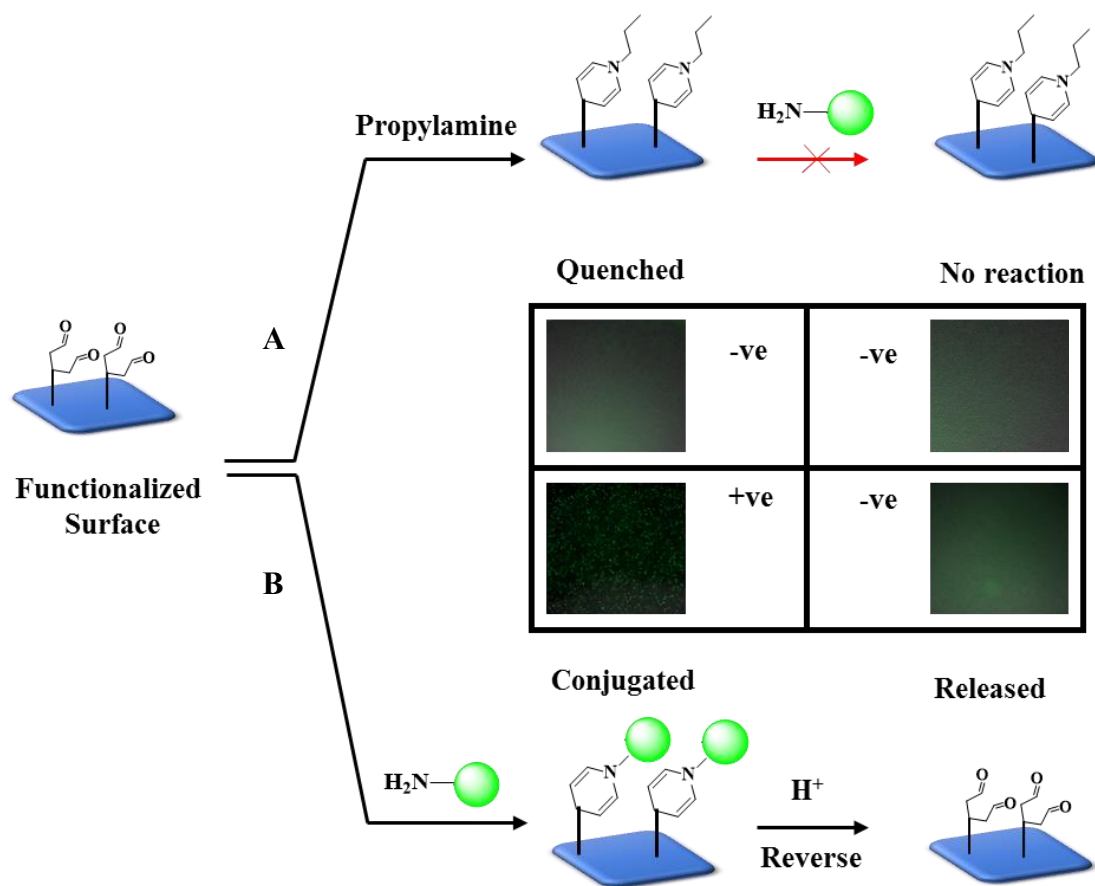


Figure 4.17 Demonstration and characterization of dialdehyde headgroup synthesized on surface via conjugation to fluorescent reporter beads

**Pathway A** Dialdehyde functionalized surface was quenched with propylamine to inactivate the amine-trapping headgroups, therefore any future conjugations with attacking amine reporters will remain ineffective. **Pathway B** Dialdehyde functionalized surface is treated with amine-beads and immobilized the fluorescent particles through ligation with dialdehyde moiety. The fluorescent microscopic analysis confirms the presence of amine-beads on dialdehyde functionalized surface, in contrast, quenched surface did not display any fluorescent signal.

This system could be easily reproduced using other surface material to deliver highly specialized purposes. The downstream application for such surfaces are predominantly determined by the field of study, however, the synthesis would only require the precursor material to be nucleophilic and chemically compatible with our tether

carboxylic acid moiety. In addition to the experiments explained above, there have been many attempts to use dialdehyde headgroup to conjugate a probe to antibodies of various kinds. However, all attempts were inconclusive and require a more reproducible protocol.

## **4.3 Materials and Method**

### **4.3.1 General Dialdehyde Liposomes (Pathway A) (Figure 4.2)**

The Dialdehyde substrate **42** (0.6451 mmol, 3.2 mg) in chloroform was aliquoted into a 5 mL autoclaved glass vial, followed by the addition of 295  $\mu$ L of POPC (10 mg/mL) in chloroform (Avanti Polar Lipids) and 25.6  $\mu$ L of DOTAP (10 mg/mL) in chloroform (Avanti Polar Lipids). The lipid solution was then evaporated under a stream of air for 1 hour to dryness. Then 1.92 mL of culture grade PBS (Sigma Aldrich) was added to the dried lipids and immediately tip sonicated (Fisher Scientific) for 10 minutes at 30 Watts in an ice bath. The resulting lipid suspension was used within 24 hours and stored at 4 °C until use.

### **4.3.2 General Blank Liposomes (Figure 4.2)**

Into an autoclaved 5 mL glass vial 295  $\mu$ L of POPC (10 mg/mL) in chloroform (Avanti Polar Lipids) and 25.6  $\mu$ L of DOTAP (10mg/mL) in chloroform (Avanti Polar Lipids) were added, followed by evaporation using a stream of air for 1 hour. Then 1.92 mL of culture grade PBS (Sigma Aldrich) was added to the dried lipids and immediately tip sonicated (Fisher Scientific) for 10 minutes at 30 Watts in an ice bath. The resulting lipid suspension was used within 24 hours and stored at 4 °C until use.

#### **4.3.3 General Control Liposomes (No Dialdehyde) (Figure 4.2)**

Into an autoclaved 5 mL glass vial reporter-amine (0.9677 mmol) was added followed by 295  $\mu$ L of POPC (10 mg/mL) in chloroform (Avanti Polar Lipids) and 25.6  $\mu$ L of DOTAP (10 mg/mL) in chloroform (Avanti Polar Lipids) were added, followed by evaporation using a stream of air for 1 hour. Then 1.92 mL of culture grade PBS (Sigma Aldrich) was added to the dried lipids and immediately tip sonicated (Fisher Scientific) for 10 minutes at 30 Watts in an ice bath. The resulting lipid suspension was used within 24 hours and stored at 4 °C until use.

#### **4.3.4 General Quenched Dialdehyde Liposomes (Figure 4.2)**

The Dialdehyde substrate **42** (0.6451 mmol, 3.2 mg) in chloroform was treated with excess propylamine and stirred for 4h. The excess reagents and all other volatiles were evaporated. The content was aliquoted into a 5 mL autoclaved glass vial, followed by the addition of 295  $\mu$ L of POPC (10 mg/mL) in chloroform (Avanti Polar Lipids) and 25.6  $\mu$ L of DOTAP (10 mg/mL) in chloroform (Avanti Polar Lipids). The lipid solution was then evaporated under a stream of air for 1h to dry. Then 1.92 mL of culture grade PBS (Sigma Aldrich) was added to the dried lipids and immediately tip sonicated (Fisher Scientific) for 10 minutes at 30 Watts in an ice bath. The resulting lipid suspension was used within 24h and stored at 4°C until use.

#### **4.3.5 DNP-Dialdehyde Conjugation Liposome Preparation (Pathway A) (Figure 4.2)**

Liposome nanostructure functionalized with dialdehyde headgroup was transferred into a 5 mL autoclaved glass vial and treated with DNP-amine (0.9677 mmol, 4.8 mg). The batch was incubated at room temperature for 2h on a shaker.

#### **4.3.6 Biotin-Dialdehyde Conjugation Liposome Preparation (Pathway A) (Figure 4.2)**

Liposome nanostructure functionalized with dialdehyde headgroup was transferred into a 5 mL autoclaved glass vial and treated with molecules biotin-amine (0.9677 mmol, 4.6 mg). The batch was incubated at room temperature for 2h on a shaker.

#### **4.3.7 FLAG-Dialdehyde Conjugation Liposome Preparation (Pathway A) (Figure 4.2)**

liposome nanostructure functionalized with dialdehyde headgroup was transferred into a 5 mL autoclaved glass vial and treated with peptide FLAG (4.0 mg). The batch was incubated at room temperature overnight on a shaker.

#### **4.3.8 DNPC-Dialdehyde Conjugation Liposome Preparation (Pathway B) (Figure 4.2)**

The dialdehyde substrate **42** (0.6451 mmol, 3.2 mg) was transferred into a 5 mL autoclaved glass vial and dissolved through the addition of 1.5 mL of a mixed solvent system (1:3) of THF and methanol respectively. To this solution, molecule **59** DNP-amine

(0.9677 mmol, 4.8 mg) was added, along with a magnetic stir bar and reacted for 2h at room temperature. The product was then obtained by evaporating the solvent under a stream of air and was immediately used to form a single batch of liposomes.

To the 5 mL glass vial of synthesized DNP-Dialdehyde conjugate 295  $\mu$ L of POPC (10 mg/mL) in chloroform (Avanti Polar Lipids) and 25.6  $\mu$ L of DOTAP (10 mg/mL) in chloroform (Avanti Polar Lipids) were added, followed by evaporation using a stream of air for 1h. Then 1.92 mL of culture grade PBS (Sigma Aldrich) was added to the dried lipids and immediately tip sonicated (Fisher Scientific) for 10 minutes at 30Watts in an ice bath. The resulting lipid suspension was used within 24 hours and stored at 4 °C until use.

#### **4.3.9 Biotin-Dialdehyde Conjugation Liposome Preparation (Pathway B) (Figure 4.2)**

The dialdehyde substrate **42** (0.6451 mmol, 3.2 mg) was transferred into a 5 mL autoclaved glass vial and dissolved through the addition of 1.5 mL of a mixed solvent system (1:3) of THF and methanol respectively. To this solution, biotin-amine (0.9677 mmol, 4.6 mg) was added, along with a magnetic stir bar and reacted for 2h at room temperature. The product was then obtained by evaporating the solvent under a stream of air. The product was then immediately used to form a single batch of liposomes.

To the 5 mL glass vial of synthesized biotin-Dialdehyde conjugate 295  $\mu$ L of POPC (10 mg/mL) in chloroform (Avanti Polar Lipids) and 25.6  $\mu$ L of DOTAP (10 mg/mL) in chloroform (Avanti Polar Lipids) were added, followed by evaporation using a stream of air for 1 hour. Then 1.92 mL of culture grade PBS (Sigma Aldrich) was added to the dry

lipids and immediately tip sonicated (Fisher Scientific) for 10 minutes at 30 Watts in an ice bath. The resulting lipid suspension was used within 24h and stored at 4 °C until use.

#### **4.3.10 FLAG-Dialdehyde Conjugation Liposome Preparation (Pathway B) (Figure 4.2)**

The dialdehyde substrate **5** (0.6451 mmol, 3.2 mg) was transferred into a 5 mL autoclaved glass vial and dissolved through the addition of 1.5 mL of a mixed solvent system (1:1) of H<sub>2</sub>O and methanol respectively. To this solution, molecule FLAG peptide (4.0 mg) was added, along with a magnetic stir bar and reacted overnight (16h) at room temperature. The product was then obtained by evaporating the solvent under a stream of air. The product was then immediately used to form a single batch of liposomes.

To the 5 mL glass vial of synthesized FLAG-Dialdehyde conjugate 295 µL of POPC (10 mg/mL) in chloroform (Avanti Polar Lipids) and 25.6 µL of DOTAP (10 mg/mL) in chloroform (Avanti Polar Lipids) were added, followed by evaporation using a stream of air for 1h. Then 1.92 mL of culture grade PBS (Sigma Aldrich) was added to the dry lipids and immediately tip sonicated (Fisher Scientific) for 10 minutes at 30 Watts in an ice bath. The resulting lipid suspension was used within 24 hours and stored at 4 °C until use.

#### **4.3.11 DNPC-Dialdehyde Conjugate Liposome Delivery (Mammalian Cell) (Figure 4.3)**



C3H 10T1/2 cells (ATCC) were cultured using DMEM media (Sigma Aldrich) supplemented with 10% FBS (Sigma Aldrich) and 1% P/S (Sigma Aldrich) to passage 3 in 10 cm plastic culture plates. For experiments, the cells were treated with 3 mL trypsin (Sigma Aldrich) for 3 minutes to remove the cells from suspension and then quenched using 6 mL of growth media. The suspension of cells was then centrifuged at 67 RCF for 5 minutes and the media was decanted and the cells resuspended in 500  $\mu$ L of PBS. To the prepared cell suspension, 500  $\mu$ L of the liposomal solution of pathway **A** or **B** DNP-dialdehyde was added and incubated at room temperature for 10 minutes followed by the addition of 9 mL of PBS and centrifuged at 67 RCF for 5 minutes, followed by decanting of the supernatant. The resulting pellet was then suspended in 500  $\mu$ L of PBS and 40  $\mu$ L of 2 mg/mL anti-dinitrophenyl-KLH, Alexa Fluor 488 conjugate (Life Technologies) and was incubated at room temperature for 1 hour. After incubation, the samples were diluted with 9 mL of PBS and centrifuged and the resulting pellet was washed again using 9 mL of PBS and centrifuged. The pellet was then suspended in 500  $\mu$ L of PBS. Flow cytometry and fluorescence microscopy were used to characterize the resulting cell suspension.

#### **4.3.12 Biotin-Dialdehyde Conjugate Liposome Delivery (Mammalian Cell) (Figure 4.3)**

C3H 10T1/2 cells (ATCC) were cultured using DMEM media (Sigma Aldrich) supplemented with 10% FBS (Sigma Aldrich) and 1% P/S (Sigma Aldrich) to passage 3 in 10 cm plastic culture plates. For experiments, the cells were treated with 3 mL trypsin (Sigma Aldrich) for 3 minutes to remove the cells from suspension and then quenched using 6 mL of growth media. The suspension of cells was then centrifuged at 67 RCF for

5 minutes and the media was decanted and the cells resuspended in 500  $\mu$ L of PBS. To the prepared cell suspension, 500  $\mu$ L of the liposomal solution **A** or **B** biotin-dialdehyde was added and incubated at room temperature for 10 minutes followed by the addition of 9 mL of PBS and centrifuged at 67 RCF for 5 minutes, followed by decanting of the supernatant. The resulting pellet was then suspended in 500  $\mu$ L of PBS and 40  $\mu$ L of Streptavidin-(FITC) 1.0 mg/mL and was incubated at room temperature for 1 hour. After incubation, the samples were diluted with 9 mL of PBS and centrifuged and the resulting pellet was washed again using 9 mL of PBS and centrifuged. The pellet was then suspended in 500  $\mu$ L of PBS. Flow cytometry and fluorescence microscopy were used to characterize the resulting cell suspension.

#### **4.3.13 FLAG-Dialdehyde Conjugate Liposome Delivery (Mammalian Cell) (Figure 4.3)**

C3H10T1/2 cells were cultured in 10 cm for 2 days until 90% confluent using High Glucose DMEM supplemented with 10% FBS and 1% PS at 37 °C and 5% CO<sub>2</sub>. The cells were removed using 3 mL Trypsin for 4 minutes followed by addition of 6 mL media. The cells were collected and centrifuged at 67 RCF for 5 minutes followed by decanting. The cells were resuspended in 500  $\mu$ L PBS and treated with 500  $\mu$ L of the pathway **A** or **B** FLAG-dialdehyde prepared liposome suspension. The content was incubated for 10 minutes followed by dilution with 9 mL of PBS and centrifuged followed by decantation. The pellet was resuspended in 500  $\mu$ L of PBS. The resulting pellet was then suspended in 500  $\mu$ L of PBS 10T cells and was treated with 5  $\mu$ L of 2 mg/mL Anti-FLAG peptide (Life Technologies) and incubated at room temperature for 1 hour followed by dilution with 9

mL of PBS. The content was centrifuged and resuspended in 500  $\mu$ L of PBS further characterized by Flow cytometry and fluorescence microscopy.

#### **4.3.14 Biotin-Dialdehyde Conjugate Liposome Delivery (Bacteria Cell) (Figure 4.3)**

Bacteria *E. coli* B121 were grown to  $OD^{650} = 0.6$ , corresponding to approximately  $4 \times 10^8$  CFU/mL. The cells were harvested by centrifugation at 4000 RCF for 10 minutes, washed with 100 mM  $CaCl_2$  and resuspended in 6 mL of 100 mM  $CaCl_2$  for 2h at 4 °C. Aliquot cells were suspended in 10 mL of 0.5 mM HEPES buffer pH 4.3. Cells were then treated with 6  $\mu$ L EDTA 50 mM pH 8.4 and incubated at 37 °C for 1h. 550  $\mu$ L of the liposomal solution obtained from pathway **A** or **B** was added to the cell culture and incubated at room temperature for 30 minutes. Cells were then spun down and the resulting pellet was suspended in 500  $\mu$ L of PBS and 40  $\mu$ L of Streptavidin-(FITC) 1 mg/mL. The content was incubated at room temperature for 1 hour or 15 minutes at 37 °C. After incubation, cells were centrifuged and the resulting pellet was washed x3 using 2 mL of fresh PBS. The pellet was then suspended in 500  $\mu$ L of PBS. Flow cytometry and fluorescence microscopy were used to characterize the resulting cell suspension.

#### **4.3.15 General Dodecylamine Liposomes (Pathway A) (Figure 4.6)**

The dodecylamine molecule (0.02702 mmol, 5.0 mg) in chloroform was aliquoted into a 5 mL autoclaved glass vial, followed by the addition of 295  $\mu$ L of POPC (10 mg/mL) in chloroform (Avanti Polar Lipids) and 25.6  $\mu$ L of DOTAP (10 mg/mL) in chloroform (Avanti Polar Lipids). The lipid solution was then evaporated under a stream of air for 1

hour until dry. Then 1.92 mL of culture grade PBS (Sigma Aldrich) was added to the dry lipids and immediately tip sonicated (Fisher Scientific) for 10 minutes at 30 Watts in an ice bath. The resulting lipid suspension was used within 24 hours and stored at 4 °C until use.

#### **4.3.16 General Blank Liposomes (Pathway A) (Figure 4.6)**

Into an autoclaved 5 mL glass vial 295  $\mu$ L of POPC (10 mg/mL) in chloroform (Avanti Polar Lipids) and 25.6  $\mu$ L of DOTAP (10mg/mL) in chloroform (Avanti Polar Lipids) were added, followed by evaporation using a stream of air for 1 hour. Then 1.92 mL of culture grade PBS (Sigma Aldrich) was added to the dry lipids and immediately tip sonicated (Fisher Scientific) for 10 minutes at 30Watts in an ice bath. The resulting lipid suspension was used within 24 hours and stored at 4 °C until use.

#### **4.3.17 General Control Liposomes (No Dodecylamine) (Figure 4.6)**

Into an autoclaved 5 mL glass vial reporter-dialdehyde (0.4054 mmol) was added followed by 295  $\mu$ L of POPC (10mg/mL) in chloroform (Avanti Polar Lipids) and 25.6  $\mu$ L of DOTAP (10 mg/mL) in chloroform (Avanti Polar Lipids) were added, followed by evaporation using a stream of air for 1 hour. Then 1.92 mL of culture grade PBS (Sigma Aldrich) was added to the dry lipids and immediately tip sonicated (Fisher Scientific) for 10 minutes at 30 Watts in an ice bath. The resulting lipid suspension was used within 24 hours and stored at 4 °C until use.

#### **4.3.18 General Quenched Dodecylamine Liposomes (Pathway A) (Figure 4.6)**

The dodecylamine molecule (0.1081 mmol, 20.0 mg) in DCM was treated with excess acid chloride and stirred for 1h. The excess reagents and all other volatiles were evaporated. The content was aliquoted into a 5 mL autoclaved glass vial, followed by the addition of 295  $\mu$ L of POPC (10 mg/mL) in chloroform (Avanti Polar Lipids) and 25.6  $\mu$ L of DOTAP (10 mg/mL) in chloroform (Avanti Polar Lipids). The lipid solution was then evaporated under a stream of air for 1h until dry. Then 1.92 mL of culture grade PBS (Sigma Aldrich) was added to the dry lipids and immediately tip sonicated (Fisher Scientific) for 10 minutes at 30 Watts in a room temperature water bath. The resulting lipid suspension was used within 24 hours and stored at 4 °C until use.

#### **4.3.19 DNPC-Dialdehyde-Dodecylamine Conjugation Liposome Preparation (Pathway A) (Figure 4.6)**

liposome nanostructure functionalized with dodecylamine was transferred into a 5 mL autoclaved glass vial and treated with molecule **62** DNP-dialdehyde (0.04054 mmol, 2.0 mg). the batch was incubated at room temperature for 2h on a rocker.

#### **4.3.20 Biotin-Dialdehyde-Dodecylamine Conjugation Liposome Preparation (Pathway A) (Figure 4.6)**

liposome nanostructure functionalized with primary amine headgroup was transferred into a 5 mL autoclaved glass vial and treated with molecules **57** biotin-dialdehyde (0.04054 mmol, 1.9 mg). The batch was incubated at room temperature for 2h on a rocker.

#### **4.3.21 DNPC-Dialdehyde Conjugation Liposome Preparation (Pathway B) (Figure 4.6)**

Dodecylamine molecule (0.02688 mmol, 5.0 mg) was transferred into a 5 mL autoclaved glass vial and dissolved through the addition of 1.5 mL of a mixed solvent system (1:3) of THF and methanol respectively. To this solution, molecule **61** DNP-dialdehyde (0.04032 mmol, 18 mg) was added, along with a magnetic stir bar and reacted for 2 h at room temperature. The product was then obtained by evaporating the solvent under a stream of air. The product was then immediately used to form a single batch of liposomes.

To the 5 mL glass vial of synthesized DNP-Dialdehyde-dodecylamine conjugate, 295  $\mu$ L of POPC (10 mg/mL) in chloroform (Avanti Polar Lipids) and 25.6  $\mu$ L of DOTAP (10 mg/mL) in chloroform (Avanti Polar Lipids) were added, followed by evaporation using a stream of air for 1 hour. Then 1.92 mL of culture grade PBS (Sigma Aldrich) was added to the dry lipids and immediately tip sonicated (Fisher Scientific) for 10 minutes at 30 Watts in an ice bath. The resulting lipid suspension was used within 24 hours and stored at 4 °C until use.

#### **4.3.22 Biotin-Dialdehyde-Dodecylamine Conjugation Liposome Preparation**

##### **(Pathway A) (Figure 4.6)**

Dodecylamine molecule (0.02688 mmol, 5.0 mg) was transferred into a 5 mL autoclaved glass vial and dissolved through the addition of 1.5 mL of a mixed solvent system (1:3) of THF and methanol respectively. To this solution, molecule **57** biotin-dialdehyde (0.04032 mmol, 20 mg) was added, along with a magnetic stir bar and reacted for 2h at room temperature. The product was then obtained by evaporating the solvent under a stream of air. The product was then immediately used to form a single batch of liposomes.

To the 5 mL glass vial of synthesized biotin-dialdehyde-dodecylamine conjugate 295  $\mu$ L of POPC (10 mg/mL) in chloroform (Avanti Polar Lipids) and 25.6  $\mu$ L of DOTAP (10 mg/mL) in chloroform (Avanti Polar Lipids) were added, followed by evaporation using a stream of air for 1 hour. Then 1.92 mL of culture grade PBS (Sigma Aldrich) was added to the dry lipids and immediately tip sonicated (Fisher Scientific) for 10 minutes at 30 Watts in an ice bath. The resulting lipid suspension was used within 24 hours and stored at 4 °C until use.

#### **4.3.23 DNPC-Dialdehyde-Dodecylamine Conjugate Liposome Delivery**

##### **(Mammalian Cell) (Figure 4.7)**

C3H 10T1/2 cells (ATCC) were cultured using DMEM media (Sigma Aldrich) supplemented with 10% FBS (Sigma Aldrich) and 1% P/S (Sigma Aldrich) to passage 3 in

10 cm plastic culture plates. For experiments, the cells were treated with 3 mL trypsin (Sigma Aldrich) for 3 minutes to remove the cells from suspension and then quenched using 6 mL of growth media. The suspension of cells was then centrifuged at 67 RCF for 5 minutes and the media was decanted and the cells resuspended in 500  $\mu$ L of PBS. To the prepared cell suspension, 500  $\mu$ L of the liposomal solution of pathway **A** or **B** DNP-dialdehyde-dodecylamine was added and incubated at room temperature for 10 minutes followed by the addition of 9 mL of PBS and centrifuged at 67 RCF for 5 minutes, followed by decanting of the supernatant. The resulting pellet was then suspended in 500  $\mu$ L of PBS and 40  $\mu$ L of 2 mg/mL anti-dinitrophenyl-KLH, Alexa Fluor 488 conjugate (Life Technologies) and was incubated at room temperature for 1 hour. After incubation, the samples were diluted with 9 mL of PBS and centrifuged and the resulting pellet was washed again using 9 mL of PBS and centrifuged. The pellet was then suspended in 500  $\mu$ L of PBS. Flow cytometry and fluorescence microscopy were used to characterize the resulting cell suspension.

#### **4.3.24 Biotin-Dialdehyde-Dodecylamine Conjugate Liposome Delivery (Mammalian Cell) (Figure 4.7)**

C3H 10T1/2 cells (ATCC) were cultured using DMEM media (Sigma Aldrich) supplemented with 10% FBS (Sigma Aldrich) and 1% P/S (Sigma Aldrich) to passage 3 in 10 cm plastic culture plates. For experiments, the cells were treated with 3 mL trypsin (Sigma Aldrich) for 3 minutes to remove the cells from suspension and then quenched using 6 mL of growth media. The suspension of cells was then centrifuged at 67 RCF for 5 minutes and the media was decanted and the cells resuspended in 500  $\mu$ L of PBS. To the



prepared cell suspension, 500  $\mu$ L of the liposomal solution **A** or **B** biotin-dialdehyde-dodecylamine was added and incubated at room temperature for 10 minutes followed by the addition of 9 mL of PBS and centrifuged at 67 RCF for 5 minutes, followed by decanting of the supernatant. The resulting pellet was then suspended in 500  $\mu$ L of PBS and 40  $\mu$ L of Streptavidin-(FITC) 1mg/mL and was incubated at room temperature for 1 hour. After incubation, the samples were diluted with 9 mL of PBS and centrifuged and the resulting pellet was washed again using 9 mL of PBS and centrifuged. The pellet was then suspended in 500  $\mu$ L of PBS. Flow cytometry and fluorescence microscopy were used to characterize the resulting cell suspension.

#### **4.3.25 DNP-Dialdehyde-dodecylamine Conjugate Liposome Delivery (Bacteria Cell) (Figure 4.7)**

Bacteria *E. coli* B121 were grown to  $OD^{650} = 0.6$ , corresponding to approximately  $4 \times 10^8$  CFU/mL. The cells were harvested by centrifugation at 4000 RCF for 10 minutes, washed with 100 mM  $CaCl_2$  and resuspended in 6 mL of 100 mM  $CaCl_2$  for 2h at 4 °C. Aliquot cells were suspended in 10 mL of 0.5 mM HEPES buffer pH 4.3. Cells were then treated with 6  $\mu$ L EDTA 50 mM pH 8.4 and incubated at 37 °C for 1h. 550  $\mu$ L of the liposomal solution obtained from pathway **A** or **B** was added to the cell culture and incubated at room temperature for 30 minutes. Cells were then spun down and the resulting pellet was then suspended in 500  $\mu$ L of PBS and 40  $\mu$ L of 2 mg/mL anti-dinitrophenyl-KLH, Alexa Fluor 488 conjugate (Life Technologies) and was incubated at room temperature for 1 hour. The content was incubated at room temperature for 1 hour or 15 minutes at 37 °C. After incubation, cells were centrifuged and the resulting pellet was washed x3 using 2 mL of

fresh PBS. The pellet was then suspended in 500  $\mu$ L of PBS. Flow cytometry and fluorescence microscopy were used to characterize the resulting cell suspension.

#### **4.3.26 Biotin-Dialdehyde-dodecylamine Conjugate Liposome Delivery (Bacteria Cell) (Figure 4.7)**

Bacteria *E. coli* B121 were grown to  $OD^{650} = 0.6$ , corresponding to approximately  $4 \times 10^8$  CFU/mL. The cells were harvested by centrifugation at 4000 RCF for 10 minutes, washed with 100 mM  $CaCl_2$  and resuspended in 6 mL of 100 mM  $CaCl_2$  for 2h at 4 °C. Aliquot cells were suspended in 10 mL of 0.5 mM HEPES buffer pH 4.3. Cells were then treated with 6  $\mu$ L EDTA 50 mM pH 8.4 and incubated at 37 °C for 1h. 550  $\mu$ L of the liposomal solution obtained from pathway **A** or **B** was added to the cell culture and incubated at room temperature for 30 minutes. Cells were then spun down and the resulting pellet was suspended in 500  $\mu$ L of PBS and 40  $\mu$ L of Streptavidin-(FITC) 1.0 mg/mL. The content was incubated at room temperature for 1 hour or 15 minutes at 37 °C. After incubation, cells were centrifuged and the resulting pellet was washed x3 using 2 mL of fresh PBS. The pellet was then suspended in 500  $\mu$ L of PBS. Flow cytometry and fluorescence microscopy were used to characterize the resulting cell suspension.

#### **4.3.27 Conjugation of L-lysine ethyl ester dihydrochloride with dialdehyde substrate **53** (Scheme 4-1)**

In a 10 mL round bottom flask, 30 mg of L-lysine ethyl ester dihydrochloride (Sigma Aldrich 62880) was mixed with 40 mg of substrate **53** and excess bicarbonate in

water for 30 minutes at RT. The mixture was dried under vacuum to strip of any residual, then re-dissolved in  $\text{CDCl}_3$  solvent and filtered through a layer of silica gel, further analyzed by NMR spectroscopy.

#### **4.3.28 Decoupling of L-Lysine Ethyl Ester Dihydrochloride with Dialdehyde**

##### **Substrate 53 (Scheme 4-3)**

The conjugate product of (Scheme 4-1) was recovered from NMR tube and stripped off of solvent under vacuum. The afforded crystals were dissolved in MeOD and been exposed to a dilute solution of 0.1N DCl and analyzed with NMR spectroscopy for the signals of interest.

#### **4.3.29 Crosslinking of Protein LAR D1D1 and CS2 Domain (Figure 4.11)**

20  $\mu\text{L}$  of Protein LAR D1D1 18.5  $\mu\text{M}$  was mixed with 20  $\mu\text{L}$  of CS2 domain 20  $\mu\text{M}$  (courtesy of Donaldson Lab) and incubated for 30 minutes for complete interactive binding, to which, 20  $\mu\text{L}$  of homobifunctional crosslinker dialdehyde (**70**) 20 mg/mL was added. The mixture was further diluted to a total of 50  $\mu\text{L}$  volume using PBS pH 8.4 buffer and incubated at 25  $^\circ\text{C}$  and 37  $^\circ\text{C}$  for 15 minutes.

*Control protein (Crosslinker Deficient):* A native control experiment was also conducted by mixing 20  $\mu\text{L}$  of Protein LAR D1D2 18.5  $\mu\text{M}$  and 20  $\mu\text{L}$  of CS2 20  $\mu\text{M}$  (courtesy of Donaldson Lab), incubated for 30 minutes for complete interactive binding to form the complex.

*Control Crosslinker reagent (Quenched Head Groups):* A native control experiment was also conducted using quenched linker with propylamine, presenting a terminated head group dialdehyde functional group. 20  $\mu$ L of homobifunctional crosslinker dialdehyde (**70**) 20 mg/mL was mixed with excess propylamine in a 1 mL vial and incubated at room temperature for 5 hours to ensure both head groups are terminated. The solvent and excess volatile reagents were evaporated using a stream of air for overnight. The content was resolved in 20  $\mu$ L of fresh PBS pH 8.4 and added to 20  $\mu$ L of protein complex further diluted to a total of 50  $\mu$ L volume using PBS pH 8.4 buffer and incubated at 25 °C and 37 °C for 15 minutes.

*Positive Control Crosslinker reagent (Glutaraldehyde):* To investigate the extent of crosslinking, a positive control experiment was also performed conventional 50% glutaraldehyde consistent with the total concentration of the protein-protein complex. 20  $\mu$ L of Protein LAR D1D2 was mixed with 20  $\mu$ L of CS2 20  $\mu$ M (courtesy of Donaldson Lab) and incubated for 30 minutes for complete interactive binding, to which, 5  $\mu$ L of homobifunctional crosslinker glutaraldehyde was added, further diluted to a total of 50  $\mu$ L volume using PBS pH 8.4 buffer and incubated at 25 °C and 37 °C for 15 minutes.

#### **4.3.30 Crosslinking/Stapling of Protein EA22 (Figure 4.12)**

3  $\mu$ L of Protein EA22 1mg/mL (courtesy of Donaldson Lab) was mixed with 15  $\mu$ L of homobifunctional crosslinker dialdehyde (**72**) 20 mg/mL, further diluted to a total of 50  $\mu$ L volume using PBS pH 8.4 buffer and incubated at 25 °C for 15 minutes.

*Control Crosslinker reagent (Quenched Head Groups):* A native control experiment was also conducted using quenched linker with propylamine, presenting a terminated head group dialdehyde functional group. 3  $\mu$ L of homobifunctional crosslinker dialdehyde (**70**) 20 mg/mL was mixed with excess propylamine in a 1 mL vial and incubated at room temperature for 5 hours to ensure both head groups are terminated. The solvent and excess volatile reagents were evaporated using a stream of air for overnight. The content was resolved in 10  $\mu$ L of PBS pH 7.8 and added to 3  $\mu$ L of protein EA22 further diluted to a total of 50  $\mu$ L volume using PBS pH 8.4 buffer and incubated at 25 °C for 15 minutes.

#### **4.3.31 Crosslinking of Protein PP16 (Figure 4.12)**

3  $\mu$ L of Protein PP16 1 mg/mL (courtesy of Donaldson Lab) was mixed with 15  $\mu$ L of homobifunctional crosslinker dialdehyde (**70**) 20 mg/mL, further diluted to a total of 50  $\mu$ L volume using PBS pH 8.4 buffer and incubated at 25 °C for 15 minutes.

*Control Crosslinker reagent (Quenched Head Groups):* A native control experiment was also conducted using quenched linker with propylamine, presenting a terminated head group dialdehyde functional group. 15  $\mu$ L of homobifunctional crosslinker dialdehyde (**70**) 20 mg/mL was mixed with excess propylamine in a 1 mL vial and incubated at room temperature for 5 hours to ensure both head groups are terminated. The solvent and excess volatile reagents were evaporated using a stream of air for overnight. The content was resolved in 10  $\mu$ L of PBS pH 7.8 and added to 3  $\mu$ L of protein PP16 further diluted to a total of 50  $\mu$ L volume using PBS pH 8.4 buffer and incubated at 25 °C for 15 minutes.

*SDS Gel Electrophoresis Analysis:* A 20  $\mu\text{L}$  aliquot of each complex above was mixed with equal volume of 2X SDS dye and resolved on a 12 % SDS-PAGE gel. The gel was stained with Coomassie Brilliant Blue staining solution and developed.

#### **4.3.32 Dialdehyde Crosslinking of Commercial Latex-Amine Beads in Aqueous**

##### **Solution (Figure 4.13)**

In a 5 mL test tube, 10  $\mu\text{L}$  of L1030 (Sigma Aldrich) amine presenting latex beads in aqueous solution were aliquoted and diluted with 500  $\mu\text{L}$  of ddH<sub>2</sub>O and gently agitated. An aqueous solution of crosslinking TEG dialdehyde (**70**) in 250  $\mu\text{L}$  (0.011 mM) using ddH<sub>2</sub>O OR methanolic solution of crosslinker dialdehyde (**66**) in methanol was made. 250  $\mu\text{L}$  of either solution of crosslinker dialdehyde was aliquoted into the latex-amine bead suspension, gently agitated and reacted overnight at room temperature. Examination upon overnight reaction yielded precipitated beads.

*Blank Control Liposomes, dialdehyde deficient:* In a 5 mL test tube 10  $\mu\text{L}$  of L1030 (Sigma Aldrich) amine presenting latex beads in aqueous solution were aliquoted and diluted with 500  $\mu\text{L}$  of ddH<sub>2</sub>O and gently agitated. Then 100  $\mu\text{L}$  of ddH<sub>2</sub>O was aliquoted into the latex-amine bead suspension and reacted overnight at room temperature. No change in opaque suspension of beads.

*N-propylamine Quenched Aldehyde Control:* An aqueous solution of crosslinking TEG containing dialdehyde (**70**) in 250  $\mu\text{L}$  (0.011 mM) was made using ddH<sub>2</sub>O AND solution of crosslinker (**66**) in 250  $\mu\text{L}$  of methanol (0.011 mM) were made. N-propylamine was

added and reacted at room temperature for one hour to both solutions separately. Then 250  $\mu\text{L}$  of the quenched crosslinking dialdehyde was added to a suspension of latex amine presenting beads from through the dilution of 15  $\mu\text{L}$  of L1030 (Sigma Aldrich) beads diluted using 500  $\mu\text{L}$  of ddH<sub>2</sub>O. No change in opaque suspension of beads.

*Crosslinked Dialdehyde Acid Release:* First a precipitated crosslinked bead sample was produced using a 5 mL test tube 10  $\mu\text{L}$  of L1030 (Sigma Aldrich) amine presenting latex beads in aqueous solution were aliquoted and diluted with 500  $\mu\text{L}$  of ddH<sub>2</sub>O and gently agitated. An aqueous solution of (**70**) in 250  $\mu\text{L}$  (0.011 mM) was made using ddH<sub>2</sub>O. The similar methanolic solution was made using (**66**). 250  $\mu\text{L}$  of crosslinker solution was aliquoted into the latex-amine bead suspension, gently agitated and reacted overnight at room temperature. Examination upon overnight reaction yielded precipitated beads. The remaining liquid was decanted using a micropipette leaving behind the precipitated beads. To the aggregated beads 450  $\mu\text{L}$  of ddH<sub>2</sub>O treated with 1M HCl to pH 2.0 was added and agitated. The suspension was then allowed to react and visualized to determine if the beads continued to precipitate or remained in suspension. The after 12 hour reaction of the crosslinked beads with pH 2.0 water the bead suspensions were centrifuged at 7000 RCF for 10 minutes followed by decanting of the supernatant and the addition of fresh 500  $\mu\text{L}$  of pH 2.0 ddH<sub>2</sub>O and resuspended. The beads were allowed to react for a further 30 minutes and then centrifuged at 7000 RCF for 10 minutes followed by decanting of the supernatant and the addition of fresh 500  $\mu\text{L}$  of ddH<sub>2</sub>O and resuspended. The beads were allowed to sit for 16 hours and images were obtained of the final suspension with controls along with fluorescent microscopy.

*Fluorescent Microscopy of Dialdehyde Crosslinking of Amine Beading in Solution:* In a 5 mL test tube 10  $\mu$ L of L1030 (Sigma Aldrich) amine presenting latex beads in aqueous solution were transferred and diluted with 500  $\mu$ L of ddH<sub>2</sub>O and gently agitated. An aqueous solution of crosslinker TEG containing dialdehyde (**70**) in 250  $\mu$ L (0.011 mM 1.5 mg) was made using ddH<sub>2</sub>O AND solution of crosslinker (**66**) in 250  $\mu$ L of methanol (0.011 mM, 1.5mg) were made. 250  $\mu$ L of the crosslinker solution was aliquoted into the latex-amine bead suspension, gently agitated and reacted overnight at room temperature. Examination upon overnight reaction yielded precipitated beads. The beads were transferred unto glass slides and imaged using phase contrast and fluorescent microscopy to visualize aggregation.

#### **4.3.33 Crosslinker Dialdehyde Generation of Tissue Constructs (Figure 4.15)**

Cell Culture: GFP NIH 3T3 cells, RFP HDNF cells, C3H10T1/2

C3H/10T1/2 were cultured in petri dishes at 37 °C and 5% CO<sub>2</sub> with DMEM media containing 10% fetal bovine serum (FBS) and 1% penicillin/streptomycin (P/S). RFP Expressing Human Neonatal Dermal Fibroblasts (RFP) were maintained in DMEM containing 5% FBS and 1% P/S. The cell cultures used for experiments were between 3 and 8 passages. GFP expressing NIH3T3 (GFP) cells were cultured in DMEM (high glucose), with 10% FBS, 0.1 mM MEM Non-Essential Amino Acids, 2 mM L-glutamine, 1% P/S, and 10  $\mu$ g/mL Blasticidin. 3T3 Swiss albino mouse fibroblasts were cultured in Dulbecco's Modified Eagle Medium (Gibco) containing 10 % calf bovine serum (CBS) and 1 % penicillin/streptomycin at 37 °C in 5% CO<sub>2</sub>



*General Tissue Formation through Dialdehyde Crosslinking:* Cells were cultured in 10cm tissue for 2 days until 90% confluent using optimal growth media, when needed the cells cultures were suspended using 3 mL Trypsin for 4 minutes followed by addition of 6 mL media. The cells were collected and centrifuged at 67 RCF for 5 minutes followed by decanting. The pellet was resuspended in approximately 650  $\mu$ L of serum free media to obtain a cell concentration of 4 million cells/mL using a hemacytometer. For the C3H10T1/2 cells, 2  $\mu$ L of a 20 mg/mL dialdehyde crosslinker solution was added to the suspension. Then 200  $\mu$ L of the treated suspension was carefully added on top of a sterile 1 cm<sup>2</sup> glass slide and incubated for 1 hour 37 °C and 5% CO<sub>2</sub>. The glass slides were then washed once with PBS and fresh serum containing media was added and the plates were further incubated for 16 hours (overnight) and then washed twice with PBS and fixed with 4% formalin solution. For confocal microscopy, the cells were stained with DAPI and TRITC for 3D visualization using manufacturers protocol. The images were obtained by mounting onto thin glass slides with Light Diagnostics Mounting Fluid (Millipore) for 3D confocal microscopy using a Zeiss LSM 700.

Tissues were also formed using RFP and GFP expressing cell lines by using our general protocol, while the cells were combined in suspension with 1:1 ratio and an overall cell concentration of 4 million cells/mL. These tissues were visualized without staining by mounting onto thin glass slides with Light Diagnostics Mounting Fluid (Millipore) for 3D confocal microscopy using a Zeiss LSM 700.

*Cell Viability Assay of C3H10T1/2 cells with Crosslinker Dialdehyde:* The cell viability assay was performed using C3H10T1/2 cells using the general tissue engineering protocol. After treatment of the cells with the crosslinker dialdehyde molecule (70), wash and given

fresh serum media, after 16 hours of incubation (overnight) the cells were resuspended and the cell viability assay was performed using Trypan Blue (Sigma Aldrich) staining following standard provided protocol.

#### **4.3.34 Functionalization of a Solid Surface with Dialdehyde Headgroup (Figure 4.16)**

A (1x1 cm) glass SuperAmine substrate was carefully cut and submerged in a solution of excess bicarbonate and water. The content of the vial was stirred at RT for 30 min to generate a free-base amine surface. In another vial, excess DCC/*N*-hydroxysuccinimide and bicarbonate was mixed in THF and stirred for 15 minutes to which, (244 mg, 1 mmol) of the substrate (**46**) was added. Once the activated ester of the substrate (**46**) is generated, the glass substrate is submerged into the vial to allow for the formation of the amide bond between the substrate (**46**) and the surface over 3h at RT. The glass substrate is removed and rinsed with MeOH/H<sub>2</sub>O to remove all by-products and impurities behind. Since it's a protected diol surface, it could be stored at 4-8 °C and further deprotected upon demand.

The substrate is submerged in a mixture of MeOH/H<sub>2</sub>O (1:9) to which, 1 drop of dilute HCl acid is added and stirred for 4h to ensure the acetonide residue is completely cleaved off. It was then removed from the solution and rinsed with MeOH/H<sub>2</sub>O multiple times. The resulting surface displays a 1,2 vicinal diol and is submerged into a vial containing excess NaIO<sub>4</sub> in MeOH/H<sub>2</sub>O and stirred for 4h at RT. The glass is then rinsed thoroughly with MeOH/H<sub>2</sub>O and used for immobilization applications.

#### 4.3.35 Immobilization of Beads on the Functionalized Dialdehyde Surface Substrate

(Figure 4.17)

*Pathway A:* Synthesized surface displaying dialdehyde headgroup was submerged into a 12 mL vial charged with MeOH and treated with excess propylamine for 4h. Then it was removed and washed with MeOH/H<sub>2</sub>O thoroughly. The dried surface was then submerged into a fresh vial a 1,2 vicinal diol and is submerged into a vial containing excess NaIO<sub>4</sub> in MeOH/H<sub>2</sub>O and stirred for 4h at RT. The glass substrate was submerged into a 12 mL vial containing 10 µL of L1030 (Sigma Aldrich) amine presenting latex beads in an aqueous solution for 4h. The resulting solid surface was rinsed and images were obtained on the final surface with fluorescent microscopy.

*Pathway B:* Synthesized surface displaying dialdehyde headgroup was submerged into a 12 mL vial charged with 10 µL of L1030 (Sigma Aldrich) amine presenting latex beads in an aqueous solution for 4h. It was removed and rinsed with an aqueous solution to remove any non-specific and non-covalent interaction from the surface. Then it was treated with dilute HCl solution to investigate the reverse process. The resulting solid surface was rinsed and the images of both steps were obtained using fluorescent microscopy.

#### 4.3.36 Streptavidin-FITC Adhesion to Liposomes Functionalized with Dialdehyde

**Lipid (42)**

In an autoclaved 5 mL glass vial 460 µL of POPC (10 mg/mL in CHCl<sub>3</sub>) (Avanti Polar Lipids Lipids), 20 µL of DOTAP (10mg/mL in CHCl<sub>3</sub>) (Avanti Polar Lipids Lipids)

and 100  $\mu\text{L}$  of **(42)** (10 mg/mL in  $\text{CHCl}_3$ ) were combined and gently mixed. The solvent was then removed using a gentle stream of air for 1h. To the resulting lipid film 3 mL of molecular grade RNase/DNase free water was added and the resulting mixture was immediately tip sonicated for 10 minutes using a room temperature water in an ice bath at 30 Watts. Immediately 500  $\mu\text{L}$  of the resulting liposome suspension was aliquoted into a 1.5 mL Eppendorf tube and to the liposome aliquot, 1000  $\mu\text{L}$  of streptavidin-FITC (1 mg/mL in ddH<sub>2</sub>O) (Sigma Aldrich) was added. The mixed suspensions were then placed on a rocker at 4 °C for 4 days. 500  $\mu\text{L}$  of the liposomal solution was added to a suspension of C3H 10T1/2 cells (ATCC) and incubated at room temperature for 10 minutes followed by the addition of 9 mL of PBS and centrifuged at 67 RCF for 5 minutes, followed by decanting of the supernatant. The resulting pellet was washed again using 9 mL of PBS and centrifuged. The pellet was then suspended in 500  $\mu\text{L}$  of PBS. Flow cytometry and fluorescence microscopy were used to characterize the resulting cell suspension.

#### **4.3.37 Rabbit IgG-FITC Adhesion to Liposomes Functionalized with Dialdehyde**

##### **Lipid (42)**

In an autoclaved 5 mL glass vial 460  $\mu\text{L}$  of POPC (10 mg/mL in  $\text{CHCl}_3$ ) (Avanti Polar Lipids Lipids), 20  $\mu\text{L}$  of DOTAP (10 mg/mL in  $\text{CHCl}_3$ ) (Avanti Polar Lipids Lipids) and 100  $\mu\text{L}$  of **(42)** (10 mg/mL in  $\text{CHCl}_3$ ) were combined and gently mixed. The solvent was then removed using a gentle stream of air for 1h. To the resulting lipid film 3 mL of molecular grade RNase/DNase free water was added and the resulting mixture was immediately tip sonicated for 10 minutes using a room temperature water in an ice bath at 30 Watts. Immediately 500  $\mu\text{L}$  of the resulting liposome suspension was aliquoted into a

1.5 mL Eppendorf tube and to the liposome aliquot, 1000  $\mu$ L of IgG-FITC (rabbit) (1 mg/mL in ddH<sub>2</sub>O) (Sigma Aldrich) was added. The mixed suspensions were then placed on a rocker at 4 °C for 4 days. 500  $\mu$ L of the liposomal solution was added to a suspension of C3H 10T1/2 cells (ATCC) and incubated at room temperature for 10 minutes followed by the addition of 9 mL of PBS and centrifuged at 67 RCF for 5 minutes, followed by decanting of the supernatant. The resulting pellet was washed again using 9 mL of PBS and centrifuged. The pellet was then suspended in 500  $\mu$ L of PBS. Flow cytometry and fluorescence microscopy were used to characterize the resulting cell suspension.

## 5 CHAPTER FIVE

---

Bio-conjugation is a rapidly growing field, which has drawn a lot of attention in the past 20 years. Its provision continues to build a variety of powerful tools through which, macro/micro biological molecules could connect to one another that otherwise were impossible to unite with sustaining native biological activity. Its invaluable use has been recognized in protein modification systems, where a delicate intact protein structure should no longer be genetically re-engineered to deliver a specialized purpose other than its intrinsic functionality. Such developments have made possible to exploit protein-protein conjugates, enzyme-linked antibodies, immunotoxins and drug-protein conjugates in more applied clinical approaches and conquer some sophisticated pathological complexities in therapeutics. This principle is not limited to protein domain and could be further expanded to any material with dependence to functional groups that craft an organic backbone.

During the first years of this study, we focused on using the already existing biorthogonal chemistry of oxyamines and ketones to re-engineer the surface of the bacterial cell. We used two most common gram-negative organisms, *Escherichia coli*, and *Pseudomonas aeruginosa*, as model systems to demonstrate the ability of liposome to deliver non-native organic functional groups via fusion. Our method offered a noninvasive, nontoxic, biocompatible and highly efficient delivery system that could embed multiple head groups on the cell surface. Our approach was a complementary technique along with other available methods to tailor bacteria cell surface; however, it proved to be the only one that does not permanently change the identity or behavior of the cell. Its wide use in

biotechnology, fluorescent tagging, microscopy and material science was partly investigated to illustrate its utility in multiple fields. We used a variety of analytical techniques to characterize and quantify the incorporated organic functional groups on the cell surface. We also isolated the surface membranes containing our reporter and analyzed via mass spectroscopy.

Although our approach was a successful demonstration of re-engineering the cell surface, it suffered from some limitations that could not be addressed using biorthogonal chemistry. Our technology was insufficient for delivery of larger biomolecules and required performing undesired chemical reactions on both analytes and cell. Although liposome fusion delivery systems is a powerful tool, it could not transfer proteins, DNA, antibodies or other biomolecules. Such limitations encouraged us to develop a method that could successfully deliver any biomolecules on the cell surface with a minimum extent of chemistry performed on the analyte. We determined that an ideal system must target the most abundant and available functional group existing on biomolecules. We determined that amines are the single most important, reactive, abundant and available nucleophiles in biological systems. This led us to design our system to target amino groups already existing on most biomolecules.

Inspired by glutaraldehyde crosslinking, we found great opportunity to manipulate its structure and generate some novel variations that could trap a primary amino group. Our system allowed for the installation of a chemical handle that could carry any reporter for different applications. Our conjugation system offered great efficiency, selectivity, yield and atom economy. The only by-product is water and therefore no purification is needed and the reaction proceeds with high atom economy. Unlike other conjugation reactions

that react with amines no activating center, background hydrolysis, need for purification nor reductive amination agents are necessary.

In the past years, we optimized the model substrates to meet all the requirements for a successful characterizable conjugation to primary amines. We fully studied the kinetics of the ligation reaction through a pseudo-first order reaction as well as stability and pH profile of the final product. In this study, we synthesized a suite of dialdehyde reagents and demonstrated their utility in several applications applied to cell surface engineering and material science. We successfully conjugated and delivered a range of ligands from small molecules to a polypeptide onto the surface of the bacterial and mammalian cell wall, further characterized them via flow cytometry, microscopy and immunostaining.

We crosslinked larger macroscopic solid beads presenting amine functional group on their surface to form aggregates and explored the reversibility of the system to release the amine, which is very valuable in antibody-drug conjugate applications. For the first time, to the best of our knowledge, a viable multilayer cellular tissue construct was formed with the addition of a small amount of only one molecule without the need to manipulate the physiology or surface chemistry of the cells. We re-functionalize material surface substrates to display dialdehyde head groups and characterized the dialdehyde headgroup using fluorescent beads via fluorescence microscopy.

Future work will expand the suite of dialdehyde reagents by tethering probes and labels including photoactive, redox, crosslinkers, alkyne, azide and fluorescent molecules. The system is general and may be used for many studies and applications including mass



spectrometry molecular tagging, the linkage of drug molecules to antibodies for antibody drug conjugates, biosensors and nanostructure, surface chemistry and for the synthesis of a broad range of dendrimers, polymers, inorganic MOFs and COFs and biomaterials. Despite many attempts to extend this technology to antibody conjugation and study the delivery of therapeutic agents, we could not generate a sustainable method to ligate any dialdehyde headgroup to an antibody molecule. Many factors and elements are yet to be explored in such studies. Insufficient results should not be perceived as an inability to obtain a conjugation to the antibody using dialdehyde system. In addition to antibody conjugations, proteins and other macro-biomolecules allowed a great opportunity to be decorated with a variety of ligands and reporters using this system.

The dialdehyde template precursor is designed to allow for the installation of a third organic functional group and act as a little Swiss army molecule. We briefly investigated this feature but were bound to leave it for future projects.

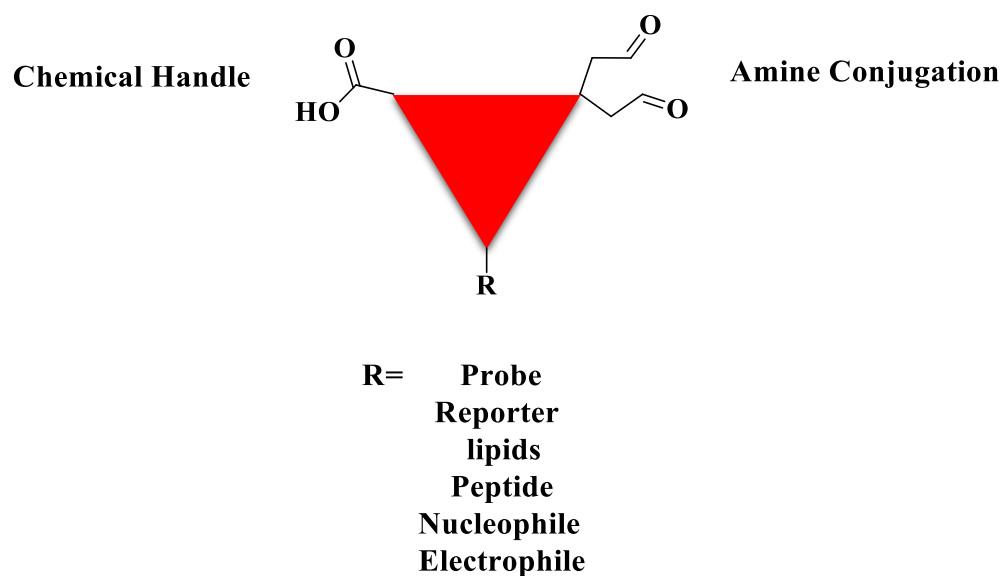


*Figure 5.1 Cartoon depiction of a Swiss army molecule with three locations for functionality*

Recent advances in our lab have established a well-defined blueprint frontier for the behavior of the dialdehyde models towards multiple variations within the structure of its linking substrate. The extent of advancement in this project is very broad; applications could be extrapolated to bead synthesis, solid state, molecular fluorescent probe, integration with other click chemistry reagent, DNA/RNA conjugation, carbohydrate chemistry and many more.

## References

1. Rup, B. & O'Hara, D. Critical ligand binding reagent preparation/selection: when specificity depends on reagents. *AAPS J.* **9**, E148-55 (2007).
2. Lavis, L. D. & Raines, R. T. Bright ideas for chemical biology. *ACS Chem. Biol.* **3**, 142–55 (2008).
3. Gonçalves, M. S. T. Fluorescent labeling of biomolecules with organic probes. *Chem. Rev.* **109**, 190–212 (2009).
4. Jannatipour M., Dion, P., Khan, S., Jindal, H., Fan, X., Laganière, J., Chishti, AH., Rouleau, GA. Schwannomin isoform-1 interacts with syntenin via PDZ domains. *J. Biol. Chem.* **276**, 33093–100 (2001).
5. Ducoux, M., Urbach, S., Baldacci, G., Hubscher, U., Koundrioukoff, S., Christensen, J., & Hughes, P. Mediation of proliferating cell nuclear antigen (PCNA)-dependent DNA replication through a conserved p21(Cip1)-like PCNA-binding motif present in the third subunit of human DNA polymerase delta. *J. Biol. Chem.* **276**, 49258–66 (2001).
6. Pellecchia, M., Sem, D. S. & Wüthrich, K. NMR in drug discovery. *Nat. Rev. Drug Discov.* **1**, 211–9 (2002).
7. Lipshutz, R. J., Fodor, S. P., Gingeras, T. R. & Lockhart, D. J. High density synthetic oligonucleotide arrays. *Nat. Genet.* **21**, 20–4 (1999).
8. Brown, P. O. & Botstein, D. Exploring the new world of the genome with DNA microarrays. *Nat. Genet.* **21**, 33–7 (1999).
9. Hoheisel, J. D. Microarray technology: beyond transcript profiling and genotype analysis. *Nat. Rev. Genet.* **7**, 200–10 (2006).
10. Jares-Erijman, E. A. & Jovin, T. M. FRET imaging. *Nat. Biotechnol.* **21**, 1387–95 (2003).
11. Jiang, Y., Ruta, V., Chen, J., Lee, A. & MacKinnon, R. The principle of gating charge movement in a voltage-dependent K<sup>+</sup> channel. *Nature* **423**, 42–8 (2003).
12. Zalipsky, S. Functionalized poly(ethylene glycol) for preparation of biologically relevant conjugates. *Bioconjug. Chem.* **6**, 150–65
13. Roberts, M. J., Bentley, M. D. & Harris, J. M. Chemistry for peptide and protein PEGylation. *Adv. Drug Deliv. Rev.* **54**, 459–76 (2002).
14. Chapman, A. P. PEGylated antibodies and antibody fragments for improved therapy: a review. *Adv. Drug Deliv. Rev.* **54**, 531–45 (2002).

15. Dunnill, P. Immobilized enzymes research and development. *Biochem. Educ.* **7**, 73 (1979).
16. Lagerlöf, E., Nathorst-Westfelt, L., Ekström, B. & Sjöberg, B. Production of 6-aminopenicillanic acid with immobilized *Escherichia coli* acylase. *Methods Enzymol.* **44**, 759–68 (1976).
17. Kobayashi, M., Nagasawa, T. & Yamada, H. Enzymatic synthesis of acrylamide: a success story not yet over. *Trends Biotechnol.* **10**, 402–8 (1992).
18. Algar, W. R., Tavares, A. J. & Krull, U. J. Beyond labels: A review of the application of quantum dots as integrated components of assays, bioprobes, and biosensors utilizing optical transduction. *Anal. Chim. Acta* **673**, 1–25 (2010).
19. Smith, M. E. B. et al. Protein Modification, Bioconjugation, and Disulfide Bridging Using Bromomaleimides. *J. Am. Chem. Soc.* **132**, 1960–1965 (2010).
20. Zhou, Q. et al. Bioconjugation by Native Chemical Tagging of C–H Bonds. *J. Am. Chem. Soc.* **135**, 12994–12997 (2013).
21. Kalia, J. & Raines, R. T. *Curr Org Chem.* **14**(2):138-147.(2012)
22. Tian, F. et al. A general approach to site-specific antibody drug conjugates. *Proc. Natl. Acad. Sci. U. S. A.* **111**, 1766–71 (2014).
23. Sochaj, A. M., Świdarska, K. W. & Otlewski, J. Current methods for the synthesis of homogeneous antibody-drug conjugates. *Biotechnol. Adv.* **33**, 775–84 (2015).
24. Shen, B.-Q. et al. Conjugation site modulates the in vivo stability and therapeutic activity of antibody-drug conjugates. *Nat. Biotechnol.* **30**, 184–9 (2012).
25. Cha, T., Guo, A. & Zhu, X.-Y. Enzymatic activity on a chip: the critical role of protein orientation. *Proteomics* **5**, 416–9 (2005).
26. Crankshaw, M. W., Grant, G. A., Crankshaw, M. W. & Grant, G. A. in *Current Protocols in Protein Science*.
27. Chalker, J. M., Bernardes, G. J. L., Lin, Y. A. & Davis, B. G. Chemical modification of proteins at cysteine: opportunities in chemistry and biology. *Chem. Asian J.* **4**, 630–40 (2009).
28. Sletten, E. M. & Bertozzi, C. R. Bioorthogonal chemistry: fishing for selectivity in a sea of functionality. *Angew. Chem. Int. Ed. Engl.* **48**, 6974–98 (2009).
29. Kalkhof, S. & Sinz, A. Chances and pitfalls of chemical cross-linking with amine-reactive N-hydroxysuccinimide esters. *Anal. Bioanal. Chem.* **392**, 305–312 (2008).
30. Hermanson, G. T. *Bioconjugate techniques*. (Academic Press, 2008).
31. Nakamura, T., Kawai, Y., Kitamoto, N., Osawa, T. & Kato, Y. Covalent modification of lysine residues by allyl isothiocyanate in physiological conditions:

- plausible transformation of isothiocyanate from thiol to amine. *Chem. Res. Toxicol.* **22**, 536–42 (2009).
32. Bednar, R. A. Reactivity and pH dependence of thiol conjugation to N-ethylmaleimide: detection of a conformational change in chalcone isomerase. *Biochemistry* **29**, 3684–90 (1990).
  33. Bernardes, G. J. L., Chalker, J. M., Errey, J. C. & Davis, B. G. Facile Conversion of Cysteine and Alkyl Cysteines to Dehydroalanine on Protein Surfaces: Versatile and Switchable Access to Functionalized Proteins. *J. Am. Chem. Soc.* **130**, 5052–5053 (2008).
  34. Henkel, M., Röckendorf, N. & Frey, A. Selective and Efficient Cysteine Conjugation by Maleimides in the Presence of Phosphine Reductants. *Bioconjug. Chem.* **27**(10), 2260–2265. (2016)
  35. Kim, Y. et al. Efficient site-specific labeling of proteins via cysteines. *Bioconjug. Chem.* **19**, 786–91 (2008).
  36. Gundlach, H. G., Moore, S. & Stein, W. H. The reaction of iodoacetate with methionine. *J. Biol. Chem.* **234**, 1761–4 (1959).
  37. Chalker, J. M. et al. Enabling olefin metathesis on proteins: chemical methods for installation of S-allyl cysteine. *Chem. Commun.* **47**, 3714 (2009).
  38. Miseta, A. & Csutora, P. Relationship between the occurrence of cysteine in proteins and the complexity of organisms. *Mol. Biol. Evol.* **17**, 1232–9 (2000).
  39. Jacob M. Hooker, Ernest W. Kovacs, and Francis, M. B. Interior Surface Modification of Bacteriophage MS2. **126**,12: 3718–719 (2004).
  40. Schlick, T. L.; Ding, Z.; Kovacs, E. W.; Francis, M. B. Journal of the American Chemical Society, **127** (11), 3718–3723, (2005)
  41. Guo, H.-M., Minakawa, M., Ueno, L. & Tanaka, F. Synthesis and evaluation of a cyclic imine derivative conjugated to a fluorescent molecule for labeling of proteins. *Bioorg. Med. Chem. Lett.* **19**, (2009).
  42. McFarland, J. M., Joshi, N. S. & Francis, M. B. Characterization of a three-component coupling reaction on proteins by isotopic labeling and nuclear magnetic resonance spectroscopy. *J. Am. Chem. Soc.* **130**, 7639–44 (2008).
  43. Gilles, M. A., Hudson, A. Q. & Borders, C. L. Stability of water-soluble carbodiimides in aqueous solution. *Anal. Biochem.* **184**, 244–248 (1990).
  44. Ishikawa, T. Guanidine chemistry. *Chem. Pharm. Bull.* **58**, 1555–64 (2010).
  45. Kent, D. R., Cody, W. L. & Doherty, A. M. Two New Reagents for the Guanylation of Primary, Secondary and Aryl Amines. *Tetrahedron Lett.* **48**, 8711–8714 (1996).
  46. Jentoft, N. & Dearborn, D. G. Labeling of proteins by reductive methylation using

- sodium cyanoborohydride. *J. Biol. Chem.* **254**, 4359–65 (1979).
47. Hooker, J. M., Esser-Kahn, A. P. & Francis, M. B. Modification of Aniline Containing Proteins Using an Oxidative Coupling Strategy. *J. Am. Chem. Soc.* **128**, 15558–15559 (2006).
  48. Tanaka, K. et al. The inhibitory mechanism of bovine pancreatic phospholipase A2 by aldehyde terpenoids. *Tetrahedron* **55**, 1657–1686 (1999).
  49. Tanaka, K., Fujii, Y. & Fukase, K. Site-Selective and Nondestructive Protein Labeling through Azaelectrocyclization-Induced Cascade Reactions. *Chem Bio Chem* **9**, 2392–2397 (2008).
  50. Nienhaus, G. U. The green fluorescent protein: a key tool to study chemical processes in living cells. *Angew. Chem. Int. Ed.* **47**, 8992–4 (2008).
  51. Hang, H. C., Yu, C., Kato, D. L. & Bertozzi, C. R. A metabolic labeling approach toward proteomic analysis of mucin-type O-linked glycosylation. *Proc. Natl. Acad. Sci.* **100**, 14846–51 (2003).
  52. Layer, R. W. The Chemistry of Imines. *Chem. Rev.* **63**, 489–510 (1963).
  53. Klopman, G., Tsuda, K., Louis, J. B. & Davis, R. E. Supernucleophiles—I. *Tetrahedron* **26**, 4549–4554 (1970).
  54. Klopman, G. & Evans, R. C. Supernucleophiles—II. *Tetrahedron* **34**, 269–273 (1978).
  55. Fina, N. J. & Edwards, J. O. The alpha effect. A review. *Int. J. Chem. Kinet.* **5**, 1–26 (1973).
  56. Dirksen, A., Hackeng, T. M. & Dawson, P. E. Nucleophilic Catalysis of Oxime Ligation. *Angew. Chemie Int. Ed.* **45**, 7581–7584 (2006).
  57. Cornish, V. W., Hahn, K. M. & Schultz, P. G. Site-Specific Protein Modification Using a Ketone Handle. *J. Am. Chem. Soc.* **118**, 8150–8151 (1996).
  58. Mahal, L. K. Engineering Chemical Reactivity on Cell Surfaces Through Oligosaccharide Biosynthesis. *Science*. **276**, 1125–1128 (1997).
  59. Hang, H. C. & Bertozzi, C. R. Ketone Isosteres of 2-N-Acetamid sugars as Substrates for Metabolic Cell Surface Engineering. *J. Am. Chem. Soc.* **123**, 1242–1243 (2001).
  60. Staudinger, H. & Meyer, J. Über neue organische Phosphorverbindungen III. Phosphinmethylderivate und Phosphinimine. *Helv. Chim. Acta* **2**, 635–646 (1919).
  61. Cartwright, I. L., Hutchinson, D. W. & Armstrong, V. W. The reaction between thiols and 8-azido adenosine derivatives. *Nucleic Acids Res.* **3**, 2331–9 (1976).

62. Staros, J. V., Bayley, H., Standring, D. N. & Knowles, J. R. Reduction of aryl azides by thiols: Implications for the use of photoaffinity reagents. *Biochem. Biophys. Res. Commun.* **80**, 568–572 (1978).
63. Reardon, J. E., Crouch, R. C. & St John-Williams, L. Reduction of 3'-azido-3'-deoxythymidine (AZT) and AZT nucleotides by thiols. Kinetics and product identification. *J. Biol. Chem.* **269**, 15999–6008 (1994).
64. Burns, J. A., Butler, J. C., Moran, J. & Whitesides, G. M. Selective reduction of disulfides by tris(2-carboxyethyl)phosphine. *J. Org. Chem.* **56**, 2648–2650 (1991).
65. Lemieux, G. A., Graffenried, C. L. D. & Bertozzi, C. R. A Fluorogenic Dye Activated by the Staudinger Ligation. *J. Am. Chem. Soc.* **125**, 4708–4709 (2003).
66. Soellner, M. B., Nilsson, B. L. & Raines, R. T. Reaction Mechanism and Kinetics of the Traceless Staudinger Ligation. *J. Am. Chem. Soc.* **128**, 8820–8828 (2006).
67. Lin, F. L., Hoyt, H. M., Halbeek, H. V., Bergman, R. G. & Bertozzi, C. R. Mechanistic Investigation of the Staudinger Ligation. *J. Am. Chem. Soc.* **127**, 2686–2695 (2005).
68. Arthur, M. A biographical Memoir. **48**, 94, (1893).
69. Huisgen, R. Kinetics and Mechanism of 1,3-Dipolar Cycloadditions. *Angew. Chemie Int. Ed.* **2**, 633–645 (1963).
70. Rostovtsev, V. V., Green, L. G., Fokin, V. V & Sharpless, K. B. A stepwise huisgen cycloaddition process: copper(I)-catalyzed regioselective "ligation" of azides and terminal alkynes. *Angew. Chem. Int. Ed.* **41**, 2596–9 (2002).
71. Tornøe, C. W., Christensen, C. & Meldal, M. Peptidotriazoles on solid phase: [1,2,3]-triazoles by regiospecific copper(i)-catalyzed 1,3-dipolar cycloadditions of terminal alkynes to azides. *J. Org. Chem.* **67**, 3057–64 (2002).
72. Himo, F. et al. Copper(I)-catalyzed synthesis of azoles. DFT study predicts unprecedented reactivity and intermediates. *J. Am. Chem. Soc.* **127**, 210–6 (2005).
73. Kolb, H. C. & Sharpless, K. B. The growing impact of click chemistry on drug discovery. *Drug Discov. Today* **8**, 1128–37 (2003).
74. Dondoni, A. Triazole: the keystone in glycosylated molecular architectures constructed by a click reaction. *Chem. Asian J.* **2**, 700–8 (2007).
75. Lutz, J.-F. & Nanotechnology for Life Science Research Group. 1,3-dipolar cycloadditions of azides and alkynes: a universal ligation tool in polymer and materials science. *Angew. Chem. Int. Ed.* **46**, 1018–25 (2007).
76. Tron, G. C. et al. Click chemistry reactions in medicinal chemistry: applications of the 1,3-dipolar cycloaddition between azides and alkynes. *Med. Res. Rev.* **28**, 278–308 (2008).

77. Fokin, V. V. Click imaging of biochemical processes in living systems. *ACS Chem. Biol.* **2**, 775–8 (2007).
78. Fournier, D., Hoogenboom, R. & Schubert, U. S. Clicking polymers: a straightforward approach to novel macromolecular architectures. *Chem. Soc. Rev.* **36**, 1369–80 (2007).
79. Wang, Q. et al. Bioconjugation by copper(I)-catalyzed azide-alkyne [3 + 2] cycloaddition. *J. Am. Chem. Soc.* **125**, 3192–3 (2003).
80. Breinbauer, R. & Köhn, M. Azide-alkyne coupling: a powerful reaction for bioconjugate chemistry. *ChemBiochem* **4**, 1147–9 (2003).
81. Link, A. J. & Tirrell, D. A. Cell surface labeling of Escherichia coli via copper(I)-catalyzed [3+2] cycloaddition. *J. Am. Chem. Soc.* **125**, 11164–5 (2003).
82. Link, A. J., Vink, M. K. S. & Tirrell, D. A. Presentation and detection of azide functionality in bacterial cell surface proteins. *J. Am. Chem. Soc.* **126**, 10598–602 (2004).
83. Alder K, S. G. . *Justus Liebigs Ann Chem.* **501**, 1, (1933).
84. Wittig G, K. A. . *Chem Ber.* **94**, 3260 (1962).
85. Agard, N. J., Prescher, J. A. & Bertozzi, C. R. A strain-promoted [3 + 2] azide-alkyne cycloaddition for covalent modification of biomolecules in living systems. *J. Am. Chem. Soc.* **126**, 15046–7 (2004).
86. Baskin, J. M. et al. Copper-free click chemistry for dynamic in vivo imaging. *Proc. Natl. Acad. Sci. U. S. A.* **104**, 16793–7 (2007).
87. Laughlin, S. T., Baskin, J. M., Amacher, S. L. & Bertozzi, C. R. In vivo imaging of membrane-associated glycans in developing zebrafish. *Science* **320**, 664–7 (2008).
88. Link, A. J., Mock, M. L. & Tirrell, D. A. Non-canonical amino acids in protein engineering. *Curr. Opin. Biotechnol.* **14**, 603–9 (2003).
89. Hendrickson, T. L., de Crécy-Lagard, V. & Schimmel, P. Incorporation of nonnatural amino acids into proteins. *Annu. Rev. Biochem.* **73**, 147–76 (2004).
90. Budisa, N. Prolegomena to future experimental efforts on genetic code engineering by expanding its amino acid repertoire. *Angew. Chem. Int. Ed.* **43**, 6426–63 (2004).
91. Dieterich, D. C., Link, A. J., Graumann, J., Tirrell, D. A. & Schuman, E. M. Selective identification of newly synthesized proteins in mammalian cells using bioorthogonal noncanonical amino acid tagging (BONCAT). *Proc. Natl. Acad. Sci. U. S. A.* **103**, 9482–7 (2006).
92. Kast, P. & Hennecke, H. Amino acid substrate specificity of Escherichia coli phenylalanyl-tRNA synthetase altered by distinct mutations. *J. Mol. Biol.* **222**, 99–124 (1991).



93. Ibba, M., Kast, P. & Hennecke, H. Substrate specificity is determined by amino acid binding pocket size in *Escherichia coli* phenylalanyl-tRNA synthetase. *Biochemistry* **33**, 7107–12 (1994).
94. Noren, C. J., Anthony-Cahill, S. J., Griffith, M. C. & Schultz, P. G. A general method for site-specific incorporation of unnatural amino acids into proteins. *Science* **244**, 182–8 (1989).
95. Ellman, J., Mendel, D., Anthony-Cahill, S., Noren, C. J. & Schultz, P. G. Biosynthetic method for introducing unnatural amino acids site-specifically into proteins. *Methods Enzymol.* **202**, 301–36 (1991).
96. Ellman, J. A., Mendel, D. & Schultz, P. G. Site-specific incorporation of novel backbone structures into proteins. *Science* **255**, 197–200 (1992).
97. Koh, J. T., Cornish, V. W. & Schultz, P. G. An experimental approach to evaluating the role of backbone interactions in proteins using unnatural amino acid mutagenesis. *Biochemistry* **36**, 11314–22 (1997).
98. Dougherty, D. A. Cys-loop neuroreceptors: structure to the rescue? *Chem. Rev.* **108**, 1642–53 (2008).
99. Dougherty, D. A. Unnatural amino acids as probes of protein structure and function. *Curr. Opin. Chem. Biol.* **4**, 645–52 (2000).
100. Chin, J. W. et al. Addition of p-azido-L-phenylalanine to the genetic code of *Escherichia coli*. *J. Am. Chem. Soc.* **124**, 9026–7 (2002).
101. Deiters, A. & Schultz, P. G. In vivo incorporation of an alkyne into proteins in *Escherichia coli*. *Bioorg. Med. Chem. Lett.* **15**, 1521–4 (2005).
102. Zhang, Z. et al. A new strategy for the site-specific modification of proteins in vivo. *Biochemistry* **42**, 6735–46 (2003).
103. Wang, L., Zhang, Z., Brock, A. & Schultz, P. G. Addition of the keto functional group to the genetic code of *Escherichia coli*. *Proc. Natl. Acad. Sci. U. S. A.* **100**, 56–61 (2003).
104. Zhang, Z., Wang, L., Brock, A. & Schultz, P. G. The selective incorporation of alkenes into proteins in *Escherichia coli*. *Angew. Chem. Int. Ed.* **41**, 2840–2 (2002).
105. Wang, L., Xie, J., Deniz, A. A. & Schultz, P. G. Unnatural amino acid mutagenesis of green fluorescent protein. *J. Org. Chem.* **68**, 174–6 (2003).
106. Santoro, S. W., Wang, L., Herberich, B., King, D. S. & Schultz, P. G. An efficient system for the evolution of aminoacyl-tRNA synthetase specificity. *Nat. Biotechnol.* **20**, 1044–8 (2002).
107. Carrico, Z. M., Romanini, D. W., Mehl, R. A. & Francis, M. B. Oxidative coupling of peptides to a virus capsid containing unnatural amino acids. *Chem. Commun.*

1205–7 (2008).

108. Brustad, E. et al. A genetically encoded boronate-containing amino acid. *Angew. Chem. Int. Ed.* **47**, 8220–3 (2008).
109. Chin, J. W., Martin, A. B., King, D. S., Wang, L. & Schultz, P. G. Addition of a photocrosslinking amino acid to the genetic code of *Escherichia coli*. *Proc. Natl. Acad. Sci. U. S. A.* **99**, 11020–4 (2002).
110. Sletten, E. M. & Bertozzi, C. R. Bioorthogonal chemistry: fishing for selectivity in a sea of functionality. *Angew. Chem. Int. Ed.* **48**, 6974–98 (2009).
111. Summerer, D. et al. A genetically encoded fluorescent amino acid. *Proc. Natl. Acad. Sci. U. S. A.* **103**, 9785–9 (2006).
112. Wang, J., Xie, J. & Schultz, P. G. A genetically encoded fluorescent amino acid. *J. Am. Chem. Soc.* **128**, 8738–9 (2006).
113. Keppler, O. T., Horstkorte, R., Pawlita, M., Schmidt, C. & Reutter, W. Biochemical engineering of the N-acyl side chain of sialic acid: biological implications. *Glycobiology* **11**, 11R–18R (2001).
114. Keppler, O. T. et al. Biosynthetic modulation of sialic acid-dependent virus-receptor interactions of two primate polyoma viruses. *J. Biol. Chem.* **270**, 1308–14 (1995).
115. Yarema, K. J., Mahal, L. K., Bruehl, R. E., Rodriguez, E. C. & Bertozzi, C. R. Metabolic delivery of ketone groups to sialic acid residues. Application To cell surface glycoform engineering. *J. Biol. Chem.* **273**, 31168–79 (1998).
116. Jacobs, C. L. et al. Substrate specificity of the sialic acid biosynthetic pathway. *Biochemistry* **40**, 12864–74 (2001).
117. Martin, D. D. O. et al. Rapid detection, discovery, and identification of post-translationally myristoylated proteins during apoptosis using a bio-orthogonal azidomyristate analog. *FASEB J.* **22**, 797–806 (2008).
118. Kostiuk, M. A. et al. Identification of palmitoylated mitochondrial proteins using a bio-orthogonal azido-palmitate analogue. *FASEB J.* **22**, 721–32 (2008).
119. Rose, M. W. et al. Enzymatic incorporation of orthogonally reactive prenylazide groups into peptides using geranylazide diphosphate via protein farnesyltransferase: implications for selective protein labeling. *Biopolymers* **80**, 164–71 (2005).
120. Labadie, G. R., Viswanathan, R. & Poulter, C. D. Farnesyl diphosphate analogues with omega-bioorthogonal azide and alkyne functional groups for protein farnesyl transferase-catalyzed ligation reactions. *J. Org. Chem.* **72**, 9291–7 (2007).
121. Xu, J. et al. Synthesis and reactivity of 6,7-dihydrogeranylazides: reagents for primary azide incorporation into peptides and subsequent Staudinger ligation. *Chem. Biol. Drug Des.* **68**, 85–96 (2006).

122. Nguyen, U. T. T. et al. Exploiting the substrate tolerance of farnesyltransferase for site-selective protein derivatization. *Chembiochem* **8**, 408–23 (2007).
123. Kalia, J. & Raines, R. T. Advances in Bioconjugation. *Curr. Org. Chem.* **14**, 138–147 (2010).
124. Stephanopoulos, N. & Francis, M. B. Choosing an effective protein bioconjugation strategy. *Nat. Chem. Biol.* **7**, 876–884 (2011).
125. Mayer, A. Membrane fusion in eukaryotic cells. *Annu. Rev. Cell Dev. Biol.* **18**, 289–314 (2002).
126. Ebara, M. et al. Temperature-responsive cell culture surfaces enable & quote on-off quote affinity control between cell integrins and RGDS ligands. *Biomacromolecules* **5**, 505–10
127. Zareie, H. M., Boyer, C., Bulmus, V., Nateghi, E. & Davis, T. P. Temperature-Responsive Self-Assembled Monolayers of Oligo(ethylene glycol): Control of Biomolecular Recognition. *ACS Nano* **2**, 757–765 (2008).
128. Sletten, E. M. & Bertozzi, C. R. Bioorthogonal Chemistry: Fishing for Selectivity in a Sea of Functionality. *Angew. Chemie Int. Ed.* **48**, 6974–6998 (2009).
129. Silhavy, T. J., Kahne, D. & Walker, S. The bacterial cell envelope. *Cold Spring Harb. Perspect. Biol.* **2**, a000414 (2010).
130. Lee, S. Y., Choi, J. H. & Xu, Z. Microbial cell-surface display. *Trends Biotechnol.* **21**, 45–52 (2003).
131. Desvaux, M., Dumas, E., Chafsey, I. & Hébraud, M. Protein cell surface display in Gram-positive bacteria: from single protein to macromolecular protein structure. *FEMS Microbiol. Lett.* **256**, 1–15 (2006).
132. Cross, A. et al. Nosocomial infections due to *Pseudomonas aeruginosa*: review of recent trends. *Rev. Infect. Dis.* **5 Suppl 5**, S837-45
133. Croxen, M. A. & Finlay, B. B. Molecular mechanisms of *E. coli* pathogenicity. *Nat. Rev. Microbiol.* **8**, 26 (2009).
134. Wu, C. H., Mulchandani, A. & Chen, W. Versatile microbial surface-display for environmental remediation and biofuels production. *Trends Microbiol.* **16**, 181–8 (2008).
135. Fan, S., Hou, C., Liang, B., Feng, R. & Liu, A. Microbial surface displayed enzymes based biofuel cell utilizing degradation products of lignocellulosic biomass for direct electrical energy. *Bioresour. Technol.* **192**, 821–5 (2015).
136. Schüürmann, J., Quehl, P., Festel, G. & Jose, J. Bacterial whole-cell biocatalysts by surface display of enzymes: toward industrial application. *Appl. Microbiol. Biotechnol.* **98**, 8031–8046 (2014).

137. van Bloois, E., Winter, R. T., Kolmar, H. & Fraaije, M. W. Decorating microbes: surface display of proteins on Escherichia coli. *Trends Biotechnol.* **29**, 79–86 (2011).
138. Georgiou, G. et al. Display of heterologous proteins on the surface of microorganisms: from the screening of combinatorial libraries to live recombinant vaccines. *Nat. Biotechnol.* **15**, 29–34 (1997).
139. Holliger, P. & Hudson, P. J. Engineered antibody fragments and the rise of single domains. *Nat. Biotechnol.* **23**, 1126–36 (2005).
140. Lee, J. S., Shin, K. S., Pan, J. G. & Kim, C. J. Surface-displayed viral antigens on Salmonella carrier vaccine. *Nat. Biotechnol.* **18**, 645–8 (2000).
141. Etz, H. et al. Identification of in vivo expressed vaccine candidate antigens from Staphylococcus aureus. *Proc. Natl. Acad. Sci. U. S. A.* **99**, 6573–8 (2002).
142. O'Hara, A. M. & Shanahan, F. The gut flora as a forgotten organ. *EMBO Rep.* **7**, 688–93 (2006).
143. Cho, C. M.-H., Mulchandani, A. & Chen, W. Bacterial cell surface display of organophosphorus hydrolase for selective screening of improved hydrolysis of organophosphate nerve agents. *Appl. Environ. Microbiol.* **68**, 2026–30 (2002).
144. Benhar, I. Biotechnological applications of phage and cell display. *Biotechnol. Adv.* **19**, 1–33 (2001).
145. Linnebacher, M., Maletzki, C., Klier, U. & Klar, E. Bacterial immunotherapy of gastrointestinal tumors. *Langenbeck's Arch. Surg.* **397**, 557–68 (2012).
146. Casadevall, A. & Pirofski, L. A. Host-pathogen interactions: redefining the basic concepts of virulence and pathogenicity. *Infect. Immun.* **67**, 3703–13 (1999).
147. Finlay, B. B. & Cossart, P. Exploitation of mammalian host cell functions by bacterial pathogens. *Science* **276**, 718–25 (1997).
148. Torchilin, V. P. Recent advances with liposomes as pharmaceutical carriers. *Nat. Rev. Drug Discov.* **4**, 145–60 (2005).
149. Gao, W., Hu, C.-M. J., Fang, R. H. & Zhang, L. Liposome-like Nanostructures for Drug Delivery. *J. Mater. Chem. B. Mater. Biol. Med.* **1**, (2013).
150. Chan, Y.-H. M. & Boxer, S. G. Model membrane systems and their applications. *Curr. Opin. Chem. Biol.* **11**, 581–7 (2007).
151. Bertozzi, C. R. A decade of bioorthogonal chemistry. *Acc. Chem. Res.* **44**, 651–3 (2011).
152. McKay, C. S. & Finn, M. G. Click chemistry in complex mixtures: bioorthogonal bioconjugation. *Chem. Biol.* **21**, 1075–101 (2014).
153. Dieterich, D. C. et al. Labeling, detection and identification of newly synthesized

- proteomes with bioorthogonal non-canonical amino-acid tagging. *Nat. Protoc.* **2**, 532–40 (2007).
154. Patterson, D. M., Nazarova, L. A. & Prescher, J. A. Finding the Right (Bioorthogonal) Chemistry. *ACS Chem. Biol.* **9**, 592–605 (2014).
  155. Rashidian, M., Song, J. M., Pricer, R. E. & Distefano, M. D. Chemoenzymatic reversible immobilization and labeling of proteins without prior purification. *J. Am. Chem. Soc.* **134**, 8455–67 (2012).
  156. Park, S., Westcott, N. P., Luo, W., Dutta, D. & Yousaf, M. N. General Chemoselective and Redox-Responsive Ligation and Release Strategy. *Bioconjug. Chem.* **25**, 543–551 (2014).
  157. Desjardins, A., Chen, T., Khalil, H., Sayasith, K. & Lagacé, J. Differential behaviour of fluid liposomes toward mammalian epithelial cells and bacteria: restriction of fusion to bacteria. *J. Drug Target.* **10**, 47–54 (2002).
  158. Düzgüneş, N., Faneca, H. & Lima, M. C. Methods to monitor liposome fusion, permeability, and interaction with cells. *Methods Mol. Biol.* **606**, 209–32 (2010).
  159. Wilschut, J. & Hoekstra, D. Membrane fusion: from liposomes to biological membranes. *Trends Biochem. Sci.* **9**, 479–483 (1984).
  160. Yang, J. et al. Drug Delivery via Cell Membrane Fusion Using Lipopeptide Modified Liposomes. *ACS Cent. Sci.* **2**, 621–630 (2016).
  161. Çağdaş, M., Sezer, A. D. & Bucak, S. in *Application of Nanotechnology in Drug Delivery* (InTech, 2014).
  162. Tamkun, J. W. et al. Structure of integrin, a glycoprotein involved in the transmembrane linkage between fibronectin and actin. *Cell* **46**, 271–82 (1986).
  163. Danilov, Y. N. & Juliano, R. L. (Arg-Gly-Asp)<sub>n</sub>-albumin conjugates as a model substratum for integrin-mediated cell adhesion. *Exp. Cell Res.* **182**, 186–96 (1989).
  164. Brown, L., Wolf, J. M., Prados-Rosales, R. & Casadevall, A. Through the wall: extracellular vesicles in Gram-positive bacteria, mycobacteria and fungi. *Nat. Rev. Microbiol.* **13**, 620–630 (2015).
  165. Vaara, M. Agents that increase the permeability of the outer membrane. *Microbiol. Rev.* **56**, 395–411 (1992).
  166. Driessen, A. J., Hoekstra, D., Scherphof, G., Kalicharan, R. D. & Wilschut, J. Low pH-induced fusion of liposomes with membrane vesicles derived from *Bacillus subtilis*. *J. Biol. Chem.* **260**, 10880–7 (1985).
  167. Tomlinson, S., Taylor, P. W. & Luzio, J. P. Transfer of phospholipid and protein into the envelope of Gram-negative bacteria by liposome fusion. *Biochemistry* **28**, 8303–8311 (1989).

168. Dagert, M. & Ehrlich, S. D. Prolonged incubation in calcium chloride improves the competence of *Escherichia coli* cells. *Gene* **6**, 23–28 (1979).
169. Alexander, C. & Rietschel, E. T. Bacterial lipopolysaccharides and innate immunity. *J. Endotoxin Res.* **7**, 167–202 (2001).
170. Tzeng, Y.-L., Datta, A., Kolli, V. K., Carlson, R. W. & Stephens, D. S. Endotoxin of *Neisseria meningitidis* composed only of intact lipid A: inactivation of the meningococcal 3-deoxy-D-manno-octulosonic acid transferase. *J. Bacteriol.* **184**, 2379–88 (2002).
171. Castuma, C. E., Huang, R., Kornberg, A. & Reusch, R. N. Inorganic polyphosphates in the acquisition of competence in *Escherichia coli*. *J. Biol. Chem.* **270**, 12980–3 (1995).
172. Dutta, D., Pulsipher, A., Luo, W. & Yousaf, M. N. Synthetic Chemoselective Rewiring of Cell Surfaces: Generation of Three-Dimensional Tissue Structures. *J. Am. Chem. Soc.* **133**, 8704–8713 (2011).
173. Dutta, D., Pulsipher, A., Luo, W., Mak, H. & Yousaf, M. N. Engineering Cell Surfaces via Liposome Fusion. *Bioconjug. Chem.* **22**, 2423–2433 (2011).
174. Luo, W., Pulsipher, A., Dutta, D., Lamb, B. M. & Yousaf, M. N. Remote control of tissue interactions via engineered photo-switchable cell surfaces. *Sci. Rep.* **4**, 6313 (2014).
175. Pulsipher, A., Dutta, D., Luo, W. & Yousaf, M. N. Cell-Surface Engineering by a Conjugation-and-Release Approach Based on the Formation and Cleavage of Oxime Linkages upon Mild Electrochemical Oxidation and Reduction. *Angew. Chemie Int. Ed.* **53**, 9487–9492 (2014).
176. O'Brien, P. J., Luo, W., Rogozhnikov, D., Chen, J. & Yousaf, M. N. Spheroid and Tissue Assembly via Click Chemistry in Microfluidic Flow. *Bioconjug. Chem.* **26**, 1939–1949 (2015).
177. Luo, W. et al. A Dual Receptor and Reporter for Multi-Modal Cell Surface Engineering. *ACS Chem. Biol.* **10**, 2219–2226 (2015).
178. Daugherty, P. S. Protein engineering with bacterial display. *Curr. Opin. Struct. Biol.* **17**, 474–80 (2007).
179. Tamma, P. D., Cosgrove, S. E. & Maragakis, L. L. Combination therapy for treatment of infections with gram-negative bacteria. *Clin. Microbiol. Rev.* **25**, 450–70 (2012).
180. Parsek, M. R., Val, D. L., Hanzelka, B. L., Cronan, J. E. & Greenberg, E. P. Acyl homoserine-lactone quorum-sensing signal generation. *Proc. Natl. Acad. Sci. U. S. A.* **96**, 4360–5 (1999).
181. Chandki, R., Banthia, P. & Banthia, R. Biofilms: A microbial home. *J. Indian Soc.*

*Periodontol.* **15**, 111–4 (2011).

182. Reardon, S. Bacteria implicated in stress-related heart attacks. *Nature*. 1539 (2014).
183. Hancock, R. E. Resistance mechanisms in *Pseudomonas aeruginosa* and other nonfermentative gram-negative bacteria. *Clin. Infect. Dis.* **27**, 1, S93-9 (1998).
184. Pulsipher, A., Westcott, N. P., Luo, W. & Yousaf, M. N. Rapid in Situ Generation of Two Patterned Chemoselective Surface Chemistries from a Single Hydroxy-Terminated Surface Using Controlled Microfluidic Oxidation. *J. Am. Chem. Soc.* **131**, 7626–7632 (2009).
185. Pulsipher, A., Westcott, N. P., Luo, W. & Yousaf, M. N. Rapid Microfluidic Generation of Patterned Aldehydes from Hydroxy-Terminated Self-Assembled Monolayers for Ligand and Cell Immobilization on Optically Transparent Indium Tin Oxide Surfaces. *Adv. Mater.* **21**, 3082–3086 (2009).
186. Kuehn, M. J. Bacterial outer membrane vesicles and the host-pathogen interaction. *Genes Dev.* **19**, 2645–2655 (2005).
187. Matsumoto, K., Kusaka, J., Nishibori, A. & Hara, H. Lipid domains in bacterial membranes. *Mol. Microbiol.* **61**, 1110–1117 (2006).
188. Mugabe, C., Halwani, M., Azghani, A. O., Lafrenie, R. M. & Omri, A. Mechanism of enhanced activity of liposome-entrapped aminoglycosides against resistant strains of *Pseudomonas aeruginosa*. *Antimicrob. Agents Chemother.* **50**, 2016–22 (2006).
189. Shorr, A. F. Review of studies of the impact on Gram-negative bacterial resistance on outcomes in the intensive care unit. *Crit. Care Med.* **37**, 1463–1469 (2009).
190. Vasoo, S., Barreto, J. N. & Tosh, P. K. Emerging issues in gram-negative bacterial resistance: an update for the practicing clinician. *Mayo Clin. Proc.* **90**, 395–403 (2015).
191. Xu, Z.-Q., Flavin, M. T. & Flavin, J. Combating multidrug-resistant Gram-negative bacterial infections. *Expert Opin. Investig. Drugs* **23**, 163–82 (2014).
192. Schembri, M. A., Givskov, M. & Klemm, P. An Attractive Surface: Gram-Negative Bacterial Biofilms. *Sci. Signal.* **2002**, (2002).
193. Clayden, J., Greeves, N., Warren, S. & Wothers, P. Organic Chemistry. *Am. Nat.* **40**, 1990–1992 (2001).
194. Stork, G. & Dowd, S. R. A New Method for the Alkylation of Ketones and Aldehydes: the C-Alkylation of the Magnesium Salts of N-Substituted Imines. *J. Am. Chem. Soc.* **85**, 2178–2180 (1963).
195. Carlson, R. et al. Improved Titanium Tetrachloride Procedure for Enamine Synthesis. II. Scope of the Reaction. *Acta Chem. Scand.* **38b**, 49–53 (1984).

196. Capon, B. & Wu, Z. P. Comparison of the tautomerization and hydrolysis of some secondary and tertiary enamines. *J. Org. Chem.* **55**, 2317–2324 (1990).
197. White, W. A. & Weingarten, H. A versatile new enamine synthesis. *J. Org. Chem.* **32**, 213–214 (1967).
198. Meyers, A. I. & Williams, D. R. Asymmetric alkylation of acyclic ketones via chiral metallo enamines. Effect of kinetic vs. thermodynamic metalations. *J. Org. Chem.* **43**, 3245–3247 (1978).
199. Seufert, W. & Effenberger, F. Zur Halogenierung von Enaminen — Darstellung von  $\beta$ -Halogen-iminium-halogeniden. *Chem. Ber.* **112**, 1670–1676 (1979).
200. Mastracchio, A., Warkentin, A. A., Walji, A. M. & MacMillan, D. W. C. Direct and enantioselective  $\{\alpha\}$ -allylation of ketones via singly occupied molecular orbital (SOMO) catalysis. *Proc. Natl. Acad. Sci. U. S. A.* **107**, 20648–51 (2010).
201. Li, Q. et al. One-Pot AgOAc-Mediated Synthesis of Polysubstituted Pyrroles from Primary Amines and Aldehydes: Application to the Total Synthesis of Purpurone. *Org. Lett.* **12**, 4066–4069 (2010).
202. Guo, F., Clift, M. D. & Thomson, R. J. Oxidative Coupling of Enolates, Enol Silanes, and Enamines: Methods and Natural Product Synthesis. *European J. Org. Chem.* **2012**, 4881–4896 (2012).
203. Pidathala, C., Hoang, L., Vignola, N. & List, B. Direct Catalytic Asymmetric Enolexo Aldolizations. *Angew. Chemie Int. Ed.* **42**, 2785–2788 (2003).
204. Mukherjee, S., Yang, J. W., Hoffmann, S. & List, B. Asymmetric Enamine Catalysis. *Chem. Rev.* **107**, 5471–5569 (2007).
205. Casiraghi, G. et al. Selective step-growth phenol-aldehyde polymerization, 1. Synthesis, characterization and X-ray analysis of linear all-ortho oligonuclear phenolic compounds. *Die Makromol. Chemie* **183**, 2611–2633 (1982).
206. Vogl, O. & Bryant, W. M. D. Polymerization of higher aldehydes. VI. Mechanism of aldehyde polymerization. *J. Polym. Sci. Part A Gen. Pap.* **2**, 4633–4645 (1964).
207. Vogl, O. Kinetics of Aldehyde Polymerization. *J. Macromol. Sci. Part C Polym. Rev.* **12**, 109–164 (1975).
208. North, A. M. & Richardson, D. Entropy of stereoregularity in aldehyde polymerization. *Polymer (Guildf)*. **6**, 333–338 (1965).
209. Bullock, G. R. The current status of fixation for electron microscopy: A review. *J. Microsc.* **133**, 1–15 (1984).
210. Hopwood, D. Theoretical and practical aspects of glutaraldehyde fixation. *Histochem. J.* **4**, 267–303 (1972).
211. Russell, A. & Hopwood, D. 4 The Biological Uses and Importance of



Glutaraldehyde. *Prog Med Chem.* 271–301 (1976).

212. Hopwood, D. The reactions of glutaraldehyde with nucleic acids. *Histochem. J.* **7**, 267–276 (1975).
213. Adami, R. C. & Rice, K. G. Metabolic stability of glutaraldehyde cross-linked peptide dna condensates. *Journal of Pharmaceutical Sciences* **88**, 739–746 (1999).
214. Weetall, H. H. Immobilized Enzymes: Analytical Applications. *Anal. Chem.* **46**, 602A–615A (1974).
215. Zahn, H. Bridge reactions in amino acids and fibrous proteins. *Angew. Chem* 561–572. (1955).
216. Quijcho, F. A. & Richards, F. M. Intermolecular Crosslinking Of A Protein In The Crystalline State: Carboxypeptidase-A. *Proc. Natl. Acad. Sci. U. S. A.* **52**, 833–9 (1964).
217. Arthur Robertson, E. & Schultz, R. L. The impurities in commercial glutaraldehyde and their effect on the fixation of brain. *J. Ultrastruct. Res.* **30**, 275–287 (1970).
218. Scouten, W. H. *Solid phase biochemistry : analytical and synthetic aspects*. (Wiley, 1983).
219. Avrameas, S. & Ternynck, T. The Cross-linking of Proteins with Glutaraldehyde and its use for the preparation of immunoadsorbents. *Immunochemistry* **6**, 53–66 (1969).
220. Weetall, H. H. Immobilized Enzymes: Analytical Applications. *AnalChem.* **46**, (1974).
221. Jansen, E. F., Tomimatsu, Y. & Olson, A. C. Cross-linking of  $\alpha$ -chymotrypsin and other proteins by reaction with glutaraldehyde. *Arch. Biochem. Biophys.* **144**, 394–400 (1971).
222. Ottesen, M. & Svensson, B. Modification of papain by treatment with glutaraldehyde under reducing and non-reducing conditions. *C. R. Trav. Lab. Carlsberg* **38**, 171–85 (1971).
223. Tomimatsu, Y., Jansen, E. ., Gaffield, W. & Olson, A. Physical chemical observations on the  $\alpha$ -chymotrypsin glutaraldehyde system during formation of an insoluble derivative. *J. Colloid Interface Sci.* **36**, 51–64 (1971).
224. Jansen, E. F. & Olson, A. C. Properties and enzymatic activities of papain insolubilized with glutaraldehyde. *Arch. Biochem. Biophys.* **129**, 221–227 (1969).
225. Sabatini, D. D., Bensch, K. & Barnett, R. J. Cytochemistry and electron microscopy. The preservation of cellular ultrastructure and enzymatic activity by aldehyde fixation. *J. Cell Biol.* **17**, 19–58 (1963).
226. Bowes, J. H. & Cater, C. W. The interaction of aldehydes with collagen. *Biochim.*

*Biophys. Acta - Protein Struct.* **168**, 341–352 (1968).

227. Hopwood, D., Allen, C. R. & McCabe, M. The reactions between glutaraldehyde and various proteins. An investigation of their kinetics. *Histochem. J.* **2**, 137–150 (1970).
228. Alexa, G., D. Chisalita, and G. C. Reaction of aldehyde with functional groups in collagen. *Rev. Tech. Ind. Cuir* **63**, 5–6 (1971).
229. Okuda, K., Urabe, I., Yamada, Y. & Okada, H. Reaction of glutaraldehyde with amino and thiol compounds. *J. Ferment. Bioeng.* **71**, 100–105 (1991).
230. Hardy, P. M., Nicholls, A. C. & Rydon, H. N. The nature of glutaraldehyde in aqueous solution. *J. Chem. Soc. D Chem. Commun.* 565 (1969).
231. Aso, C. & Aito, Y. Studies on the polymerization of bifunctional monomers. II. Polymerization of glutaraldehyde,. *Die Makromol. Chemie* **58**, 195–203 (1962).
232. Richards, F. M. & Knowles, J. R. Glutaraldehyde as a protein cross-linking reagent. *J. Mol. Biol.* **37**, 231–233 (1968).
233. Korn, A. H., Feairheller, S. H. & Filachoine, E. M. Glutaraldehyde: Nature of the reagent. *J. Mol. Biol.* **65**, 525–529 (1972).
234. Whipple, E. B. & Ruta, M. Structure of aqueous glutaraldehyde. *J. Org. Chem.* **39**, 1666–1668 (1974).
235. Monsan, P., Puzo, G. & Mazarguil, H. Étude du mécanisme d'établissement des liaisons glutaraldéhyde-protéines. *Biochimie* **57**, 1281–1292 (1976).
236. Margel, S. & Rembaum, A. Synthesis and Characterization of Poly(glutaraldehyde). A Potential Reagent for Protein Immobilization and Cell Separation. *Macromolecules* **13**, 19–24 (1980).
237. Tashima, T., Imai, M., Kuroda, Y., Yagi, S. & Nakagawa, T. Structure of a new oligomer of glutaraldehyde produced by aldol condensation reaction. *J. Org. Chem.* **56**, 694–697 (1991).
238. Gruen, L. C. & McTigue, P. T. Hydration equilibria of aliphatic aldehydes in H<sub>2</sub>O and D<sub>2</sub>O. *J. Chem. Soc.* 5217 (1963).
239. Kawahara, J., Ohmori, T., Ohkubo, T., Hattori, S. & Kawamura, M. The structure of glutaraldehyde in aqueous solution determined by ultraviolet absorption and light scattering. *Anal. Biochem.* **201**, 94–98 (1992).
240. Kawahara, J., Ishikawa, K., Uchimar, T. & Takaya, H. in *Polymer Modification* 119–131 (Springer US, 1997).
241. Boucher, R. M. Advances in sterilization techniques: state of the art and recent breakthroughs. *Am. J. Hosp. Pharm.* **29**, 661–72 (1972).

242. Boucher, R. M. Potentiated acid 1,5 pentanedial solution--a new chemical sterilizing and disinfecting agent. *Am. J. Hosp. Pharm.* **31**, 546–57 (1974).
243. Ruijgrok, J. M., Boon, M. E. & De Wijn, J. R. The effect of heating by microwave irradiation and by conventional heating on the aldehyde concentration in aqueous glutaraldehyde solutions. *Histochem. J.* **22**, 389–93
244. Hardy, P. M., Nicholls, A. C. & Rydon, H. N. The nature of the cross-linking of proteins by glutaraldehyde. Part I. Interaction of glutaraldehyde with the amino-groups of 6-aminohexanoic acid and of alpha-N-acetyl-lysine. *J. Chem. Soc. Perkin I* 958–62 (1976).
245. Lubig, R., Kusch, P., Raper, K. & Zahn, H. Zum Reaktionsmechanismus von Glutaraldehyde mit Proteinen. *Monatshefte for Chemie* **112**, 1313–1323 (1981).
246. Walt, D. R. & Agayn, V. I. The chemistry of enzyme and protein immobilization with glutaraldehyde. *TrAC Trends Anal. Chem.* **13**, 425–430 (1994).
247. Earle, M. et al. in *Ionic Liquids in Synthesis* 265–568 (2008).
248. Wade, L. G. Organic Synthesis: The Disconnection Approach (Warren, Stuart). *J. Chem. Educ.* **61**, A248 (1984).
249. Girard, J. E. Practical organic chemistry. *Nature* **284**, 83–83 (1980).
250. Kohlpaintner, C. et al. in *Ullmann's Encyclopedia of Industrial Chemistry* (Wiley-VCH Verlag GmbH & Co. KGaA, 2008).
251. Zhu, Q. et al. A novel green process for the synthesis of glutaraldehyde by WS<sub>2</sub> @HMS material with aqueous H<sub>2</sub>O<sub>2</sub>. *RSC Adv.* **3**, 1744–1747 (2013).
252. Milas, N. A. & Sussman, S. The Hydroxylation of the Double Bond. *J. Am. Chem. Soc.* **58**, 1302–1304 (1936).
253. Milas, N. A., Trepagnier, J. H., Nolan, J. T. & Iliopoulos, M. I. A Study of the Hydroxylation of Olefins and the Reaction of Osmium Tetroxide with 1,2-Glycols. *J. Am. Chem. Soc.* **81**, 4730–4733 (1959).
254. *Comprehensive Organic Name Reactions and Reagents* (John Wiley & Sons, Inc., 2010).
255. Kim, S., Chung, J. & Kim, B. M. Recycling of osmium catalyst in oxidative olefin cleavage: a chemoentrappment approach. *Tetrahedron Letters* **52**, (2011).
256. Whitehead, D. C., Travis, B. R. & Borhan, B. The OsO<sub>4</sub>-mediated oxidative cleavage of olefins catalyzed by alternative osmium sources. *Tetrahedron Letters* **47**, (2006).
257. Wensheng Yu, Yan Mei, Ying Kang, Zhengmao Hua, and Jin, Z. Improved Procedure for the Oxidative Cleavage of Olefins by OsO<sub>4</sub>–NaIO<sub>4</sub>. (2004).

258. VanRheenen, V., Kelly, R. C. & Cha, D. Y. An improved catalytic OsO<sub>4</sub> oxidation of olefins to cis-1,2-glycols using tertiary amine oxides as the oxidant. *Tetrahedron Lett.* **17**, 1973–1976 (1976).
259. Eames, J. et al. An efficient protocol for Sharpless-style racemic dihydroxylation. *J. Chem. Soc. Perkin Trans. 1* **37**, 1095–1104 (1999).
260. Jacobsen, E. N., Marko, I., Mungall, W. S., Schroeder, G. & Sharpless, K. B. Asymmetric dihydroxylation via ligand-accelerated catalysis. *J. Am. Chem. Soc.* **110**, 1968–1970 (1988).
261. Kolb, H. C., VanNieuwenhze, M. S. & Sharpless, K. B. Catalytic Asymmetric Dihydroxylation. *Chem. Rev.* **94**, 2483–2547 (1994).
262. Gonzalez, J., Aurigemma, C. & Truesdale, L. Synthesis of (1S,2R) and (–)-(1R,2S)-trans-2-Phenylcyclohexanol Via Sharpless Asymmetric Dihydroxylation (AD). *Org. Synth* 93–93 (2003).
263. Yang, D. & Zhang, C. Ruthenium-Catalyzed Oxidative Cleavage of Olefins to Aldehydes. *J. Org. Chem.* **66**, 4814–4818 (2001).
264. Parks, B. W., Gilbertson, R. D., Domaille, D. W. & Hutchison, J. E. Convenient Synthesis of 6,6-Bicyclic Malonamides: A New Class of Conformationally Preorganized Ligands for f-Block Ion Binding. *J. Org. Chem.* **71**, 9622–9627 (2006).
265. Grieco, P. A., Clark, D. S. & Withers, G. P. Direct conversion of carboxylic acids into amides. *J. Org. Chem.* **44**, 2945–2947 (1979).
266. Rao, Y., Li, X., Nagorny, P., Hayashida, J. & Danishefsky, S. J. A Simple Method for the Conversion of Carboxylic Acids into Thioacids with Lawesson's Reagent. *Tetrahedron Lett.* **50**, 6684–6686 (2009).
267. Ainsworth, C. The Conversion of Carboxylic Acid Hydrazides to Amides with Raney Nickel. *J. Am. Chem. Soc.* **76**, 5774–5775 (1954).
268. Jagdmann, G. , Randall, H & Gero, T. A Mild Efficient Procedure for the Conversion of Carboxylic Acid Esters to Primary Amides Using Formamide/Methanolic Sodium Methoxide. *Synth. Commun.* **20**, 1203–1208 (1990).
269. Wang, W. B. & Roskamp, E. J. Tin(II) amides: new reagents for the conversion of esters to amides. *J. Org. Chem.* **57**, 6101–6103 (1992).
270. Zacharie, B., Connolly, T. P. & Penney, C. L. A Simple One-Step Conversion of Carboxylic Acids to Esters Using EEDQ. *J. Org. Chem.* **60**, 7072–7074 (1995).
271. Anelli, P. L., Brocchetta, M., Palano, D. & Visigalli, M. Mild conversion of primary carboxamides into carboxylic esters. *Tetrahedron Lett.* **38**, 2367–2368 (1997).

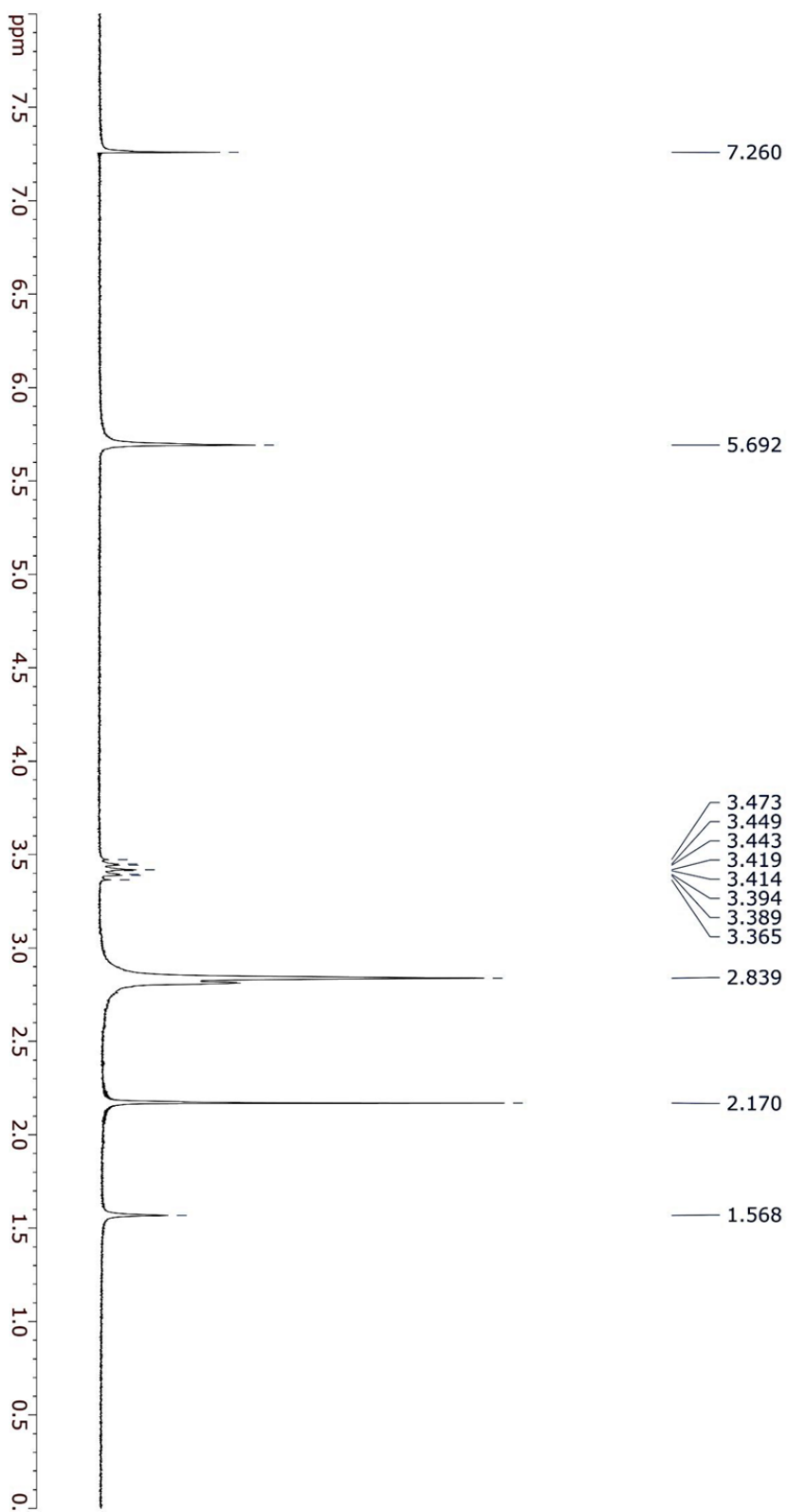
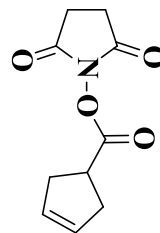
272. Zoete, M. D., Dalen, A. K.-V., Rantwijk, F. V. & Sheldon, R. A new enzymatic one-pot procedure for the synthesis of carboxylic amides from carboxylic acids. *J. Mol. Catal. B: Enzym.* **2**, 19–25 (1996).
273. Li, B. et al. Aqueous Phosphoric Acid as a Mild Reagent for Deprotection of *tert* -Butyl Carbamates, Esters, and Ethers. *J. Org. Chem.* **71**, 9045–9050 (2006).
274. Filali, E., Lloyd-Jones, G. & Sale, D. Cleavage of *tert*-Butyl Benzoates with NaH in DMF: Comments on the -Mechanism and a Simple and Safe Alternative Procedure. *Synlett* **2009**, 0205–0208 (2009).
275. Marcantoni, E. et al. Selective Deprotection of N-Boc-Protected *tert* -Butyl Ester Amino Acids by the  $\text{CeCl}_3 \cdot 7\text{H}_2\text{O}$ –NaI System in Acetonitrile. *J. Org. Chem.* **66**, 4430–4432 (2001).
276. Sayer, J. M., Pinsky, B., Schonbrunn, A. & Washtien, W. Mechanism of carbinolamine formation. *J. Am. Chem. Soc.* **96**, 7998–8009 (1974).
277. Green, N. M. Avidin. *Adv. Protein Chem.* **29**, 85–133 (1975).
278. Sachon, E., Tasseau, O., Lavielle, S., Sagan, S. & Bolbach, G. Isotope and affinity tags in photoreactive substance P analogues to identify the covalent linkage within the NK-1 receptor by MALDI-TOF analysis. *Anal. Chem.* **75**, 6536–43 (2003).
279. Sanger, F. The free amino groups of insulin. *Biochem. J.* **39**, 507–15 (1945).
280. Schaefer, T. The Proton Magnetic Resonance Spectrum Of 1-Fluoro-2,4-Dinitrobenzene. *Can. J. Chem.* **40**, 431–433 (1962).
281. Nageswara Rao, B. D. The  $^1\text{H}$  and  $^{19}\text{F}$  resonance spectra of 1-fluoro-2,4-dinitrobenzene. *Mol. Phys.* **7**, 307–310 (1964).
282. Wilkins, A., Small, R. W. H. Structure of 1-fluoro-2,4-dinitrobenzene. *Acta Crystallogr. Sect. C Cryst. Struct. Commun.* **47**, 220–221 (1991).
283. Murelli, R. P., Zhang, A. X., Michel, J., Jorgensen, W. L. & Spiegel, D. A. Chemical Control over Immune Recognition: A Class of Antibody-Recruiting Small Molecules That Target Prostate Cancer. *J. Am. Chem. Soc.* **131**, 17090–17092 (2009).
284. McEnaney, P. J., Parker, C. G., Zhang, A. X. & Spiegel, D. A. Antibody-Recruiting Molecules: An Emerging Paradigm for Engaging Immune Function in Treating Human Disease. *ACS Chem. Biol.* **7**, 1139–1151 (2012).
285. McEnaney, P. J., Parker, C. G., Zhang, A. X. & Spiegel, D. A. Antibody-recruiting molecules: an emerging paradigm for engaging immune function in treating human disease. *ACS Chem. Biol.* **7**, 1139–51 (2012).
286. Genady, A. R. et al. Preparation and Evaluation of Radiolabeled Antibody Recruiting Small Molecules That Target Prostate-Specific Membrane Antigen for

- Combined Radiotherapy and Immunotherapy. *J. Med. Chem.* **59**, 2660–73 (2016).
287. Murelli, R. P., Zhang, A. X., Michel, J., Jorgensen, W. L. & Spiegel, D. A. Chemical control over immune recognition: a class of antibody-recruiting small molecules that target prostate cancer. *J. Am. Chem. Soc.* **131**, 17090–2 (2009).
  288. Lamb, B. M. & Yousaf, M. N. Redox-Switchable Surface for Controlling Peptide Structure. *J. Am. Chem. Soc.* **133**, 8870–8873 (2011).
  289. Elahipanah, S. et al. Rewiring Gram-Negative Bacteria Cell Surfaces with Bio-Orthogonal Chemistry via Liposome Fusion. *Bioconjug. Chem.* **27**, 1082–1089 (2016).
  290. Ducry, L. & Stump, B. Antibody–Drug Conjugates: Linking Cytotoxic Payloads to Monoclonal Antibodies. *Bioconjug. Chem.* **21**, 5–13 (2010).
  291. Heydarkhan-Hagvall, S. et al. Three-dimensional electrospun ECM-based hybrid scaffolds for cardiovascular tissue engineering. *Biomaterials* **29**, 2907–2914 (2008).
  292. Horch, R. E., Kopp, J., Kneser, U., Beier, J. & Bach, A. D. Tissue engineering of cultured skin substitutes. *J. Cell. Mol. Med.* **9**, 592–608 (2005).
  293. Santos, M. I. et al. Endothelial cell colonization and angiogenic potential of combined nano- and micro-fibrous scaffolds for bone tissue engineering. *Biomaterials* **29**, 4306–4313 (2008).
  294. Agarwal, P. & Bertozzi, C. R. Site-Specific Antibody–Drug Conjugates: The Nexus of Bioorthogonal Chemistry, Protein Engineering, and Drug Development. *Bioconjug. Chem.* **26**, 176–192 (2015).
  295. Wang, Q. et al. Bioconjugation by Copper(I)-Catalyzed Azide-Alkyne [3 + 2] Cycloaddition. *J. Am. Chem. Soc.* **125**, 3192–3193 (2003).
  296. Hoffman, A. S. & Stayton, P. S. Bioconjugates of smart polymers and proteins: synthesis and applications. *Macromol. Symp.* **207**, 139–152 (2004).
  297. Raindllová, V., Pohl, R. & Hocek, M. Synthesis of Aldehyde-Linked Nucleotides and DNA and Their Bioconjugations with Lysine and Peptides through Reductive Amination. *Chem. Eur. J.* **18**, 4080–4087 (2012).
  298. Rogozhnikov, D., Luo, W., Elahipanah, S., O'Brien, P. J. & Yousaf, M. N. Generation of a Scaffold-Free Three-Dimensional Liver Tissue via a Rapid Cell-to-Cell Click Assembly Process. *Bioconjug. Chem.* **27**, 1991–1998 (2016).
  299. Rogozhnikov, D. et al. Scaffold Free Bio-orthogonal Assembly of 3-Dimensional Cardiac Tissue via Cell Surface Engineering. *Sci. Rep.* **6**, 39806 (2016).
  300. Massia, S. P. & Hubbell, J. A. Covalent surface immobilization of Arg-Gly-Asp- and Tyr-Ile-Gly-Ser-Arg-containing peptides to obtain well-defined cell-adhesive substrates. *Anal. Biochem.* **187**, 292–301 (1990).

301. Homola, J. Surface Plasmon Resonance Sensors for Detection of Chemical and Biological Species. (2008).
302. Filler, M. A. & Bent, S. F. The surface as molecular reagent: organic chemistry at the semiconductor interface. *Prog. Surf. Sci.* **73**, 1–56 (2003).
303. Ma, Z. & Zaera, F. Organic chemistry on solid surfaces. *Surf. Sci. Rep.* **61**, 229–281 (2006).
304. Fowkes, F. M. Determination Of Interfacial Tensions, Contact Angles, And Dispersion Forces In Surfaces By Assuming Additivity Of Intermolecular Interactions In Surfaces. *J. Phys. Chem.* **66**, 382–382 (1962).
305. Onda, T., Shibuichi, S., Satoh, N. & Tsujii, K. Super-Water-Repellent Fractal Surfaces. *Langmuir* **12**, 2125–2127 (1996).
306. Irwin, M. D. et al. Consequences of Anode Interfacial Layer Deletion. HCl-Treated ITO in P3HT:PCBM-Based Bulk-Heterojunction Organic Photovoltaic Devices. *Langmuir* **26**, 2584–2591 (2010).
307. Xia, Y., Sun, K. & Ouyang, J. Solution-Processed Metallic Conducting Polymer Films as Transparent Electrode of Optoelectronic Devices. *Adv. Mater.* **24**, 2436–2440 (2012).
308. Kim, H. et al. Electrical, optical, and structural properties of indium–tin–oxide thin films for organic light-emitting devices. *J. Appl. Phys.* **86**, 6451 (1999).
309. Du, J. et al. Highly transparent and conductive indium tin oxide thin films for solar cells grown by reactive thermal evaporation at low temperature. *Appl. Phys. A* **117**, 815–822 (2014).

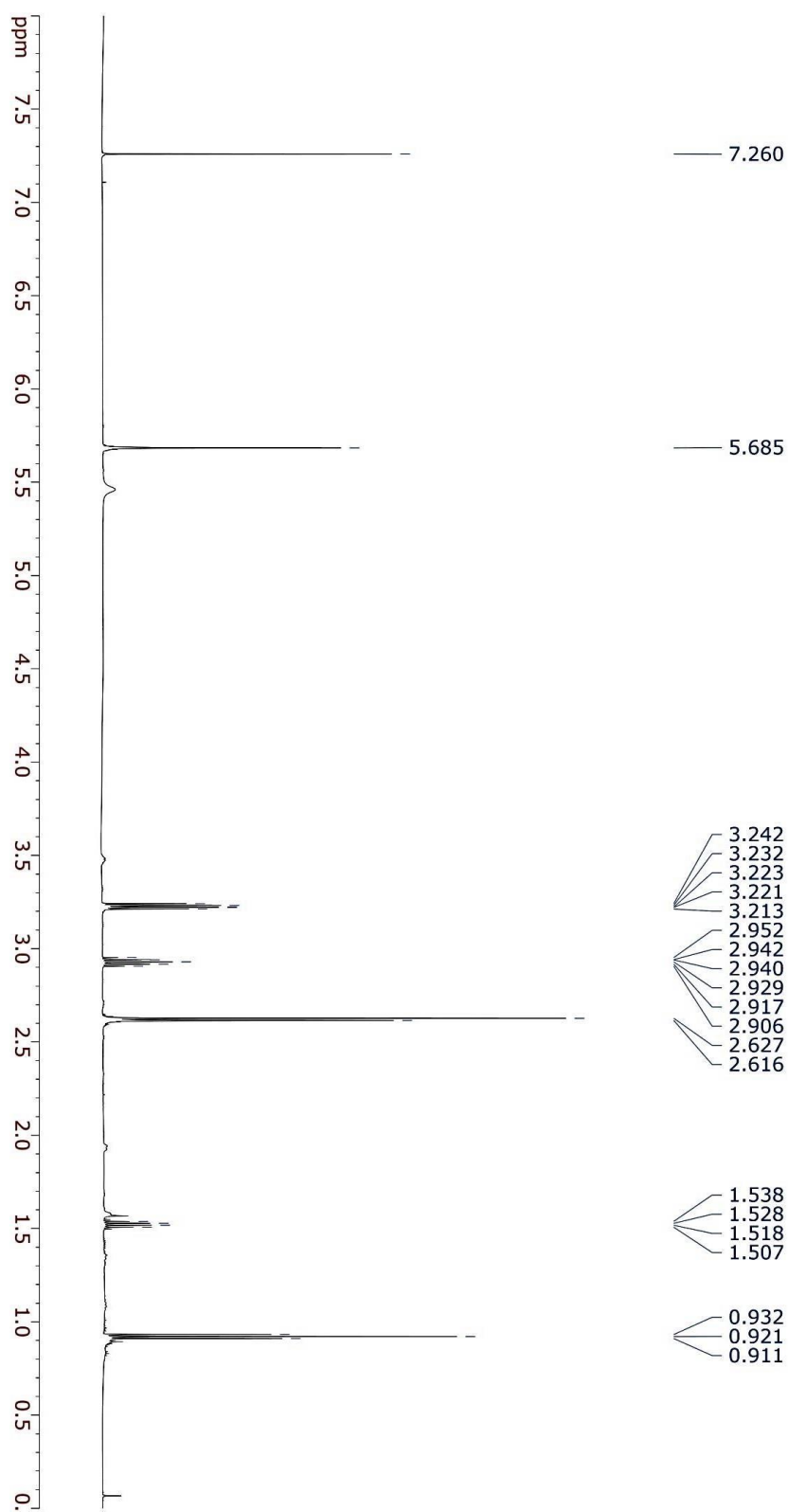
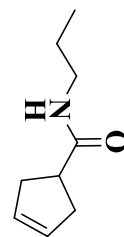
## Appendix (NMR Spectroscopy)

<sup>1</sup>H-NMR data for compound (**1**) Recorded on 300 MHz spectrometer (CDCl<sub>3</sub>)

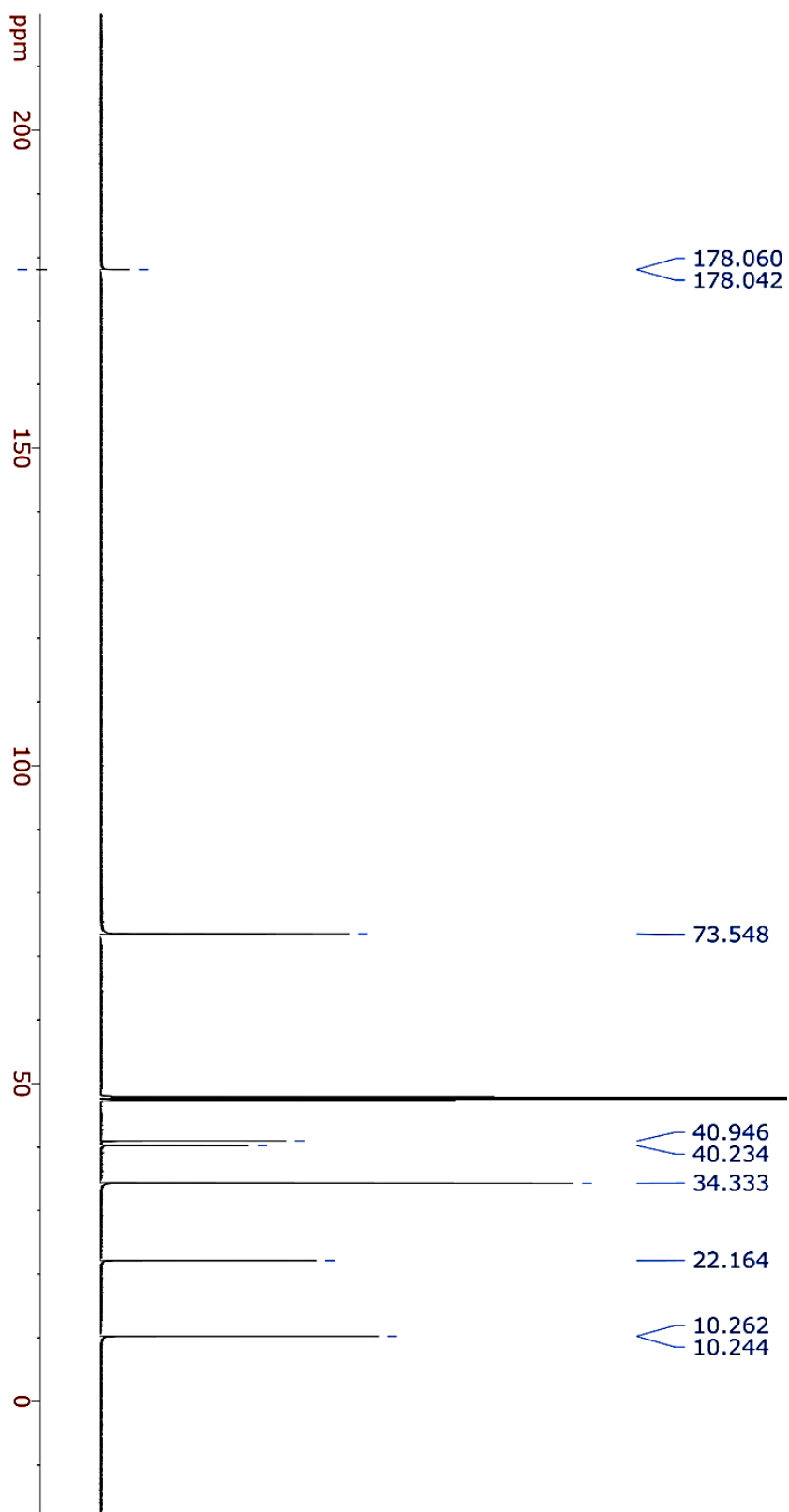
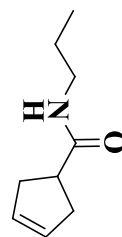




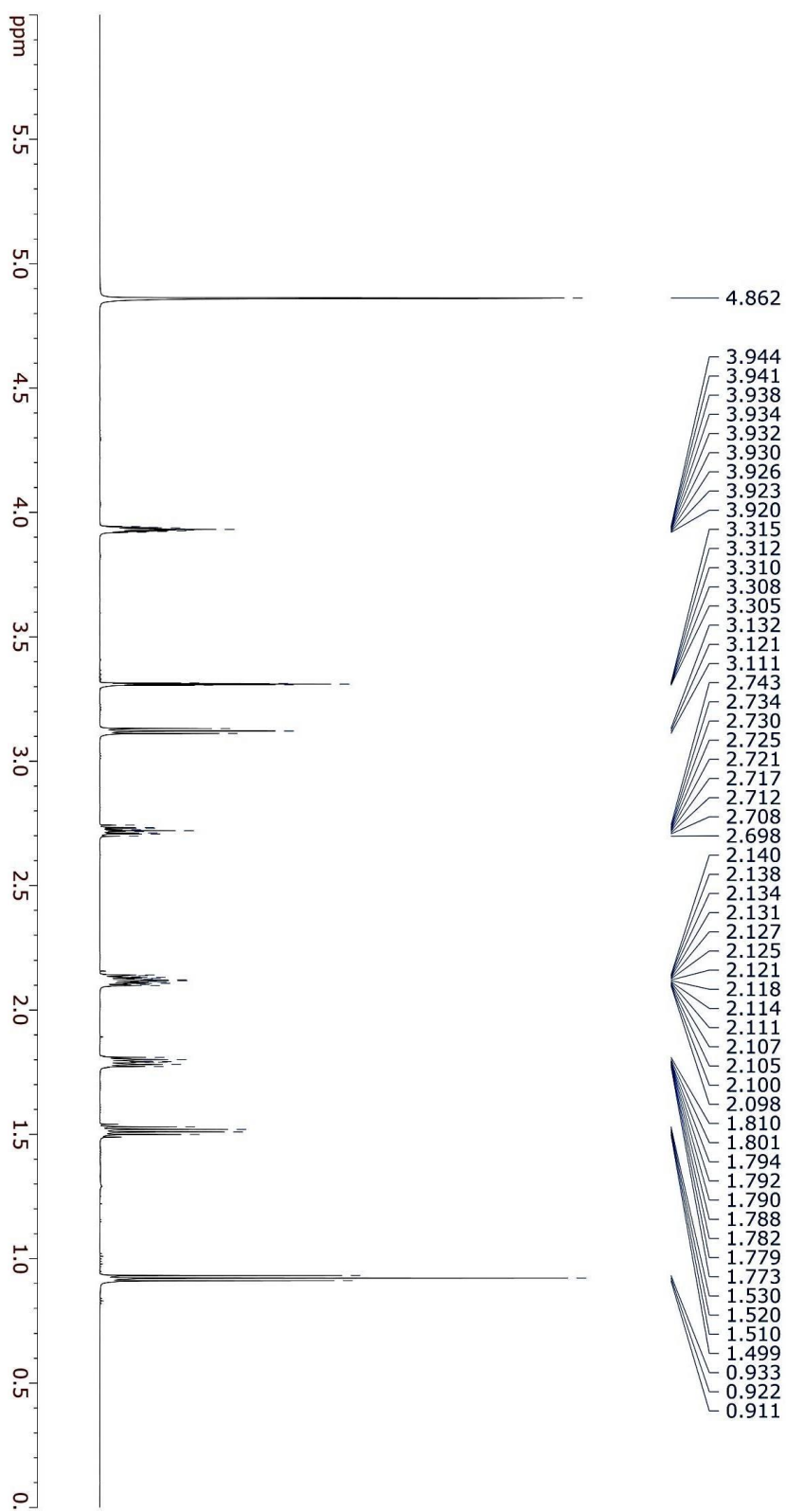
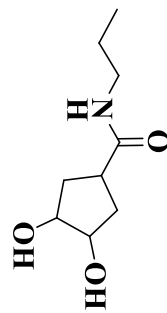
<sup>1</sup>H-NMR data for compound (**2**) Recorded on 300 MHz spectrometer (CDCl<sub>3</sub>)



$^{13}\text{C}$ -NMR data for compound (**2**) Recorded on 300 MHz spectrometer ( $\text{CDCl}_3$ )

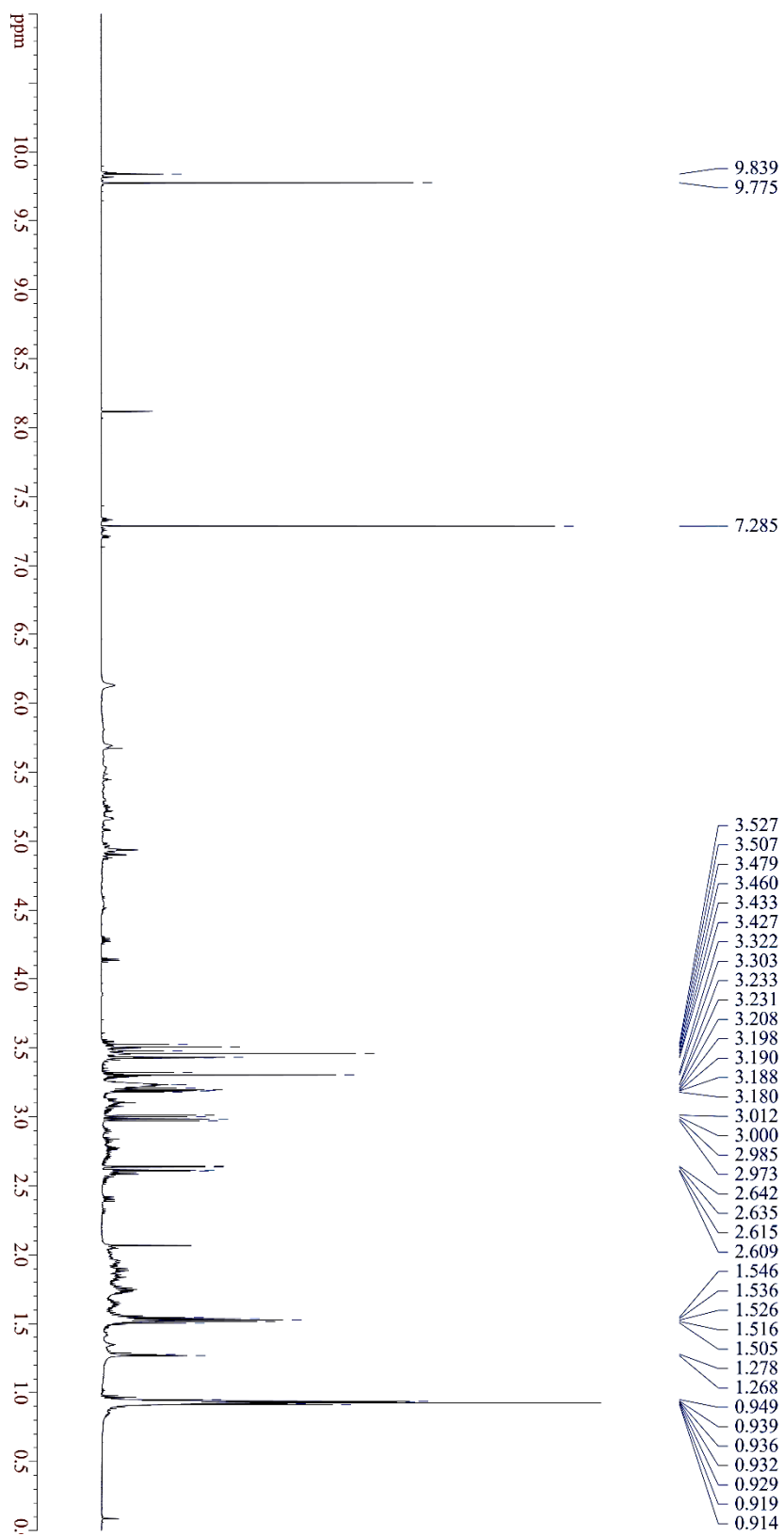
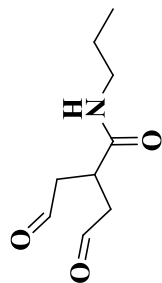


<sup>1</sup>H-NMR data for compound (3) Recorded on 700 MHz spectrometer (MeOD)



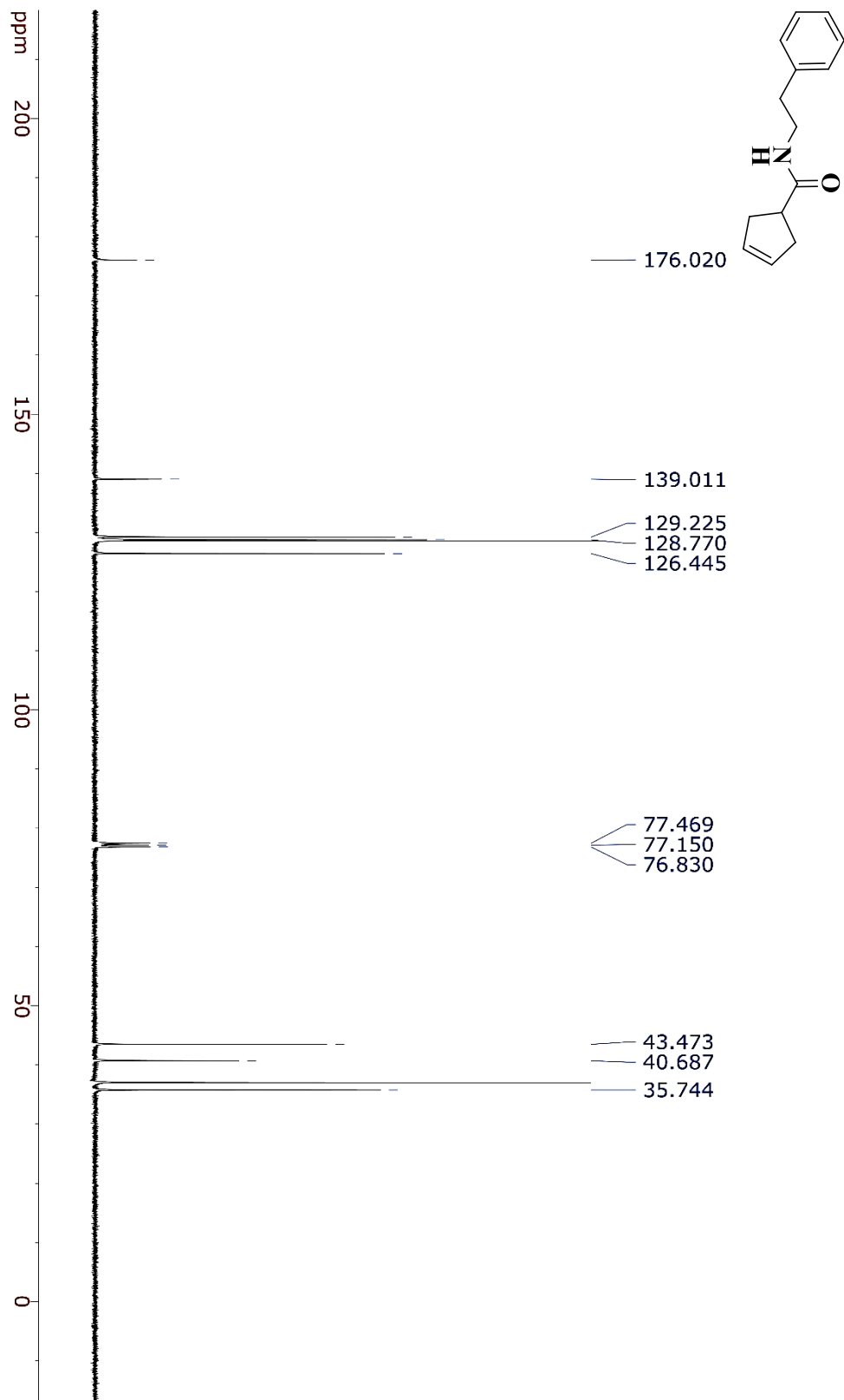


<sup>1</sup>H-NMR data for compound (4) Recorded on 700 MHz spectrometer (CDCl<sub>3</sub>)

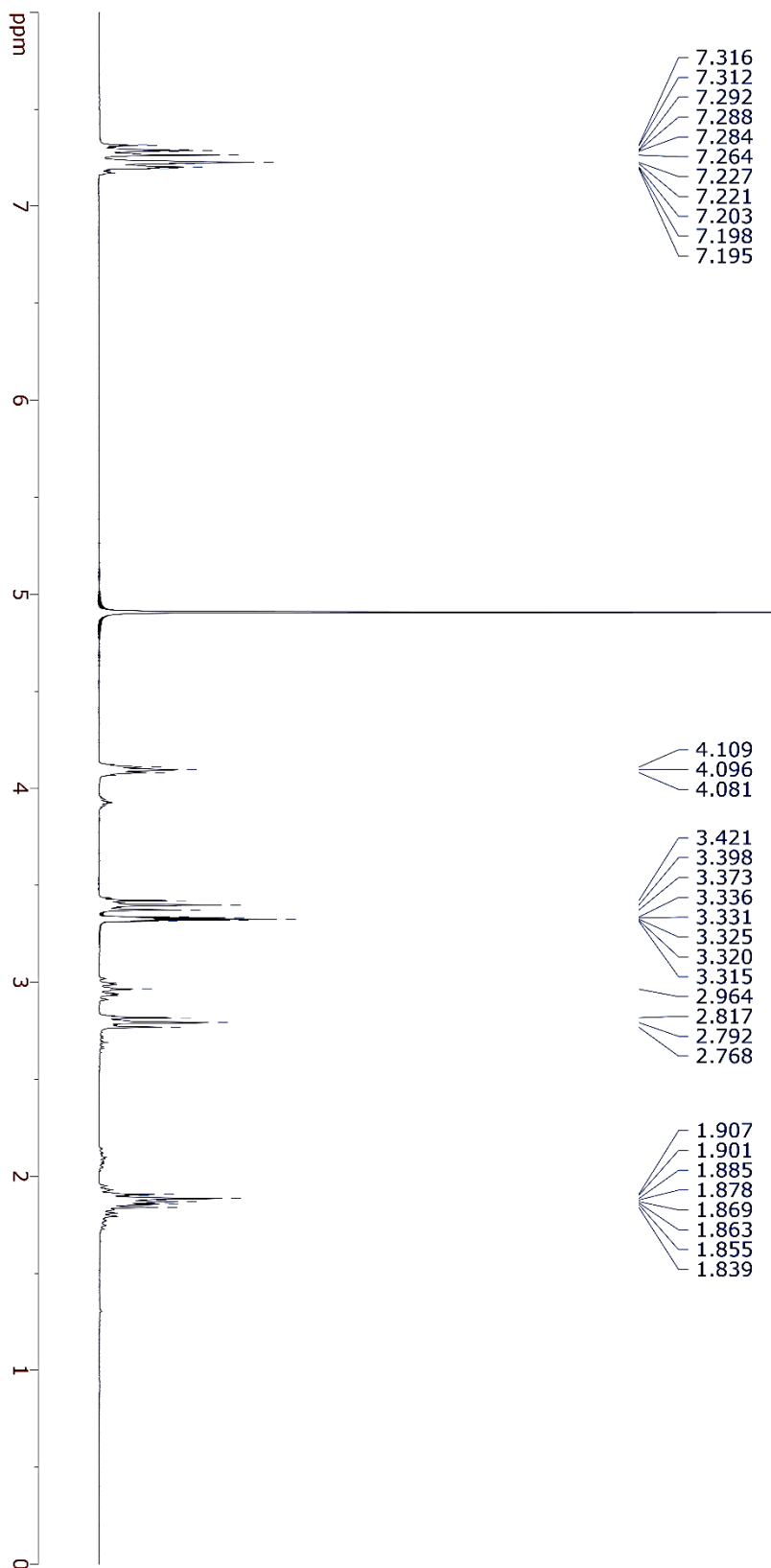
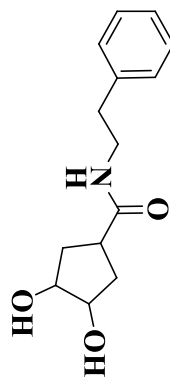




<sup>13</sup>C-NMR data for compound (**5**) Recorded on 400 MHz spectrometer (CDCl<sub>3</sub>)

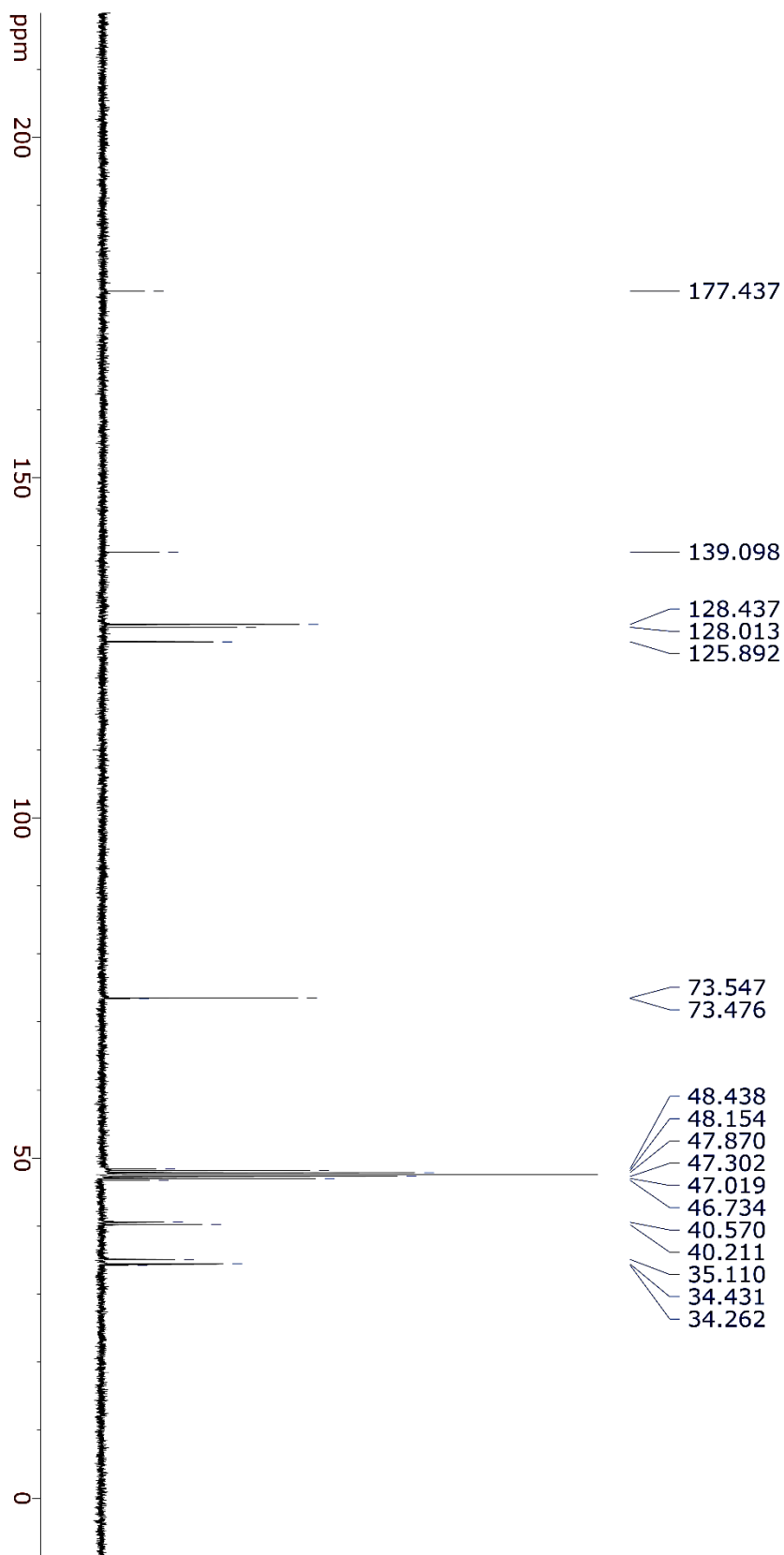
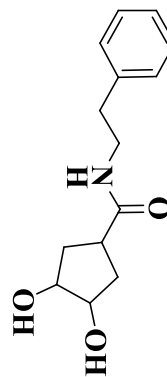


<sup>1</sup>H-NMR data for compound (**6**) Recorded on 300 MHz spectrometer (MeOD)



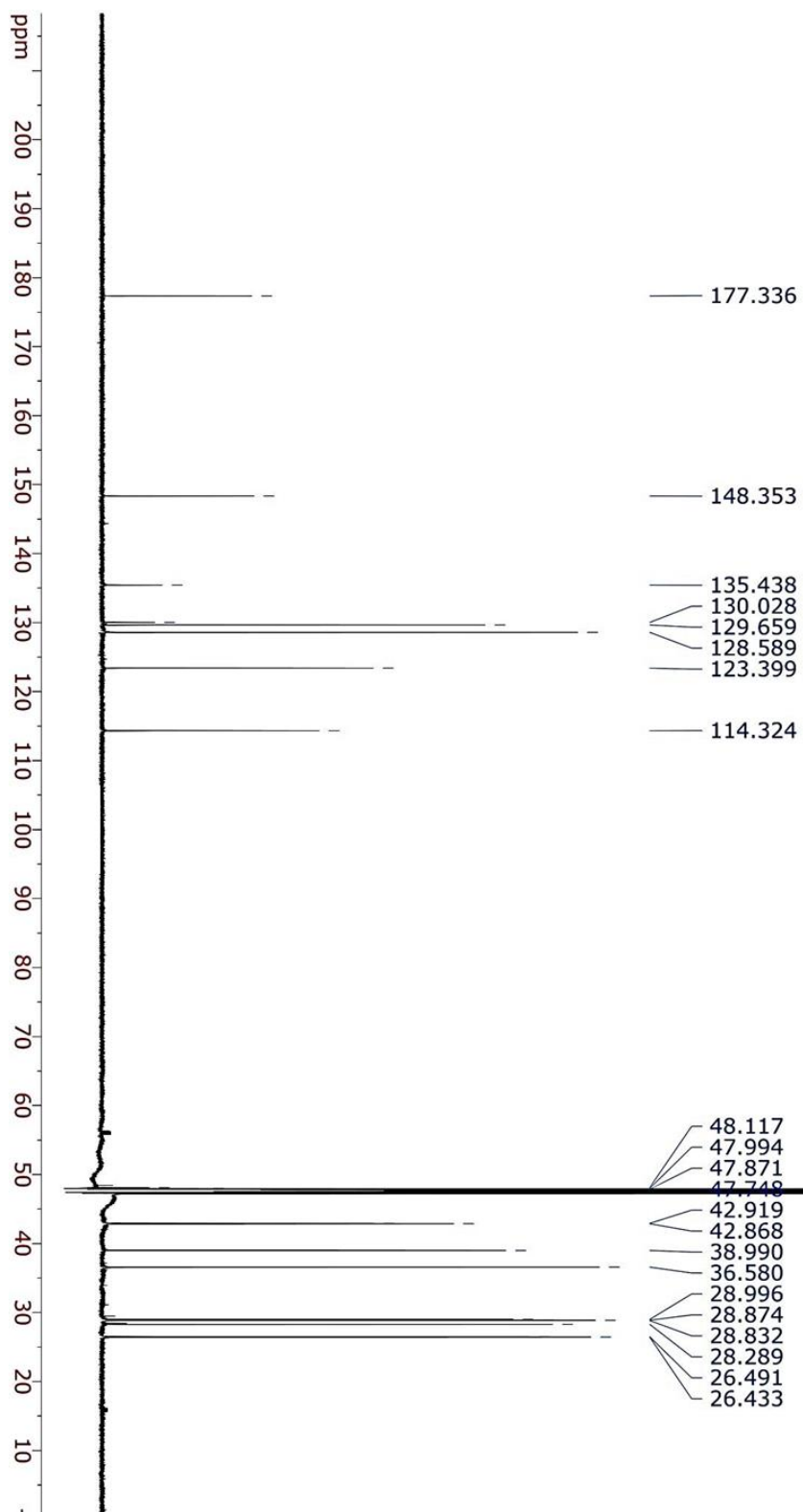
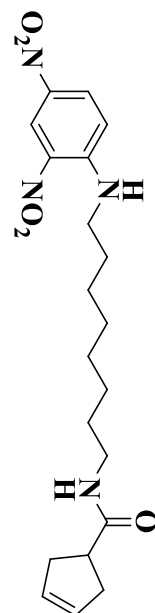


$^{13}\text{C}$ -NMR data for compound (**6**) Recorded on 300 MHz spectrometer (MeOD)





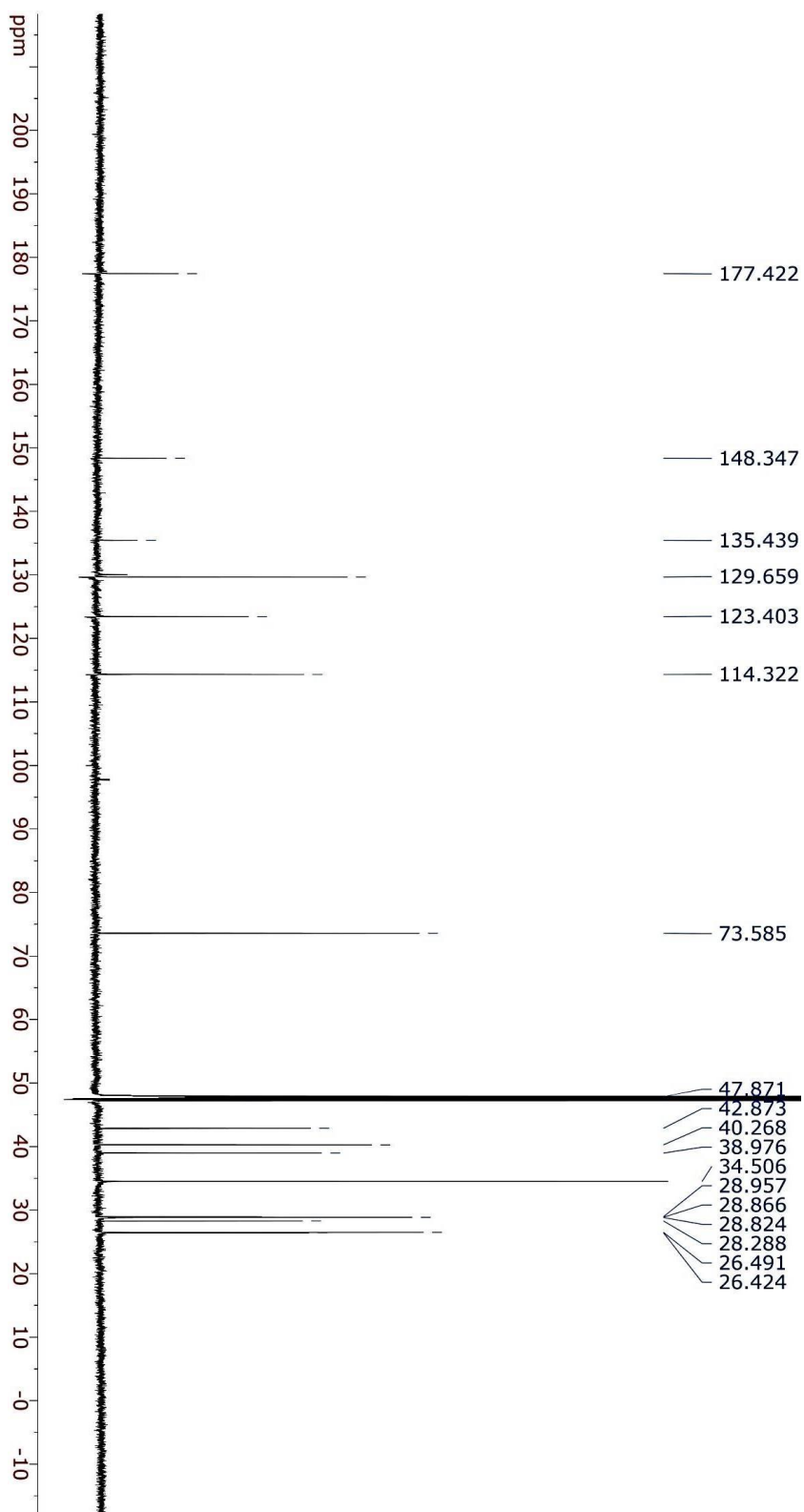
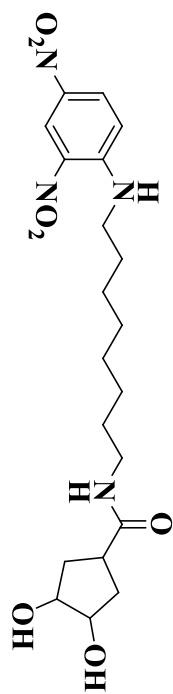
<sup>13</sup>C-NMR data for compound (8) Recorded on 700 MHz spectrometer (MeOD)





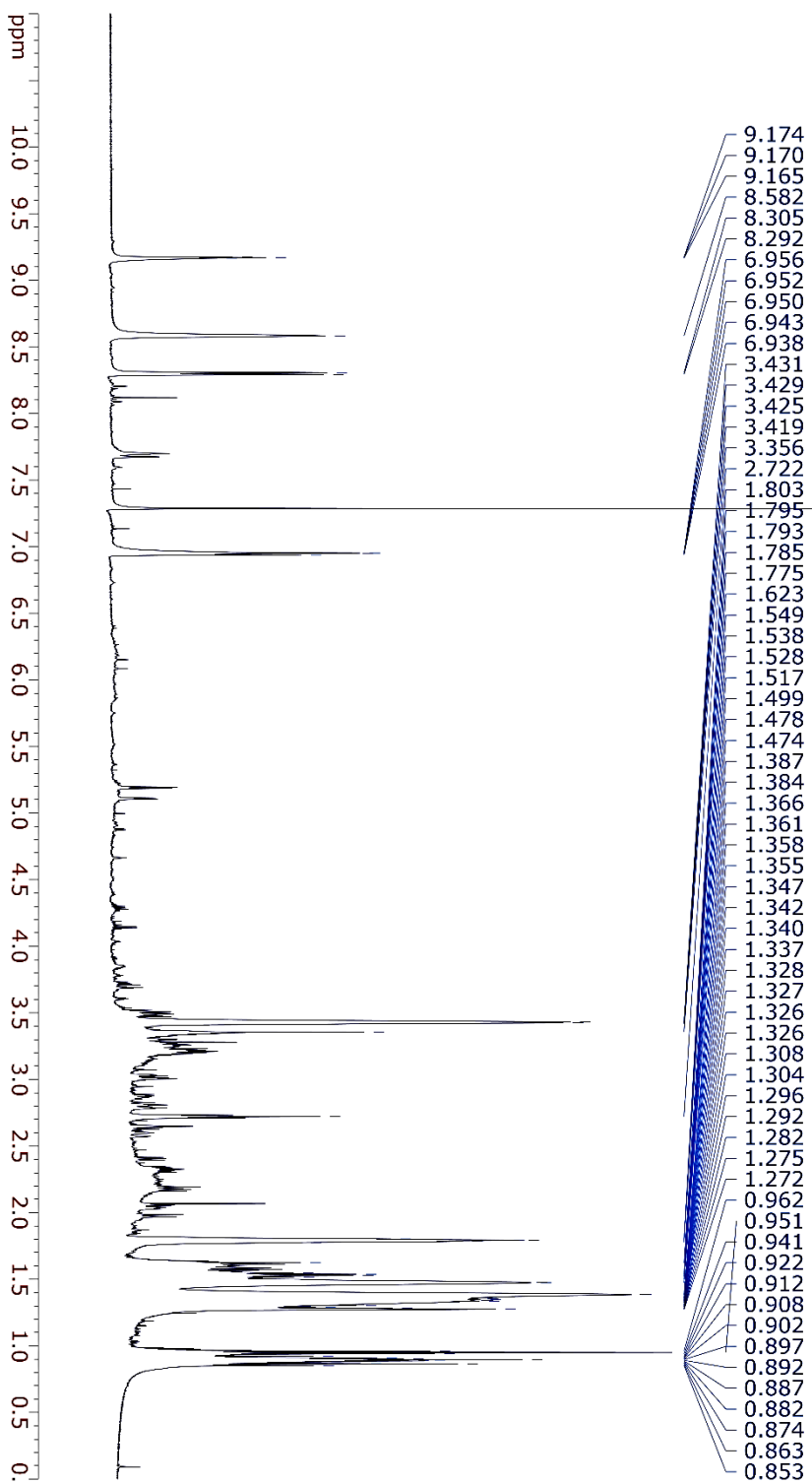
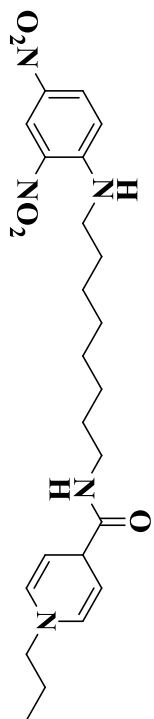


<sup>13</sup>C-NMR data for compound (9) Recorded on 700 MHz spectrometer (MeOD)



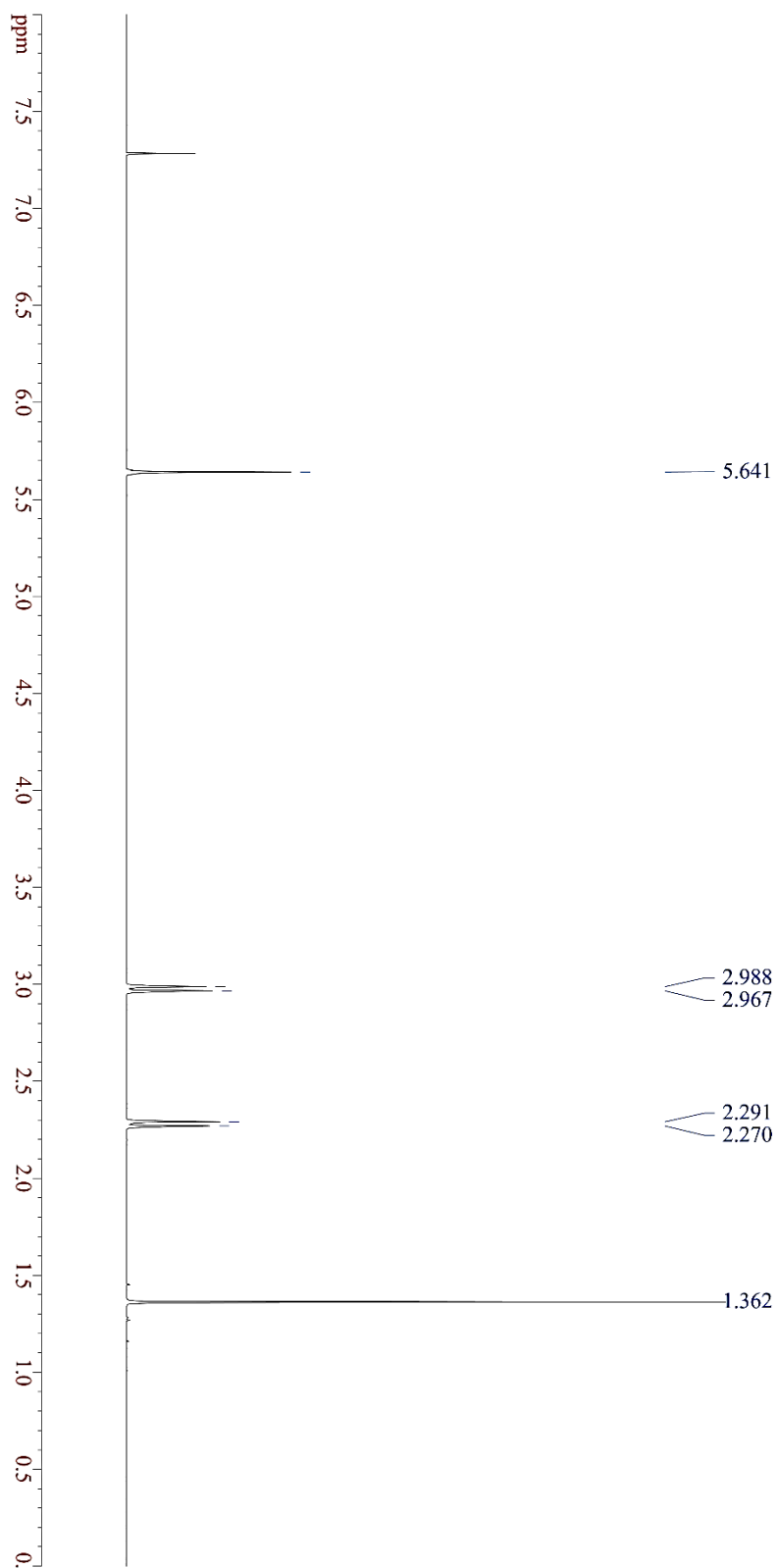
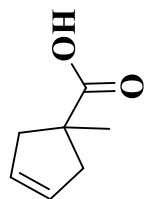


<sup>1</sup>H-NMR data for compound (Attempted Conjugation 11) Recorded on 700 MHz spectrometer

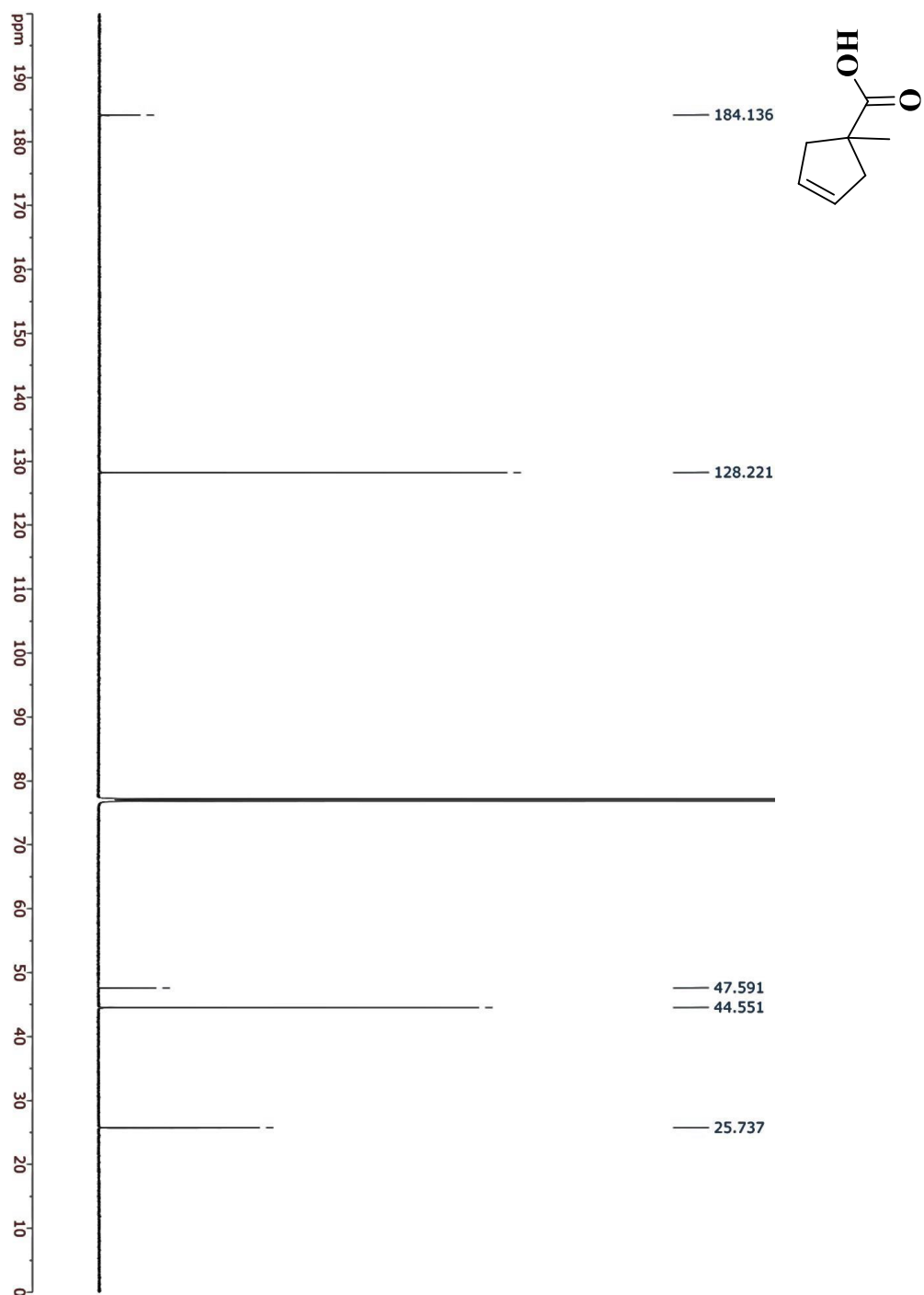




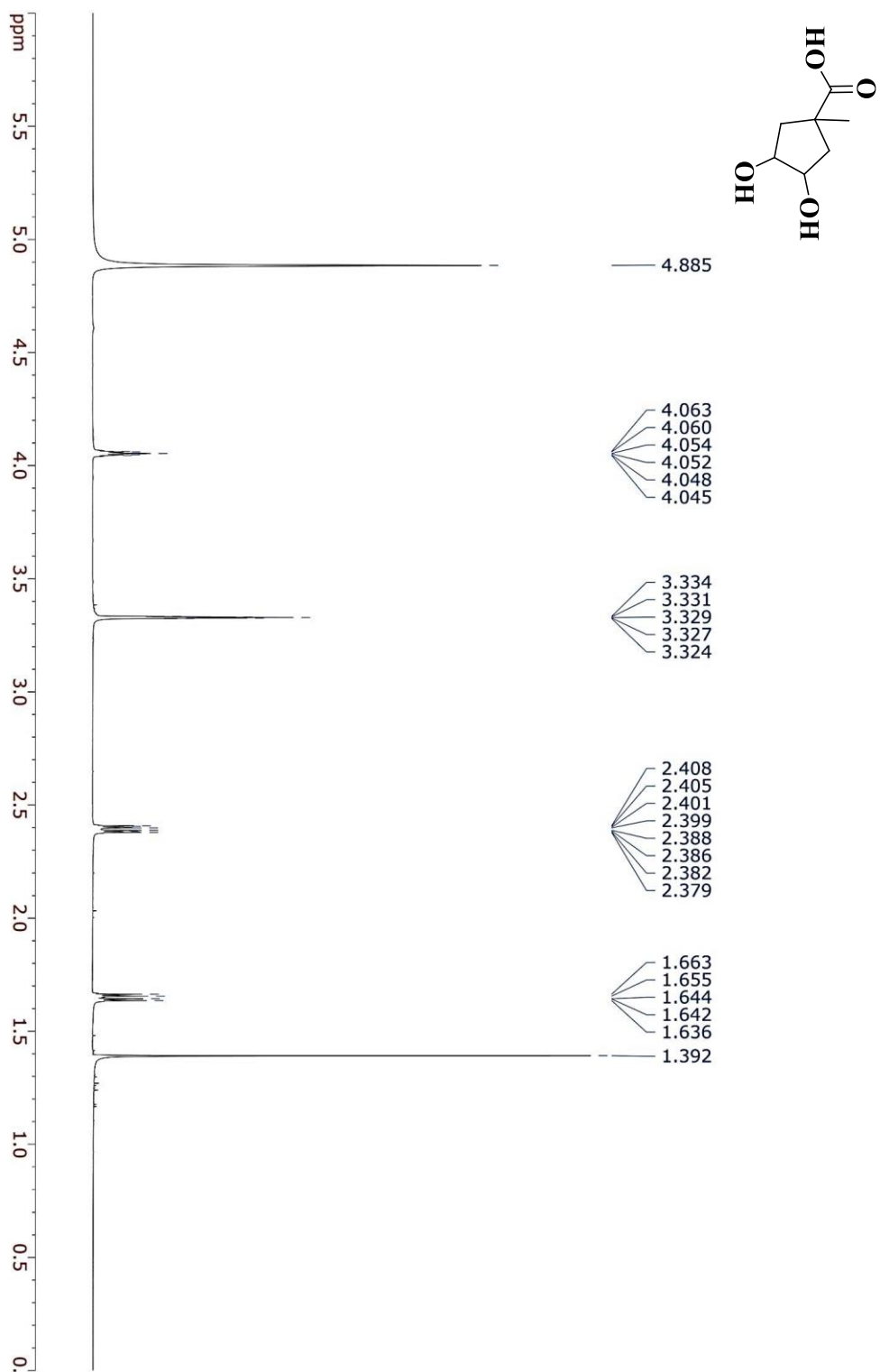
<sup>1</sup>H-NMR data for compound (**12**) Recorded on 700 MHz spectrometer (CDCl<sub>3</sub>)



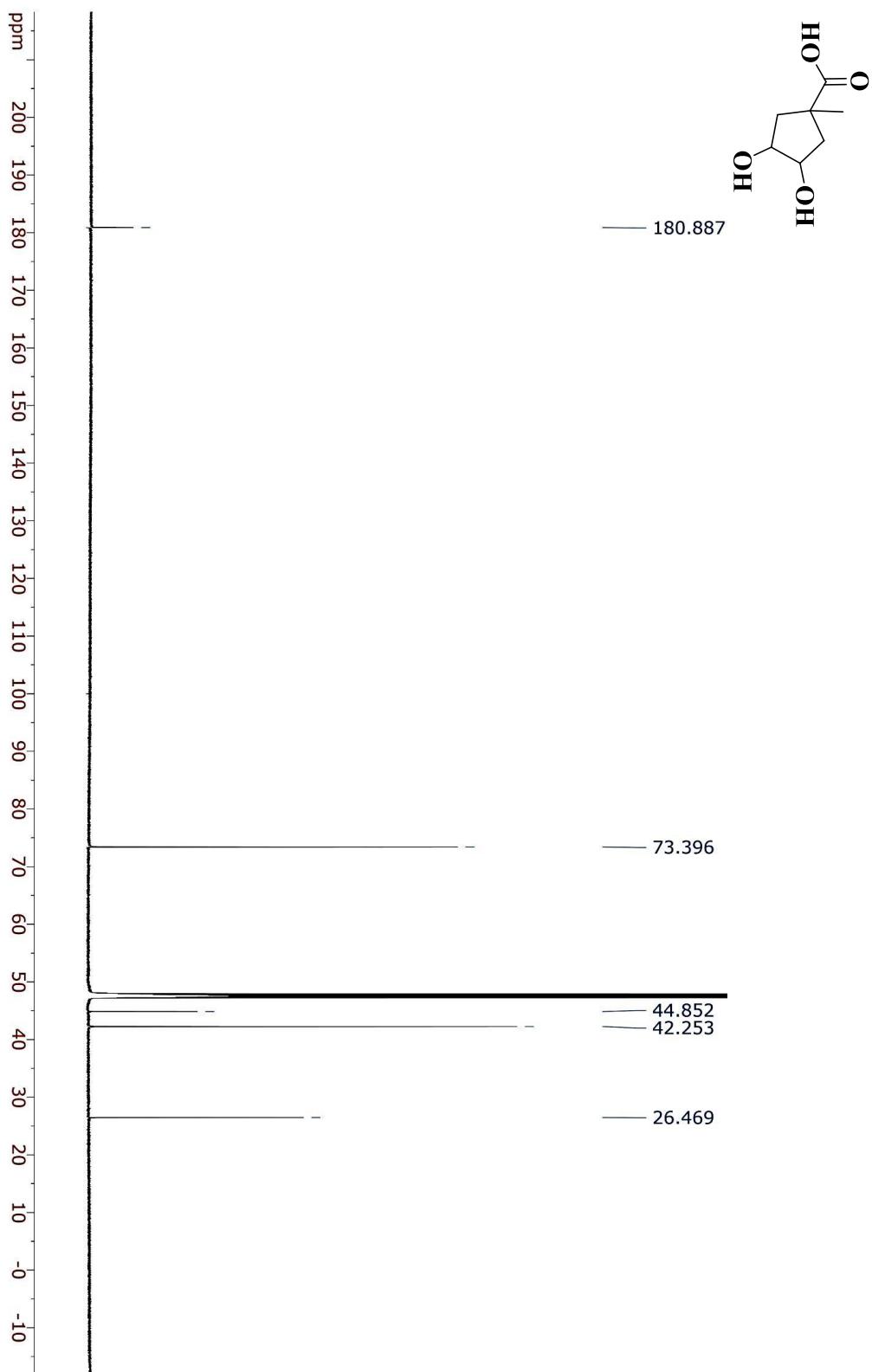
$^{13}\text{C}$ -NMR data for compound (**12**) Recorded on 700 MHz spectrometer ( $\text{CDCl}_3$ )



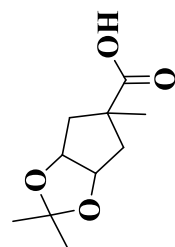
<sup>1</sup>H-NMR data for compound (**13**) Recorded on 700 MHz spectrometer (MeOD)



$^{13}\text{C}$ -NMR data for compound (**13**) Recorded on 700 MHz spectrometer (MeOD)



<sup>1</sup>H-NMR data for compound (**14**) Recorded on 700 MHz spectrometer (CDCl<sub>3</sub>)



7.260

4.743  
4.739  
4.735

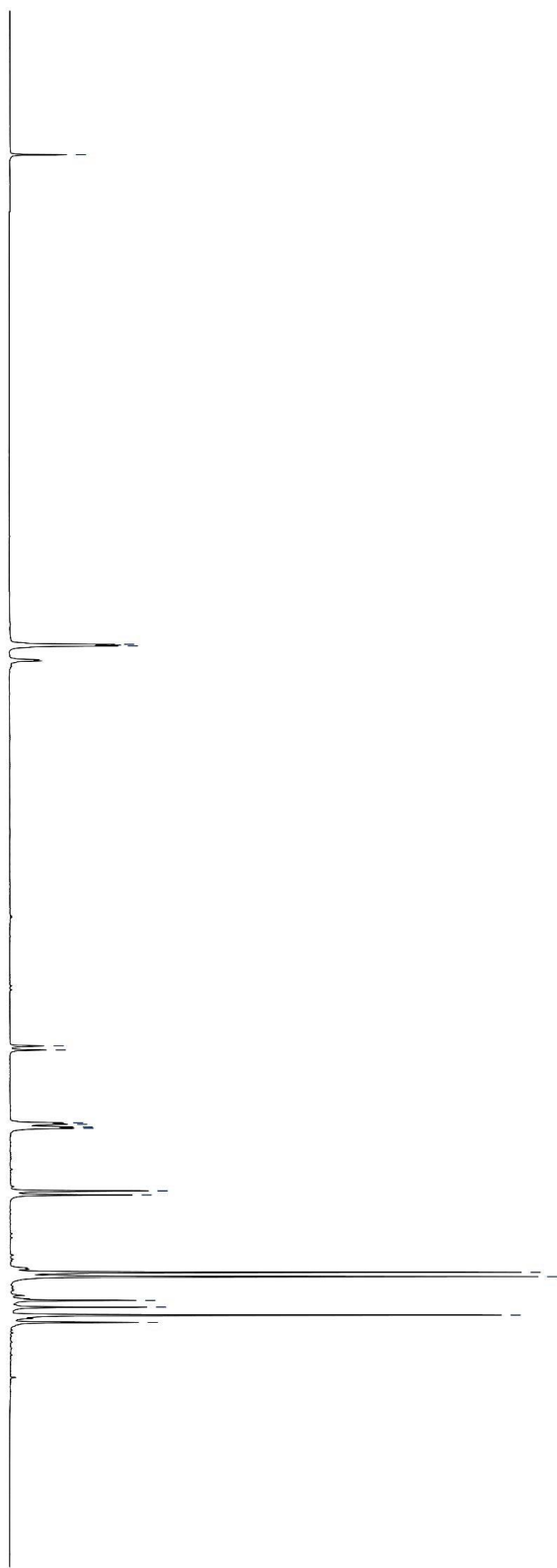
2.679  
2.658

2.284  
2.277  
2.263  
2.256

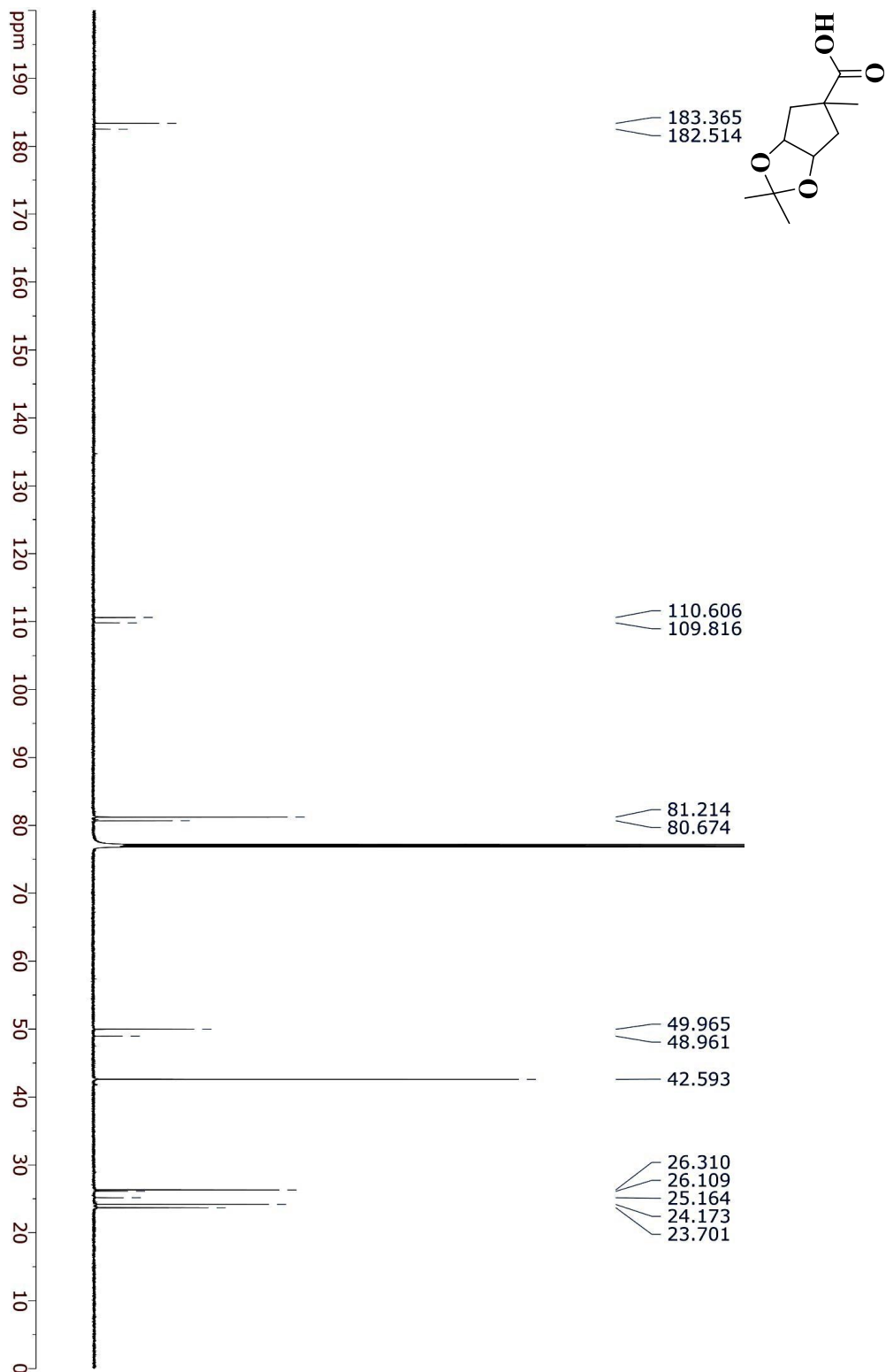
1.934  
1.913

1.516  
1.493  
1.371  
1.337  
1.296  
1.259

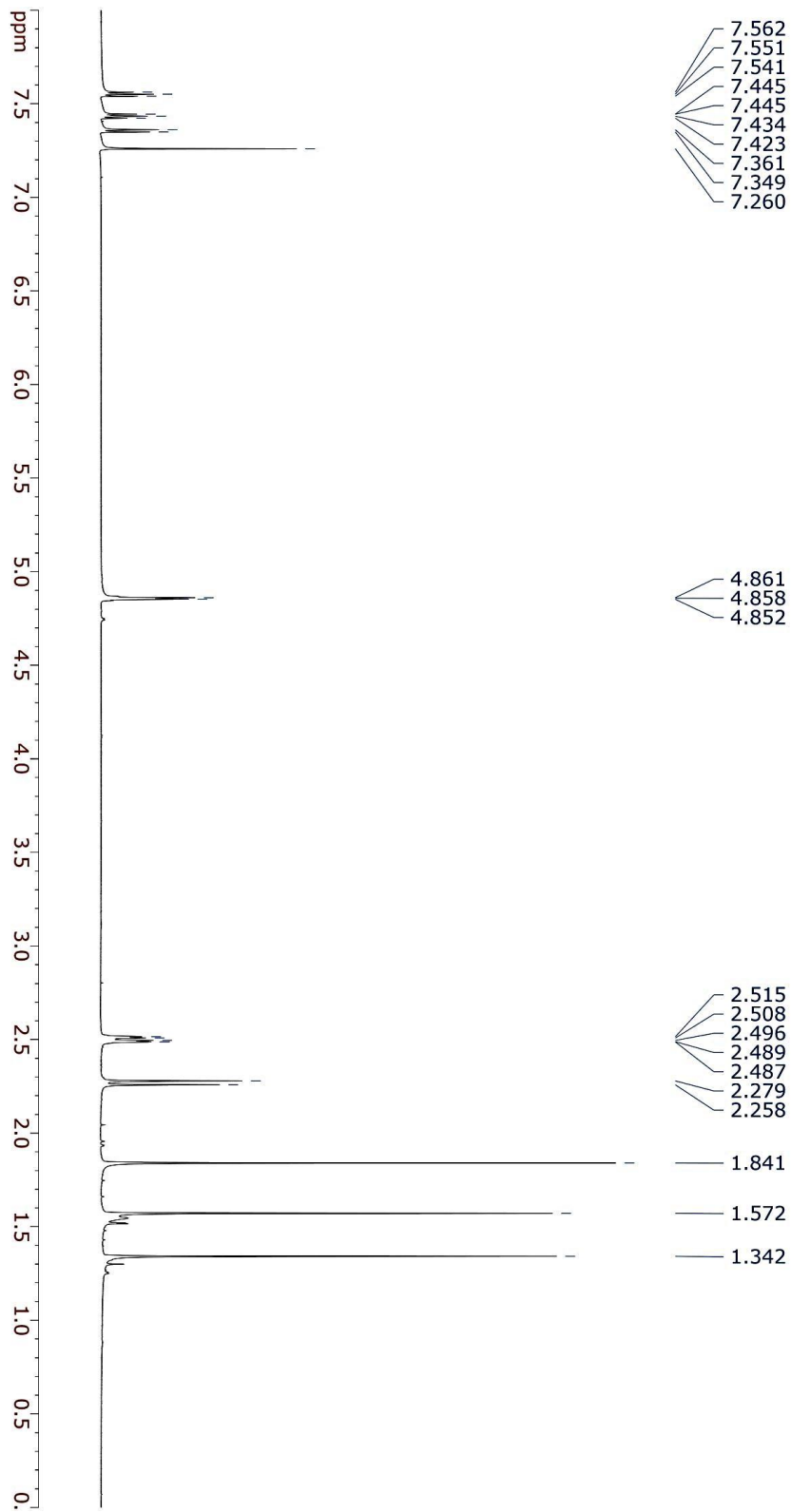
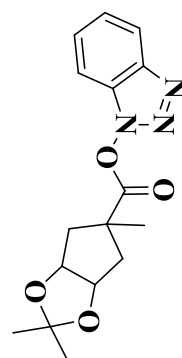
ppm 7.5 7.0 6.5 6.0 5.5 5.0 4.5 4.0 3.5 3.0 2.5 2.0 1.5 1.0 0.5 0.



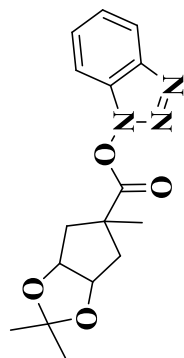
$^{13}\text{C}$ -NMR data for compound (**14**) Recorded on 700 MHz spectrometer ( $\text{CDCl}_3$ )



<sup>1</sup>H-NMR data for compound (**15**) Isomer I Recorded on 700 MHz spectrometer (CDCl<sub>3</sub>)



<sup>1</sup>H-NMR data for compound (**15**) Isomer II Recorded on 700 MHz spectrometer (CDCl<sub>3</sub>)

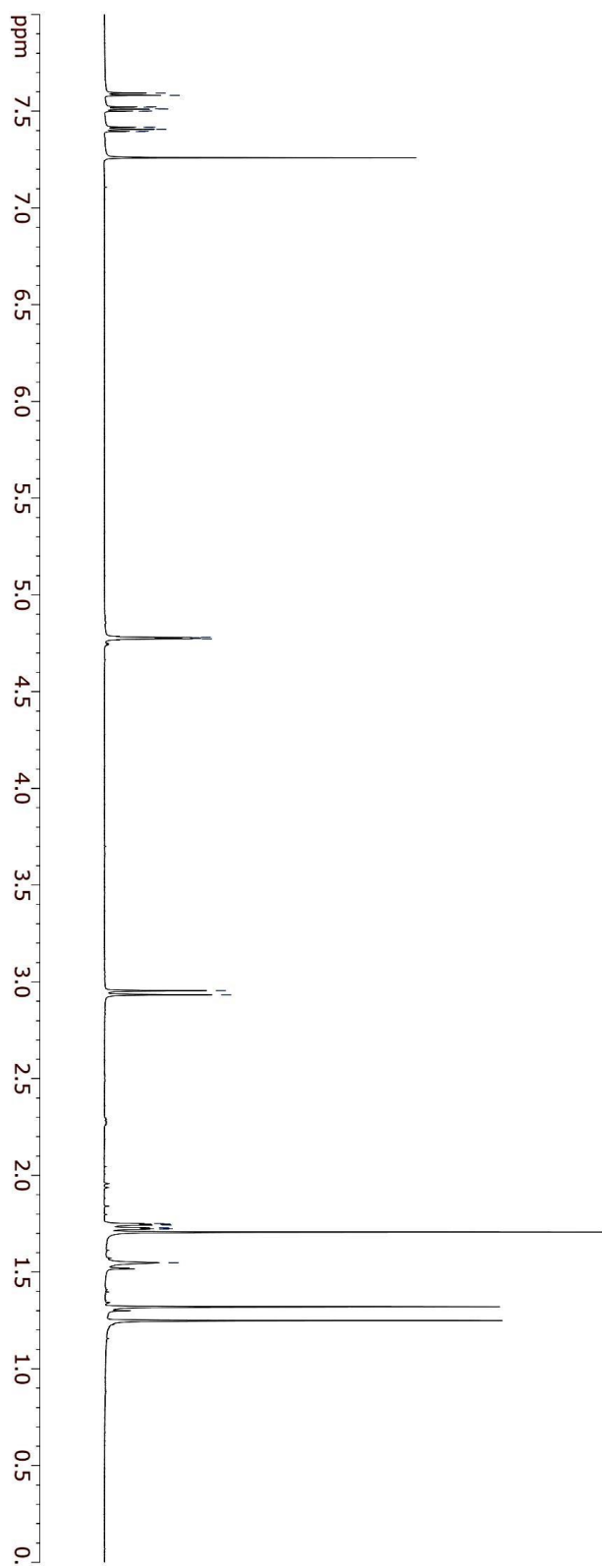


7.594  
7.582  
7.523  
7.522  
7.513  
7.511  
7.510  
7.501  
7.500  
7.419  
7.417  
7.409  
7.407  
7.405  
7.397  
7.395

4.781  
4.779  
4.775  
4.773

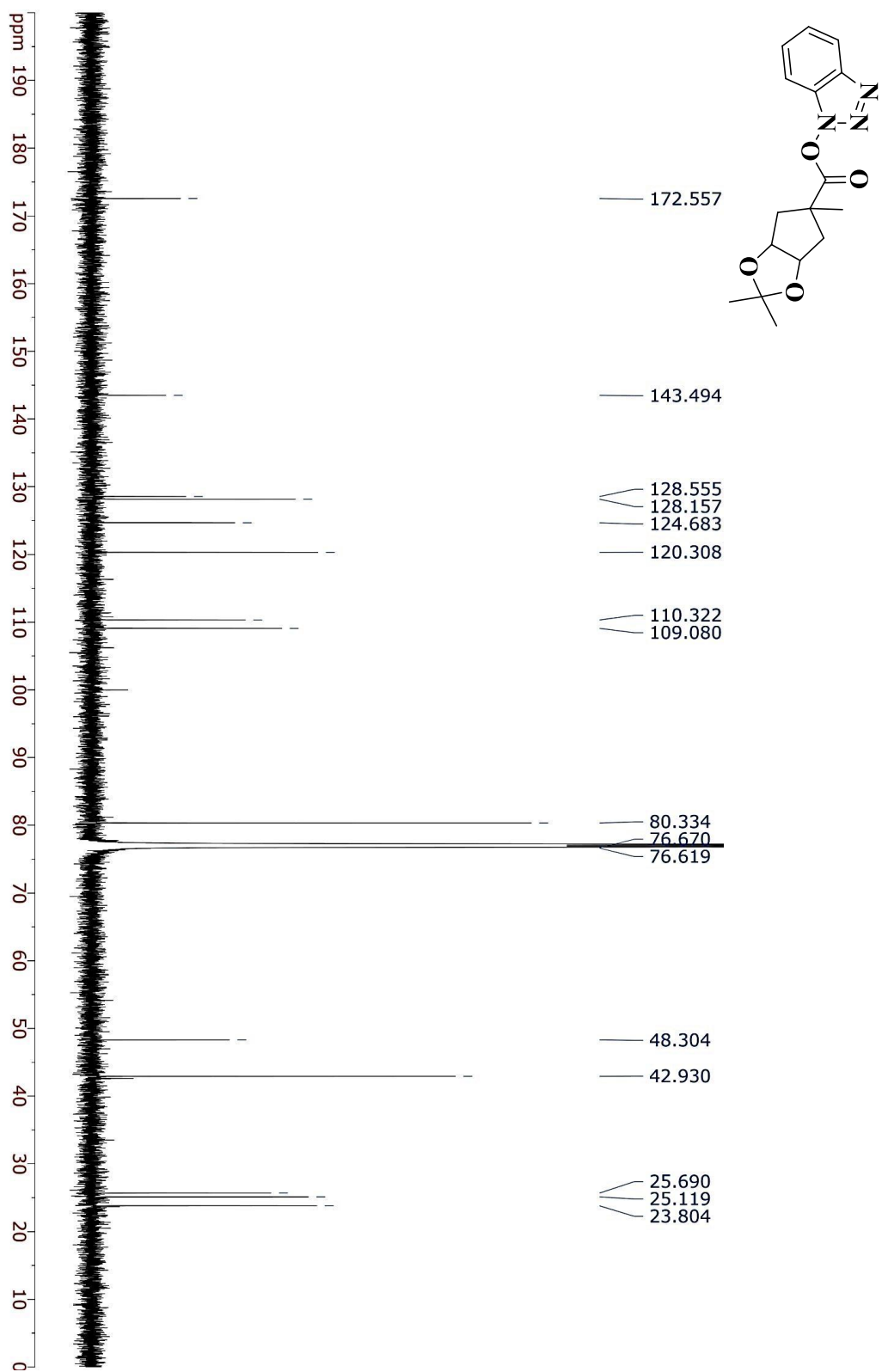
2.955  
2.933

1.751  
1.749  
1.745  
1.743  
1.729  
1.728  
1.724  
1.722  
1.548

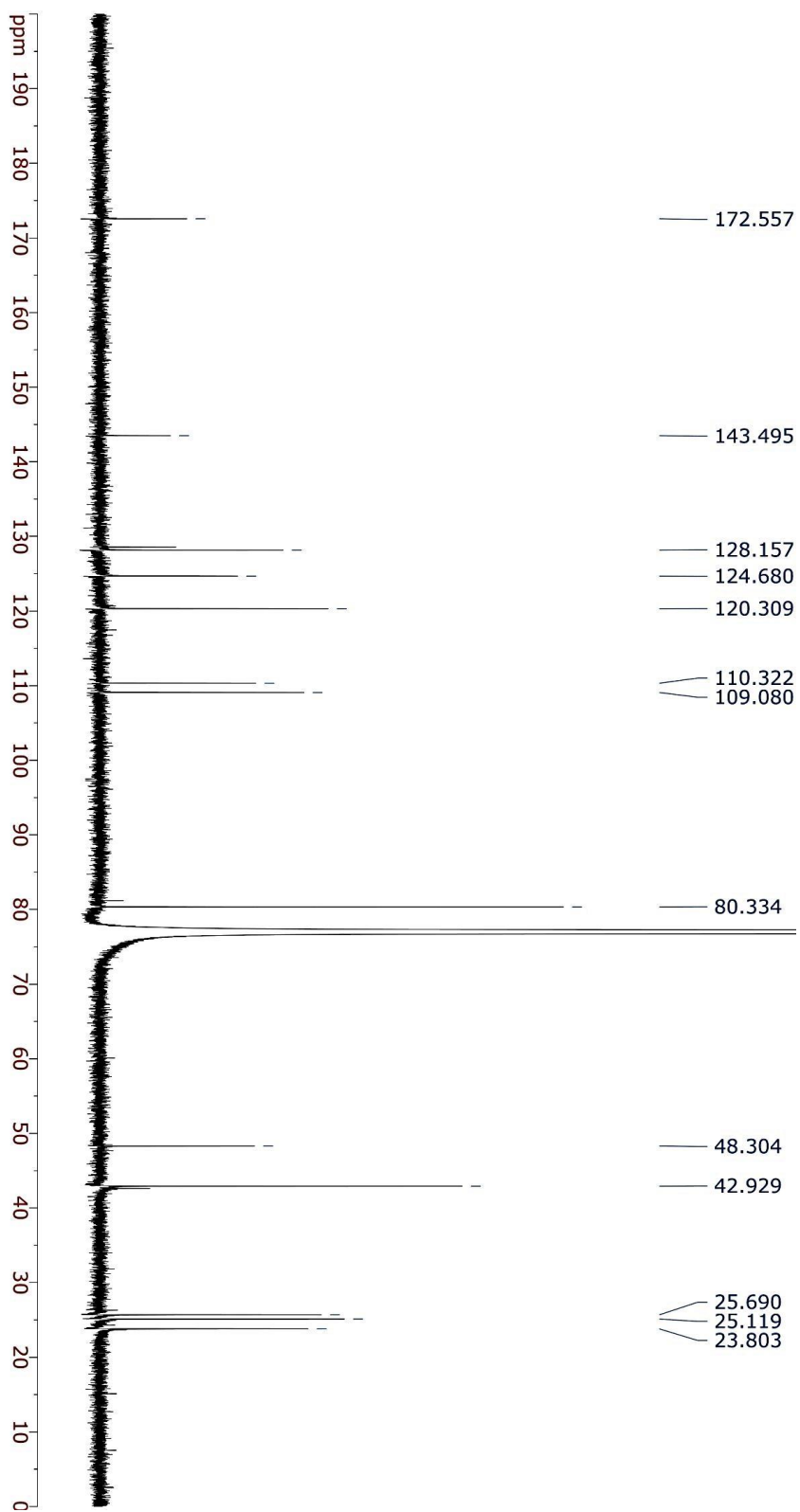
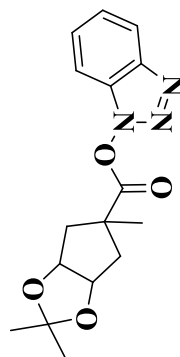




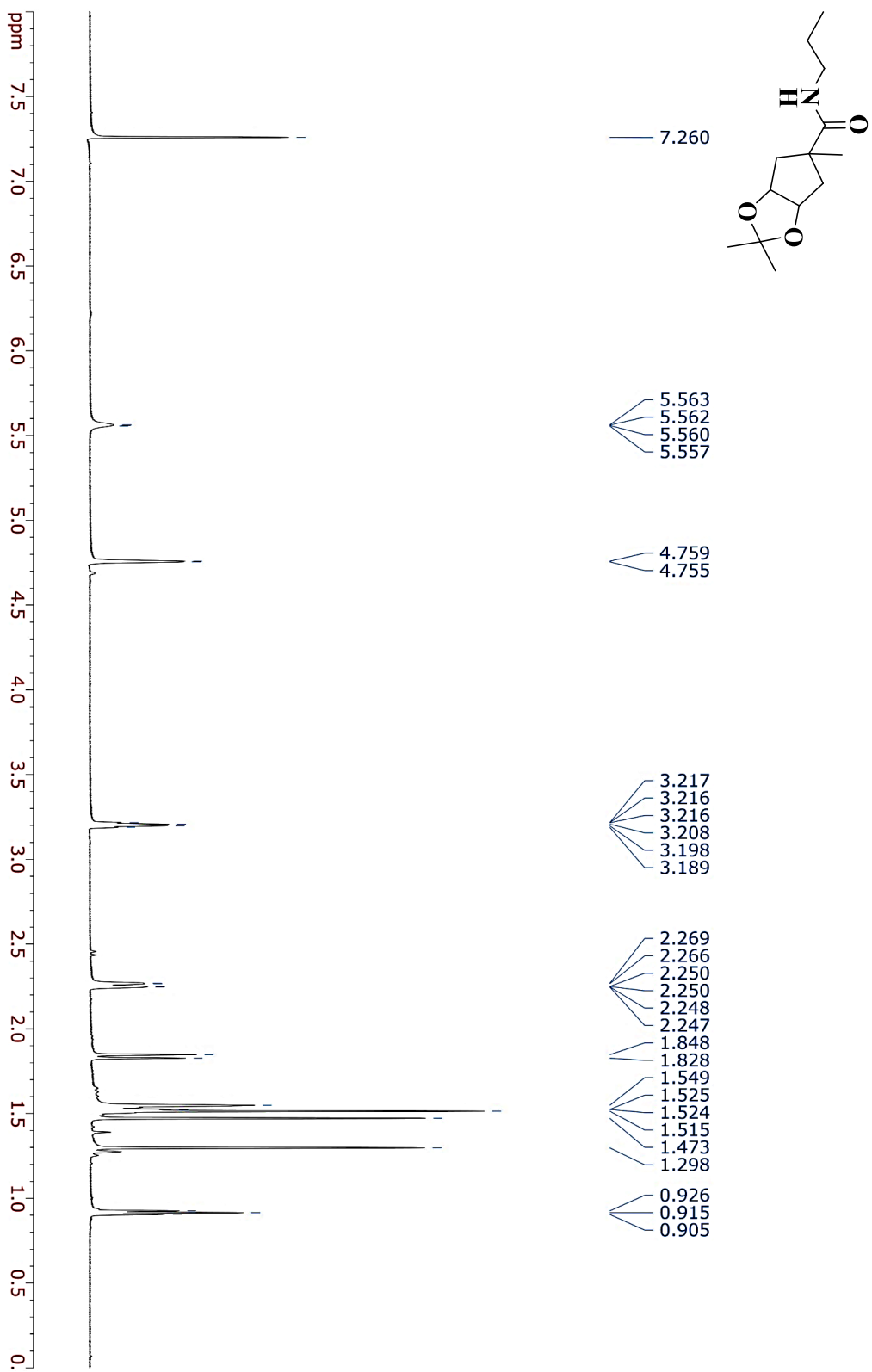
<sup>13</sup>C-NMR data for compound (**15**) Isomer I Recorded on 700 MHz spectrometer (CDCl<sub>3</sub>)



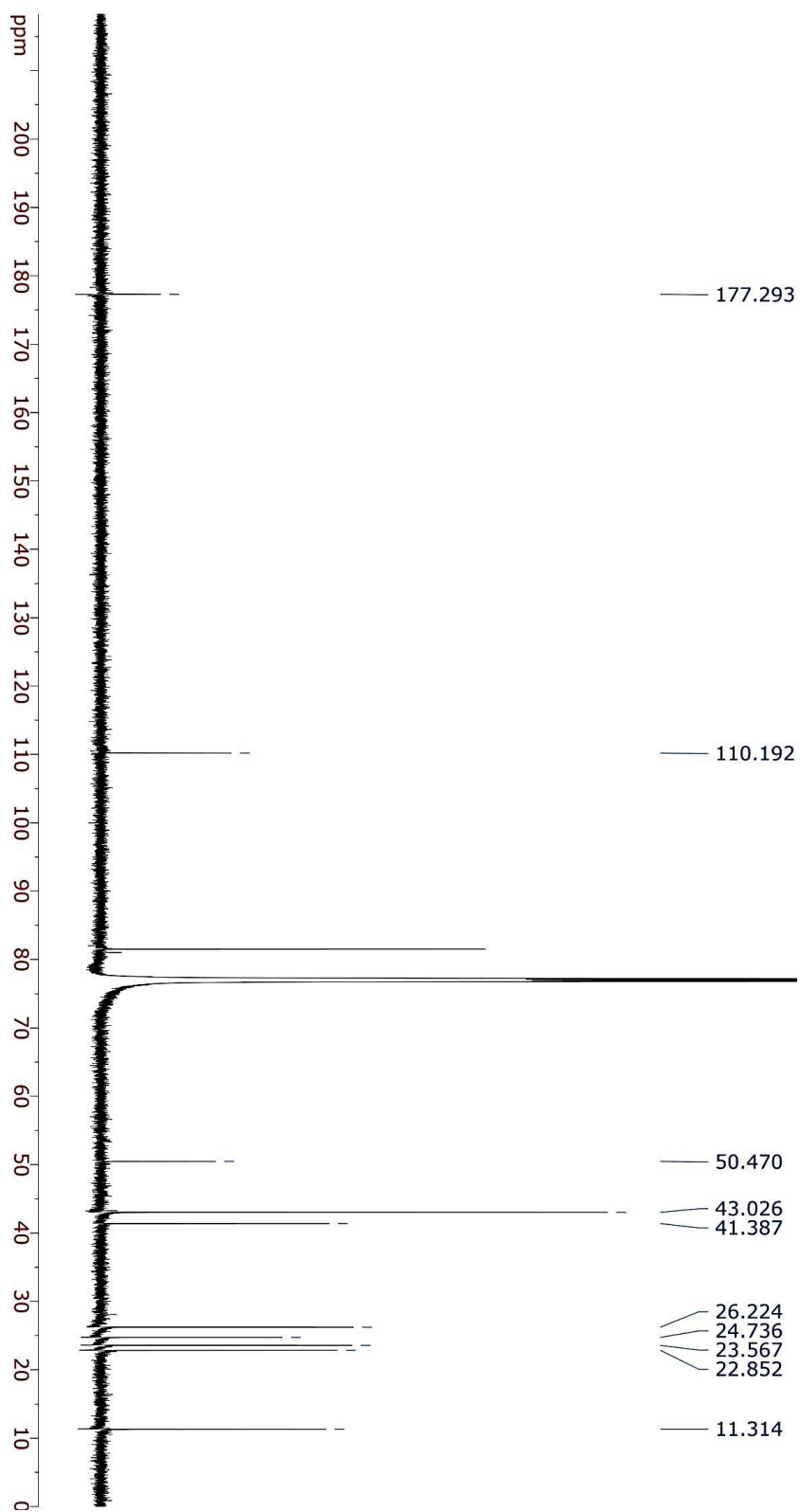
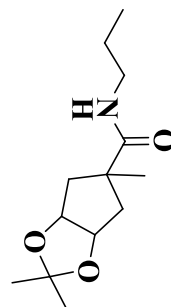
<sup>13</sup>C-NMR data for compound (**15**) Isomer II Recorded on 700 MHz spectrometer (CDCl<sub>3</sub>)



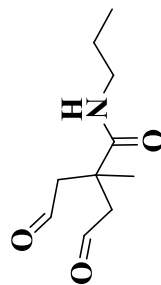
<sup>1</sup>H-NMR data for compound (**16**) Recorded on 700 MHz spectrometer (CDCl<sub>3</sub>)



$^{13}\text{C}$ -NMR data for compound (**16**) Recorded on 700 MHz spectrometer ( $\text{CDCl}_3$ )

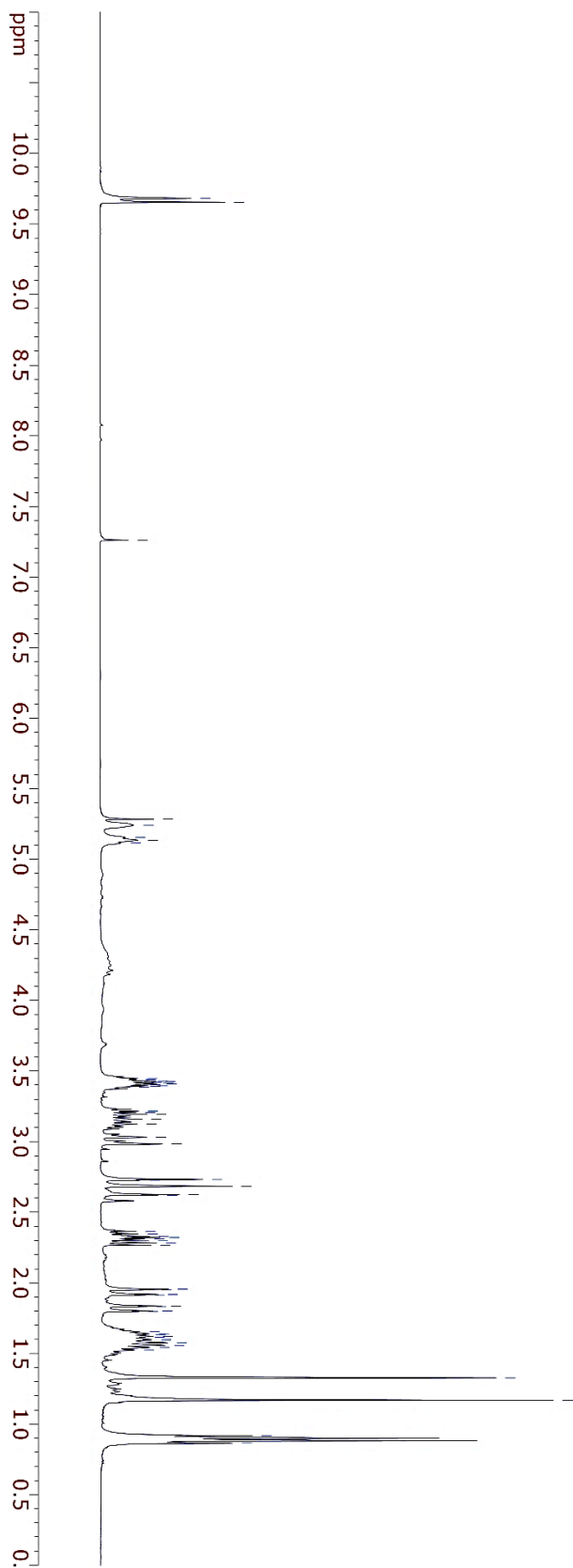


<sup>1</sup>H-NMR data for compound (**18**) Recorded on 400 MHz spectrometer (CDCl<sub>3</sub>)



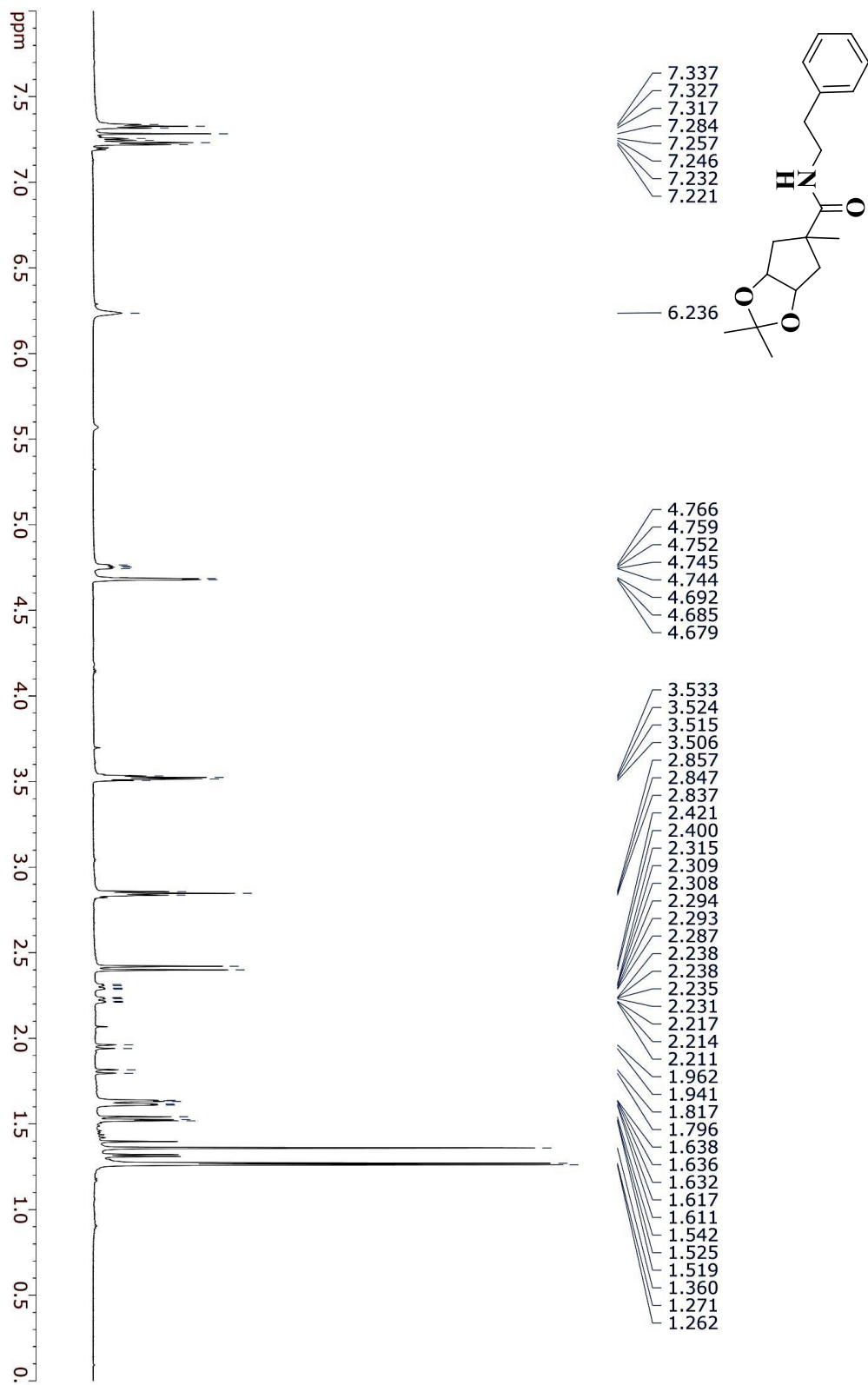
9.681  
9.654

7.260  
5.284  
5.241  
5.155  
5.135  
5.115  
3.447  
3.441  
3.436  
3.429  
3.425  
3.419  
3.413  
3.407  
3.402  
3.395  
3.391  
3.386  
3.215  
3.208  
3.195  
3.160  
3.124  
3.032  
2.984  
2.732  
2.727  
2.684  
2.625  
2.621  
2.365  
2.348  
2.330  
2.321  
2.313  
2.302  
2.284  
2.266  
1.955  
1.950  
1.919  
1.913  
1.836  
1.832  
1.802  
1.797  
1.653  
1.640  
1.634  
1.621  
1.613  
1.600  
1.594  
1.576  
1.558  
1.542  
1.524  
1.327  
1.167  
0.917  
0.863

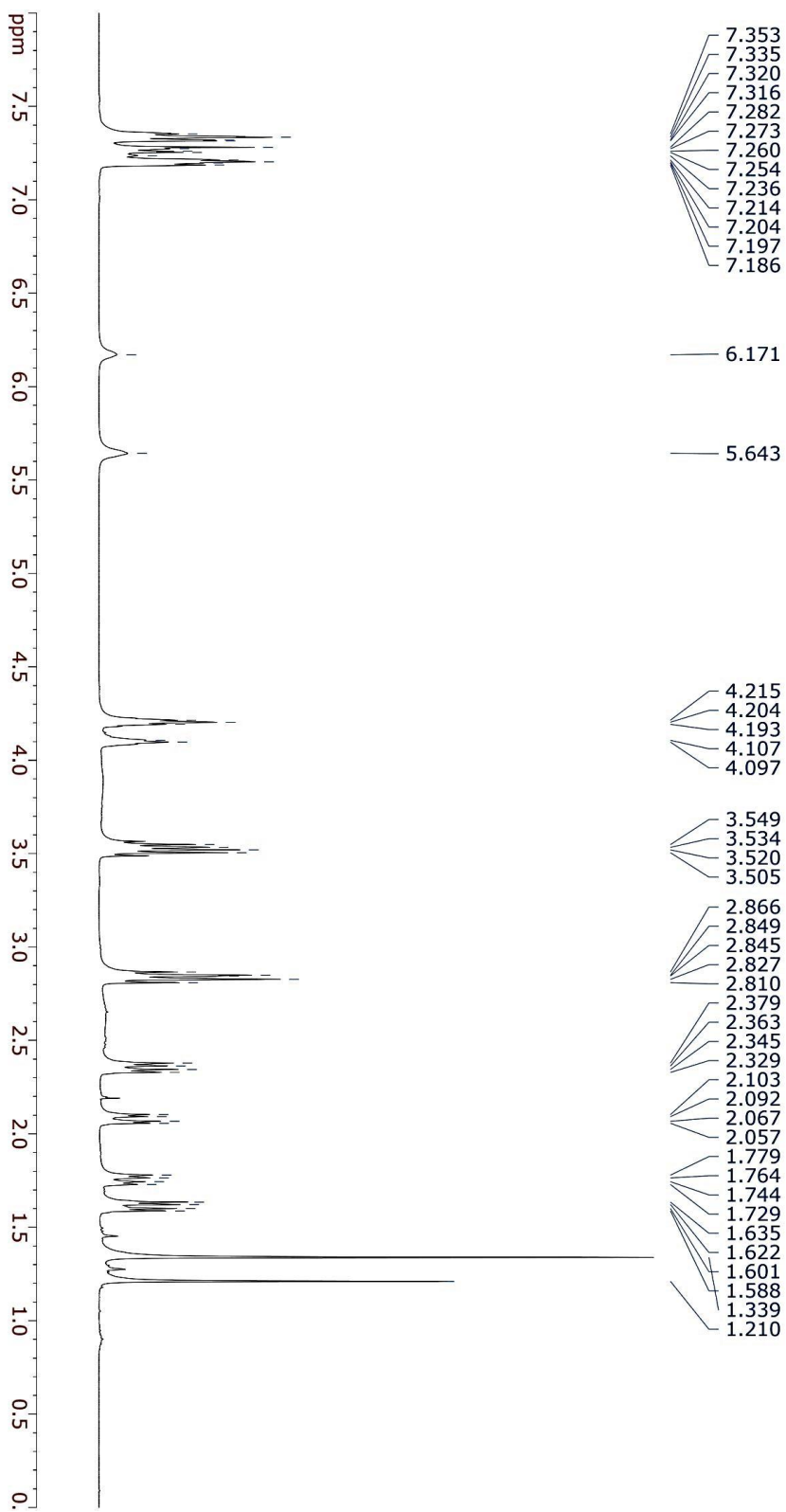
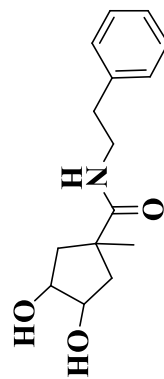




<sup>1</sup>H-NMR data for compound (**20**) Recorded on 700 MHz spectrometer (CDCl<sub>3</sub>)

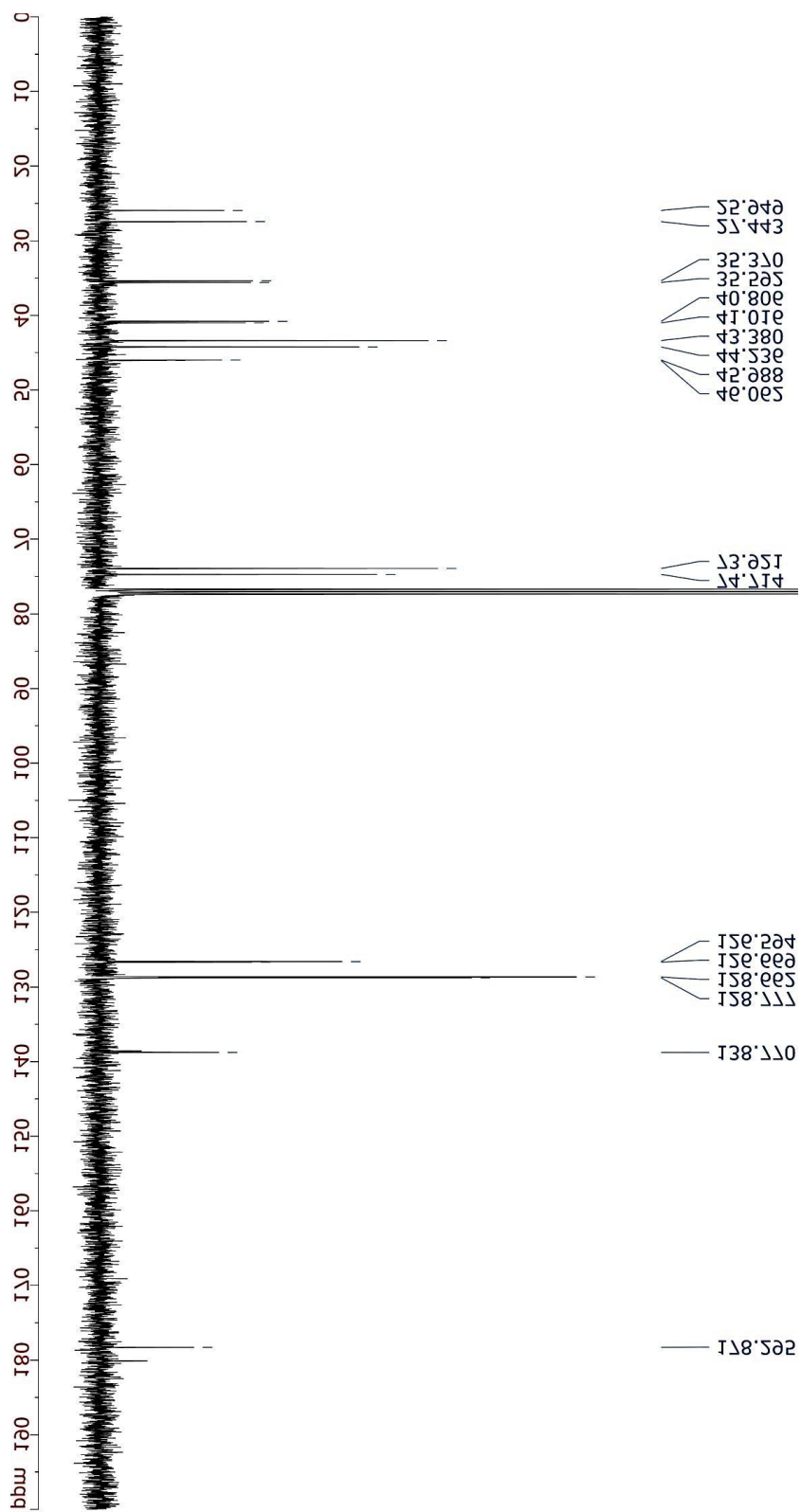
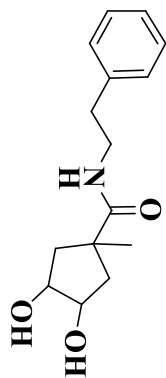


<sup>1</sup>H-NMR data for compound (**21**) Recorded on 400 MHz spectrometer (CDCl<sub>3</sub>)

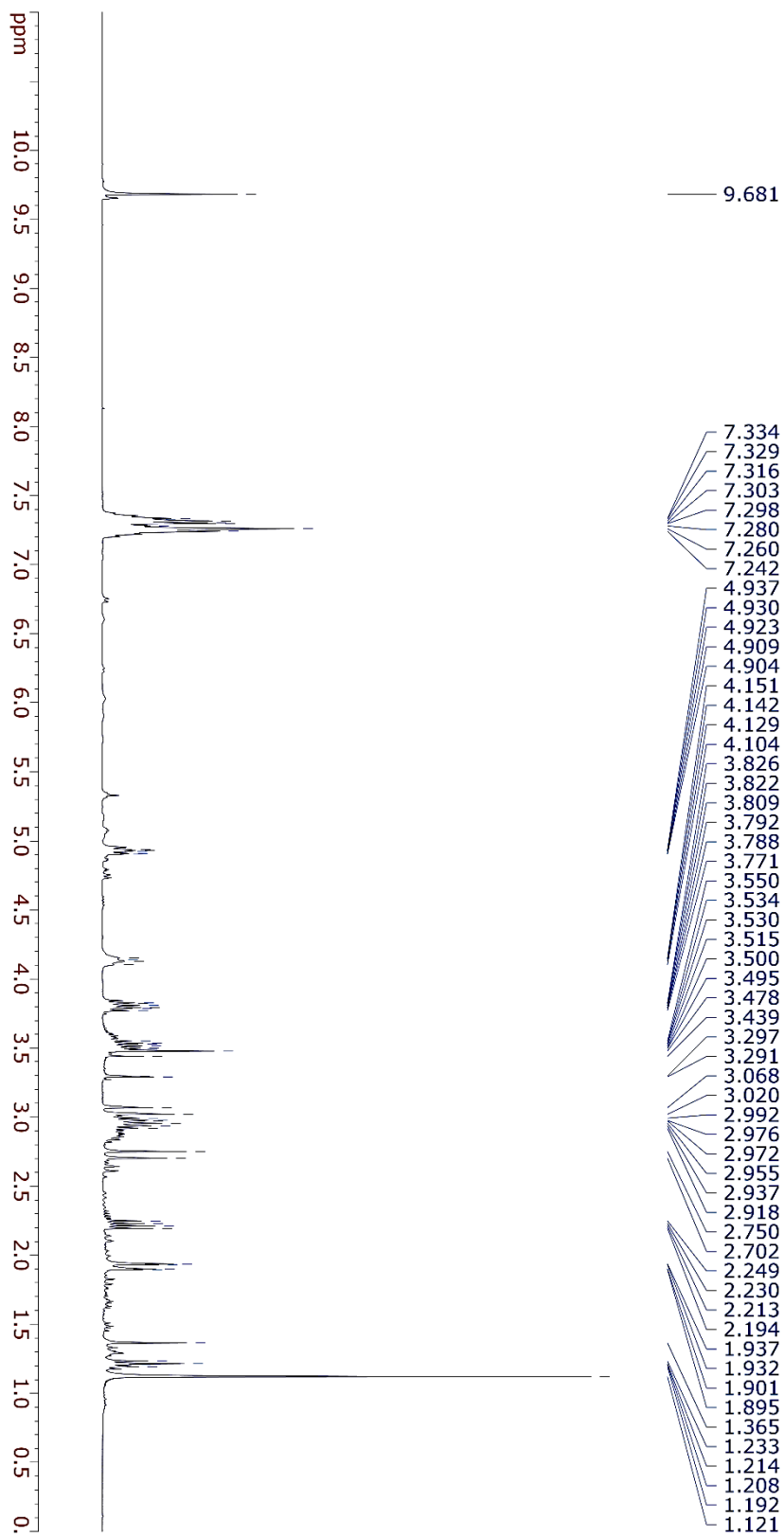
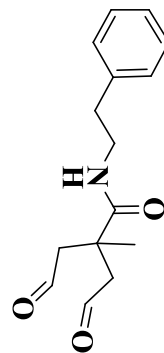




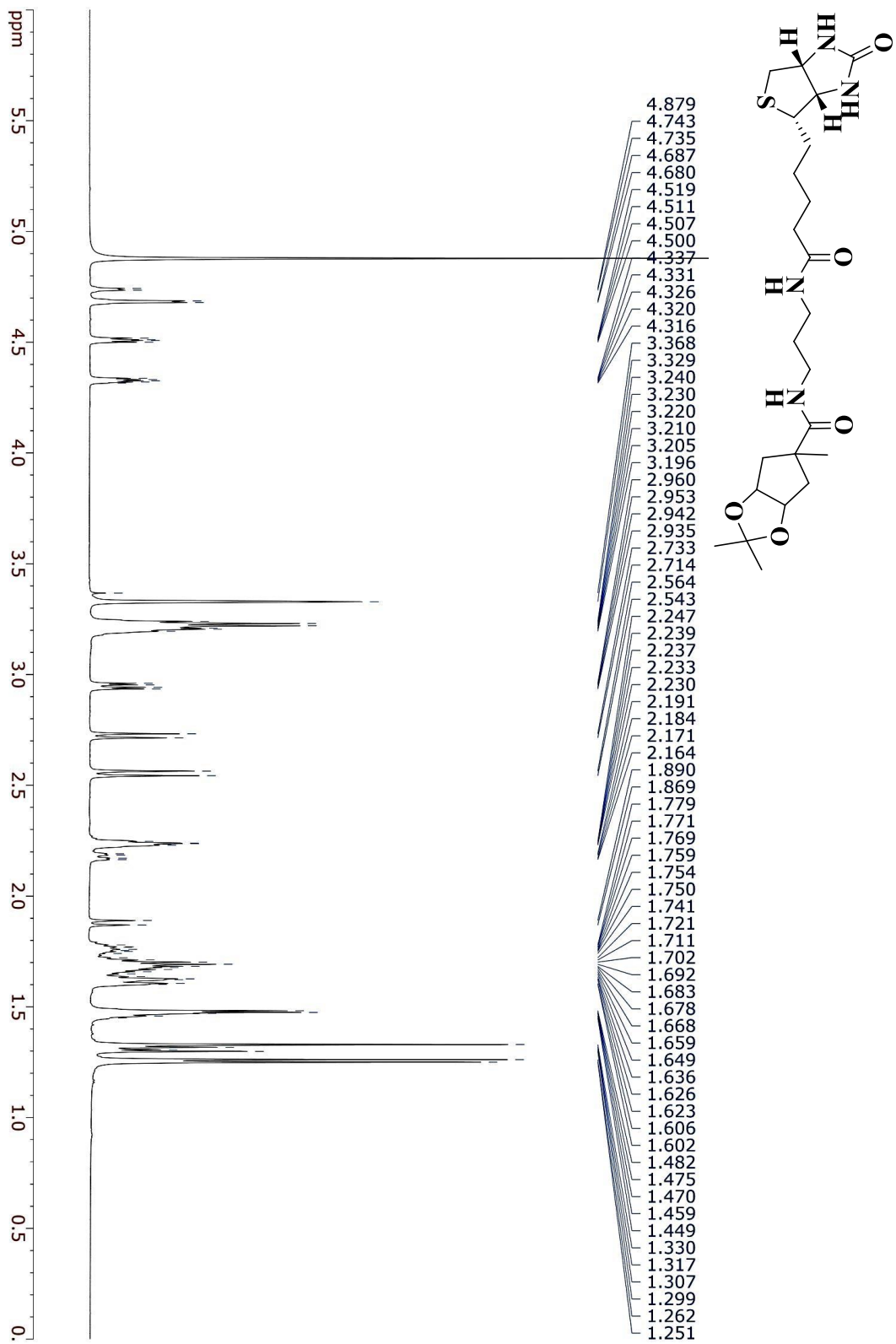
<sup>13</sup>C-NMR data for compound (21) Recorded on 400 MHz spectrometer (CDCl<sub>3</sub>)



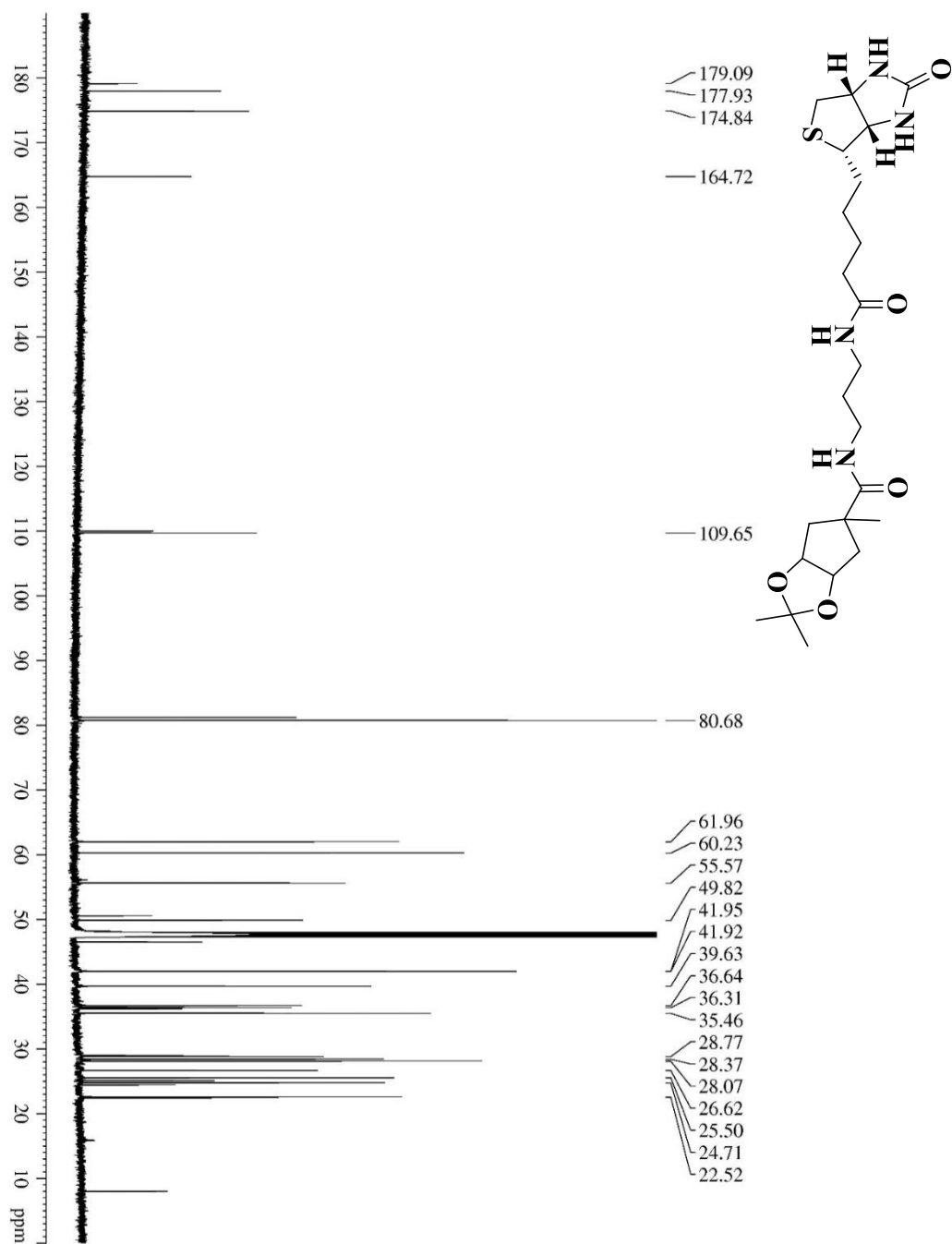
<sup>1</sup>H-NMR data for compound (**22**) Recorded on 700 MHz spectrometer (CDCl<sub>3</sub>)



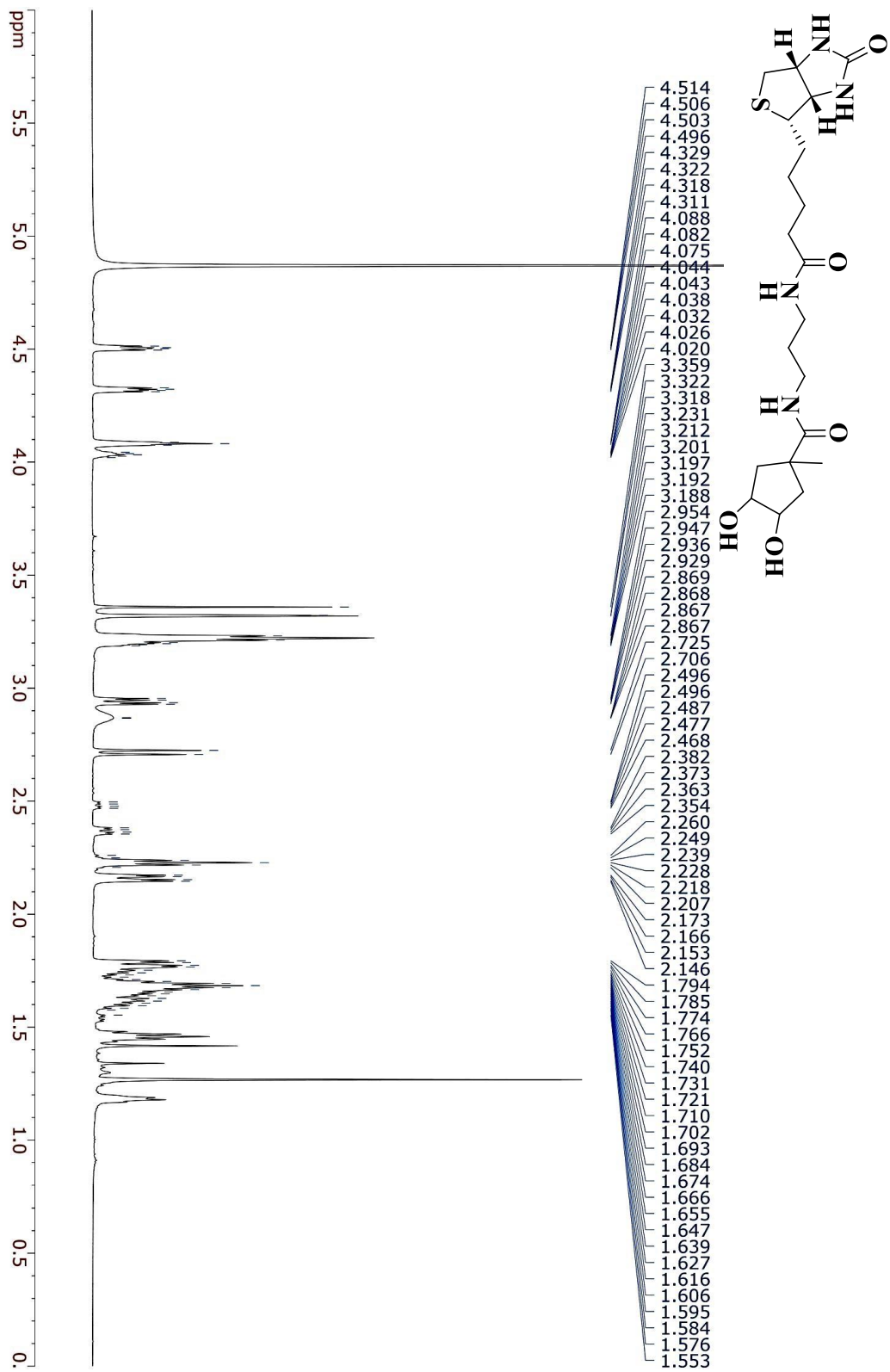
<sup>1</sup>H-NMR data for compound (**24**) Recorded on 700 MHz spectrometer (MeOD)



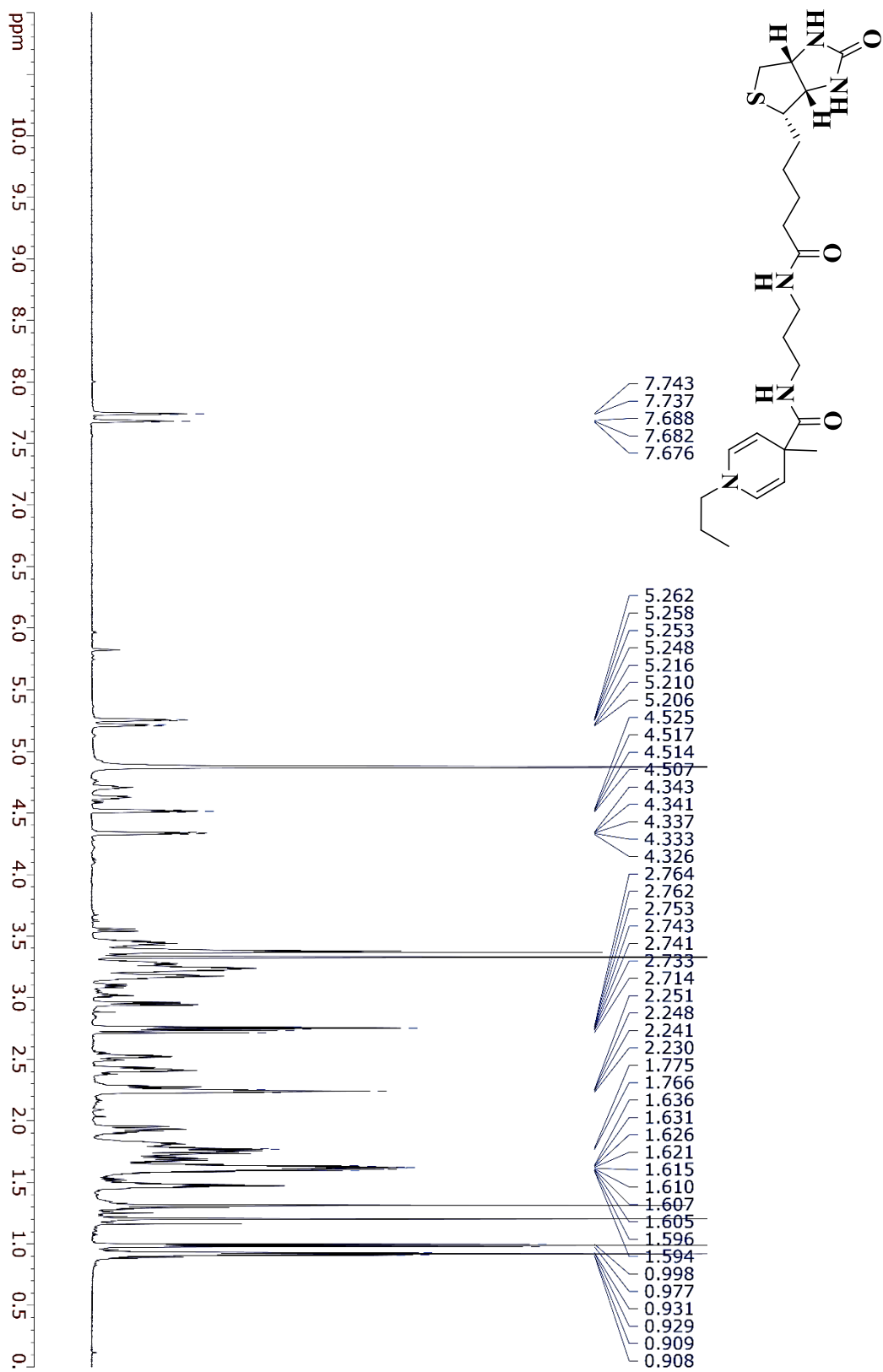
$^{13}\text{C}$ -NMR data for compound (**24**) Recorded on 700 MHz spectrometer (MeOD)



<sup>1</sup>H-NMR data for compound (**25**) Recorded on 700 MHz spectrometer (MeOD)

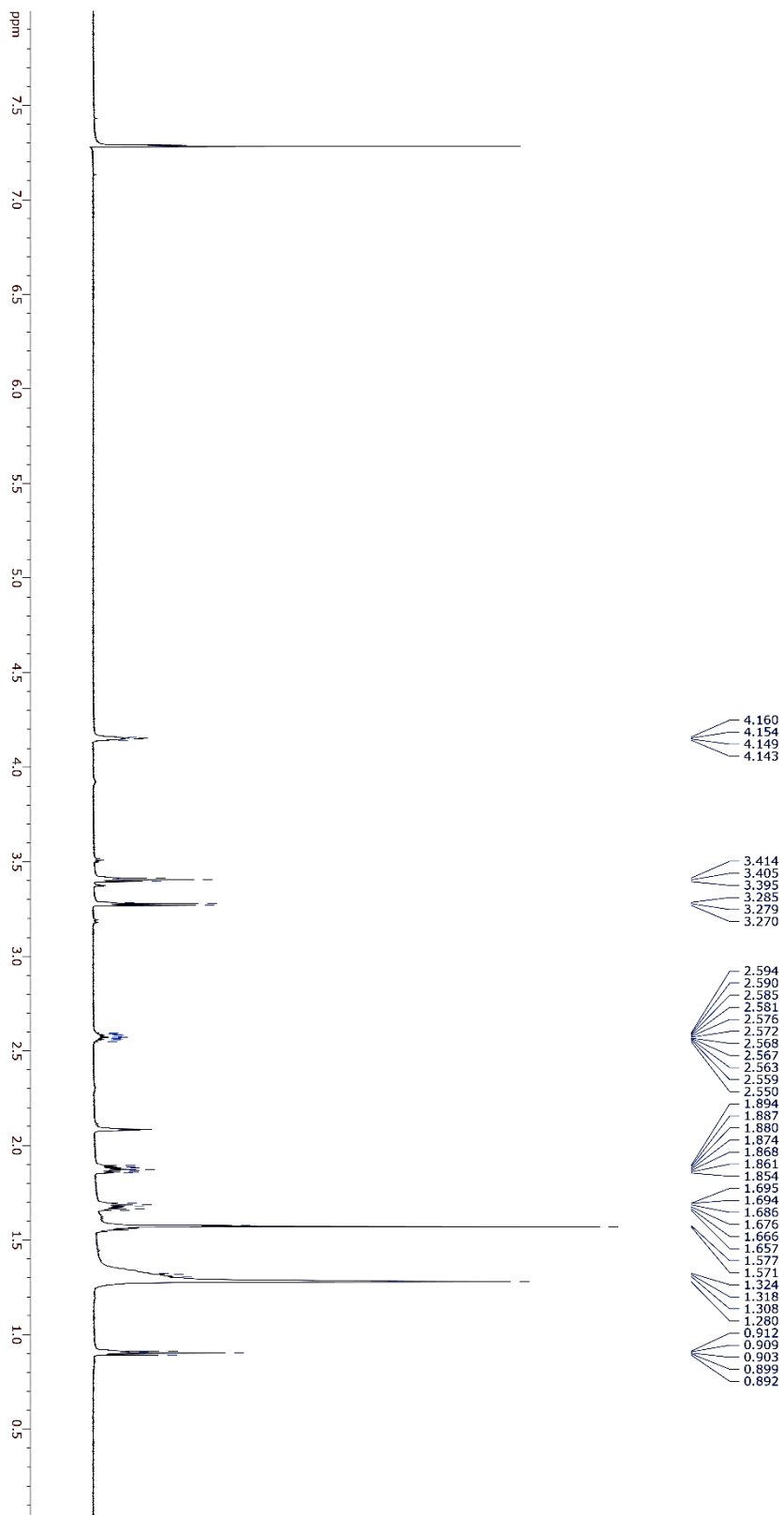


<sup>1</sup>H-NMR data for compound (**Attempted Conjugation 27**) Recorded on 700 MHz spectrometer



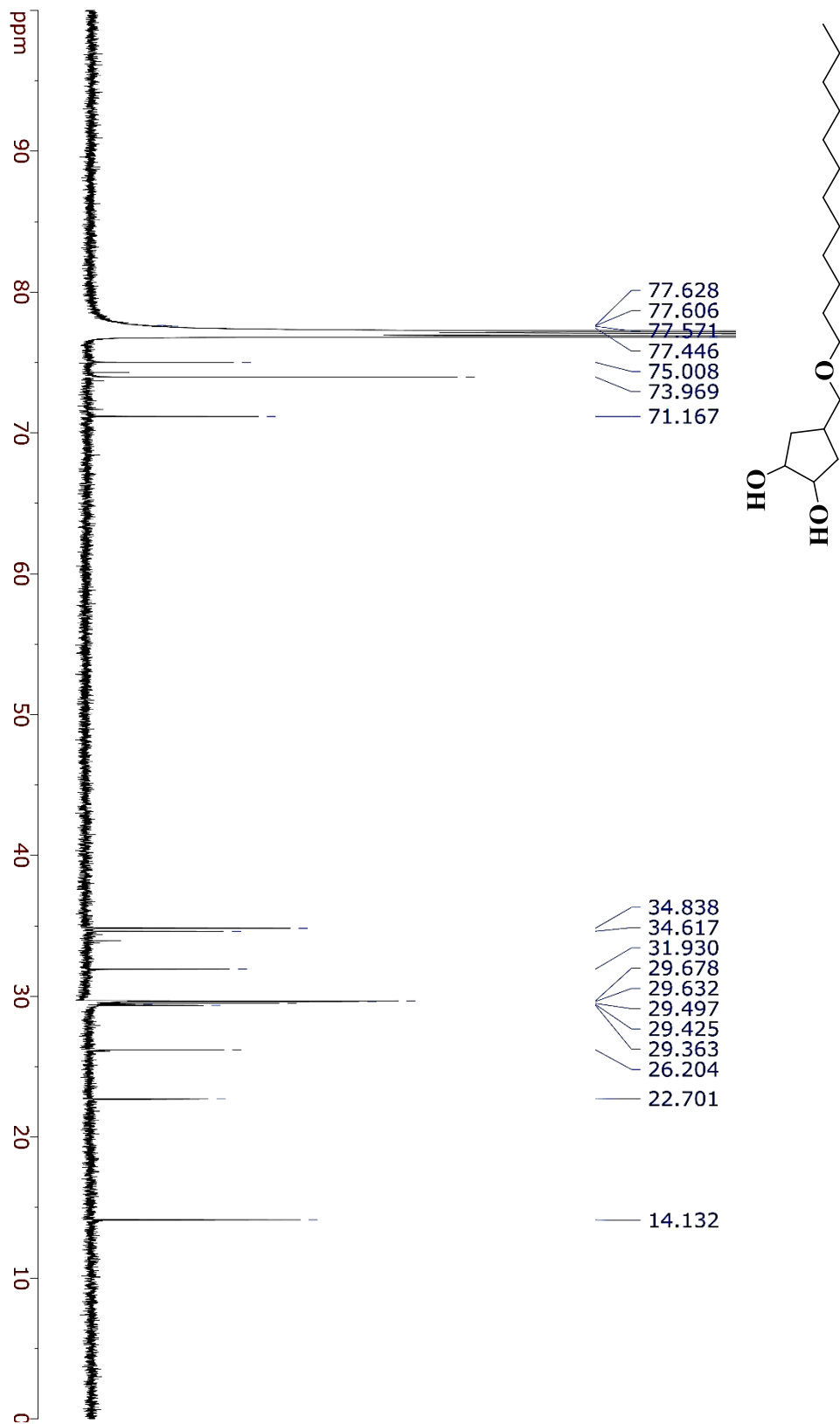


<sup>1</sup>H-NMR data for compound (30) Recorded on 700 MHz spectrometer (CDCl<sub>3</sub>)

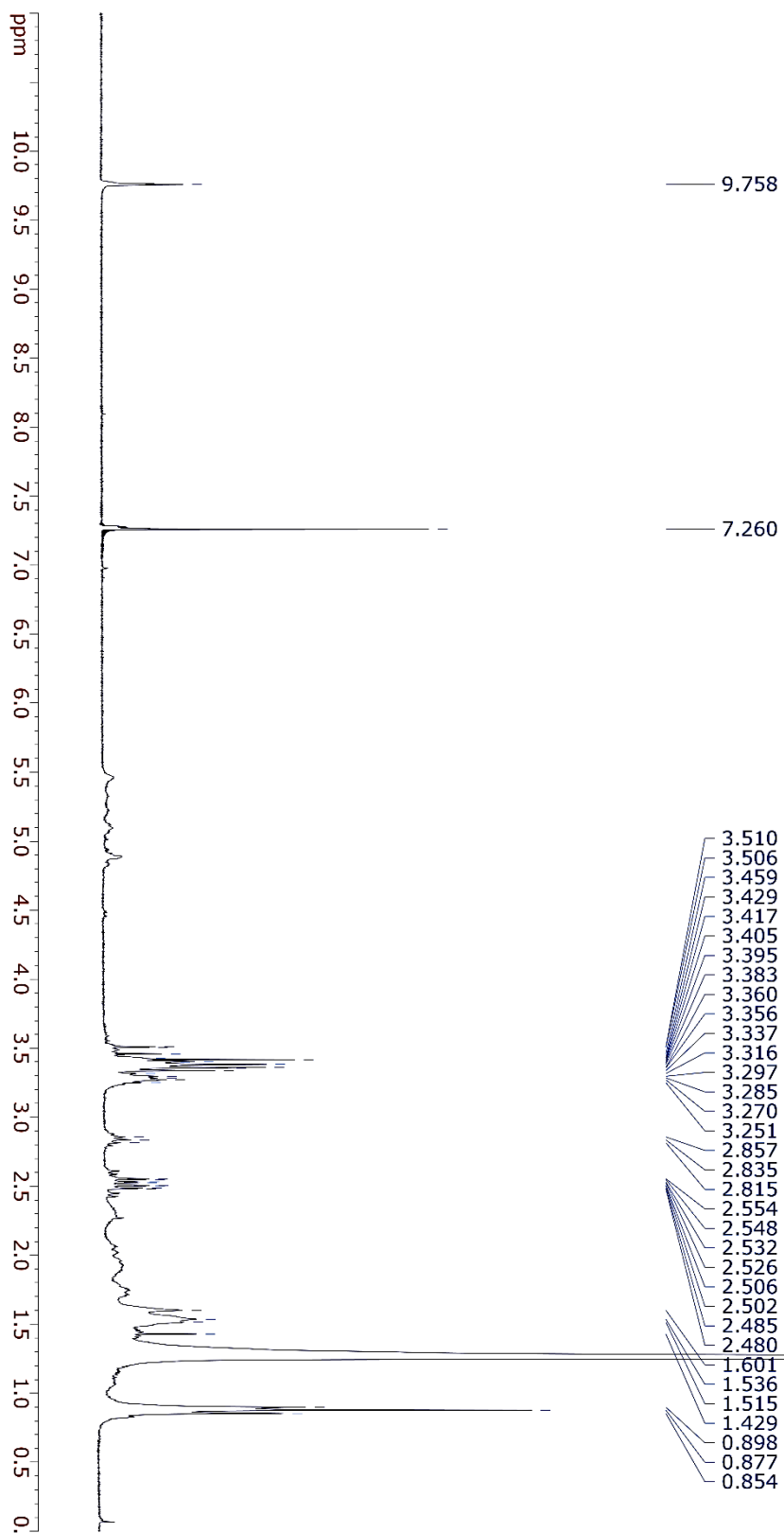
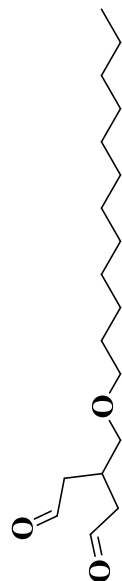




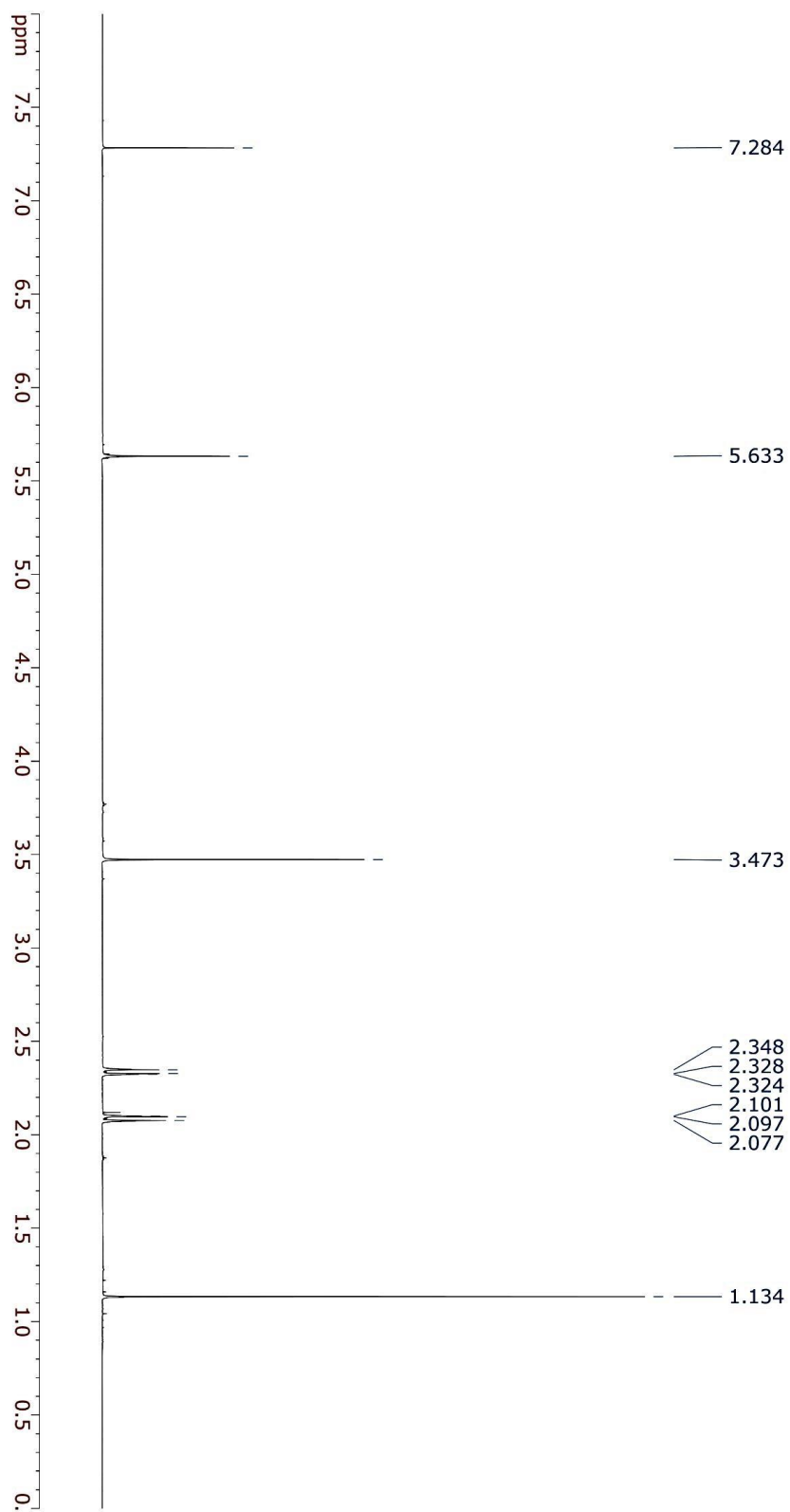
$^{13}\text{C}$ -NMR data for compound (**30**) Recorded on 700 MHz spectrometer ( $\text{CDCl}_3$ )



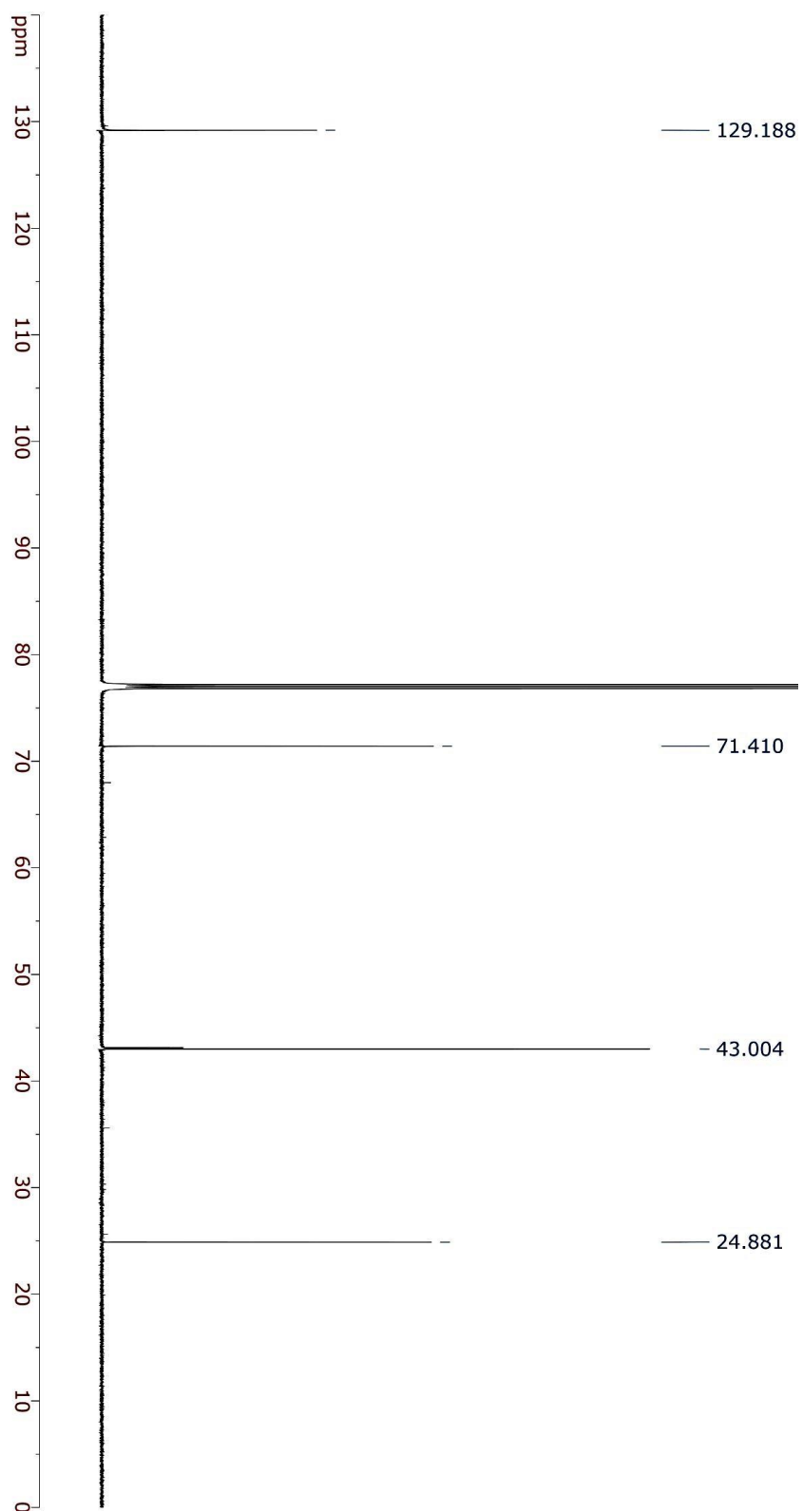
<sup>1</sup>H-NMR data for compound (**31**) Recorded on 300 MHz spectrometer (CDCl<sub>3</sub>)



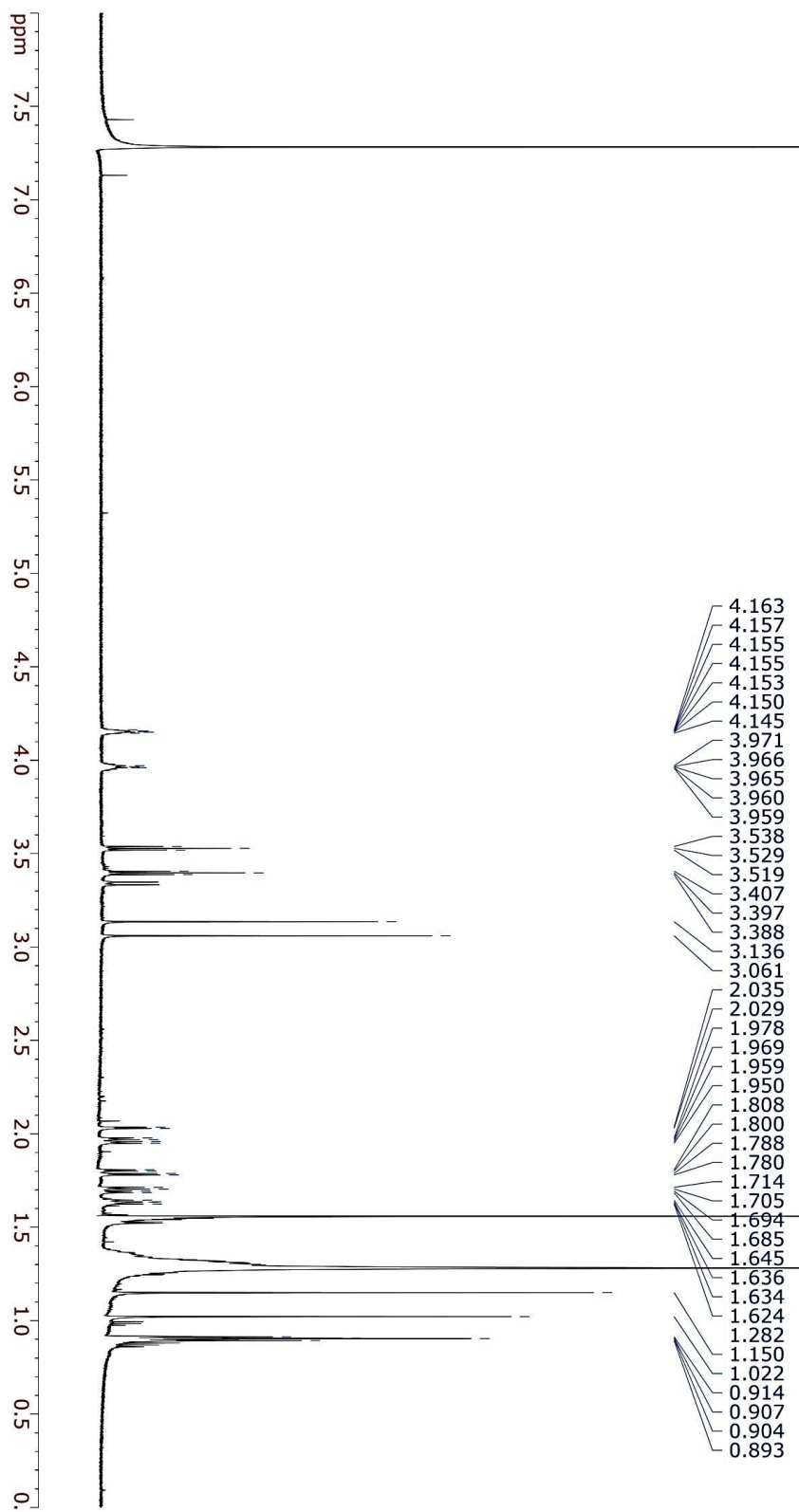
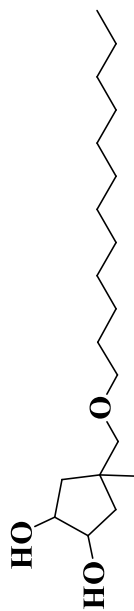
<sup>1</sup>H-NMR data for compound (**33**) Recorded on 700 MHz spectrometer (CDCl<sub>3</sub>)



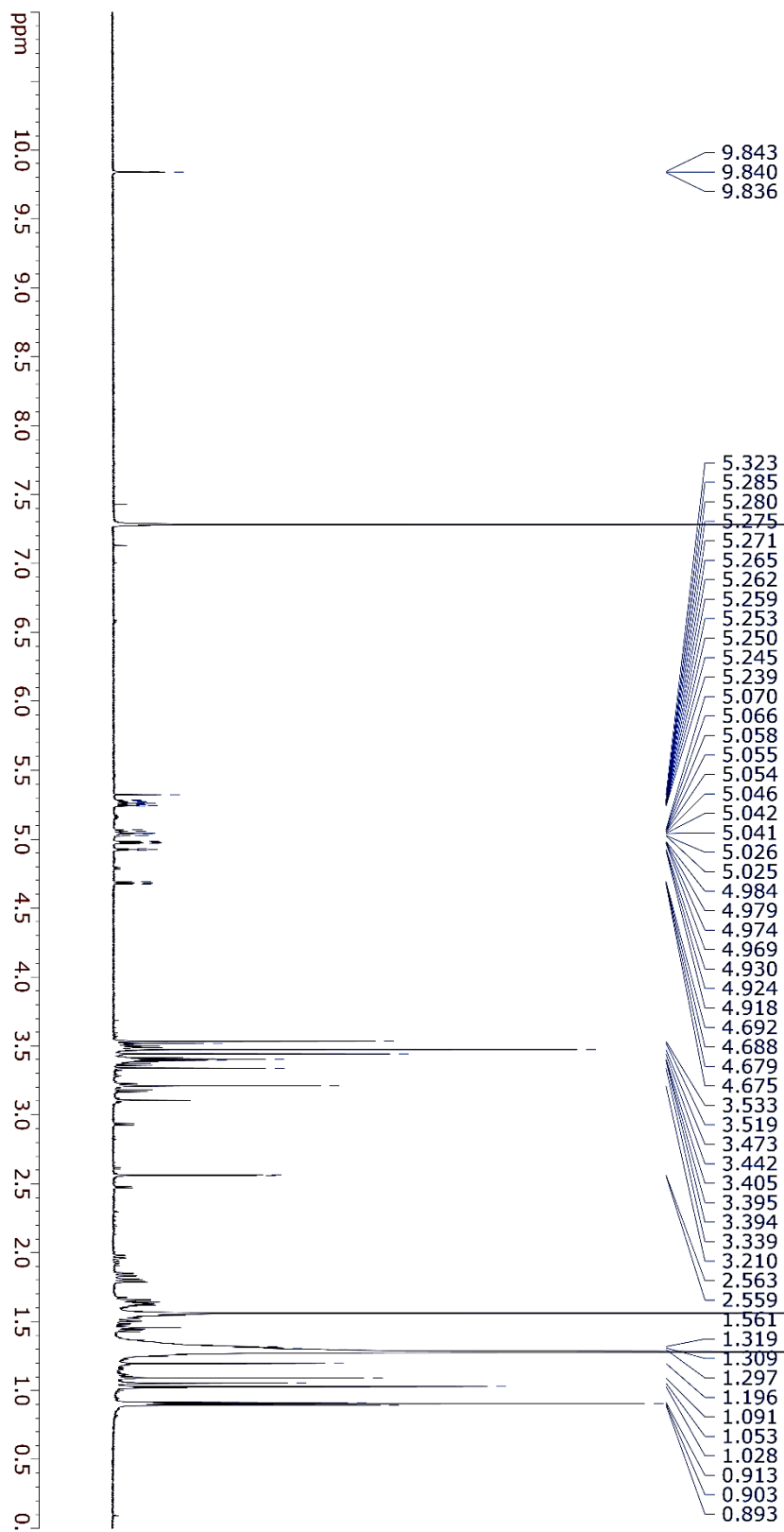
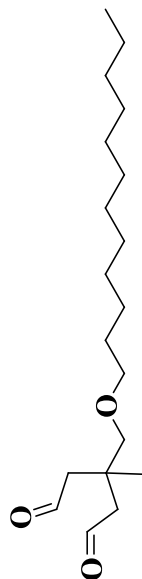
$^{13}\text{C}$ -NMR data for compound (**33**) Recorded on 700 MHz spectrometer ( $\text{CDCl}_3$ )



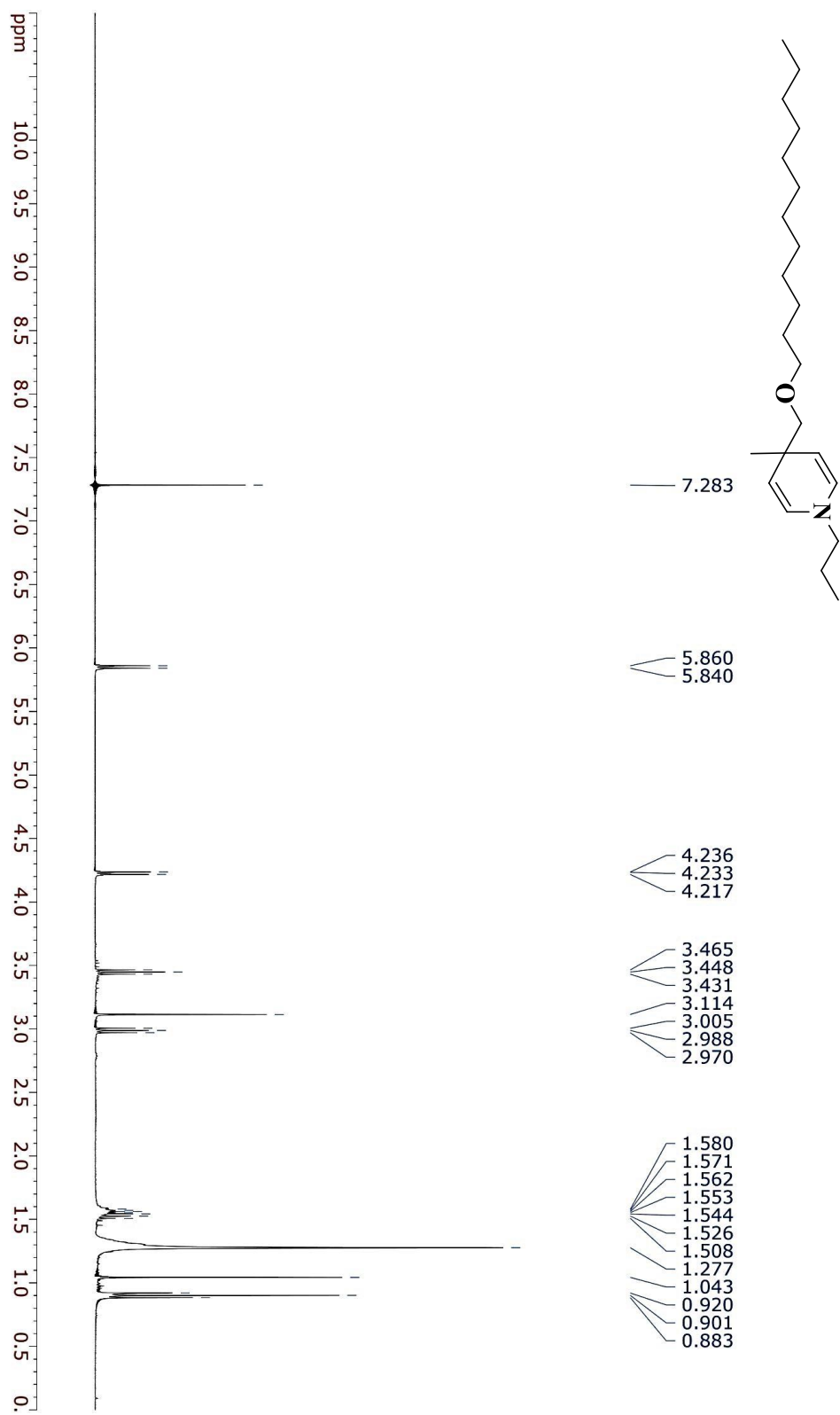
<sup>1</sup>H-NMR data for compound (35) Recorded on 700 MHz spectrometer (CDCl<sub>3</sub>)



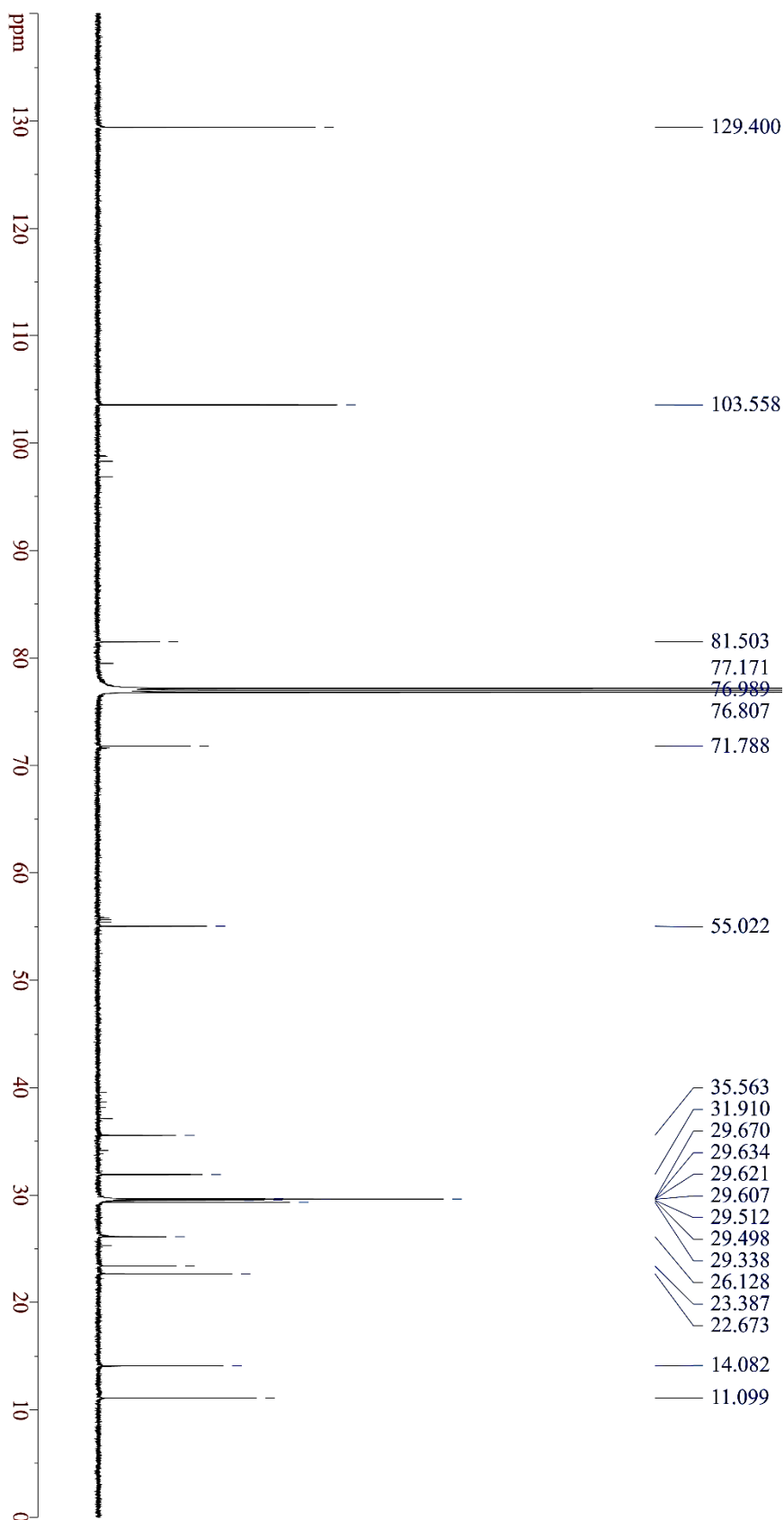
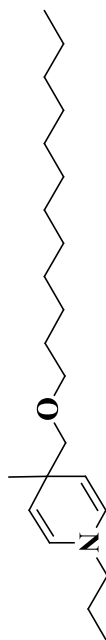
<sup>1</sup>H-NMR data for compound (**36**) Recorded on 700 MHz spectrometer (CDCl<sub>3</sub>)



<sup>1</sup>H-NMR data for compound (**37**) Recorded on 700 MHz spectrometer (CDCl<sub>3</sub>)

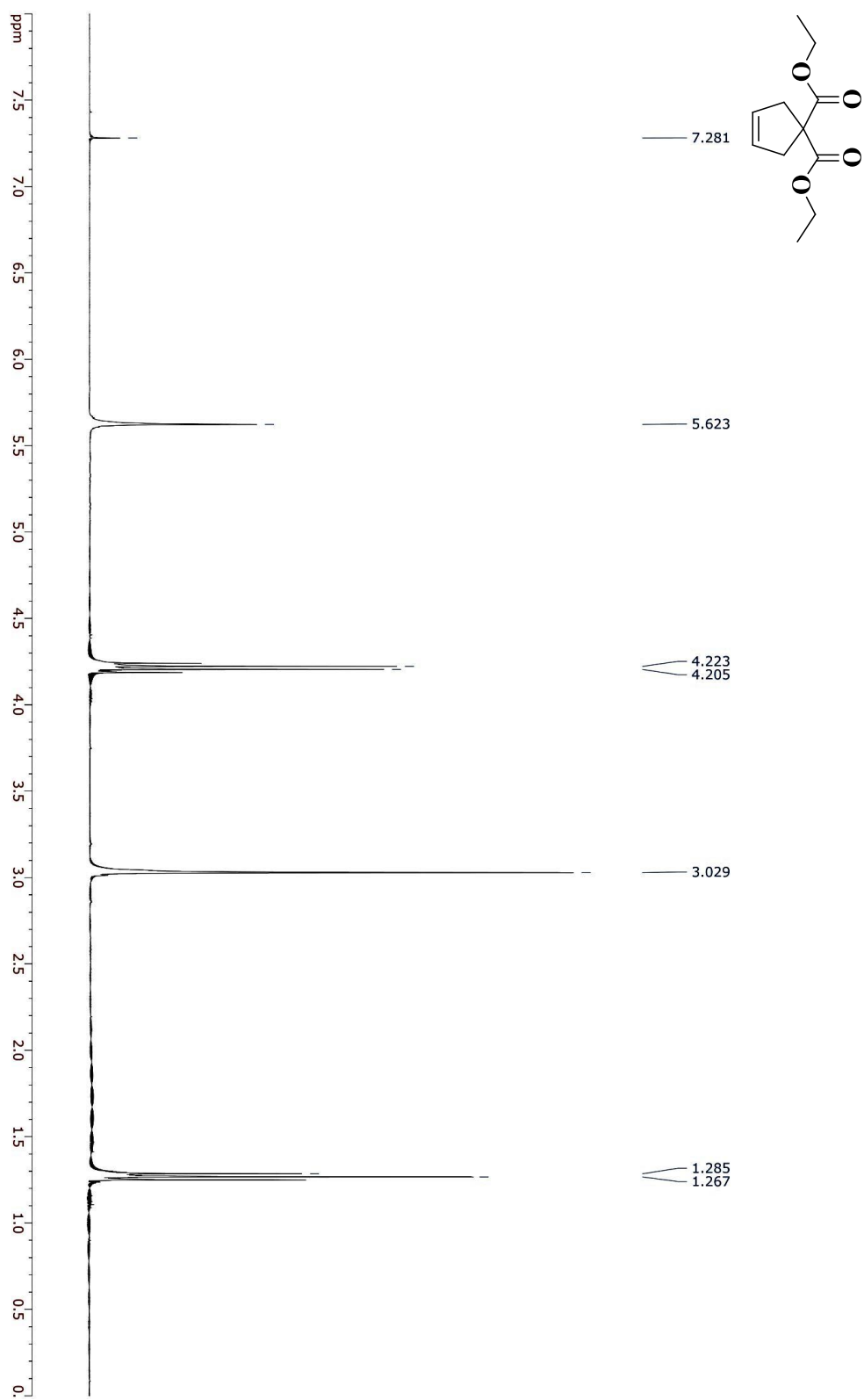


<sup>1</sup>H-NMR data for compound (37) Recorded on 700 MHz spectrometer (CDCl<sub>3</sub>)

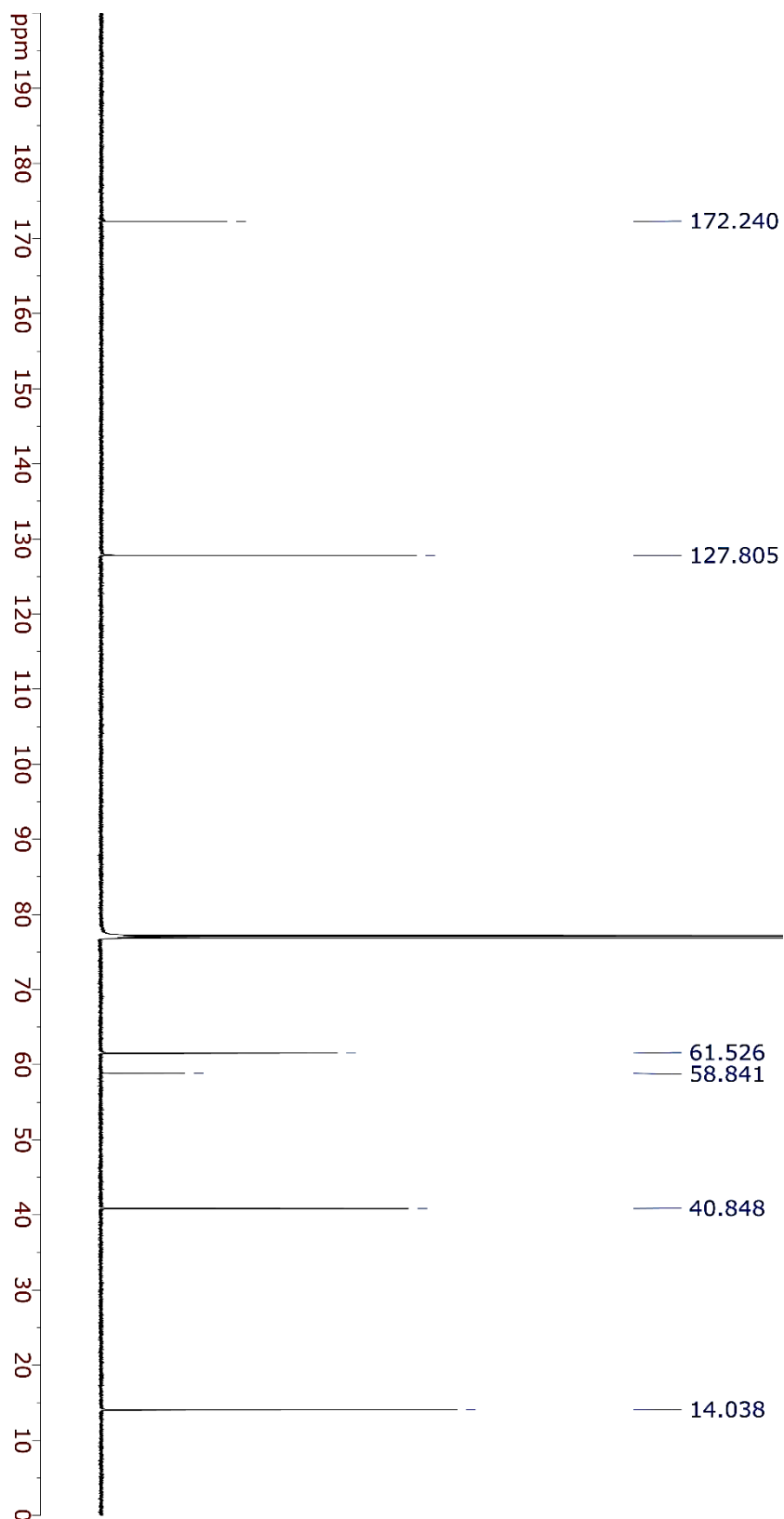
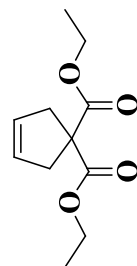




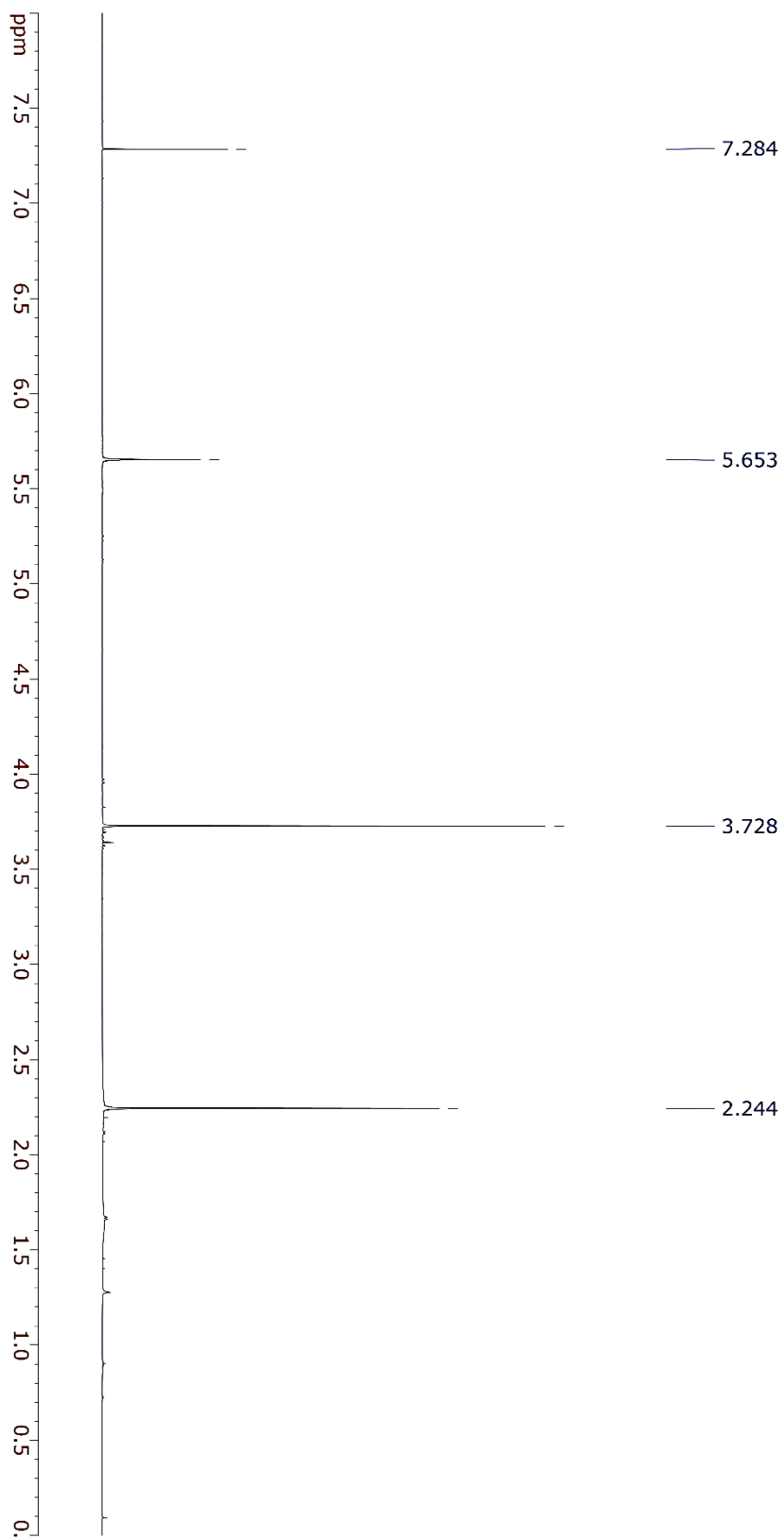
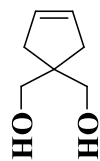
<sup>1</sup>H-NMR data for compound (38) Recorded on 400 MHz spectrometer (CDCl<sub>3</sub>)



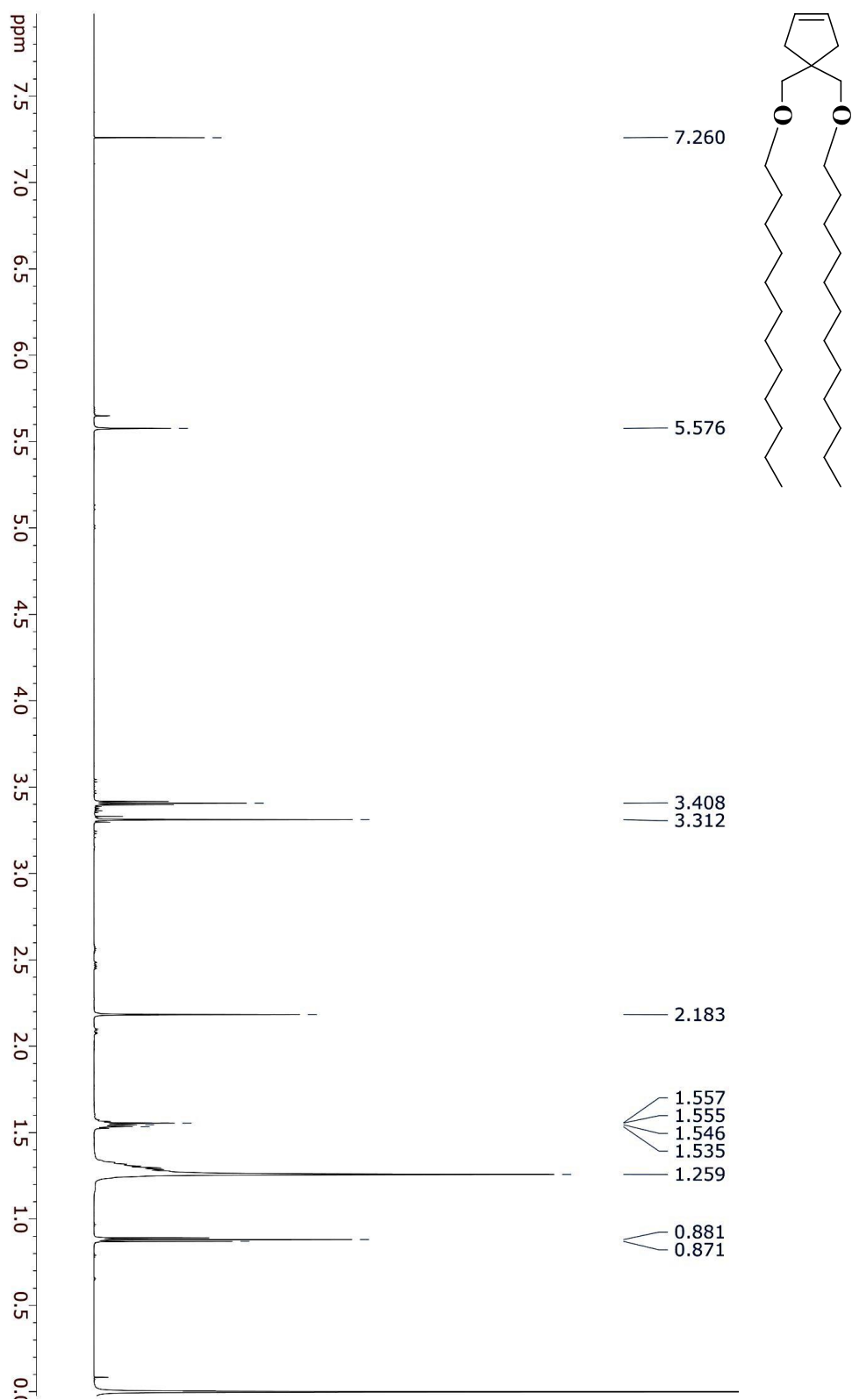
$^{13}\text{C}$ -NMR data for compound (38) Recorded on 400 MHz spectrometer ( $\text{CDCl}_3$ )



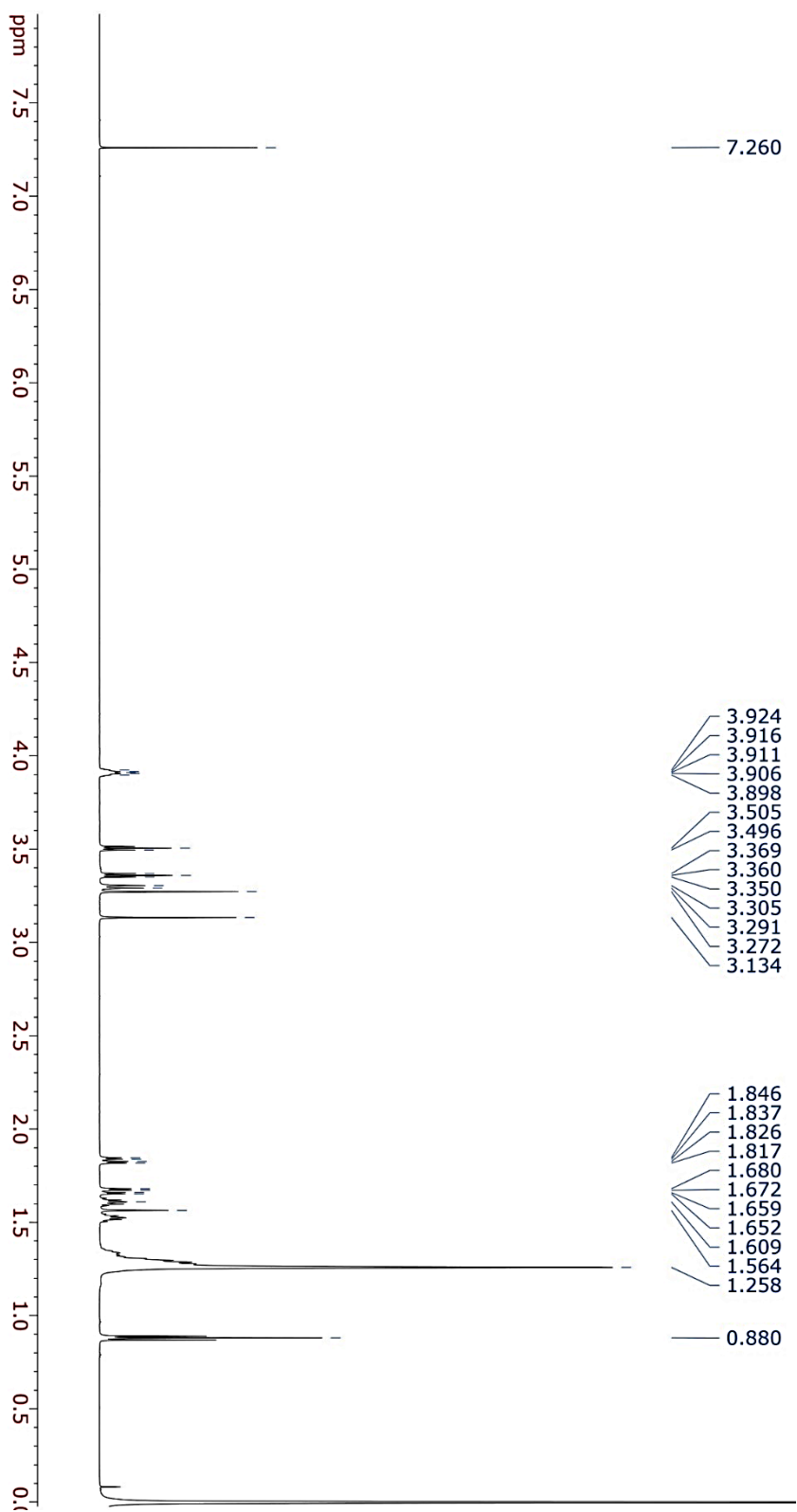
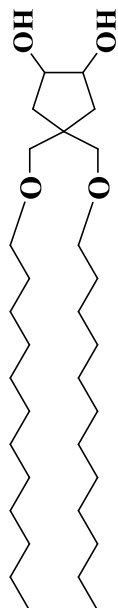
<sup>1</sup>H-NMR data for compound (39) Recorded on 700 MHz spectrometer (CDCl<sub>3</sub>)



<sup>1</sup>H-NMR data for compound (**40**) Recorded on 700 MHz spectrometer (CDCl<sub>3</sub>)



<sup>1</sup>H-NMR data for compound (**41**) Recorded on 700 MHz spectrometer (CDCl<sub>3</sub>)



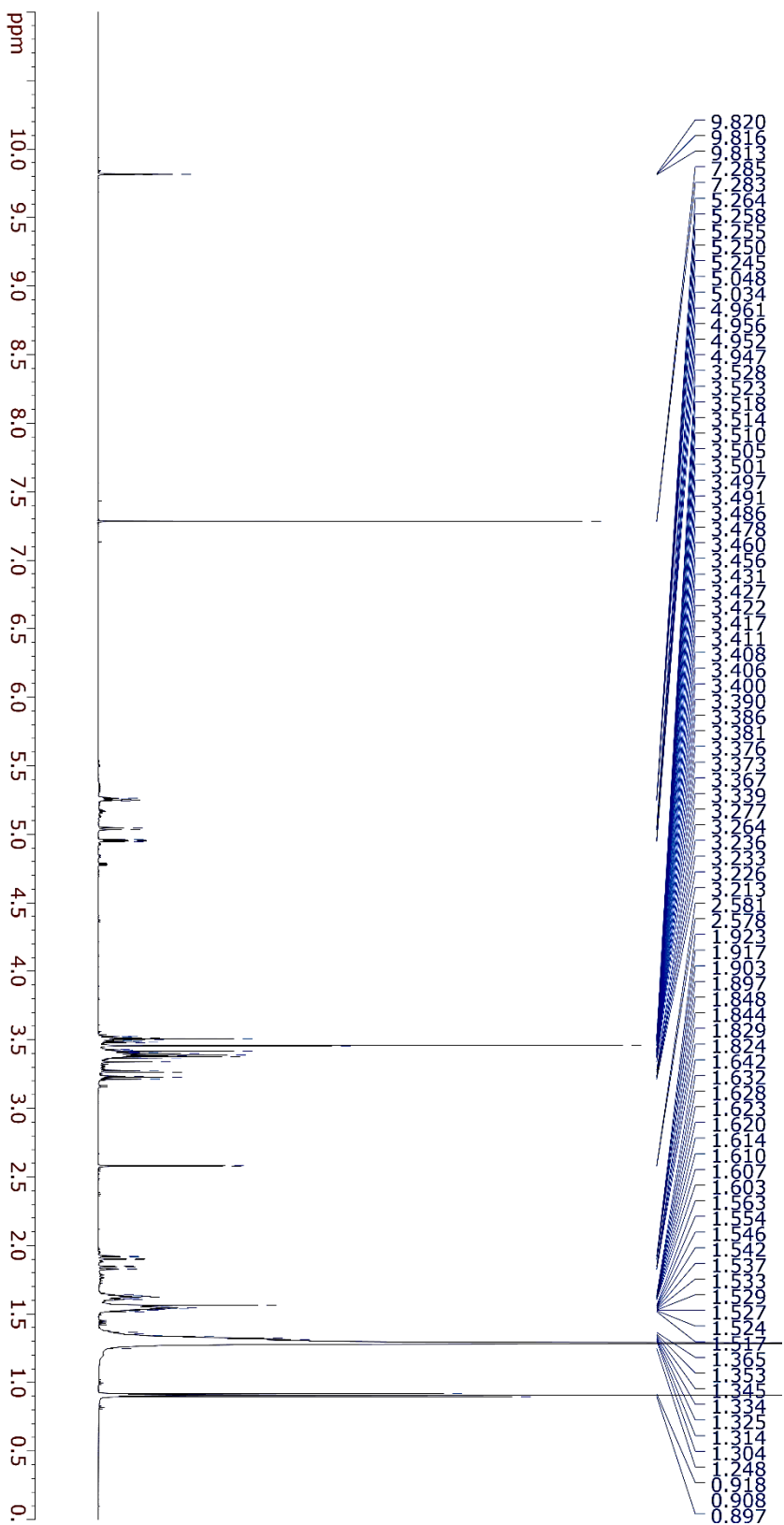
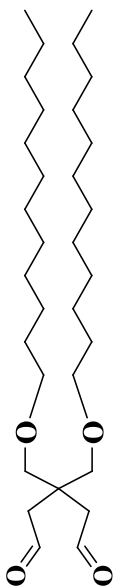




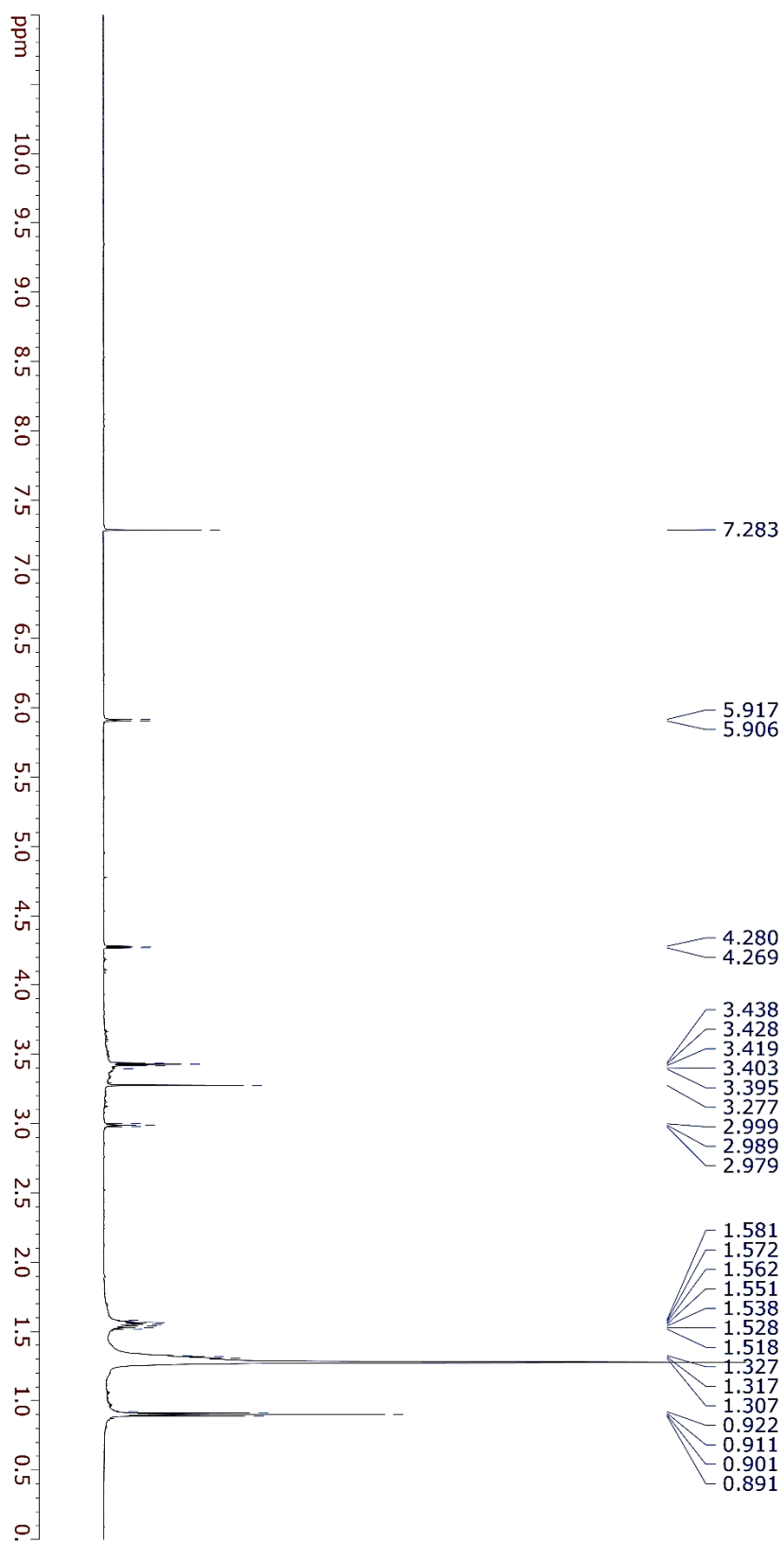
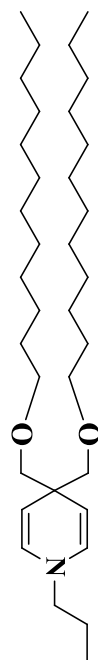




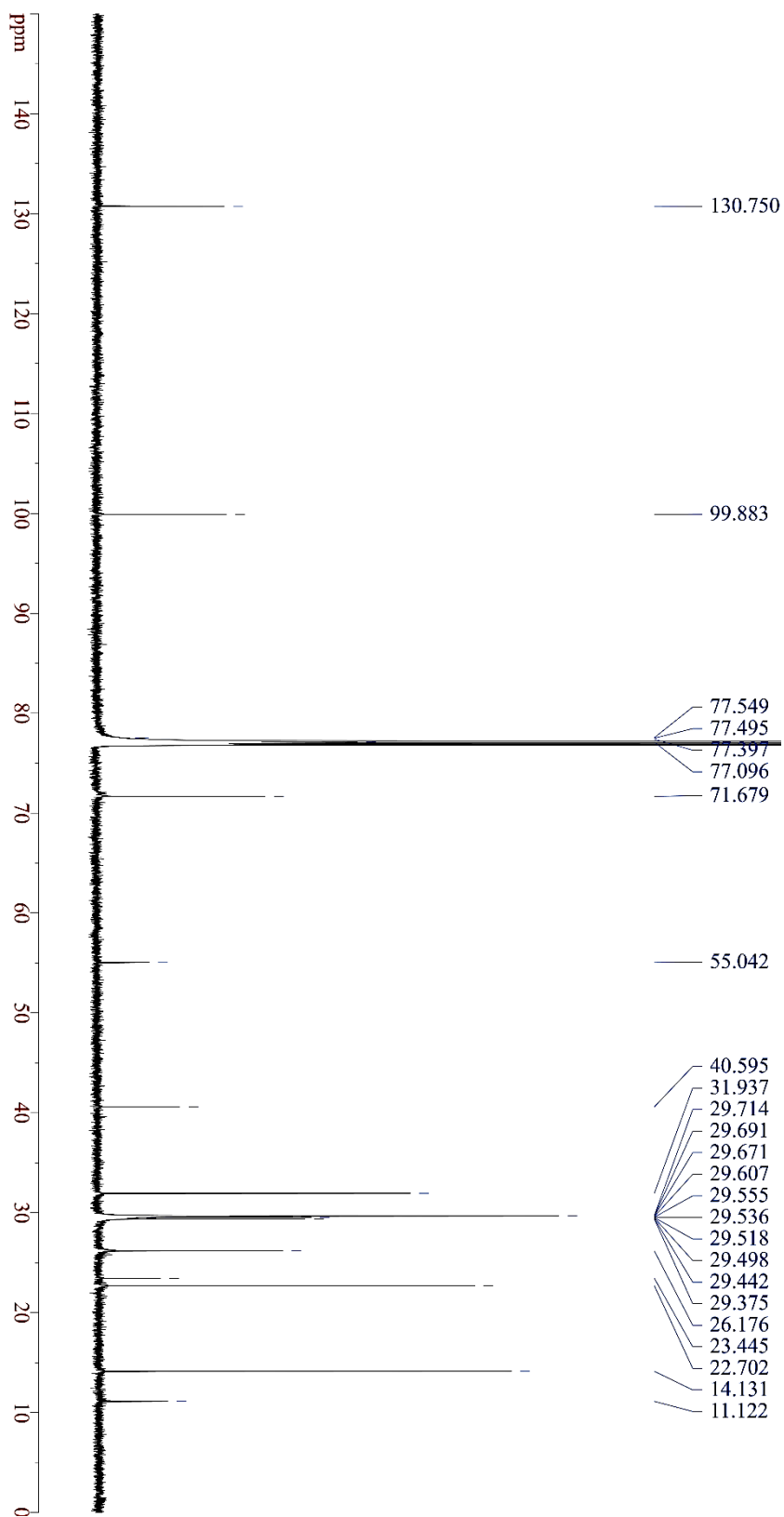
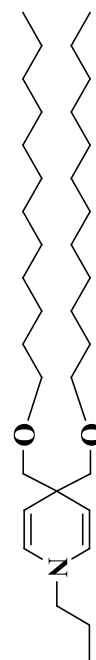
$^1\text{H}$ -NMR data for compound (**42**) Recorded on 400 MHz spectrometer ( $\text{CDCl}_3$ )



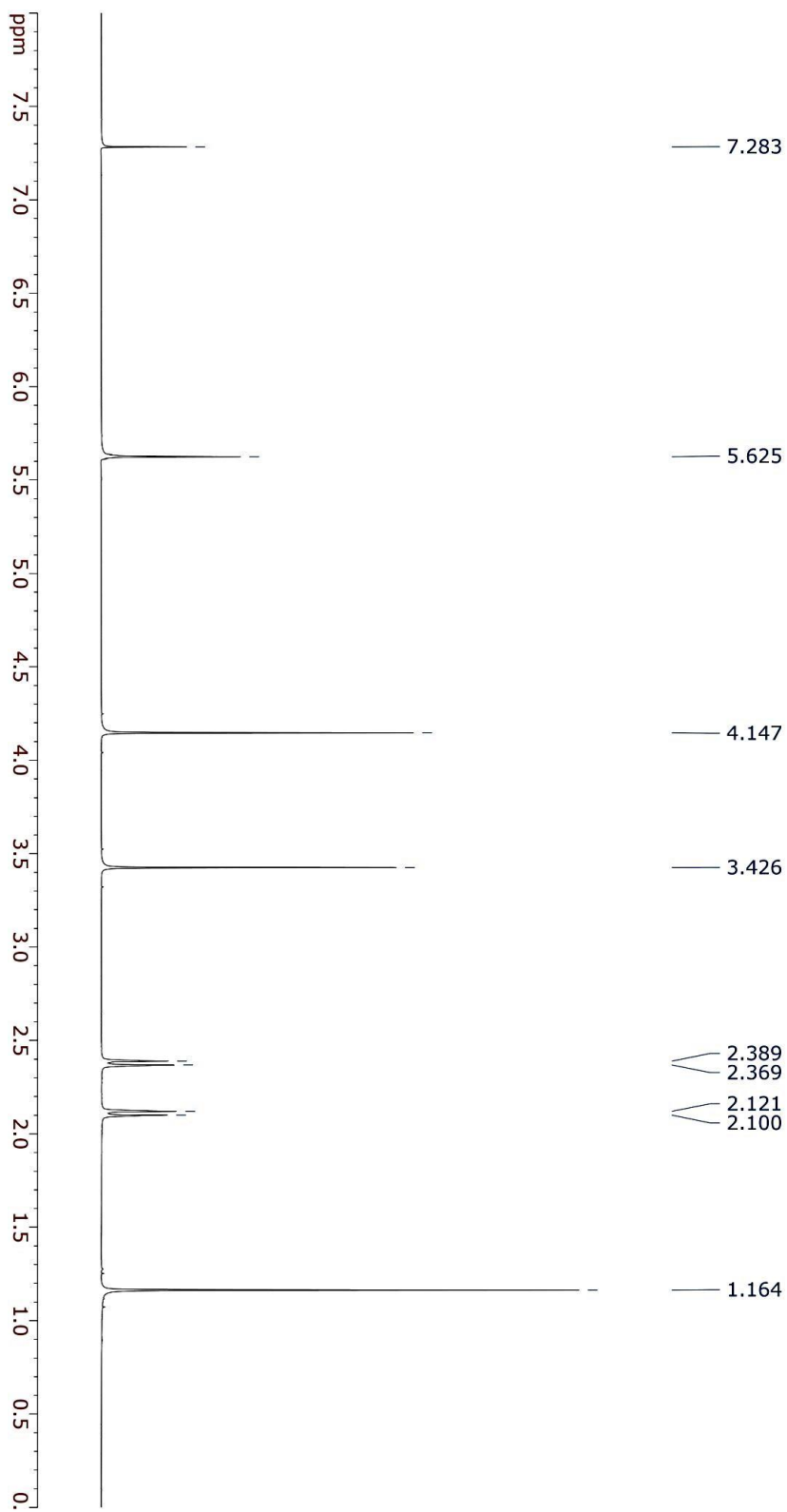
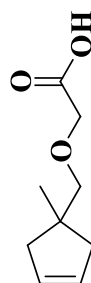
<sup>1</sup>H-NMR data for compound (**43**) Recorded on 700 MHz spectrometer (CDCl<sub>3</sub>)



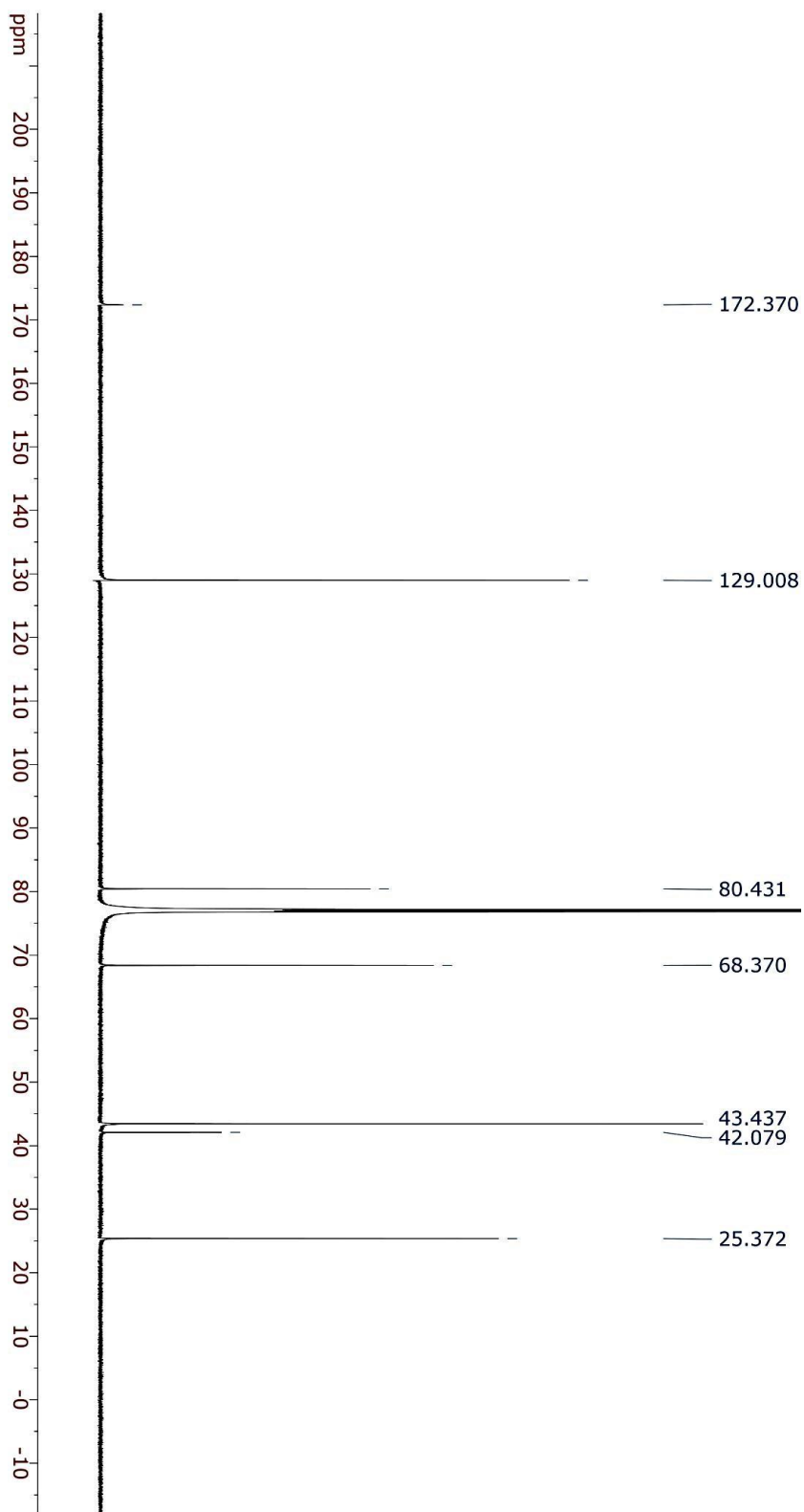
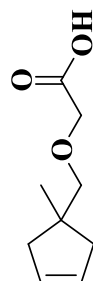
$^{13}\text{C}$ -NMR data for compound (**43**) Recorded on 700 MHz spectrometer ( $\text{CDCl}_3$ )



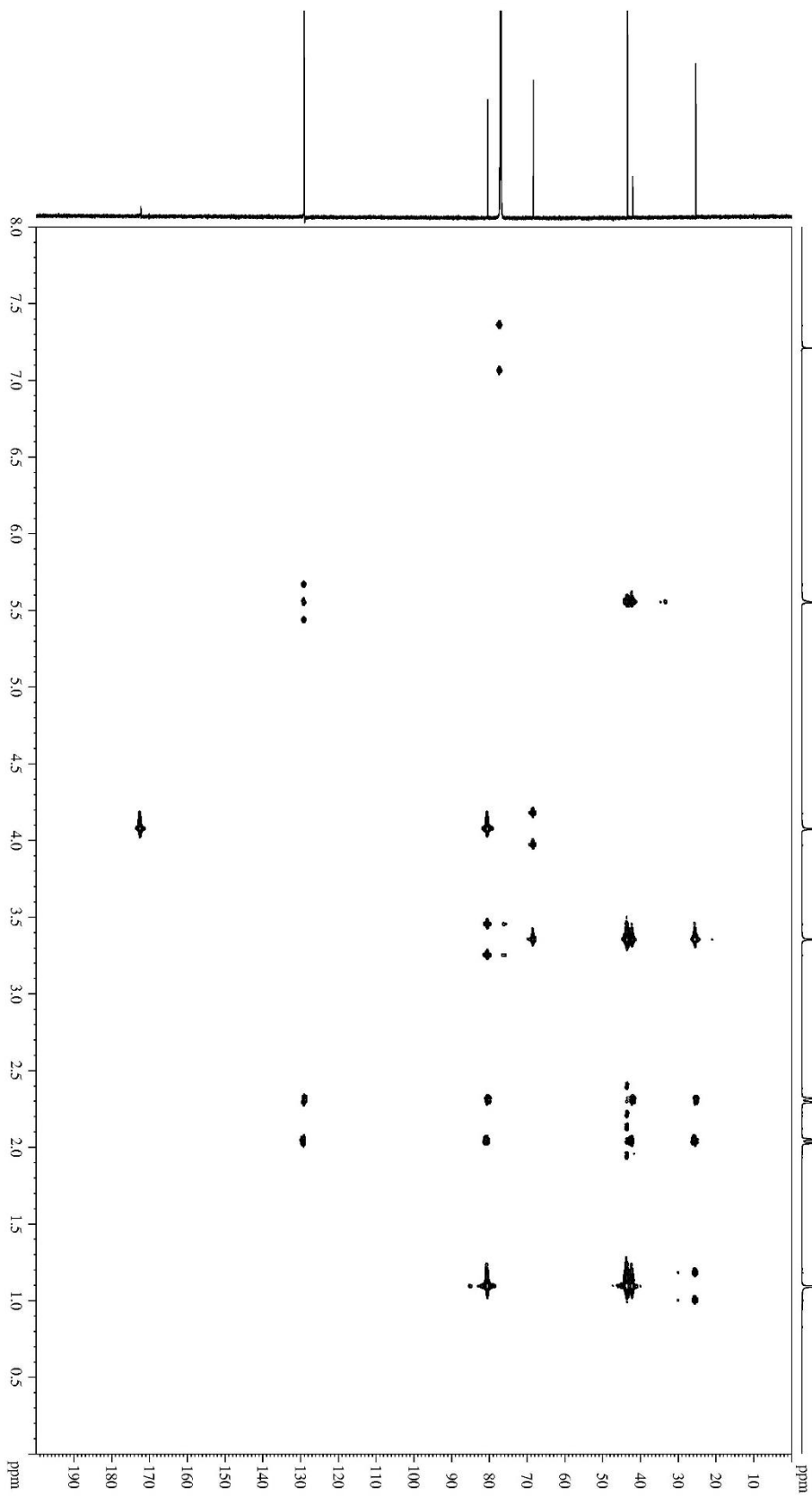
<sup>1</sup>H-NMR data for compound (**44**) Recorded on 700 MHz spectrometer (CDCl<sub>3</sub>)



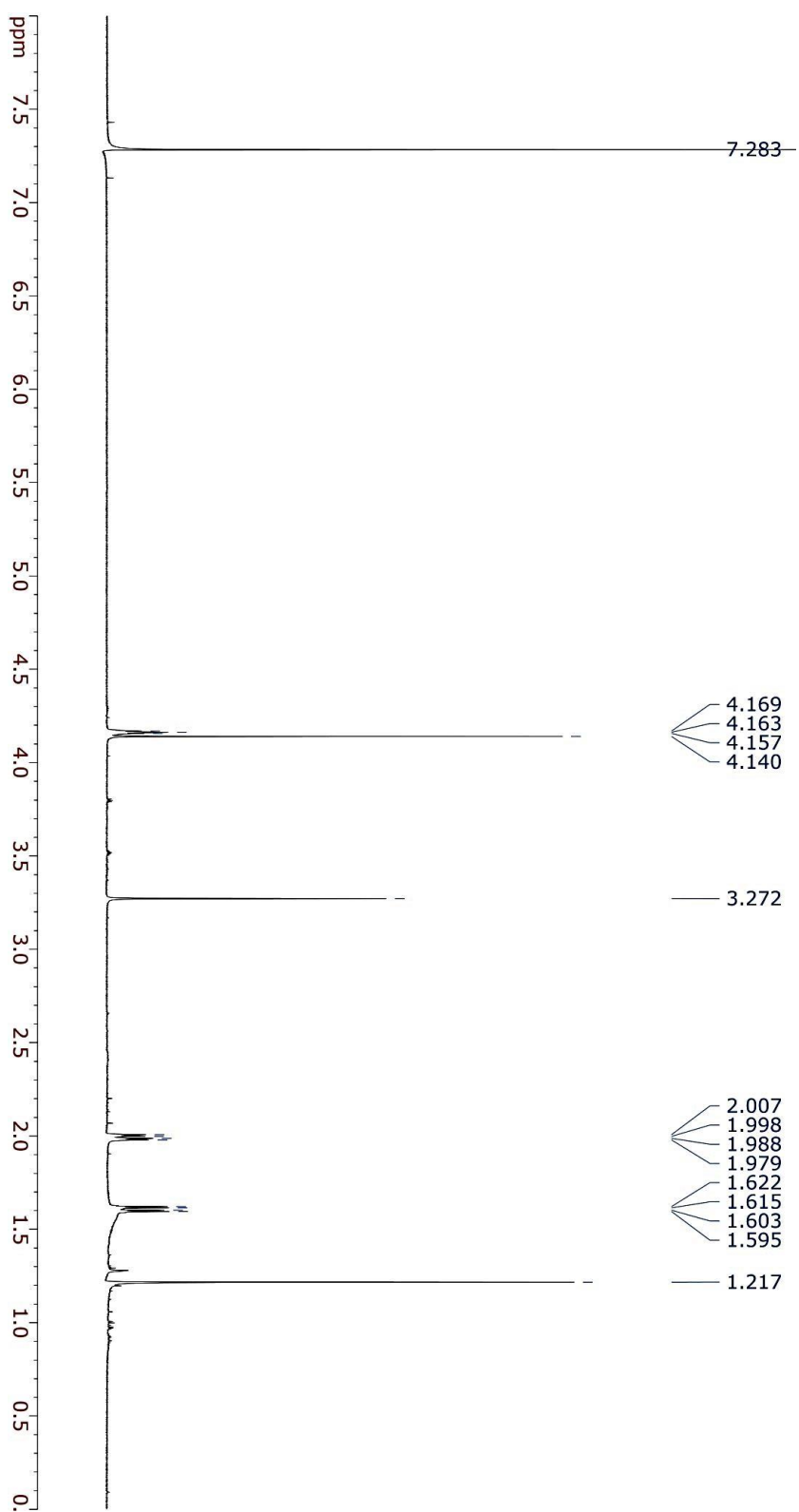
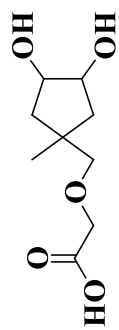
$^{13}\text{C}$ -NMR data for compound (**44**) Recorded on 700 MHz spectrometer ( $\text{CDCl}_3$ )



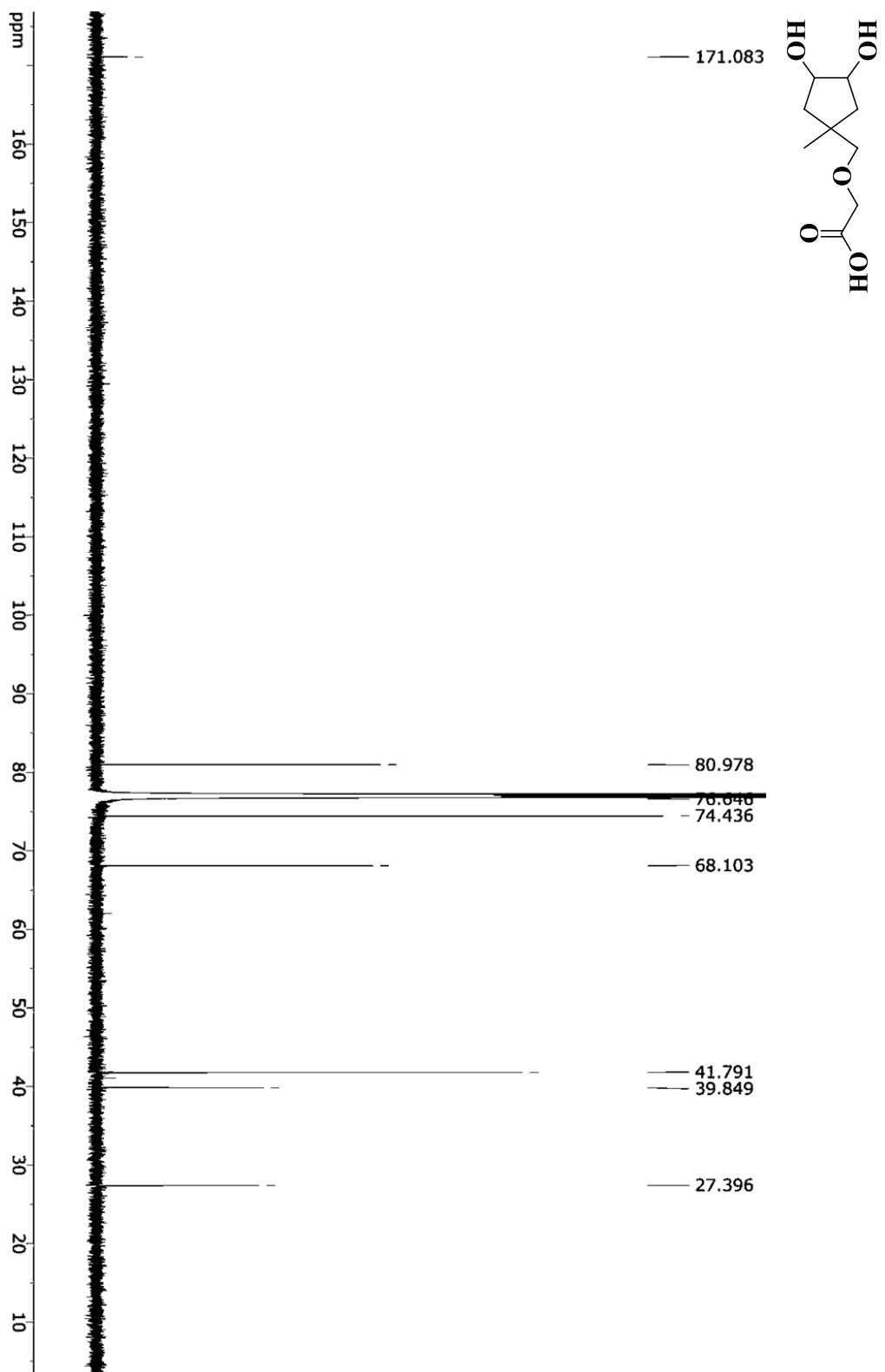
Heteronuclear multiple-bond correlation 2D spectroscopy (**HMBC**) for compound (**44**) Recorded



<sup>1</sup>H-NMR data for compound (**45**) Recorded on 700 MHz spectrometer (CDCl<sub>3</sub>)



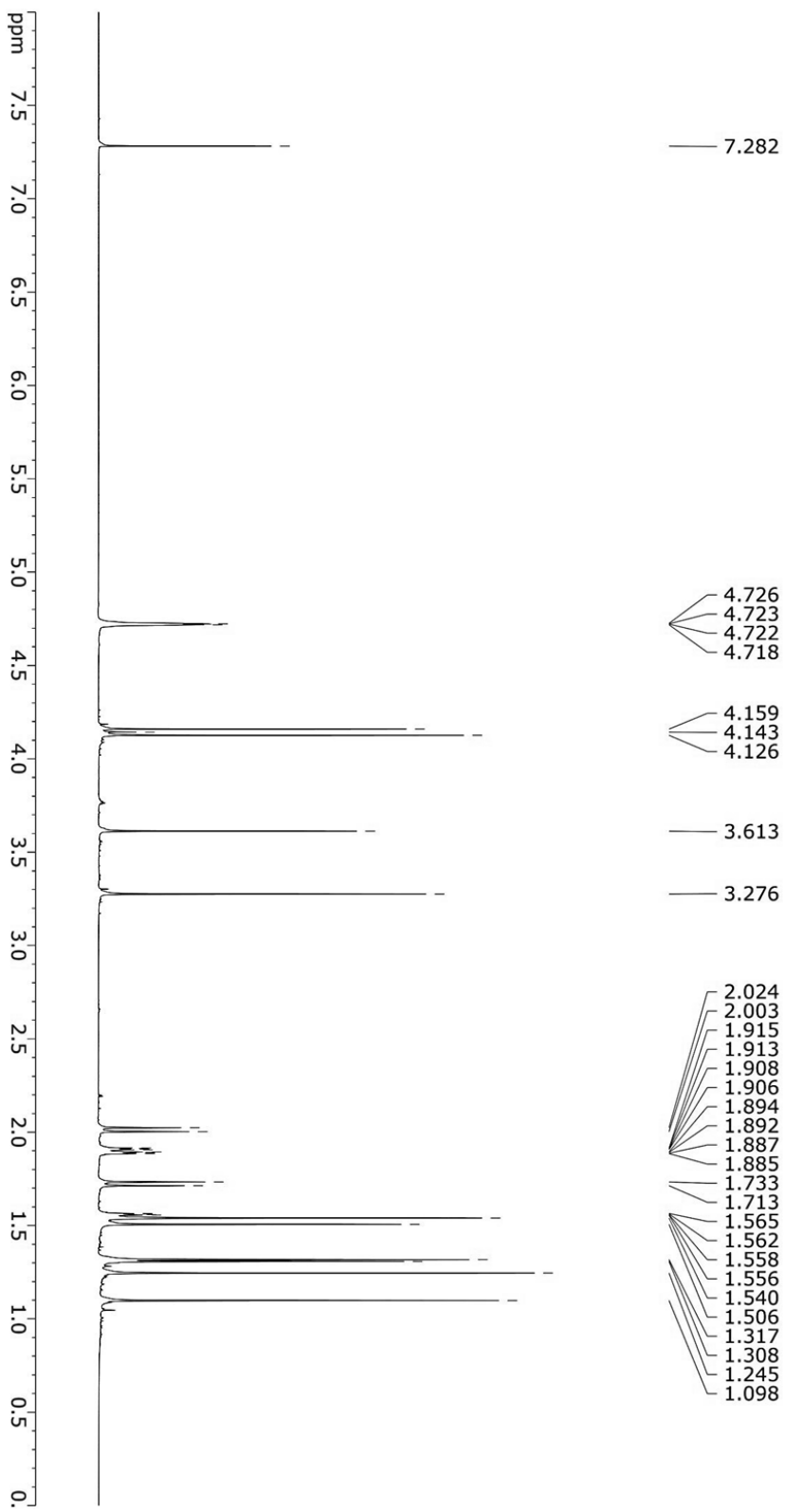
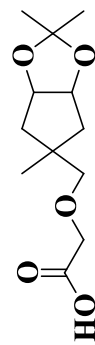
$^{13}\text{C}$ -NMR data for compound (**45**) Recorded on 700 MHz spectrometer ( $\text{CDCl}_3$ )



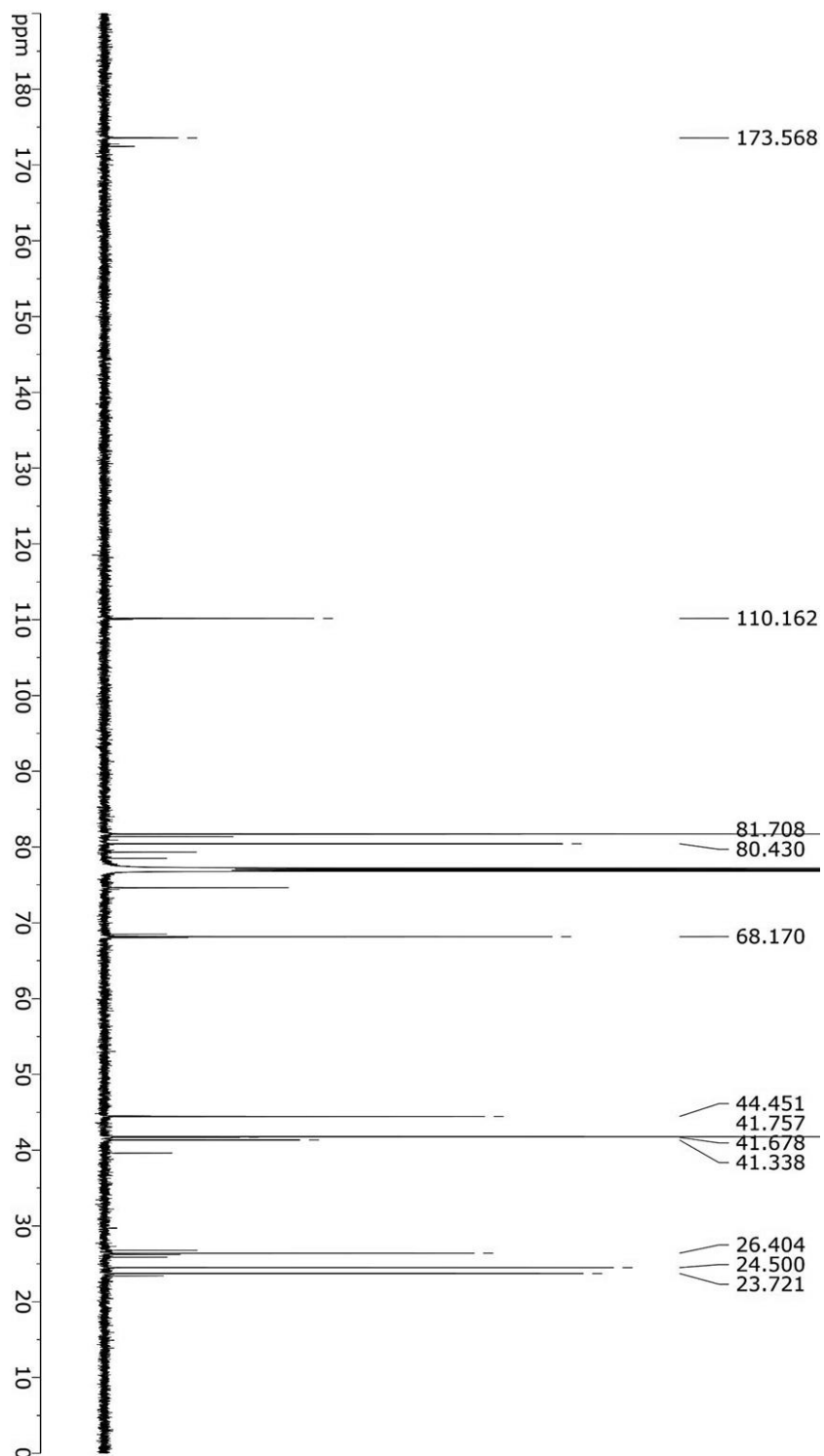




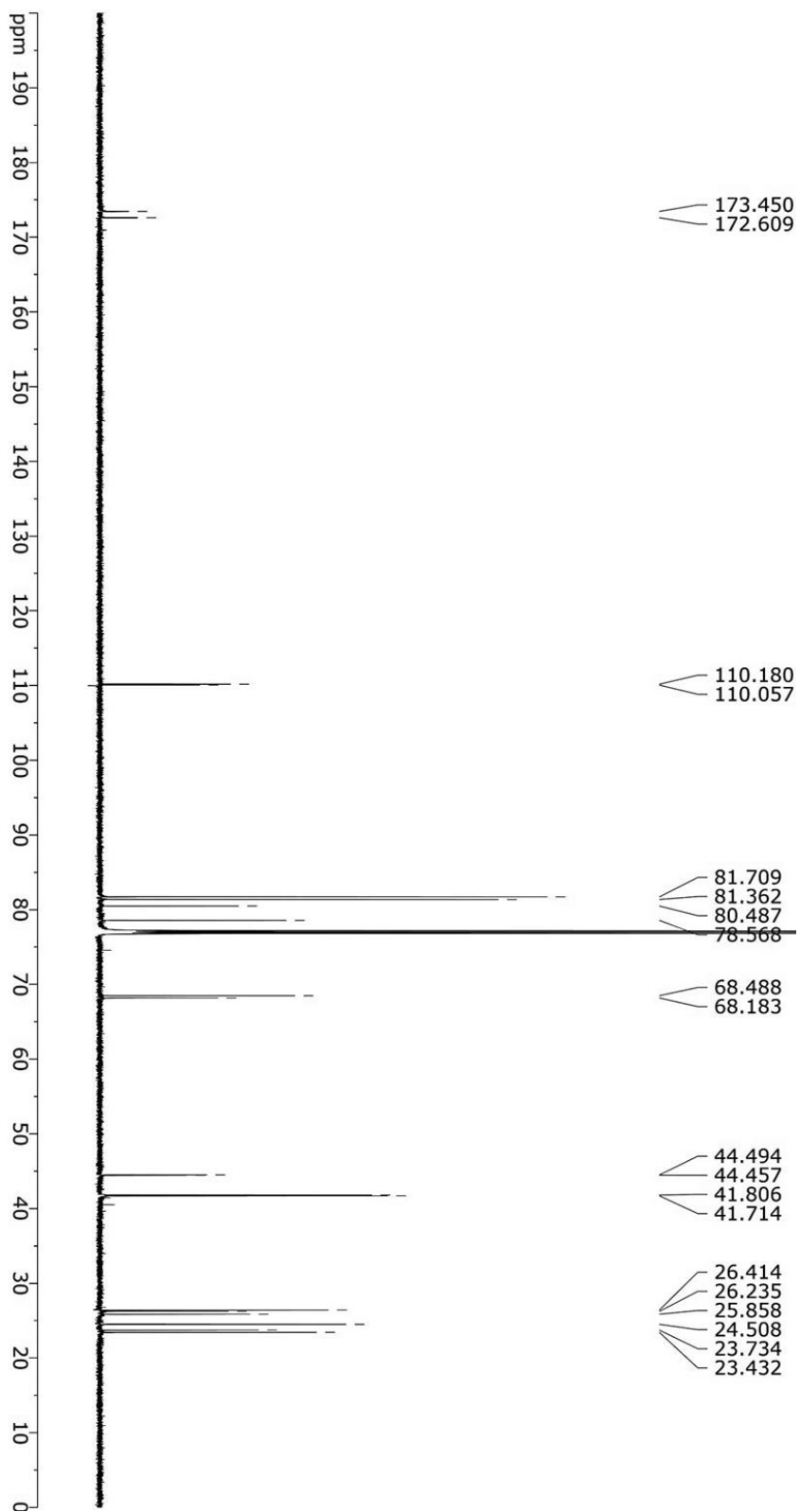
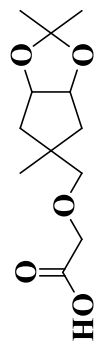
<sup>1</sup>H-NMR data for compound (**46**) Isomer II Mixture Recorded on 700 MHz spectrometer (CDCl<sub>3</sub>)



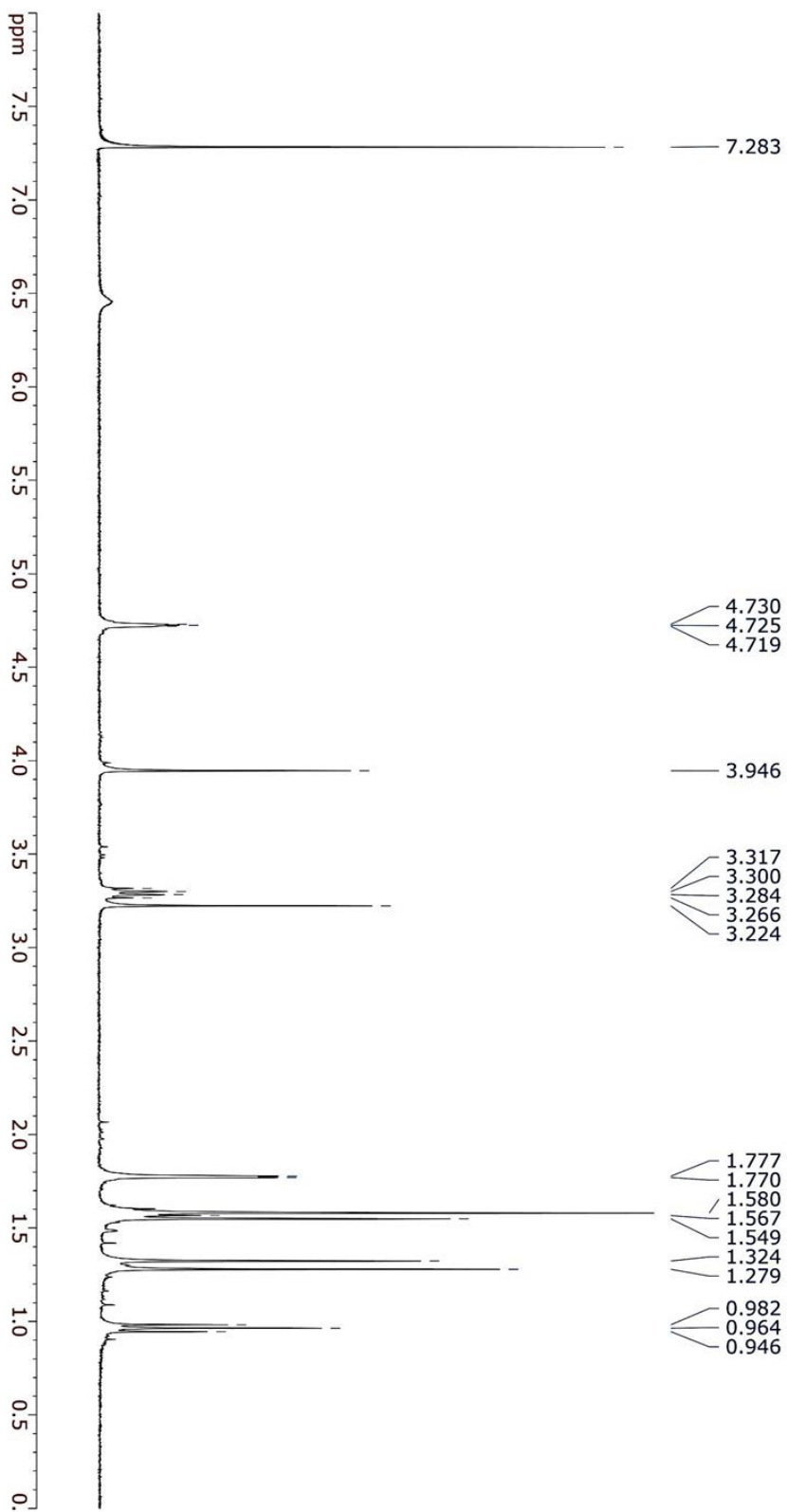
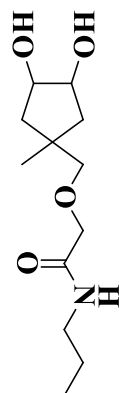
$^{13}\text{C}$ -NMR data for compound (**46**) Isomer I Recorded on 700 MHz spectrometer ( $\text{CDCl}_3$ )



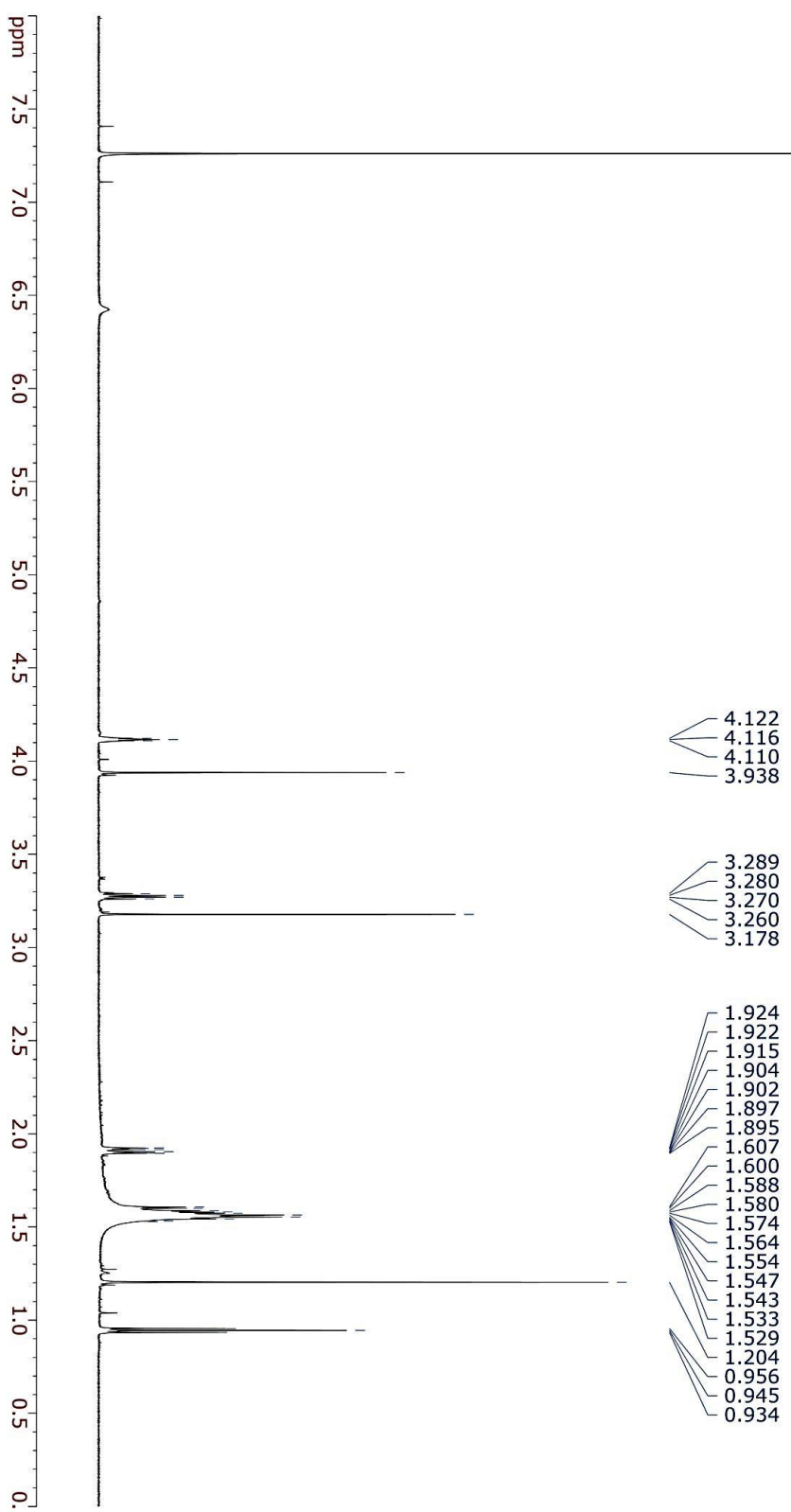
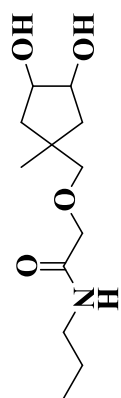
$^{13}\text{C}$ -NMR data for compound (46) Isomer mixture recorded on 700 MHz spectrometer ( $\text{CDCl}_3$ )



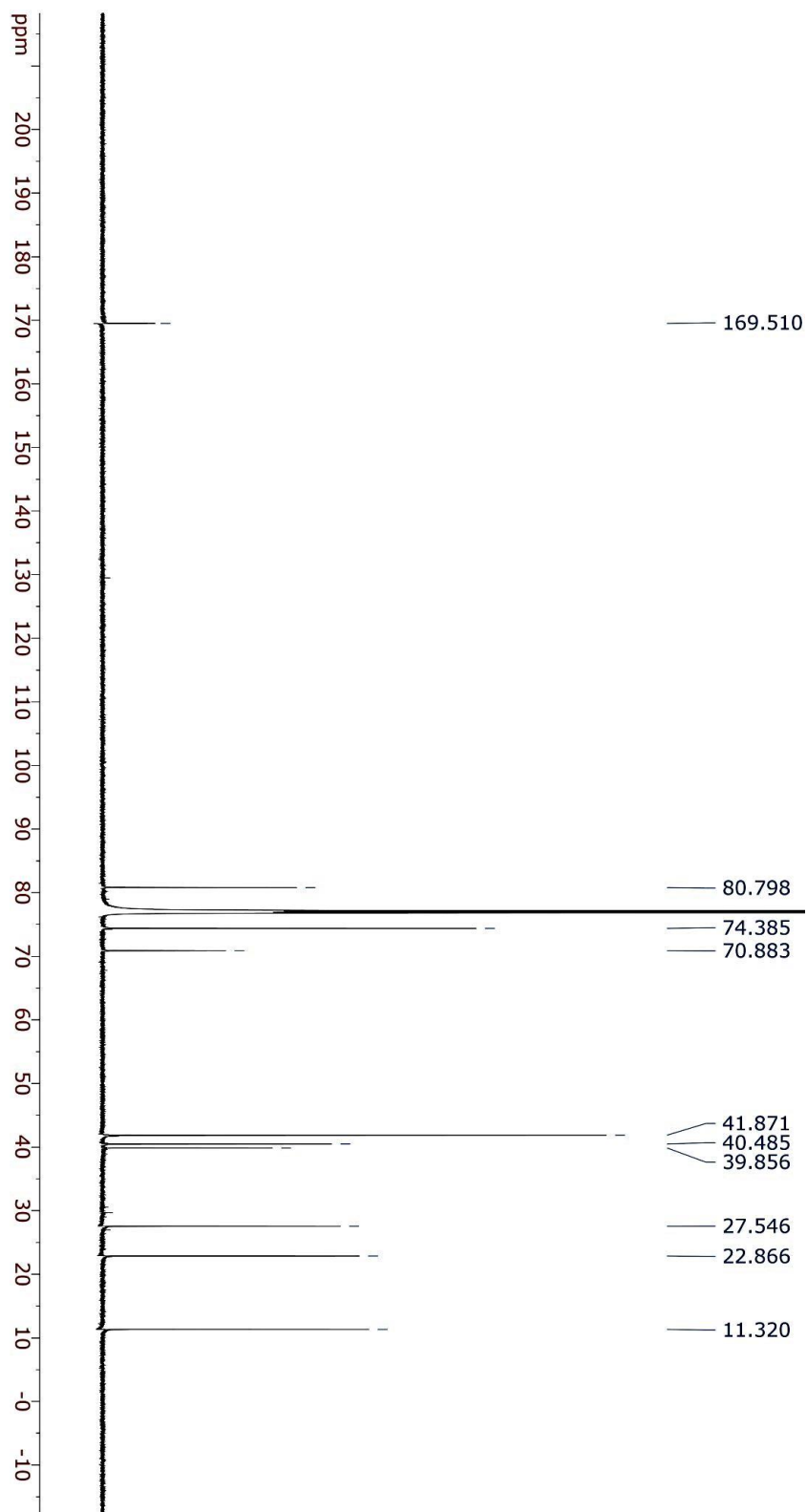
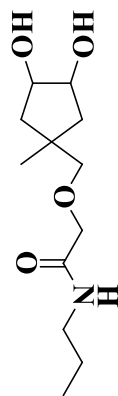
<sup>1</sup>H-NMR data for compound (48) Isomer I Recorded on 400 MHz spectrometer (CDCl<sub>3</sub>)



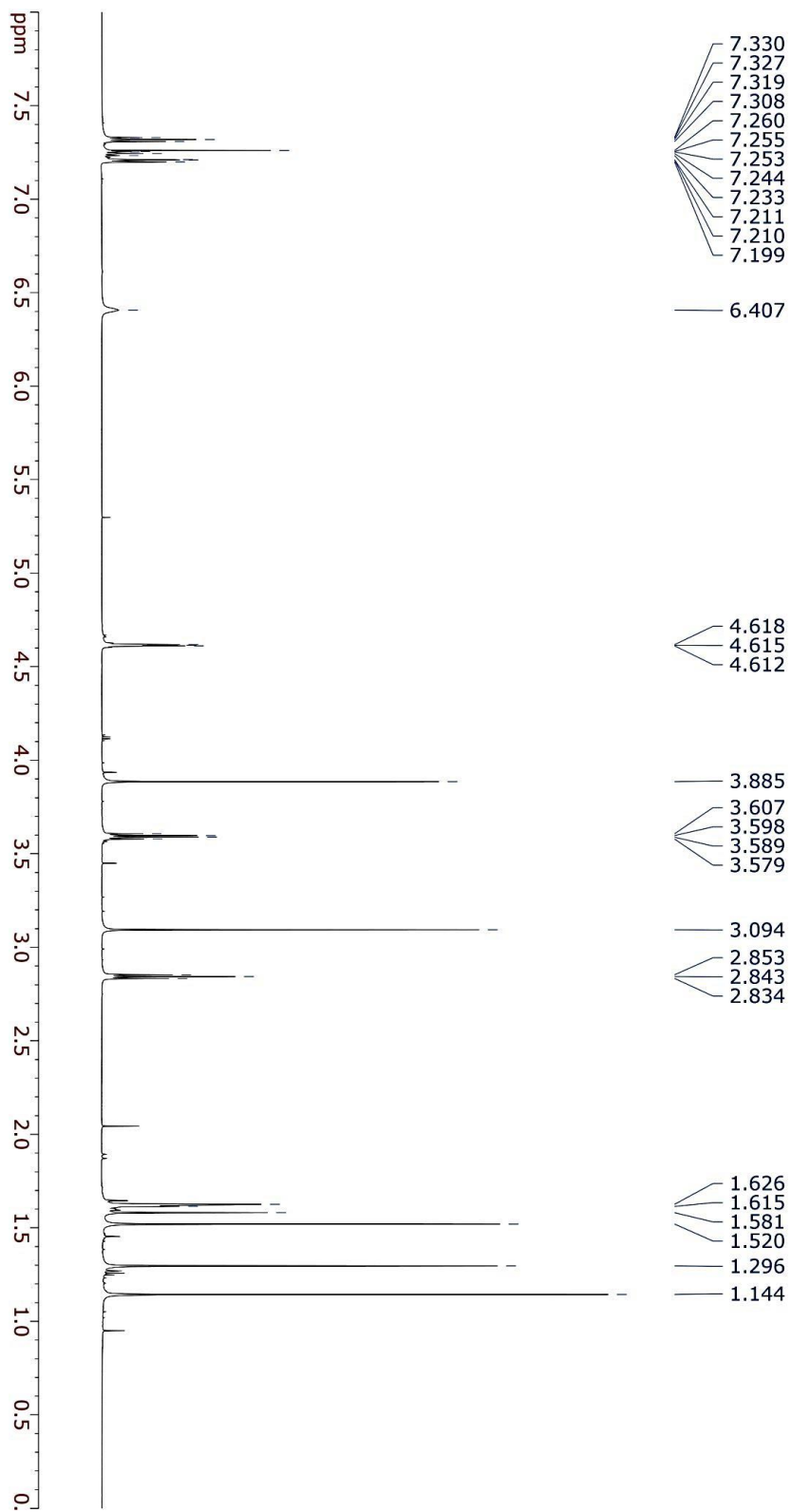
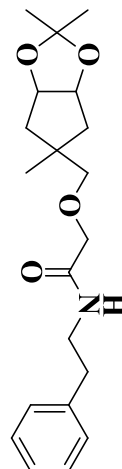
<sup>1</sup>H-NMR data for compound (**48**) Isomer II Recorded on 700 MHz spectrometer (CDCl<sub>3</sub>)



$^{13}\text{C}$ -NMR data for compound (48) Recorded on 700 MHz spectrometer ( $\text{CDCl}_3$ )

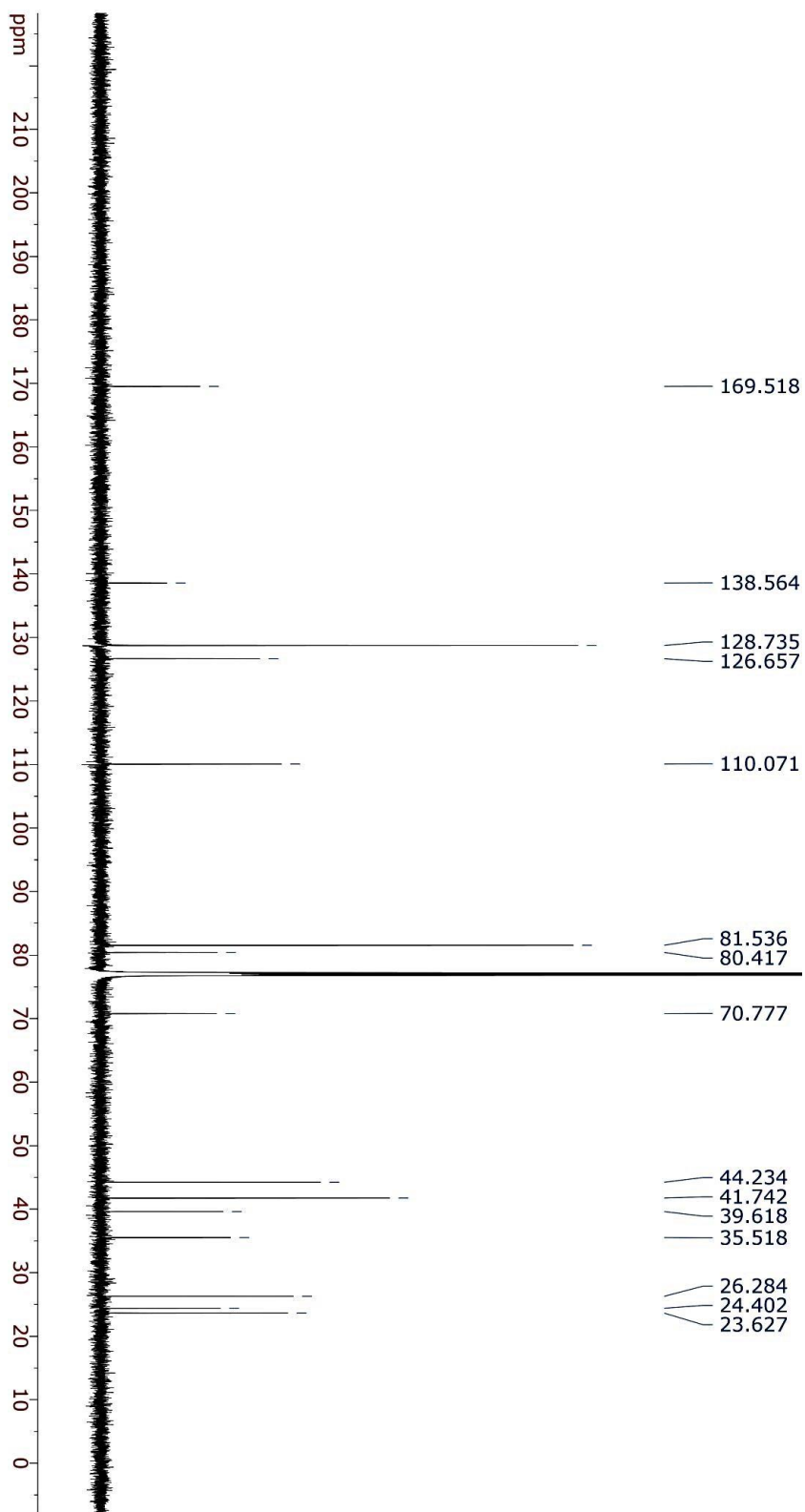
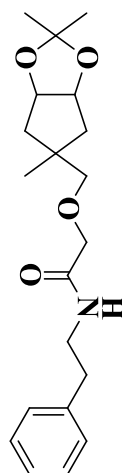


<sup>1</sup>H-NMR data for compound (**51**) Recorded on 700 MHz spectrometer (CDCl<sub>3</sub>)

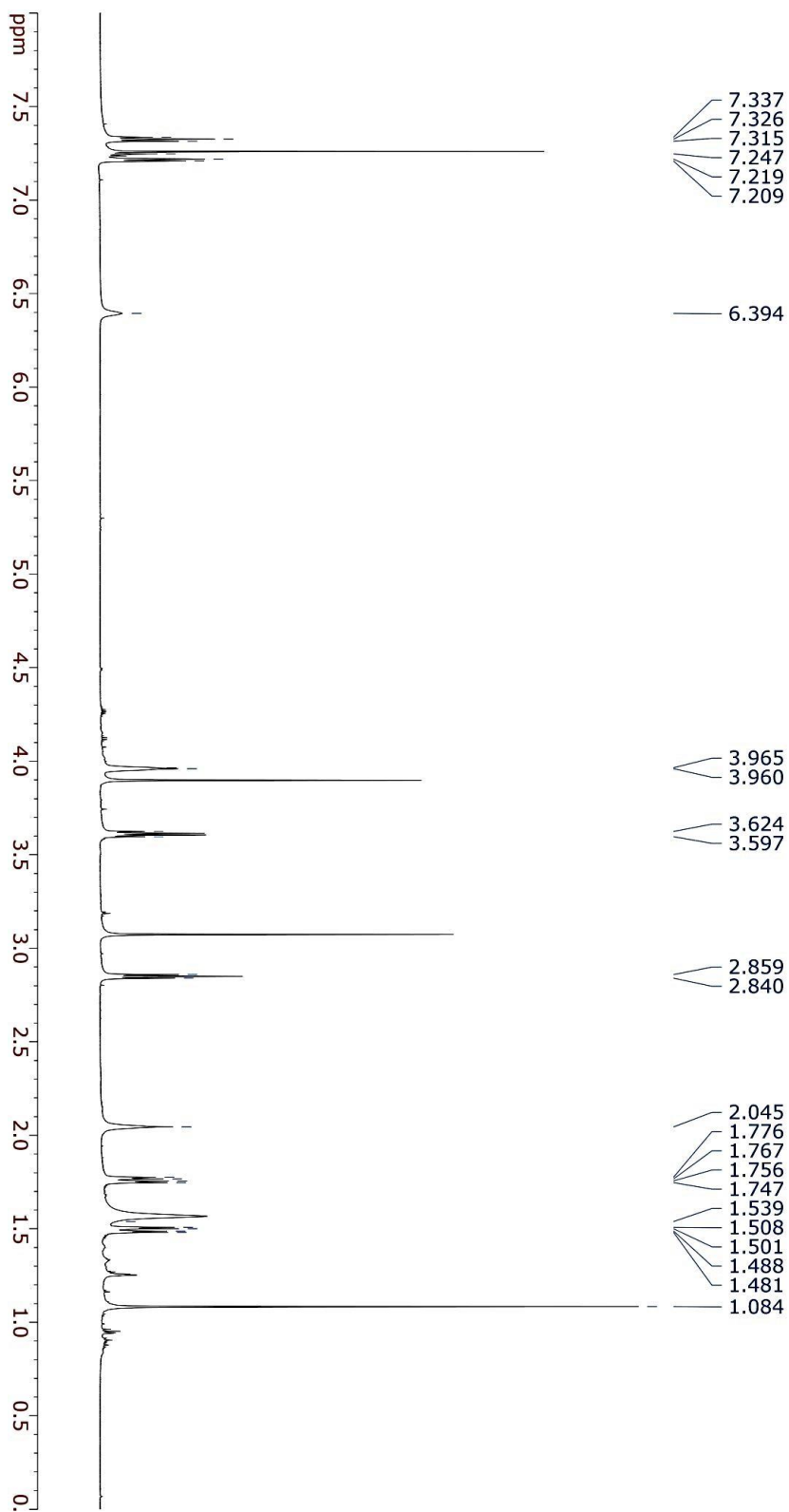
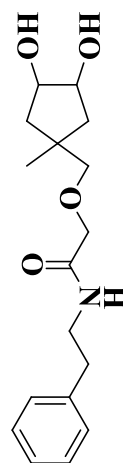




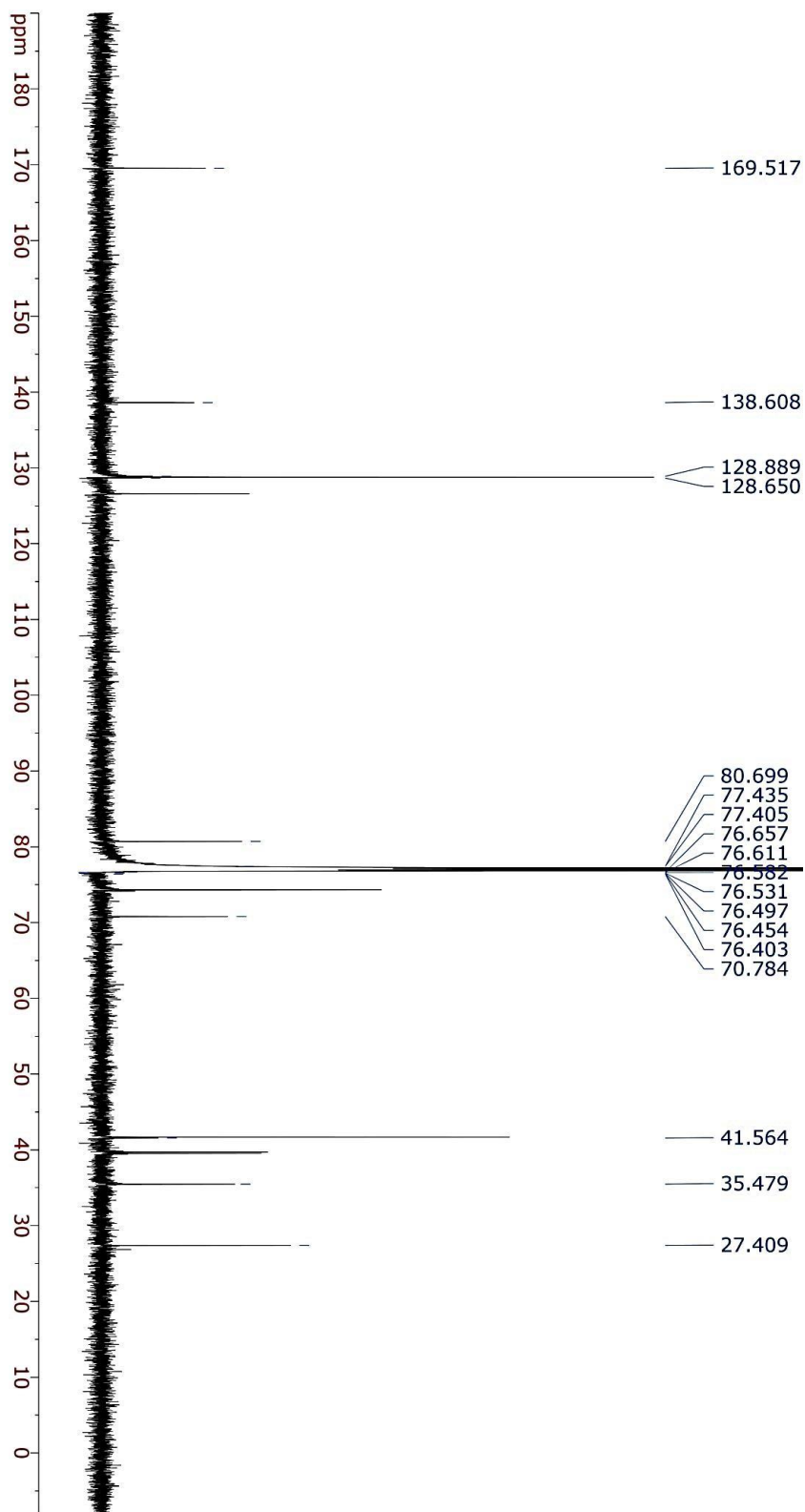
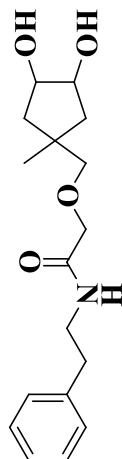
$^{13}\text{C}$ -NMR data for compound (**51**) Recorded on 700 MHz spectrometer ( $\text{CDCl}_3$ )



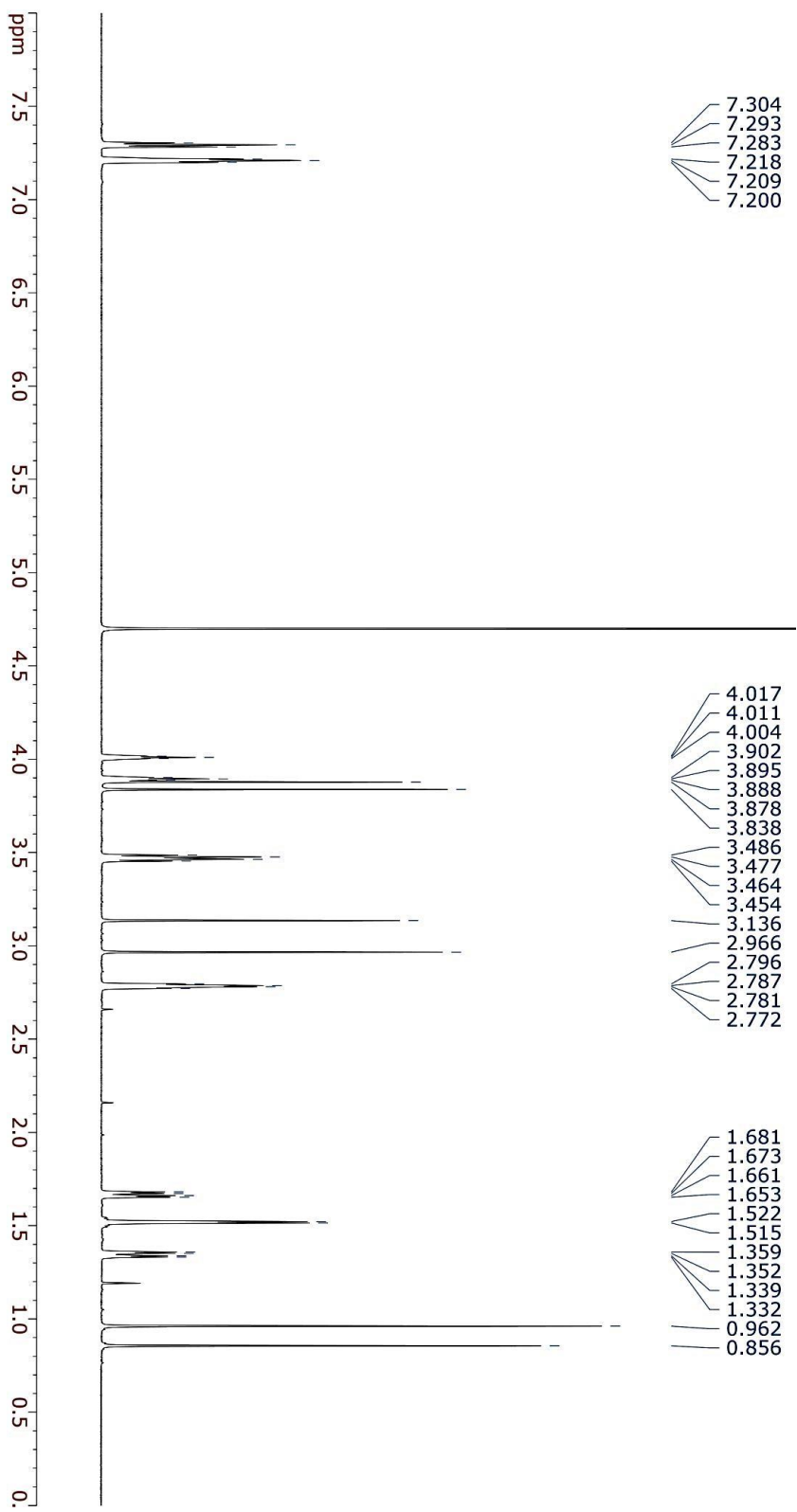
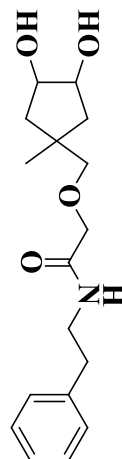
<sup>1</sup>H-NMR data for compound (**52**) Recorded on 700 MHz spectrometer (CDCl<sub>3</sub>)



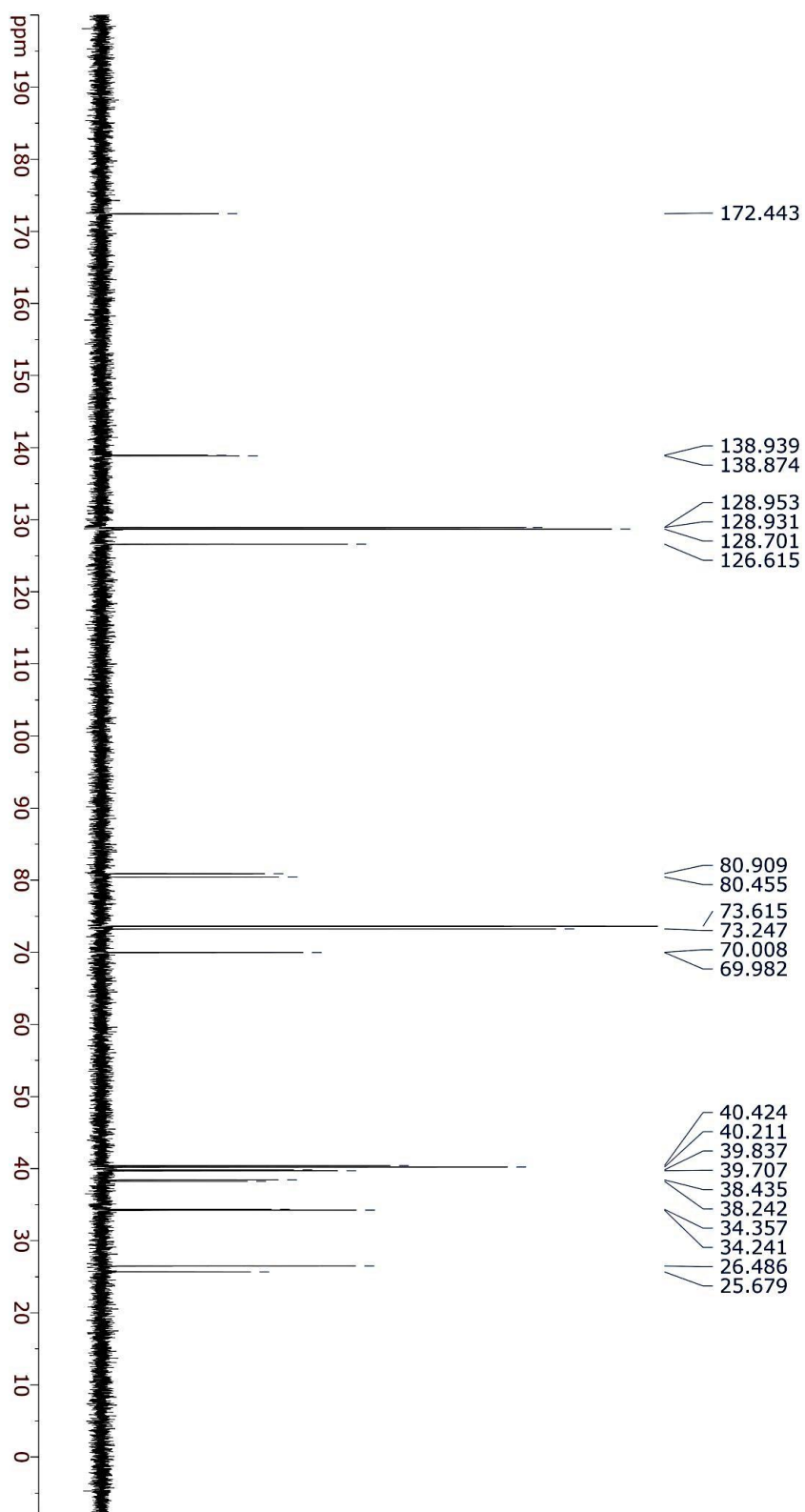
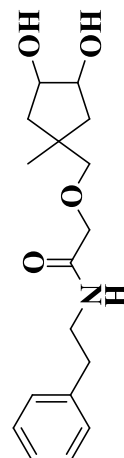
$^{13}\text{C}$ -NMR data for compound (**52**) Recorded on 700 MHz spectrometer ( $\text{CDCl}_3$ )



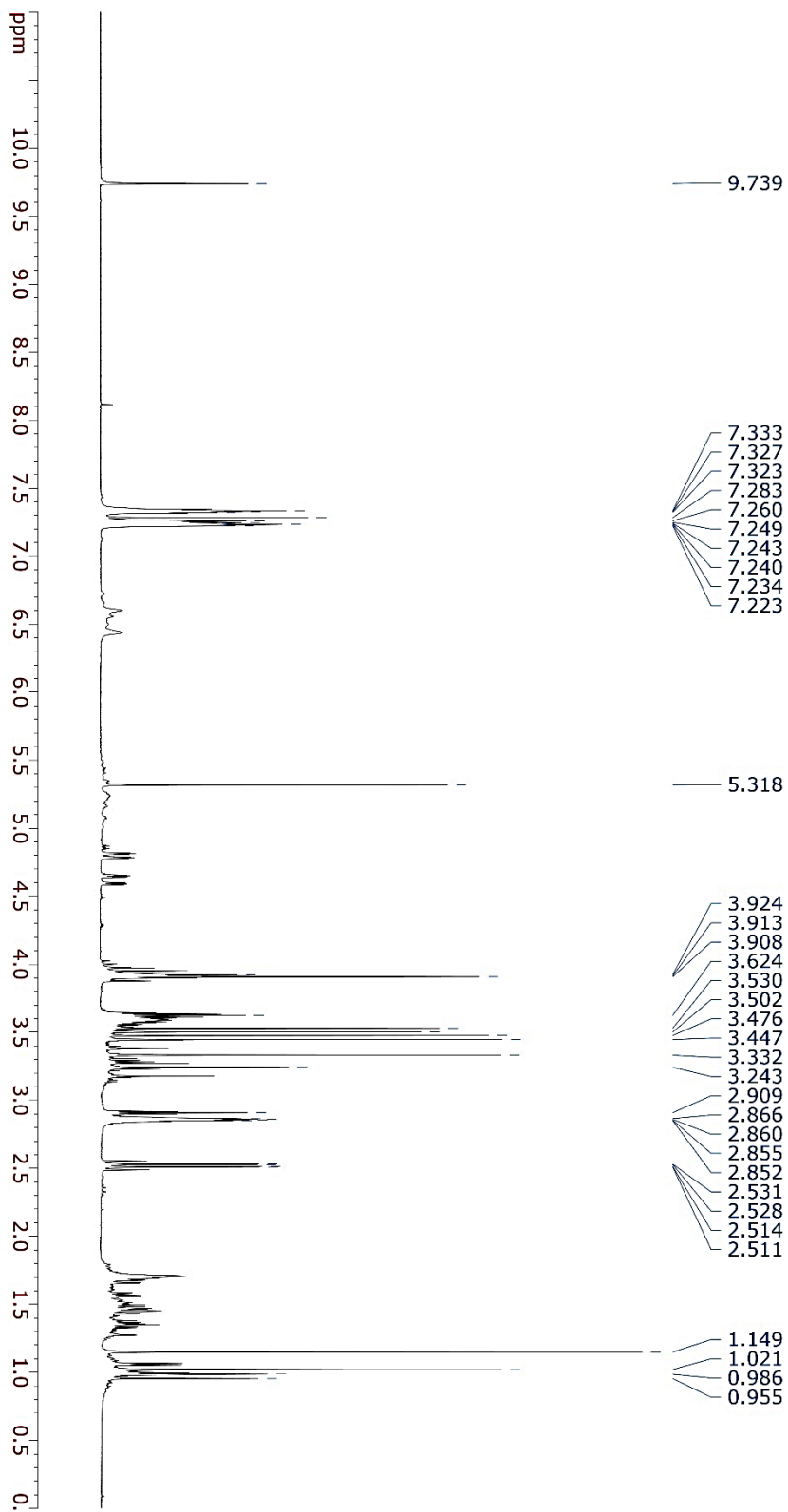
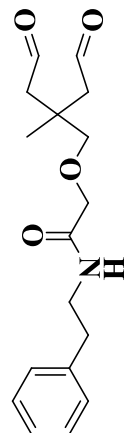
<sup>1</sup>H-NMR data for compound (**52**) Recorded on 700 MHz spectrometer (D<sub>2</sub>O)



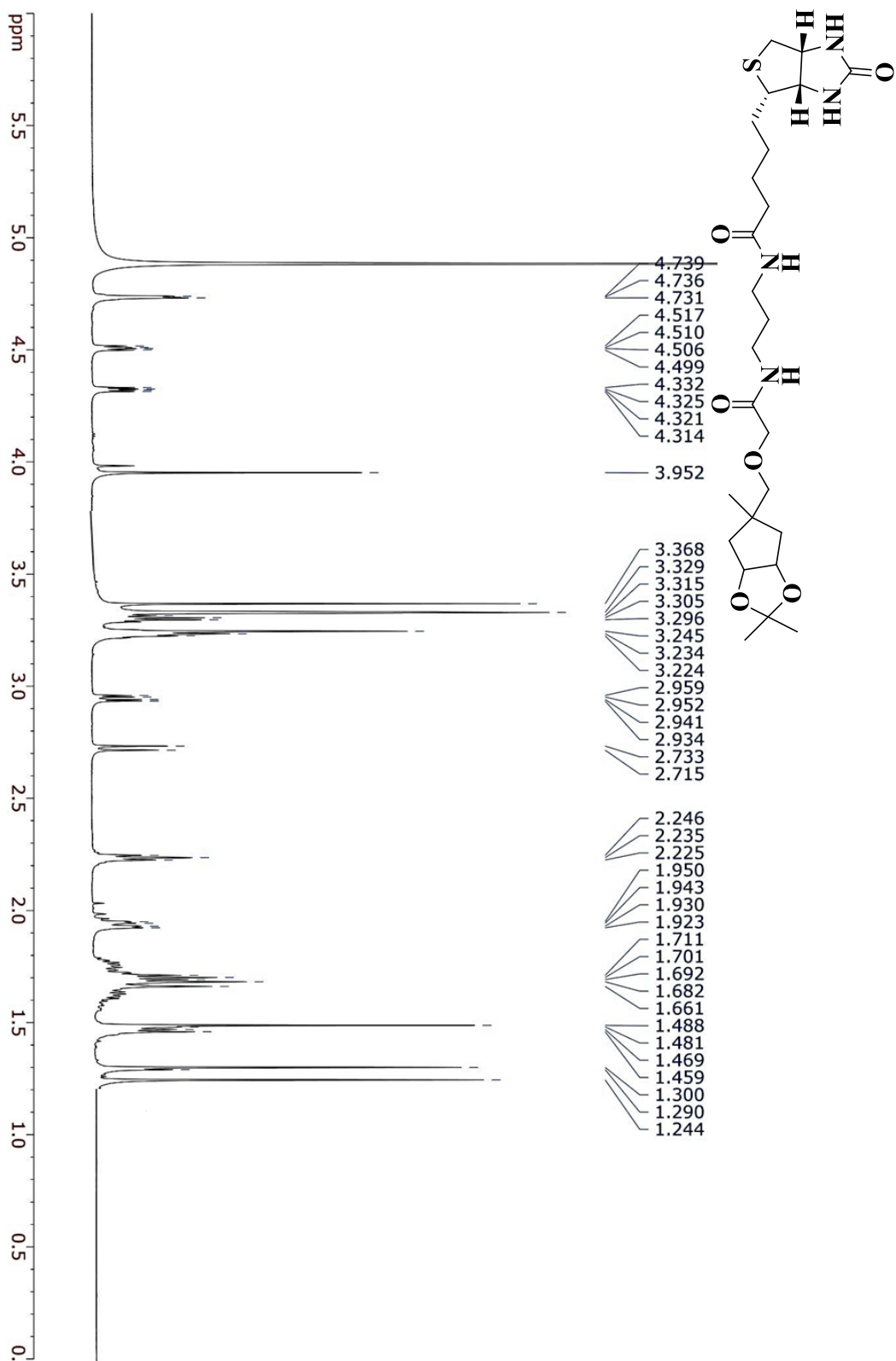
$^{13}\text{C}$ -NMR data for compound (**52**) Recorded on 700 MHz spectrometer ( $\text{D}_2\text{O}$ )



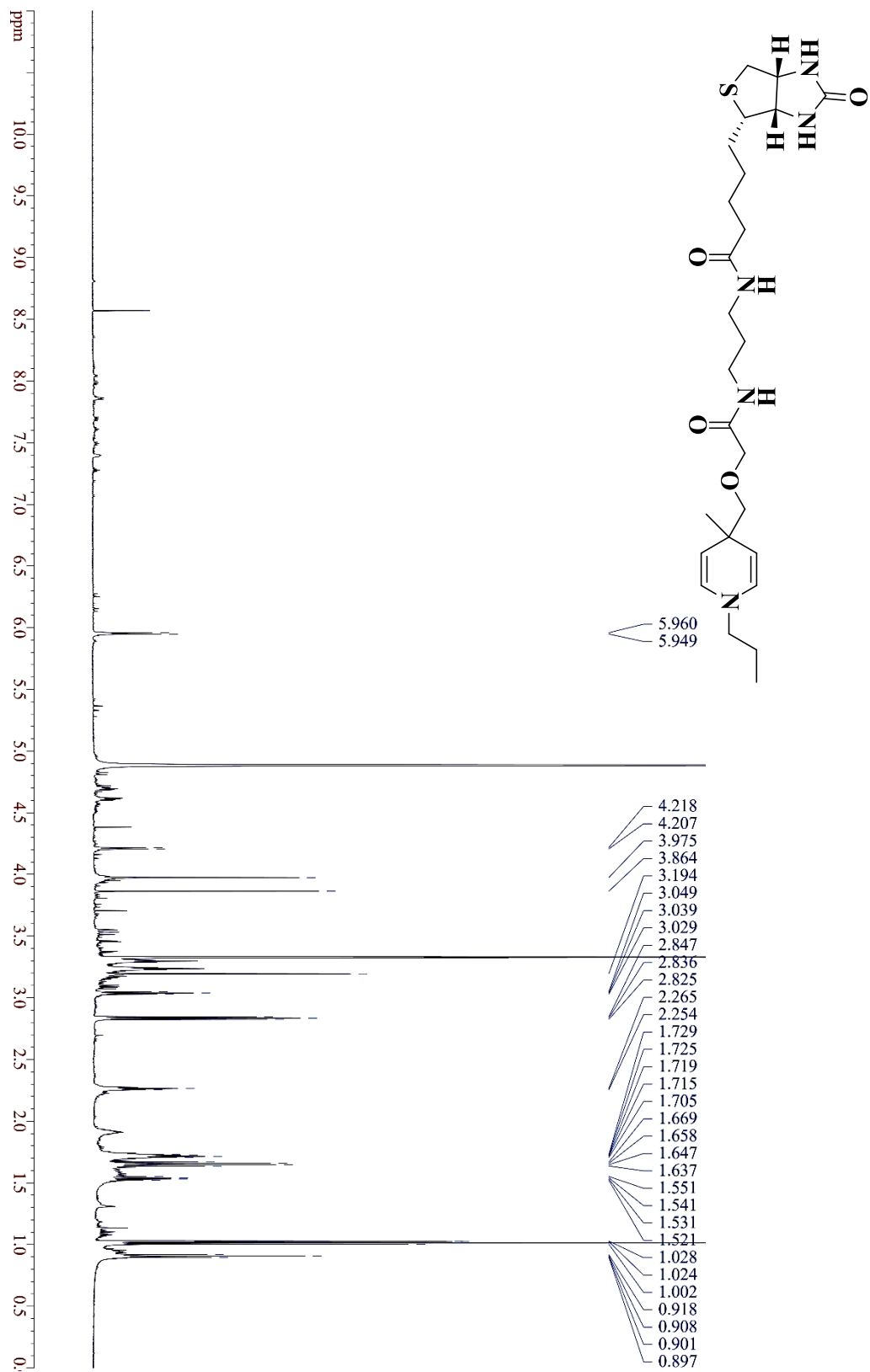
<sup>1</sup>H-NMR data for compound (**53**) Recorded on 700 MHz spectrometer (CDCl<sub>3</sub>)



<sup>1</sup>H-NMR data for compound (**55**) Recorded on 700 MHz spectrometer (MeOD)

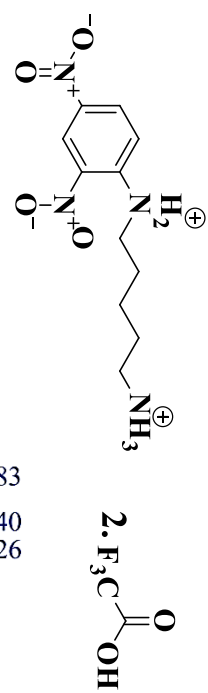


<sup>1</sup>H-NMR data for compound (**Attempted Conjugation 58**) Recorded on 700 MHz spectrometer





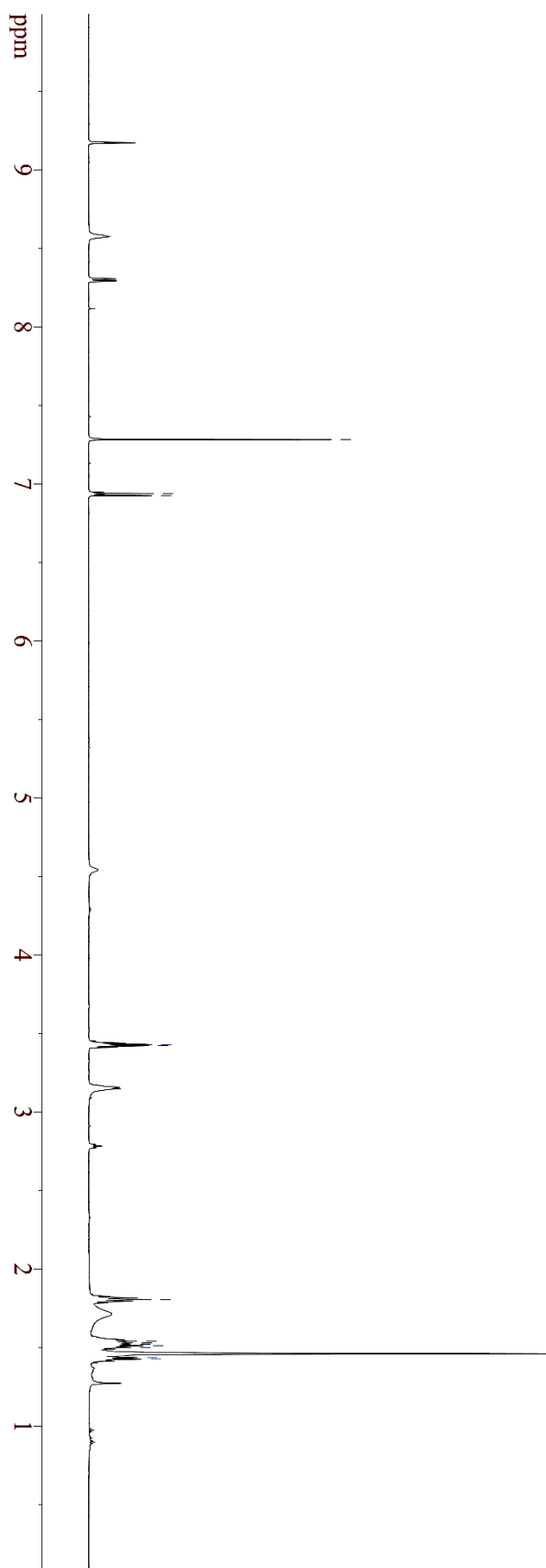
<sup>1</sup>H-NMR data for compound (**59**) Recorded on 700 MHz spectrometer (CDCl<sub>3</sub>)



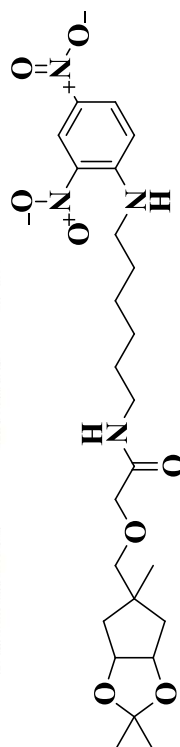
7.283  
6.940  
6.926

3.431  
3.424

1.808  
1.543  
1.533  
1.525  
1.523  
1.514  
1.503  
1.438  
1.428



<sup>1</sup>H-NMR data for compound (**60**) Recorded on 700 MHz spectrometer (CDCl<sub>3</sub>)

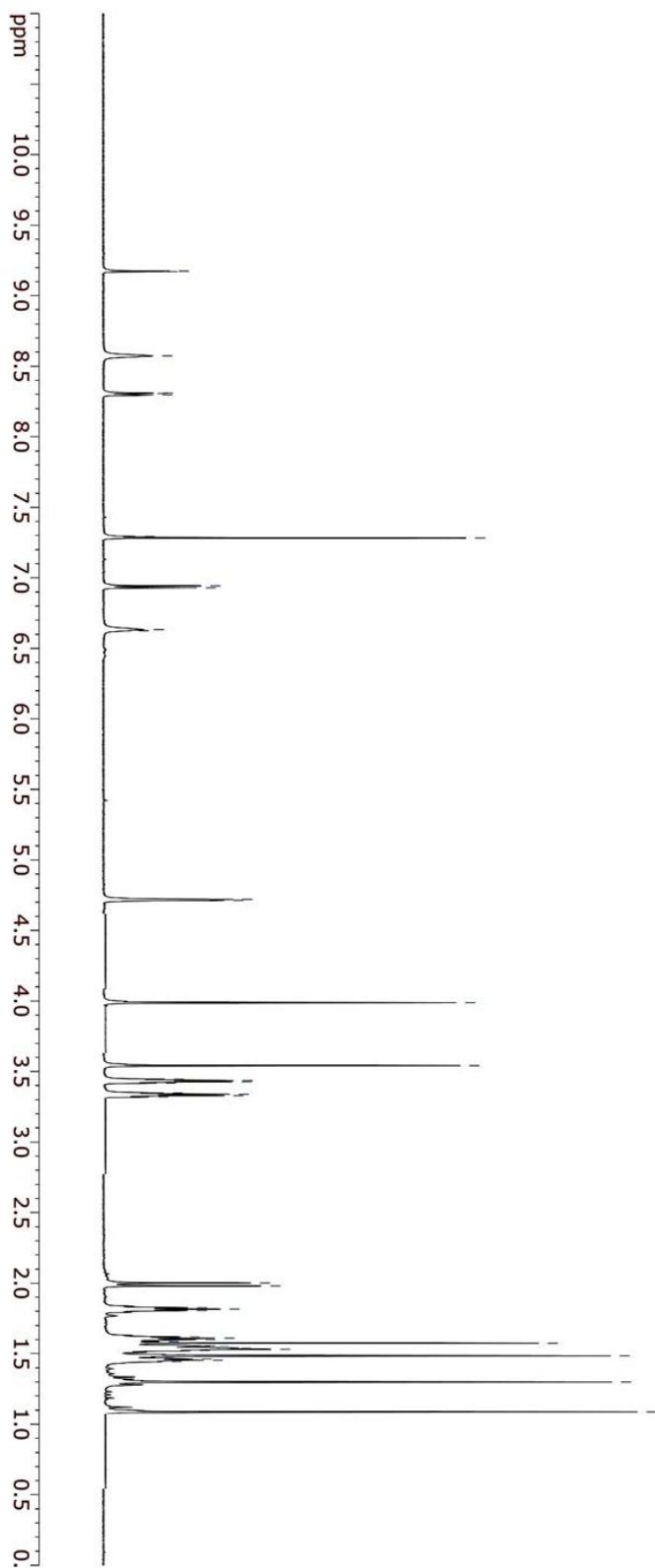


9.174  
9.171

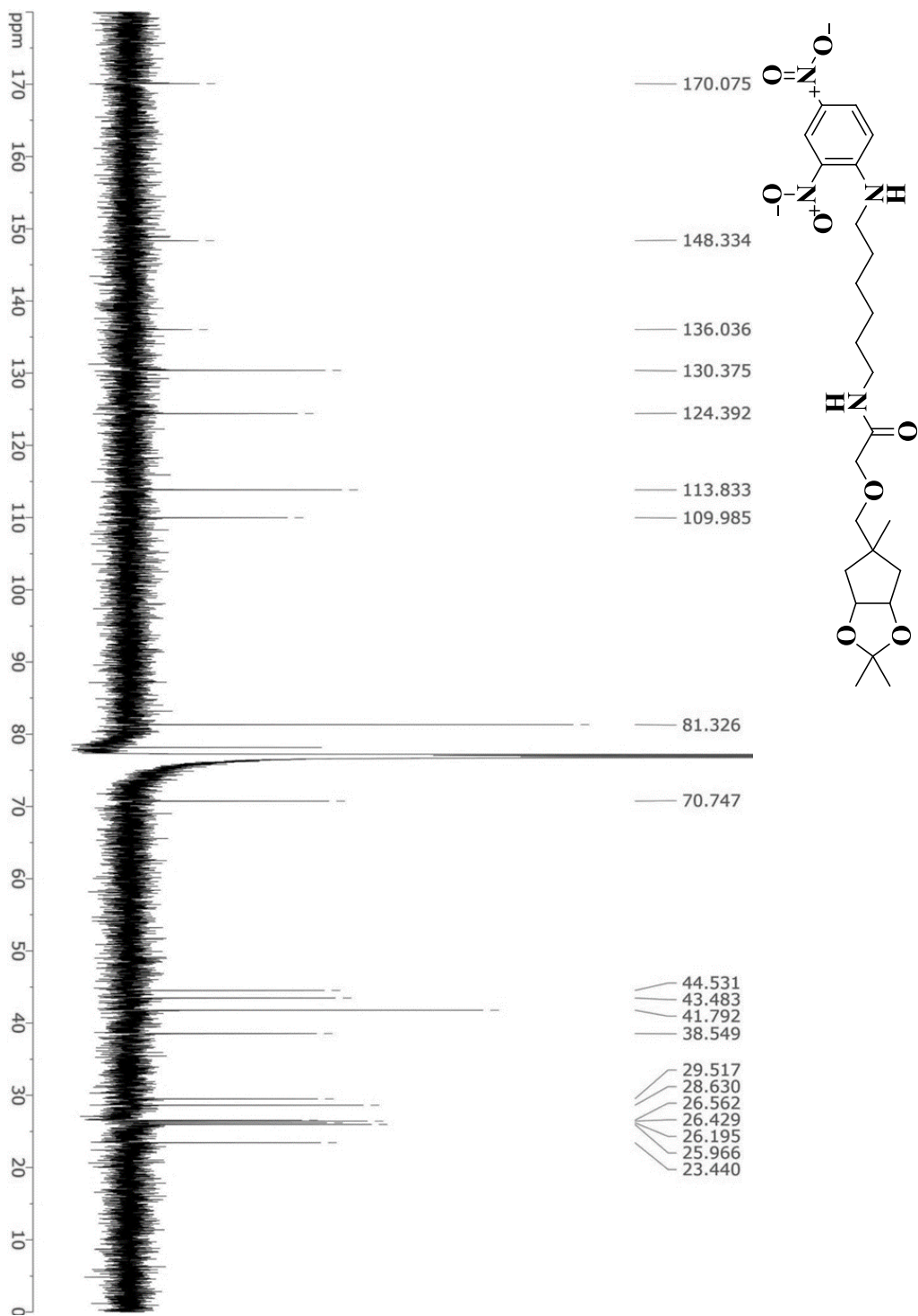
8.573  
8.310  
8.307  
8.296

7.293  
7.290  
7.282  
6.943  
6.929  
6.633  
6.625

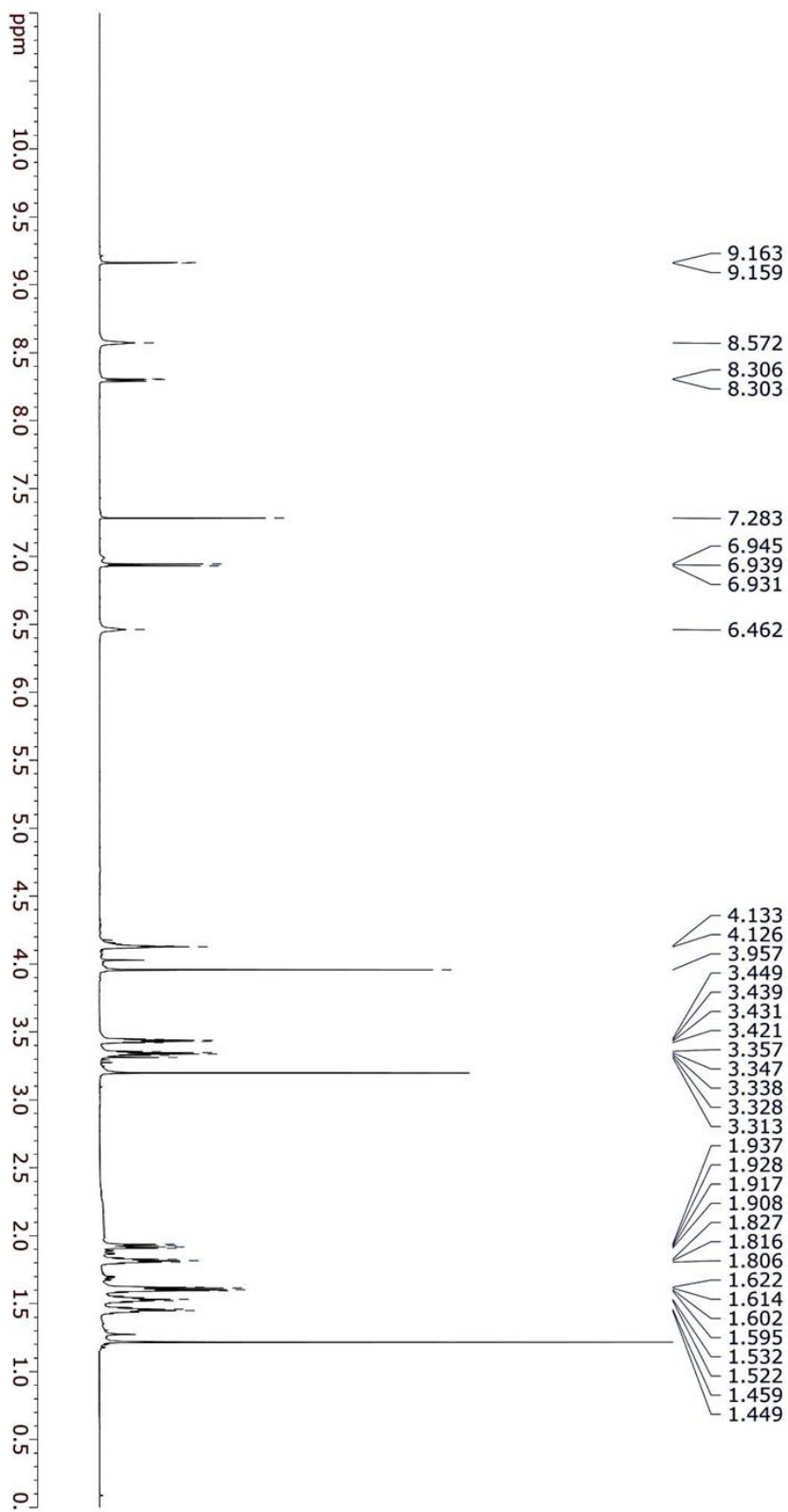
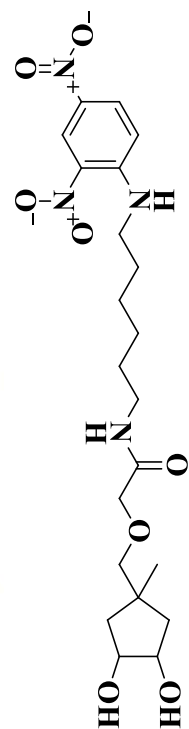
4.720  
4.713  
3.988  
3.542  
3.446  
3.437  
3.428  
3.418  
3.348  
3.339  
3.329  
3.319  
2.001  
1.980  
1.826  
1.815  
1.805  
1.619  
1.609  
1.598  
1.587  
1.585  
1.574  
1.556  
1.552  
1.542  
1.537  
1.531  
1.521  
1.493  
1.485  
1.476  
1.464  
1.453  
1.443  
1.299  
1.087



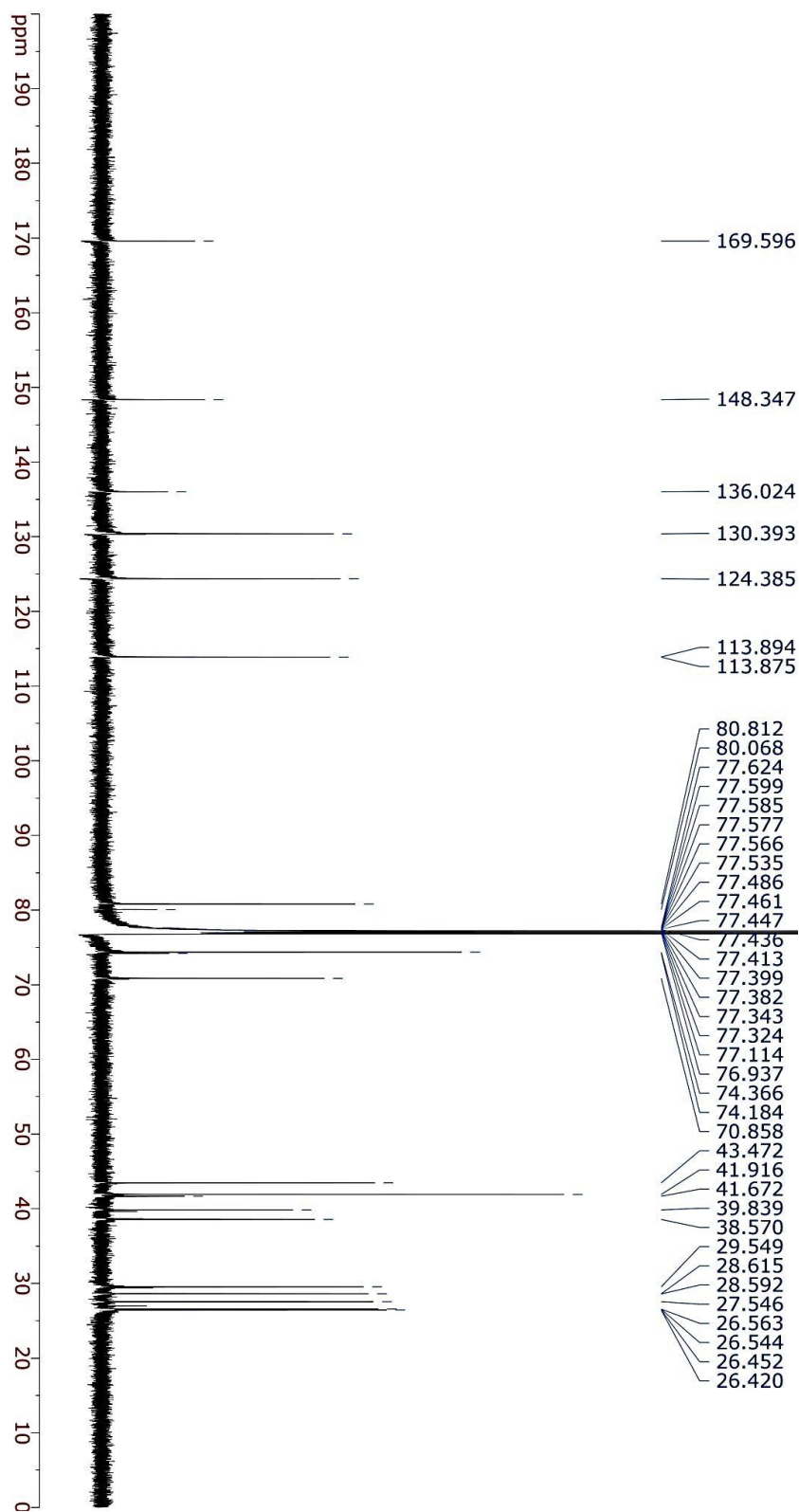
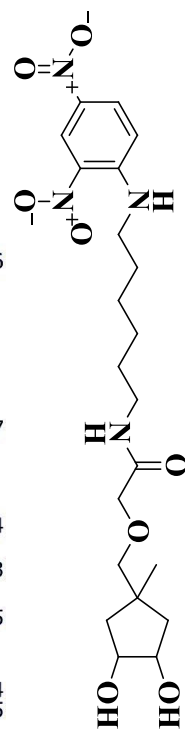
$^{13}\text{C}$ -NMR data for compound (**60**) Recorded on 700 MHz spectrometer ( $\text{CDCl}_3$ )



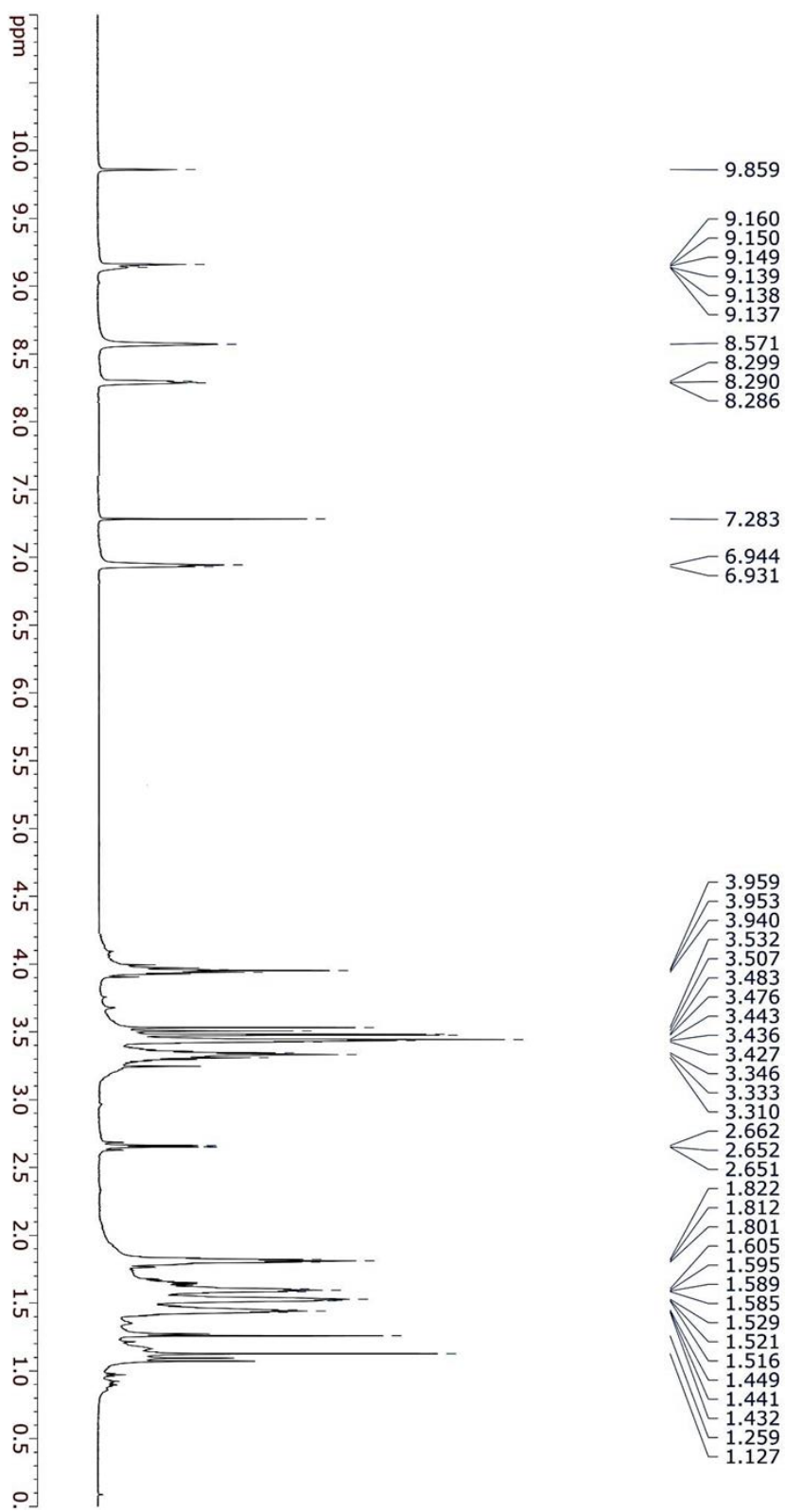
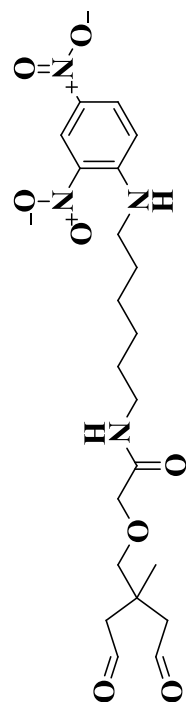
<sup>1</sup>H-NMR data for compound (**61**) Recorded on 700 MHz spectrometer (CDCl<sub>3</sub>)



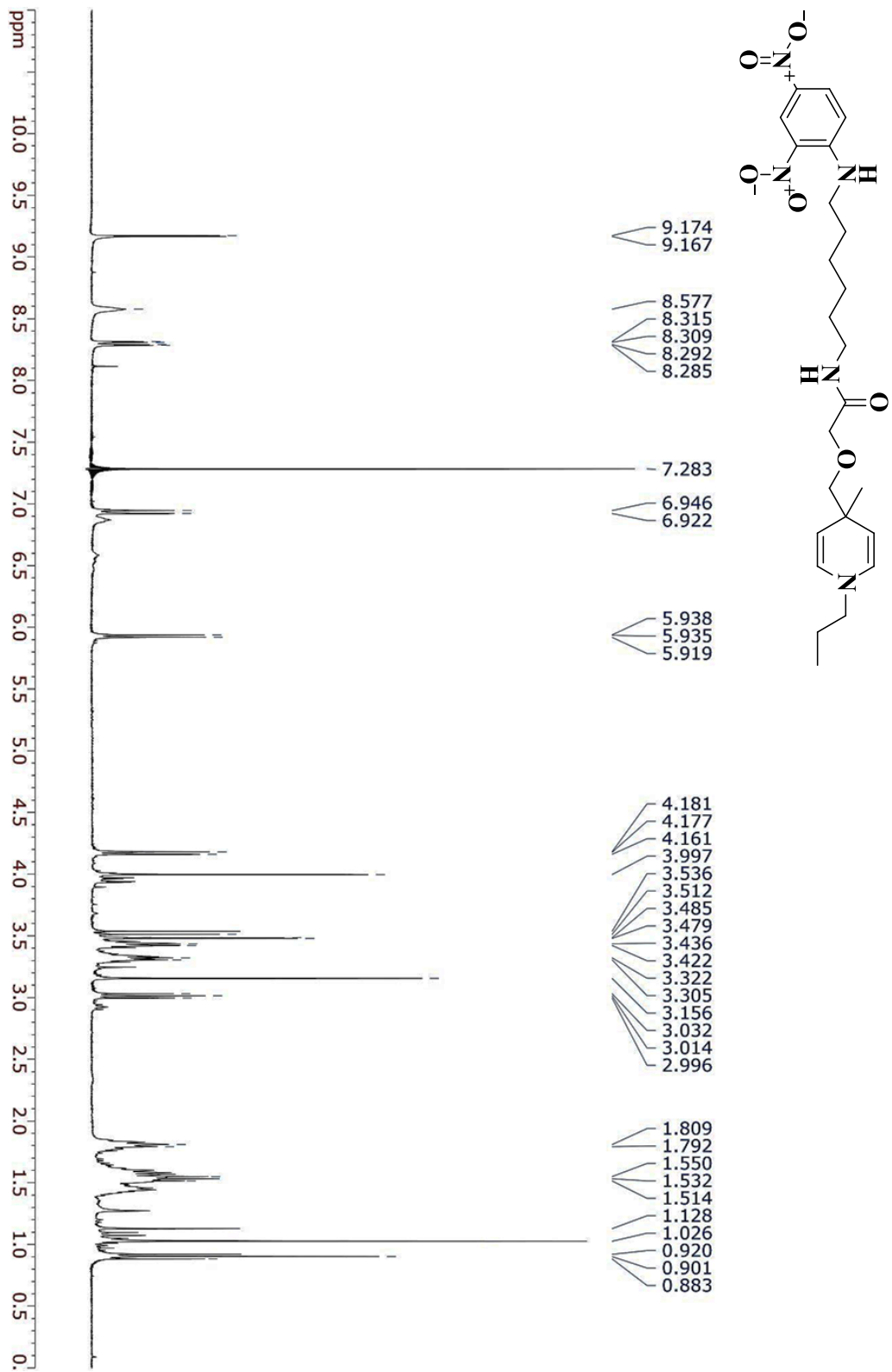
$^{13}\text{C}$ -NMR data for compound (**61**) Recorded on 700 MHz spectrometer ( $\text{CDCl}_3$ )



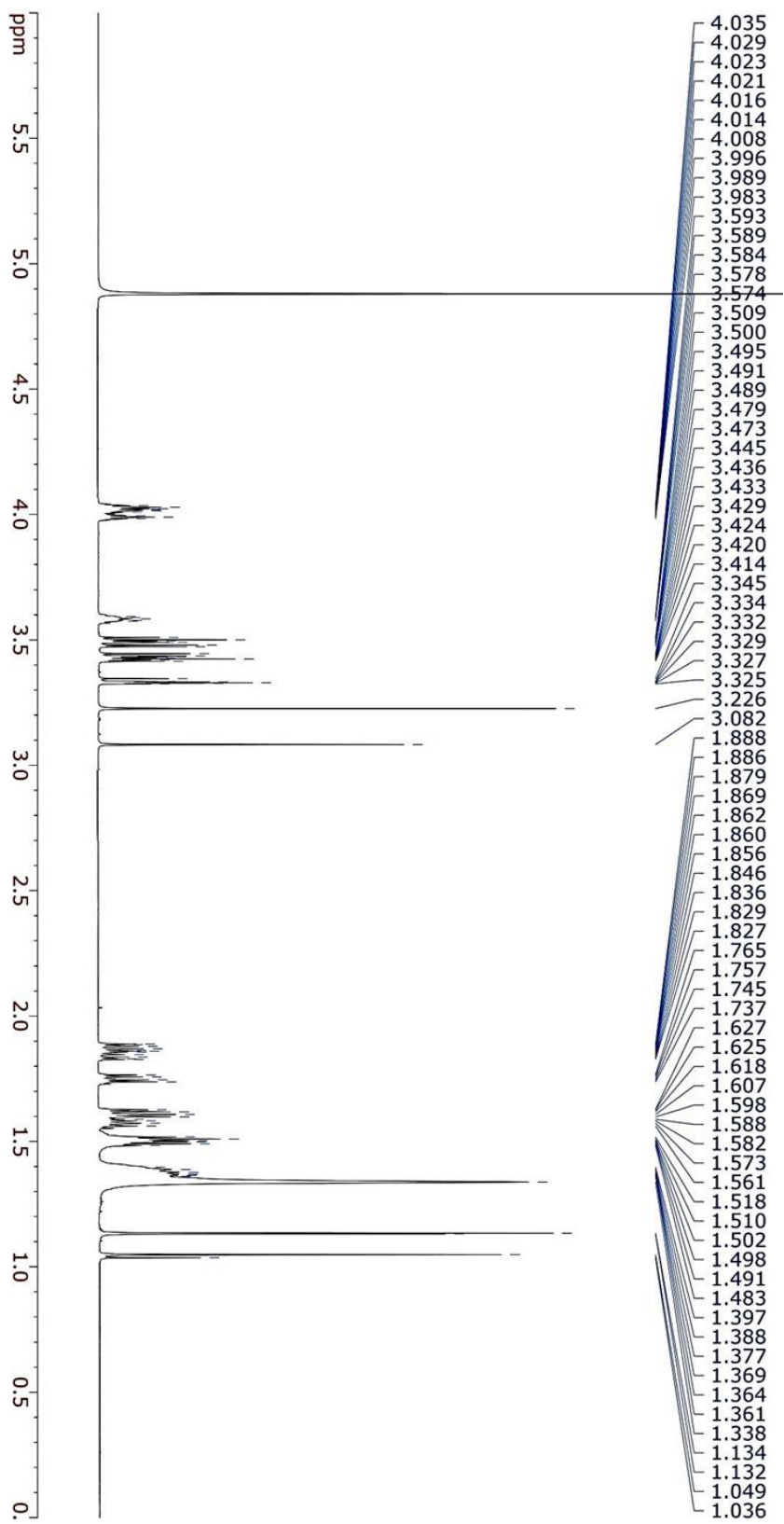
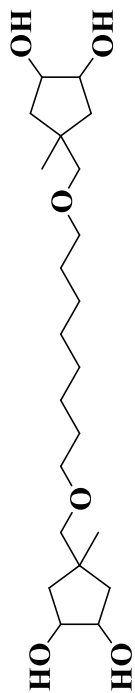
<sup>1</sup>H-NMR data for compound (**62**) Recorded on 700 MHz spectrometer (CDCl<sub>3</sub>)



<sup>1</sup>H-NMR data for compound (**Attempted Conjugation 63**) Recorded on 700 MHz spectrometer

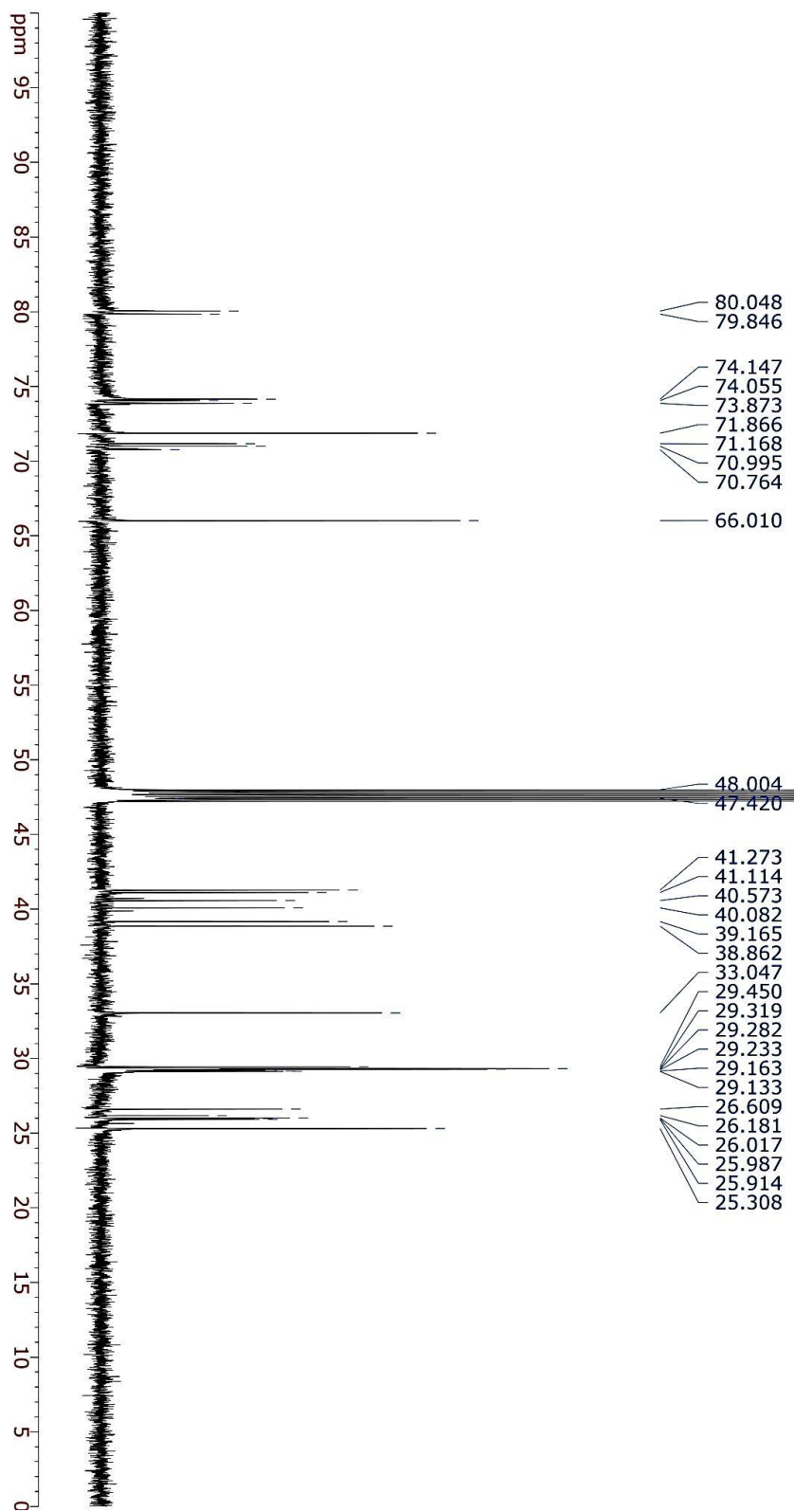
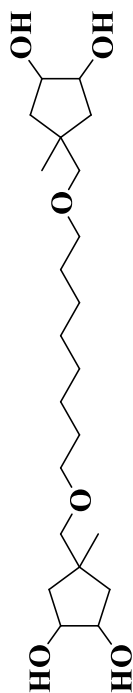


<sup>1</sup>H-NMR data for compound (**65**) Recorded on 700 MHz spectrometer (MeOD)

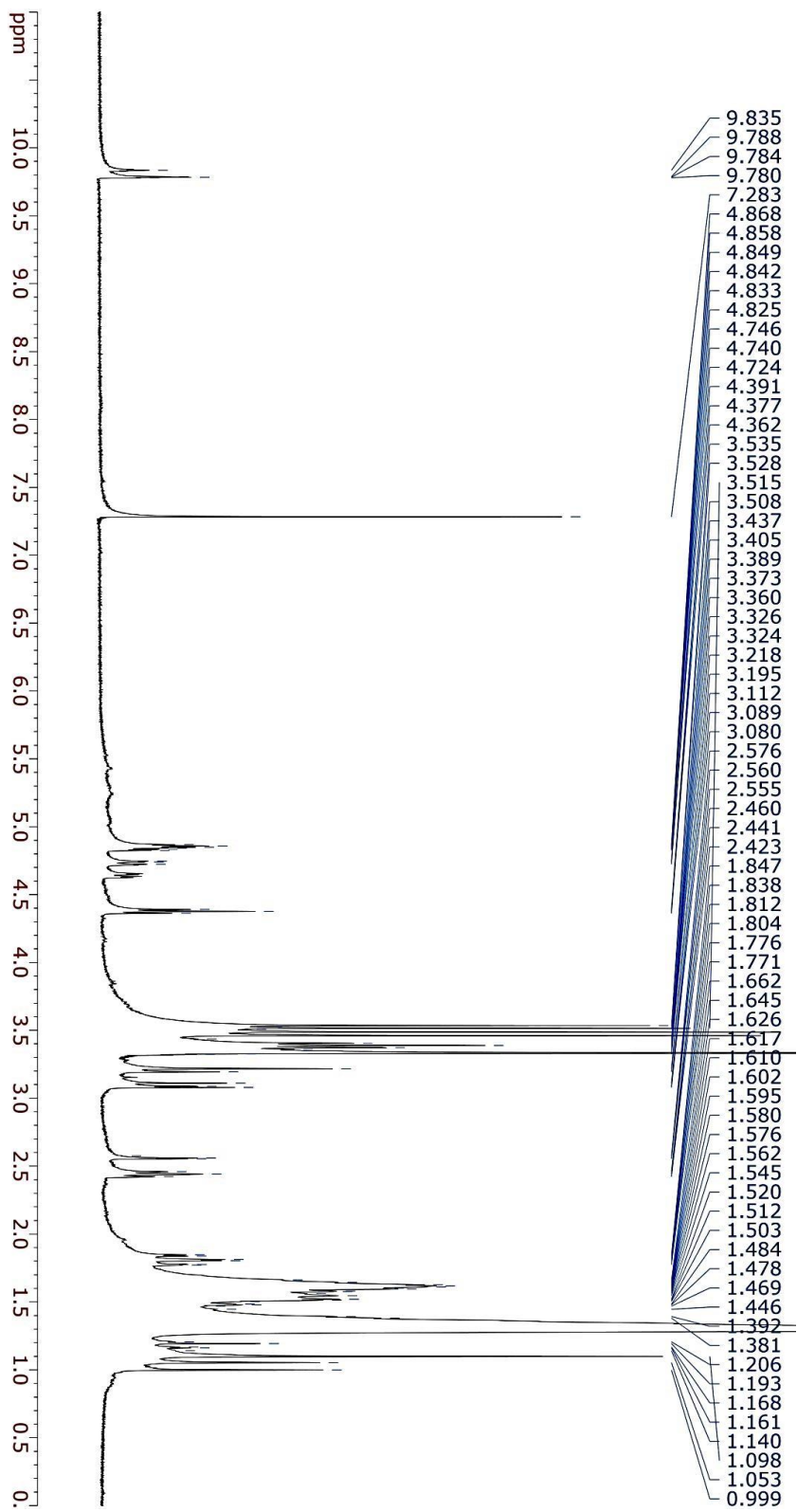
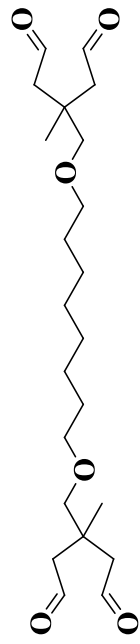




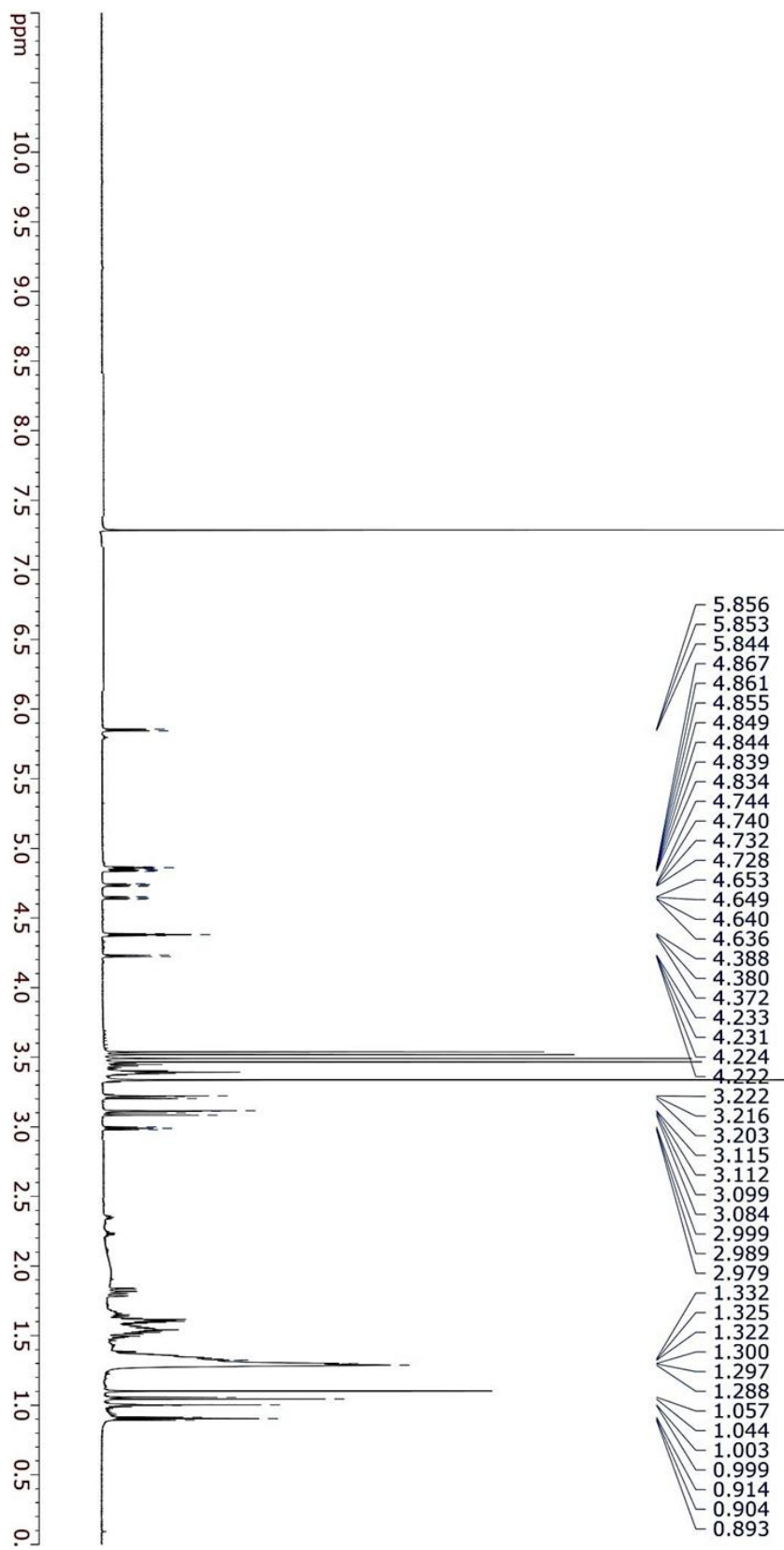
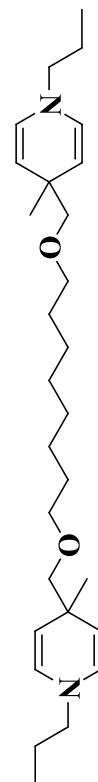
$^{13}\text{C}$ -NMR data for compound (**65**) Recorded on 700 MHz spectrometer (MeOD)



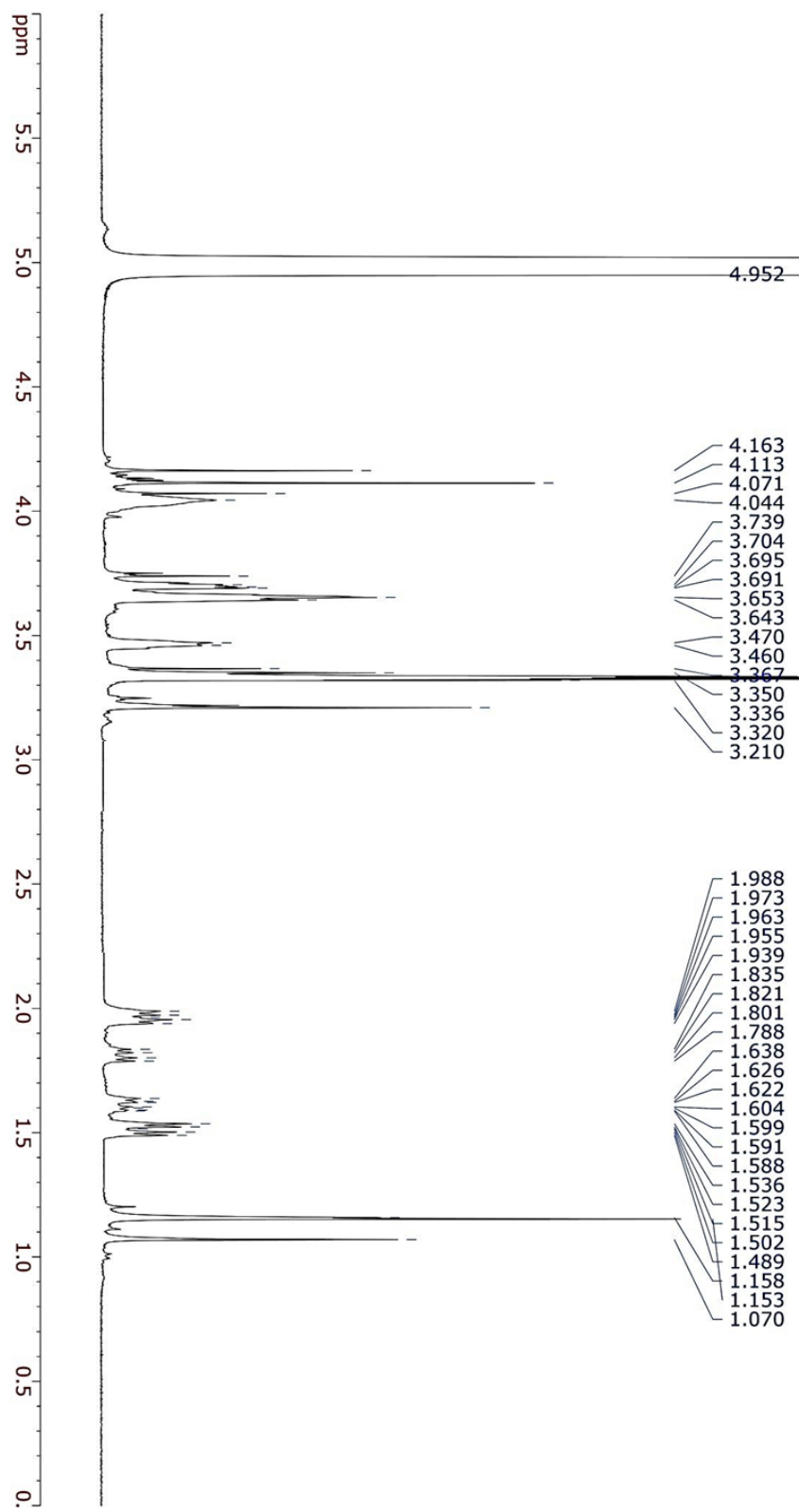
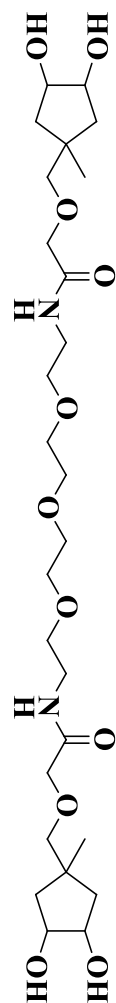
<sup>1</sup>H-NMR data for compound (66) Recorded on 700 MHz spectrometer (CDCl<sub>3</sub>)



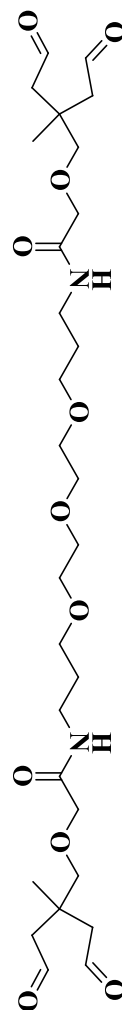
<sup>1</sup>H-NMR data for compound (Attempted Conjugation 67) Recorded on 700 MHz spectrometer



<sup>1</sup>H-NMR data for compound (**69**) Recorded on 700 MHz spectrometer (MeOD)



<sup>1</sup>H-NMR data for compound (**70**) Recorded on 300 MHz spectrometer (CDCl<sub>3</sub>)

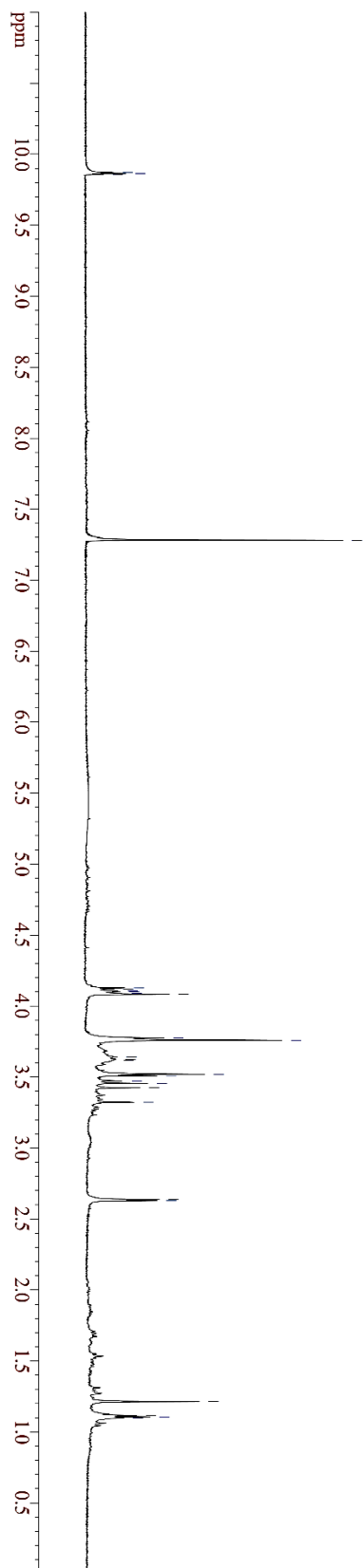


9.872  
9.865  
9.858

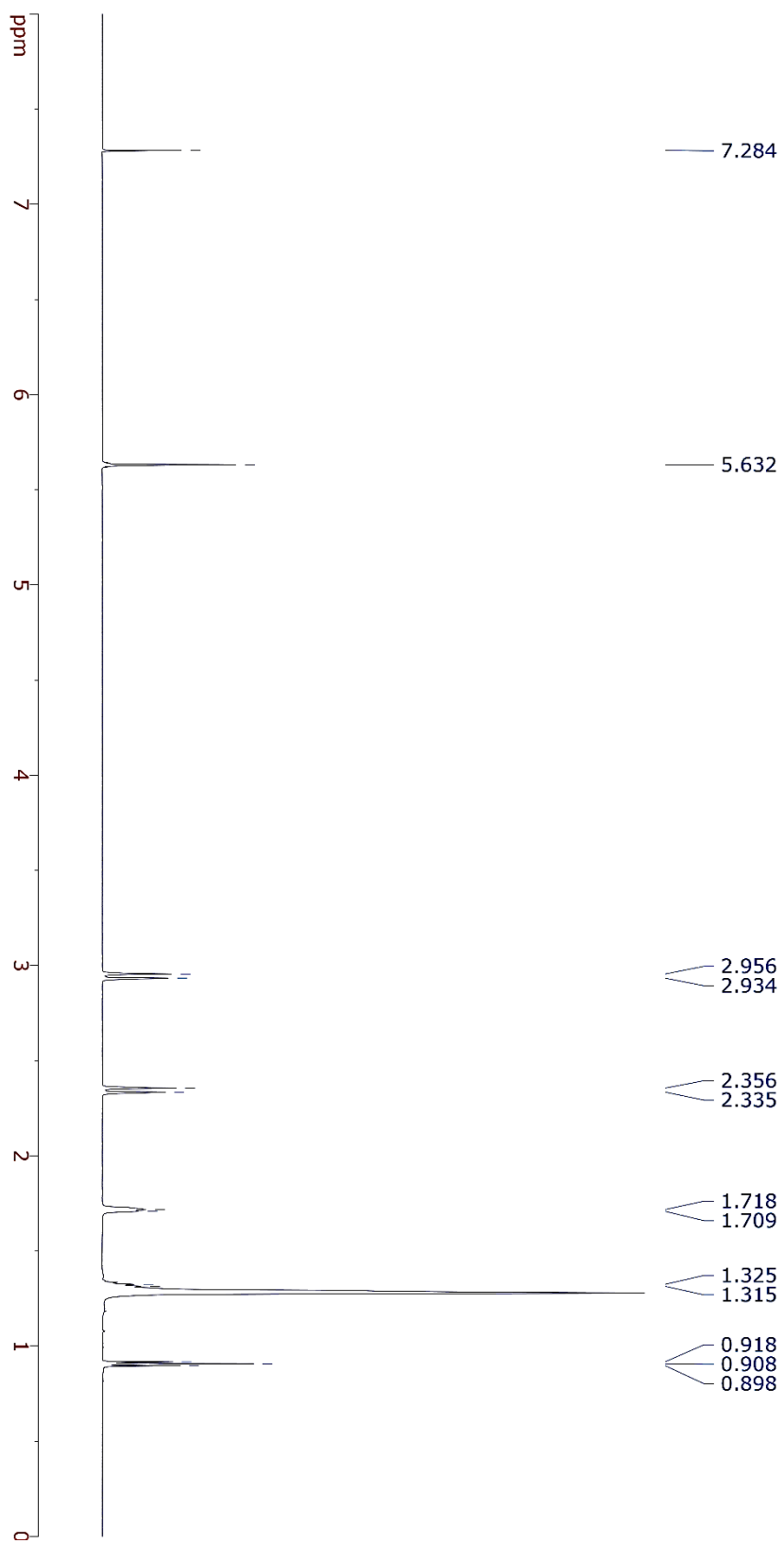
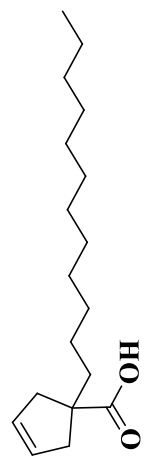
7.281

4.128  
4.119  
4.106  
4.101  
4.089  
4.083  
3.776  
3.759  
3.642  
3.626  
3.623  
3.617  
3.520  
3.509  
3.473  
3.455  
3.424  
3.323  
2.637  
2.630

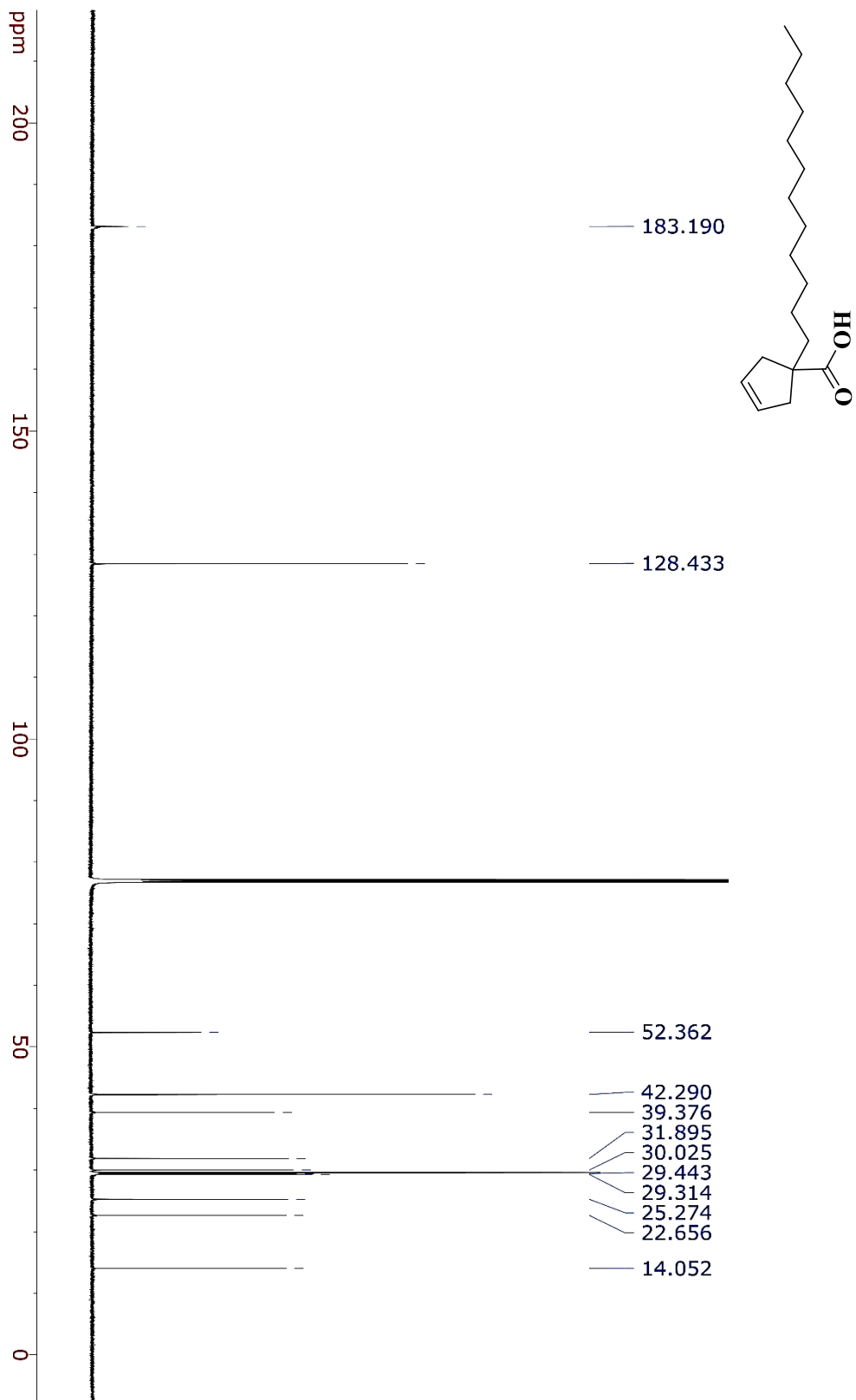
1.214  
1.116  
1.106  
1.099



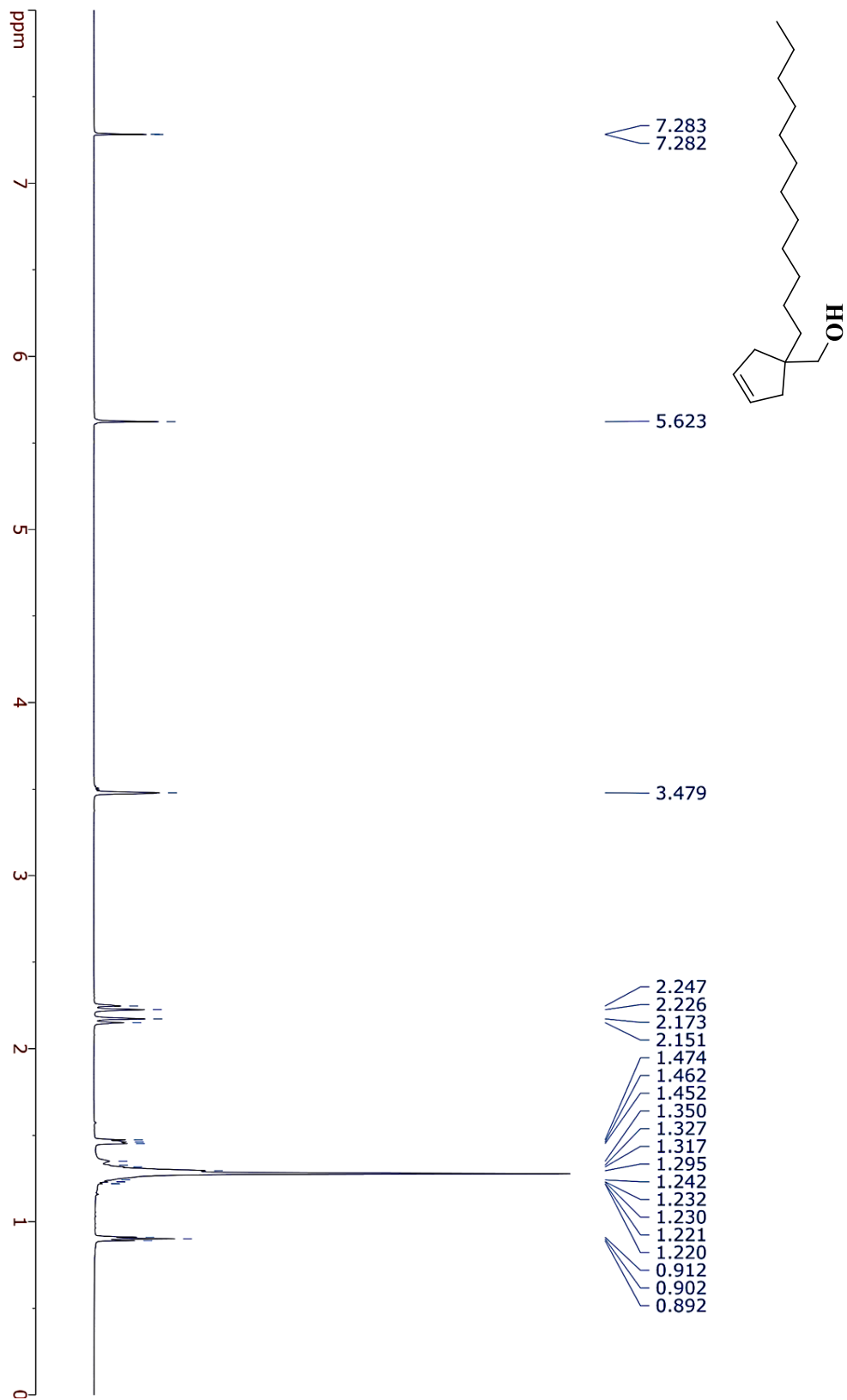
<sup>1</sup>H-NMR data for compound (72) Recorded on 700 MHz spectrometer (CDCl<sub>3</sub>)



$^{13}\text{C}$ -NMR data for compound (**72**) Recorded on 700 MHz spectrometer ( $\text{CDCl}_3$ )

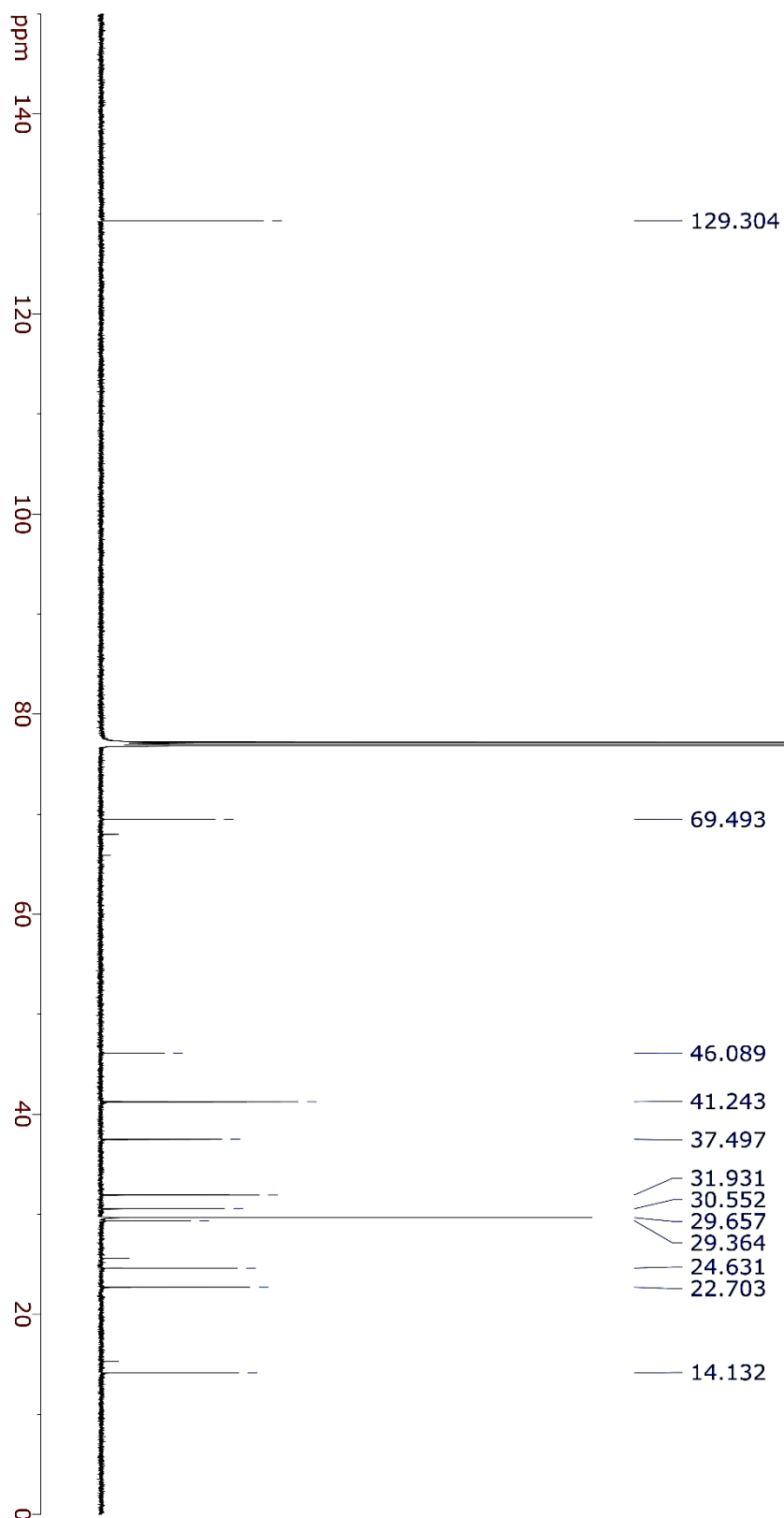
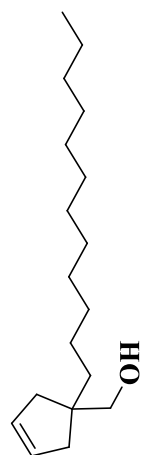


$^1\text{H}$ -NMR data for compound (73) Recorded on 700 MHz spectrometer ( $\text{CDCl}_3$ )

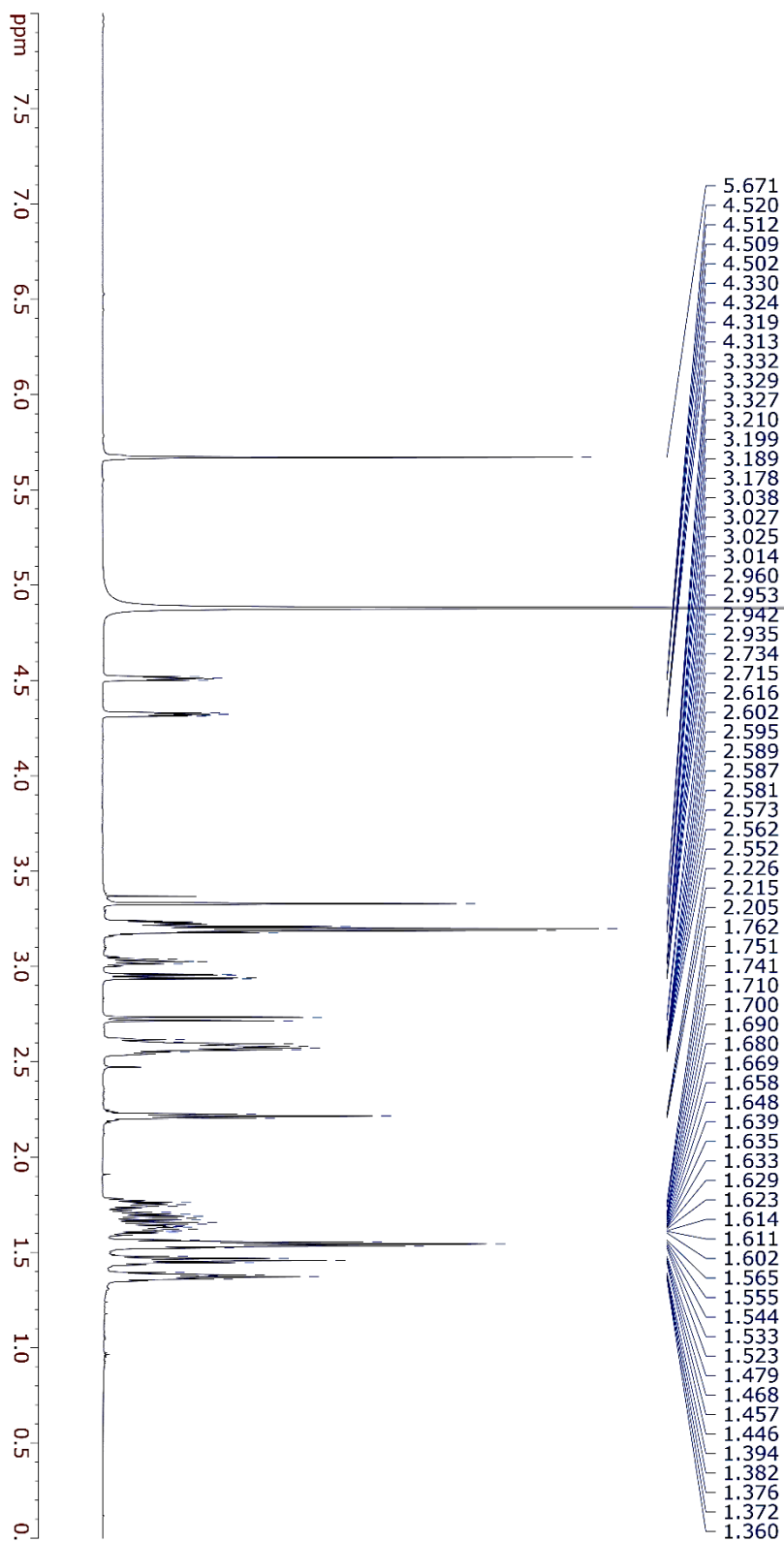
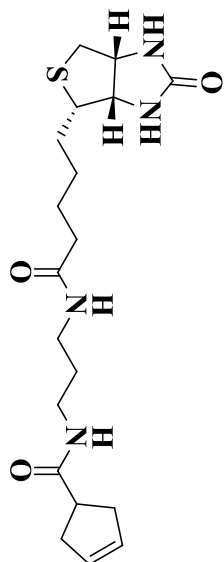




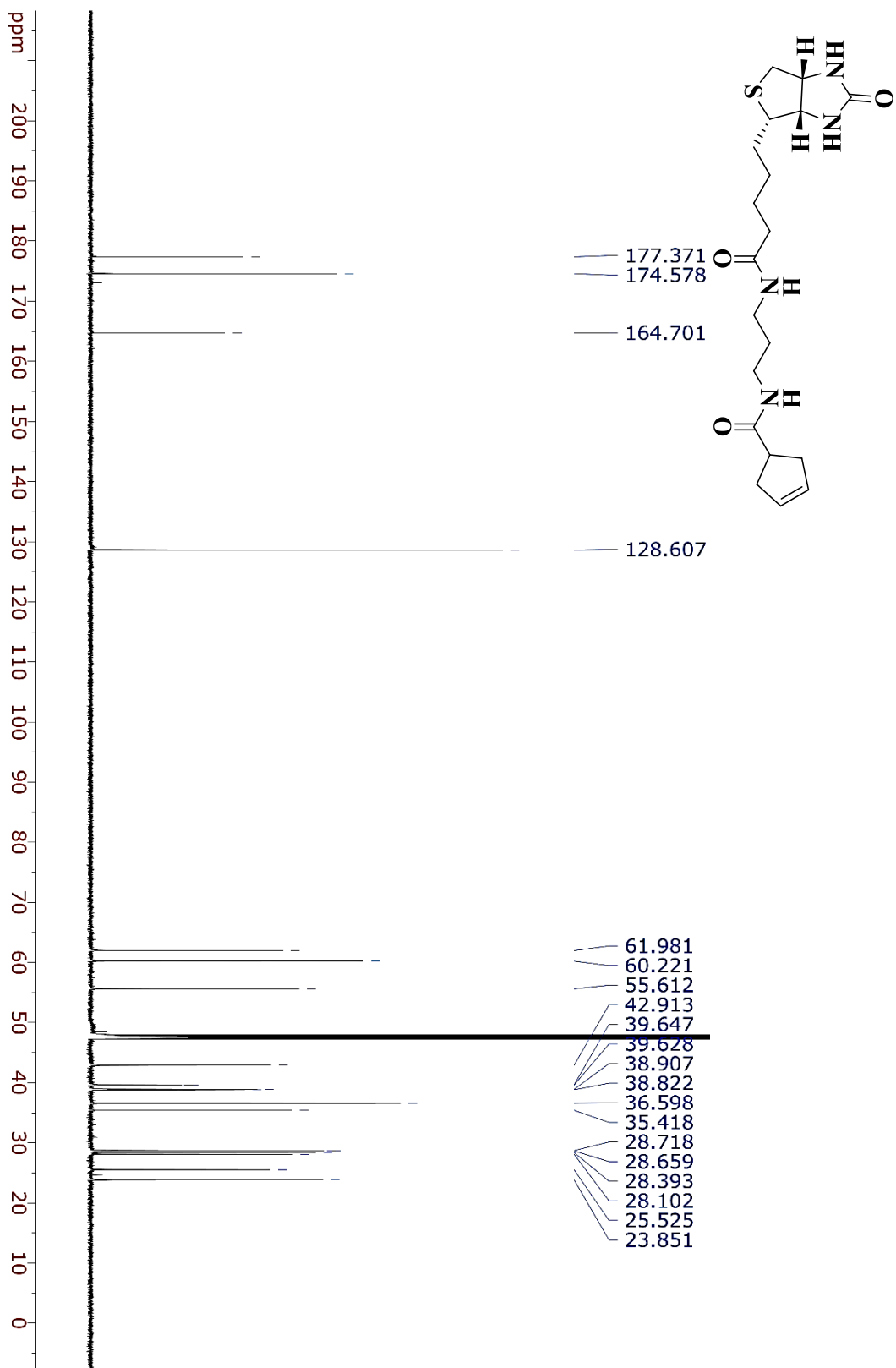
$^{13}\text{C}$ -NMR data for compound (**73**) Recorded on 700 MHz spectrometer ( $\text{CDCl}_3$ )



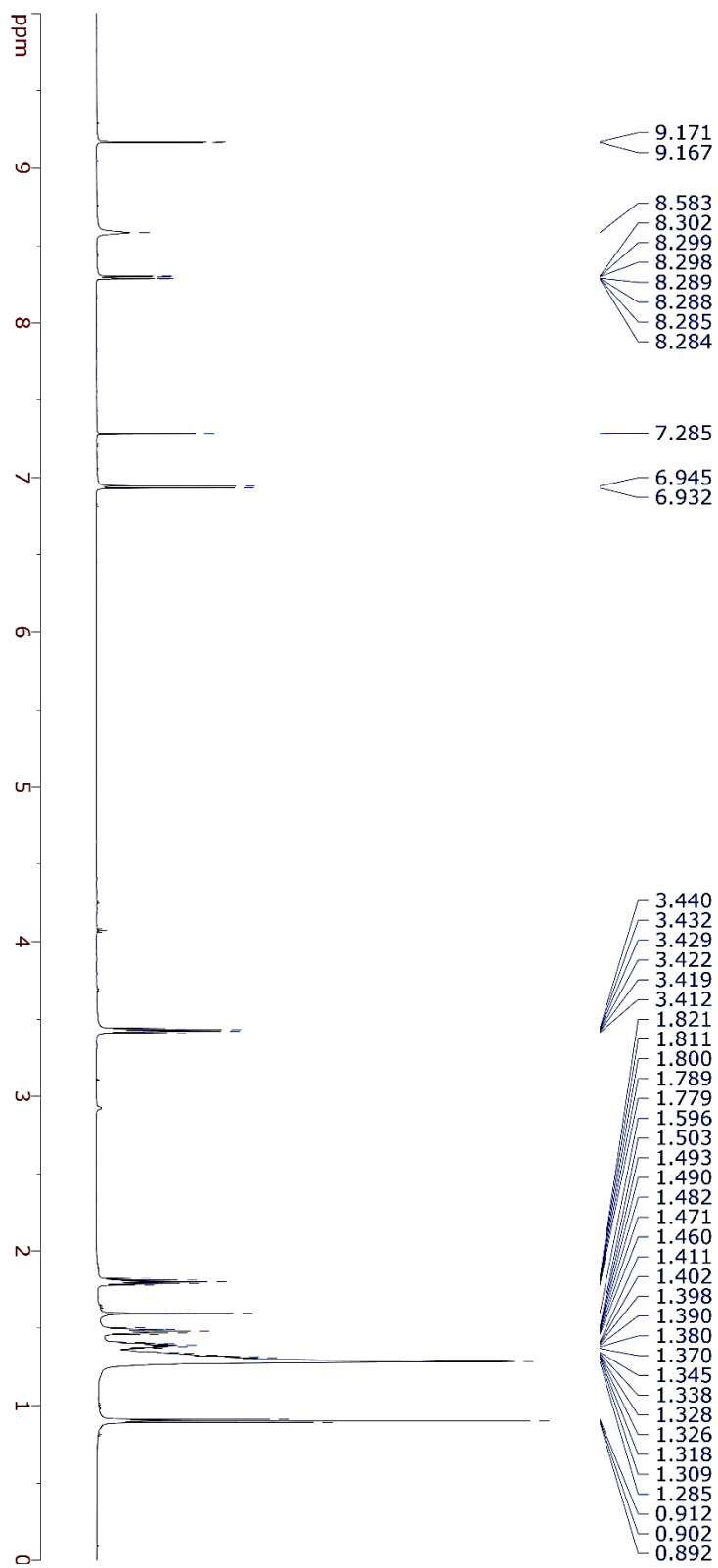
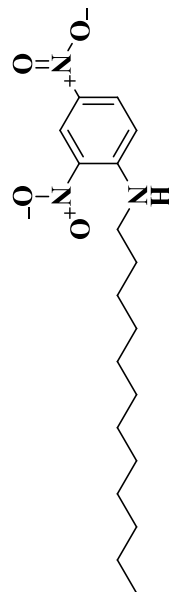
<sup>1</sup>H-NMR data for compound (74) Recorded on 700 MHz spectrometer (MeOD)



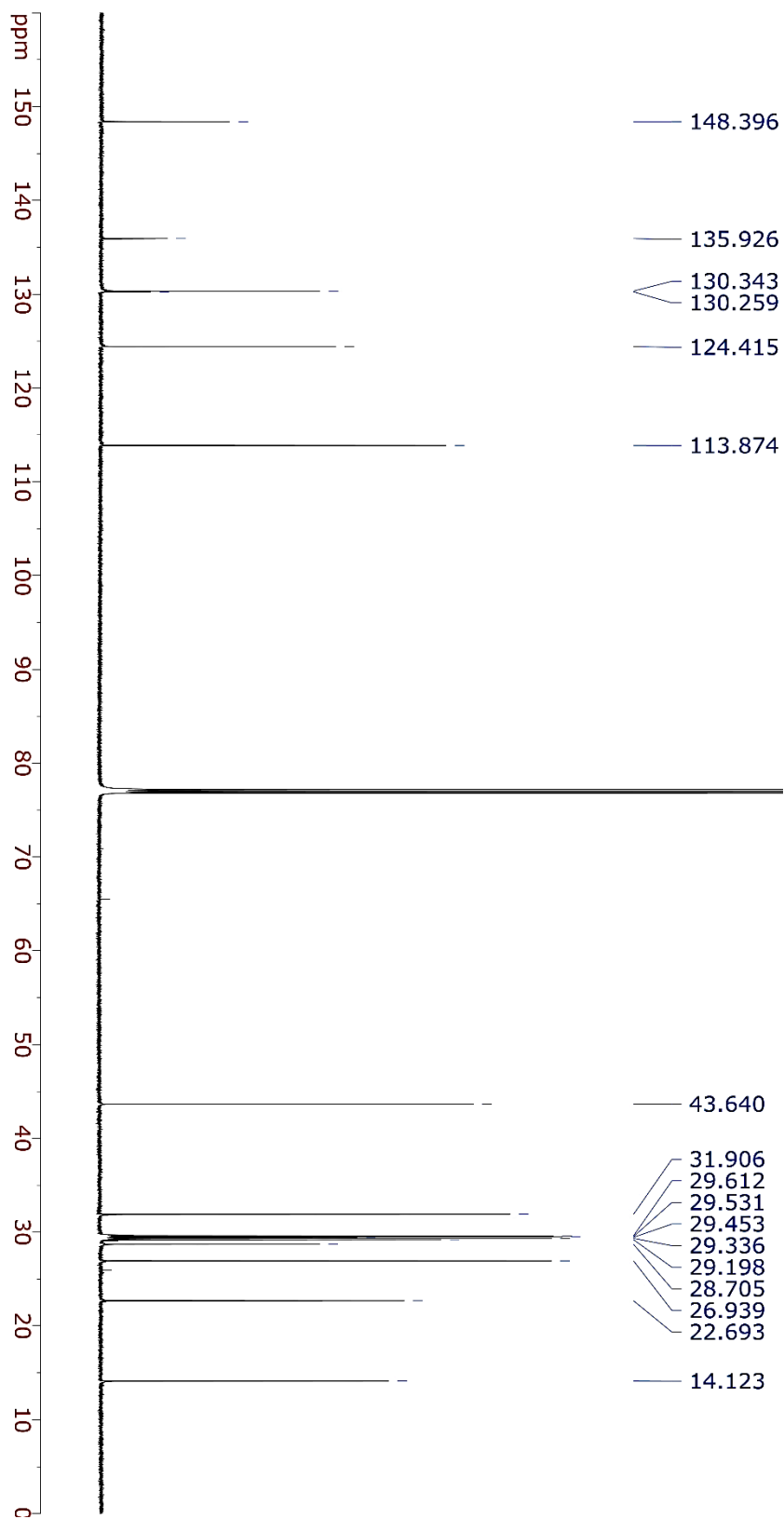
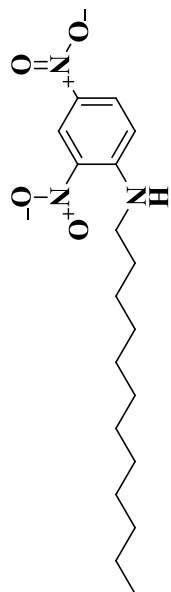
$^{13}\text{C}$ -NMR data for compound (**74**) Recorded on 700 MHz spectrometer (MeOD)

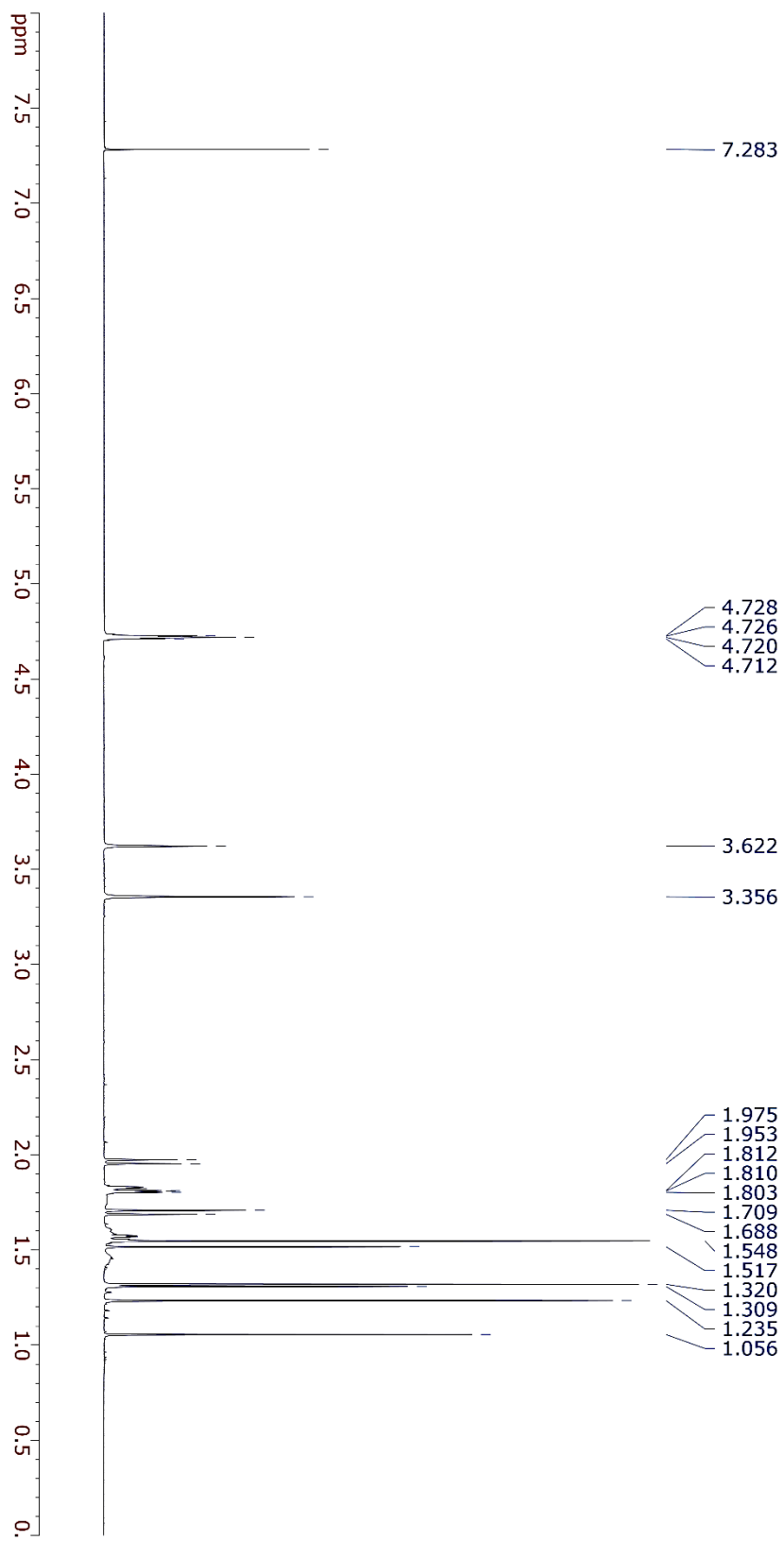
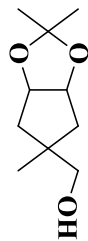


<sup>1</sup>H-NMR data for compound (**75**) Recorded on 400 MHz spectrometer (CDCl<sub>3</sub>)

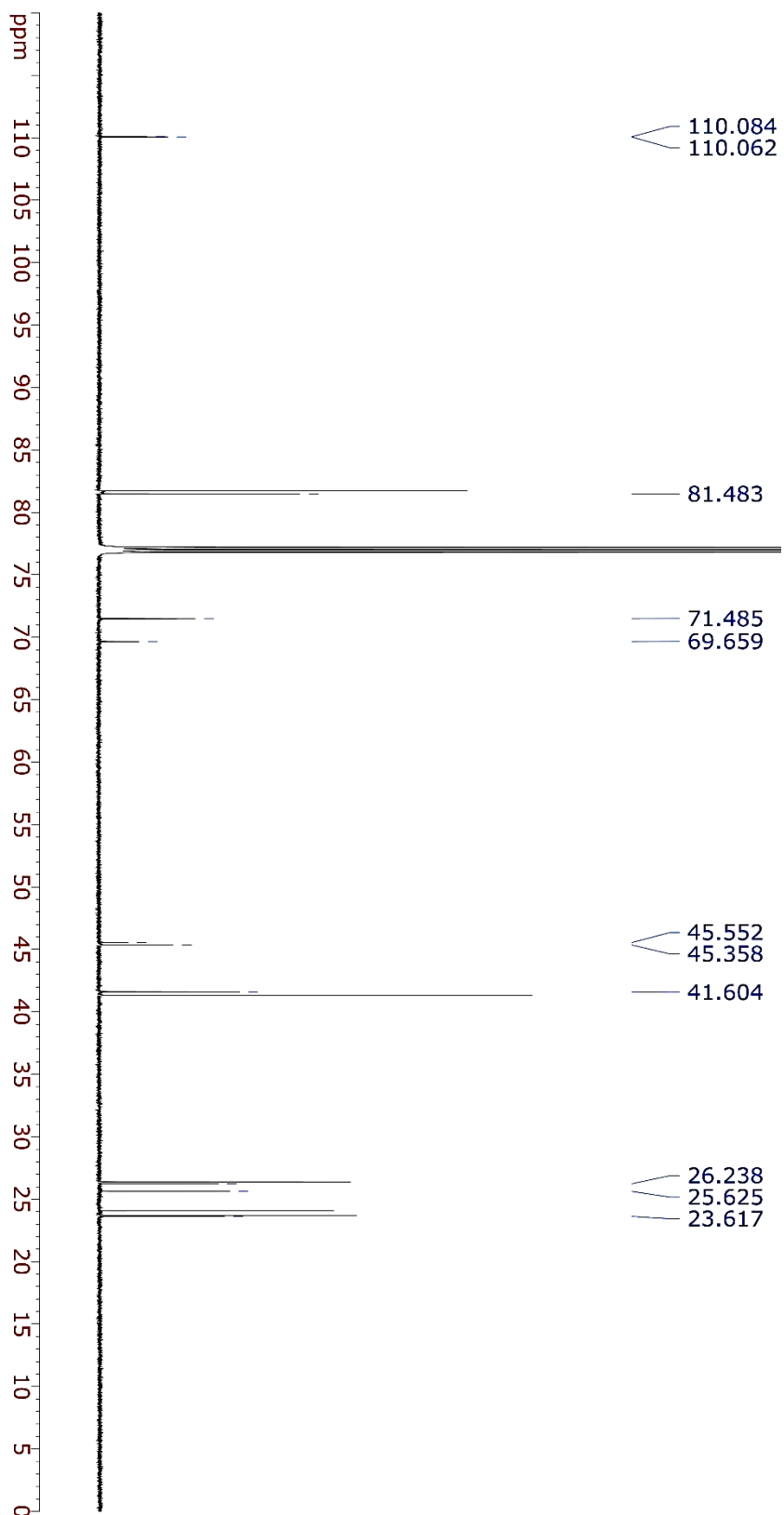
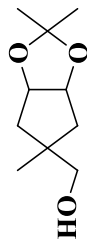


$^{13}\text{C}$ -NMR data for compound (**75**) Recorded on 400 MHz spectrometer ( $\text{CDCl}_3$ )





$^{13}\text{C}$ -NMR data for compound (**76**) Recorded on 700 MHz spectrometer ( $\text{CDCl}_3$ )



<sup>1</sup>H-NMR data for L-Lysine ethyl ester dihydrochloride Recorded on 700 MHz spectrometer

